The role B cells in ANCA-associated vasculitis

Sarah Katrina Todd

UCL

Thesis submitted for the degree of Doctor of Philosophy

Declaration of originality

I, Sarah Katrina Todd confirm that the work presented in this thesis is my own. Where information has been derived from other sources, I confirm that this has been indicated in the thesis

Dedicated to Liam Edmonds, for his unwavering love and support

15 wonderful years, with my hand in yours

Looking forward to the next chapter, of our lives together

Acknowledgements

This work was supported by grants from Kidney Research UK (grant number RP32/2011) and The Wellcome Trust (grant number 090048/B/09/Z).

Sincere thanks to my supervisor Professor Alan Salama, who always had faith in me, even when I doubted myself. Also, to my secondary supervisor Professor Claudia Mauri.

With deep gratitude to Brian Todd, Vicky Strzelczyk, Mark Dyne and Scott Henderson, you have been the very best and most patient of friends. I could not have done it without you.

Thank you to Doctor Simon Wolf, for your care.

Abstract

B cells are central to the pathology of ANCA-associated vasculitis (AAV), a disease characterized by autoantibodies and effectively treated by rituximab. In addition to promoting inflammation, a subset of B cells act to suppress harmful autoimmune responses. The balance of effector and regulatory B cell subsets in AAV is not known. This study was conducted to assess the relative frequency of these subsets during different states of disease activity.

B regulatory cells are reduced in AAV, whether defined as CD5+ or $CD24^{high}$ $CD38^{high}$. There is an imbalance in B regulatory (Breg) and B memory (Bmem) cells, which represents a proinflammatory B cell profile. Bmem augment Th1 differentiation *in vitro*, whilst Breg do not. Breg positively correlate with IL-10 competent B cells and, inversely with TNFα production in B cells. The converse was observed with Bmem. There was no functional defect in Breg from AAV patients, assessed by effect on Th1 differentiation and IL-10 induction *in vitro*.

The imbalance in Bmem and Breg was represented as ratio, calculated from the number of memory cells divided by number regulatory cells in flow cytometry gate (M:Rn).

M:Rn has potential for to be used as a predictive measure of clinical outcome. This imbalance may contribute to the high rate of relapse observed in AAV. Higher ratios were observed in PR3-ANCA patients (who have greatest propensity to relapse), compared to MPO-ANCA patients with the same disease activity. Tolerant patients and those treated with rituximab, had low M:Rn. Rituximab resets the balance of effector and regulatory B cells in AAV, including a tolerogenic state.

Detection of proinflammatory and inhibitory immune mediators in B cells by intracellular flow cytometry, warranted additional analysis to better define the cytokine profile. 15 analytes were measured in cell supernatants. IL-10, IL-6, IL-1β, TNFα, IL-17A, IFNγ and IL-2 were significantly induced in PBMC, stimulated for maximum IL-10 induction in B cells. The net effect of these supernatants was to limit T cell TNFα production *in vitro,* this was not impaired on blockade of IL-10 with an agonistic antibody.

Highly activated CD4 cells were increased in AAV, whilst Treg were reduced. There was no relationship between Breg and Treg frequency in AAV. Patients had reduction in Breg or Treg, but not both (frequency lower than the mean of the healthy controls, minus 2 standard deviations).

Further investigation was conducted in an MPO animal model of disease, in which passive transfer of antibodies or B cells are reported to be pathogenic. Limited disease was observed on cell transfer, despite equivalent autoantibody titres to MPO null, immunised mice.

B cells or antibody alone are insufficient to cause disease, an initiating event is crucial with deposition of MPO on the microvasculature and tissue damage elicited by innate immune cells previously described. Without this inciting damage, adaptive immune ignorance is maintained and renal function unaffected.

Impact statement

Antineutrophil cytoplasmic antibody (ANCA)-associated vasculitidies (AAV) are systemic autoimmune diseases, managed by immunosuppressive therapy. Treatment is inadequate in some incidences, 20% relapse annually and 30% of patients become dialysis dependent. In others the burden of treatment is too much, with increased risk of infection and cancer.

At the time of undertaking this study, rituximab a B cell depleting therapy had been approved for treatment. New effector and functions had been attributed to B cells, but we did not yet know what role B cells may have in AAV beyond antibody production or why rituximab might be beneficial, since the CD20 target is absent from plasma blasts.

A subset of B cells was reported to be immunoregulatory (Breg) and functionally defective in Systemic Lupus Erythematous (SLE) (Blair, Norena et al. 2010). SLE like AAV, is a systemic autoimmune disease, defined by the presence of pathological antibodies and often presenting with glomerulonephritis.

We had identified a rare subset of patients who re-established immune tolerance, becoming ANCA-negative and demonstrating prolonged, disease-free remission after withdrawal of all treatment ($\geq$2 years). B cell subset frequency and function had not previously been assessed in autoimmune patients, who re-establish immune tolerance.

The study represents one of the most comprehensive assessments of B cell phenotype and function in AAV. It is the only one to include functional assessment of unstimulated B cells, with effects on Th1 differentiation investigated. In addition to B

cell IL-10 induction, B cell production of TNFα and TGFβ was demonstrated and soluble mediators measured in cell supernatants.

The results presented here, add to the cumulating evidence that Breg are numerically deficient in AAV. Immunophenotyping revealed an imbalance in memory B cells (Bmem) and Breg, predicted to be proinflammatory.

The balance of Bmem and Breg subsets was presented as a ratio (M:Rn), and proposed as a prognostic indicator in AAV. M:Rn was profoundly different in tolerant patients or following rituximab therapy. Rituximab resets the balance of effector and regulatory cells, inducing a tolerogenic state.

M:Rn might be predictive of whether rituximab treatment is likely to be successful in other autoimmune diseases. Clinical trials in SLE (LUNAR NCT00282347 and EXPLORER NCT00137969 studies) did not meet threshold for clinical efficacy. Treatment of rituximab continues off label; as an expensive biological therapy it would be useful to have to an indicator of success.

I suggest revisiting the cell transfer model of disease, considering the newly appreciated functions of B cells in human disease. This would permit the role of antibody, effector and regulatory B cells in AAV to be resolved.

This work has been widely disseminated, with poster presentations at the 8th International Conference on Autoimmunity, Granada, Spain, 2012 and The 17th ANCA Workshop in London, 2015 (Todd, Henderson et al. 2015). The immunophenotyping and functional characterisation of B cell subsets was selected for an oral presentation at The 16th ANCA Workshop in Paris, 2013 (Todd, Pepper et al.

2013) and published in Oxford Journal of Rheumatology, 51 citations to-date (Todd, Pepper et al. 2014).

Table of contexts

Acknowledgements 4

Abstract 5

Impact statement 7

Table of contexts 10

Index of figures 16

Index of tables 20

Chapter 1 Introduction 21

1.1 Innate and adaptive immunity 23

1.2 Antigen receptor diversity 24

1.3 Immunological tolerance 27

1.4 Classification of B cells 44

1.5 Effector B cell functions 46

1.6 Regulatory B cells 50

1.7 Anti-neutrophil cytoplasm antibody (ANCA)-associated vasculitidies 61

Hypothesis and aims 70

Chapter 2 Methods 71

2.1 Human Studies 71

2.2 MPO protein production 83

2.3 *In vivo* murine methods 88

2.4 *In vitro* murine methods 92

Chapter 3 CD24 and CD38 B cell immunophenotyping 100

3.1 Background 100

3.2 Aims 104

3.3 Methods in brief 104

3.4 Patient and healthy control samples 104

3.5 Results 106

3.5.1 Patient demographics 106

3.5.2 Comparison relative to disease controls **Error! Bookmark not defined.**

3.5.3 Differences in B cell subsets according to disease activity 118

3.5.4 Analysis of B cells according to disease activity and ANCA ..... **Error! Bookmark not defined.**

3.5.5 Relative B cell frequencies 128

3.5.6 Effects of rituximab on B cell subsets.. **Error! Bookmark not defined.**

3.5.7 Outcome data 133

3.6 Key findings 136

3.6.1 B subsets altered in AAV and differ according to disease activity 136

3.6.2 Frequency of B cell subsets differs according to ANCA specificity . 136

3.6.3 B cell changes after rituximab treatment 136

3.7 Discussion 137

3.7.1 Rationale for CD24 CD38 gating strategy 137

3.7.2 Cumulative evidence for an imbalance in B cell subsets in AAV 138

3.7.3 Discussion of treatment effects 145

Chapter 4 Additional B cell immunophenotyping 150

4.1 Background 150

4.2 Aims 152

4.3 Methods in brief 152

4.4 Patient and healthy control samples 153

4.5 Results 157

4.5.1 CD1d immunophenotyping 157

4.5.2 CD5 immunophenotyping 167

4.5.3 Flow cytometry to verify that the 3 B cell subsets, defined by relative expression of CD24 and CD38 are phenotypically distinct 179

4.6 Key findings 199

4.6.1 There is little differential expression in CD1d in B cells 199

4.6.2 CD5 B cells are reduced in AAV, but CD5 expression not limited to a single B cell subset and CD5 expression is inducible 199

4.6.3 CD24 and CD38 B cell subsets are distinct 199

4.7 Discussion 202

Chapter 5 Assessment of B cell function 208

5.1 Background 208

5.2 Aim 210

5.3 Methods in brief 210

5.4 Results 212

5.4.1 Co-culture of B cell subsets and T cells 212

5.4.2 Intracellular flow cytometric detection of B cell cytokines 220

5.4.3 Soluble mediators detected in supernatants of PBMC stimulated with CPG alone or in combination with CD154 235

5.4.4 Net effect of supernatants on T cells 246

5.5 Key findings 249

5.5.1 Bmem and Bnaive cells augment Th1 differentiation, Breg do not 249

5.5.2 IL-10 B cell frequency is comparable in AAV remission patients and healthy controls 249

5.5.3 Conditions favouring B cell IL-10 production also induce TNFα and TGFβ 249

5.5.4 Balance of B cell subsets, linked to B cell cytokine production 250

5.5.5 CD24 and CD38 immunophenotyping after stimulation 250

5.5.6 Immune mediators detected in supernatants of PBMCs 251

5.5.7 Correlation between soluble analytes and B cell subsets at baseline 251

5.5.8 Effect of supernatants from PBMCs, stimulated for IL-10 induction 252

5.5.9 Summary 252

5.6 Discussion 253

5.6.1 B cell co-cultures 253

5.6.2 IL-10, TNFα and TGFβ induction in B cells 254

5.6.3 Soluble mediators detected in supernatants 256

Chapter 6 Relationship with CD4 subsets 258

6.1 Background 258

6.2 Aims 259

6.3 Methods in brief 261

6.4 Results 268

6.4.1 Treg frequency is reduced in AAV patients compared to controls 268

6.4.2 Treg and B cell subset regression analysis 271

6.4.3 AAV patients had an increased frequency of highly activated CD4 T cells 275

6.4.4 Expression of CD39 and CD73 in PBMC 279

6.4.5 Regression analysis of ATPase positive Treg, B cell subsets and cytokines ..... **Error! Bookmark not defined.**

6.5 Discussion 291

Chapter 7 Investigation of the role of B cells in an *in vivo* model 298

7.1 Background 298

7.2 Aims 303

7.3 Methods in brief 303

7.4 Results 304

7.4.1 Assessment of B cell phenotype in mice 304

7.4.2 Challenges of the MPO cell transfer model 320

7.4.3 Investigation of the role of B cells in the MPO cell transfer model 329

7.5 Key findings 353

7.5.1 Phenotyping of candidate immunoregulatory B cells 353

7.5.2 Precursor B cells are present in Rag2 mouse spleen 353

7.5.3 Successful cell transferral into Rag2 mice 353

7.5.4 Disease penetrance and severity less, than previously described. 354

7.5.5 B cells alone are unlikely to be pathological 354

7.6 Discussion 355

Chapter 8 Final summary 362

References 367

Appendix Summary of all tests conducted in AAV patientsError! Bookmark not defined.

Index of figures

Figure 1.1 Lymphocyte antigen receptors 30

Figure 1.2 CD4 T cell subsets 34

Figure 1.3 The process of B cell devlopment 39

Figure 1.4 Key mechansims in immunoregulatory B cells 60

Figure 1.5 Key pathogeneic mechanisms in AAV 65

Figure 2.1 Modified Ig subtyping ELISA 96

Figure 3.1 Frequency of B cell subsets in patients and controls 109

Figure 3.2 Refinement of patient cohort after collection of clinical data 111

Figure 3.3 Differences in B cell subsets according to disease activity 119

Figure 3.4 B cell subsets according to disease activity 123

Figure 3.5 Comparison of patients according to disease activity and ANCA 125

Figure 3.6 Comparison of B cell profile in tolerant patients and other 127

Figure 3.7 Comparison of relative cell numbers in patients 129

Figure 3.8 Effects of rituximab on B cell profile, paired analysis and 131

Figure 3.9 Relapsing and non-relapsing PR3-ANCA patients 135

Figure 4.1 Little differential expression of CD1d on biaxial plots 158

Figure 4.2 Consistent staining with 51.1 or CD1d42 clone 162

Figure 4.3 CD1d extracellular and intracellular staining at baseline 165

Figure 4.4 CD5 variation in paired fresh and frozen samples 168

Figure 4.5 B cell immunophenotyping in paired fresh and frozen samples 170

Figure 4.6 CD24 and CD38 consistent on freeze-thawing 171

Figure 4.7 CD5 B cells are reduced in AAV 175

Figure 4.8 Correlation between CD5+ B cells and Breg 178

Figure 4.9 CD5 B cells, no line between age or lymphocyte count 180

Figure 4.10 No differential expression of CD1d in B cell subsets 184
Figure 4.11 Breg highest CD5 expresion but CD5+ not limitted to a subset 185
Figure 4.12 Bmem cells are highly enriched in the CD27+ gate 186
Figure 4.13 Breg, Bnaive and Bmem populations correspond well with CD5 187
Figure 4.14 CD24 and CD38 gates applied to CD5 or CD27 B cells, data..... 188
Figure 4.15 IgD and IgM staining combined with CD19, CD24 and CD38 192
Figure 4.16 Positive correlation between Bmem and CD95 B cells, no relationship between CD10 B cells and Bmem or Breg 195
Figure 4.17 Graphical summary of CD10 and CD95 flow cytometry data..... 197
Figure 4.18 Flow cytometry plots of CD10 and CD95 expression profiles 198
Figure 4.19 Verification that CD24 and CD38 B cell subsets are distinct 201
Figure 5.1 Breg limited CD4 cell proliferation in the 5-day culture system 213
Figure 5.2 Purity of magnetically isolated CD4+ CD25- T cells 214
Figure 5.3 Purity of FACS sorted B cell subsets 215
Figure 5.4 Cytokine MFI in T cells cultured with B cell subsets 216
Figure 5.5 Comparison of cytokine positive T cells in B cell co-cultures 219
Figure 5.6 IL-10 induction, also results in TNFα and TGFβ production 221
Figure 5.7 Remission patients' cytokine profile not significantly different..... 222
Figure 5.8 B cell production of TGFβ 223
Figure 5.9 Regression a of Bmem and Breg, with IL-10 B cell frequency 225
Figure 5.10 Regression analysis starting frequency of Bmem and Breg, with 226
Figure 5.11 Stability of B cell subsets on stimulation..... 227
Figure 5.12 B cell profile in unstimulated cells compared with IL-10+ B cells, after maximum stimulation..... 229
Figure 5.13 Different intensity of intracellular staining, in the B cell subsets 230

Figure 5.14 B cell cytokine intensity, in CPG stimulated PBMC 232
Figure 5.15 Differences in patients and controls, upon CPG stimulation 233
Figure 5.16 B cell cytokine intensity in CPG and CD154 stimulated PBMC..... 234
Figure 5.17 Detection of soluble cytokines in PBMC supernatants..... 237
Figure 5.18 Cytokines detected in supernatants of stimulated PBMCs 238
Figure 5.19 IL-9 not induced and approaching the limit of detection..... 239
Figure 5.20 Comparsion of soluble cytokines in patients and healthy controls 241
Figure 5.21 Net cytokine profile in supernatants from stimulated PBMC 243
Figure 5.22 Cytokine profile, represented as percentage of all analytes detected 244
Figure 5.23 Linear regression of B cell subsets with soluble cytokines..... 245
Figure 5.24 Net effect of PBMC supernatants on T cells..... 248
Figure 6.1 Gating strategy for CD4, CD25 and CD127 stained PBMC..... 263
Figure 6.2 Gating strategy for CD39 and CD73, within Treg 264
Figure 6.3 Treg reduced in AAV, frequency not affected by age 270
Figure 6.4 Treg correlation with B cell subsets..... 272
Figure 6.5 Colour coding to denote of ANCA specificity and disease activity .. 273
Figure 6.6 Highly activated T cells are increased in AAV, balance with Treg is perturbed and there is relationship with B cell subsets 277
Figure 6.7 Comparison of CD39 and CD73 expression in T cell subsets 284
Figure 6.8 Regression analysis of ATPase positive Treg..... 290
Figure 7.1 IL-10 induction in murine splenocytes, 5-hour stimulation..... 306
Figure 7.2 IL-10 induction in mice, 48-hour stimulation with LPS 307
Figure 7.3 Immunophenotyping of mouse splenocytes..... 310
Figure 7.4 Comparison of bone marrow, splenic and peritoneal B cells..... 311
Figure 7.5 Extended immunophenotyping in splenic B cells..... 314

Figure 7.6 Comparison of CD1d+ and CD1d- splenic B cells 315
Figure 7.7 TIM-1 expression in mouse splenocytes 316
Figure 7.8 Magnetic isolation of CD1d B splenocytes 318
Figure 7.9 Magnetic enrichment of CD19+ B splenocytes and flow cytometry . 319
Figure 7.10 Successful B cell transfer and pathology on initial testing 323
Figure 7.11 Low MPO antibodies titres in the initial experiment 324
Figure 7.12 Quality assessment of a new batch of murine MPO 326
Figure 7.13 Response upon immunisation, with the new batch of MPO 327
Figure 7.14 MPO titres of mice, used for final splenocyte transfer experiment ... 328
Figure 7.15 Transfer of splenocytes into Rag2 mice 331
Figure 7.16 Verification of cell transfer in Rag2 mouse blood 332
Figure 7.17 Verification of cell transfer in Rag2 mouse spleen 334
Figure 7.18 Different frequency of CD19+ and B220+ B cells in spleen 335
Figure 7.19 Phenotype of the $B220^{low}$ $CD19^{high}$ splencoytes 336
Figure 7.20 Variable MPO response in MPO-/- immunised and Rag2 mice 338
Figure 7.21 MPO antibody levels in Rag2 mice and $MPO^{-/-}$ immunised 339
Figure 7.22 Overview of pulmonary pathology observed in Rag2 mice 341
Figure 7.23 Further characterisation of lung pathology 342
Figure 7.24 Summary of renal pathology in rag2 mice 343
Figure 7.25 Pathological renal findings in Rag2 mice 344
Figure 7.26 Enumeration of infiltrating T cells in Rag2 kidney 346
Figure 7.27 Increase in splenic mass and restoration of normal architecture 348
Figure 7.28 Analysis of B and T cell splenic composition in Rag2 mice 350
Figure 7.29 Total IgG levels and Ig subtyping in Rag2 mice 351

Index of tables

Table 2.1 Analytes measured in PBMC supernatants 82

Table 2.2 Polyacrylamide gel preparation..... 87

Table 2.3 Immunisation schedule in MPO null mice..... 90

Table 2.4 Antibodies used for B cell immunophenotyping in mice..... 97

Table 3.1 Refined patient cohort, compared according to disease activity..... 115

Table 3.2 Details of patients with acute disease..... 116

Table 3.3 B cell subsets following rituximab therapy..... 132

Table 3.4 Evidence for reduced frequency of regulatory B cells in AAV 143

Table 4.1 CD5 cohort, patients compared according to disease activity .....**Error! Bookmark not defined.**

Table 4.2 Geometric MFI for CD1d in B cells, across various conditions..... 166

Table 4.3 Verification that CD24 and CD38 B cell subsets are distinct..... 200

Table 6.1 Treg cells are numerically or functionally deficient in AAV 260

Table 6.2 Patient cohort 266

Table 6.3 Summary of analysis of CD39 and CD73 expression in PBMC 286

Table 7.1 *In vivo* models of MPO-ANCA vasculitis 299

Chapter 1 Introduction

Foreword

In this opening chapter I will discuss how B and T cells operate within the adaptive immune system. Random rearrangement of B and T cell receptor gene segments, result in millions of different antigen specificities, conferring broad protection from pathogens. As antigen receptor gene rearrangement proceeds by chance, it can also result in cells that react with self. B and T cells are subject to selection during development and additional mechanisms exist to remove or tame these cells in the periphery. Both central and peripheral tolerance must be overcome for autoimmunity to ensue. Productive cells, that recognise cognate antigen are maintained in the memory pool and consequently, autoimmune conditions are lifelong and debilitating.

The terminal function of B cells is classically considered antibody production, with autoantibodies central to the pathogenesis of many autoimmune diseases. B cells also produce a wide range of cytokines, both pro-inflammatory and immunoregulatory. B regulatory cells (Breg) were first characterised by production of interleukin 10 (IL-10), with additional attributes and cell surface markers subsequently defined. Breg defined by high surface expression of CD24 and CD38, were shown to be functionally perturbed in Systemic Lupus Erythematous (SLE) a prototypic autoimmune disease (Blair, Norena et al. 2010).

Antineutrophil cytoplasmic antibody (ANCA)-associated vasculitis (AAV) like SLE, is an autoimmune disease characterised by autoantibody production. Detection of ANCA has a very high diagnostic sensitivity and specificity for disease, whilst B cells

from ANCA positive mice or antibody transfer alone, is pathological in mice (Xiao, Heeringa et al. 2002).

Following 2 large clinical trials (RITUXVAS and RAVE), the anti-CD20 B cell depleting agent Rituximab received clinical approval for treatment of AAV (Jones, Tervaert et al. 2010, Stone, Merkel et al. 2010). CD20 expression is down modulated in antibody producing plasma cells and serum immunoglobulins have long half-lives. Collectively this suggested that the role of B cells beyond antibody production, is important in AAV pathogenesis.

At the time of undertaking this research B cells had not been extensively studied in AAV. There was no phenotypic characterisation of B cell subsets in AAV based on relative CD38 and CD24 expression; there was one study reporting a reduction in Breg in active disease and restoration in remission, with Breg characterised as CD25+ and CD86+ (Eriksson, Sandell et al. 2010). No functional assessment of B cell subsets had been conducted, and so my work focussed on better defining the role of B cells, and specifically Breg, in AAV

AAV is typically a chronic disease, with a relapsing-remitting course. However, we also identified a rare subset of patients who re-established immune tolerance, becoming ANCA-negative and demonstrating prolonged, disease-free remission after withdrawal of all treatment ($\geq$2 years). Newell *et al* previously described a B cell signature in tolerant renal transplant recipients (Newell, Asare et al. 2010); this was surprising because B cells are typically considered pathological in solid organ transplantation, with alloantibodies attacking the graft. B cell subset frequency and function has not previously been assessed in autoimmune patients, who re-establish immune tolerance.

1.1 Innate and adaptive immunity

The immune system can be broadly classified into native responses, present at birth and adaptive responses, which are learnt and evolve throughout a lifetime. Innate immune cells include neutrophils, monocytes, macrophages, dendritic cells (DC) and natural killer (NK) T cells. Other components of the native immune system include the complement system, physical and chemical barriers.

The cells of innate immune system do not have the same exquisite specificity as the adaptive immunity but do have pathogen selectivity, binding common molecular targets via pattern recognition receptors (PRR). The functions of the innate immune system include clearance of immune complexes and cellular debris, production of reactive oxygen species (ROS), release of proteolytic enzymes, direct cell killing via death receptors, production of chemokines and cytokines. Innate immune cells respond immediately, but there is no refinement of the response during the course of infection and no enhancement, upon subsequent exposure. They are crucial for the recruitment and activation of adaptive immune cells.

The adaptive immune system has a much broader range of reactivity and is more potent. Response are delayed relative to innate immunity, but are honed during an infection, with memory cells retained, to more rapidly deal with subsequent exposure. Although autoimmune diseases are initiated by innate immune system, overt disease is a consequence of a misdirected adaptive immune response, with life-long, destructive reactivity specifically towards self. The central cells of the adaptive immune system are lymphocytes, B and T cells.

B and T cells are so named, because of their initial characterisation in the Bursa of Fabricius and Thymus (Cooper, Peterson et al. 1965). In mammals, the bone marrow

(BM) is equivalent to the bursa of Fabricius, the latter only being present in birds. The thymus and BM are together referred to as the primary lymphoid organs, the sites where lymphocytes are formed and mature. After birth this is true, with all immature lymphocytes originating from a common lymphoid precursor in BM, and T cell maturation proceeding in the thymus. However, in embryogenesis lymphopoiesis initially occurs in the yolk sac, moving to the mesoderm and then the liver, spleen and BM. Some of these lymphocytes of foetal origin form long-lived, self-sustaining populations: B1 B cells and innate lymphoid cells (ILC). These cells are evolutionary ancient but share morphology, functional characteristics or markers, with classical lymphocytes. Critically these cells have limited or no antigen restriction and are maintained without refinement in specificity (Artis and Spits 2015). From now on, the term lymphocyte will only be used to refer to the antigen restricted B and T cells of the adaptive immune system.

1.2 Antigen receptor diversity

Lymphocytes have exquisite specificity and are highly potent, with activation, resulting in clonal expansion and life-long immunological memory. The adaptive immune system can protect against a diverse range of pathogens because there is a large repertoire of lymphocytes. The number of specificities is estimated to be greater than $x10^{12}$ (Dongen, Szczepanski et al. 2002), which far exceeds the total number of genes in the human genome. This breadth of protective immunity is possible through random recombination of discrete variable, diversity and joining gene segments (V, D and J segments respectively). The recombinase enzyme complex is critical for combining the discrete gene segments and removing the intervening material. The two proteins which comprise this complex are called RAG1 and RAG2, encoded by *recombination activating gene 1 and 2*. In the absence of these proteins, VDJ

recombination cannot occur and no mature B or T cells are formed (Shinkai, Rathbun et al. 1992). Additional levels of complexity are conferred by random insertion of nucleotides between the gene segments (junctional diversity), mediated by terminal deoxynucleotide transferase (TdT); receptor editing and combination of two V(D)J encoded protein chains. Each V(D)J heterodimer, encodes a unique membrane bound antigen receptor, T cell receptor (TCR) or B cell receptor (BCR). TCR are comprised of alpha and beta (αβ) or gamma and delta chains (γδ), whilst the BCR is formed through the combination of heavy and light chains. The α, γ and light chains are composed of V and J segments only, whereas the β, δ and heavy chains comprise V, D and J gene segments. Light chains may be kappa (κ) or lambda (λ) specificity; κ segments are rearranged first and if the rearrangement is non-productive or auto-reactive, λ rearrangement can proceed in the same cell.

Antigen was first defined as a substance resulting in antibody, or immunoglobulin production. When B cells encounter their cognate antigen, they undergo terminal differentiation to plasma cells and produce antibody of the same antigen-specificity as their BCR. For this reason, the BCR is also referred to as surface immunoglobulin (sIg). Long-term antibody production requires cooperation of antigen specific T and B lymphocytes. High affinity antibodies are a marker of a co-ordinated, refined adaptive immune response, as are antigen-specific T cell responses. For example: circulating neutralising antibodies in the blood upon immunisation and T cell interferon gamma (IFN-γ) production *in vitro*, upon incubation of cells with the same live-attenuated viral vaccine.

The BCR binds antigen in its native confirmation, interacting with small epitopes or immunoreactive residues on the tertiary structure. In contrast, the TCR recognises

processed peptide presented within the major binding groove of the Major Histocompatibility Complex (MHC) (Figure 1.1, Panel A). Both peptide and MHC are integral for TCR binding. There are two major subset of T cells, CD4 helper T cells and CD8 cytotoxic T cells (CD prefix stands for cluster of differentiation, a nomenclature system for cell markers). CD4 cells recognise exogenous antigen processed into peptide and presented on MHC class II. Expression of MHC class II is limited to specialised antigen presenting cells (APC): macrophages, DC (dendritic cells) and B cells. CD8 cells recognise peptide in the context of MHC class I. All nucleated cells express MHC class I, permitting detection of intracellular pathogens and cancer (endogenous antigens).

Primary immune responses are initiated in the secondary lymphoid tissues of the spleen, lymph node and MALT (mucosal associated lymphoid tissue). These tissues may be distal from the initial encounter of pathogen, so although all cells express MHC class I, CD8 activation also requires specialised migratory APCs. B cells are thought be the critical APC, for instigation of all immune responses (Janeway, Ron et al. 1987).

In the secondary lymphoid tissue, the B cells undergo another receptor editing process called somatic hypermutation (SHM); this involves single nucleotide mutations, deletions and insertions, within the coding regions of the V(D)J genes. B cells are then selected on the basis on increased avidity to cognate antigen, a process called affinity maturation. The effector functions can also be refined, by immunoglobulin class switching, a process that requires T cell help in the form of CD154-CD40 co-stimulation. This modifies of the constant part of the immunoglobulin molecule but does not affect antigen specificity. In total, there 5 classes of immunoglobulin: IgA, IgD, IgE, IgM and IgG.

Naïve B cells, that have not encountered their corresponding antigen, express immunoglobulin M (IgM). In hyper-IgM syndrome patients have a defect in CD40 B cell signalling and cannot produce high affinity class-switched immunoglobulins, consequently they have increased susceptibility to infection.

B cells are most potent with cognate T cell interaction. When multiple antigen receptors on the B cell surface become cross-linked by binding to repetitive epitopes, T-cell independent activation can also proceed however, without T cell help, antibody responses tend to low affinity, cross-reactive and wanes quickly.

1.3 Immunological tolerance

The process of antigen receptor rearrangement is random and consequently, it can result in generation of non-productive or harmful antigen receptors. Lymphocytes have an absolute requirement for low level or tonic antigen signalling for their survival; this ensures only advantageous rearrangements are retained in the repertoire, whilst other lymphocytes die by neglect. Therefore, by definition some autoreactive clones will be generated and could be released into the periphery. Auto-antigens are ubiquitous, therefore additional control mechanisms must exist to remove or regulate these harmful, cells that target self.

Central tolerance removes immature cells from the repertoire before they are released into the periphery, this selection process occurs in the primary lymphoid organs. Peripheral tolerance refers to the mechanisms that limit autoreactivity of mature B and T cells after release from the BM and thymus, both within the blood and tissue.

Autoimmunity can be considered a failure in both pathways of immune tolerance. Autoreactive cells escape following antigen receptor rearrangement, bypassing the

central tolerance checkpoints. The mechanisms that would normally limit the action of these cells in the periphery are also defective, permitting survival and expansion of the deleterious clones.

1.3.1 T cell selection

T cells arise from a common lymphoid progenitor cell in the bone marrow, which can also give rise to B cells and Natural Killer (NK) cells. Cells that migrate to the thymus are initially negative for CD4 and CD8, acquiring expression of both markers in the cortex. The TCR must bind self-MHC on cortical epithelial cells, to ensure continued T cell survival; cell fate is determined based on relative affinity for MHC class I (CD8) or II (CD4). This process is called positive selection.

T cells subsequently undergo negative selection in the thymic medulla, this process is dependent on the transcription factor AIRE (AutoImmune REgulator). AIRE induces the ectopic expression of tissue restricted antigens by medullary epithelial cells. Those T cells which bind self-antigen weakly are retained within the TCR repertoire, they may still be advantageous in terms of immunological protection. If the TCR binds these auto-antigens with high avidity, T cells undergo apoptosis; this process is not absolute, and some auto-reactive clones will escape. In addition, some highly reactive CD4 T cells in the thymus are fated to become T regulatory cells (Tregs), under the control the transcription factor forkhead box P3 (FoxP3). These cells are referred to as central or natural Tregs (nTreg), distinguishing them from inducible Treg (iTreg), generated in the periphery.

1.3.2 T cell peripheral tolerance

1.3.2.1 3-signal hypothesis

The context in which the TCR signal is received is an important tolerogenic mechanism in the periphery, with a 3-signal hypothesis is proposed (Figure 1.1, Panel A). Signal 1 is provided by the antigen complex, cognate peptide and MHC. A preceding innate immune response is required, permitting cytokine and chemokine directed migration of T cells to the site of inflammation. T cells might otherwise remain ignorant of their cognate antigen, in the periphery or lymphoid tissue.

An initiating event is believed to be necessary for autoimmunity to occur; a viral infection, bacterial infection or environmental factor, which results in the recruitment of immune cells from the periphery to the target tissue. Nasal carriage of *Staphylococcal aureus* and exposure to silica have been implicated in pathogenesis of AAV (Stegeman, Tervaert et al. 1994, Hogan, Cooper et al. 2007), with LPS (lipopolysaccharide) exacerbating disease in an *in vivo* model (Huugen, Xiao et al. 2005).

Damage to the tissue is incidental and can lead to bystander activation of APC, with uptake and processing of self-protein alongside exogenous proteins. Selection of autoreactive clones may be favoured if they cross react with the exogenous antigen, a process referred to as molecular mimicry. Modification of self-protein can also occur under this stress, generating novel autoantigens not presented in the thymus; examples described in the literature include transglutamination of gluten in celiac disease (Molberg, McAdam et al. 1998), and generation of hybrid peptides in type 1 diabetes (Delong, Wiles et al. 2016).

Signal 2 is co-stimulation, the reciprocal interaction of cell surface markers on

Figure 1.1 Lymphocyte antigen receptors

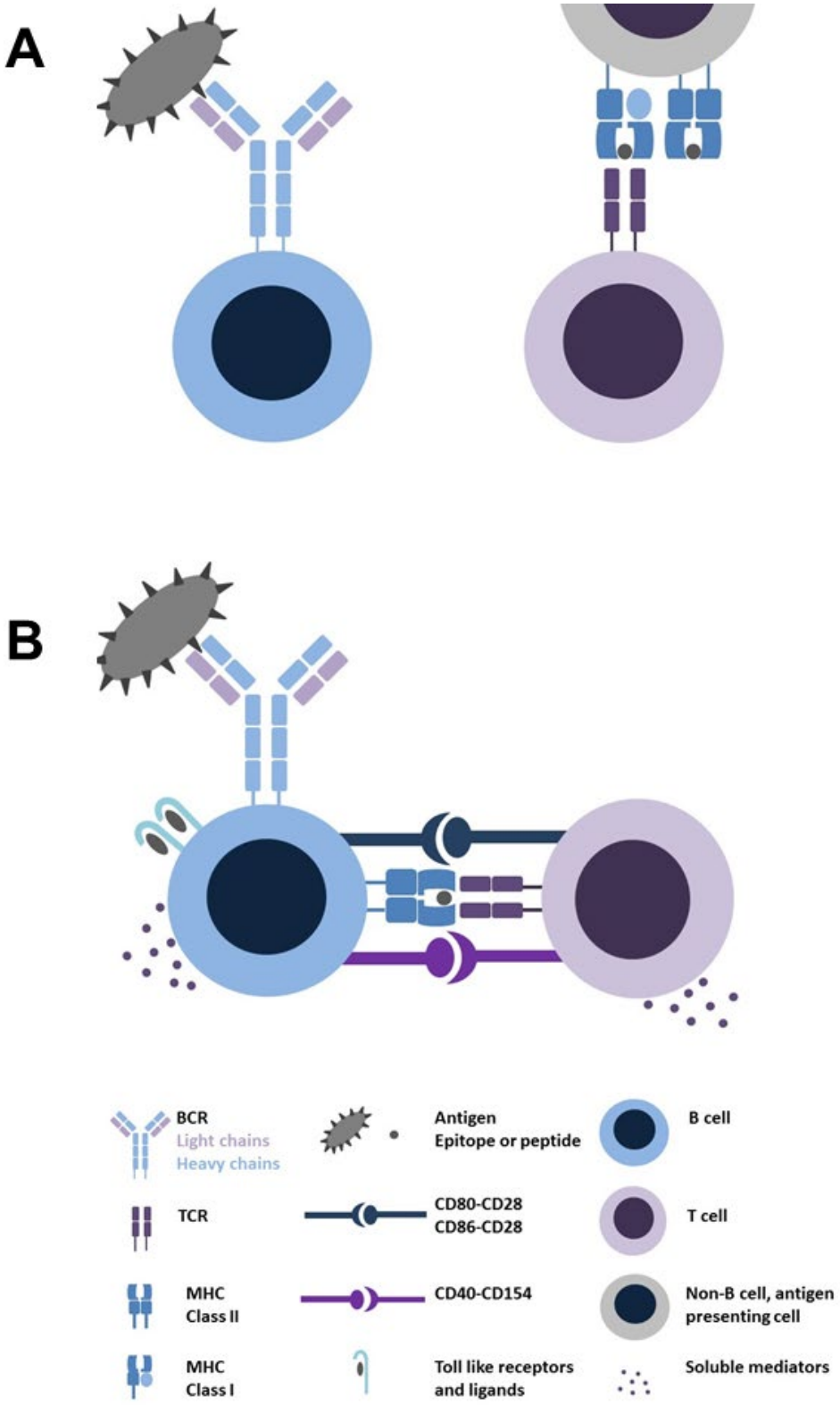

[A] B cell depicted on the left, and T cell on the right. The BCR binds native antigen, whilst the TCR binds peptides, presented by specialised antigen presenting cells (APC), in the context of MHC CI or CII. [B] APC additionally provide co-stimulatory signals and soluble factors for T cells (signal 2 and 3). B cells are APC, with uptake of antigen via the BCR. BCR integrate signals received from the BCR and toll like receptors (TLR). This can fine tune the immune response, by influencing the soluble mediators they produce. The balance of cytokines determines T cell fate or polarisation, on encountering antigen.

activated T cells and mature APC (e.g. CD28 and CD86). DC (DC) are the archetypal APC and their maturation is also dependent on inflammatory stimuli.

Signal 3 is provided by soluble mediators, specifically cytokines which permit T cell survival and clonal expansion (e.g. type I interferons, IL-2 and IL-12 for CD8 cells). The second and third signals are depicted in Figure 1.1, Panel B.

If the signal is received in the wrong context and weak, T cells can be rendered anergic; they are retained in the repertoire but are unable to respond. If the TCR signal is very strong and in the wrong context, the antigen may be ubiquitous or self, T cells undergo activation induced cell death (AICD) and are removed from the repertoire.

1.3.2.2 Th1:Th2 paradigm

Another mechanism of T cell tolerance is the reciprocal action of CD4 subsets with one other. The model was first proposed in the mid-1980s and initially referred to as the Th1:Th2 paradigm (Mosmann, Cherwinski et al. 1986). The 'Th' prefix is used to designate CD4 or T helper subsets. This classification system has subsequently been extended to include other CD4 subsets (Th17, Th9, Th22 and Treg). In its most basic derivation, the prototypic Th1 and Th2 cytokines interferon gamma (IFN-γ) and interleukin 4 (IL-4), act in an autocrine manner to further augment differentiation of Th1 or Th2 cells. These cytokines also act on the opposing cell type, limiting proliferation and induction from uncommitted Th0 cells. In health, this negative feedback loop ensures cellular and humoral immunity are in balance. In cell mediated autoimmunity, where there is an essential pathological role for CD8 cells the balance is proposed to be skewed in favour of Th1. Whilst in humoral autoimmunity, where antibodies have a pathological role, the balance would be skewed in favour of Th2. This model did not always hold true, especially in humans, and more recently, a critical

role for Th1 and Th17 cells has been shown in most autoimmune conditions. This has been described in GPA specifically, with Th1 or Th2 responses differing dependent on localised or generalised disease, but Th17 responses in all patients (Sanders, Stegeman et al. 2003). Treg have been shown to be critically important in limiting both proinflammatory cell types, this is in part mediated by prototypic cytokines, IL-10 and tumour growth factor beta (TGFβ) (Figure 1.2).

1.3.2.3 T regulatory cells

Treg are essential for maintenance of tolerance. In the absence of the FoxP3 transcription factor, patients develop an aggressive autoimmune disease called Immune dysregulation Polyendocrinopathy Enteropathy X-linked syndrome (IPEX). IPEX results in early death, it is associated with very high incidence of type 1 diabetes, inflammatory bowel disease (IBD) and allergy. In addition to FoxP3, Treg can be defined by high expression of CD25, CLTA4 (cytotoxic T-lymphocyte-associated protein 4) and GITR (glucocorticoid-induced TNFR family related gene), with low expression of CD127.

The principle method of suppression is the production of IL-10, TGFβ and IL-35 cytokines. Treg are also outcompete effector cells for IL-2 the critical T cell survival factor, due to higher relative expression of CD25 (the high affinity IL-2 receptor); this results in cytokine-deprivation mediated apoptosis of effector T cells (absence of signal 3).

Other mechanisms of Treg suppression can be broadly classified as: cytolytic, metabolic and the targeting of DC (Vignali, Collison et al. 2008). In terms of cytolysis, Treg can kill T effector cells and myeloid cells by production of the cell toxins: granzyme A, granzyme B and perforin. Another mechanism of inducing cell death is

Figure 1.2 CD4 T cell subsets

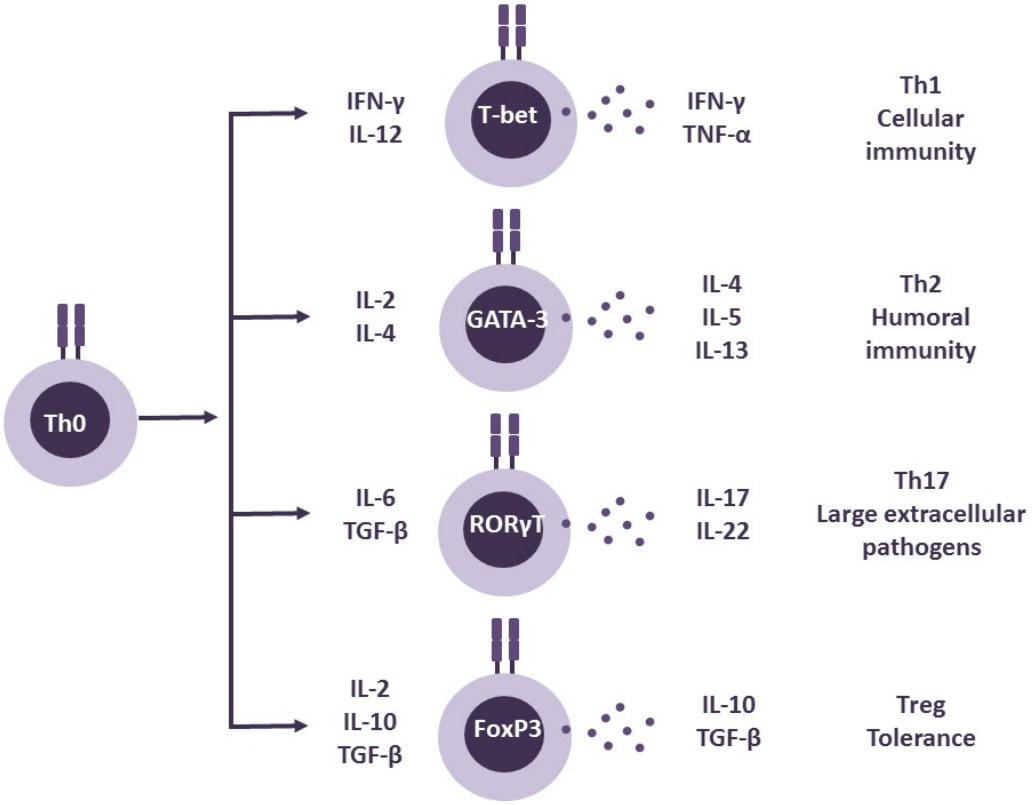

Uncommitted CD4 T cells (Th0) have 4 alternative fates after antigen encounter, polarization into Th1, Th2, Th17 or Treg. These cells are defined by mode of induction, the transcription factors they express and cytokine profile. Th1 and Th2 cells produce the cytokines, required for their own maintenance; IL-4 and IFNγ also block differentiation of the opposing cell type. Th2 cells provide help to antibody producing cells. Th17 and Th1 cells are proinflammatory and implicated in pathogenesis of autoimmunity. Treg cells suppress differentiation of both cell types.

through interaction of death receptors and their cognate ligands e.g. Fas and Fas-ligand, TNF-related apoptosis-inducing ligand (TRAIL) and death receptor 5, programmed death 1 (PD-1) and its ligand (PD-L1). Treg express high levels of the ectoenzymes CD39 and CD73, which dephosphorylate ATP (adenosine triphosphate) to generate extracellular adenosine. ATP promotes Th17 differentiation by binding to the purinergic receptors (P2X, P2Y), catabolism to adenosine limits this process. Adenosine also directly suppresses effector T cells and DC, by binding to the adenosine receptor 2A (A2AR) (Cekic and Linden 2016). The net effect is to augment Treg differentiation and limit Th17 induction, through sustained TGFβ production and suppression of IL-6 (Zarek, Huang et al. 2008).

Treg interactions with DC, are reciprocal and can be classified as direct (cell-to-cell contact required) or indirect (mediated by soluble factors). A subset of DC are classified as tolerogenic, favouring polarisation toward Treg (IL-10 producing DC) opposed to Th1 (IL-12 producing DC). Tolerogenic DC are typically immature, lacking the cytokine milieu or danger signals, for full maturation. Some conditions, positively favour the induction of tolerogenic DC, including: rapamycin, corticosteroids, retinoic acid, vitamin D3 or IL-10 (Gordon, Ma et al. 2014).

Treg express CTLA4 in preference to CD28, which has much greater affinity for the co-stimulatory molecules CD80 and CD86. Treg acquire these molecules, ripping them from the surface of APCs, a process called trogocytosis, resulting in loss of signal 2 for T effector cells (Gu, Gao et al. 2012). A subset additionally express LAG-3 (Lymphocyte activating gene 3, CD223). LAG-3 is a CD4 homologue, which binds MHC CII with high affinity, blocking T cell interaction with APCs (Vignali, Collison et al. 2008).

The classical FoxP3+ CD4+ Treg population discussed herein, are the major regulatory T cell subset, both in terms of number and functional significance. However, FoxP3- Treg and CD8+ Treg subsets have additionally been described.

1.3.3 B cell selection

The mechanisms of B cell central tolerance are less well resolved than T cells. Development proceeds in a step-wise fashion in the BM (Figure 1.3); maturation can halt at any point, with cells undergoing apoptosis. This process is referred to as negative selection by clonal deletion.

Before any gene recombination can commence, precursor cells must express CD79a and CD79b (also called Igα and Igβ). The BCR only has a short cytoplasmic tail and must partner with these molecules for downstream signal transduction. The VDJ gene segment encoding the heavy chain rearranges first and must pair successfully an invariant surrogate light chain (SLH), forming a pre-BCR before light chain rearrangement proceeds. If there is a failure to pair with the SLH, no signal transduction or if the BCR is strongly autoreactive, B cells can be removed from the repertoire at this point.

Some features of the Ig heavy chain have been associated with inherent autoreactivity, including use of the VH2-34 gene segment and generation of a long complementary determining region (CDR) 3. A long CDR3 is indicative of extensive rearrangement, with many nucleotide insertions.

Expression of the SLH is an important negative selection checkpoint; mice that lack expression of SLH do not have a complete halt in B cell development but form spontaneous germinal centres and have increased levels of autoantibodies to

deoxyribonucleic acid (DNA) (Keenan, De Riva et al. 2008, Grimsholm, Ren et al. 2015). Low gene copy number of the surrogate light chain component CD179a, has also been linked with rheumatoid arthritis in man (Yim, Chung et al. 2011). Interestingly, the role of the SLH may not be limited to central tolerance in the BM; when expression is prolonged in the periphery of mice, it improves tolerance to self in a dose-dependent manner, with enhanced clonal deletion and anergy (Kil, Corneth et al. 2015, Ren, Grimsholm et al. 2015). The commencement of Ig light chain rearrangement is transcriptionally controlled, with downmodulation of IL-7 and up regulation of interferon regulatory factor 4 (Johnson, Hashimshony et al. 2008). Light chains may be kappa (κ) or lambda (λ) specificity; κ segments are rearranged first and if the initial heavy chain (VDJ) and light chain (VJ) combination is autoreactive or non-productive, the other germline copies of the light chain gene segments will undergo recombination in a process called receptor rearrangement. This is thought to be the principle mechanism of B cell central tolerance, with gene rearrangement in up to 50% of peripheral B cells (Casellas, Shih et al. 2001).

When receptor editing is complete, B cells express the prototypic BCR or surface IgM. BCR interaction with antigen is essential for their continued survival (clonal selection). Immature cells that are weakly self-reactive, have a survival advantage and are actively retained in the repertoire (Gaudin, Hao et al. 2004). If cells remain strongly autoreactive two alternative fates are possible: clonal deletion or release into the periphery, with the inability to respond to antigen (anergy). Anergic cells are limited in their ability to traffic, instead they are retained in lymphoid tissues and excluded from entry of the germinal centre (Cyster, Hartley et al. 1994). In this sense, encounter with cognate antigen and specific T cells, is inhibited spatially (ignorance).

Intracellular antigens are common targets of systemic autoimmunity; B cells that recognise intracellular antigens are more likely to bypass tolerance checkpoints, differentiate to plasma cells and produce autoantibodies (Ferry, Jones et al. 2003). This is compounded by failure to clear apoptotic cells in SLE and production of Neutrophil Extracellular Traps (NETs) in AAV, which leads to persistence of extracellular auto-antigens (Kessenbrock, Krumbholz et al. 2009, Hakkim, Furnrohr et al. 2010).

Autoreactive cells can be rescued from cell death by the presence of pro-survival or anti-apoptotic factors. Mice transgenic for the anti-apoptotic factor bcl-2 (B-cell lymphoma 2) or with mutations in the death receptor Fas (*lpr* mutation), have a higher frequency of autoreactive B cells. Cells are rescued from clonal deletion and as a consequence the mice spontaneously develop a disease, resembling human systemic lupus erythematous (SLE) (Cohen and Eisenberg 1991, Strasser, Whittingham et al. 1991).

B cell survival factors include BAFF (B lymphocyte activating factor) and APRIL (a proliferation-inducing ligand). Elevated levels are thought to enable persistence and maturation of autoreactive B cells in the periphery. BAFF transgenic mice develop B cell hyperplasia and produce pathological autoantibodies that result in salivary gland destruction and impairment of renal function (Mackay, Woodcock et al. 1999, Khare, Sarosi et al. 2000, Groom, Kalled et al. 2002).

Overexpression has also been described in human autoimmune disease, leading to the development of novel immunotherapies to block APRIL and BAFF (Nakayamada and Tanaka 2016). Clinical trials have been conducted in patients with SLE, rheumatoid arthritis (RA), Primary Sjörgen's syndrome and Multiple sclerosis (MS)

Figure 1.3 The process of B cell devlopment

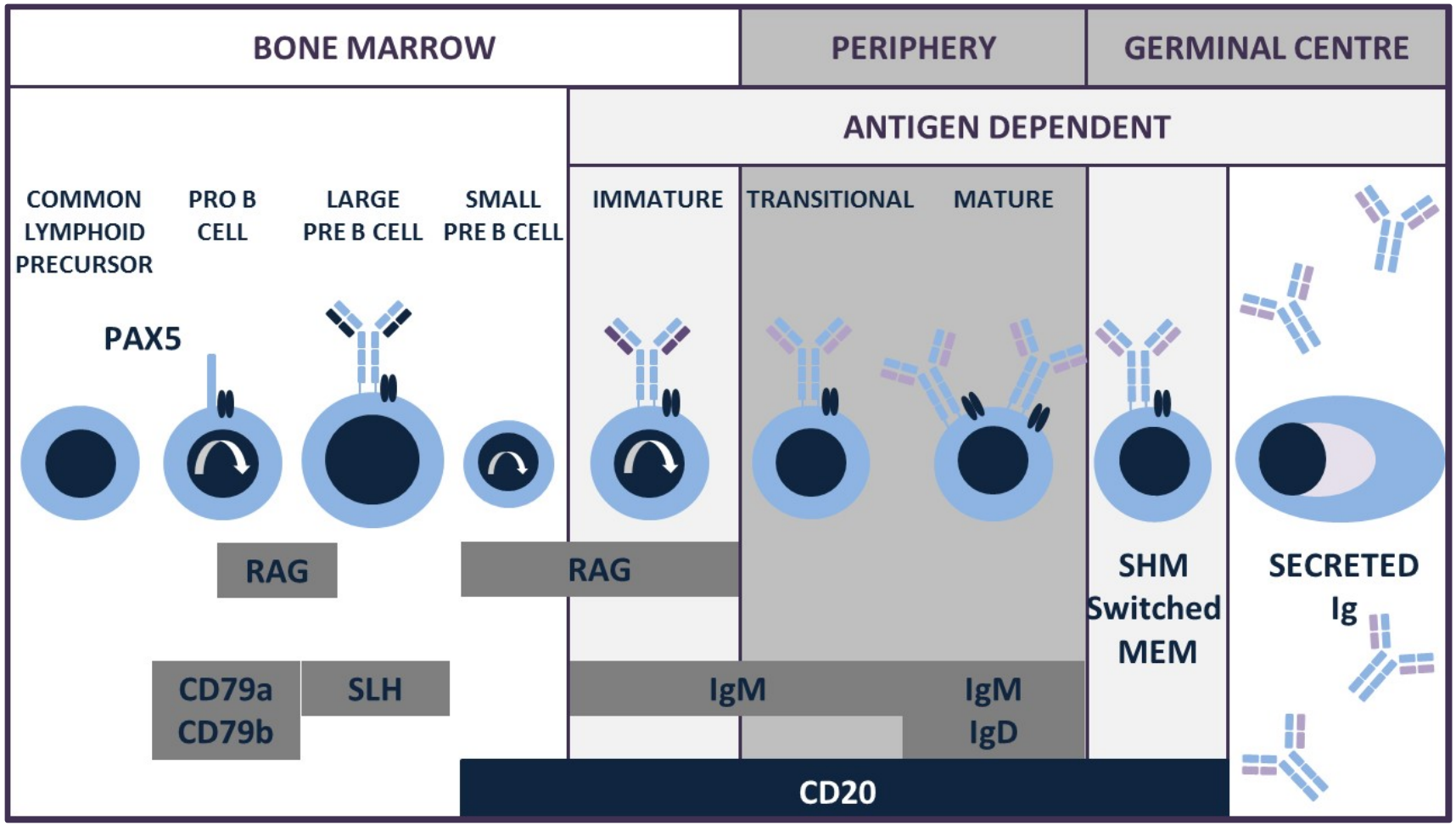

Key stages in B cell development are shown. Pax 5 is essential B cell lineage commitment from the common lymphoid precursor. The BCR has no intrinsic capacity for intracellular signalling, which is instead mediated by CD79a and CD79b. Recombination-activating genes (RAG) permit the heavy chain gene segments of the BCR are rearranged, the intervening DNA is excised, and the gene segments are spliced together. The VDJ heavy chain they must successfully pair with the surrogate light chain before light chain rearrangement can proceed. At this stage in development the pre-BCR is expressed on the cell surface. The kappa light chain is then rearranged, if this is unproductive the lambda light chain is rearranged. When the BCR is expressed at the cell surface, cells undergo a process of negative selection and receptor editing prior to release into the periphery. The transitional B cell is an important target of negative selection in the periphery. When cells encounter cognate antigen, they migrate to secondary lymphoid organs; with T cell help, they form germinal centres, differentiate into long lived memory B cells and plasma cells, which produce high affinity class switched antibody.

[*ClinicalTrials.gov registry and results database*]. The trial in MS had to terminated early, due to worsening disease in the treated cohort relative to the placebo

1.3.4 B cell peripheral tolerance

The process of negative B cell selection in the BM favours the retention of autoreactive heavy chain gene segments in the repertoire (Hayakawa, Asano et al. 1999). It seems counterintuitive that these immature auto-reactive B cells would be released into the periphery at all, but they are thought to be required for breadth of protective immunity. Transitional B cells are an important checkpoint (Carsetti, Kohler et al. 1995), with a gradual reduction in auto-reactivity as B cells mature. This was demonstrated by cloning human BCR genes, into 239A human embryonic kidney fibroblast cells and testing the recombinant antibodies produced. Reactivity of these antibodies with human epithelial type 2 (HEp-2) cells was 75% for immature B cells in the BM, 40% for new B cell emigrants in the periphery and 20% in mature B cells (Wardemann, Yurasov et al. 2003).

Immature B cells spontaneously produce low affinity, highly cross-reactive IgM antibodies, in a T cell independent manner. These natural antibodies neutralise blood borne pathogens, in the absence of prior immunity. This prevents overwhelming disease in the early phase of infection, when there is no effective adaptive immune response (Ochsenbein, Fehr et al. 1999). Natural autoantibodies may even protect against autoimmune disease, through FcR mediated clearance of apoptotic cells (Vas, Gronwall et al. 2013) and neutralisation of pro-inflammatory cytokines in autoimmune polyendocrinopathy candidiasis-ectodermal dystrophy (APECED) [*Meyer 2016*].

The type of antigen, stage of B cell maturation and requirement for T cell help, is critical in determining cell fate. In contrast to spontaneous IgM production on tonic BCR signalling, immature B cells undergo clonal deletion when they encounter their specific antigen and this avidly crosslinks the BCR (Norvell, Mandik et al. 1995). With the same stimulus, mature cells become activated, undergo clonal expansion and produce class-switched antibodies. The threshold and duration of BCR signalling required for deletion of immature cells is also lower, relative to that required for proliferation of mature cells (Sater, Sandel et al. 1998). In addition to BCR signal strength, immature B cells also have an increased requirement for BAFF (Hsu, Harless et al. 2002).

Signalling strength is mediated by differences in the co-receptors engaged in tandem with the BCR: FcγRIIB, CD5, CD21, CD22, CD19, CD11b, CD45 and CD72 differentially modulate outcome. CD5 negatively modulates BCR signalling, expression is higher on immature B cell subsets and it is important in maintenance of anergy in these cells (Hippen, Tze et al. 2000).

Upon BCR engagement with a high avidity ligand, there are dynamic changes to cell biology; the antigen is internalised and processed, with peptide presented in the context of MHC CII. Reciprocal interaction with an antigen specific T cell, is critical to further B cell survival, differentiation and class-switch recombination. T helper cells licence B cells to produce high affinity antibody, by CD154 engagement of CD40, provision of IL-10 and IL-4. Entry to the germinal centre in secondary lymphoid tissues, is controlled and continued maturation, is competitive (limited spatially, by availability of antigen, survival factors and cytokines like IL-21). Selection is based of increased

avidity of the BCR for the inciting antigen, lower affinity B cells die by neglect. The resultant plasma blasts produce class-switched antibodies, which not only bind antigen more avidly but also have different effector functions and longer half-life, mediated by class switching to different Fc domain. A pool of long-lived plasma and memory B cells is generated, which reduces time to respond on subsequent exposure. These cells are life-long, residing in a specialised BM niche.

Germinal centre formation and plasma cell differentiation is controlled on a genetic and epigenetic level. Whilst PAX-5 (paired box protein 5) is essential to B cell differentiation from a central lymphoid precursor BM, entry to the germinal centre and terminal differentiation is under the control of BLIMP1, with miRNA (micro ribonucleic acid) 155 also implicated (Thai, Calado et al. 2007, Vigorito, Perks et al. 2007).

TLR agonists are reported to enhance antigen presentation, proliferation, antibody production and class switch recombination by augmenting initial BCR signalling (He, Qiao et al. 2004, Pasare and Medzhitov 2005, Jiang, Lederman et al. 2007, Eckl-Dorna and Batista 2009). In contrast, anergic cells do not proliferate or produce antibody on engagement of TLR ligand.

This might be an important pathogenic mechanism in autoimmunity. TLR-9 B cells are present at higher frequency in SLE patients (Papadimitraki, Choulaki et al. 2006) and combined CPG and IL-2 stimulation *in vitro,* results in ANCA production in AAV patients (Tadema, Abdulahad et al. 2011). Endogenous TLR ligands are increased in serum of patients with AAV (Bruchfeld, Wendt et al. 2011, Pepper, Hamour et al.

2013) and LPS administration, exacerbates disease in an *in vivo* model of disease (Huugen, Xiao et al. 2005).

Interestingly, LPS-activated B cells actually limit autoimmune pathology in animal model of type 1 diabetes (Tian, Zekzer et al. 2001). Protection from an SLE-like disease in FcγRIIb knock out mice, is conferred by transfer of TLR-9 positive B cells (Stoehr, Schoen et al. 2011). This is thought to be mediated by IL-10, a key immunoregulatory cytokine, produced on TLR ligation (Yanaba, Bouaziz et al. 2009). Not only are B cells subject to central and peripheral mechanism of tolerance, limiting autoimmunity, they can also act as mediators of inflammation themselves.

1.4 Classification of B cells

B cells can be classified based on ontogeny and maturation. In addition to classical BM development a self-sustaining population of cells arise in foetal life, populating the pleural and peritoneal cavities. These cells are classified as B1, with the B1a subset expressing high levels of CD5; they tend to produce low affinity cross-reactive antibodies (Baumgarth 2011). B cells can be broadly defined by anatomical location, they reside in pleural or peritoneal cavities, tonsils, lymph nodes, spleen, mucosa, blood and BM. Within tissues, regulatory and inflammatory B cells have been described, sometimes forming highly organized structures (ectopic germinal centers or lymphoid like organoids). Within secondary lymphoid organs, B cells are defined as marginal or follicular based on their distribution; different cell surface markers and functions are also described.

In terms of maturation in the bone marrow, central lymphoid precursors commit to a B cell fate and progressively rearrange the V(D)J gene segments. The sequential steps of development are: early pro-B (V-D joining), late pro-B (VD-J joining), large pre-B cell (heavy chain expressed with SLH at the surface, pre-BCR), small pre-B (no surface BCR, light chain rearrangement), immature B cells (rearranged BCR). Mature B cells migrate from the marrow to the periphery, they have undergone negative selection and BCR editing. These stages of development were also designated fractions A-F, based on expression of cells surface markers, including CD24, CD249 and CD43 (Hardy, Carmack et al. 1991).

Immature B cells are also called transitional B cells, they express IgD and CD21 *de novo.* These cells have a higher proportion of autoreactive B cells and in mice, they initially home to the spleen, where they undergo further selection. On continued maturation they acquire expression of CD23, with T1 and T2 classification proposed (Carsetti, Rosado et al. 2004).

The role of the spleen in human B cell development is less well characterised, the most profound effect of asplenia is increased susceptibility to blood borne infection, caused by encapsulated bacteria. Protection is normally conferred by marginal zone B cells, which are effective at capturing antigen and produce broadly neutralising antibodies to the polysaccharide bacterial capsule, preventing overwhelming infection prior to induction of a high affinity B cell response.

Transitional B cells are defined in man as $CD24^{high}$ $CD38^{high}$, these are the first to re-emerge after haematopoietic stem cell transplant (Marie-Cardine, Divay et al. 2008) or B cell depletion therapy with the CD20 monoclonal agent Rituximab (Palanichamy,

Barnard et al. 2009). CD24 and CD38 antigens are expressed on a continuum in peripheral B cell subsets, permitting definition of 3 subsets, which differ in expression of other surface markers (Blair, Norena et al. 2010). The $CD24^{int}$ $CD38^{int}$ subset is naïve, having not yet encountered cognate antigen or undergone class-switch, these cells are IgD+ IgM+ (Bnaive). The $CD24^{high}$ $CD38^{low}$ B cell subset corresponds to a memory B cell population (Bmem), which also has high expression of CD27, a marker which is upregulated after the germinal centre reaction, class switch and downmodulation of IgD. B cell subsets are also classified as Bm1-5, based on relative expression of CD38 and IgD (Pascual, Liu et al. 1994).

In terms of antibody production, B cells can be classified based on isotope of immunoglobulin expressed at the cell surface or produced *ex vivo* (IgM, IgD, IgG, IgA, IgE, κ or λ). Plasmablasts can be detected in the periphery by downmodulation of CD20 and expression of CD138. Other functional classification strategies are discussed below, with cells broadly categorised as effector or regulatory.

1.5 Effector B cell functions

1.5.1 Antibody production

B cell responses are categorized as T dependent or independent. With T cell help, B cells produce class switched antibodies and long-lived memory B cells. Class switched immunoglobulin binds native antigen with high affinity, a process called opsonization. The downstream effector functions are primarily mediated by innate immune cells.

Myeloid and granulocytic cells express Fc receptors (FcR), with uptake of antibody and antigen complexes via the immunoglobulin Fc domain. Antigen and antibody

complexes are cleared in steady state, but if additional inflammatory stimuli are present, the antigen is processed and presented to T cells in the context of MHC. Activated APC also express increased co-stimulatory molecules. B cells additionally capture membrane-bound whole antigen, from other APCs (Bergtold, Desai et al. 2005). The net effect is T and B cell activation, epitope spreading and diversification of the immune response.

Cells coated with antibody can be killed directly by antibody-dependent cell-mediated cytotoxicity (ADCC) or complement dependent cytotoxicity (CDC). CD16 (FcγRII) is highly expressed on NK cells, upon interaction with antibody coated cells, NK release their cytolytic contents resulting in ADCC. In CDC, immunoglobulin fixes complement to the cell surface, with cells lysed on assembly of the terminal membrane attack complex (MAC). During this cascade, fragments of complement proteins called anaphylatoxins are released, which enhance recruitment of other innate cells.

1.5.2 Antigen presentation and T cell co-stimulation

B cells are the essential APC, for initiation of all primary CD4 cells responses (Janeway, Ron et al. 1987, Crawford, Macleod et al. 2006). B cells also determine the breadth of immune response, with a key role in diversification of the CD4 T cell repertoire (Merkenschlager, Ploquin et al. 2016). In addition to antigen presentation in the context of MHC CII, antigen presentation on MHC CI and CD1d, to CD8 and iNKT cells has additionally been described (Barral, Eckl-Dorna et al. 2008, Marino, Tan et al. 2012).

With exquisite specificity, B cells are particularly adept at capturing and concentrating

low levels of antigen (Rivera, Chen et al. 2001, Rodriguez-Pinto 2005). B cells can acquire soluble and particulate antigen, functions attributed to follicular and marginal zone subsets (Carrasco and Batista 2007, Pape, Catron et al. 2007). Uptake of membrane bound antigen by the BCR is a dynamic process, with immunological synapse formed. Cells become polarised with redistribution of cells surface markers in lipid rafts and cytoskeletal rearrangement (Harwood and Batista 2010).

In addition to BCR uptake of soluble, particulate or membrane bound antigen, phagocytosis is reported in B1 cells (Gao, Ma et al. 2012). B cells express many other markers implicated in antigen uptake, including: Fc (FcγRIIB and FcεRII), c-type lectin (CD23, CD72, Dectin 1, Dectin 2, CLEC4A and CD205), complement (CD21, CD11b) and scavenger receptors (CD5, CD6, CSCL16, CD68, CD46, SR-A and SR-B1). B cells are also highly effective at activating T cells (Lanzavecchia 1985), having many co-stimulatory molecules in common with DC, including: CD40, CD80, CD86, CD83, ICOSL (inducible co-stimulator ligand), ICAM1 (Intercellular Adhesion Molecule 1, CD54) and OX40L (CD252).

1.5.3 Cytokine production

Production of multiple cytokines by B cells is well established (Pistoia 1997). Naïve B cells can differentiate into B effector (Be) 1 and 2 cells *in vitro*, reciprocating the cytokine profile of the Th1 or Th2 cells they are cultured with (Harris, Haynes et al. 2000). Be1 cells produce IFNγ and IL-2, whilst Be2 cells produce IL-4, IL-5, IL-6, IL-10 and IL-13. These cytokines are essential for maintaining T cell polarisation, limiting differentiation of the opposing subset (Figure 1.2).

Cytokines are renowned for pleiotropy, with multiple outcomes observed with a single mediator. Both synergistic and antagonistic effects, can be observed on combination of cytokines. It is therefore essential to consider net cytokine production, and no 1 cytokine in isolation.

In mice a deletion in IFNγ restricted to B cells, results in less severe experimental arthritis and improved Treg frequency (Olalekan, Cao et al. 2015). However, in *Mycobacterium tuberculosis* infection, IFNγ competent B cells induce regulatory macrophages (Benard, Sakwa et al. 2018). Production of IFNγ by B cells is accompanied by acquisition of Tbet expression *in vitro* (Harris, Goodrich et al. 2005). B cells expressing T-bet accumulate with age and are implicated in pathogenesis of autoimmunity (Rubtsova, Rubtsov et al. 2015).

Exposure to autoantigen induces B cell IL-6, in combination with IL-10 and TNFα (Langkjaer, Kristensen et al. 2012). TNFα and IL-6 are considered proinflammatory, whilst IL-10 is considered anti-inflammatory. Cells that produce IL-10 are also designated B10 (Tedder 2015). Relative B cell production of TNFα and IL-10, determine graft outcome in allogeneic kidney transplant (Cherukuri, Rothstein et al. 2014). An imbalance of GM-CSF (granulocyte colony stimulating factor) or IL-6 B cells, relative to IL-10 B cells is implicated in the pathogenesis of MS (Barr, Shen et al. 2012, Li, Rezk et al. 2015). GM-CSF induces proinflammatory myeloid cells.

IL-6 has profound autocrine effects on B cells and is also called B cell stimulatory factor 2. IL-6 causes terminal differentiation of B cells and antibody production *in vitro* (Matsuda, Hirano et al. 1988), with spontaneous GC formation in an animal

model of SLE (Arkatkar, Du et al. 2017). IL-6 in combination with IL-1β is essential to the maintenance of IL-10 competent B cells in mice (Rosser, Oleinika et al. 2014).

In addition to IL-10, B cells also produce IL-35 and TGFβ anti-inflammatory cytokines (Tian, Zekzer et al. 2001, Parekh, Prasad et al. 2003, Natarajan, Singh et al. 2012, Lee, Stott et al. 2014, Shen, Roch et al. 2014). These negative mediators of immune response are a key mechanism of regulatory B cells.

1.6 Regulatory B cells

In the preceding section, I discussed how B cells contribute to inflammation by production of antibody and provision of all 3 signals, required for an antigen-specific T cell response (peptide and MHC, co-stimulation and soluble mediators). However, there is evidence that B are also involved in the maintenance of tolerance limiting harmful T cell responses in the periphery.

B cell depletion has proven safe and effective for treatment of autoimmune disease overall, but there is some evidence that it may worsen disease. Rituximab treatment has been reported to cause increased severity of ulcerative colitis and lead to onset of psoriasis (Dass, Vital et al. 2007, Goetz, Atreya et al. 2007). Whilst blockade of B cell survival factors BAFF and APRIL (a proliferation-inducing ligand), worsened disease in multiple sclerosis (NCT00642902, http://clinicaltrials.gov)

1.6.1 Initial characterisation in mice

The immunomodulatory potential of B cells was first described in the mid-1970s; B cell depleted splenocytes did not resolve delayed type hypersensitivity response in

guinea pigs (Katz, Parker et al. 1974). It was over 20 years before the regulatory role of B cells was revisited.

In a model of chronic colitis, mice that completely lacked B cells (μMT), had an earlier onset of disease and severity was worse. Disease was equivalent to wild type mice after transfer of B cells or immunoglobulin, consequently the protection was thought to be conferred by antibody mediated clearance of apoptotic cells (Mizoguchi, Mizoguchi et al. 1997). Subsequently, anti-inflammatory potential was shown to be dependent on CD40 or B7 co-stimulatory receptors on the B cell surface (Mizoguchi, Mizoguchi et al. 2000).

Experimental Autoimmune Encephalomyelitis (EAE) is an animal model of MS, in which mice are immunised with Myelin Basic Protein (MBP) or immunodominant peptide (MOG 35-55). Disease spontaneously resolves in wild type mice, but follows a progressive course μMT mice (Wolf, Dittel et al. 1996). B cells from wildtype mice, produced IL-10 on stimulation with peptide *ex vivo*. When B cells were present but lacked capacity to produce IL-10, mice did not recover from EAE and Th1 cytokine production was enhanced in splenocytes (Fillatreau, Sweenie et al. 2002). IL-10 competency was subsequently attributed to a CD5+ $CD1d^{high}$ subset of splenocytes; this subset was absent in CD19-/- mice, which have increased inflammatory response on oxazolone challenge (Yanaba, Bouaziz et al. 2008). Adoptive transfer of 2 million CD5+ $CD1d^{high}$ B cells, resulted in remission in EAE, whilst transfer of whole B cells exacerbated disease (Matsushita, Yanaba et al. 2008). In mice deficient in STIM (stromal interaction molecule) 1 and 2, calcium flux after BCR engagement is reduced and B cells fail to produce IL-10, resulting in higher clinical scores on EAE induction

(Matsumoto, Fujii et al. 2011).

B cell IL-10 is induced by TLR or CD40 ligation (Yanaba, Bouaziz et al. 2009). B cells stimulated with LPS produce TGF-β and express Fas-L, a death ligand which induces apoptosis in cells expressing the cognate receptor (Fas). These LPS stimulated B cells, prevented disease in an animal model of type 1 diabetes by limiting the Th1 response (Tian, Zekzer et al. 2001). Transfer of B cells treated with an agonistic CD40 antibody, prevented disease in an animal model of arthritis (Mauri, Gray et al. 2003). IL-10 production on CD40 ligation and prevention of disease, was subsequently attributed to an immature, T2-MZP (transitional 2 mantle zone precursor) B cell subset, defined as CD19+ $CD21^{high}$ $CD23^{high}$ $CD24^{high}$ and $CD1d^{high}$ (Evans, Chavez-Rueda et al. 2007). In mice with deficiency in IL-10 limited to B cells, more severe disease develops, with reduced Treg but increased Th1 and Th17 response (Carter, Vasconcellos et al. 2011, Carter, Rosser et al. 2012).

These initial studies showed that B cells could limit antigen mediated autoimmunity. Interaction with T cells was important, with blockade of co-stimulation impairing function (CD40 or B7 antibodies). In terms of maintenance, BCR signalling was implicated because there was loss of regulatory B cells in CD19-/- mice (CD19 forms part of BCR complex) and in STIM1/2 knock out. Cells were inducible by TLR or CD40 ligation, which suggested they integrated innate and adaptive immune responses. Mechanisms of action included antibody mediated cell clearance, induction of cell death in effector cells, production of immunoregulatory cytokines IL-10 and TGFβ. Overall the effect was to limit harmful autoimmune Th1 and Th17 responses *in vivo*.

1.6.2 First description in man

1.6.2.1 CD5 B cells

Regulatory function had been attributed to CD5+ B cells, this marker down modulates BCR signalling (Berland and Wortis 2002) and is important in the maintenance of B cell tolerance (Hippen, Tze et al. 2000). CD5+ cells are enriched for IL-10 competency (Gary-Gouy, Harriague et al. 2002, Lee, Noh et al. 2011) and increased in SLE (Amel Kashipaz, Huggins et al. 2003). CD5 B cells are also reported to express FoxP3+ (Noh, Choi et al. 2010) the Treg transcription factor and produce TGFβ, limiting allergic responses (Lee, Noh et al. 2011).

1.6.2.2 CD27+ or CD25^{high} B cells

IL-10 was shown to be inducible in CD24high CD27+ B cells, upon CD40 and TLR ligation. These cells were increased in autoimmunity and limit monocyte TNFα production *in vitro* to a greater extent than CD24low CD27- B cells (Iwata, Matsushita et al. 2011).

CD25^{high} CD27+ B cells are also proposed to be regulatory (Amu, Tarkowski et al. 2007). CD25^{high} B cells produce TGFβ and IL-10, they limit proliferation of CD4 cells but enhance FoxP3 and CTLA4 expression by Treg (Kessel, Haj et al. 2012). Large CD25^{high} B cells induce angery in CD4 T cells and apoptosis of activated T cells (Tretter, Venigalla et al. 2008). CD25^{high} B cells are decreased in AAV (Eriksson, Sandell et al. 2010).

1.6.2.3 Transitional B cells

$CD24^{high}$ $CD38^{high}$ B cells were shown to be immunoregulatory. IL-10 expression was inducible upon CD40 ligation. $CD24^{high}$ $CD38^{high}$ cells limited Th1 differentiation *in vitro*, this was in part dependent on IL-10, CD80 and CD86. Although number was unaffected in SLE, cells were functionally perturbed (Blair, Norena et al. 2010). $CD24^{high}$ $CD38^{high}$ (Breg) were subsequently shown to induce Treg, whilst limiting and Th17 responses (Flores-Borja, Bosma et al. 2013).

Breg are numerically reduced in autoimmune thrombocytopenia; patients with the most profound reduction in platelets also had functional impairment in Breg, with reduced B cell IL-10 competency and ability to inhibit TNFα production by monocytes (Li, Zhong et al. 2012).

Bouaziz *et al* found IL-10 to be most potently induced on combined BCR and TLR stimulation; induction was not limited to the transitional B cell population, with IL-10 competent cells also detected within the memory B cell pool. Stimulated cells inhibited T cell proliferation *in vitro*, this was only partially mediated by IL-10 (Bouaziz, Calbo et al. 2010).

Collectively, there is evidence that Breg limit T cell proliferation, Th17 and Th1 differentiation. They induce Treg and additionally limit TNFα induction by monocytes. The mechanism is in-part IL-10 dependent. However, no one B cell phenotype is associated with IL-10 induction *in vitro* (Lighaam, Unger et al. 2018) nor is B cell immunoregulation, limited to this one mechanism. This was demonstrated by addition of an IL-10 agonistic antibody *in vitro*, which only partially abrogated function (Blair, Norena et al. 2010, Iwata, Matsushita et al. 2011)

1.6.3 Additional markers, mechanisms of action and induction

Induction of B regulatory cells is not limited to IL-1β, IL-6, BCR ligation, TLR ligands and CD154 stimulation (Yanaba, Bouaziz et al. 2009, Bouaziz, Calbo et al. 2010, Poe, Smith et al. 2011, Rosser, Oleinika et al. 2014, Zhang, Wan et al. 2016). IL-10 B cells can also be induced by DC and type I interferons (Zhang, Deriaud et al. 2007, Giannoukakis and Trucco 2012, Menon, Blair et al. 2016). A regulatory B cell phenotype is also acquired on BAFF, IL-21, IL-35 or TIM-1 (T-cell immunoglobulin and mucin domain 1) stimulation (Yang, Sun et al. 2010, Ding, Yeung et al. 2011, Yoshizaki, Miyagaki et al. 2012, Wang, Yu et al. 2014, Dambuza, He et al. 2017, Zhang, Li et al. 2017). TIM-1 is a marker of regulatory cells (Ding, Yeung et al. 2011) and IL-35,a key immunoregulatory cytokine produced by B cells (Shen, Roch et al. 2014, Wang, Yu et al. 2014). IL-35 and IL-10 are also produced by plasmablasts, another immunomodulatory B cell subset (Matsumoto, Baba et al. 2014, Shalapour, Font-Burgada et al. 2015, Shen and Fillatreau 2015).

Regulatory B cells can be defined functionally, by markers other than IL-10, IL-35 and TGFβ. In addition to Fas-L, B cells also express programmed death ligand (PD-L) 1, PD-L2 and granzyme B (Klinker and Lundy 2012). By adopting this killer-like phenotype, B cells can induce cell death in effector immune cells, directly. These cells are reported to be induced by BIP (binding immunoglobulin protein), a stress protein up-regulated by conditions of reduced oxygen and glucose (Tang, Jiang et al. 2016). Hypoxia-inducible factor-1α (HIF-1α) is also induced in these conditions, and recently reported to be a transcription factor for IL-10 B cells (Meng, Grotsch et al. 2018).

PD-L1 B cells interact with PD-1 T follicular helper (TFH) cells in the secondary lymphoid tissues. The net effect is to downmodulate humoral response. PD-L1 positive B cells have higher expression of BAFF receptors and are therefore more likely to survive CD20 monoclonal depletion with Rituximab. This is proposed a mechanism whereby antibody titres are reduced, despite absence of the CD20 target on antibody producing plasma cells (Khan, Hams et al. 2015).

Antibodies themselves are proposed to be immunoregulatory (Mizoguchi, Mizoguchi et al. 1997). Efficacy of mucosal immunotherapy in bee keepers, was subsequently been attributed to antigen specific IgG4 (van de Veen, Stanic et al. 2013). Low affinity auto-reactive IgM antibodies are implicated in peripheral B cell tolerance and prevention of autoimmunity (Baker and Ehrenstein 2002, Manson, Mauri et al. 2005). Transfer of IgM antibodies delays onset of lupus nephritis in the MLR-lpr mouse, with transfer of dsDNA specific IgM reported to ameliorate disease (Zhao, Jiang et al. 2009, Mannoor, Matejuk et al. 2012).

The balance of regulatory and effector T cells is modulated by extracellular adenosine, produced by catabolism of extracellular ATP by CD39 and CD73. Adenosine production is an important mechanism in regulatory B cells (Saze, Schuler et al. 2013, Kaku, Cheng et al. 2014). CD39 expression in particular, is highly concordant with an immunomodulatory B cell phenotype (Figueiro, Muller et al. 2016, Menon, Smith et al. 2017).

B cells also modulate balance of T cells by production of IDO, this is dependent of interaction with CTLA4 a co-stimulatory molecule more highly expressed on Treg cells than T effector cells (Johnson, Kahler et al. 2010, Nouel, Pochard et al. 2015).

Another co-stimulatory molecule implicated in the induction of Treg by regulatory B cells, is glucocorticoid-induced TNFR-related protein ligand (GITRL) (Ray, Basu et al. 2012). In addition, IL-10 acts in on Breg in an autocrine manner to affect the relative balance of CD86 and CD80 (B7.1 and B7.2) on the cell surface, inhibiting T cell responses (Hussain and Delovitch 2005, Nova-Lamperti, Fanelli et al. 2016). This is in keeping with previous findings: a B7 monoclonal antibody which blocks CD80 and CD86, prevents regulatory function *in vivo* (Mizoguchi, Mizoguchi et al. 2000) and blockade *in vitro*, reduces ability of Breg to limit Th1 differentiation (Blair, Norena et al. 2010).

B cells can also affect antigen presentation and co-stimulatory signals received by T cells indirectly, by affecting monocyte or dendritic cell activation and maturation (Naumov, Bahjat et al. 2001, Matsushita, Yanaba et al. 2008, Morva, Lemoine et al. 2012, Li, Rezk et al. 2015).

Presentation of antigen in context of CD1d, is an important immunoregulatory mechanism in B cells. CD1d receptor cycling from the endocytic cell compartment is impaired in SLE and accompanied by a reduction in iNKT (Bosma, Abdel-Gadir et al. 2012). Mice with CD1d deletion restricted to B cells, develop more severe arthritis. This was shown to be dependent on presentation of glycolipid antigen in the context of CD1d, inducing tolerogenic iNKT that limited Th1 and Th17 responses (Oleinika, Rosser et al. 2018).

The evidence for B cells modulating CD8 T cell responses is more limited. LPS activated B cells induce anergy in CD8 cells in a TGFβ dependent manner (Parekh, Prasad et al. 2003). Ability of B cells to limit CD8 memory T cells responses is reduced

in ankylosing spondylitis; this was partially mediated by IL-10, with function restored on ligation of CD40 and the BCR (Chen, Zhang et al. 2016). *In vivo* studies demonstrated that the effect of B cells on CD8 T cells is antigen specific, mediated in-part by co-stimulatory molecules CD80 and CD86 (Hollsberg, Batra et al. 1996, Bennett, Carbone et al. 1998). An additional mechanism was induction of FAS-L, resulting in effector cell death (Hollsberg, Batra et al. 1996, Bennett, Carbone et al. 1998).

Some of the key mechanisms of regulatory B cells are summarised in Figure 1.4.

1.6.4 Balance of effector and regulatory cells in autoimmunity

Balance of effector and regulatory B cell subsets is likely to be important in determining outcome in autoimmunity. Memory B cells have a lower requirement for BAFF and BCR signalling, they are antigen experienced and can readily differentiate into plasmablasts, producing high affinity, class switched immunoglobulin. IgM antibodies produced by immature B cells are low affinity, wane quickly and reported to be immunomodulatory. In MS and SLE, there is an imbalance in memory and naïve B cells (Duddy, Niino et al. 2007, Jacobi, Reiter et al. 2008, Knippenberg, Peelen et al. 2011). In EAE, passive transferral of CD5+ CD1d^{high} B cells ameliorates disease, but whole B cells worsen outcome (Matsushita, Yanaba et al. 2008)

B cells are central to adaptive immune responses. They can concentrate low levels of antigen via the BCR, presenting peptides in the context of MHC to T cells. B cells are also co-stimulatory and produce soluble mediators for B cell survival. The net effect is diversification of the adaptive immune response; disease fails to resolve and

becomes progressive, with organ damage. The reciprocal interaction of B cells and CD4 cells is described as a feed-forward mechanism, whereby tolerance is broken (Lund and Randall 2010).

Be1 cells promote Th1 differentiation, Be2 cells induce Th2. In contrast IL-10 competent B cells, which are $CD38^{high}$ $CD24^{high}$, limit Th1 and Th17 and induce Treg (Blair, Norena et al. 2010, Venhoff, Niessen et al. 2014). In MS there is an imbalance in cytokine producing B cells, which is proposed to be pathogenic; IL-10 B cells are reduced and B cells which produce the proinflammatory cytokines lymphotoxin, IL-6, GM-CSF and TNF-α are increased (Duddy, Niino et al. 2007, Knippenberg, Peelen et al. 2011, Barr, Shen et al. 2012, Li, Rezk et al. 2015). The balance of TNFα and IL-10 produced by B cells, is additionally linked to graft outcome after kidney transplantation (Cherukuri, Rothstein et al. 2014)

Breg from SLE patients have reduce IL-10 competency and cannot limit Th1 responsese as efefctively as controls. This was partially meidated by CD80 and CD86, B cells can fine tune the balance of these co-stimulatory molecules, determining T cell fate.

Figure 1.4 Key mechansims in immunoregulatory B cells

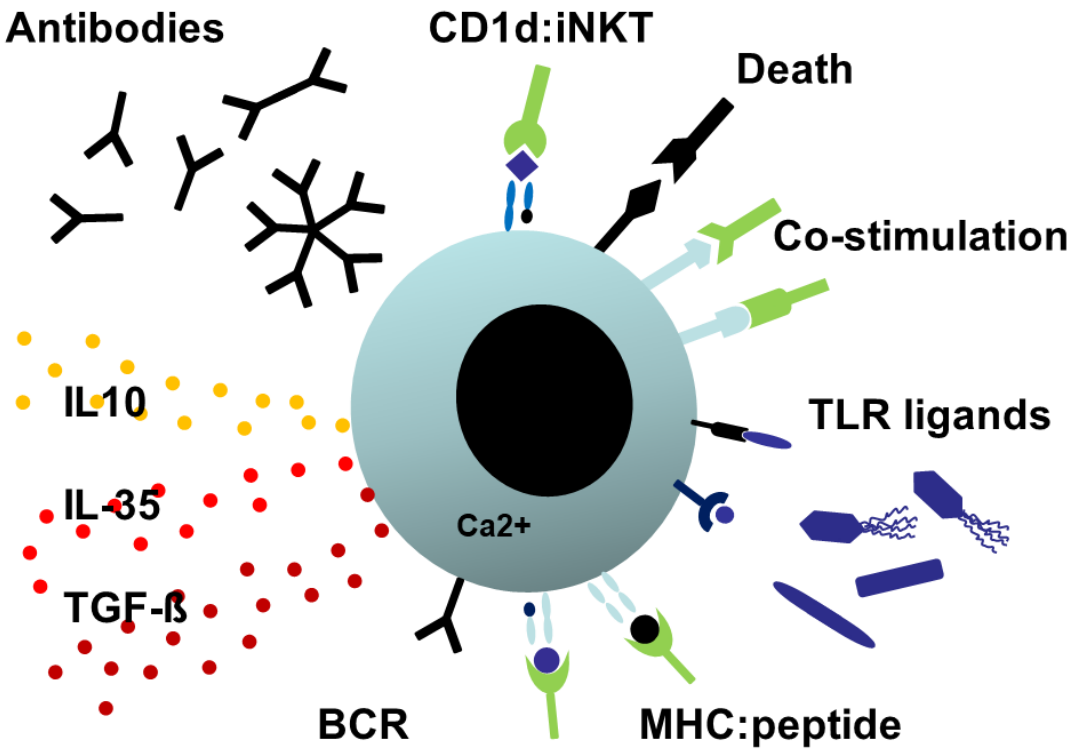

B regulatory cells exert their effects, primarily through anti-inflammatory cytokines, which include IL-10, IL-35 and TGFα. In addition, they produce inhibitory antibodies. B cells can cause effector cell death directly, adopting a killer-like phenotype defined by expression of FAS-L, granzyme B, PD-L1 and PD-L2. B regulatory cells have an intimate interaction with T cells, presenting antigen in the context of MHC CI, CII or CD1d. They also provide co-stimulatory signals, the balance of which, determines CD4 T cell fate. Breg are thought to be antigen specific, being absent in mice that cannot mount a calcium flux after BCR ligation. But they are additionally induced by the TLR ligands LPS and CPG.

1.7 Anti-neutrophil cytoplasm antibody (ANCA)-associated vasculitidies

1.7.1 Pathology, incidence and classification

AAV are a group of systemic autoimmune diseases, characterised by inflammation of small blood vessels. Three distinct clinical syndromes have been described: granulomatosis with polyangiitis (GPA), microscopic polyangiitis (MPA) and eosinophilic granulomatosis with polyangiitis (EGPA). AAV have constitutional symptoms in common and share a predilection for the kidney. Renal histopathology is characterised by fibroid necrosis, with crescents within the glomeruli, which compress the capillary tuft. Extra-renal manifestations of AAV may be respiratory, cutaneous, musculoskeletal, neurological, ocular, gastrointestinal or audio-vestibular (Berden, Goceroglu et al. 2012).

The prevalence of GPA in the United Kingdom was recently estimated at 145.9 per million and MPA, at 63.1 per million. Although prevalence of AAV is low, disease is associated with substantial morbidity and increased mortality. AAV typically follows a chronic relapsing course, necessitating renal replacement therapy in up to 30% of cases (Little, Nazar et al. 2004). Prior to the introduction of cyclophosphamide, disease resulted in almost 90% mortality at one year (Fauci, Katz et al. 1979). With current treatment protocols, survival rates are 88 and 78% at 1 and 5 years respectively. Half of deaths within the first year occur because of infection, whilst 14% can be attributed to active disease (Flossmann, Berden et al. 2011). This indicates that immunosuppression is inadequate in some patients, who die from active disease or go on to relapse, while in others the treatment regimen is too harsh, resulting in profound

reduction in immune competency, and increased risk of infection and malignancy (Turnbull and Harper 2009).

The systemic vasculitidies may be classified according to criteria or definitions, published by the American College of Rheumatologists (ACR) and Chapel Hill Consensus Conference (CHCC) respectively (Fries, Hunder et al. 1990, Jennette, Falk et al. 1994). Neither system was intended for diagnosis, but rather to standardise nomenclature and for definition of study cohorts. The ACR criteria were created prior to widespread use of ANCA testing and did not differentiate MPA from polyarteritis nodosa. The CHCC system was recently updated and was utilised to assign patients into MPA and GPA groups for this study (Jennette, Falk et al. 2013). The CHSS system defines AAV broadly, as a necrotizing inflammatory condition, which can affect veins, capillaries, venules and arterioles. It is associated with ANCA but histologically, is pauci-immune, with scant or absent deposition of immunoglobulin and complement. The three clinical syndromes overlap, however granulomatous inflammation is absent in MPA and glomerulonephritis is very common. In GPA, glomerulonephritis is relatively common and there is granulomatous inflammation within the upper and lower respiratory tract. EGPA has a unique prodrome of late onset asthma and is defined by eosinophilia; EPGA is more commonly ANCA negative than MPA or GPA.

Classification of AAV based of MPO- and PR3-ANCA specificity, may more informative than a clinical diagnosis of EGPA, GPA or MPA (Watts and Scott 2012). In Genome Wide Association Study (GWAS) there was one hit for MPO-ANCA within the MHC locus, and this differed from PR3-ANCA (Human Leukocyte Antigen DP and DQ loci respectively). PR3-ANCA was additionally associated with the gene

that encodes PR3 (*PRTN3*) and its natural inhibitor, α1-antitrypsin (*SERPINA1)* (Lyons, Rayner et al. 2012). An infectious trigger has also been proposed for PR3-ANCA, due to the cyclic pattern of disease and strong association with nasal carriage of *Staphylococcus aureus*, a pathogen which mimics the anti-sense sequence of PR3 (Stegeman, Tervaert et al. 1994, Watts, Mooney et al. 2012). Furthermore, in a large cohort of 535 AAV patients, PR3-ANCA was independently associated with increased risk of relapse (Walsh, Flossmann et al. 2012)

1.7.2 Pathological role of B cells and antibody in AAV

Detection of auto-antibodies in patient serum has high diagnostic specificity for AAV. Auto-antibodies are directed to myeloperoxidase (MPO-ANCA) or proteinase 3 (PR3-ANCA), constituents of azurophilic neutrophil granules and monocyte lysosomes. Two distinctive patterns may be observed when patient serum is incubated with neutrophils and fluorescently labelled anti-human IgG, a peri-nuclear pattern (p-ANCA) or a cytoplasmic pattern (c-ANCA). The p-ANCA staining pattern is commonly associated with MPO-ANCA and cANCA with PR3-ANCA, however this relationship is not absolute and enzyme-linked immunosorbent assay
(ELISA) is required to assign correct specificity. Identification of ANCA specificity is important, with PR3-ANCA found in most GPA patients (80-90% of cases). A rise in ANCA titre may precede an AAV relapse, and can inform treatment decision (Tervaert, Elema et al. 1990, Han, Choi et al. 2003), however titre does not correlate with disease activity (Hogan, Nachman et al. 1996, Finkielman, Merkel et al. 2007).
PR3-ANCA and MPO-ANCA have been shown to activate monocytes and neutrophils *in vitro*, through interaction with Fc receptors (Mulder, Stegeman et al. 1995) and by

Fc independent mechanisms (Falk, Terrell et al. 1990, Nowack, Schwalbe et al. 2000). Cellular activation results in the release of reactive oxygen species and proteolytic enzymes, which can cause endothelial cell damage (Varani, Ginsburg et al. 1989). ANCA enhance leukocyte recruitment, by release of proinflammatory mediators and increased expression of adhesion molecules, which promote cell adherence to the endothelium (Little, Smyth et al. 2005, Pankhurst, Nash et al. 2011, Kuravi, Bevins et al. 2012).

Some have reported that both antigen targets are available on the endothelium, making it a potential target for complement mediated lysis (Mayet, Csernok et al. 1993, De Bandt, Meyer et al. 1999, Baldus, Eiserich et al. 2001). MPO is present in renal biopsies but is proposed to be supplanted on the endothelium, by infiltrating innate immune cells (O'Sullivan, Lo et al. 2015). BM cells are sufficient, as a source of antigen, for initiation of disease in mice (Schreiber, Xiao et al. 2006)

Historically complement was not considered to have a prominent role in AAV, due to scant deposition of C3 and immune complexes within renal biopsies, which is described as pauci-immune. However, complement and immunoglobulin deposition was subsequently described in a high proportion of AAV renal biopsies, where it was associated with an increase in crescents and proteinuria (Haas and Eustace 2004, Chen, Xing et al. 2009). Factor B, a marker of the alternative pathway of complement activation is elevated in patient serum (Gou, Yuan et al. 2012), and blockade of this pathway ameliorates disease in animal models (Huugen, Van Esch et al. 2007, Xiao, Schreiber et al. 2007, Schreiber, Xiao et al. 2009).

ANCA are typically high affinity, class switched antibodies of IgG specificity and can

Figure 1.5 Key pathogeneic mechanisms in AAV

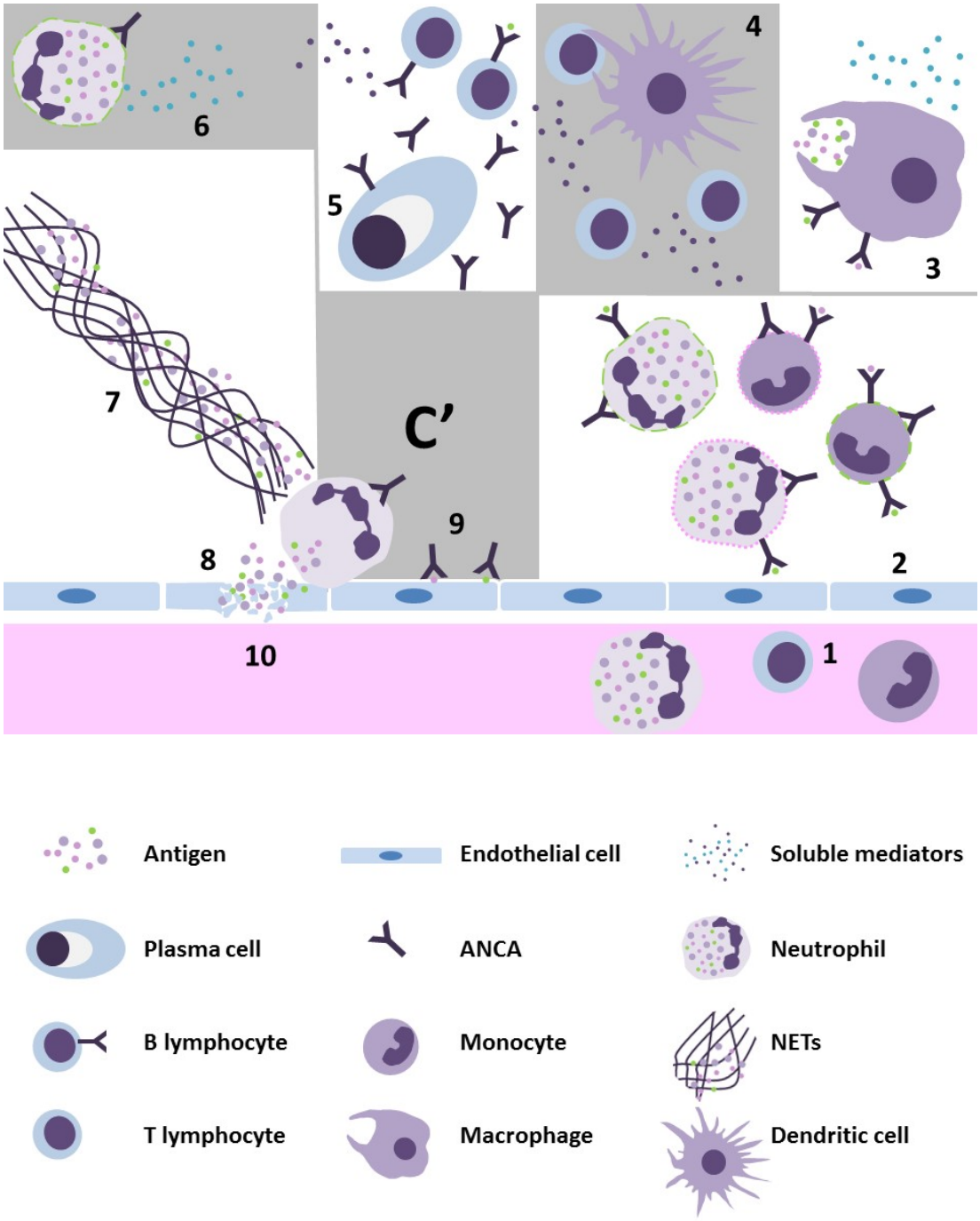

The numbers denote various stages in AAV pathogenesis, with key provided at the bottom. [1] Activated endothelium, leukocytes recruited and migrate across the endothelium. [2] Leukocyte activation induces expression of antigen on cell plasma membrane, ANCA bound via PR3, MPO and Fc receptors. [3] Macrophages take up and present antigen to T cells and release inflammatory cytokines like TNFα. [4] Pathology is mediated by Th1 and Th17, Treg fail to limit inflammation. [5] B cells differentiate to plasma cells and produce ANCA. [6] B and T cell reciprocal interaction, determines the net balance of cytokines. This is a feed-forward mechanism, which leads to diversification of the adaptive immune response. [5-6]. Neutrophils produce B cell survival factor BAFF and B cells, produce key neutrophil growth factor GM-CSF (GM-CSF also results in activation of myeloid cells, depicted in panel 1-4). [7] Neutrophil death by NETosis, persistence of antigen and innate immune stimuli. [8] Neutrophil degranulation, release of ROS, proteolytic enzymes and antigen. [9] Antibody and complement deposition. [10] Cascade cumulating in vascular damage.

therefore, be transferred across the placenta. There is only a single case report of MPO-ANCA resulting in neonatal MPA, with pulmonary haemorrhage and renal disease reported (Bansal and Tobin 2004, Schlieben, Korbet et al. 2005). However in a recent retrospective analysis of 22 pregnancies, no evidence of neonatal systemic vasculitis was found, which indicates additional risk factors may be required (Tuin, Sanders et al. 2012). The beneficial effect of plasma exchange provides further evidence, supporting a pathogenic role of antibody or other soluble plasma factors in AAV. In a randomised controlled trail, plasma exchange was associated with greater likelihood of dialysis independence at 12 months than pulsed methylprednisolone (Jayne, Gaskin et al. 2007).

Several models of MPO AAV have also been described, which result in crescentic glomerulnephritis and pulmonary haemorrhage. An immunological response to MPO, is central to the induction of disease: immunisation with human protein in combination with adjuvant in rats; passive transfer of splenocytes or immunoglobulin from MPO immunised $MPO^{-/-}$ mice; bone marrow transplants from wild type to MPO immunised $MPO^{-/-}$ mice (McAdoo, Tam et al. 2010, Heeringa and Little 2011, Salama and Little 2012).

PR3-ANCA mediated disease has been more difficult to model. Following immunisation with chimeric human and mouse PR3 proteins, antibodies to granulocytes are detected, but this does not result in pathology (van der Geld, Hellmark et al. 2007). Furthermore, transgenic mice with renal restricted expression of human PR3, develop no disease following intravenous administration of human PR3 antibodies (Relle, Cash et al. 2013). A pathogenic role for PR3-ANCA was finally

demonstrated in mice with a humanized, chimeric immune system; animals develop renal disease and punctate bleeding on the surface of lungs, however granulomatous inflammation is absent (Little, Al-Ani et al. 2012).

B lymphocytes also form part of the recruited mononuclear infiltrate in AAV, described within nasal lesions and the kidney. Cells are found in close association with antigen positive neutrophils, with organisation varying from randomly scattered cells to highly organised structures, resembling germinal centres (Steinmetz, Velden et al. 2008). Immunoglobulin gene sequencing of individual B cells from renal biopsies, demonstrates that these cells have undergone affinity maturation and have a bias for the VH4-34 gene segment, linked with autoreactivity (Voswinkel, Assmann et al. 2008). In nasal mucosal, there is proliferation of the infiltrating B cells (Ki67 positivity) and an increase in the expression of B cell survival factors locally (Zhao, Odell et al. 2012).

Soluble markers of B cell activation are also increased in AAV. B-cell activating factor (BAFF) promotes B cell survival and proliferation; serum levels are increased in AAV and inversely correlated with disease activity and ANCA titre (Bader, Koldingsnes et al. 2010, Nagai, Hirayama et al. 2011). Furthermore levels of BAFF are reduced, on commencing glucocorticoid treatment (Krumbholz, Specks et al. 2005). The increase in BAFF is accompanied by increased levels of soluble CD30 and CD25, the authors infer that this was due to T cell activation, however these markers are both also expressed on activated B cells (Mingari, Gerosa et al. 1984, Huang, Perrin et al. 1988, Shanebeck, Maliszewski et al. 1995). Interestingly, stimulation of neutrophils with ANCA has been shown to result in increased cleavage of BAFF from the cell surface,

with supernatant supporting growth of a centroblast cell line (Holden, Williams et al. 2011).

The importance of B cells in disease pathogenesis is further demonstrated by use of B cell depleting agents such as rituximab, a monoclonal antibody against CD20. Rituximab has been shown to induce clinical remission with similar efficacy to the standard induction regimen of cyclophosphamide in AAV (Stone, Merkel et al. 2010, Guerry, Brogan et al. 2012). Since, its CD20 target is absent from plasma cells, this indicates that the role of B cells extends beyond ANCA production in AAV.

The overall balance of effector and regulatory B cells is likely to contribute to disease activity in AAV. At the time of undertaking this project in October 2011, little was known about relative frequency of these subsets in AAV. During disease remission Tadema *et al* reported a reduction in memory B cell frequency (Tadema, Abdulahad et al. 2011), while Eriksson *et al* observed no difference in CD27+ memory B cells but an increase in CD25+ B cells, compared to controls, which they proposed to be immunoregulatory, but were lacking confirmatory functional phenotyping (Eriksson, Sandell et al. 2010).

Hypothesis

There is a quantitative or qualitative difference in B regulatory cells in AAV, which may explain the tendency for disease induction and relapse. This defect may be restored in a subset of tolerant AAV patients, who have become ANCA negative and demonstrated prolonged disease-free remission after withdrawal of treatment.

Aims

To assess whether any imbalance in B cell subsets exists in AAV patients relative to controls. To evaluate whether changes are linked to disease activity (in acute, tolerant and remission patients).

Testing for functional deficiency in B cell subsets in AAV, IL-10 competency and suppression of Th1 differentiation *in vitro*.

Evaluation of the role of regulatory B cells in an animal model of AAV, through adoptive transfer of whole B cells and B cells depleted of the regulatory fraction, into Rag2 immunodeficient mice.

Chapter 2 Methods

All statistical analyses were performed in Prism Graph Pad version 7.04 (GraphPad Software, San Diego, California). Tests are specified in the results chapters.

2.1 Human Studies

2.1.1 Subjects

Samples were obtained in accordance with the 1975 Declaration of Helsinki, after informed patient consent and under local ethical approval (05/Q0508/6). All AAV patients fulfilled the Chapel Hill definitions for GPA or MPA (Jennette, Falk et al. 2013). Patient demographics are presented in appendix 1, in full. A description of the cases included, is also presented at the start of the relevant results chapters.

AAV patients were categorised by disease activity. Active disease was defined as having clinical symptoms or signs due to systemic vasculitis, with consistent immunological and pathological findings. Remission patients had a Birmingham Vasculitis Activity Score (BVAS) of 0 (Mukhtyar, Lee et al. 2009), with the complete absence of clinical disease attributable to vasculitis for a minimum of one month. Tolerant patients were classified as those with a history of active AAV and positive ANCA, who subsequently became negative for ANCA by ELISA, remaining free from pathology after withdrawal of treatment for a minimum of 2 years.

2.1.2 Cell isolation

2.1.2.1 Density centrifugation

Peripheral blood mononuclear cells (PBMC) were isolated from venous blood by gradient centrifugation on lymphoprep (Alere, Stockport, UK). Blood was collected in Ethylenediaminetetraacetic acid (EDTA) vacutainer tubes (BD biosciences, Oxford, UK). Samples were diluted with an equal volume of Dulbecco's Phosphate-Buffered Saline without added magnesium or calcium (DPBS, Life Technologies, Paisley, UK). Diluted blood was layered on top of lymphoprep and cells were removed from the interface, after centrifugation at 800g for 30 minutes with no brake. PBMC were washed twice in DPBS, collected by centrifugation at 250g for 10 minutes. Cell counts were conducted on a haemocytometer and viability was assessed by trypan blue exclusion dye (Invitrogen). Only live cells float on the lymphoprep interface, so viability was consistently >95%.

2.1.2.2 PBMC cryopreservation and thawing

The majority of testing was conducted on fresh PBMC samples, where frozen samples were used, this is clearly stated in the results section.

For cryopreservation 2 freezing mixes were prepared, [A] contained equal volumes of foetal calf serum (FCS, Sigma Aldrich, Dorset, UK) and RPMI 1640 (Roswell Park Memorial Institute medium, Life Technologies,); [B] contained 20% DMSO (Dimethyl sulfoxide, Sigma Aldrich), 40% FCS and 40% RPMI 1640. PBMC concentration was adjusted to $20x10^6$ cells per ml in freezing media A in a 50ml tube and transferred onto ice.

An equal volume of ice-cold freezing mix B was adding drop-by-drop with a pastette, whilst gently swirling the cells over ice. Addition of DMSO creates an exothermic reaction, which can rupture cell membranes. The final cell concentration was $10x10^6$ cells per ml in 45% FCS, 45% RPMI and 10% DMSO. Cells were aliquoted into cryovials and placed in a Mr. Frosty™ (Thermo Fisher Scientific) in a -80 freezer for minimum of 12 hours before transferring to liquid nitrogen.

No more than 3 samples were thawed at once. RPMI containing 5% human AB serum (Life technologies) and 50U/ml benzonase (100kU, Novagen) was freshly prepared and warmed in advance. Cells were gently thawed in a 37°C water bath, without agitation.

The warm media was gradually added drop by drop, to the thawed cells, as sudden change in osmolarity can cause cells to rupture. PBMC were collected by centrifugation and washed in thaw media (250g, 10 minutes). Cells were rested in replete media 37°C and 5% CO_2 for a minimum of 1 hour prior to immunophenotyping. Replete media consisted of RPMI 1640, 10% heat inactivated FCS, 2mM L-glutamine (Life Technologies, Paisley, UK) 100U/ml penicillin and 100µg/ml streptomycin (100x solution from Life Technologies).

2.1.2.3 Magnetic enrichment of human CD25- T lymphocytes

Untouched T cells were isolated by CD25 magnetic bead isolation on MS columns, followed by CD4 or CD3 magnetic separation (Miltenyi Biotec, Surrey, UK). The method was conducted as per the manufacturer's recommendations. CD4+ CD25- cells were used for T and B cell co-cultures. CD3+ CD25- null cells were used to

assess effect of PBMC supernatants on T cells. Purity of cell subsets was assessed by flow cytometry, relative to starting populations.

2.1.2.4 Flow cytometric isolation of B cell subsets

PBMC were stained with CD19 [HIB19], CD24 [eBioSN3] and CD38 [HIT2] antibodies for flow cytometric sorting. Cells were stained at the recommended antibody concentration for 30 minutes on ice, in the dark. The antibody mix was prepared in DPBS 1% FCS and syringe filtered, prior to use (4mm diameter and 0.2µm pore size, Millipore, Watford, UK). Cells were washed twice in ice cold 1% FCS in DPBS (1000g, 3 minutes, 4°C) and resuspended in sorting media with 1% heat inactivated FCS. Sorting media was RPMI 1640 with 50µg/ml Gentamycin (Sigma Aldrich), 2mM L-Glutamine (Life Technologies), 100U/ml penicillin, 100µg/ml streptomycin, 2.5µg/ml amphotericin B (Sigma Aldrich), 25mM HEPES (Sigma Aldrich) and 2mM EDTA (Fisher Scientific). Cells were passed through a BD Falcon cell strainer tube immediately before sorting.

B cell subsets were isolated by cell sorting on a BD FACS Aria (BD Biosciences), with a 70µm nozzle. The instrument was set up with cytometer setup and tracking (CST) beads (BD Biosciences) and application settings applied. Drop delay was set using Accudrop beads. Instrument voltages adjusted on the fully stained sample (BD Biosciences). Compensation was conducted with unstained cells and mouse IgG kappa beads (BD Biosciences).

A 3-way sort was conducted based on of DAPI (4', 6-diamidino-2-phenylindole) dye exclusion (1µg/ml added immediately prior to sorting, Sigma-Aldrich, Dorset, UK) and relative expression of CD19, CD24 and CD38. Cells were collected into sort

media, with 10% added FCS. Purity of cell subsets was assessed by flow cytometry, relative to starting populations.

2.1.3 Carboxyfluorescein succinimidyl ester (CFSE) labelling of T cells

CD4+ CD25- T cells were isolated, counted and washed in 37°C DPBS (centrifugation at 250g for 10 minutes). CFSE was reconstituted in DMSO to 5mM stock and diluted to a final concentration of 2.5µM in 37°C DPBS, prior to adding to cells. Labelling protocol and dye-quenching was conducted according to the manufacturer's instructions. Round bottom 96 well tissue culture plates were coated with anti-CD3 [HIT3a], by preparing a 1 µg/ml stock in DPBS, adding 50µl per a well and incubating at 2 hours at room temperature. Plates were washed 3 time with 200µl DPBS and airdried in the laminar hood. CFSE labelled T cells were seeded with B cell subsets, in complete media with soluble anti-CD28 [CD28.8] at 2 µg/ml. Unstimulated T cells were included as the control. Cells were cultured for 5 days at 37°C in 5% CO_2. At the end of the incubation fixable viability stain was conducted (BD Biosciences) according to the manufacturer's protocol (10 minutes at room temperature, 1 in 1000 dilution prepared in DPBS), with flow cytometry cell surface staining for CD4 [RPA-T4]. Data was acquired on an LSR Fortessa instrument (BD Bioscience) and analysed using the proliferation tool in Flow Jo version 7.6.

2.1.4 Flow cytometry

2.1.4.1 Cell surface flow cytometry protocol

Up to 2 million cells were stained per a condition, with PBMC collected into wells on a 96 well v-bottom plate (Greiner bio-one, Stroud) by centrifugation at 4°C and 1000g

for 2 minutes. Cells were washed by resuspension in 200µl of ice-cold staining buffer (prepared in-house, DPBS with 1% heat inactivated FCS and 0.1% NaN_3, 0.22 micron filtered). Antibodies were combined in a master mix in staining buffer, at the manufacturer's recommended concentrations. PBMC were resuspended in antibody mix and incubated on ice for 30 minutes, wrapped in foil to protect from light. Cells were washed 3-times in staining buffer (resuspension in 200µl of staining buffer, centrifugation at 4°C and 1000g for 2 minutes). After the final wash cells were resuspended in 1% paraformaldehyde (PFA) fixative (prepared in-house in DPBS and 0.22 micron filtered), transferred to FACS tubes and total volume adjusted to 350µl. Tubes were racked and wrapped in foil, stored in fridge until analysis. Acquisition was conducted within 16 hours, to minimise dissociation of tandem dyes.

2.1.4.2 Data acquisition and analysis

Acquisition was performed on an LSR Fortessa instrument (BD Bioscience), with spectral overlap compensated in BD Diva. Differences in instrument sensitivity over time, were corrected by running CST beads (BD Biosciences) before each run. Flow cytometry analysis was conducted using FlowJo (TreeStar, Ashland).

2.1.4.3 Definition of B cell subsets on relative CD38 and CD24 expression

PBMC were stained immediately after density centrifugation isolation. The cell lineage marker chosen was CD19 [clone HIB19], because it has the widest distribution of the B cell specific markers, with expression starting in pro-B cells and continuing into the plasmablast phase of development. CD20 expression commences later and is lost before plasmablast development. Gating of B cell subpopulations was based on relative expression of CD24 [clone eBioSN3] and CD38 [clone HIT2], previously

described by Carsetti and Sims (Carsetti, Rosado et al. 2004, Sims, Ettinger et al. 2005). The gating strategy permits definition of three B cell subsets. Transitional B cells are defined as CD38 high and CD24 high. These were termed Breg, due to the immunomodulatory properties attributed to these cells (Blair, Norena et al. 2010, Flores-Borja, Bosma et al. 2013). Memory B cells are CD38 negative and CD24 high, whilst naïve B cells have intermediate expression of both markers. Staining was conducted alongside an IgG1 mouse isotype control and in each staining run, an intra-assay control was included (frozen healthy control donor cells). Single stained cells were used for compensation controls.

B cell frequencies were expressed as corrected percentages, with the sum equal to 100%, excluding the contribution of CD19+ CD24- cells, previously described (Sanz, Wei et al. 2008, Flores-Borja, Bosma et al. 2013).

2.1.4.4 Extended B cell immunophenotypic profiling

CD19+ cell expression of CD5 [clone UCHT2] and CD1d [clone 2H7 or CD1d42] was assessed, either in parallel to CD24 and CD38 immunophenotyping or on frozen cells stocks (31 patients and 17 controls).

Limited staining for CD5, CD1d, CD27 [O323], CD10 [eBioCB-CALLA], CD95 (Fas) [DX2], IgM [MHM-88] and IgD [1A6-2] was conducted in combination with CD24 and CD38.

CD1d expression was assessed intracellularly before and after stimulation (4 hours, 1µg/ml ionomycin and 50ng/ml PMA, Sigma Aldrich). Comparative cell surface and intracellular staining was conducted with the CD1d42 and 51.1 clones.

2.1.4.5 T cell immunophenotyping

Cell surface staining was conducted on PBMC with CD4 [RPA-T4], CD25 [BC96], CD127 [A019D5], CD39 [eBioA1 (A1)] and CD73 [AD2] antibodies.

2.1.4.6 Intracellular flow cytometry staining

The routine method for intracellular staining was fixation in 4% PFA prepared in DPBS, 10 minutes at room temperature. This is opposed to fixation in 1% at the end of the cell surface staining protocol. Cells were collected by centrifugation (1000g, 3 minutes), and permeabilization conducted with 0.5% saponin (Sigma-Aldrich) in DPBS, for 10 minutes at room temperature. Following another centrifugation step (100g, 3 minutes), cells were resuspended with intracellular antibodies, diluted in 0.1% saponin and 1% BSA (Bovine Serum Albumin), with incubation on ice for 40 minutes, in the dark. Cells were washed with staining buffer (0.1% saponin and 1% BSA) and 1% BSA in DPBS, prior to resuspending in 1% BSA in DPBS (collection by centrifugation in between wash steps, 1000g, 3 minutes)

Intracellular flow cytometry staining for cytokine detection in B cells, was conducted using the fixation and permeabilization buffer set (eBioscience, Hatfield, UK) and manufacturer's protocol.

2.1.5 T and B cells co-cultures

Effects on T cell activation were assessed in consecutive samples from the main cohort, 5 patients and 5 controls. $CD4^{+}CD25^{-}$ T cells were isolated by magnetic beads and cultured alone or with B cell subsets by flow cytometry sorting. Cells were combined at a fixed ratio of 1 B:4 T cells in RPMI 1640 supplemented with 2 mM L-

glutamine, 10% FCS, non-essential amino acid (NEAA) solution (Fisher, Loughborough, UK), 1 mM sodium pyruvate and penicillin/streptomycin. T cells were stimulated with soluble anti-CD28 [CD28.8] and anti-CD3 [HIT3a], as described in the preceding paragraph (2.2.2). Unstimulated T cells were included as a control. Cells were cultured for 5 days at 37°C in 5% CO_2. For the last 4 h, 50 ng/ml PMA (phorbol myristate acetate) and 1 µg/ml ionomycin were added to CD3/28-stimulated cells and Golgi-transport inhibitors brefeldin A (Golgi-Plug, BD Biosciences) and monensin (Golgi- Stop, BD Biosciences) were added to all wells. Fixable viability staining was conducted, with flow cytometry cell surface staining for CD4 [SK3], as previously described. Intracellular staining was conducted for IFN-γ [4S.B3] and TNF-α [MAb11]. Results were expressed as the percentage change relative to T cells cultured alone (normalized to zero), to assess the effect of B cell subsets on Th1 differentiation.

2.1.6 B cell intracellular cytokine detection

B cell IL-10 production was assessed in a subset of individuals from the main cohort (16 remission patients and 8 controls). PBMCs were simulated were seeded into 24-well tissue culture plates in replete RPMI 1640, 1 million cells per a well in 500µl. Cells were cultured for 48 hours at 37°C in 5% CO_2. Untreated cells were compared with CpG- stimulated cells (20µg/ml ODN 2006-G5 (InvivoGen, Toulouse, France)), with or without CD154 stimulation. The G5 modification of the CPG DNA promotes more effective cellular uptake of the TLR9 ligand. The CPG sequence was TCGTCGTTTTGTCGTTTTGTCGTTGGGGG. The CD154 stimulation comprised treatment with 4µg/ml histidine-tagged CD154 and 10 µg/ml cross-linking antibody [AD1.1.10] (R&D systems, Abingdon, UK). CD154 naturally exists as trimer, this

recombinant CD154 reagent is histidine tagged and can thus be cross-linked with antibody, forming multimers that maximally stimulate B cells. An alternative strategy is use of an irradiated or Mitomycin C treated CD154-transfected cell line. Since conducting this research multimeric recombinant CD154 reagents have become commercially available, which overcomes the need for an un-transfected cell control or antibody only control.

For the last 5 hours of the culture, brefeldin A (Golgi-Plug) was added to all wells, with 50ng/ml PMA and 1µg/ml ionomycin added to stimulated PBMC.

Fixable viability staining and CD19 [HIB19] cell surface staining was conducted. Intracellular staining was completed with the eBioscience fixation and permeabilization kit, with IL-10 [JES3-9D7], latency-associated peptide (LAP) [TW4-2F8] and TNF-α [MAb11] antibodies. LAP is secreted non-covalently linked to TGFβ, the archetypal immunoregulatory cytokine. Gates were set relative to the negative control, <1% positivity in unstimulated cells.

2.1.7 Measurement of soluble cytokine in supernatants

At the end of 48-hour PBMC culture for IL-10 induction, media was removed and centrifuged to collect cells for flow cytometry (1000g and 10 minutes). Supernatants were gently removed from cells with a pipette and then centrifuged twice at for 5 minutes at 16000g and 4°C, ensuring any cells or debris was removed, before freezing at -80ºC for future analysis. When all the samples were collected supernatants were thawed on ice, reformatted into a deep 96-well plate with 1ml capacity and daughter plates created to prevent the need for further freeze-thaw cycles.

A cytometric bead array (CBA) was conducted to compare cytokine released into the supernatants (Human Th1/Th2/Th9/Th17/Th22 kit from eBioscience). Analysis was conducted using Flow Cytomix software (Biolegend). TGFβ1 (eBioscience) and IL-35 (Biolegend) ELISA (enzyme-linked immunosorbent assay) were also performed. ELISA were conducted according the manufacturer's instructions, with absorption of capture antibody onto NUNC MaxiSorp 96 well flat bottom plates (Thermofisher Scientific). Detection method was tetramethylbenzidine (TMB) substrate, which is blue when applied and turns yellow on addition of stop solution. Ultraviolet (UV) absorbance was read on a Biochrom EZ Read 400 plate reader, with 450nm primary wavelength and 620nm reference. The complete list of analytes and limits of detection are provided below.

2.1.8 Net effect of PBMC cell supernatants on T cells

Supernatants of PBMC stimulated for B cell IL-10 induction, were pooled from patient or controls. Agonistic anti-IL-10 [JES3-9D7] (BD Biosciences) or rat IgG control was added at a final concentration of 10µg/ml. Samples were incubated for 30 minutes at room temperature and then microcentrifuge hard to remove antibody complexes (16000g, 10 minutes), the supernatant was removed, and samples were spun again. Samples were diluted 1 in 5 in ice-cold replete media, filtered to remove debris and ensure sterility.

The effect of supernatant on T cells, was tested at a final concentration of 10%. Round bottom 96-well plates coated with anti-CD3 (1µg/ml), as previously described. CD3+ CD25- cells were isolated from healthy controls using magnetic microbeads and MS columns. 75,000 T cells were added per a well in 150µl final volume and cultured for

Table 2.1 Analytes measured in PBMC supernatants

Analyte	Limit of detection (pg/ml)
IL-1β	4.2
IL-2	16.4
IL-4	20.8
IL-5	1.6
IL-6	1.2
IL-9	1.5
IL-10	1.9
IL-12 p70	1.5
IL-13	4.5
IL-17A	2.5
IL-22	43.3
IFNγ	1.6
TNFα	3.2
TGFβ1	8.6
IL-35	130

All analytes measured by Cytometric Bead Array, apart from TGFβ and IL-35 (eBioscience ELISA kits)

3 days. Brefeldin A (Golgi-Plug), PMA and ionomycin added for the final 4 hours. Intracellular staining was conducted for IFNγ and TNF-α.

2.2 MPO protein production

2.2.1 Cell culture

MPO protein was extracted from the neutrophil progenitor, mouse promyelocyte (MPRO) cell line (ATCC, CRL-11422). These cells require supplementation with GM-CSF (granulocyte-macrophage colony stimulating factor); the source of GM-CSF utilised was supernatant from the BHK (baby hamster kidney) HM5 cell line, a kind gift from Professor Robson, King's College London.

HM5 cells were cultured at 37°C and 5% CO2 in Dulbecco's Modified Eagle Medium (DMEM) supplied with GlutaMAX™, 4500 mg/L D-Glucose and 1µM Sodium Pyruvate (Life Technologies) and supplemented with 10% heat-inactivated FCS 100 units/ml penicillin and 100 µg/mL streptomycin. Cells were grown to confluency and media allowed to become yellow in colour, prior to harvesting. Media was centrifuged at 4,500g for 10 minutes to remove any cells which had detached and passed through a 0.22-micron syringe filter unit, prior to freezing at -80°C.

MPRO cells were grown in Iscove's Modified Dulbecco's Media (PAA Laboratories) with 20% heat-inactivated FCS, 100 units/ml penicillin and 100 µg/mL streptomycin and with 15% freshly thawed conditioned media from the BHK-HM5 cell line. Cells were maintained in liquid suspension at 1-2x$10^{6}$$ml^{-1}$; fresh media was added every 2-3 days and conditioned media, at 15% the final volume.

Cells were harvested by centrifugation, resuspended at $2x10^8$ cells in a final volume of 1ml of buffer A and frozen at -80°C. Buffer A was prepared as follows: 6.7mM of sodium phosphate (pH6.0 solution prepared by combining 12% by volume sodium phosphate, dibasic dihydrate and 88%, sodium phosphate, monobasic, monohydrate stock solutions), 1mM MgCl2 and 3mM NaCl (all chemicals from Sigma Aldrich). For the purpose of freezing cells, complete protease inhibitor cocktail was added to buffer A, 1 mini tablet for every 10ml of buffer (Roche Diagnostics GmbH, Mannheim Germany). In all subsequent steps, 0.5mM PMSF (phenylmethylsulfonyl fluoride, Sigma Aldrich) was used as the protease inhibitor.

2.2.2 MPRO cell and vesicle rupture

A minimum volume of 20ml cell lysate from $4x10^9$ cells was thawed at a time, this was diluted 1 in 10 in buffer A plus 0.5mM PMSF. Dounce homogenization was performed on ice, firstly 10 strokes with a large 40ml volume homogenizer and then 10 strokes with a small 10ml capacity homogenizer. The lysate was spun in an ultracentrifuge, for 30 minutes at 48,400g (20,000 rpm) and 4°C. The green pellets were retained and resuspended in 50 percent the initial volume of buffer A plus 0.5mM PMSF and 1% cetyltrimethylammonium bromide (CTAB, Sigma Aldrich), a detergent which ruptures the cell vesicles releasing MPO. This lysate was mixed vigorously on a magnetic plate for 2 hours at 4°C, then spun in an ultracentrifuge, for 20 minutes at 48,400g (20,000 rpm) and 4°C. The soluble fraction was now faintly green and the insoluble pellet, white in colour. The supernatant was dialysed in 31.7mm diameter regenerated cellulose tubing (SLS Limited, Nottingham) overnight in two large

beakers, with 5 litres of buffer B in each (100mM sodium acetate CH3COONa, pH6.3 and 100mM NaCl2, chemicals supplied by Sigma Aldrich), on a magnetic plate mixer at 4°C (100-fold higher volume of dialysis buffer than dialysate).

2.2.3 Affinity chromatography

MPO was isolated the next day by affinity chromatography on a 1ml HiTrap Con A (Concanavalin A) Sepharose 4B column (GE Healthcare, Amersham) and Äkta Prime FPLC system (GE Healthcare). All liquids were passed over the column at a fixed flow rate of $1ml/ml^{-1}$ and were degassed by filtration through a 0.45μm filter immediately prior to running. The column was first of all washed with 60ml milli-Q (18.2MΩ.cm filtered) water; then the column was equilibrated, by passing 60ml of filtered binding buffer over it. The binding buffer was buffer B, with 1mM MgCl2, McCl2 and CaCl2 added. The ions are essential in maintaining the stability of tetrameric Con A and binding to sepharose, therefore ions were also added to the dialysate. The dialysate with added ions was placed in an ice bucket and mixed occasionally by swirling, the entire volume was passed over the column 3 times after which, the column was a deep green colour.

The bound MPO was eluted with methyl-d-mannopyranoside; a 20-minute gradient elution was programmed on the Äkta Prime, buffer B with ions and no methyl-d-mannopyranoside at baseline, ramping to 1 molar methyl-d-mannopyranoside. 1ml fractions collected throughout and a further 10 fractions were collected after maximum methyl-d-mannopyranoside concentration reached. Aliquots were collected into a pre-determined volume of Tris-EDTA pH9.0, correcting final pH to 6.3 (volumetric ratio

was calculated on a larger total volume, using a pH meter).

2.2.4 Murine myeloperoxidase concentration and quality check

To determine protein concentration and purity, eluted fractions were analysed using a UV Nanodrop spectrophotometer (wavelength 280nm for protein and 430nm, green absorbance). Fractions positive for both, were pooled together and buffer exchanged into sterile PBS using PD-10 columns (GE Healthcare). Protein was concentrated to 1mg/ml using Vivaspin centrifugal concentrator (Sartorius Stedim Biotechnology, Goettingen, Germany). Visually, the concentrated protein was deep green in colour.

SDS-PAGE (sodium dodecyl sulfate polyacrylamide gel electrophoresis) was used to confirm the molecular weight and purity. Protein was resolved on hand-poured 10% polyacrylamide gel. The running gel was prepared according to Table 2.2 and overlaid with water saturated butanol; once set, the butanol was washed away with water, the stacking gel poured, and comb inserted. The extracted MPO was run alongside MPO isolated from human neutrophils (Millipore) and pre-stained precision Plus Protein™ Western C™ Standard (Biorad, Watford, UK). Samples were diluted 1 in 4 in non-reducing laemmli buffer prior to loading (Biorad). Final composition of running buffer was 0.025M Tris, 0.192M glycine, 0.1% SDS, pH 8.5 (10x solution prepared in-house, all chemicals supplied by Sigma Aldrich). The gel was run at 10mA for the first 20 minutes and 20mA thereafter, until leading band of the ladder was at the bottom edge of the gel. The gel was stained with Bio-Safe^{TM} Coomassie (Biorad), according to the manufacturer's instructions and imaged with visible light, on a gel imaging system.

Table 2.2 Polyacrylamide gel preparation

	Running gel	Stacking gel
Milli-Q 18.2µM water	4000µl	3400µl
1.5M Tris pH8.8	2500µl	0
1M Tris pH6.8	0	630µl
30% acrylamide-bis 37.5:1 (Biorad)	3340µl	750µl
10% Sodium dodecyl sulfate (Sigma Aldrich)	100µl	50µl
10% Ammonium persulfate (Sigma Aldrich)	80µl	75µl
Tetramethylethylenediamine (Sigma Aldrich)	4µl	10µl

SDS-PAGE was used to assess purity of native MPO, isolated from MPRO cells by Dounce homogenisation and Con A affinity chromatography. A 10% acrylamide gel was poured with the volumes indicated in the table.

2.3 *In vivo* murine methods

Experiments were performed in accordance with the terms of the Animals Scientific Procedures Act 1986, under UK Home Office project license 40/3228. Professor Salama was the personal license holder who conducted the procedures on live mice, whilst I assisted. Mice were euthanized by CO_2 inhalation and death confirmed by cervical dislocation.

Histological processing included preparation of wax blocks, sectioning of tissues, Periodic Acid-Schiff (PAS) and Haematoxylin and Eosin (H&E) stains. This work was outsourced to C&C Laboratory Services Ltd. London. Biochemical tests were performed by Pathology services, MRC Harwell, Oxfordshire. Histological scoring for frequency of crescents, was conducted independently by a minimum of two experimentally-blinded renal physicians.

I conducted the rest of the animal experiments independently: genotyping the MPO mice, preparing cells for transfer, making up the MPO-Freud's adjuvant emulsion, readying the metabolic cages and conducting post-mortem processing of tissues, blood and urine. This involved: photography, dissection, weighing, homogenization, red cell lysis of splenocytes and blood, CD19 magnetic cell isolation, flow cytometry cell sorting, flow cytometry immunophenotyping, MPO and immunoglobulin ELISA, urinary dipstick, immunofluorescent staining of tissue sections, light and confocal microscopy.

The details follow for the main experiment presented in Chapter 7, conducted after extensive optimisation of immunisation in MPO null mice.

2.3.1 MPO immunisation of MPO-/- mice

MPO-/- mice over 6 weeks of age were given a total dose of 30µg of native MPO (isolated from MPRO cells) and 300µg of MPO immunodominant peptide over course 10 weeks, with final immunisation 6 days before sacrifice. The peptide sequence of the T cell epitope was PRWNGEKLYQEARKIVGAMV, first described by Ooi *et al* (Ooi, Chang et al. 2012) and synthesized by Activotec Ltd, Cambridge. The first injection of 10µg and 100µg MPO immunodominant peptide was given subcutaneously into the hind flank, in an emulsion with Complete Freund's Adjuvant (CFA). The second and third injections were given with Incomplete Freund's Adjuvant (IFA). The full immunization schedule is provided in Table 2.3. Cardiac puncture was conducted post mortem, with blood collected into 0.8% sodium citrate, 10% final volume. Samples were mixed thoroughly to prevent clotting, centrifuged at 16,000g for 5 minutes and plasma removed to a fresh Eppendorf. Centrifugation was repeated to ensure no erythrocytes were carried across, which would be lysed upon freezing and interfere with downstream colorimetric assays. Plasma was aliquoted and stored at minus 80, avoiding repeat freeze-thawing cycles. Spleens were retrieved into ice cold RPMI.

2.3.2 Splenocyte injections in Rag2-/- mice

Spleens from the MPO-/- mice were dissociated and a single cell suspension obtained by passing through a 40µm cell strainer (BD Biosciences). Red blood cells were ruptured by addition of 1x commercial lysis buffer (Biolegend, San Diego, CA). The samples were mixed in 50ml tubes, with end-over-end rotation for 15 minutes at room

Table 2.3 Immunisation schedule in MPO null mice

	SEX	BIRTH	Imm 1	Imm 2	Imm 3	Age
WT	M	17/03/2014	30/09/2014	28/10/2014	26/11/2014	9.00
MPO	M	17/03/2014	30/09/2014	28/10/2014	26/11/2014	9.00
MPO	M	17/03/2014	30/09/2014	28/10/2014	26/11/2014	9.00
MPO	M	17/03/2014	30/09/2014	28/10/2014	26/11/2014	9.00
MPO	M	20/04/2013	30/09/2014	28/10/2014	26/11/2014	20.00
MPO	M	20/04/2013	30/09/2014	28/10/2014	26/11/2014	20.00
MPO	M	23/10/2013	24/09/2014	23/10/2014	26/11/2014	14.00
MPO	F	23/10/2013	24/09/2014	23/10/2014	26/11/2014	14.00
MPO	M	23/10/2013	24/09/2014	23/10/2014	26/11/2014	14.00
MPO	F	31/05/2013	24/09/2014	23/10/2014	26/11/2014	19.00
MPO	M	18/02/2014	30/09/2014	23/10/2014	26/11/2014	10.00
MPO	M	05/02/2014	24/09/2014	23/10/2014	26/11/2014	10.00
MPO	F	05/02/2014	24/09/2014	28/10/2014	26/11/2014	10.00
MPO	F	05/02/2014	24/09/2014	28/10/2014	26/11/2014	10.00
MPO	M	04/08/2014	None	None	None	4.00

The table details mouse background wild type (WT) or MPO knock out (MPO), and sex (M, male or F, female). Mice were immunised (imm) 3 times in total, subcutaneously into the hind flank (10µg native MPO and 100µg of immunodominant peptide). The first immunisation was in an emulsion prepared with an equal volume of CFA, with subsequent injections prepared with IFA. All mice were culled 6 days after final immunisation (02/12/14). Age in months at first immunisation, is provided in the last column.

temperature. Lysis was halted by topping tubes up with DPBS and centrifuging at 350g for 10 minutes, to collect cells.

B cell enriched, and depleted fractions were prepared using CD19 magnetic microbeads and LS columns (Miltenyi Biotec), according to the manufacturer's instructions. Highly purified B effector (CD1d-) and B regulatory (CD1d+) cells were isolated by 2-way flow cytometric cell sort (instrument set up, staining procedure and sorting media, as previously described).

Purity of cell fractions were assessed by flow cytometry using the cell surface protocol previously described: CD45 [30-F11], CD3 [17A2], CD19 [6D5], CD5 [53-7.3] and CD1d [1B1].

On day 1 cells were infused intravenously as detailed in Chapter 7. Mice were additionally given 0.018µg of lipopolysaccharide LPS intraperitoneally (R515 serotype, Enzo, Exeter, UK), which is reported to exacerbate antibody mediated disease (Huugen, Xiao et al. 2005). On day 6 an antigen boost was delivered, 10µg of native MPO given subcutaneously into the hind flank, in an emulsion with CFA. Mice were culled on day 15. Blood was collected by cardiac puncture (previously described), with spleen, lungs and kidneys additionally retrieved. Kidneys, lung and spleen were collected into ice-cold RPMI prior to photographing.

Kidney, lung and a portion of spleen were snap locked into histology cassettes and fixed in 10% buffered formalin overnight, then sent for histological processing.

18 hours prior to euthanasia, animals were transferred to metabolic cages for collection of urine. Samples were spun at 16,000g for 5 minutes to remove cage or cellular debris,

then transferred to clean tubes, taking care not to disrupt any sediment. Urine was aliquoted and stored at minus 20.

2.4 *In vitro* murine methods

2.4.1 Genotyping of MPO-/- mice

Ear clips were digested overnight in a lysis buffer at 55°C with end-over-end rotation. The lysis buffer was 100mM Tris HCl, 5mM EDTA, 0.2% SDS, 200mM NaCl, pH8.0, with 100µg/ml proteinase K (Thermo Fisher Scientific). After overnight digestion, samples were diluted with by a factor of 4, with distilled water and the proteinase K enzyme was inactivated by heating to 75°C for 15 minutes. PCR (polymerase chain reaction) was conducted with 2µl of the crude lysates and ReadyMix™ PCR Reaction Mix (Sigma Aldrich). Primer sequences and cycling conditions were specified by The Jackson Laboratory (Oligonucleotide synthesis, Sigma Aldrich).

Primers:	5’ TGA-CAC-CTG-CTC-AGC-TGA-AT 3’		
	5’ TGC-AGGCAG-CTG-GTC-TCG-CA- 3’		
	5’ CTA-CCG-GTG-GAT-GTG-GAA-TGT- 3’		
PCR conditions:	Hot-start	95°C for 5 minutes	
	35 cycles	Denaturation	94°C for 1 minute
		Primer annealing	60°C for 1 minute
		DNA extension	72°C for 1 minute
	Final extension	72°C for 5 minutes	
	Hold	4°C indefinitely	

Tris Borate EDTA (TBE) buffer was prepared with a final concentration of 90mM Tris-borate (Sigma Aldrich) and 20mM EDTA, pH8.3. A 2% agarose (Thermo Fisher

Scientific) with 10mg/ml ethidium bromide (Sigma Aldrich), was prepared in TBE. Gels were run in TBE buffer at 100V for 30 minutes and visualised using a UV light source.

2.4.2 Urinary and blood analysis

2.4.2.1 Urinary dipstick and biochemistry

Urine was spotted onto Multistix 10SG reagent sticks for detection of blood, leukocyte esterase and protein (Siemens Healthcare Limited, Surrey). The remaining urine was frozen at minus 20 and an aliquot sent for urinary protein and creatinine testing (MRC Harwell).

Blood was spun and plasma removed, with cell pellet retained for red cell lysis and flow cytometric analysis. Plasma aliquots were stored at –80. An aliquot was sent for urea, creatinine and albumin testing at MRC Harwell.

2.4.2.2 MPO ELISA

MaxiSorp ELISA plates (Thermo Fisher Scientific) were coated with MPO overnight at 4°C, at a concentration of 0.5µg/ml in 0.1M carbonate-bicarbonate (Sigma Aldrich) pH9.6. A wash solution of 10mM Tris, 75mM NaCl, 0.05% Tween 20, pH8 was prepared. Wells were washed with 300µl of wash solution X5 after overnight incubation with antigen.

Non-tissue culture grade PBS was made up in house, with a 10x solution prepared by combining 25.6g $NaHPO_4.7H_2O$, 80g NaCl, 2g KCl and 2g KH_2PO_4 in 1 litre total volume, milli-Q water. Final pH was adjusted to 7.4 with HCl. Blocking was conducted with 1% BSA in PBS (1 hour at room temperature on a plate mixer). Plasma

samples were diluted 1:100 in incubation buffer (PBS with 0.2% BSA, 0.05% Tween-20) and added to first column of the plate. Samples were serially diluted across the plate by a factor of 4. Samples were incubated for 1 hour at room temperature on a plate mixer. Wells were washed, as before. Plates were incubated with the secondary antibody, alkaline phosphatase labelled goat anti-mouse IgG diluted 1/000 in incubation buffer for 1 hour at room temperature before washing, as before. Detection was with p-nitrophenyl phosphate (Sigma), with reaction stopped by adding 100µl/well NaOH. Plates were read at a single wavelength of 405nm, on an ELISA plate reader (Biochrom EZ Read 400).

Native MPO protein isolated from MPRO, full length recombinant MPO (R&D Systems) and immunodominant peptide were used to coat plates. Plasma from MPO-null immunised mice and WT immunised were used as negative controls. Positive controls included native MPO and positive control serum (kindly gifted by Peter Heeringa, Groningen University).

2.4.2.3 IgG ELISA

Mouse IgG was quantified in plasma of null, immunised mice and Rag2 mice using the IgG total ELISA Ready-SET-Go! (eBioscience). Samples applied at 1 in 10,000 dilution, the standard curve range was 1.56-100ng/ml, with a lower LOD of 30pg/ml. Kit was performed according to the manufacturer's instructions.

2.4.2.4 Ig subtyping

Ig subclasses were assessed in plasma of null, immunised mice and Rag2 mice using the Mouse Ig isotyping ELISA Ready-Set-Go! (eBioscience). This is not a quantitative

assay but relative; the kit is designed for hybridoma selection, but the company verified quality assessment was also conducted with mouse serum.

MPO specific subclasses were measured using the modified protocol, outlined Figure 2.1. The initial steps were the same as the MPO ELISA (coat with recombinant or native MPO overnight, wash, block with 1% BSA, incubate with plasma and wash again). The isotype specific antibodies were then added at the concentrations stipulated for coating the plate (1 in 250 diluted in 1% BSA in PBS). Plates were washed again, and the detection antibody added, in 1% BSA PBS. The detection antibody was changed to HRP-conjugated anti-Rat Ig, normally supplied with the Rat Ig isotyping kit. The detection reagent was unaltered, plates read at 450nm absorbance with background at 570nm deducted. Results for Rag2 mice were expressed as percentage of the optical density observed in the MPO null, immunised mice (mean values used).

2.4.3 Cell surface flow cytometry murine cells

Flow cytometry was conducted on dissociated splenocytes and whole blood, after red blood cell lysis. Bone marrow and peritoneal cavity leukocytes from wild type mice were additionally used, isolated using published protocols (Ray and Dittel 2010, Liu and Quan 2015).

For in-depth B cell phenotyping, non-specific binding of antibodies was blocked by prior incubation in 20% FCS prepared in DPBS (20 minutes on ice) and addition of FcR block (anti-CD16 and anti-CD32) to the staining media (TruStain FcX,Biolegend). Wash steps, fixation and acquisition were as previously described. Full details of antigen targets and clones are provided in Table 2.4.

Figure 2.1 Modified Ig subtyping ELISA

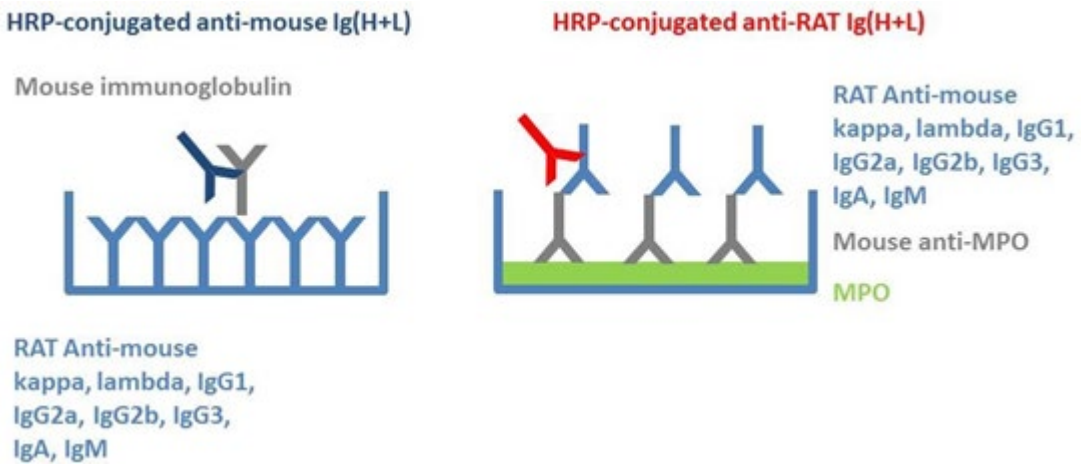

The standard protocol is shown on the left, with the modified one on the right. The plates were coated with MPO and then incubated with mouse serum. The Ig subtype antibodies, which would normally be used as the capture reagent were then added. The secondary was changed to anti-rat Ig with HRP tag. The substrate supplied with the kit was used.

Table 2.4 Antibodies used for B cell immunophenotyping in mice

Antigen	Clone
CD1d	1B1
CD5	53-7.3
B220	RA3-6B2
CD45	30-F11
CD3	17A2
IgM	II/41
IgD	11-26c.2a
CD38	90
CD24	M1/69
CD38	B3B4
CD43	S11
CD21/35	7G6
CD11b	M1/70
CD19	6D5
TIM-1	RMT 1-4
TIM-1	RMT 1-10

Full list of antibodies used for cell surface immunophenotyping of murine B cells, antigen target and clone detailed.

2.4.4 Induction of IL-10 in mouse B cells

Splenocytes or peritoneal leukocytes were cultured in replete media with 5×10^{-5}M 2-mercaptoethanol (Sigma Aldrich), 1mM sodium pyruvate and NEAA. Cells were plated at a density of 1 x $10^6 ml^{-1}$on round bottom tissue culture plates. Various conditions were tested including 48-hour stimulation with agonistic CD40 antibody [FGK45] (Enzo) and 5-hour stimulation with LPS, PMA and ionomycin (Matsushita and Tedder 2011).

The condition resulting in maximum induction of IL-10, was 48-hour stimulation with 10µg/ml LPS. Serotypes tested included R515 (Enzo), 026:B6 and 0111.B4 (Sigma Aldrich). 50ng/ml PMA, 1µg/ml ionomycin and monensin (Golgi-Plug) were added for the final 5 hours. Induction was verified by inclusion of peritoneal cells as a positive control. Fixable viability and CD19 flow cytometric cell surface staining was conducted. Intracellular staining for IL-10 [JES5-16E3] was conducted with Biolegend fixation and permeabilization buffers.

2.4.5 Immunofluorescent staining of tissue sections

Formalin Fixed Paraffin Embedded (FFPE) sections were dewaxed with xylene washes (2x 5 minutes), rehydrated through a series of alcohols (3 minutes each in a 1:1 volumetric ratio of xylene and ethanol, 100% ethanol x2 washes, 95% ethanol, 70% ethanol and 50% ethanol) and washed under cold running water. HIER (heat induced epitope retrieval) was conducted with 10mM sodium citrate and 0.05% Tween-20, pH 6.0. Slides were placed in HIER buffer warmed to 95°C in a water bath and transferred to a domestic electrical pressure cooker for 30-minutes. Slides were

cooled to the point that they could be handled and cells permeabilised in 0.5% Triton-X (Sigma Aldrich) in DPBS (30 minutes on a mixer). Tissue was outlined with a wax pen (Vector Labs, Peterborough, UK). Blocking was conducted for 30 minutes in PBS with 5% BSA, FcR block and 0.05% Triton-X for 2 hours at room temperature in a humidified chamber. The primary antibodies were stained overnight at 4°C, in the same blocking buffer: rat anti-mouse BB20 [RA3-6B2] and rabbit anti-mouse CD3 [SP7] (Abcam, Cambridge, UK).

Slides were washed in permeabilization buffer and PBS (5 minutes on a mixer). The slides were stained with Goat anti-Rabbit IgG (H+L) Alexa Fluor 488 for 1 hour at room temperature (Thermo Fisher Scientific). Slides were washed in PBS (5 minutes on plate mixer) and blocked for 15 minutes with 0.1% Triton-X and 10% goat serum (Sigma Aldrich) prepared in PBS. Goat anti-Rat IgG (H+L) Alexa Fluor 568 (Thermo Fisher Scientific), was stained for 2 hours at room temperature in the same blocking buffer. Slides were washed in PBS (5 minutes on a mixer) and counterstained with DAPI (3x 5-minute incubation with 1µg/ml solution prepared in PBS). Autofluorescence was quenched with a 0.1% solution of Sudan Black B (Sigma Aldrich), prepared in 70% alcohol (30 minutes, room temperature in a humidified chamber). Slides were flushed with a jet of HBSS (Hank's Balanced Salt Solution, Thermo Fisher Scientific). Slides mounted with Vectashield (Vector Labs) and coverslip sealed with nail polish. Slides were wrapped in foil to protect from the light and stored at 4°C prior to imaging. Imaging was on a Nikon-Ti with Nis-Elements. Confocal images were captured, in addition to large stitched fluorescent images, with a 15% overlap. Image analysis was conducted in FIJI (Schindelin, Arganda-Carreras et al. 2012).

Chapter 3 CD24 and CD38 B cell immunophenotyping

3.1 Background

Anti-neutrophil cytoplasm antibody (ANCA)-associated vasculitidies (AAV) are characterised by class-switched autoantibodies against myeloperoxidase (MPO-ANCA) or proteinase 3 (PR3-ANCA). ANCA are thought to directly contribute to pathogenesis, by activation of neutrophils and monocytes, which promotes adherence to the endothelium, release of proteolytic granule proteins, cytokines and chemokines (Jennette, Xiao et al. 2006). The importance of B cells, in addition to antibody production, is clearly demonstrated by use of B cell depleting agents such as rituximab, shown to induce clinical remission with similar efficacy to cyclophosphamide (Jones, Tervaert et al. 2010, Stone, Merkel et al. 2010, Guerry, Brogan et al. 2012). Importantly, B cells can modulate immunity independently of antibody production. They are effective antigen presenting cells (Rodriguez-Pinto 2005) and a potent source of cytokines (Harris, Haynes et al. 2000).

In the mid-1990s Janeway and colleagues demonstrated that B cells also act to limit inflammation (Wolf, Dittel et al. 1996). This function was subsequently attributed to an IL-10 competent B cell subset, capable of ameliorating or limiting autoimmune disease (Mizoguchi, Mizoguchi et al. 2002, Mauri, Gray et al. 2003). These cells were further defined as arising early in development and phenotypically, CD93+, $CD21^{high}$, CD23+, $CD24^{high}$, IgM^{high}, IgD+, CD5+ and $CD1d^{high}$ (Evans, Chavez-Rueda et al. 2007, Yanaba, Bouaziz et al. 2008). These cells were coined type 2 transitional–marginal zone precursor (T2-MZP) B cells, which denotes their early phase in

maturation, divergent development pathway to follicular B cells, with distinct spatial niche and antigen-processing function in secondary lymphoid tissue (Petro, Gerstein et al. 2002, Evans, Chavez-Rueda et al. 2007).

With a growing body of evidence for such regulatory B cells in animal models, the equivalent was sought in man. Classification on IL-10 competency, revealed that these cells were enriched in the circulating marginal zone pool, phenotypically classified as $CD24^{high}$ CD27+. IL-10 positive frequency was determined after short or prolonged stimulation and cells, were consequently called B10 or pro-B10 B cells. They limited monocyte TNFα production *in vitro* and were increased in frequency in multiple autoimmune diseases (Iwata, Matsushita et al. 2011).

B regulatory function was also attributed to CD11b+ (Griffin and Rothstein 2012) and CD5+ B cells (Noh, Choi et al. 2010), which straddle innate and adaptive immunity (CD11b is a subunit of the complement 3 receptor and CD5, a scavenger receptor). CD5 negatively regulates B cell receptor signalling and subset of CD5+ B cells are even reported to express the archetypal Treg transcription factor FoxP3 (Noh, Choi et al. 2010); other putative markers of immunoregulatory B cells, analogous to those on Treg include CD25 and CD27 (Amu, Tarkowski et al. 2007).

Another candidate regulatory population was the CD19+ $CD38^{hi}$ $CD24^{hi}$ population of transitional B cells, the first to repopulate the blood after stem cell transplant or rituximab depletion (Anolik, Friedberg et al. 2007, Marie-Cardine, Divay et al. 2008, Palanichamy, Barnard et al. 2009). Blair *et al* showed that these immature, CD19+ $CD38^{hi}$ $CD24^{hi}$ B cells were increased in frequency but not absolute number in SLE. These cells had a unique cell surface phenotype, were IL-10 competent and could limit

Th1 differentiation *in vitro*. Function was partly dependent on cell-cell contact, as effect was reduced on addition of antibodies to CD86 or CD80; these antibodies prevent ligation of CD28 on the T cell surface, suggesting that Breg are antigen dependent. Critically, these cells were functionally impaired in SLE (Blair, Norena et al. 2010), a multisystemic autoimmune disease, which frequently presents with glomerulonephritis.

CD24 and CD38 immunophenotyping permits 3 distinct B cell populations, which differ in maturation, to be resolved simultaneously: B memory cells, $CD19^{+}$ $CD24^{high}$ and $CD38^{low}$ (Bmem), B naive cells, $CD19^{+}$ $CD24^{intermediate}$ and $CD38^{intermediate}$ (Bnaive) and B regulatory cells, $CD19^{+}$ $CD24^{high}$ and $CD38^{high}$ (Breg). This gives a global overview of B cell populations in peripheral blood. As classification relies on cell surface markers, cells can be isolated from blood and function assessed, without prior stimulation or permeabilization.

AAV typically follows a chronic relapsing course, necessitating maintenance immunosuppression. However, we had identified a small cohort of "tolerant" patients who had history of active disease and ANCA positivity, who subsequently became negative for ANCA by ELISA, remaining free from pathology after withdrawal of all treatment, essentially re-establishing normal immunity. The concept of tolerance is not often used in the setting of autoimmunity but is used in field of transplantation. Renal transplant rejection is also an antibody mediated process, with B cells considered pathological. Like AAV, patients require life-long immunosuppressive therapy. Some patients do not comply with treatment, however they do not always mount an immune response to the foreign antigens and proceed to rejection, instead they enter a state of

operational tolerance. B cells have been shown to be important in maintaining tolerance to the renal allograft in these patients (Newell, Asare et al. 2010, Le Texier, Thebault et al. 2011, Silva, Takenaka et al. 2012). This led me to propose the overall balance of effector and regulatory B cells, contributes to disease activity in AAV.

At the time this project was undertaken, little was known about the relative frequency of B cell subsets in AAV (samples isolated between March 2011 and April 2013). Dysregulated expression in CD19 was shown in SLE and AAV relative to controls, with CD19 expression reduced in naïve B cells and enhanced in subset of memory B cells (Culton, Nicholas et al. 2007). Increased frequency of $CD38^{high}$ B cells was observed in active GPA and proposed to be a marker of B cell activation (Popa, Stegeman et al. 1999). During disease remission Tadema *et al* reported a reduction in memory B cell frequency (Tadema, Abdulahad et al. 2011), while Eriksson *et al* observed no difference in CD27+ memory B cells but an increase in CD25+ B cells, compared to controls. CD25+ B cells were proposed to be immunoregulatory, but this study lacked confirmatory functional phenotyping (Eriksson, Sandell et al. 2010).

3.2 Aims

To define memory, naïve and regulatory B cells based on relative expression of CD24 and CD38, assessing the balance of these subsets in an AAV cohort during different disease states.

3.3 Methods in brief

Peripheral blood mononuclear cells (PBMC) were isolated by gradient centrifugation on lymphoprep (Alere, Stockport, UK). PBMC were stained with CD19 [HIB19], CD24 [eBioSN3] and CD38 [HIT2] antibodies (eBioscience Ltd, Hatfield, UK). Data analysis was conducted using FlowJo (TreeStar, Ashland, OR). B cell frequencies were expressed as corrected percentages, with the sum equal to 100%, excluding the contribution of CD19+ CD24- cells (Sanz, Wei et al. 2008, Flores-Borja, Bosma et al. 2013). Relative B cell numbers were calculated from full blood count (lymphocytes per litre) and flow cytometry data (raw percentages). Full blood counts were not conducted on healthy controls, so comparison was only possible between patient groups.

3.4 Patient and healthy control samples

Samples were obtained in accordance with the 1975 Declaration of Helsinki, under local ethical approval (05/Q0508/6). Patients fulfilled the Chapel Hill definitions for

granulomatosis with polyangiitis (GPA) or microscopic polyangiitis (MPA) (Jennette, Falk et al. 2013). The study group comprised 19 healthy controls and 61 unique AAV patients. Clinical samples were isolated between 02/03/11 and 29/04/2013; clinical data collection was performed by consultant nephrologists Doctor Ruth Pepper and Doctor Juliana Draibe, after flow cytometric analysis (testing conducted blind).

Active disease was defined as having clinical symptoms or signs due to systemic vasculitis, with consistent immunological and pathological findings. The active group were further classified as acute (new onset, $\leq$17days since initial presentation) and grumbling (on-going disease or relapse). Remission was defined as the complete absence of clinical disease attributable to vasculitis, for a minimum of one month (BVAS equal to zero). Tolerant patients were classified as those with a history of active AAV, who subsequently became negative for ANCA by ELISA, remaining free from pathology after withdrawal of treatment for a minimum of 2 years.

3.5 Results

3.5.1 Patient demographics

3.5.1.1 Healthy controls and AAV patient groups

The control group comprised 10 males and 9 females, sex distribution did not differ from the AAV cohort (27 males and 34 females, Fishers exact test conducted P=0.4306). The median age of the controls was 50 years (Inter Quartile Range, IQR 40-60), this differed significantly from patients, with a median of 64 years and IQR 49-72 (Mann Whitney test P=0.0030**).

3.5.1.2 No relationship between B cell subsets and age

To assess whether age might skew results, regression analysis was conducted for the patient cohort (n=56, excluding rituximab treated individuals). There was no relationship between age and B cell subsets (Bmem P=0.9872, Breg 0.6887 and Bnaive 0.9214). In this study CD24- CD38- B cells were excluded from analysis, this putative population of plasmablasts were previously shown to be expanded in aged subjects with no changes in the other CD24 CD38 B cell subsets (Buffa, Pellicano et al. 2013). This population was rarely visible on flow cytometry biaxial plots.

3.5.1.3 Lymphocyte number declines with age, but there is no relationship with B cell subsets in AAV patients

Lymphocyte count declined with age (P=0.0088**), however there was no relationship between B cell frequencies and lymphocyte count (Bmem P=0.8384, Breg 0.9584 and Bnaive 0.8297). Results do not seem to be affected by generalised lymphopenia,

however full blood counts were only conducted in patients and it would be interesting to assess this in a healthy cohort.

3.5.1.4 No relationship between ANCA positivity or sex and B cell subsets

There was no difference in B cell subsets when patients were segregated by sex (35 female and 26 male) or ANCA positive titre at the time of testing (24 negative, 37positive). This was assessed for all B cell subpopulations by Mann Whitney U.

3.5.2 B cell subsets in a mixed AAV cohort compared to healthy controls

3.5.2.1 Breg reduced in AAV

The first result was observational, with flow cytometry plots revealing a striking and unexpected loss of the Breg in a subset of AAV patients (Figure 3.3). This necessitated inclusion of an intraassay control; for consistency in staining an antibody master mix was prepared, with staining conducted on v-bottom plates (Greiner Bio-one, Austria).

Analysis was first conducted in the mixed AAV cohort (n=61), relative to the healthy controls (n=19). When D'Agostino and Pearson normality test was conducted, the distribution pattern for all B cell subsets was normal in healthy controls but the frequency of Breg and Bmem cells did not have a normal distribution in patients. This is likely due to heterogeneity in the patient cohort, necessitating further analysis based on treatment, disease activity and ANCA specificity.

Breg were significantly reduced in AAV patients (median 2.89%, range 0.00-41.99%), compared to controls (median 6.18%, range 2.06-12.54). The patient data was negatively skewed, with some extremely high outliers. Mann Whitney U was used to compare data sets, data presented in Figure 3.1, Panel A (P=0.0005***).

3.5.2.2 Bmem frequency reduced in AAV compared to healthy controls

Bmem were significantly reduced in AAV patients (median 20.80%, range 1.53-69.27%), compared to controls (median 33.4%, range 4.40-48.38). Mann Whitney U was used to compare data sets because patient data did not have a normal distribution pattern (P=0.0486*, Figure 3.1, Panel B).

3.5.2.3 Bnaive frequency increased in AAV compared to healthy controls

The frequency of Breg, Bmem and Bnaive cells were corrected to 100%, excluding any CD24 null cells (putative plasmablasts). The reduction in Breg and Bmem, was therefore reciprocated with an increase in naive B cells. Whether this represents reduction of Breg and Bmem concomitantly or reduction of one population over another dependent on patient subclassification, remained to be determined.

Patient and control data both fitted a normal distribution pattern, consequently unpaired two-tailed t-test with Welch's correction was performed. Bnaive frequency was higher in patients than controls (P=0.0288*). The mean Bnaive frequency was 70.25% (SD 15.02%) in patients and 62.41% (SD 12.44) in controls. The spread of data was much wider for patients than controls, AAV range was 29.91-95.48% and this was 44.27-87.51% in controls (Figure 3.1, Panel C).

3.5.2.4 Refinement of the patient cohort and comparison of subgroups

The patient group was subsequently refined to just 51 unique patients and 53 samples, after collection of clinical data (patients initially tested blind) (Todd, Pepper et al. 2014). The refinement of the final case series is detailed in Figure 3.2, this cohort comprised 39 remission patients, 12 patients with acute disease and 2 replicate samples (tested in remission after rituximab treatment, also in the acute phase of disease).

Figure 3.1 Frequency of B cell subsets in patients and controls

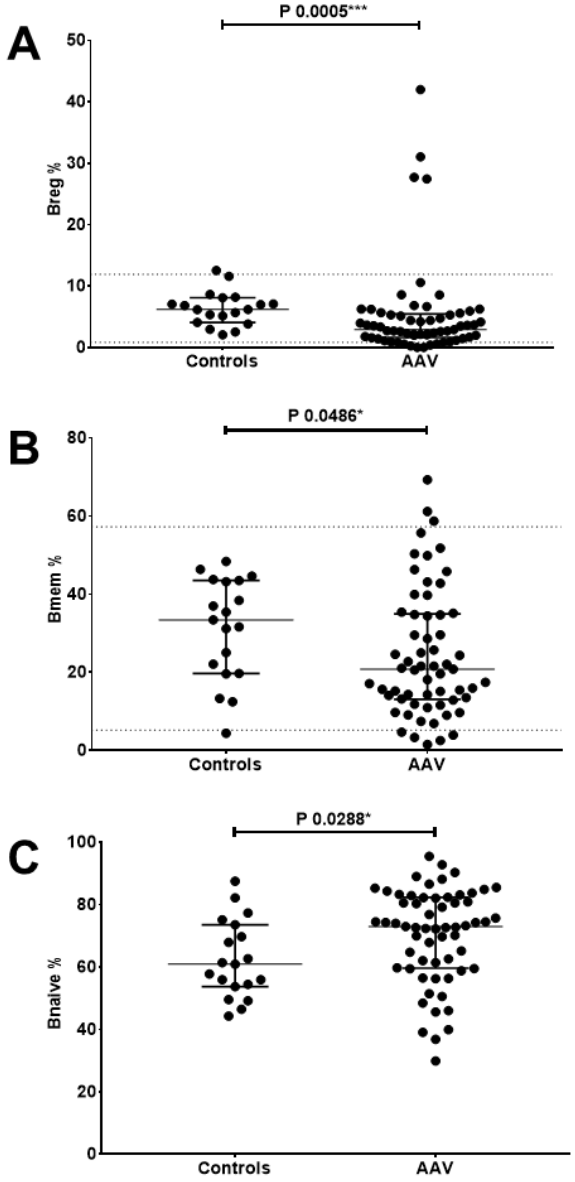

Corrected frequency of Breg, Bmem and Bnaive cells shown for healthy controls (n=19) and AAV mixed cohort (n=61). Error bars denote median, 25th and 75th percentiles. Dashed lines represent healthy control mean plus and minus 2 standard deviations. [A-B] Percentage frequency of Breg and Bmem was reduced in AAV patients compared to healthy controls, whilst Bnaive frequency was increased [C].

3.5.2.4.1 Subclassification of patients with active disease

Patients with active disease not only include those at initial presentation, but also those with flares or grumbling disease. This distinction in these 2 active disease groups was made because patients with grumbling disease had variable disease duration, 0.5-16 years in grumbling disease compared to ≤17days in acute patients (latter detailed in Table 3.2). Longstanding disease is associated with higher cumulative burden of immunosuppression. Grumbling patients also differed clinically, they had significantly lower BVAS (P=0.0192*), ANCA titre (p=0.0023*) and serum creatinine (P=0.0136*), compared to patients presenting acutely. Ultimately a mixed active cohort might affect the validity of results (those presenting acutely and those with grumbling persistent disease); in mice immunoregulatory B cells are reported to limit autoimmunity in the initiation phase but cannot limit pathogenesis in the chronic phase of disease (Matsushita, Yanaba et al. 2008).

When acute (n=12) and grumbling patient (n=5) B cell subsets were compared by MannWhitney U, the grumbling group had lower Breg (IQR 1.2-2.9 and 2.7-5.9, P=0.0357*) and higher Bnaive (IQR 83.3-90.0 and 74.1-82.8, P=0.0194*) than patients at initial presentation. Bmem did not differ significantly (IQR 8.3-14.9 and IQR 12.6-20.7, P=0.1037)

Upon 3-way analysis (Kruskal-Wallis and Dunn's multiple comparison), Bnaive were significantly higher and Bmem significantly lower in both acute and grumbling disease, compared to remission. Breg were significantly higher in acute disease, compared to remission. Frequency of Breg in patients with grumbling disease, did not differ from acute patients or remission patients. This profile of B cell subsets in

Figure 3.2 Refinement of patient cohort after collection of clinical data

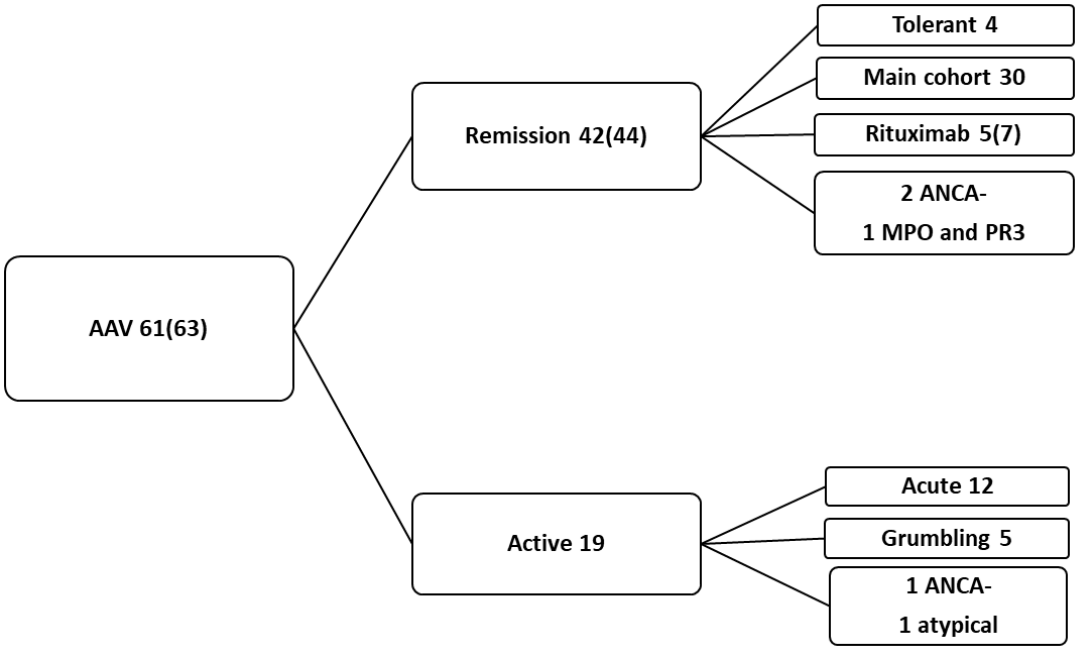

61 unique patients were originally tested, with 2 replicate samples (indicated in brackets, above). The final cohort was refined to 53 samples and 51 unique patients: 4 tolerant patients, 7 rituximab treated patients (2 replicates, also tested in the acute phase of disease), 30 patients in clinical remission (non-tolerant, no history of rituximab treatment) and 12 acute patients (tested within 17 days of initial presentation). This excluded 5 grumbling patients, with on-going disease or relapse and 5 patients without single positivity for MPO or PR3-ANCA (no ANCA detected (n=3), atypical (n=1) and double positive for MPO- and PR3-ANCA (n=1)).

grumbling disease (low Bmem), more closely resembles acute disease than remission (restored Bmem).

3.5.2.4.2 Subclassification of remission patients

There were outlying values for Breg, when separated according to disease activity these high Breg values were all within the remission group. The remission subgroups were therefore compared by Kruskal Wallis and Dunn's Multiple comparison (30 patients in remission, non-tolerant and no prior rituximab treatment; 4 tolerant patients and 7 patients who had historical rituximab treatment). Breg differed significantly across these subgroups, Breg were significantly higher in tolerant patients (P=0.0303*) and those who received prior rituximab treatment (P<0.0001****), compared to the main remission cohort. The latter was not unexpected, Breg are known to be the first to recover after rituximab treatment (Anolik, Friedberg et al. 2007, Palanichamy, Barnard et al. 2009).

3.5.2.4.3 Removal of patients without single ANCA positivity

Patients without single positivity for MPO- or PR3-ANCA were excluded. These 5 patients included 1 individual with atypical ANCA and acute disease, 1 ANCA negative acute, 2 ANCA negative remission, and 1 remission patient who was positive for both MPO- and PR3-ANCA (Figure 3.2).

I limited the final cohort to patients with a history of ANCA positivity, following suggestion by the reviewers (Todd, Pepper et al. 2014) and, a seminal publication proving PR3-ANCA and MPO-ANCA vasculitides are genetically distinct (Lyons, Rayner et al. 2012). ANCA specificity also better predicts patient outcome than

clinical manifestations of disease (GPA or MPA diagnosis is more subjective) (Lionaki, Blyth et al. 2012, Unizony, Villarreal et al. 2016), furthermore MPO-ANCA and PR3-ANCA patients have distinct cytokine profiles (Berti, Warner et al. 2018).

3.5.2.5 Characteristics of the refined cohort

Characteristics of the refined cohort of 51 patients is provided in Tables 3.1, 3.2 and 3.3. Rituximab treated patients were in clinical remission; 7 data points, 2 of which were replicate samples, also tested in the acute phase of disease (Figure 3.2). Analysis was performed separately, due to the profound effects of therapy on B cell homeostasis (Figure 3.8).

Within the patient subgroups (remission, acute, rituximab-treated and tolerant), there was no difference in frequency of individuals with GPA or MPA diagnosis, MPO- or PR3-ANCA (P=0.2197 and 0.2621, Chi-square, Table 3.1). Furthermore, age and lymphocyte count did not differ significantly (P=0.1480 and P=0.3754, Mann Whitney, Table 3.1). When these 4 patient groups were compared relative to healthy controls, only the remission group were significantly older (Mann Whitney P=0.0143* and Dunn's multiple comparison test P=0.0129*). With age spanning 16-86 years and disease duration up to 33 years, it was hard to control for this level of variance.

There was no significant difference in the frequency of men and women in the respective groups (P=0.1432, Chi-square, Table 3.1), nor compared to healthy controls (Chi-square, P=0.1645). The frequency of patients who were ANCA positive at the time of testing differed significantly between the groups (P=0.0023**, Chi-square, Table 3.1). All tolerant patients (TOL) were ANCA negative by definition, all acute

patients were ANCA positive, 60% of remission and 71% of rituximab patients were ANCA positive at the time of testing.

Dunn's multiple comparison test was used to compare all columns, whenever Mann Whitney U was significant (Table 3.1). Creatinine was higher in acute patients compared to remission (REM P=0.0193*) and tended to be higher in acute patients, compared to ritxumab treated patients (RTX P=0.0520). Disease duration was significantly lower in acute patients compared to remission (P<0.0001****), tolerant patients (TOL P=0.0003***) and ritxumab treated patients (RTX 0.0024**).

Standard induction therapy in acute patients was high dose prednisolone and cyclophosphamide. Maintenance therapy in remission comprised azathioprine or mycophenolate mofetil, in combination with low dose prednisolone. There were significantly more acute patients on cyclophosphamide and fewer on azathioprine (P=0.0002*** and P=0025**, Chi-square, Table 3.1). Prednisolone dose was also significantly higher in acute patients compared to remission (P=0.0011**, Mann Whitney and Dunn's multiple comparison).

Acute patients invariably had high BVAS and ANCA titre, further clinical details of these 12 individuals is provided in Table 3.2.

Table 3.1 Refined patient cohort, compared according to disease activity[KT1]

Patient characteristics		REM	ACUTE	RTX	TOL	P-value
Sample number	53	30	12	7	4	
Age	Median	66	64	48	73	0.1480
	IQR	49-77	43-70	34-65	52-83	
Sex %	Male:Female	30:70	67:33	57:43	75:25	0.1432
Lymphocyte count	Median ($x10^9$/L)	1.4	0.9	1.36	1.5	0.3754
	IQR	0.8-1.9	0.6-1.5	0.7-1.7	1.1-1.8	
ANCA %	Negative:Positive	40:60	0:100	29:71	100:0	**0.0023**
Serum creatinine	Median (mg/dL)	98	216	89	220	**0.0038**
	IQR	62-165	144-522	70-102	134-316	
Diagnosis %	MPA:GPA	57:43	75:25	29:71	75:25	0.2197
Disease duration	Median (years)	6	0	7	11	**<0.0001**
	Range	0.2-33	0-0.08	0.3-13	7-17	
ANCA specificity %	PR3	60	58	86	25	0.2621
	MPO	40	42	14	75	
Treatment %	None	7	17	29		0.2437
	Cyclophosphamide	3	50	0		**0.0002**
	Mycophenolate	20	0	14		0.2466
	Methotrexate	7	8	14		0.8025
	Azathioprine	53	8	0		**0.0025**
	Corticosteroids	63	83	57		0.3780
Oral prednisolone	Median dose (mg)	5.0	40.0	5.0		0.0017

*Statistical analyses were performed to compare patient groups: Chi-square for discrete variables (percentage frequency shown) and 1-way ANOVA for continuous variables. Significant differences between patient groups shown in **bold**.*

Table 3.2 Details of patients with acute disease

	Days since presentation	BVAS score	ANCA titre	Creatinine mg/dL	Lymphocyte $x10^9$/L	Current treatment	M:R(n)	Bmem%	Breg%
MPO_1	3	12	58	633	0.86	CYC, PRED	2.0	17.4	8.6
MPO_2	2	14	>100	383	0.74	MP, single dose	3.6	15.2	4.2
MPO_3	1	12	>100	665	0.37	CYC, PRED	0.9	9.1	10.6
MPO_4	0	14	37	142	1.63	CYC, PRED	3.3	19.6	5.9
MPO_5	4	14	>100	279	1.44	MP, single dose	2.7	11.0	4.1
PR3_1	15	13	44	150	0.61	CYC, PRED	7.9	21.6	2.7
PR3_2	17	13	176	67	1.49	NONE	3.7	21.0	5.7
PR3_3	6	13	23	74	0.86	MTX, PRED	4.1	11.8	2.9
PR3_4	0	17	96	151	2.62	NONE	9.0	16.0	1.8
PR3_5	17	12	>177	153	0.78	CYC, PRED	9.0	24.3	2.7
PR3_6	0	12	92	531	1.23	MP, single dose	7.6	15.1	2.0
PR3_7	14	14	35	494	0.37	CYC, PRED	6.8	18.1	2.7

All acute patients were tested within 17 days of initial presentation (median 3.5 days). At the time of sampling, median BVAS was 13 and patients were strongly positive for ANCA. There was no significant difference in creatinine or lymphocyte count between MPO-ANCA and PR3-ANCA, assessed by Mann Whitney U (P=0.2020 and P=0.9747, respectively). Breg frequency was significantly lower in PR3-ANCA acute patients, compared to MPO-ANCA (Figure 1, P=0.0101); although treatment varied, there was no trend apparent relative to B cell subset frequency or lymphocyte count (abbreviations used: CYC, cyclophosphamide; PRED, oral prednisolone; MP, intravenous methylprednisolone; MTX, methotrexate).

3.5.3 Comparison of B cell subsets in the refined AAV cohort, relative to healthy controls

The profound differences in the patient groups, are shown with representative flow cytometric plots in Figure 3.3. There was such a great reduction in the Breg subset in some individuals (both in the remission and acute phase of disease), that this necessitated incorporation of an intraassay control in each staining batch. The plots show a clear reduction in Bmem in the tolerant and acute patient, but not in the remission patient.

3.5.3.1 Breg are reduced in remission irrespective of ANCA specificity, with tendency for a reduction in PR3-ANCA acute disease

Breg frequency was compared in remission, acute and tolerant patients, relative to healthy controls (Mann Whitney and Dunn's multiple comparison). Breg frequency was significantly lower in remission patients (IQR 0.87-3.63%) compared to controls (P<0.0001****, Figure 3.4). Breg frequency in tolerant patients (IQR 6.22–8.01) and acute patients (IQR 2.68-5.86), did not differ significantly to controls (IQR 4.09–8.10). As Breg values were much higher in rituximab treated patients, separate analysis of this cohort was conducted relative to the healthy controls (Figure 3.8 and Table 3.3).

When subdivided by ANCA specificity, MPO- and PR3-ANCA remission patients did not differ significantly from one another, both had significantly lower Breg frequency than healthy controls. Breg frequency was significantly lower in PR3-ANCA acute patients relative to acute MPO-ANCA patients (P=0.0101, Figure 3.5). PR3-ANCA acute patients tended to have lower Breg frequency than healthy controls (IQR 1.99-2.89, P=0.0563) but MPO-ANCA acute patients did not (IQR 4.17-9.56, Table 3.2).

Figure 3.3 Differences in B cell subsets according to disease activity[KT2]

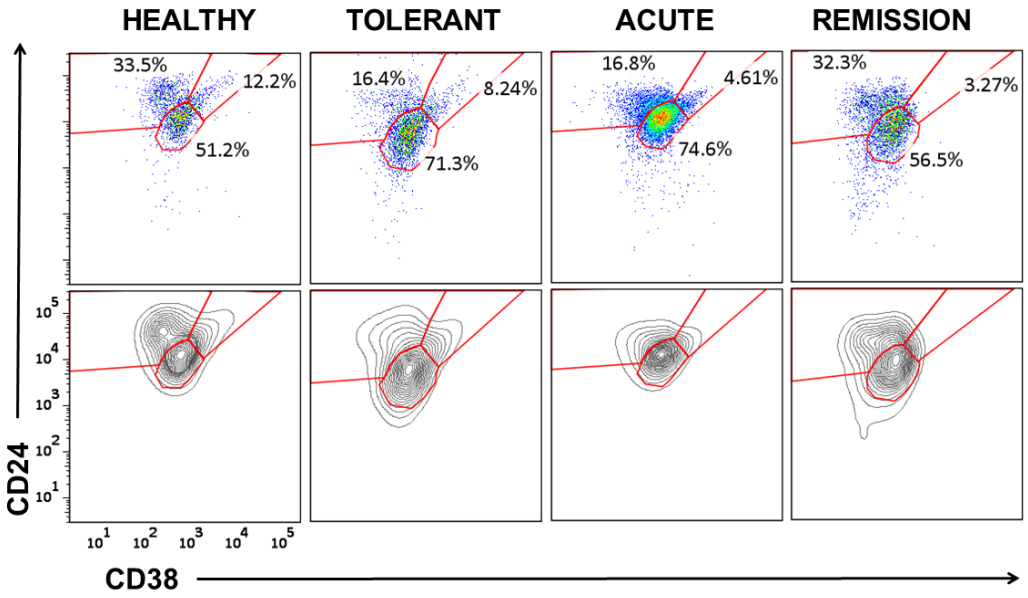

Representative flow cytometry plots for 1 healthy control, 1 tolerant AAV patient, 1 AAV patient with acute disease and 1 AAV patient disease remission. Samples run with an intraassay control and data viewed on multiple plots to improve gating accuracy, paired pseudocolour dot plot (top row) and contour plot (bottom row) shown. Breg were diminished in remission and active disease, Bmem reduced in active disease and tolerance.

3.5.3.2 Reduction in Bmem in acute AAV and trend towards a reduction in tolerant patients. Highest Bmem frequency in PR3-ANCA remission patients.

Bmem frequency was reduced in acute patients relative to controls (P=0.0121*) and showed a trend towards a reduction in tolerant patients (P=0.0624). When separated according to ANCA specificity, acute MPO-ANCA patients (IQR 10.03–18.51) did not differ significantly from acute PR3-ANCA patients (IQR 15.10–21.58). Overall Bmem frequency in remission was comparable to controls (Figure 3.4). However, frequency was higher in PR3-ANCA (IQR 27.69-52.75) than MPO-ANCA remission patients (IQR 9.70-40.93, P=0.0382, Figure 3.5).

PR3-ANCA patients have the highest propensity to relapse, this led me to hypothesise that the balance in Bmem and Breg, might be important in determining clinical outcome, especially since the converse is observed in tolerant individuals (normal Breg frequency without restoration in Bmem frequency). The relationship between these 2 cell types, was therefore represented as a ratio (results discussed in section 3.5.3.3).

Why might Bmem be reduced in acute disease? CD24low B cell subsets were seldom observed in biaxial plots (sum of raw B cell frequencies median 90% and IQR 83-93%); however, it is possible the reduction in Bmem might be due to differentiation to plasmablasts (more reliably defined as CD20low, CD138+). Bmem, might also be recruited to inflammatory sites or retained in secondary lymphoid tissue in an active immune response. Ectopic lymphoid structures, similar to germinal centres are reported in kidney and nasal lesion in AAV and would be of great interest (Steinmetz,

Velden et al. 2008, Voswinkel, Assmann et al. 2008) unfortunately, many studies in patients are limited to sampling peripheral blood.

3.5.3.3 Increased memory: regulatory ratio in remission

The imbalance in effector and regulatory subsets was represented by a memory:regulatory ratio, denoted M:R_n (Figure 3.4 and 3.5). This was derived by dividing the absolute number of cells within the Bmem gate by the number within the Breg gate. M:R_n was increased in remission (IQR 7.77-43.75), compared to controls (IQR 2.9-9.4, P<0.0001). When separated according to ANCA and disease activity, the highest M:R_n values were observed in MPO-ANCA remission (IQR 3.496-103.60, Figure 3.5), however, the median was only statistically higher than controls in PR3-ANCA remission patients (IQR 10.38-29.85, P=0.0006***).

Differences were observed between MPO-ANCA and PR3-ANCA patients with similar disease activity and treatment. Bregs were reduced in acute PR3-ANCA but not acute MPO-ANCA patients. In remission, Bmem frequency was higher in PR3-ANCA patients than in MPO-ANCA patients. The results suggest that the role of B cells in pathogenesis may differ between PR3- and MPO-ANCA disease. This is perhaps not surprising, with variations in genetics, cytokine-profile, pathology and outcome also reported (Lionaki, Blyth et al. 2012, Lyons, Rayner et al. 2012, Walsh, Flossmann et al. 2012, Unizony, Villarreal et al. 2016, Berti, Warner et al. 2018)

3.5.3.4 Increased Bnaive in acute disease

Bnaive cells were increased in acute disease relative to healthy controls (IQR 74.15-82.75 and 53.73-73.57%, P=0.0039**) but did not differ significantly in remission (IQR 50.08-74.35 P>0.9999) or tolerant patients (IQR 72.74-90.14 P=0.0945). When

segregated according to ANCA specificity, statistical significance was preserved for acute patients with PR3-ANCA (higher Bmem frequency, relative to healthy controls).

The relationship of these 3 B cell subpopulations are reciprocal, they are linked not only in terms of their development but for the purposes of analysis, the sum of the 3 populations was corrected to 100% (removing any confounding effect of CD24low putative plasmablasts). In acute disease, there is a reduction in both Bmem and Breg in acute disease; Bmem are typically more abundant than Breg and reduction in this subset would inevitably be accompanied by an increase in Bnaive (the largest B cell population).

Homeostatic proliferation is a well characterised phenomenon in mature T cells, but this process is not well elucidated in B cells. It would be interesting to see if clonotypic expansion contributes to the high frequency of Bnaive in patients. If this process occurred in an analogous manner to T cells, it would result in reduced BCR diversity, with peripheral maintenance of the B cell number (turnover of the naïve subset), due to low egress of precursors from the marrow.

3.5.3.5 Tolerant patients are distinct from other patients

Tolerant patients are defined by long term remission, with no requirement for continued immunosuppression and history of ANCA positivity, with subsequent reversion to negative status. Consequently, tolerant patients were compared to other ANCA positive and ANCA negative patients (Figure 3.6). Corrected Breg frequency was significantly higher in the tolerant group compared to ANCA negative and positive patient groups.

Figure 3.4 **B cell subsets according to disease activity**

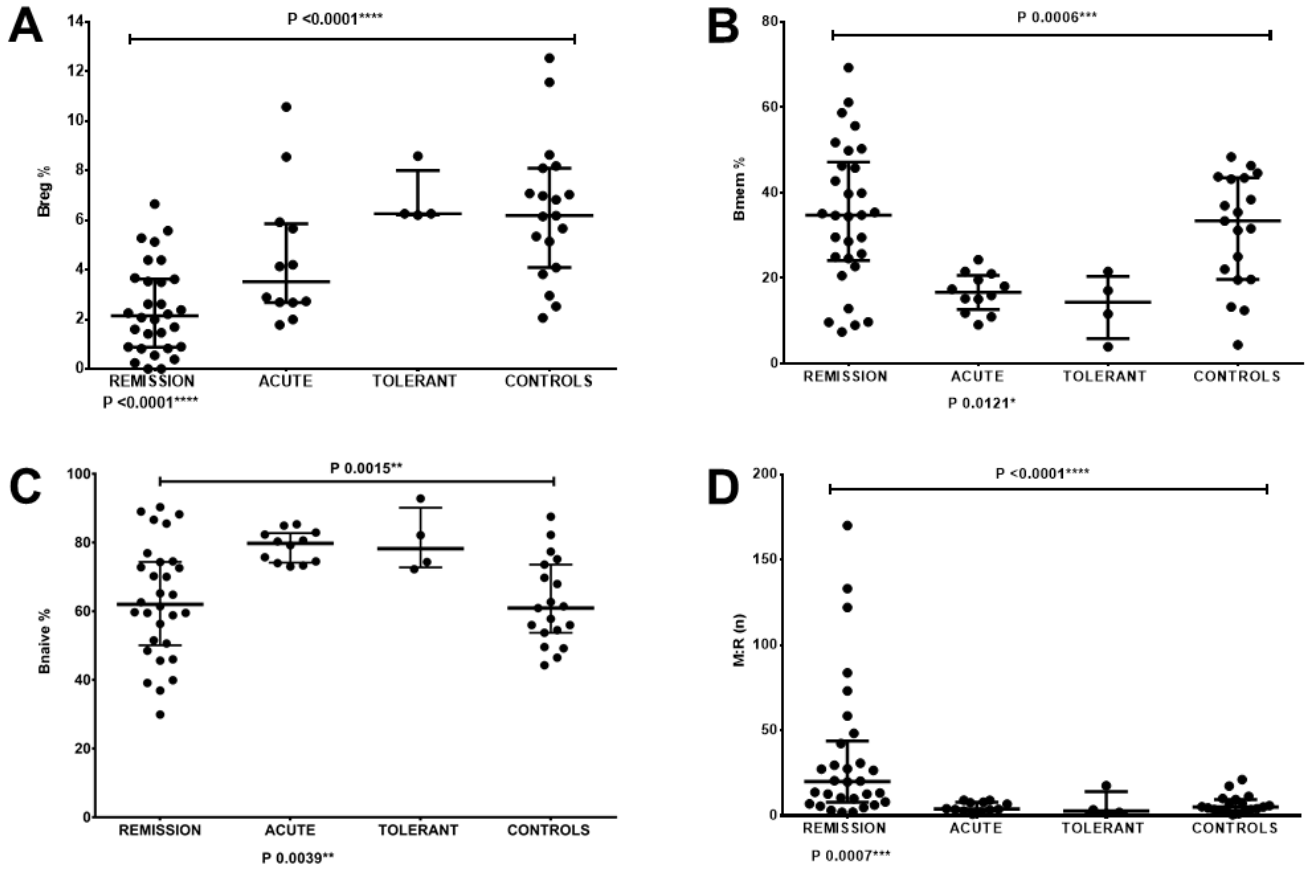

*Kruskal Wallis and Dunn's multiple comparison tests were conducted, to assess whether there was any difference in the patient groups, relative to healthy controls. [A] Breg were significantly reduced in the remission cohort (IQR 0.87-3.63, n=30) compared to healthy controls (IQR 4.09-8.10, n=19, P<0.0001****). [B]Bmem were reduced in acute disease (IQR 12.65-20.68, n=12) relative to healthy controls (IQR 19.71-43.47, n=19, P=0.0121*). Bmem typically rebound in remission (IQR 24.14-47.18), but not in tolerant individuals (IQR 5.87-20.46). [C] Low Breg and Bmem frequency in the acute cohort resulted in significantly higher Bnaive frequency (IQR 74.13-82.75) than healthy controls (IQR 53.73-73.57, P=0.0039**). [D] The imbalance of memory and regulatory cells may predispose to relapse in non-tolerant patients. A ratio was calculated by dividing the number of cells in the Bmem gate by the number in Breg gate (denoted M:Rn).High M:Rn values were only observed in a subset of remission patients (range 2.05-170.00); this group differed significantly from healthy controls (range 0.54-21.16, P=0.0007***)*

Figure 3.5 **Comparison of patients separated according to disease activity and ANCA**

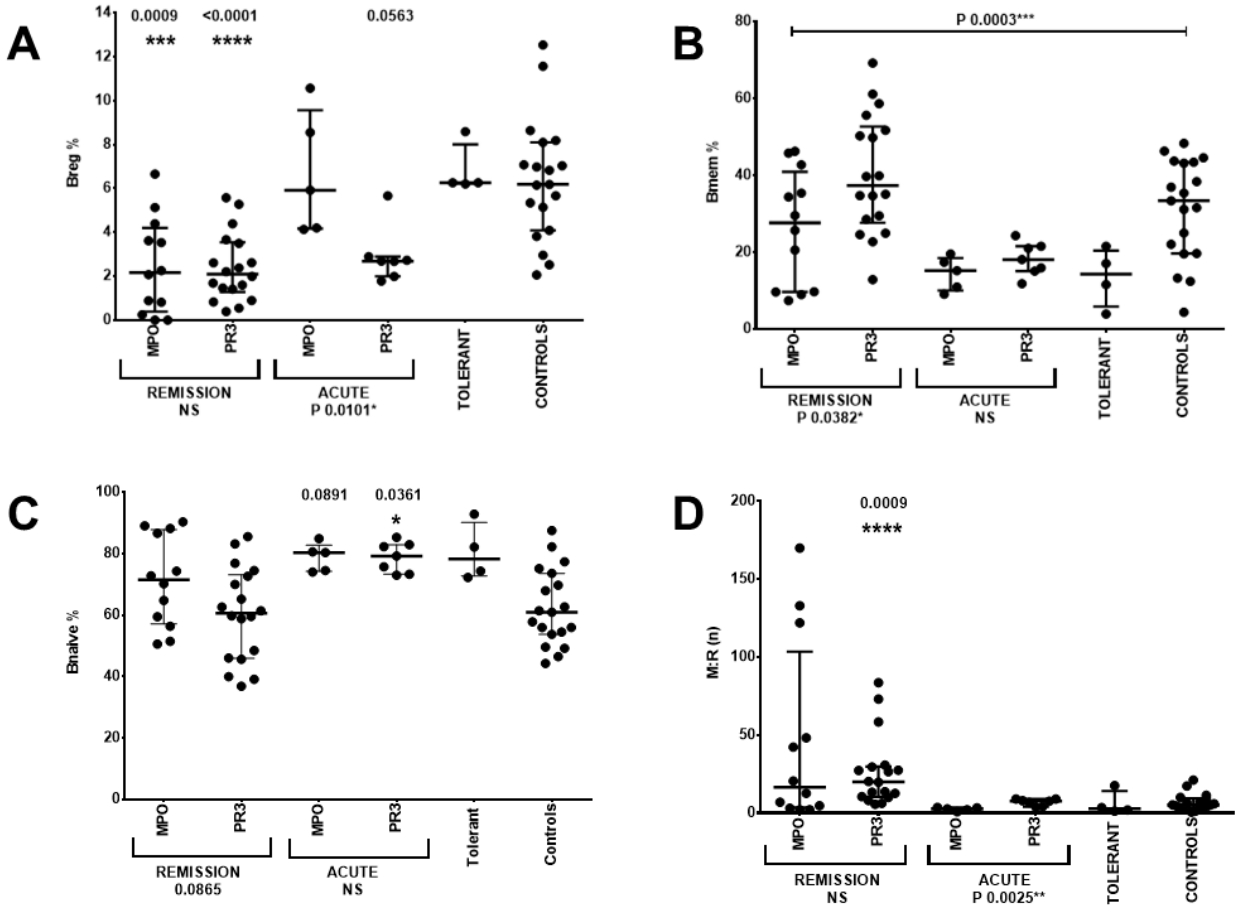

Patient cohorts were further separated according to ANCA specificity, Kruskal Wallis and Dunn's Multiple comparison conducted relative to healthy controls. Mann Whitney test was additionally used to compare remission and acute patients, segregated by ANCA (significance shown below the X-axes). [A] Breg were significantly reduced in MPO-ANCA (n=12) and PR3-ANCA (n=18) remission patients, compared to healthy controls. Acute PR3-ANCA patients tended to have lower Breg (IQR 1.99-2.89, n=7) than healthy controls (IQR 4.09-8.10) and had significantly lower Breg than MPO-ANCA acute patients (IQR 4.17-9.56, n=5, Mann Whitney P=0.0101). [B]Bmem were previously shown to be significantly reduced in acute AAV patient compared to controls. Bmem did not differ between acute patients with MPO-ANCA or PR3-ANCA. Bmem frequency was higher in PR3-ANCA remission patients (IQR 27.69-52.75), compared to MPO-ANCA patients (IQR 9.70-40.93, P0.0382*). This resulted in a trend towards lower Bnaive frequency in PR3-ANCA remission patients [C]. Bnaive frequency did not differ in acute patients with MPO-ANCA or PR3-ANCA. [D] The ratio of memory and regulatory B cells (M:Rn) was significantly higher in PR3-ANCA remission patients than controls (IQR control 2.9-9.4 and PR3 remission IQR 10.4-30.0). PR3-ANCA acute patients also had higher M:Rn than MPO-ANCA acute patients (IQR MPO 1.5-3.5 and PR3 4.1-9.0, Mann Whitney, P0.0025**)*

Figure 3.6 Comparison of B cell profile in tolerant patients and other ANCA negative or untreated individuals

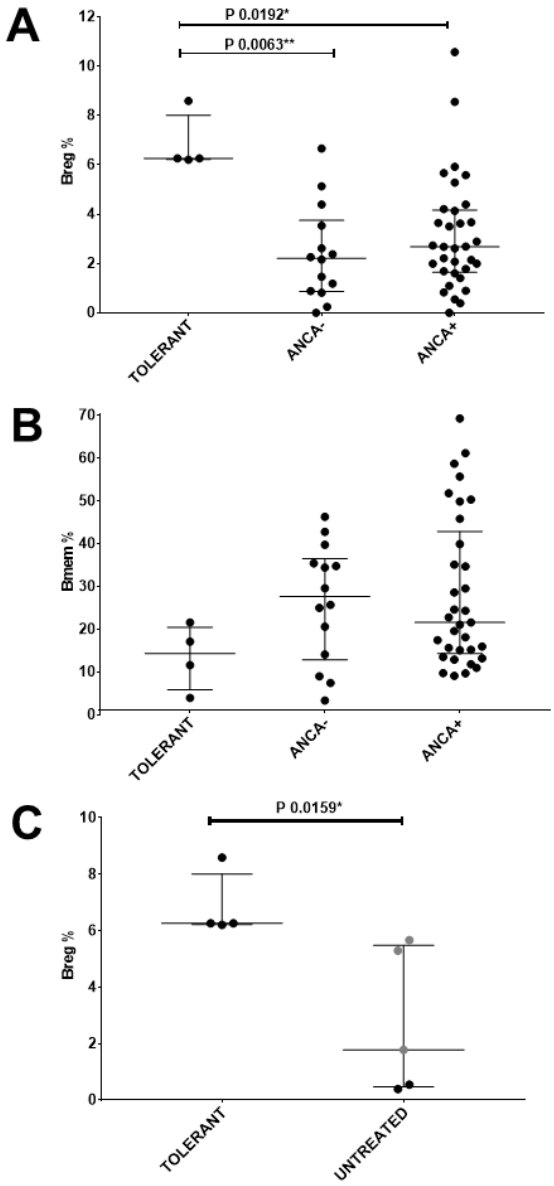

Tolerant patients are ANCA negative and not on any treatment. Breg are significantly increased in tolerance compared to other patients, irrespective of ANCA positivity. Bmem did not differ significantly, when comparator groups were defined by ANCA positivity alone. Breg were higher relative to a limited cohort of 3 acute (grey data points) and 2 remission patients (black data points), not on any treatment [Panel C].

Tolerant patients were also compared to other untreated individuals (Figure 3.6 panel C). Breg were significantly higher in the tolerance cohort compared to other untreated patients (3 acute and 2 remission data points), Mann Whitney P=0.0159*.

3.5.4 Relative B cell frequencies

3.5.4.1 No difference in relative B cell number in the patient groups

In patient samples relative B cell number was calculated from lymphocyte count and frequency of CD19+ lymphocytes on flow cytometry. There was no difference in B cells per litre across the patient groups (Kruskal Wallis test P=0.5689). The IQR overlapped for all groups: remission 0.86-4.82 $x10^7$, acute 1.50-9.30 $x10^7$, tolerant 0.67-7.61 $x10^7$and rituximab treated patients 0.26-6.87 $x10^7$.

3.5.4.2 Breg number lower in remission compared to acute disease

Raw percentages of Bmem, Bnaive and Breg, were then used to determine the number of these B cell subsets per litre of blood. Changes in relative Breg number showed a similar trend to corrected frequency, with fewer Breg per litre in remission (IQR 0.10-1.03 x 10^6), compared to acute disease (IQR 0.36-4.71 x 10^6). On paired analysis remission and acute patients differed significantly (Mann Whitney, P=0.0360*)

3.5.4.3 Breg increased in number in the rituximab treated group

When 4-way analysis was conducted for tolerance, remission, acute and rituximab-treated patient groups (Kruskal Wallis and Dunn's multiple comparison, with all groups compared relative to one another), the only significant result was an increased number of Breg in the rituximab cohort, relative to the main remission cohort (Figure 3.7, P=0.0041**).

Figure 3.7 Comparison of relative cell numbers for patients separated according to disease activity

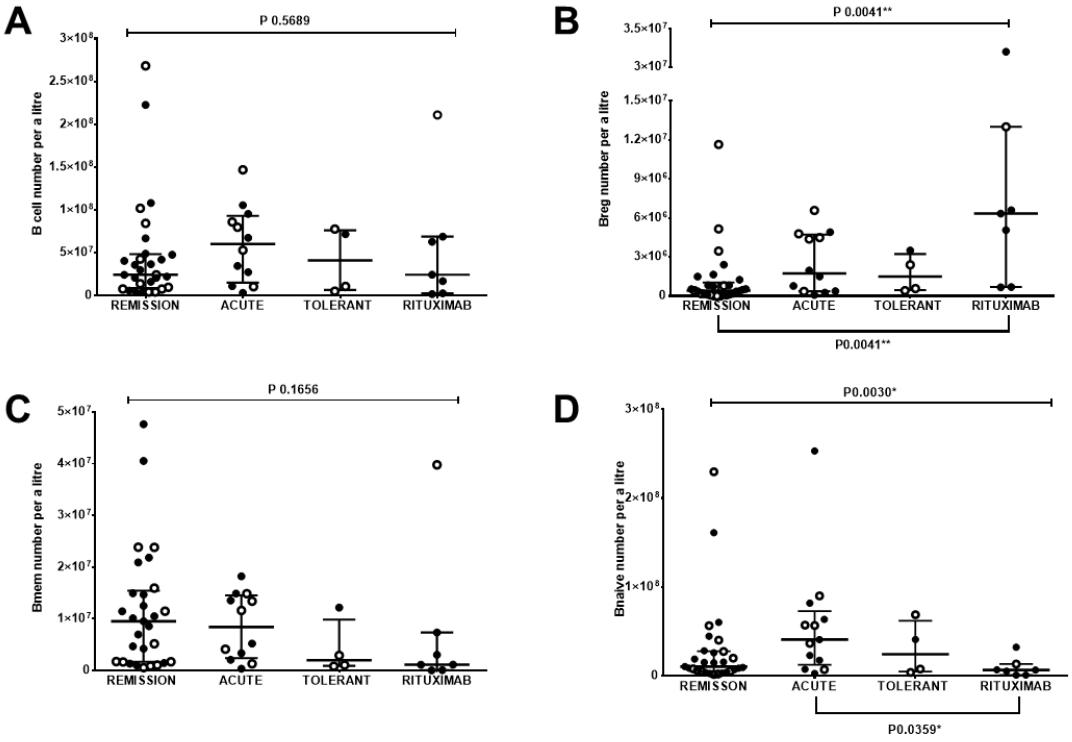

MPO-ANCA patients are shown with unfilled data points, PR3-ANCA patients with data points filled in black. Breg and Bnaive relative number differed significantly across the patient groups, total B cell number and relative Bmem number did not. When Dunn's Multiple comparison was conducted across all groups, rituximab patients had significantly higher Breg number and significantly lower Bnaive number, than remission patients and acute patients respectively.

3.5.4.4 Breg number lower in acute PR3-ANCA AAV

Breg numbers were also lower in acute PR3-ANCA (IQR 0.26-1.96 x 10^6) compared with acute MPO-ANCA (IQR 2.37-5.68 x 10^6) but this did not reach statistical significance.

3.5.4.5 Highest Bmem numbers observed in remission

There was no significant difference in relative Bmem number when patients were compared however, the highest Bmem numbers were still observed in remission. The distribution pattern was normal in acute disease and positively skewed in remission (skewness 1.711, D'Agostino and Pearson test P=0.0003).

Overall the trends in B cell subsets were similar for relative counts; the data was spread over a much greater range than percentage frequency (0-300,000,000), so it is not surprising that statistical significance was not reached.

3.5.5 Effects of rituximab on B cell subsets

Flow cytometry plots before and after rituximab illustrate the profound changes that occur within the B cell populations (Figure 3.8, panel A). The reduction in Bmem and increase in Breg were statistically significant compared with controls (Figure 3.8, Panel B). The median time from treatment with rituximab was 16 months, range 0.5-7 years (Table 3.3). Effects were sometimes long-lasting, with increased Breg frequency observed in one patient 5 years after rituximab treatment, longer than previously reported (Palanichamy, Barnard et al. 2009). Indeed, rituximab seems to be particularly efficacious in AAV, with clinical approval, whilst use remains off-label for SLE. At the point of sampling, relative B cell number in rituximab treated patients did not differ significantly from other patient groups (Figure 3.7, Panel A).

Figure 3.8 Effects of rituximab on B cell profile, paired analysis and comparison to healthy controls

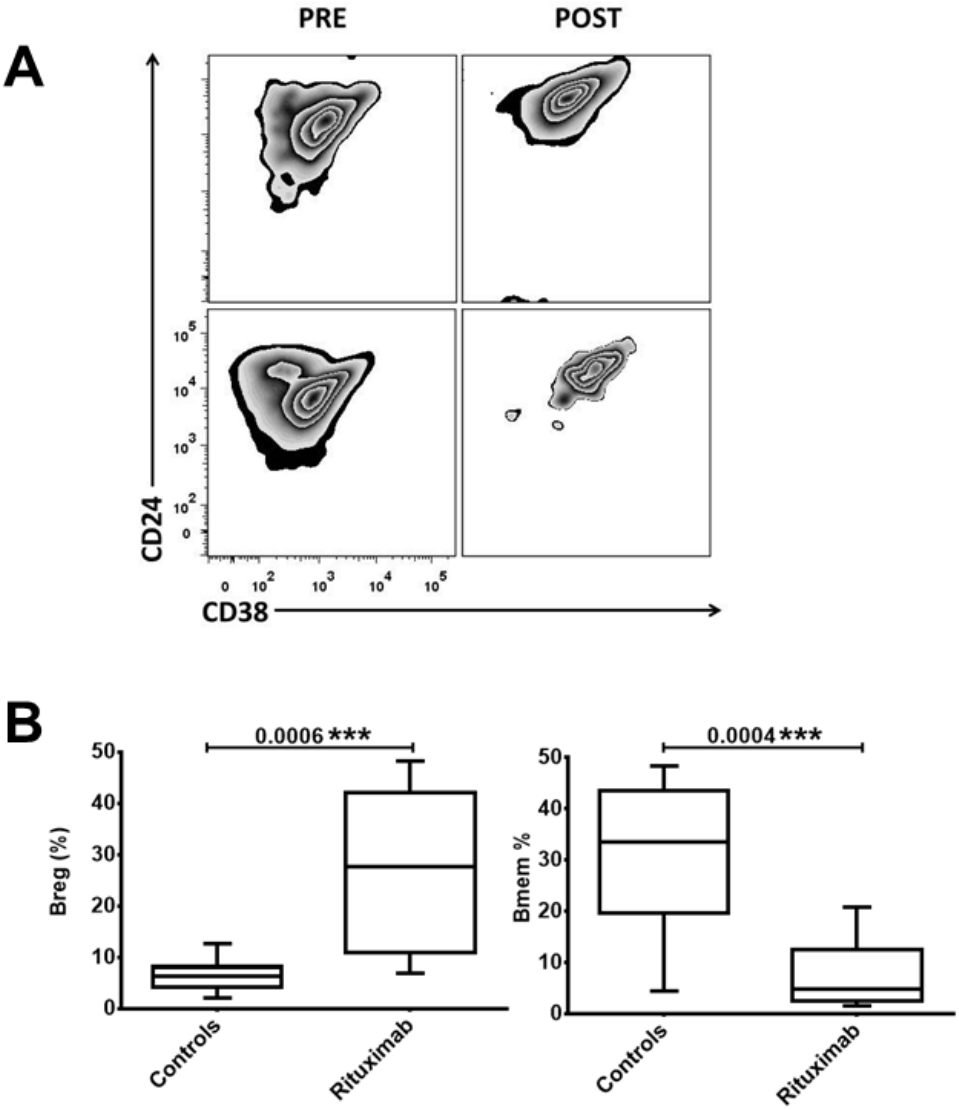

Flow cytometry plots from 2 patients before (left hand side) and after rituximab treatment (right hand side). After B cell repopulation most B cells have a regulatory phenotype ($CD24^{hi}$ $CD38^{hi}$). Rituximab treated patients have statistically lower frequency of Bmem (P=0.0004) and higher frequency of Breg (P=0.0006) than controls (n=19); Mann Whitney U test. Box and whiskers plots show minimum and maximum values, rituximab data points also provided in Table 3.3 *(n=7).*

Table 3.3 **B cell subsets following rituximab therapy**

Age	Sex	ANCA	Time Since RTX	CD19 %	Bmem %	Breg %	M:R_n
48	F	PR3	1.2	0.359	2.6	27.7	0.092
34	M	PR3	0.6	0.095	1.5	42.0	0.036
71	M	PR3	5	1.75	4.7	27.5	0.171
65	M	PR3	1.2	4.2	6.9	31.0	0.223
47	M	PR3	8	4.61	12.6	10.9	1.161
52	F	PR3	1	5.77	4.6	48.2	0.095
16	F	MPO	7	7.89	20.8	6.8	3.052

Time since last rituximab (RTX) infusion shown in years, median 16 months. CD19 percentage corresponds to frequency of B cells within the lymphocyte gate. Bmem and Breg shown as corrected percentages, M:R_n calculated as previously described.

3.5.6 Outcome data

At the time of publishing, 12-month clinical follow up was available for a subset of remission patients (Todd, Pepper et al. 2014). Bmem frequency was significantly higher and Breg tended to be lower in relapsing PR3-ANCA patients (n=3), relative to non-relapsing PR3-ANCA patients (n=6, non-overlapping IQR).

More relapses were subsequently recorded within the remission cohort (2 MPO-ANCA and 5 PR3-ANCA in total); 12-month data available for 25 out of 30 patients, with 5 lost to follow-up, due to moving away or death. M:Rn tended to be higher in PR3-ANCA relapsing patients (IQR 21.14-65.78, n=5), compared to non-relapsing PR3-ANCA patients (IQR 10.27-29.14, n=9), but this did not reach statistical significance (P=0.1898). One of the patients who did not relapse had a high M:Rn of 84 and persistently high ANCA titre (129 at time point zero and 77 at 12 months), when this data point was removed from the analysis the P value was reduced to 0.0653 (data point shown in red in Figure 3.9, Panel A). High M:Rn, may therefore reflect general state of B cell activation. Bmem cells have a lower threshold of activation than naïve cells and can readily differentiate in plasmablasts, producing immunoglobulin. A larger data series, with longitudinal measurements would be required to resolve the effect of B cell subsets in determining clinical outcome and persistence of ANCA.

There was no difference in Bmem with the additional data points, IQRs were 26.56-50.81 and 25.03-55.73 respectively (Mann Whitney P=0.8512, Figure 3.9, Panel B). Breg frequency still tended to lower in relapsing patients (IQR 0.467-2.150), compared to non-relapsing PR3-ANCA patients (IQR 1.179-3.584) but did not reach statistical significance (Mann Whitney P=0.1119, Figure 3.9, Panel C). This was a relatively small data set, with outcome data recorded up to 12 months.

With a larger cohort, longer follow-up and longitudinal measurements, predictive value of B cell immunophenotyping in AAV, would be more robustly assessed. This is certainly warranted. B cells are linked to operation tolerance in renal allograft recipients and associated with improved survival in haemodialysis patients (Newell, Asare et al. 2010, Molina, Allende et al. 2018). In AAV, Bunch *et al* found that frequency of CD5 B cells, a putative immunoregulatory subset, predicted clinical outcome after rituximab treatment (Bunch, McGregor et al. 2013). Land *et al* assessed B cells in 84 GPA patients, presenting data from 13 individuals who went on to relapse, with 13 age and sex-matched matched non-relapsing patients (Land, Abdulahad et al. 2016). Consecutive samples were available for 11 patients, IL-10 producing B cells were significantly reduced at relapse compared to baseline. However, B cell subsets at initial sampling were not predictive of relapse in the 13 paired samples (Breg, CD5+, CD38high CD27+). Why might this be? Firstly, time to relapse varied from 14-157 days after initial sampling; those with shortest times to relapse may have already had some immunological changes related to active disease. Current immunotherapy was specified, but history of B cell depletion was not listed as an exclusion criterion. Disease activity was not clearly specified, 5 individuals out of 26 were reported to have severe disease at the time of sampling and ANCA titre, exceeded 640 in some instances. In one individual with persistently high ANCA titre, I observed high M:Rn. Prediction of relapse would likely be more accurate, with serial measurement of multiple cellular, serological and urinary biomarkers: Breg, ANCA, urinary MCP-1 and soluble CD163, for example (Tervaert, Elema et al. 1990, Han, Choi et al. 2003, Moran, Monach et al. 2018).

Figure 3.9 Relapsing and non-relapsing PR3-ANCA patients

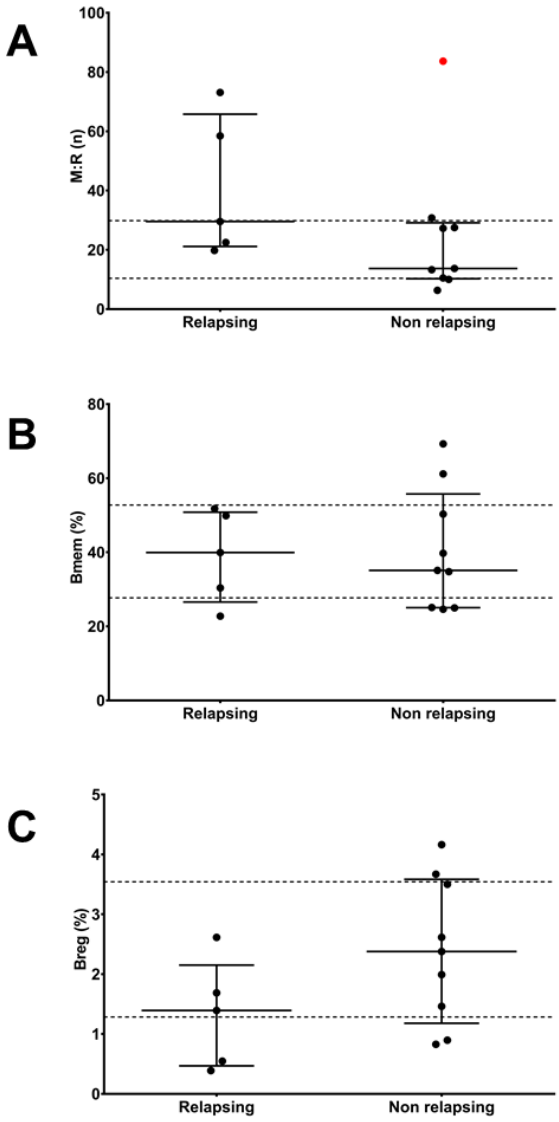

Graphs show PR3-ANCA patients who went on to relapse in 12 months after B cell phenotyping, relative to those who did not. Dashed lines represent IQR of the main PR3-ANCA remission cohort (n=18, 25th and 75th percentile values show). Relapsing patients tend to have lower Breg and higher M:Rn, with similar Bmem frequency. One patient who did not go on to relapse had very high M:Rn, shown in red in Panel A. This individual had persistency high ANCA titre, 129 baseline and 77 at 12 months.

3.6 Key findings

3.6.1 B cell subsets are altered in AAV and differ according to disease activity

In a larger mixed cohort of 61 patients, frequency of Breg and Bmem was reduced, whilst Bnaive were increased relative to healthy controls (n=19). When separated according to disease activity, Bmem were low in active disease but rebounded in remission, whilst Breg did not. Breg did not differ in the tolerant cohort relative to healthy controls, whilst Bmem remained low. Imbalance in regulatory and effector B cells in remission, may predispose a subset of patients to relapse.

3.6.2 Frequency of B cell subsets differs according to ANCA specificity

When patients were separated according to disease activity and ANCA, remission patients had low Breg irrespective of ANCA specificity. Acute PR3-ANCA patients had reduced Breg, whilst acute MPO-ANCA patients did not. PR3-ANCA patients have the greatest propensity to relapse. Interestingly, Bmem cells were significantly higher in PR3-ANCA remission patients compared to MPO-ANCA remission patients and M:Rn, was significantly higher in acute PR3-ANCA patients relative to MPO-ANCA acute patients.

3.6.3 B cell changes after rituximab treatment

B cell changes after rituximab therapy are profound and long-lasting. This may represent a tolerogenic state, explaining why this treatment is particularly efficacious in AAV.

3.7 Discussion

3.7.1 Rationale for CD24 CD38 gating strategy

At the time of undertaking this study there was emerging evidence that several B cell subsets could limit inflammation. This function was attributed to CD5+, CD25+ CD27+ and $CD24^{high}$B cells; the relationship and overlap between these cells was not established. Reported mechanisms of action included: negative regulation of BCR signalling, preferential release of the immunomodulatory cytokine IL-10, inhibition of CD4 responses, suppression of monocyte TNFα production, induction of FoxP3 and CTLA4 expression in Treg (Hippen, Tze et al. 2000, Gary-Gouy, Harriague et al. 2002, Brisslert, Bokarewa et al. 2006, Blair, Norena et al. 2010, Iwata, Matsushita et al. 2011, Kessel, Haj et al. 2012).

The surface phenotype $CD24^{high}$ CD27+ was assigned to IL-10+ cells, after stimulation. Subsequently cells were isolated on the expression of these markers; a higher proportion of $CD24^{high}$ CD27+ B cells produced IL-10, compared to $CD24^{low}$ CD27- B cells. $CD24^{high}$ CD27+ B cells limited monocyte TNFα production in an IL-10 dependent manner, whist effect of $CD24^{low}$ CD27- B cells on monocytes varied. Both cell subsets could limit T cell TNFα production, independently of IL-10. Interestingly, the phenotype of IL-10 competent B cells was not uniform, with mixed IgM expression at 5 hours (Iwata, Matsushita et al. 2011).

Blair *et al* classified Breg based on high surface expression of CD24 and CD38 (Blair, Chavez-Rueda et al. 2009). These cells were immature and expressed high levels of IgM and IgD. Breg were increased in frequency but not absolute number in SLE. Critically this study was the first to show a functional defect in autoimmunity, with reduced ability to limit Th1 differentiation in lupus patients, compared to controls. The

suppression of Th1 cytokine production was dose-dependent and inferred to be antigen specific, as it was lessened upon blockade of CD80 and CD86 (costimulatory ligands for CD4 T cells). SLE like AAV, is a systemic autoimmune disease, defined by the presence of pathological antibodies and often presenting with glomerulonephritis.

The ability to limit T cell antigen dependent response and, proven defect in a similar pathology, provided very good rationale for using this classification criteria to define B regulatory in AAV. Furthermore, CD24 and CD38 immunolabelling enables three B cell subsets to be defined, permitting the total balance of peripheral blood B cells to be assessed simultaneously.

3.7.2 Cumulative evidence for an imbalance in B cell subsets in AAV

3.7.2.1 Historic evidence

At the point of commencing this study relatively little was known about the balance of peripheral B cell subsets in AAV. In GPA patients, transitional Bm2' ($CD38^{high}$ IgD+) cells had been shown to be reduced in active disease, with an inverse relationship with PR3-ANCA and BVAS (Eriksson, Sandell et al. 2010). Bm3/4 memory cells (IgD– $CD38^{high}$ 27+) were also reduced in active disease. These results are concordant with the data presented in this chapter, with low $CD38^{high}$ $CD24^{high}$ B cells in acute PR3-ANCA patients and reduction in Bmem in acute disease, rebounding on induction of remission. I additionally found $CD38^{high}$ $CD24^{high}$ B cells to be reduced in clinical remission.

In the same study, CD25+ B cells were increased in remission compared to controls, predominantly CD27+ and proposed to be immunoregulatory. This subset of CD25+

CD27+ B cells was previously shown to produce more of the key immunoregulatory cytokine IL-10 and, less IL-2 than other B cell subsets (Amu, Tarkowski et al. 2007).

CD27+ CD5+ B cells were also shown to be diminished and may correspond to an immunoregulatory subset (Eriksson, Sandell et al. 2010). CD27+ $CD24^{high}$ B cells limit monocyte TNFα production (Iwata, Matsushita et al. 2011) and CD5+ B cells are enriched for IL-10 competency (Gary-Gouy, Harriague et al. 2002). However, the increase in CD5 and CD25 B cells in GPA might equally correspond with the cell activation; indeed CD86+ B cells were also increased (Eriksson, Sandell et al. 2010).

In both SLE and AAV, a CD19 high B cell population is described (Culton, Nicholas et al. 2007). These cells were further characterised as somatically mutated memory B cells, without any BCR bias (variable CDR3 length and V_H chain use); they were deemed to be activated, due to large size, increased granularity and high expression of CD86 and MHC Class II. Although some mechanisms are common to both SLE and AAV, TLR-9 upregulation is observed in the former but not the latter (Papadimitraki, Choulaki et al. 2006, Tadema, Abdulahad et al. 2011).

Popa *et al* observe an increase in $CD38^{high}$ B cells in GPA, which they also infer was due to cell activation. These cells might also correspond to circulating plasmablasts, as they were seemingly absent in healthy controls (Popa, Stegeman et al. 1999).

3.7.2.2 New evidence

CD5 was suggested as a surrogate marker for Breg, with correlation shown (Bunch, McGregor et al. 2013). In a mixed cohort of 54 patients, CD5 B cells were shown to be lower in active disease and restored in remission. In rituximab-treated patients with more than 30% CD5 B cells on repopulation and low dose maintenance immunosuppression, relapse was significantly reduced, both total time and months

after B cell repopulation. These findings were verified in a larger cohort of 50 rituximab treated patients (Bunch, Mendoza et al. 2015). They subsequently showed no difference in Breg frequency in different disease states, only the CD5 fraction therein (Aybar, McGregor et al. 2015). In the last study, rituximab treated patients were not analysed separately, controls were not age-matched to remission or active disease groups.

CD5 B cell frequency may only predict outcome in rituximab treated patients (Unizony, Lim et al. 2015). Serial analysis was conducted in the RAVE cohort, 197 patients randomized to receive either rituximab or cyclophosphamide and azathioprine. CD5 frequency was reduced at disease onset and progressively increased in the rituximab cohort but remained low in the control arm.

Land *et al* also looked at B cell subset in 13 relapsing and 13 non-relapsing GPA patients; frequency of transitional, naïve and memory B cells were determined, and 3 cell surface phenotypes associated with immunoregulatory B cells defined (CD5+, $CD24^{high}$ CD27+ and $CD24^{high}$ $CD38^{high}$). No B cell subsets were predictive of relapse. Patients had significantly lower memory B cells (CD27+), CD24high CD27+ B cells and higher frequency of naïve B cells (CD38+ CD27-), relative to controls (Land, Abdulahad et al. 2016). The ratio of memory and regulatory B cells was not calculated in this study.

Thiel *et al* extensively characterised B cells subsets in a mixed cohort of GPA (n=38), MPA (n=7) and EGPA (n=16) patients (Thiel, Salzer et al. 2013). Treatment resulted in a generalised B cell lymphopenia. Percentage of transitional B cells tended to lower in patients than controls (defined as $CD27^{-}$ $CD10^{+}$ $CD38^{+}$ IgM^{high} IgD^{high}).

Relative frequencies were not presented but the numbers of plasmablasts were increased in AAV ($CD19^{+}$ $CD20^{-}$ $CD38^{high}$ $IgM^{-/low}$), whilst naïve and memory B cells were reduced. Marginal zone B cells (IgD^{+} IgM^{high} $CD27^{+}$), memory B cells and plasmablasts correlated with plasma concentrations of immunoglobulin. In 25% of patients, CD21 low B cells were increased in number (marker of age-related B cells, linked to chronic inflammation).

Lepse *et al* characterised frequency of B cell subsets in a mixed AAV cohort, composed predominately of GPA patients (94%) (Lepse, Abdulahad et al. 2014). Bmem (CD27+) were reduced irrespective of disease activity and naïve B cell increased. Transitional B cells (CD27- $CD24^{high}$ $CD38^{high}$) and Breg were reduced in active disease, but not remission. The CD27+ $CD24^{high}$ population was reduced in both active and remission (more profoundly than the CD27+ parent population). Frequency of Breg, transitional and CD27+ $CD24^{high}$ B cells were not affected by treatment (67% not on any therapy).

In another publication, immunoregulatory B cells were defined based on induction of IL-10 (Wilde, Thewissen et al. 2013). The cohort were predominantly PR3-ANCA positive (78%). IL-10 B cells were diminished in remission and active disease, independent of treatment (54% not on any therapy). These authors subsequently demonstrated that granzyme B positive B cells are also diminished in AAV (Wilde, Jiqiao et al. 2016).

In summary, B cells have an activated phenotype in AAV, with increased frequency of $CD21^{low}$ cells, high expression of CD19, CD86, CD25, CD38, CD5 and MHC CII (Popa, Stegeman et al. 1999, Culton, Nicholas et al. 2007, Eriksson, Sandell et al. 2010, Thiel, Salzer et al. 2013). Despite differences in the classification strategies

used, there is convincing evidence that Breg are reduced in active GPA (Table 3.2 and Figure 3.5). Bmem are also reduced and this is concomitant with an increase in naïve B cells. The evidence is less clear for remission and MPA patients. Aybar *et al* report no difference in Breg, only the frequency of CD5+ cells therein (Aybar, McGregor et al. 2015). The other studies prior to this, have relatively few MPA patients included, due to the predominance of GPA in Northern Europe. The proporportions of patients on treatment, with localised or systemic disease, also differs across the various remission cohorts.

The case series presented here, were recruted from a renal unit and were more likely to have glomerulonephritis (opposed to a mixed specality or rheumatology clinic). It is unclear what affect uraemia might have on B cell subsets. Blair *et al* described increased frequency of Breg in SLE but Heinemann *et al* subsequently discovered a reduction in IL-10 competent B cells in SLE, which was particulary profound in patients with lupus nephritis (Blair, Norena et al. 2010, Heinemann, Wilde et al. 2016).

Breg are reduced and Bmem increased in patients with ESRF prior to commencing haemodialysis and restored afterwards (Kim, Chung et al. 2012); furthermore higher B cell number, is associated with better renal function and lower mortality in Chronic Kidney Disease (Xiang, Zhu et al. 2016, Molina, Allende et al. 2018).

MPO-ANCA patients are more likely to present with renal manifestations and had significantly lower Breg in remission in this cohort (compared to controls). Creatinine was recorded but eGFR was not calculated. Lymphocyte count had a negative correlation with creatinine (P=0.0033**), there was no relationship with B cell subsets. Outlying data points were removed, with creatinine greater than 500µmol/litre (analysis conducted for 52 out of 55, refined cohort Table 3.1).

Table 3.4 Evidence for reduced frequency of regulatory B cells in AAV

Phenotype	Author	Key findings
Transitional	*Thiel*	**Tendency to be reduced (MPA 7, GPA 38, EGPA 16)**
Bm2'	*Erikkson*	**Reduced in active AAV (MPA 4, GPA 16)**
$CD24^{high}$ $CD38^{high}$	*Todd*	**Reduced in AAV (MPA 29, GPA 17)**
	Lepse	**Low in active AAV (MPA 3, GPA 45)**
	Land	**No difference, 13 relapsing and non-relapsing GPA**
	Aybar	**No difference, only CD5+ subset (MPA 31, GPA 23)**
$CD24^{high}$ CD27+	*Land*	**Lower in GPA patients than controls**
	Lepse	**Reduced in active and remission**
CD25+	*Erikkson*	**Increased in remission compared to controls**
CD5+	*Bunch*	**Low in active disease (MPA 18, GPA 18)**
	Unizony	**CD5 reduced, remain low with conventional treatment but not rituximab (MPA 48, GPA 151)**
CD27+ CD5+	*Eriksson*	**Diminished in AAV**
IL-10 competent	*Wilde*	**Diminished in AAV (9 MPO-ANCA, 32 PR3-ANCA)**
Granzyme B	*Wilde*	**Diminished in AAV (19 AAV patients, diagnosis nor ANCA specificity provided in meeting abstract)**

Various B cell classification strategies have been employed in AAV. The evidence for a reduction in regulatory B cells in systemic disease is convincing, whether classified as IL-10 competent, CD5+, $CD24^{high}$ $CD38^{high}$ or $CD24^{high}$ CD27+. Frequency has now been in assessed in more than 500 individuals, with data presented in nine peer-reviewed journals and 1 meeting abstract.

3.7.2.3 Breg imbalance in other multiple autoimmune conditions

In this study a numerical defect in Breg was demonstrated in AAV, previously Breg were shown to be increased in frequency in SLE but dysfunctional. Further defects in Breg cells have since been characterised in SLE (Bosma, Abdel-Gadir et al. 2012, Menon, Blair et al. 2016). $CD24^{high}$ $CD38^{high}$ B cells have also been shown to be numerically or functionally disturbed in other autoimmune conditions (recently reviewed by Mauri and Menon 2017, Sakkas, Daoussis et al. 2018).

Breg are reduced in frequency in dermatomyositis, ulcerative colitis, rheumatoid arthritis (RA), multiple sclerosis and immune thrombocytopenia (ITP) (Li, Zhong et al. 2012, Flores-Borja, Bosma et al. 2013, Wang, Zhu et al. 2016, Kim, Kim et al. 2018). In RA Breg are impaired in their ability to limit Th17 differentiation and induce Treg and in ITP, they are defective at limiting monocyte TNFα production. In ankylosing spondylitis, Sjögren's syndrome and pemphigus, Breg are increased in frequency but have reduced IL-10 production, impaired ability to suppress CD8 T cells and limit Th1 differentiation of CD4+ CD25- T cells.

The evidence for a role of $CD24^{high}$ $CD38^{high}$ in pathogenesis of autoimmunity is compelling. However, it is also becoming clear that regulatory function does not reside in a single B cell type (Mauri and Menon 2015). In the next chapter, I verify that CD24 and CD38 staining is stable and cell subsets are phenotypically unique, before proceeding to functional characterisation in patients and controls. This functional testing is of paramount importance, as there is no one definitive marker for regulatory B cells. Furthermore, numerical and functional abnormalities can co-exist in immunopathology.

3.7.3 Discussion of treatment effects

3.7.3.1 A limitation of this study

It is hard to control for treatment effects, in a chronic, debilitating disease like AAV. Prior to the introduction of cyclophosphamide, disease resulted in almost 90% mortality at one year (Fauci, Katz et al. 1979). With current treatment protocols, survival rate is 88% at 1 year, with 20% of deaths attributed to active disease (Flossmann, Berden et al. 2011). Relapse occurs in 34% of patients, with a median time of 13 months, from remission induction (Booth, Almond et al. 2003). Disease may follow a progressive course, necessitating renal replacement therapy in 30% of cases (Little, Nazar et al. 2004). It is therefore not surprising that there were only 9 patients receiving no treatment at the time of sampling, 4 tolerant, 3 acute and 2 remission patients. Breg were still significantly higher in the tolerant group, compared to other untreated patients (Figure 3.6). Frequency of Breg, Bmem and Bnaive cells did not correlate with generalised lymphopenia when regression analysis was performed, nor was there any difference in lymphocyte count between the patient groups (Table 3.1).

Acute patients had minimal cumulative burden of immunosuppression, testing conducted within 17 days of initial presentation (Table 3.2). Breg and Bmem frequencies were not discordant in patients with grumbling disease, despite significantly higher BVAS, ANCA titre and serum creatinine in the acute cohort. .Differences were additionally resolved in patients with the same disease activity, when separated according to ANCA (higher Bmem in PR3-ANCA remission patients, lower Breg in MPO-ANCA acute disease). These patients have similar disease duration and immunosuppressive regimen.

Other studies in AAV have included more untreated patients. Breg, memory, naïve or transitional B cells did not differ in a cohort of 14 treated and 34 untreated AAV patients, predominately with GPA diagnosis (Lepse, Abdulahad et al. 2013). Reduction in $CD24^{high}$ $CD27^{high}$ cells in GPA, was not affected by treatment (Lepse, Abdulahad et al. 2013, Land, Abdulahad et al. 2016). Reduction IL-10 B cells was observed in active and remission AAV, irrespective of whether patients were on immunosuppression or not (20 untreated and 21 treated) (Wilde, Thewissen et al. 2013).

Unizony *et al* report that low CD5 count may predict outcome in rituximab treated individuals, but not in patients receiving conventional treatment. CD5 B cells are ablated and remain low after induction with cyclophosphamide and methylprednisolone (Unizony, Lim et al. 2015). The Chapel Hill group have shown correlation between CD5+ B cells and Breg (Bunch, McGregor et al. 2013). With this in-mind, I assessed frequency CD5+ B cells in parallel testing (presented in the next chapter).

Thiel *et al* reported specifically on the effects of immunomodulatory treatment on B cell subsets (Thiel, Salzer et al. 2013). Transitional B cells, defined as CD27- CD10+ $CD38+IgM^{high}$ IgD^{high} were significantly reduced in number irrespective of prior cyclophosphamide treatment. This was accompanied by deficiency in other B cell subsets and a generalised B cell lymphopenia, making it difficult to interpret the importance of this finding (relative frequencies were calculated but not reported).

Breg frequency is reported to be reduced in rheumatoid arthritis and most profoundly in active disease; this difference was maintained, when patients were segregated according to disease activity and treatment. Specifically, significance was retained for

untreated patients (n=15), those on steroid treatment (n=20), methotrexate treatment (n=76) and for patients on biological therapy (n=44) (Flores-Borja, Bosma et al. 2013).

To further resolve the effects of treatment on B cell subsets a very large cohort or longitudinal study would be required. The latter would permit patients to be monitored during transition in disease activity, when treatment is changed or withdrawn. This might now be possible for steroids, with a move towards steroid sparing treatment regimens and tapering doses (Kondo and Amano 2018). It would still be incredibly challenging, because the effects of rituximab on B cell subsets are profound and its use, is now much more common in clinic for both induction and maintenance regimens.

3.7.3.2 Role of rituximab in AAV

Rituximab has been approved by The US Food and Drug Administration (FDA) and the European Medicines Agency (EMEA) for treatment of AAV. It has been shown to induce clinical remission with similar efficacy to the standard induction regimen of cyclophosphamide in AAV (Jones, Tervaert et al. 2010, Stone, Merkel et al. 2010). Compared to azathioprine, disease-free and overall survival is superior (Terrier, Pagnoux et al. 2018); likelihood of progression to ESRF is also reduced (McAdoo, Medjeral-Thomas et al. 2018). Following treatment, the number of CD19 B cells and ANCA titre do not predict prognosis (Roubaud-Baudron, Pagnoux et al. 2012).

The exact mechanism of rituximab action is not fully elucidated, plasma cells downmodulate CD20 and are therefore not directly targeted. Despite this, hypogammaglobinaemia often ensues rituximab treatment in AAV patients and is particularly profound in patients that have had historic treatment with cyclophosphamide (Venhoff, Effelsberg et al. 2012). Low Ig levels and delayed B cell

reconstitution (up to 44 months), was exclusively observed in AAV, not rituximab treated patients with rheumatoid arthritis or other connective tissue tissues (Thiel, Rizzi et al. 2017).

The overall balance of B cells is likely to be important in determining outcome. In a letter, Benjamin Wilde suggested measuring proinflammatory and inflammatory cytokines to predict outcome after rituximab; preliminary data showed imbalance in Th17 and IL-10 competent lymphocytes (Wilde, Witzke et al. 2014). In mice, rituximab ameliorates EAE by depletion of IL-6 competent B cells (Barr, Shen et al. 2012), a critical cytokine for induction of Th17 cells. Interestingly, Breg were subsequently shown to limit Th17 differentiation in man (Flores-Borja, Bosma et al. 2013). In an abstract presented at The Annual European Congress of Rheumatology, Breg are reported to negatively correlate with Th17 cells in AAV (Borstel, Lintermans et al. 2018).

I report low Bmem and increased ratio of Breg in rituximab treated patients in remission, also observed in tolerant individuals (represented as a ratio, M:Rn). This is likely to confer good prognosis. Venhoff *et al* report a lower proportion of naïve B cells (IgD^{high} IgM+ CD27-) and higher frequency of switched memory B cells (IgD- IgM- CD27+) in AAV patients who go on to relapse after rituximab (Venhoff, Niessen et al. 2014). High transitional B cells and low memory B cells at reconstitution, decrease likelihood of relapse in rheumatoid arthritis, partly because switched memory B cells preferentially produce the proinflammatory cytokine TNFα over IL-10 (Adlowitz, Barnard et al. 2015). Breg cells were previously shown to be enriched for IL-10 competency and to limit CD4 cell responses (Blair, Norena et al. 2010, Bouaziz, Calbo et al. 2010). Low CD5 frequency after B cell repopulation has also

been linked to relapse in rituximab treated AAV patients, a cell population also enriched for IL-10 competency (Gary-Gouy, Harriague et al. 2002, Bunch, McGregor et al. 2013, Aybar, McGregor et al. 2015). However, CD5 frequency was not predictive of clinical outcome in the RAVE cohort (NCT00748644 (Unizony, Lim et al. 2015)).

Efficacy of rituximab treatment is also adversely affected by high CD95 B cell frequency prior to commencing treatment and persistence of a Ki67 positive memory B cell population after treatment (Adlowitz, Barnard et al. 2015).

Rituximab may also affect the balance of GM-CSF and SDF-1 B cells, resulting in a reduction in circulating neutrophils and myeloid cells (Dunleavy, Hakim et al. 2005, Li, Rezk et al. 2015).

3.7.3.3 Alemtuzumab can also alter the balance of B cell subsets

Altered balance in transitional and memory B cell subsets is associated with relapse in MS (Knippenberg, Peelen et al. 2011). Alemtuzumab (anti-CD52), has also been shown to favourably alter the proportion of memory and immature B cells in multiple sclerosis and renal transplantation (Thompson, Jones et al. 2010, Heidt, Hester et al. 2012, Kim, Kim et al. 2018). Whilst B memory cells express the highest levels of CD52, alemtuzumab broadly depletes lymphoid and myeloid cells (Rao, Sancho et al. 2012). Alemtuzumab was associated with a high rate of relapse and adverse events in AAV (infection, malignancy and thyroid disease) (Walsh, Chaudhry et al. 2008). Rituximab is a more selective therapy, inducing a prolonged change in the balance of peripheral B cell subsets in AAV, which may represent a tolerogenic state.

Chapter 4 Additional B cell immunophenotyping

4.1 Background

In the preceding chapter a numerical deficiency in Breg (CD19+ $CD24^{high}$ $CD38^{high}$) was described in AAV, both at onset and in clinical remission. Breg frequency was equivalent to healthy controls in tolerant patients and after rituximab treatment, Breg were highly enriched. Bmem frequency was low at initial presentation but was restored in remission. The perturbed balance of memory and regulatory cells may predispose to relapse.

Immunoregulatory function has been attributed to B cell subsets other than $CD24^{high}$ $CD38^{high}$ cells. Murine splenic CD5+ $CD1d^{high}$ cells have potent suppressive capacity (Yanaba, Bouaziz et al. 2008). Human Breg are reported also to have higher expression of CD5 and CD1d than other B cells (Blair, Norena et al. 2010), with concordance with B10 cells in experimental models inferred (Mauri 2010). CD1d and CD5 biaxial flow cytometry plots have even been applied to B cells isolated from human blood (Flores-Borja, Bosma et al. 2013, Ma, Liu et al. 2014, Cui, Zhang et al. 2015, Habib, Deng et al. 2015). CD5 negatively regulates BCR signalling and CD5+ B cells produce more IL-10 than CD5 null cells on stimulation (Gary-Gouy, Harriague et al. 2002). An impairment in CD1d cycling has been described in patients with SLE (Bosma, Abdel-Gadir et al. 2012); an important functional role for CD1d+ B cells was recently shown *in vivo,* the induction of tolerogenic iNKT (Oleinika, Rosser et al. 2018).

There have been two large studies on frequency of CD5 B cells in AAV. A numerical deficiency in CD5+ B cells was demonstrated in active AAV, restored in remission and following rituximab therapy (Bunch, McGregor et al. 2013). CD5+ B cells were suggested as a predictive measurement of relapse and CD5, a surrogate marker for Breg. However, in the RAVE clinical trial CD5 B cell frequency did not correspond to risk of earlier relapse in AAV patients; the authors concluded that a single marker was inadequate for classification of Breg and for determining clinical outcome (Unizony, Lim et al. 2015).

In additional to testing CD5 and CD1d in parallel to CD24 and CD38, CD24 and CD38 were co-stained with CD1d, CD5, CD27, CD95, CD10, IgM and IgD. CD10 is the classical transitional B cell marker (Sims, Ettinger et al. 2005) and CD27 is widely accepted to be a marker of memory B cells, that have been involved in a germinal centre reaction. Recently CD95 was been suggested to be a biomarker in autoimmune disease, induced in exhausted cells and upon differentiation of naïve B cells into memory B cells and plasmablasts (Ducreux, Nieuwland et al. 2014, Adlowitz, Barnard et al. 2015). IgD is a marker of naïve B cells, sIgM is expressed on B cells on egress from the marrow but is most highly expressed on immature B cells. IgM and IgD double negative cells are only observed in the Bmem population in peripheral blood (B cells that undergone Ig class switch), however as many as 50% of memory B cells express IgM with or without IgD (Seifert and Kuppers 2016). There are no definite markers of memory, with CD27 null and IgD+ cells described (Shi, Agematsu et al. 2003, Fecteau, Cote et al. 2006).

4.2 Aims

To assess CD5 and CD1d B cell expression in a subset of patients and controls. Testing conducted in parallel with CD24 and CD38 immunolabelling, to evaluate whether CD5 is a good surrogate marker for Breg.

Additional phenotyping, to verify that Breg ($CD38^{hi}$ $CD24^{hi}$), B memory (Bmem, $CD38^{lo}$ $CD24^{hi}$) and naïve B cells (Bnaive, $CD38^{int}$ $CD24^{int}$ (Carsetti, Rosado et al. 2004, Blair, Norena et al. 2010) are distinct cell subsets.

4.3 Methods in brief

PBMC isolation, flow cytometry staining, FACS acquisition and analysis were described in the preceding chapter. Additional immunophenotyping was conducted with the following antibodies: CD5 [UCHT2], CD1d [CD1d42], CD1d [51.1], CD27 [O323], CD10 [eBioCB-CALLA], CD95 (Fas) [DX2], IgM [MHM-88] and IgD [1A6-2].

In 2 patients (P_055 and P_056), CD1d expression was assessed intracellularly. PBMC also stained after stimulation *in vitro* for 4 hours, at a density of 1 million cells per ml in complete media with 1µg/ml ionomycin and 50ng/ml PMA (Sigma Aldrich Ltd.). Complete media comprised RPMI-1640, 2mM L-glutamine and penicillin/streptomycin (Life Technologies Ltd) and 10% heat inactivated FCS (Sigma Aldrich Ltd.).

4.4 Patient and healthy control samples

4.4.1 CD5 and CD1d expression

CD19, CD5 and CD1d staining was conducted alongside CD19, CD24 and CD38 in 31 patients and 17 controls (Table 4.1). 22 were presented in the Rheumatology manuscript, 21 tests conducted in parallel on fresh PBMC and 1 on a frozen sample (P_026, tolerant). An additional 9 samples were included in this CD5 CD1d data set. Testing was conducted on frozen cells for P_033 and P_035 (1 active, 1 acute ANCA negative). A summary of all the testing conducted in the patient samples, is provided in Appendix 1.

Validity of staining on frozen cells was assessed by testing fresh and cryopreserved PBMC in 5 patients (P_030, P_034, P_040, P_042 and P_043). Some additional samples were tested from frozen but not included in final cohort due to poor cell recovery (P_037, P_038, P_039, P_046 and P_049).

To further resolve the pattern of CD1d staining observed, staining was conducted with CD1d [CD1d42] and CD1d [51.1] clones in parallel (3 patients and 4 controls). Two of the patients had acute disease and diagnosis of MPA, 1 had GPA in clinical remission and prior treatment with rituximab.

In addition, CD1d expression was assessed intracellularly before and after stimulation (4 hours, 1µg/ml ionomycin and 50ng/ml PMA). Testing conducted in 2 patients with the CD1d42 and 51.1 clones. Both patients were male, in clinical remission, with a diagnosis of MPA and MPO-ANCA (P_055 and P_056). The first was 80 years old, with ANCA titre of 52, renal and pulmonary involvement, receiving no treatment. The second was 63, ANCA negative, with renal involvement, receiving 10mg of

prednisolone and 50mg of azathioprine daily. This was conducted because there was little differential expression of CD1d: 2 clones increases confidence in results; stimulation and permeabilization was conducted because a defect with CD1d cycling was shown in SLE, with membrane expression restored on PMA and ionomycin stimulation (Bosma, Abdel-Gadir et al. 2012).

4.4.2 Additional markers in combination with CD24 and CD38

Phenotype of CD24, CD38 B cell subsets was further assessed in a small group of patients and controls. Firstly, CD27 and CD5 was tested in combination with CD24 and CD38 in 4 healthy controls (34-year-old female, 31-year-old male, 41-year-old female and 36-year-old female). IgM and IgD was tested in combination with CD24 and CD38 in 2 patients (P_055 and P_056).

Finally, CD95 and CD10 expression was assessed in combination with CD24 and CD38 in 9 AAV patients (samples not assigned unique patient numbers, bled between 28/07/14 and 18/08/14). The sex distribution was 3 male and 6 females; 5 had PR3-ANCA and diagnosis of GPA, 4 had MPO-ANCA and diagnosis of MPA. The age range was 21-65 years, median 56 and mean 50 years (passed d' Agostino and Pearson normal distribution test).

Table 4.1 CD5 cohort, patients compared according to disease activity

Characteristics		Rem	Active	Tolerant	Rtx	P-value
Number		17	8	3	3	
Overlap with CD24 CD38 cohort		13/30	3/12	3/4	3/7	
Age	Median	63	54	75	48	0.0352
	IQR	51-69	44-63	70-85	47-52	
Sex %	Male:Female	8:9	6:2	3:0	1:2	0.1945
Lymphocyte count	Median ($x10^9$/L)	1.58	1.33	1.34	1.19	0.5203
	IQR	1.4-2.2	0.8-2.5	1.1-1.8	1.1-1.8	
Serum creatinine	Median (mg/dL)	85	123.5	268	85	0.0925
	IQR	62-121	76-151	171-332	70-99	
Diagnosis %	MPA:GPA	53:47	38:62	67:33	67:33	0.7543
Disease duration	Median (years)	2.0	0.3	10.0	7.0	0.1065
	Range	0.2-12	0-16	7-11	0.3-13	
ANCA %	PR3	53	50	22	100	0.3708
	MPO	41	50	67	0	
	Double positive	6	0	0	0	
Treatment	None	12	13	100	0	0.0028
%	Cyclophosphamide	6	38	0	0	0.1145
	Mycophenolate	18	0	0	0	0.4343
	Methotrexate	12	25	0	33	0.5854
	Azathioprine	41	0	0	0	0.0590
	Corticosteroids	100	88	0	67	0.0340
Prednisolone	Median dose (mg)	3.75	17.5			0.0846

Statistical analyses were performed to compare patient groups: Chi-square for discrete variables, 1-way ANOVA for continuous variables and Mann-Whitney test for prednisolone dose, significance assumed at $P \leq 0.05$. Tolerant patients tended to be older than patients with active disease ($P=0.0609$) or remission patients with history of rituximab treatment ($P=0.0626$). Patients with grumbling disease represent a more heterogenous group, compared to those with acute presentation (treatment, creatinine level and time since diagnosis no longer differs significantly from the remission cohort).

4.5 Results

4.5.1 CD1d immunophenotyping

4.5.1.1 Absence of CD1dhigh B cell subpopulation

CD5+ CD1d^{high} cells are reduced in frequency in rheumatoid arthritis (Flores Borja, Ma, Cui). Despite using a bright fluorophore to enhance detection of CD1d (phycoerythrin, PE), a discrete CD5+ CD1d^{high} population could not be robustly detected in this data set (Figure 4.1).

On reviewing the literature, where CD1d and CD5 biaxial plots are shown, there is not a striking CD5+ CD1d^{high} population of B cells (Cui, Zhang et al. 2015, Habib, Deng et al. 2015). In fact, CD19- cells are often used to set the quadrant gate for B cells, which could not otherwise be confidently assigned (Habib, Deng et al. 2015).

It was previously reported that Breg have higher expression of CD1d (Blair, Norena et al. 2010). In this case series CD38/CD24 and CD5/CD1d testing was conducted in 2 parallel tests, therefore relative CD1d expression was not routinely assessed in Breg, Bmem and Bnaive subsets. To address this CD19, CD38, CD24 CD1d and CD5 were tested together, in 4 healthy controls (in section 4.5.3).

4.5.1.2 Detection not impaired by choice of CD1d 51.1 clone

Testing was conducted with CD1d clone 51.1 (Biolegend), which differs from some of the preceding publications using (CD1d42, BD Biosciences). To verify that detection was not impaired with clone 51.1, testing with both clones was conducted in a subset of patients and controls (Figure 4.2). CD38 and CD24 immunophenotyping revealed more diversity across this mixed cohort, particularly evident in the rituximab

Figure 4.1 Little differential expression of CD1d on biaxial plots

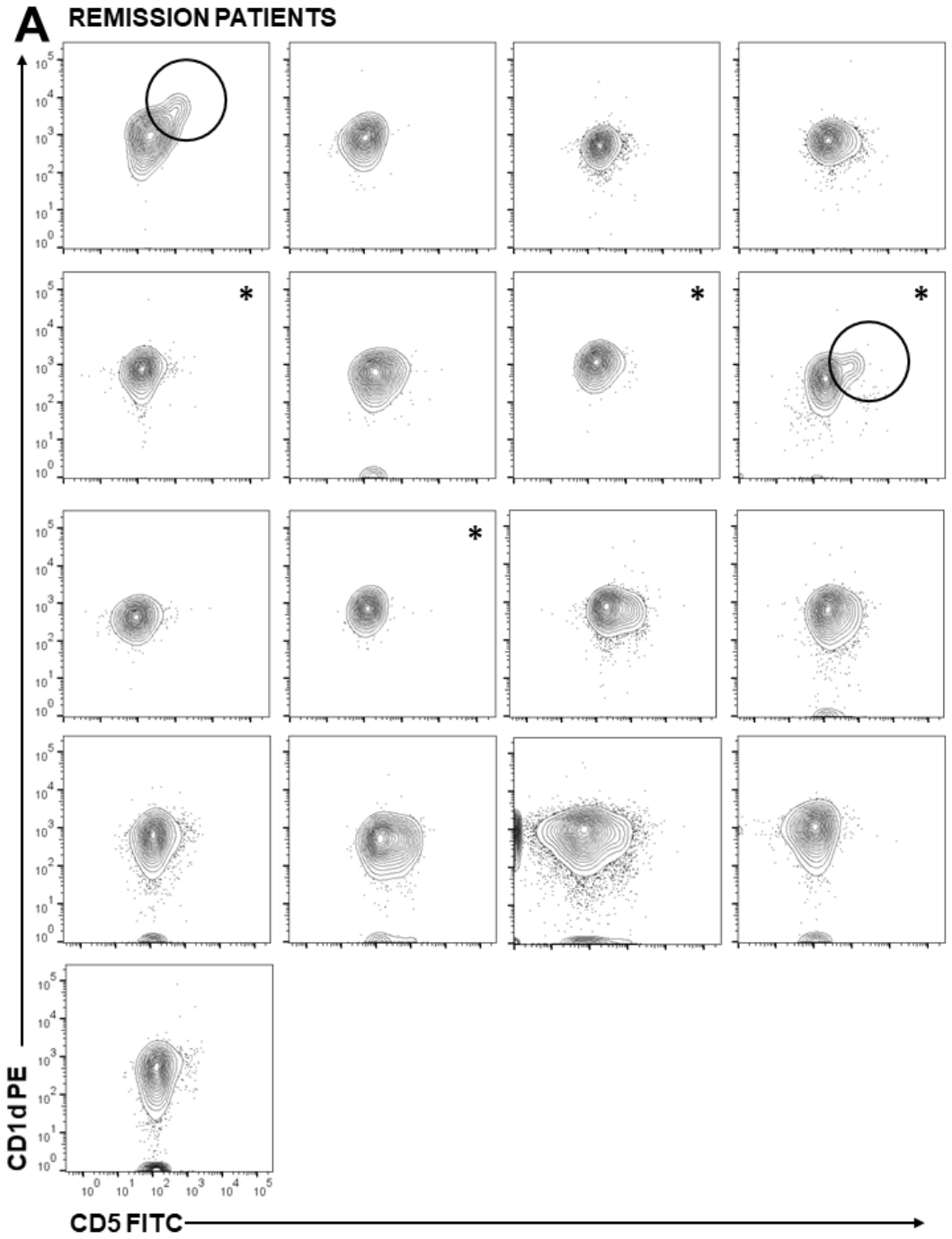

2 remission patients had a prominent CD5+ CD1d^{high} population circled. Asteriks denote patient samples tested together, verifying that this population was not an artefact of batch-processing or staining.

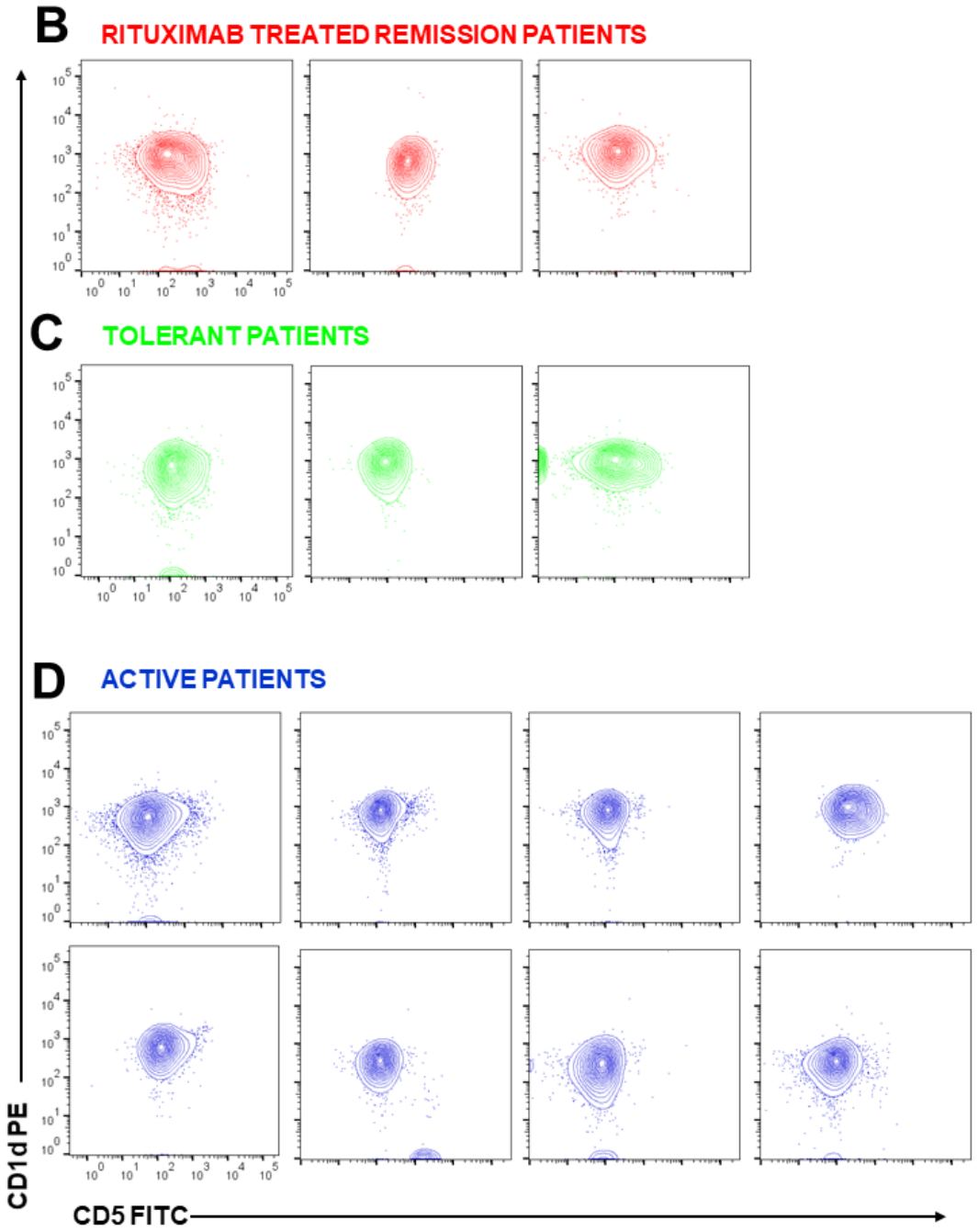

No prominent CD1dhigh populations were observed in tolerant, rituximab treated patients or in those, with active disease.

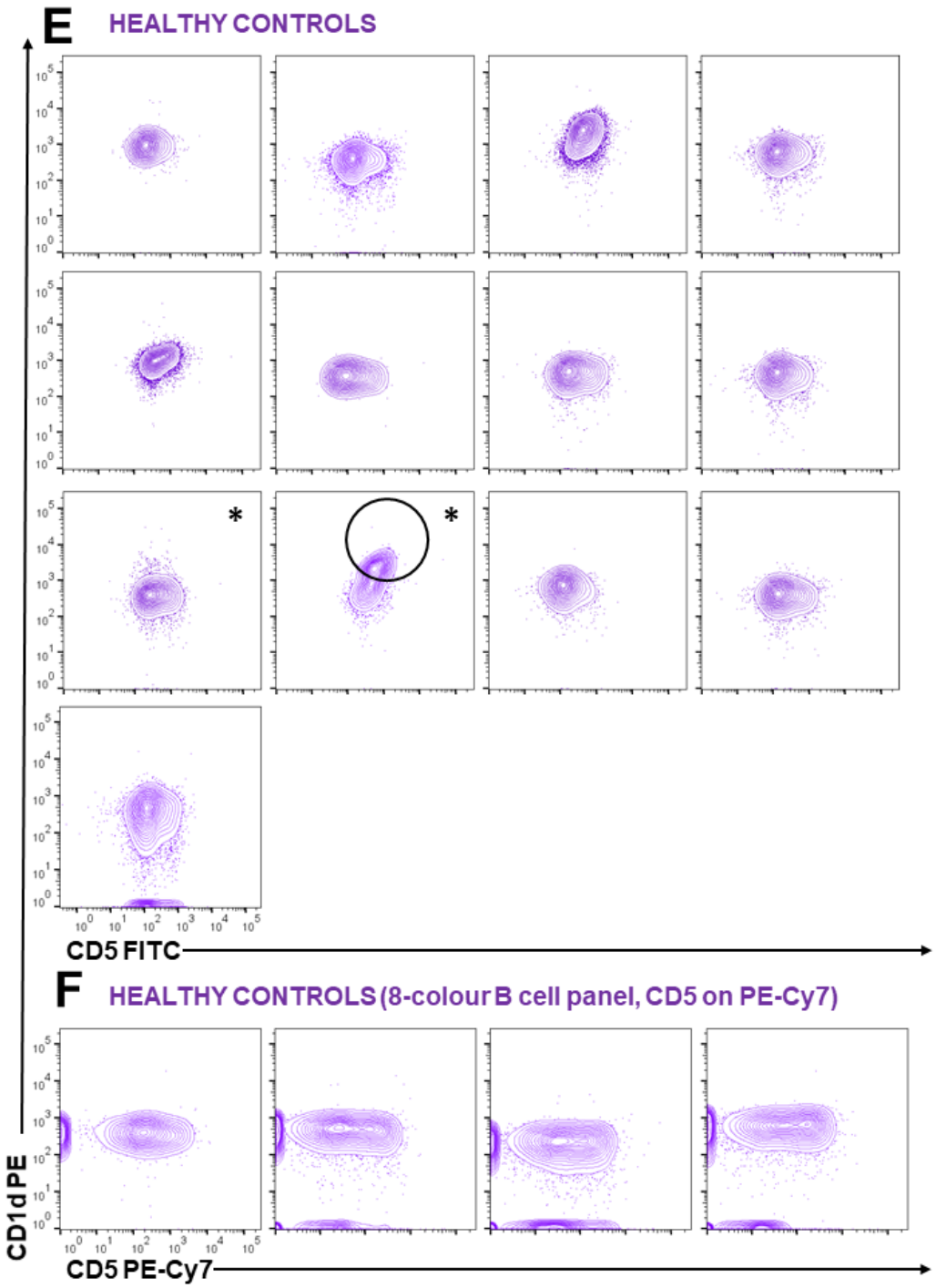

Plots for healthy controls shown, a discrete CD5+ CD1d^{high} population is circled. Asteriks denote a second sample tested alongside this one, was not an artefact of batch-processing or staining. The CD5+ cell population is better resolved on the bright fluorphore PE-Cy7 [E]

treated patient. Both CD1d42 and 51.1 CD1d clones gave equivalent staining.

4.5.1.3 B cells express high levels of CD1d, relative to CD19 null lymphocytes

Although a CD1d high subset of B cells was not consistently detected, B cells were positive relative to CD19 negative lymphocytes. The median value for CD1d geometric MFI for non-CD19 cells was 300 and for CD19+ lymphocytes, was 702 (combined patient and control data series, 48 data points). A 2-tailed Wilcoxon matched-pairs signed rank test was conducted, and the difference was highly significant P<0.0001****.

4.5.1.4 No reduction in CD1d expression in AAV, compared to controls

Fold difference in CD1d MFI, was calculated by dividing MFI for CD19+ cells by MFI for CD19 null lymphocytes, on average B cell CD1d MFI was 3.45 times greater (median). Patients and controls did not differ significantly, median 4.99 in patients and 2.51 in controls (Mann Whitney test P=0.2632). Delta MFI was also calculated (geometric MFI of CD19+ lymphocytes, minus geometric MFI of CD19 null lymphocytes). Delta MFI had a wider spread in controls compared to patients (range 50-2092 compared to 83-968), with the median tending to be lower in controls than patients (214 and 482, Mann Whitney U P=0.0538). When geometric MFI for patients and controls was compared, without correction there was no significant difference (622 and 739, Mann Whitney U P=0.7168). Overall the differences in CD19 cell CD1d expression between patients and controls were modest and did not reach statistical significance.

Figure 4.2 Consistent staining with 51.1 or CD1d42 clone

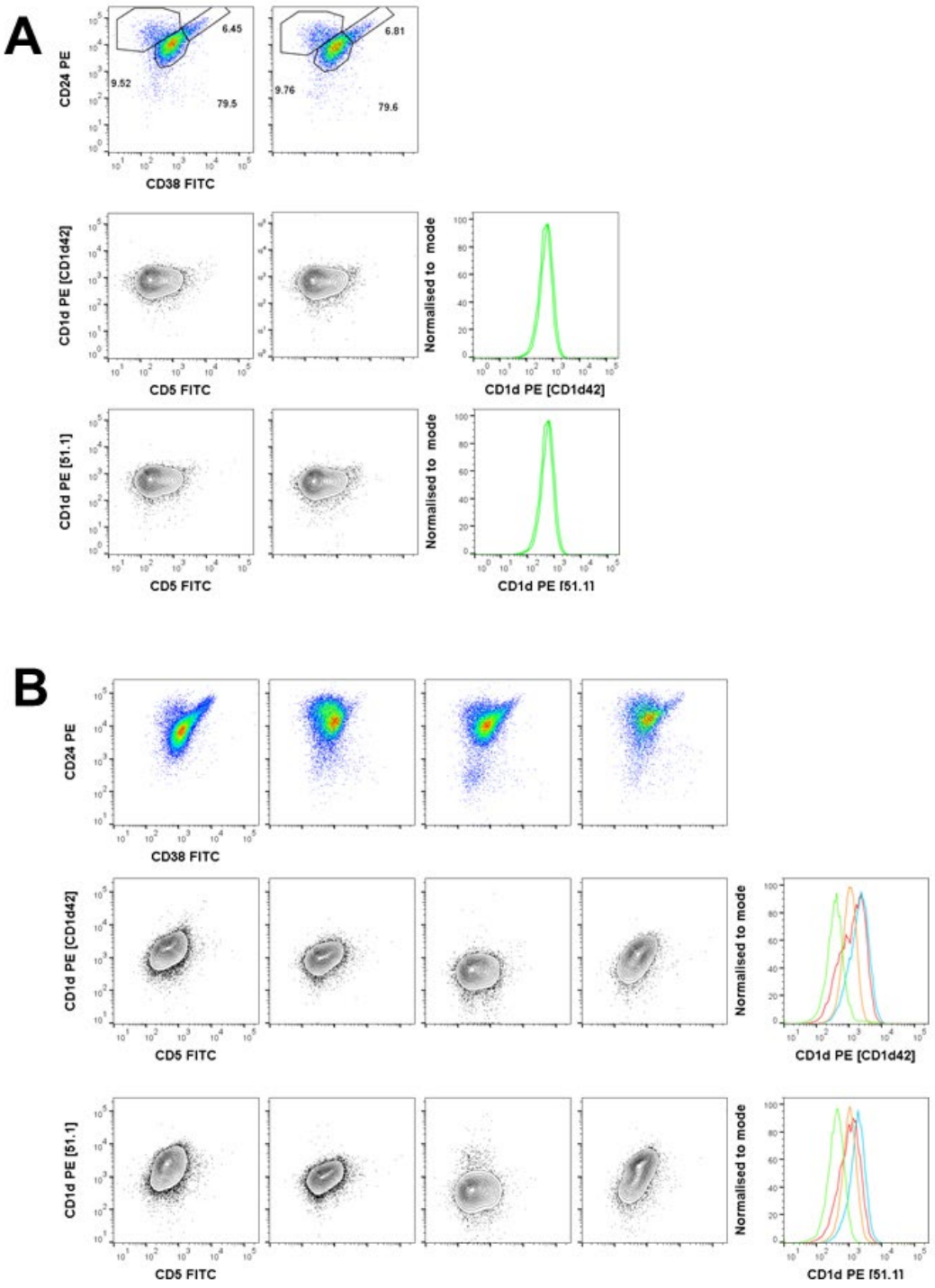

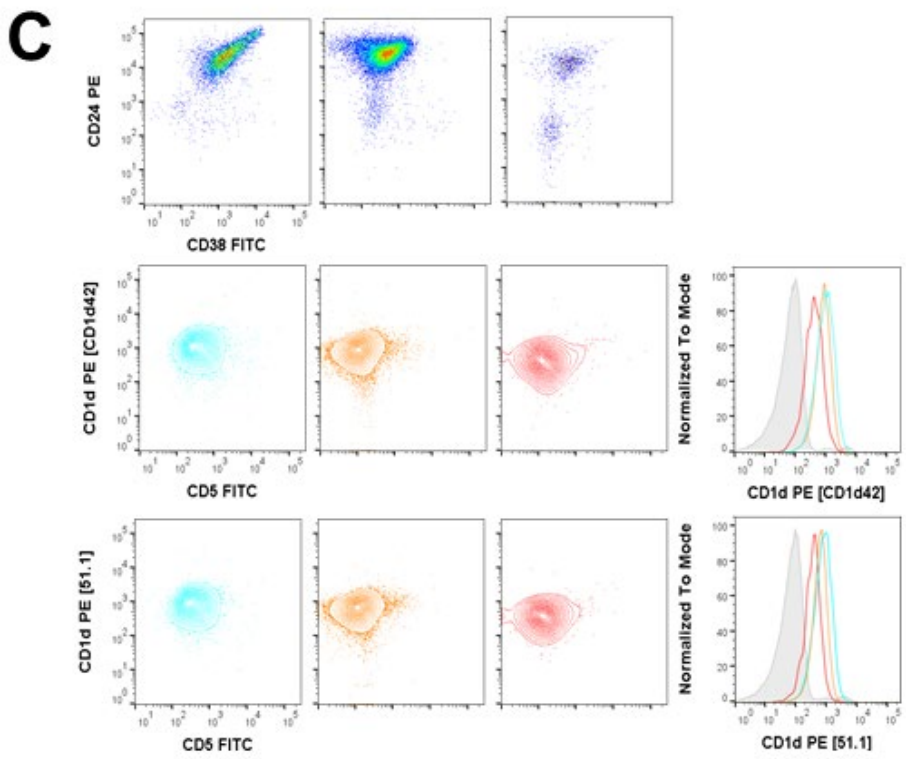

CD24 and CD38 staining is presented in the top row of each panel, with paired CD5 and CD1d immunolabelling in the next 2 rows. [A] Highly comparable staining in the same frozen sample, tested 1 week apart. [B] Flow cytometry plots for healthy controls showing considerable heterogeneity in CD1d MFI but lack of a discrete CD1d^{high} subpopulation. Detection not hampered by use of the 51.1 clone. [C] Plots for 1 rituximab treated AAV patient (column 1) and 2 acute AAV patients. The heterogeneity in CD24 and CD38 expression is not reflected in CD1d expression in the contour plots. The overlaid histograms show a CD19 negative lymphocyte population in filled grey (rituximab patient, column 1) and CD19+ cells for each of the patients (same colour at the contour plots). B cells are not negative for CD1d and express relatively high levels, compared to other major lymphocyte subsets (CD4, CD8 cells).

4.5.1.5 CD1d highest on the B cell surface, prior to any stimulation

Intracellular and extracellular CD1d staining was conducted for 2 MPA patients, to assess whether detection of $CD1d^{high}$ B cells was impaired by looking at membrane expression alone. By fixing and permeabilising the cells, not only are you able to detect surface antigen but also any CD1d trapped within the cell. PBMC were assessed immediately after isolation and after 4-hour stimulation with PMA and ionomycin. The rationale was based on evidence showing impaired endocytic cycling and low membrane expression of CD1d in SLE; PMA and ionomycin stimulation induced redistribution of CD1d to the cell surface (Bosma, Abdel-Gadir et al. 2012).

On comparing intracellular and extracellular for both clones at baseline, extracellular stained B cells had higher CD1d MFI (Figure 1.4). Furthermore, CD1d intracellular MFI at baseline was not greater than isotype control (Table 1.2). It was unexpected that MFI was reduced in fixed and permeabilised cells, the CD1d antigenic epitope might be affected by this process (some antigenic epitopes are particularly susceptible to fixation). After 4 hours PMA and ionomycin stimulation, there was a reduction in extracellular CD1d MFI, which might be expected upon cell activation however, this was not accompanied by an increase in intracellular MFI (Table 1.2). In addition, the MFI of the paired intracellular isotype control was also reduced. PBMC were stimulated in replete media with 10% FCS, which might block any non-specific antibody binding.

Testing was limited but it does not indicate that CD1d detection is impaired by looking at cell surface expression alone, nor that CD1d is trapped in the endocytic compartment, due to a defect in receptor cycling.

Figure 4.3 CD1d extracellular and intracellular staining at baseline

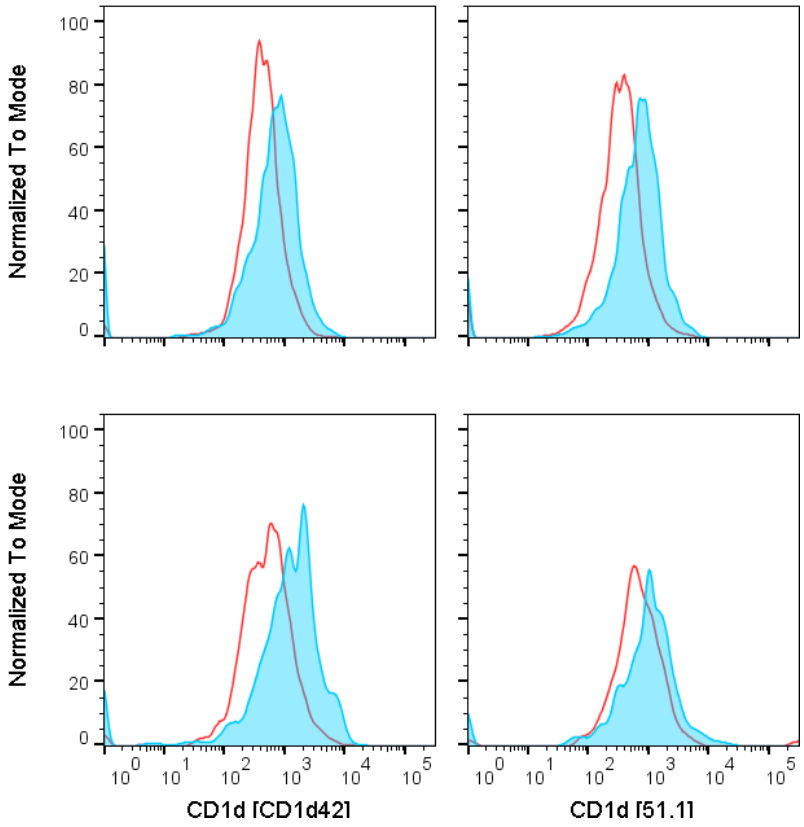

Results from two patients depicted, cell surface staining (filled blue histograms) overlaid with intracellular staining (red histograms). MFI higher prior to fixation and permeabilization.

Table 4.2 Geometric MFI for CD1d in B cells, across various conditions

CD1d geometric MFI in CD19+ cells	CD1d42 or IgG1		51.1 or IgG2bκ	
	P_055	P_056	P_055	P_056
Extracellular baseline	552	971	570	798
Intracellular baseline	393	472	299	449
Intracellular isotype baseline	578	644	293	446
Extracellular 4 hours PMA/ino	325	382	323	403
Intracellular 4 hours PMA/ino	385	729	216	433
Intracellular isotype 4 hours PMA/ino	243	593	25.2	115

Geometric MFI for all the test conditions, MFI was lower after fixation and permeabilization without any stimulation (extracellular and intracellular staining at baseline). Detection of CD1d was not enhanced upon PMA and ionomycin stimulation either. This may be indicative of a fixation-labile epitope. Geometric MFI is shown for CD1d antibodies in the unfilled rows, and for paired isotype controls in the grey rows.

4.5.2 CD5 immunophenotyping

4.5.2.1 A CD5+ subset of B cells can be characterised

There was variation in CD5 expression (Figure 4.1), which permitted a positive gate to be assigned to 48 individuals (17 healthy controls and 31 AAV patients). Because CD5 is expressed on a continuum and FITC is not a very bright fluorophore, percentage frequency was calculated by gating against 2 markers, with average calculated for improved accuracy (i.e. 2 biaxial plots with CD19, FSC-A or CD1d versus CD5).

The frequency of CD5+ B cells of the combined patient and control cohort did not meet the statistical threshold for an abnormal distribution pattern (D'Agostino and Pearson normality test P=0.0687). The frequency of CD5 B cells therein, was variable, ranging from 3.77-38.00%, with a mean value of 16.18% and standard deviation of 9.45%.

4.5.2.2 CD5 induced in a subset of samples, upon freeze-thawing

The final patient cohort for CD5 and CD1d immunophenotyping is limited (8 with active disease, 23 patients in clinical remission, 3 of whom were tolerant and 3 had prior treatment with rituximab). To better represent the CD24 CD38 cohort, an additional 11 samples were tested from frozen (tolerant and active disease). Five replicate tests were conducted at the same time, to assess validity of this approach (paired with historic testing in fresh PBMC, all from individuals with active disease). Out the 16 tests, 7 were considered invalid. In the paired testing CD5 was clearly seen to be induced, when cell recovery from frozen was suboptimal (2 out of 5 samples tested). No viability marker was included, but poor recovery could be defined on

Figure 4.4 CD5 variation in paired fresh and frozen samples

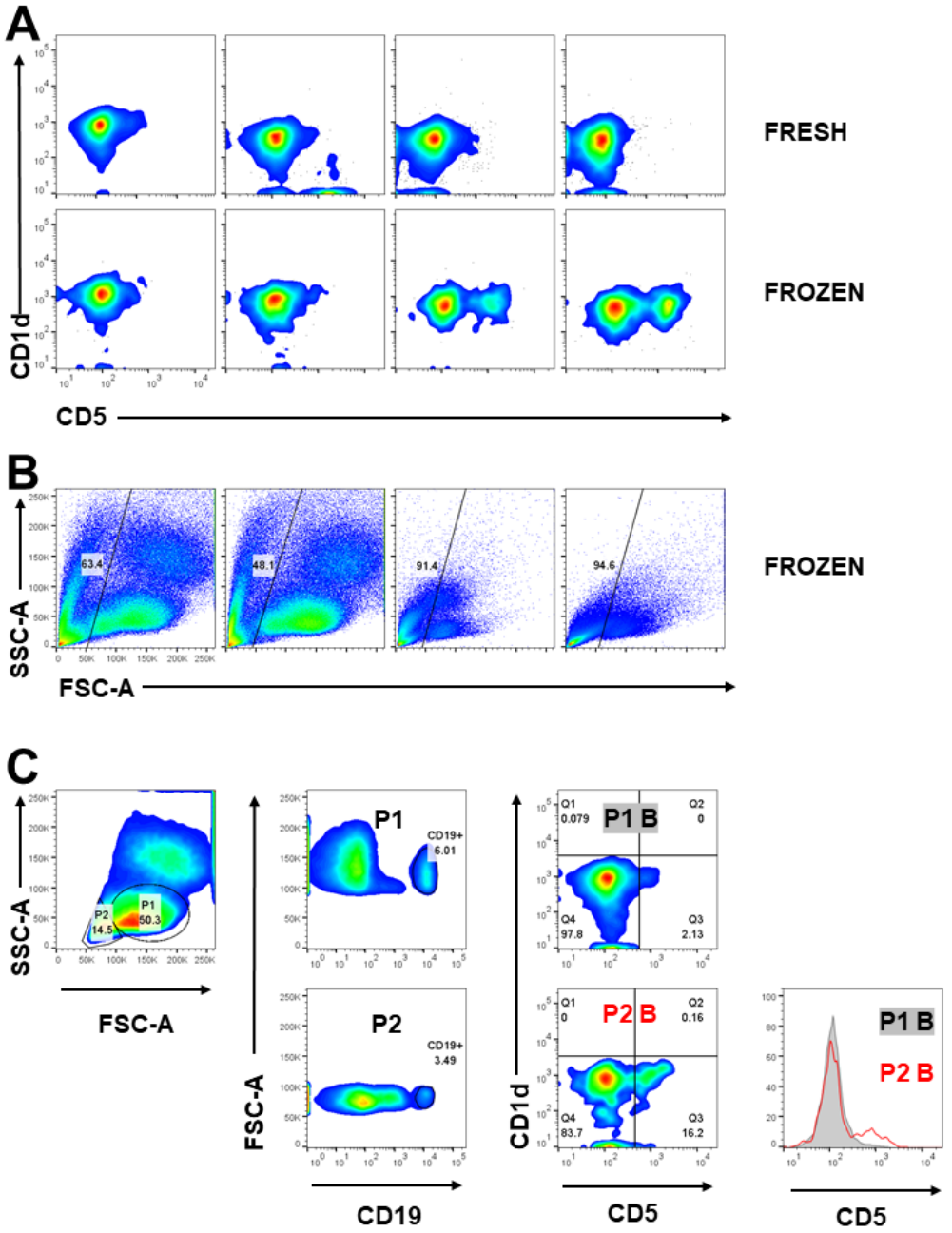

[A]. Biaxial plots for CD5 and CD1d, paired fresh and frozen patient samples. CD5 was induced in 2 samples, with poor recovery after thawing. [B]. Poor recovery resulted in a lot of debris, loss of the monocyte population and contraction of lymphocyte population. [C]. Differential staining in CD5 can also been observed within the same sample. Two gates were drawn on the FSC-A:SSC-A biaxial plot. P1 corresponds to a small, granular leukocyte population and P2, the main lymphocyte population. CD19+ cells were gated within these populations (P1-B and P2-B). Small granular CD19 events (P2 B population), had differential expression of CD5.

acquisition, with cellular debris constituting a high proportion of total acquired events, a profound loss of monocytes and a general contraction of the cells, on the FCS-A and SSC-A biaxial plot (relative to other samples). Furthermore, differentiational expression of CD5 could be detected within the same sample, when small apoptotic lymphocytes were compared to the main population (Figure 4.4, panel C).

Fresh samples were preferentially selected when frozen replicates were also available and only 3 frozen samples, included in the entire cohort (1 tolerant, 1 active and 1 acute). Inclusion was carefully considered, the samples had excellent cell recovery and none of the final CD5 frequencies were data outliers (7.615%, 9.565% and 15.550%); the final cohort would otherwise be limited to 6 active and 2 tolerant patients.

4.5.2.3 CD24 and CD38 stable, on freeze-thawing and repeat testing

B cell subpopulations based on relative expression of CD24 and CD38, were compared in fresh and frozen samples (5 control and AAV patients). Biaxial plots show raw data (Figure 4.5), further analysis was conducted on corrected frequencies (sum of 3 populations corrected to 100%). Samples were ranked from lowest to highest with paired frozen and fresh samples depicted in a line graph, which showed very good concordance (Figure 4.6, Panel A). Similarity was further assessed on the combined patient and control cohort, for the smallest B cell population (Breg). Correlation was highly significant (R^2 =0.9119, P<0.0001****) and pairing highly effective (paired t-test P<0.0001****) (Figure 4.6, Panel B).

The intraassay control further demonstrates that frozen samples are highly stable over time, data was assessed for 1 individual, 2 samples, tested 9 and 7 times respectively (Figure 4.6, Panel C). The co-efficient of variations for the 2 samples was: 18.26 and 16.23% for Bmem, 8.82 and 10.70% for Breg, 3.98 and 4.66% for Bnaive cells. The

Figure 4.5 Comparision of B cell immunophenotyping in paired fresh and frozen samples

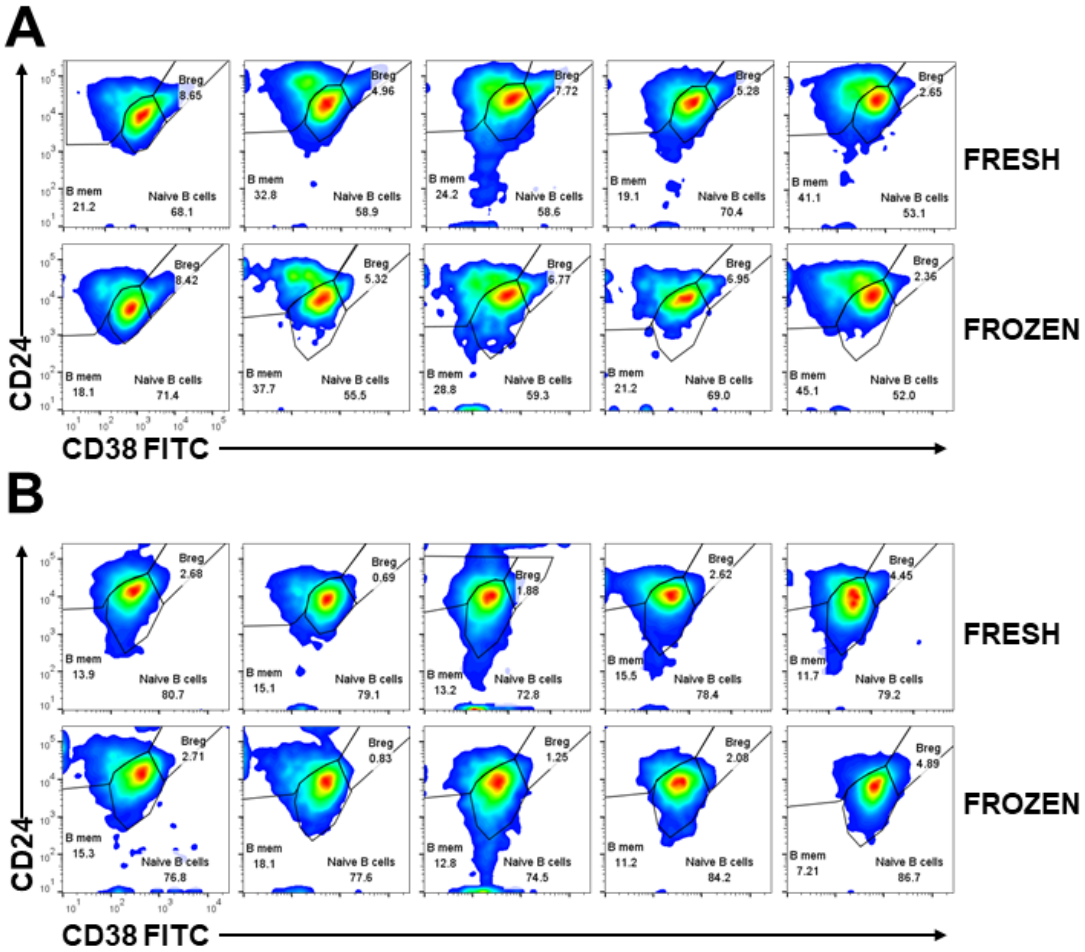

[A]. Biaxial CD24 and CD38 plots for fresh and frozen healthy controls (CD19 parent population). [B]. Fresh and frozen AAV patient samples. Very good concordance for both.

Figure 4.6 CD24 and CD38 staining is very consistent on freeze-thawing and repeat testing (intraassay control shown)

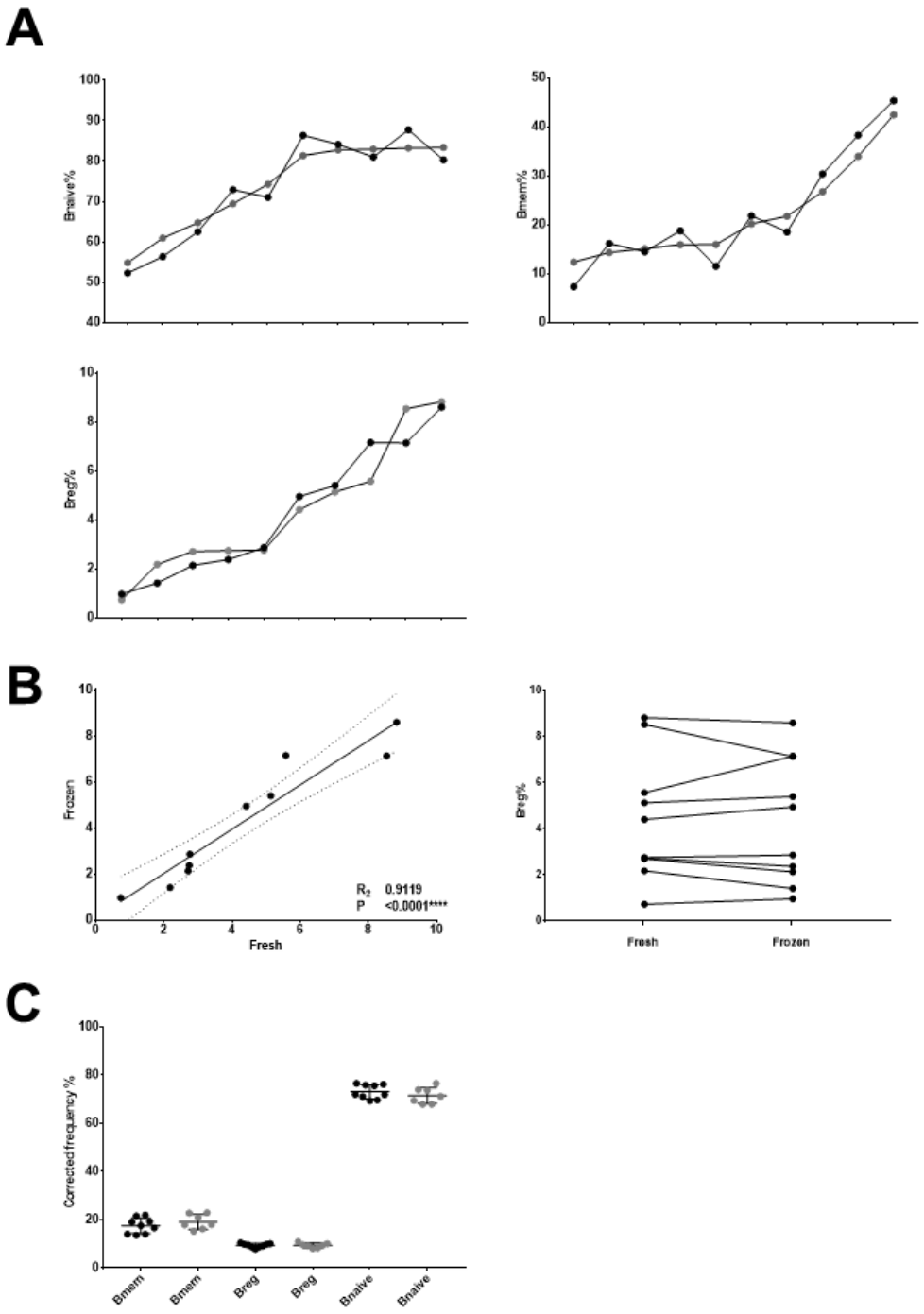

*[A]. Graphs show a mixed cohort of 5 control and AAV patients, with sum of B cell subsets corrected to 100%. Testing conducted in fresh (grey filled circles) and frozen samples (black filled circles). Graphs show good concordance. [B]. Linear regression was conducted for Breg in fresh and frozen samples (Y= 0.6231*X + 0.107, R^2 =0.9119) and correlation was highly significant P<0.0001****. Paired t test was also*

*conducted for Breg (normal distribution as assessed by D'Agostino and Pearson test), there was no significant difference between fresh and frozen samples (P=0.8264), despite the wide range of frequencies assessed (Breg range = 0.727-8.822%), furthermore, pairing was highly effective (P<0.0001****). [C]. The intraassay control further demonstrates that frozen samples are highly stable over time (sample 1 in black, tested 9 times and sample 2 in grey, tested 7 times). There was no significant difference when serial samples were compared by Mann Whitney U.*

median frequencies 17.56 and 17.98% for Bmem, 9.63 and 9.30% for Breg, 72.01 and 71.20% for Bnaive cells. There was no significant difference when serial samples were compared by Mann Whitney U (too few data points for the second sample to assess if normal distribution).

4.5.2.4 CD5+ B cell frequency is reduced in AAV patients, relative to controls

CD5 B cells were reduced in the mixed cohort of AAV patients (n=31), relative to healthy controls (n=17) (Figure 4.7, Panel A). Data was normally distributed for controls but not for patients (D'Agostino and Pearson P=0.0025**), datapoints were more likely to be distributed below the median value (skewness +1.449). The median frequency for CD5+ B cells in controls was 19.35% (range 6.37-35.75%) and 9.575% in AAV patients (range 3.77-38.00%), the difference was significant (Mann Whitney test P=0.0017**).

The skew in the patient data, might be due to the heterogeneity of the patient group. Sub-categorisation of the patient group was conducted to assess whether any relationships existed for CD5+ B cells. A reduction in Breg was previously observed in all patients in clinical remission and in active patients with PR3-ANCA, but not active patients with MPO-ANCA.

4.5.2.5 CD5 B cells significantly lower in MPA diagnosis or MPO-ANCA

This was a limited cohort, so initial analysis was conducted for patients categorised according to diagnosis or ANCA-specificity, irrespective of disease activity (Figure 4.7, Panel B). This maximised the number of patients in each group. The first observation was that CD5 frequency was significantly lower in patients with MPA diagnosis (P=0.0016**) or MPO-ANCA (P=0.0230*), relative to healthy controls.

There was also a tendency for lower CD5 frequency in GPA patients and those with PR3-ANCA, but this did not reach the threshold for statistical significance ($P \leq 0.0500$).

4.5.2.6 CD5 B cells reduced in active disease and remission

Analysis was subsequently conducted, for patients grouped according to disease activity. Tolerant and rituximab patients did not differ significantly from the main remission cohort. This was surprising, as profound differences in Breg frequency upon repopulation were described in the preceding results chapter, with similar findings published (Marie-Cardine, Divay et al. 2008, Palanichamy, Barnard et al. 2009).

CD5 B cell frequency was significantly lower in active disease (P=0.0331*) and the combined remission group, which included 3 tolerant patients and 3 rituximab treated patients, compared to healthy controls (P=0.0106*). The median for remission and active patients was very similar, 9.64% for remission (range 3.77-33.35) and 8.59% for active disease (range 4.44-38.00). This is not in keeping with the study by Donna O'Bunch *et al*, who found that CD5 frequency was reduced in active disease, with decline preceding clinical relapse (Bunch, McGregor et al. 2013). However, results are in keeping with a later study, which did not find any relationship between CD5 B cell frequency and disease activity in AAV (Unizony, Lim et al. 2015).

Patients were further classified according to disease activity and ANCA-specificity or diagnosis. Graphs are presented in Figure 4.7 Panel C, Kruskal Wallis and Dunn's multiple comparison tests were conducted. It was difficult to confidently resolve further differences, due to the wide spread of the data and the low number of patients with active disease (3 MPA diagnosis, 2 MPO-ANCA, 5 GPA diagnosis and 4 PR3-ANCA). All comparisons were conducted relative to healthy controls. Patients in clinical remission with PR3-ANCA and those with active disease and MPO-ANCA

Figure 4.7 CD5 B cells are reduced in AAV

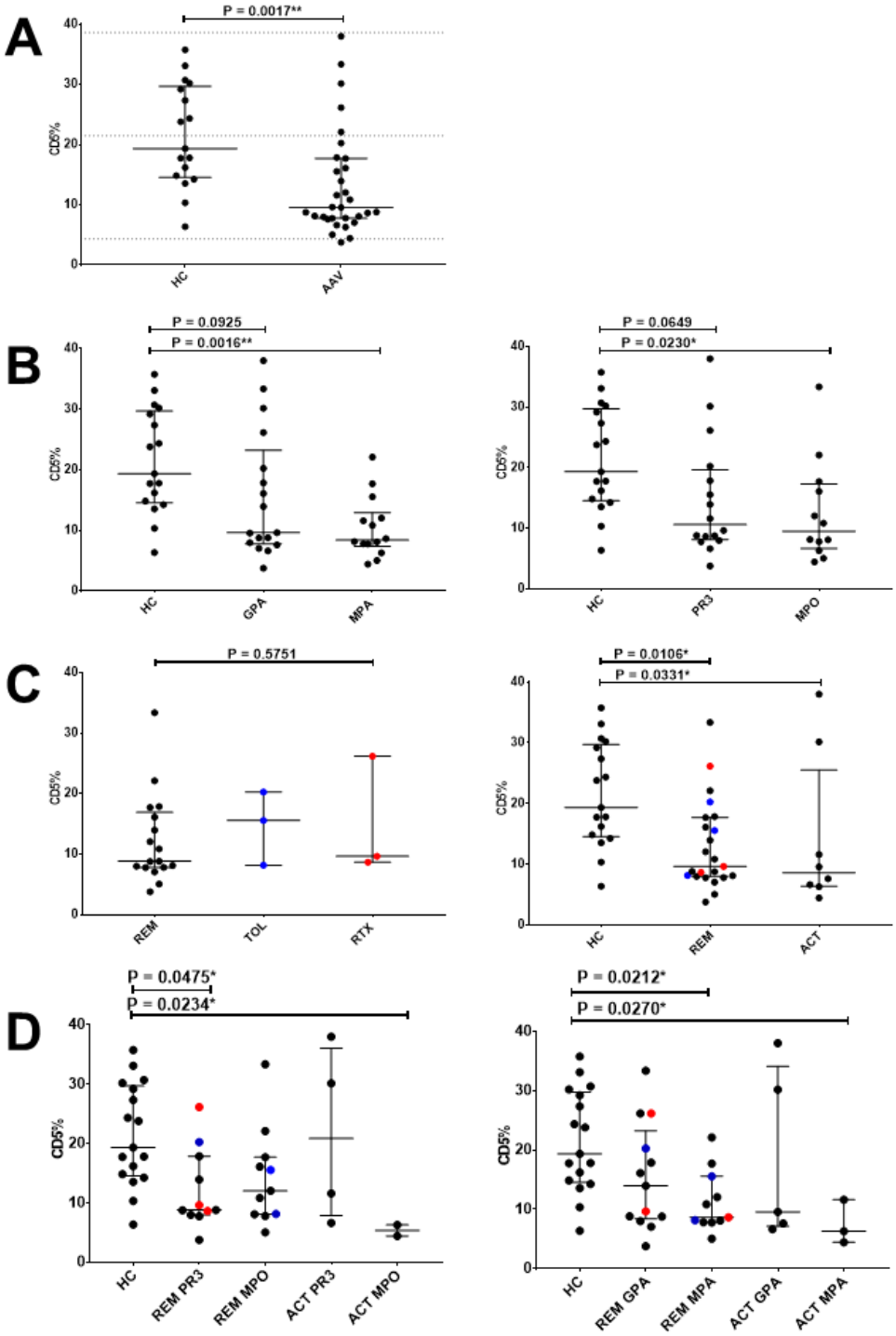

*[A]. CD5 B cell are reduced in AAV compared to controls (Mann Whitney test P=0.0017**). [B]. Patients separated according to ANCA specificity or diagnosis. Those with MPA diagnosis (P=0.0016**) or MPO-ANCA (P=0.0230*), differed significantly from healthy controls (1-way ANOVA and Dunnett's multiple comparison test). [C]. There was no significant difference between subgroups of patients in clinical remission, permitting data to be combined in subsequent graphs (tolerant patients*

shown in blue and patients who had prior rituximab treatment, shown in red). CD5 B cells are reduced in AAV, irrespective of whether disease is active or quiescent. [D]. Patients further classified according to disease activity and ANCA-specificity or diagnosis. Patients in clinical remission with PR3-ANCA and those with active disease and MPO-ANCA had significantly lowly CD5 B cell frequency. Those with a diagnosis of MPA, have reduced CD5 B cell frequency irrespective of disease activity (Kruskal Wallis and Dunn's multiple comparison test).

had significantly lower CD5 B cell frequencies. Those with a diagnosis of MPA, have reduced CD5 B cell frequency irrespective of disease activity.

Overall CD5 changes did not mirror those observed in Breg. The patient cohort was more heterogenous, with inclusion of ANCA negative individuals and patients with grumbling disease (not limited to acute patients, with blood collected at initial presentation). The distribution of CD5 is wide and a much larger data set would be required to verify whether there is any difference in active and remission subgroups.

4.5.2.7 Positive correlation between CD5+ B cells and Breg in patients

Bunch *et al* suggest CD5 as a surrogate marker for Breg (Bunch, McGregor et al. 2013). I therefore assessed the relationship between CD5 and CD24highCD38high Breg. There was a positive relationship, in the mixed cohort of patients and controls ($R^2$0.1273 and P=0.0161*, Figure 4.8). Significance was not diminished when the same test was applied to patients alone ($R^2$0.2001 and P=0.0150*) however, significance was completely lost in healthy controls ($R^2$0.01066 and P=0.6933).

Significance might be lost because there were fewer data points for controls and the range of the data was modestly narrower compared to patients. Breg frequency range was 2.06-10.45% in controls, compared to 0.00-13.26% in patients; CD5 frequency range was 6.37-35.75% in controls, compared to 3.77-38.00% in patients.

Most strikingly, there were no data points in the lower left corner of the graph for controls (Figure 4.8, Panel C), with Breg frequency $\leq$ 5% and CD5 frequency $\leq$ 10%. Unizony *et al* suggest that the frequency of Breg and CD5 may only be related when the donor is profoundly lymphopenic because of immunosuppressive treatment (Unizony, Lim et al. 2015). To test this, CD5 frequency was plotted against lymphocyte count, however, no relationship was apparent (Figure 4.9, Panel C).

Figure 4.8 Correlation between CD5+ B cells and Breg

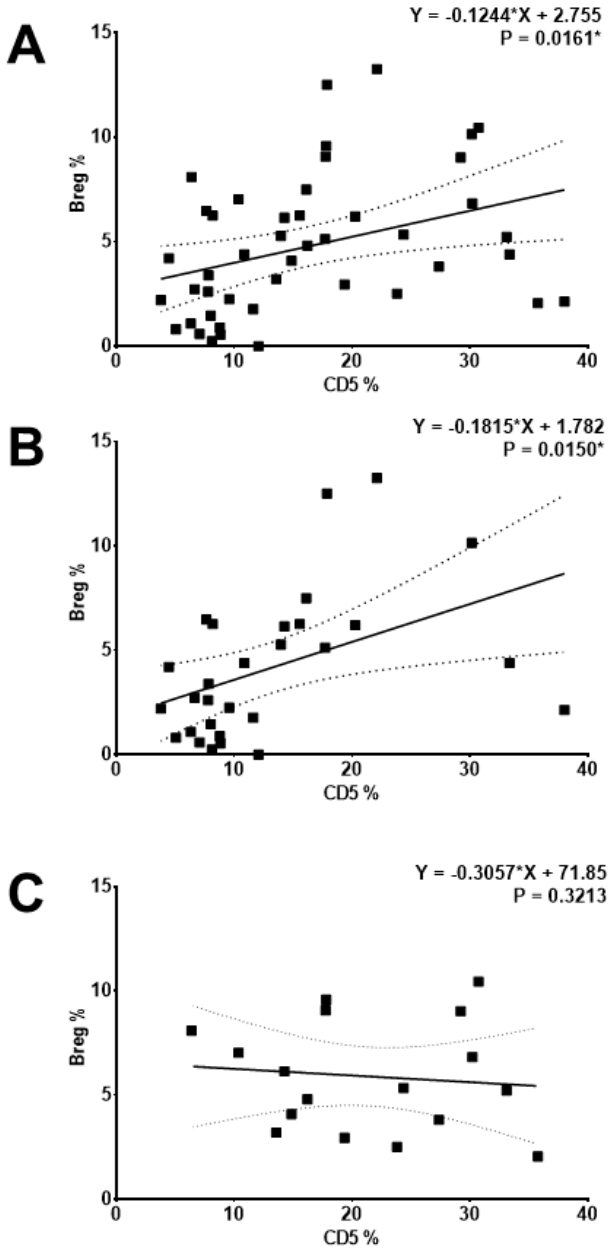

[A]. CD5 B cells showed positive correlation with Breg, in a mixed cohort of patients and controls (n=48). [B]. Correlation was also observed in AAV patients alone (n=31) but lost in healthy controls (Panel C, n=17).

Although CD5 expression levels are higher on Breg or transitional B cells, it is not uniquely expressed by these B cells. In fact, it is not even stable within the same sample; I have shown that CD5 is inducible in apoptotic B cells, due to poor recovery after freeze-thawing.

The patient group was also known to be older than the control group; to check that the low CD5 frequencies and correlation with Breg, were not related to aging, further analyses were conducted. Firstly, the active disease group was not significantly older than controls, but CD5 B cell frequency was still lower than controls (Figure 4.9, Panel A). Secondly, there was no correlation between CD5 frequency and age, with low CD5 frequencies observed across the entire age range of the patients (17-85 years) (Figure 4.9, Panel B).

4.5.3 Flow cytometry to verify that the 3 B cell subsets, defined by relative expression of CD24 and CD38 are phenotypically distinct

CD24 and CD38 are very stable markers, with regulatory function previously demonstrated *in vitro* for the $CD24^{high}CD38^{high}$ subset *(Blair, Norena et al. 2010)*.

CD5 alone is a poor surrogate for Breg cells, induced in apoptotic cells after freeze-thawing and, there is no correlation between CD5 expressing B cells and $CD24^{high}CD38^{high}$ Breg in healthy controls. Differences in CD5 and Breg in the patient subgroups were also discordant; there was a significant reduction in CD5+ B cells in patients with MPO-ANCA and grumbling disease, but no significant reduction in Breg in acute MPO-ANCA patients.

CD38 and CD24 subsets looked to be the best markers to isolate peripheral B cells on, for functional studies but prior to this, it was essential to verify that the 3 subsets were

Figure 4.9 No relationship between CD5 B cells and age or lymphocyte count

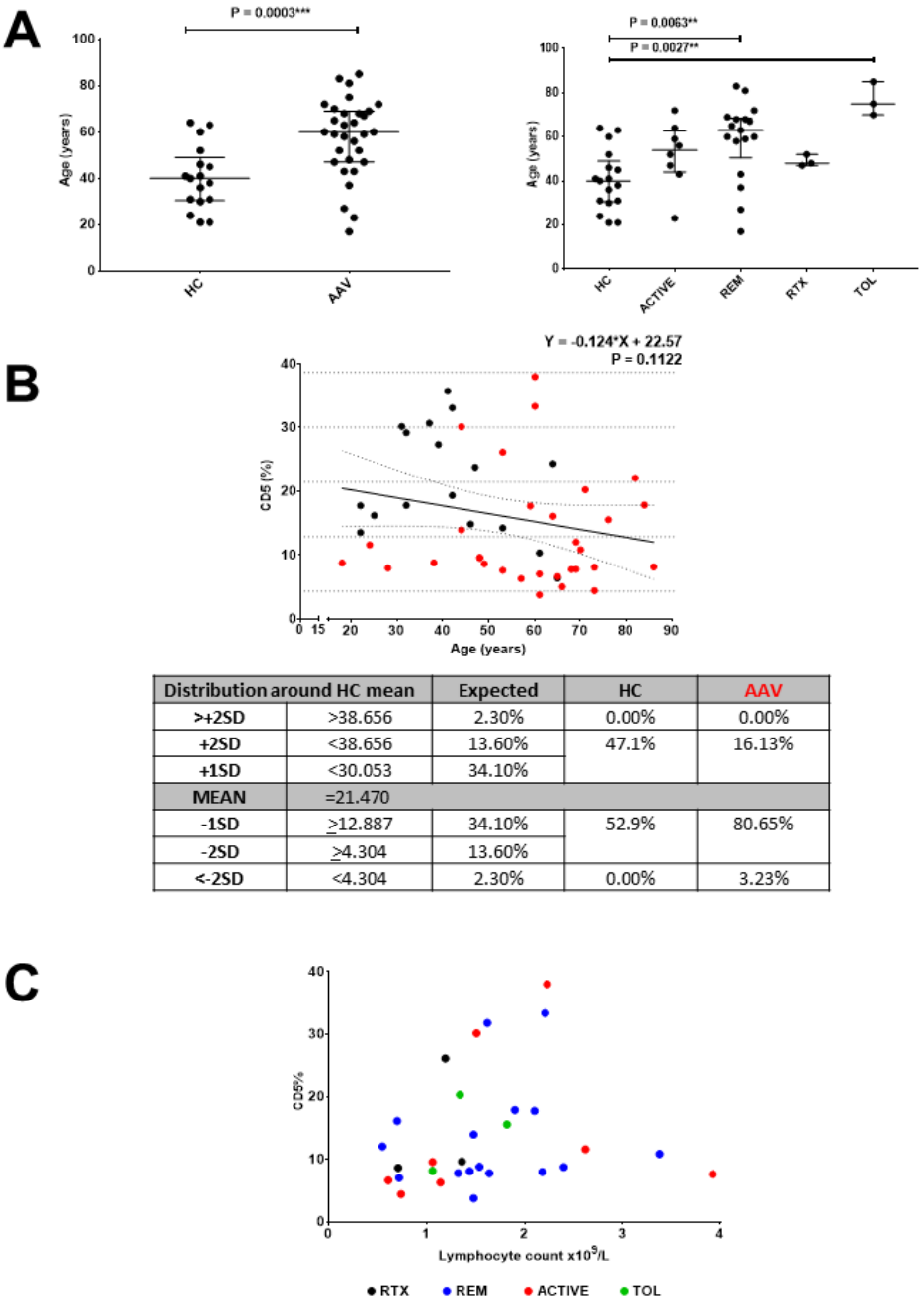

Distribution around HC mean		Expected	HC	AAV
>+2SD	>38.656	2.30%	0.00%	0.00%
+2SD	<38.656	13.60%	47.1%	16.13%
+1SD	<30.053	34.10%		
MEAN	=21.470			
-1SD	≥12.887	34.10%	52.9%	80.65%
-2SD	≥4.304	13.60%		
<-2SD	<4.304	2.30%	0.00%	3.23%

*[A]. AAV patients were older than controls (unpaired t-test with Welch's correction performed, P=0.0003***). The difference was predominately in tolerant and remission groups (median 75 and 63 years). Median ages for rituximab patients and active disease did not differ significantly from controls (Kruskal-Wallis and Dunn's multiple comparison). [B]. There was no relationship between age and CD5 B cell*

frequency. Line of best fit for combined patient and control data, with 95% confidence interval is shown, HC data points in black and patients in red. The additional lines, transecting the Y axis are the HC mean, +/- 1SD and 2SD. Patients with low CD5 frequency are observed across entire age range. Patient CD5 frequency was negatively skewed relative to controls, 84% of AAV data points lower than the HC mean (summarised in the table under the graph). [C]. There was no trend between CD5+ B cell frequency and lymphopenia.

phenotypically distinct. This was essential, since both CD24 and CD38 antigens are expressed on a continuum, with no discrete positive and negative cell populations. With this aim, CD24 and CD38 staining was conducted in combination with CD27, CD1d, CD5, IgM, IgD, CD95 and CD10.

4.5.3.1 There is limited variation in expression of CD1d within B cell subsets, defined by relative expression of CD24 and CD38

These results verify CD1d expression is high in B cells, relative to CD19- cells with similar size and intracellular complexity, which I infer to be T cells. Overlaid histograms for the 4 healthy donors, revealed little differential expression of CD1d in Breg, Bnaive and Bmem subsets, with peaks tightly aligned on top of one-another (Figure 4.10).

4.5.3.2 Breg all express high surface levels of CD5, but expression of this marker is not limited to a single B cell type

Overlaid histograms for B cell subsets show that Breg invariably express high levels of CD5, however a subset Bnaive cells also express high levels of CD5 (Figure 4.11, dashed histogram). Contour plots show lack of a discrete positive and negative population. Many markers are expressed in a continuum like CD5 and this can often correspond with maturation or functional status.

CD5+ and CD5- B cells were assigned, with populations backgated based on CD24 and CD38 expression. Breg represent 20-40.9% of the total cells within CD5+ B cells, compared to 6.7-13.6% within the CD5- population. Although enriched, it must be stated that 60-80% of the CD5+ cells are not Breg. This is likely why no correlation was observed in between CD5 and Breg in an extended healthy control dataset. Bmem are much more likely to be CD5- than CD5+ (25.9-37.0% in CD5- B cells, compared

to 4.7-7.3% in CD5+).

4.5.3.3 CD27+ cells are found within the Bmem population

Overlaid histograms for B cell subsets show that CD27+ expression is highest in Bmem (Figure 4.12). A gate defining CD27+ and CD27- B cells could be confidently assigned on contour plots. When CD27+ cells were backgated based on CD24 and CD38 expression, Bmem represented 67.9-88.3% of the total cells within CD27+ B cells, compared to 6.7-14.0% within the CD27- population. Breg and Bnaive cells are reduced in the CD27+ B cell population and enriched in CD27- population.

The relationship between Bmem and CD27 was not absolute. CD27 is the most commonly used marker for Bmem, denoting cells which have transited a germinal centre reaction. More recently, CD27- Ig class switched B cells have been described. To resolve whether any of these CD27- Ig class switched B cells were present, an IgD antibody would have to be included in the test panel. CD27+ Breg subsets have also been described (Iwata, Matsushita et al. 2011), however these do not seem prevalent; only 0.48-1.47% of CD27+ cells fell within the Breg gate, compared to 6.7-13.6% Bregs within the parental CD19+ population.

4.5.3.4 CD27 and CD5 immunolabelling correspond well with Breg, Bnaive and Bmem gates in fresh, healthy control samples

Quadrant gates were drawn on CD5 and CD27 biaxial plots for CD19+ cells (Figure 4.13). The same gates were then applied to B cell subsets, based on relative CD24 and CD38 expression. Breg are CD27 null and CD5+, Bmem are CD5- with the majority expressing CD27. Bnaive are predominantly CD27- but have variable expression of CD5. When this is expressed as percentage of the parent population, they do not appear to be enriched or decreased within the CD5+ or CD5- B cell populations (Figure 4.14,

Figure 4.10 No differential expression of CD1d in B cell subsets

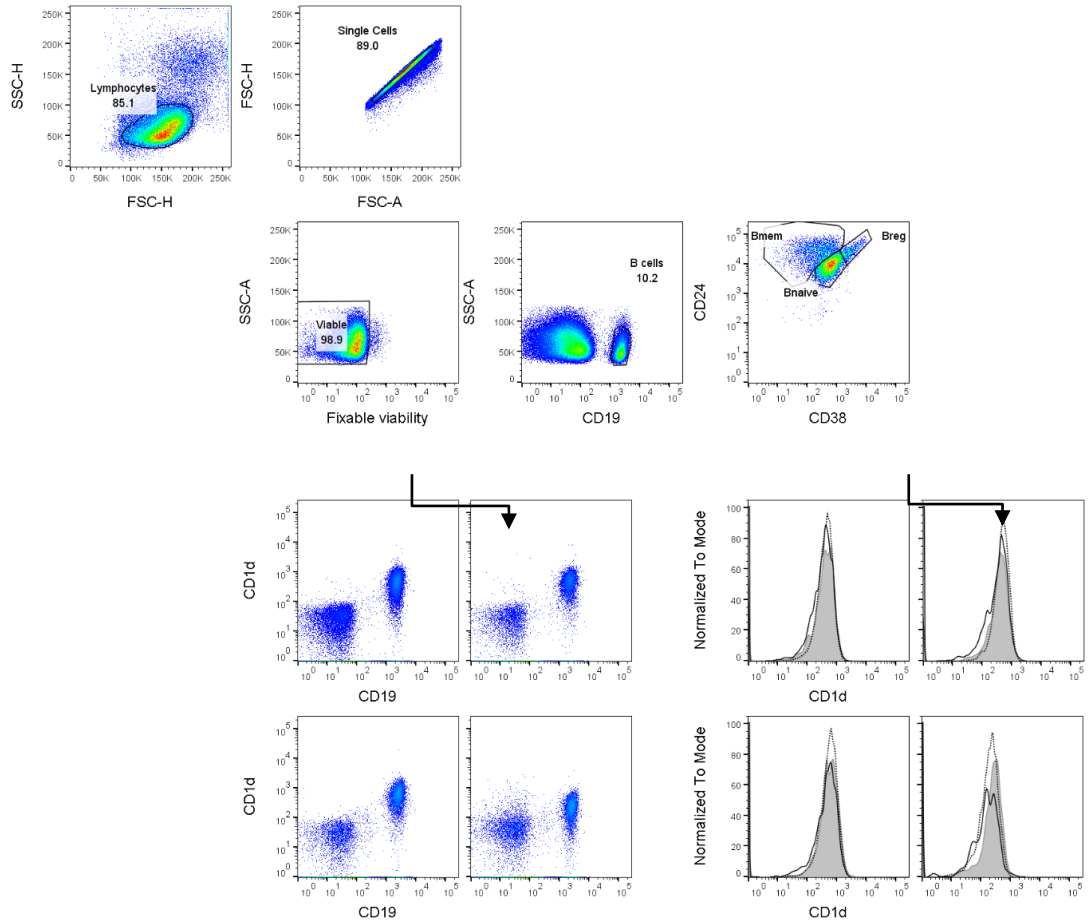

Figure shows gating strategy, firstly a threshold was set to exclude debris, lymphocytes were selected, single cells resolved by gating on the FSC area and height parameters, dead cells were excluded from analysis, B cells assigned CD19+, finally Breg, Bnaive and Bmem gates were drawn. Plots show CD1d expression is high within the CD19+ subset, relative to CD19 null cells. Expression of CD1d in Bmem (solid black line), Breg (filled grey histogram) and Bnaive (dotted black line) subsets, is shown in overlaid graphs. There is little variability in expression of CD1d in these B cell subsets.

Figure 4.11 Breg have highest CD5 expresion but CD5+ B cells not limitted to a single B cell subset

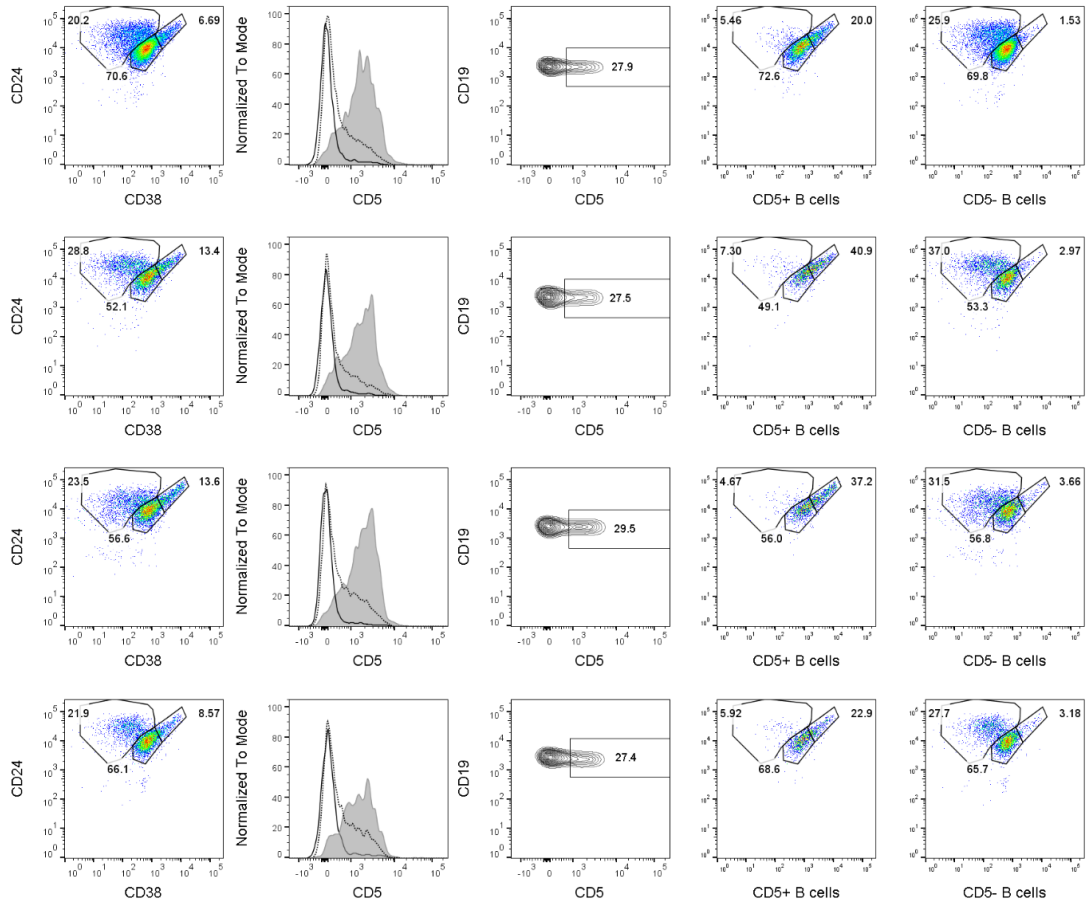

Each row shows data for 1 healthy control. Bmem, Breg and Bnaive gates were assigned (column 1). Expression of CD5 in Bmem (solid black line), Breg (filled grey histogram) and Bnaive (dotted black line) subsets, is shown in overlaid histograms in the second column. CD5+ cells were gated on a contour plot and a "not-gate" created (column 3). CD5+ and null cells were then backgated onto the CD24 and CD38 pseudocolour dot-plot, the same gates were applied to CD5+ and CD5- B cells, as those used for total B cells in column 1. Breg are highly enriched in the CD5+ gate, compared to the CD19+ population or the CD5- subset.

Figure 4.12 Bmem cells are highly enriched in the CD27+ gate

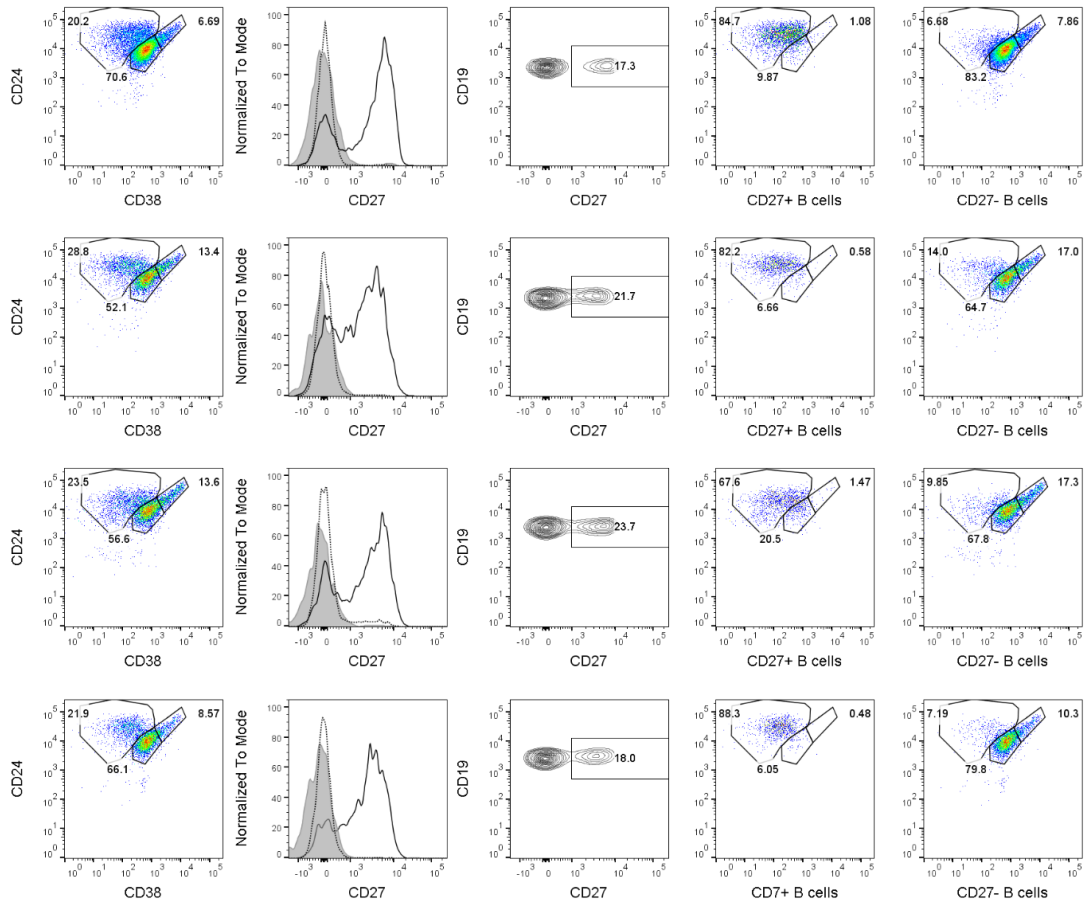

Each row shows data for 1 healthy control. Bmem, Breg and Bnaive gates were assigned (column 1). Expression of CD27 in Bmem (solid black line), Breg (filled grey histogram) and Bnaive (dotted black line) subsets, is shown in the second column. CD27+ cells were gated on a contour plot and a "not-gate" created (column 3). CD27+ and null cells were then backgated onto the CD24 and CD38 pseudocolour dot-plot, the same gates were applied to CD27+ and CD27- B cells, as those used for total B cells in column 1. Bmem are highly enriched in the CD27+ gate, compared to the CD19+ population or the CD27- subset.

Figure 4.13 Breg, Bnaive and Bmem populations correspond well with CD5 and CD27 staining pattern

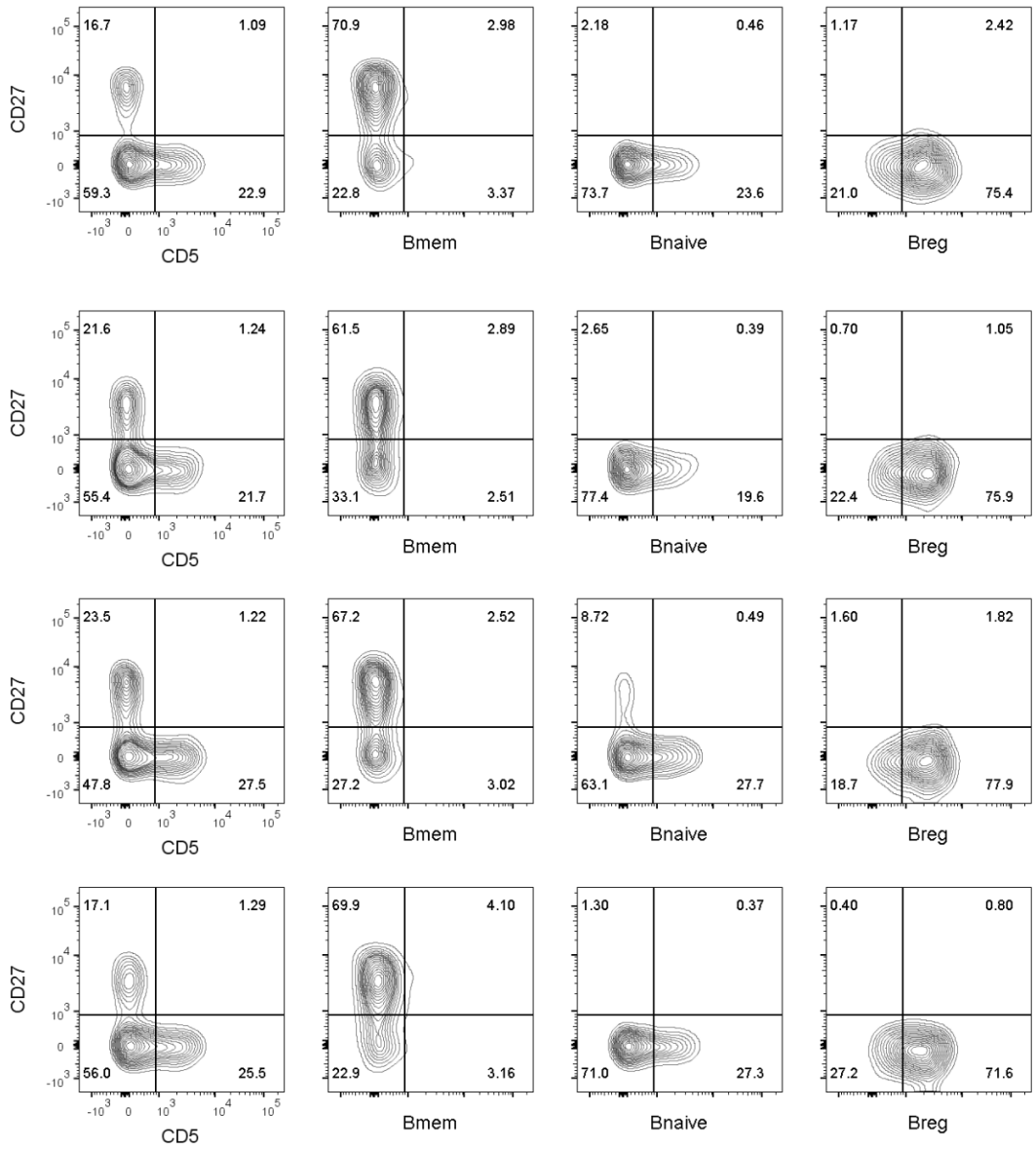

Each row shows data for 1 healthy control. A quadrant gate was created for CD5 and CD27, for total B cells (column 1). The same CD27 and CD5 quadrant gates were then applied to Bmem, Bnaive and Breg subsets (columns 2-4). Broadly speaking Bmem are CD27+ and CD5-, Breg are CD27- and CD5+, Bnaive are CD5- and CD27-.

Figure 4.14 CD24 and CD38 gates applied to CD5 or CD27 B cells, data presented as as frequency of parent and frequency of Breg, Bnaive or Bmem

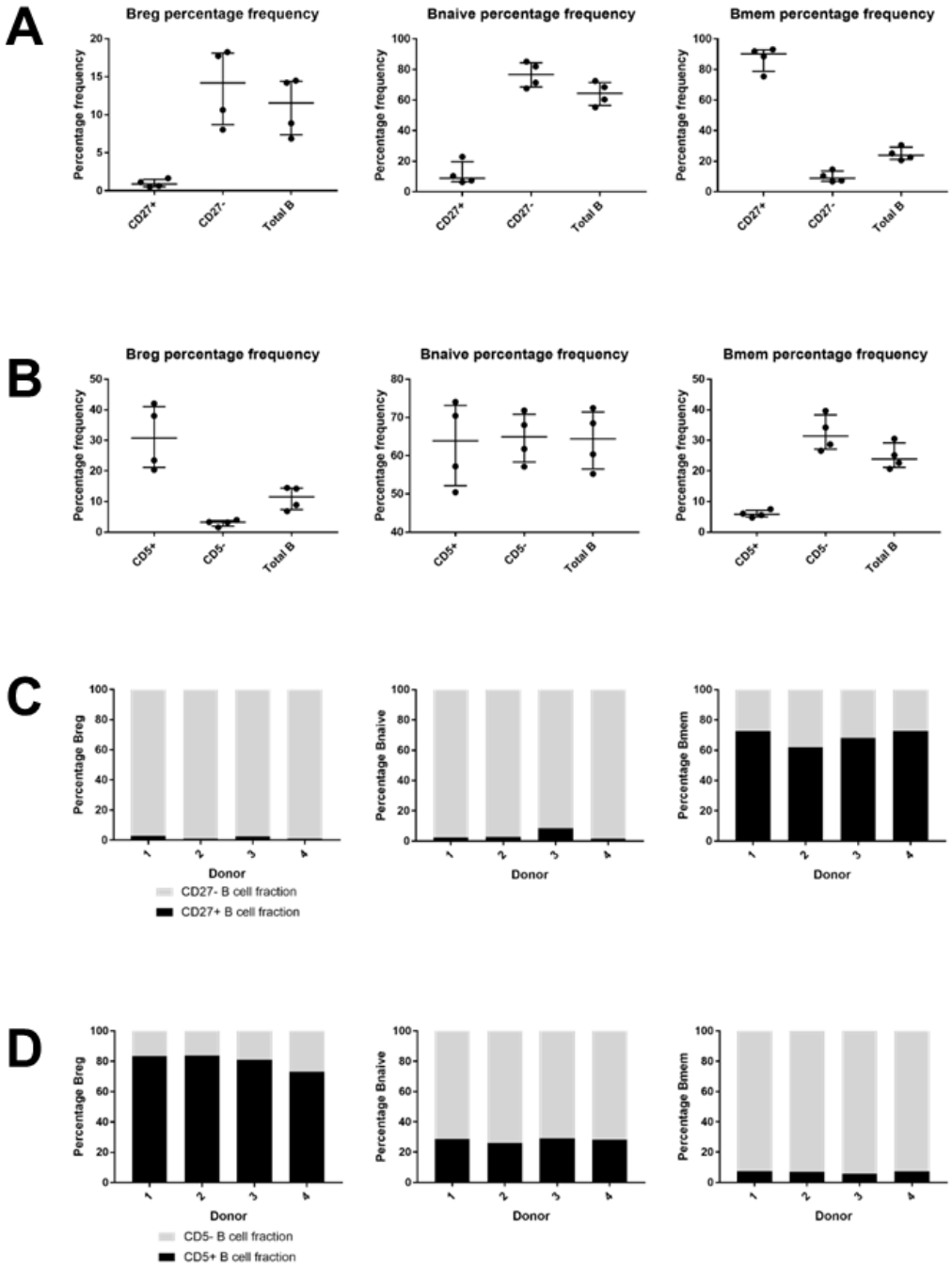

[A-B]. Frequency of Breg, Bnaive and Bmem cells in total B cells, compared to the CD27 or CD5 B cell subpopulations. Breg and Bnaive cells are reduced in CD27+ B cells, whilst Bmem frequency is higher. Bmem are enriched in the CD5- population and Breg in CD5+ population, the frequency of naïve B cells does not differ

(percentage of total B cells, CD5+ or CD5- B cells). In panels C and D the data is presented as total frequency of Breg, Bnaive and Bmem cells within the CD27 and CD5 B cell subpopulations. The majority of Bmem cells are within the CD27+ population, the majority of Breg within the CD5+ population and the majority of Bnaive cells fall within the CD5- CD27- populations. Although Bnaive frequency is similar when expressed as a percentage of parent, the CD5 null population is larger so the majority of Bnaive cells are still CD5-.

Panel A and B). However, when the data is presented as a percentage of total Bnaive cells within the CD5+ and CD5- populations, the majority of Bnaive cells fall within the CD5- gate this is because most B cells are not CD5+ (Figure 4.14, Panel C)

4.5.3.5 CD27 and CD5 immunolabelling correspond well with Breg, Bnaive and Bmem gates in fresh, healthy control samples

Quadrant gates were drawn on CD5 and CD27 biaxial plots for CD19+ cells (Figure 4.13). The same gates were then applied to B cell subsets, based on relative CD24 and CD38 expression. Breg are CD27 null and CD5+, Bmem are CD5- with the majority expressing CD27. Bnaive are predominantly CD27- but have variable expression of CD5. When this is expressed as percentage of the parent population, they do not appear to be enriched or decreased within the CD5+ or CD5- B cell populations (Figure 4.14, Panel A and B). However, when the data is presented as a percentage of total Bnaive cells within the CD5+ and CD5- populations, the majority of Bnaive cells fall within the CD5- gate this is because most B cells are not CD5+ (Figure 4.14, Panel C)

4.5.3.6 Breg are IgD+, have the highest expression of IgM and are assigned Bm2' B cells

IgD and IgM staining was conducted in 2 patients in a 5-colour flow cytometry panel with CD19, CD24 and CD38 (Figure 4.15). Results verify previous findings, Breg have a distinct immunophenotype, corresponding to an early phase in B cell maturation. Breg are IgD+ and have the highest surface expression of IgM. These markers are expressed on a continuum, with gradual downmodulation of IgM as transitional B cells mature to naïve B cells and declining IgD expression, as naïve B cells mature into memory B cells. In keeping with this, IgD null cells are only observed in the Bmem cell population. Breg correspond to the Bm2' subset ($CD38^{high}$ and in the

Bmem cell population. Breg correspond to the Bm2' subset ($CD38^{high}$ and IgD+), these cells are also referred to as GC-founder, immature or transitional B cells.

Bm2' ($CD38^{high}$ IgD+) cells have been shown to be predominately germline, with few mutations in Ig gene segments (Pascual, Liu et al. 1994); they are known to have a higher expression of CD10, CD5 and greater propensity to undergo apoptosis (Bohnhorst, Bjorgan et al. 2001, Sims, Ettinger et al. 2005). This subset of cells is the first to recover after rituximab treatment or HSCT, marking them as the earliest BM emigrants (Anolik, Friedberg et al. 2007, Palanichamy, Barnard et al. 2009). Relative enrichment after rituximab treatment was shown in the preceding chapter and absence of CD27 expression above, further demonstrating that Breg are pre-germinal centre, immature cells.

4.5.3.7 Positive correlation between CD95 and Bmem frequency in patients

CD95 and CD10 staining was conducted in 9 patients in a 5-colour flow cytometry panel with CD19, CD24 and CD38. The patient group comprised 5 individuals with PR3-ANCA and diagnosis of GPA, 4 with MPO-ANCA and diagnosis of MPA. The sex distribution was 3 male and 6 female, patients' age ranged from 21-65 years (median age was 56 and mean 50.4 years, data had a normal distribution as assessed by D'Agostino and Pearson test).

CD95 is the Fas death receptor, expression increases susceptibility of the cell to apoptosis. CD95 is induced in persistent states of immune activation and is a marker of exhaustion. CD95 expression on naive B cells is observed in SLE and associated with a switch to double negative memory B cells (CD27- IgD-) or plasma cells (Ducreux, Nieuwland et al. 2014). CD27- IgD- CD95+ B cells also correlate with clinical score and C' consumption in SLE (Jacobi, Reiter et al. 2008). Higher CD95+

Figure 4.15 IgD and IgM staining in combination with CD19, CD24 and CD38

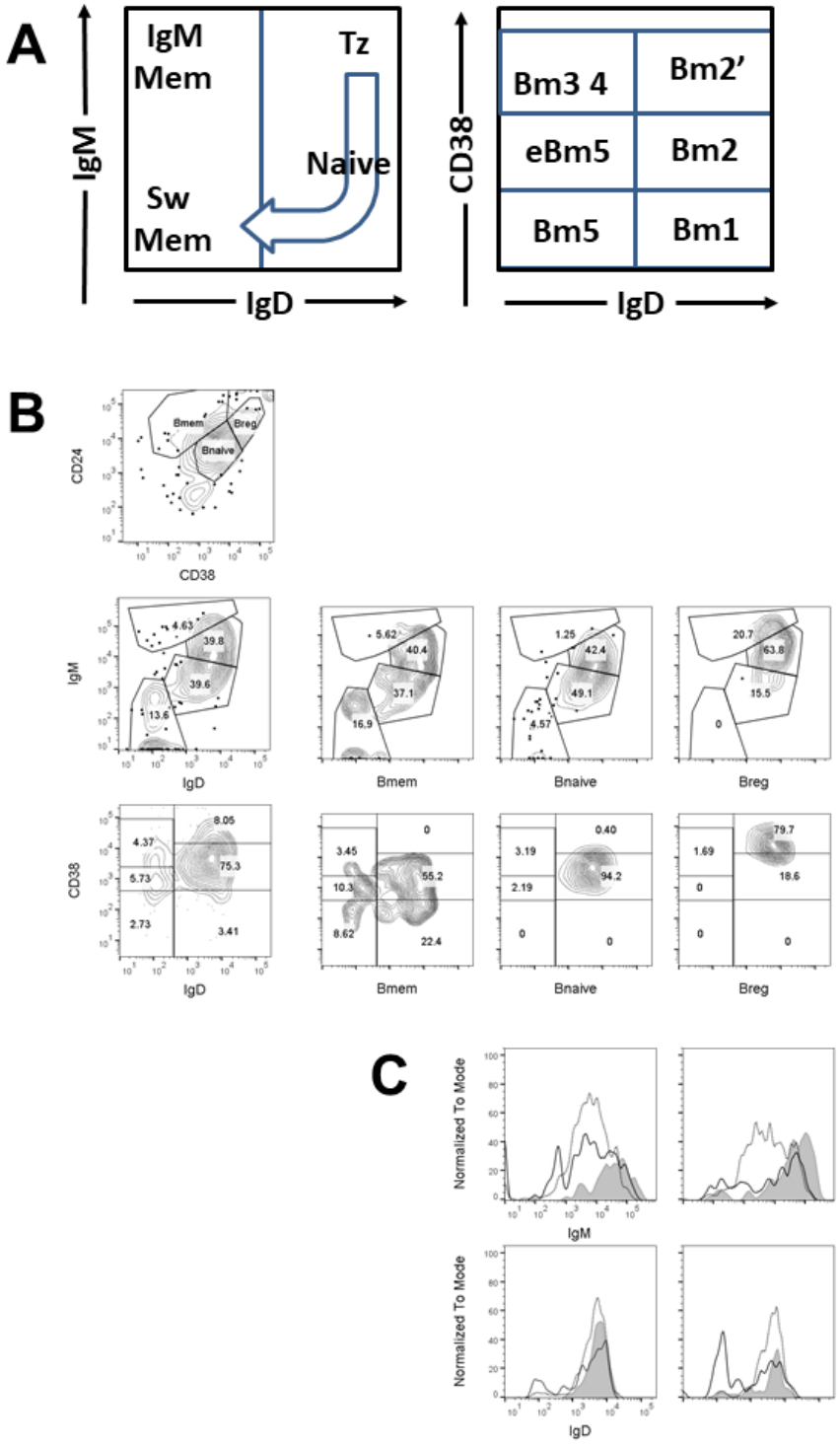

[A.] Gating strategy shown in diagram. [B]. Contour plots for 1 patient shown. Bmem, Breg and Bnaive gates assigned (top row). B cells assessed for relative of expression of IgM and IgD; 4 gates were drawn, and subsequently applied to the Bmem, Bnaive and Breg subpopulations. Breg are IgD+ and have the highest expression of IgM. IgD null cells are only observed in the Bmem cell population. In row 3, the Bm1-5 gating

strategy was applied. Breg are in the top right corner and using this designation, would be assigned Bm2' B cells. [C] IgD and IgM overlaid histograms shown for both patients. Bmem (solid black line), Breg (filled grey histogram) and Bnaive (dotted black line) subsets. IgD null cells are only observed in the Bmem population and Breg cells express the highest levels of IgM.

B cells frequency at baseline, is associated with worse prognosis after rituximab treatment in RA; this might be because CD95 is expressed on plasmablasts, which downmodulate CD20 making them resistant to treatment (Adlowitz, Barnard et al. 2015). Breg are usually defined as CD95 low and CD10 high (Sims, Ettinger et al. 2005), however CD95+ Breg have been reported in UC, with expression thought to indicate exhaustion in this subset (Wang, Zhu et al. 2016).

Regression analysis was performed for CD95 or CD10+ B cells (compared to Breg, Bnaive and Bmem). Graphs for Bmem and Breg are shown in Figure 4.16. CD95+ B cells had a positive correlation with Bmem (P=0.0323*, n=9) and tended towards an inverse relationship with Breg (P=0.0535, n=8). This was only when one outlying Breg sample was excluded (32.2%), when reincluded significance was lost (P=0.2387, n=9). Surprisingly there was no statistical relationship between Breg and CD10+ B cells (P=0.2615, n=9 and P=0.2999, n=8), this warranted further investigation.

4.5.3.8 CD10 expression is highest in Breg and CD95 in CD24 null B cells

Firstly, geometric MFI was compared for Breg, Bnaive, Bmem and CD24 null B cells (Kruskal-Wallis and Dunn's multiple comparison test). Breg had significantly higher CD10 MFI than all other B cells populations. CD24- B cells which are putative plasma blasts, had significantly higher CD95 MFI than Breg or Bnaive cells (Figure 4.17, Panel A).

Next, CD95 and CD10 gates were applied to B cell subsets. CD24- B cells had a significantly higher proportion of CD95+ cells than Breg or Bnaive; Breg had a higher proportion of CD10+ cells than any of the other subsets (Figure 4.17, Panel B). Then the CD24 and CD38 gates were applied to CD10 or CD95 B cells (Figure 4.17, Panel C). The frequency of Breg within the CD10 population varied widely (mean

Figure 4.16 Positive correlation between Bmem and CD95 B cells, no relationship between CD10 B cells and Bmem or Breg

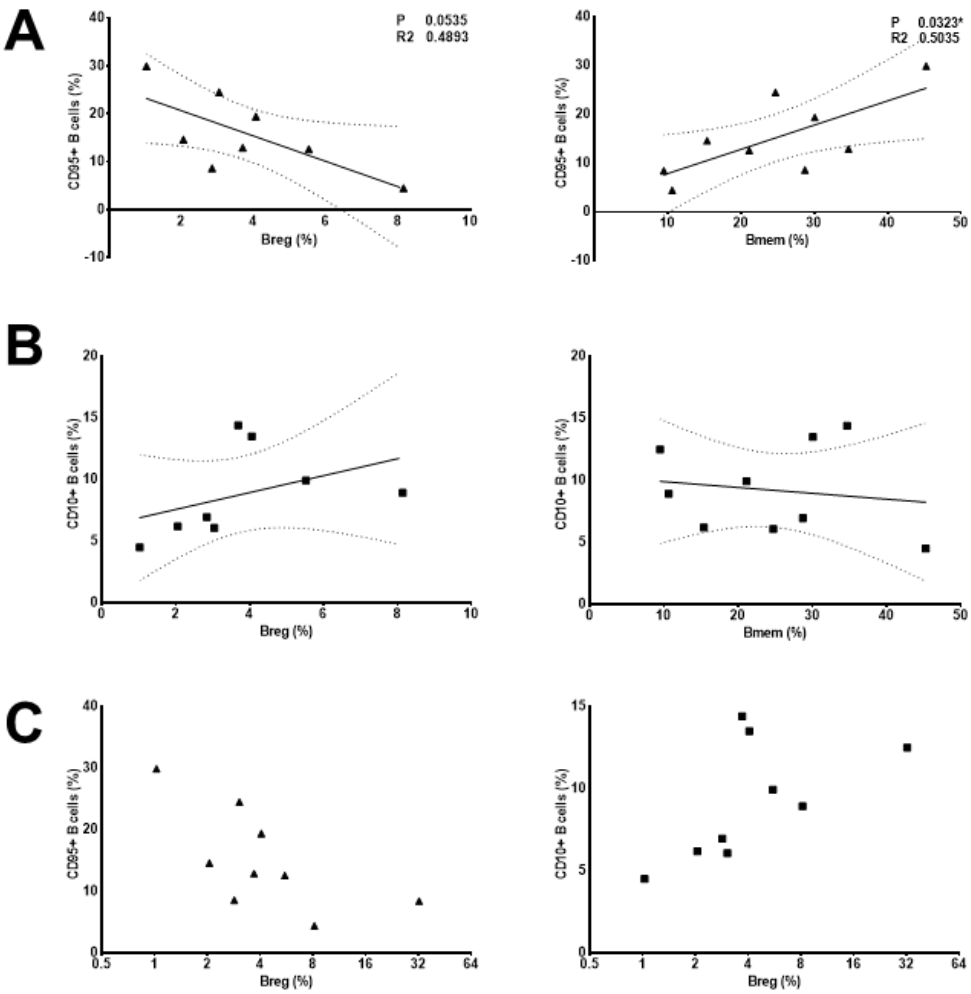

[A].CD95 B cells had a positive correlation with Bmem and trend towards an inverse relationship with Breg. [B]. There was no relationship between CD10 B cells and Breg or Bmem. In panels A and B, one outlying data point was excluded (very high Breg frequency after rituximab therapy). Panel [C] shows all 9 Breg data points (natural log, on the X axis). Results still did not reach the threshold for statistical significance.

frequency 37.29%, standard deviation 27.43% and ranged from 4.71-90.38%). This is likely due to the use of patients' samples, which sometimes have very few Breg and CD10+ B cell frequency.

Finally, flow cytometric data is presented (Figure 4.18). Overlaid histograms show that CD10 is highly expressed on Breg, this is a shift and does not represent a discrete positive cell population (Breg histograms overlap those of the other B cell populations). CD95 expression is low on Breg but variable on Bmem and CD24- cell (CD95 high cells can be identified). CD24 and CD38 biaxial contour plots are also shown, data shown for total B cells, CD10+ B cell and CD95+ B cells and 3 patients. CD10+ B cells are predominately Breg; within CD95+ B cells, Bmem and CD24- B cell populations become more prominent (Figure 4.18, Panel C).

Figure 4.17 Graphical summary of CD10 and CD95 flow cytometry data

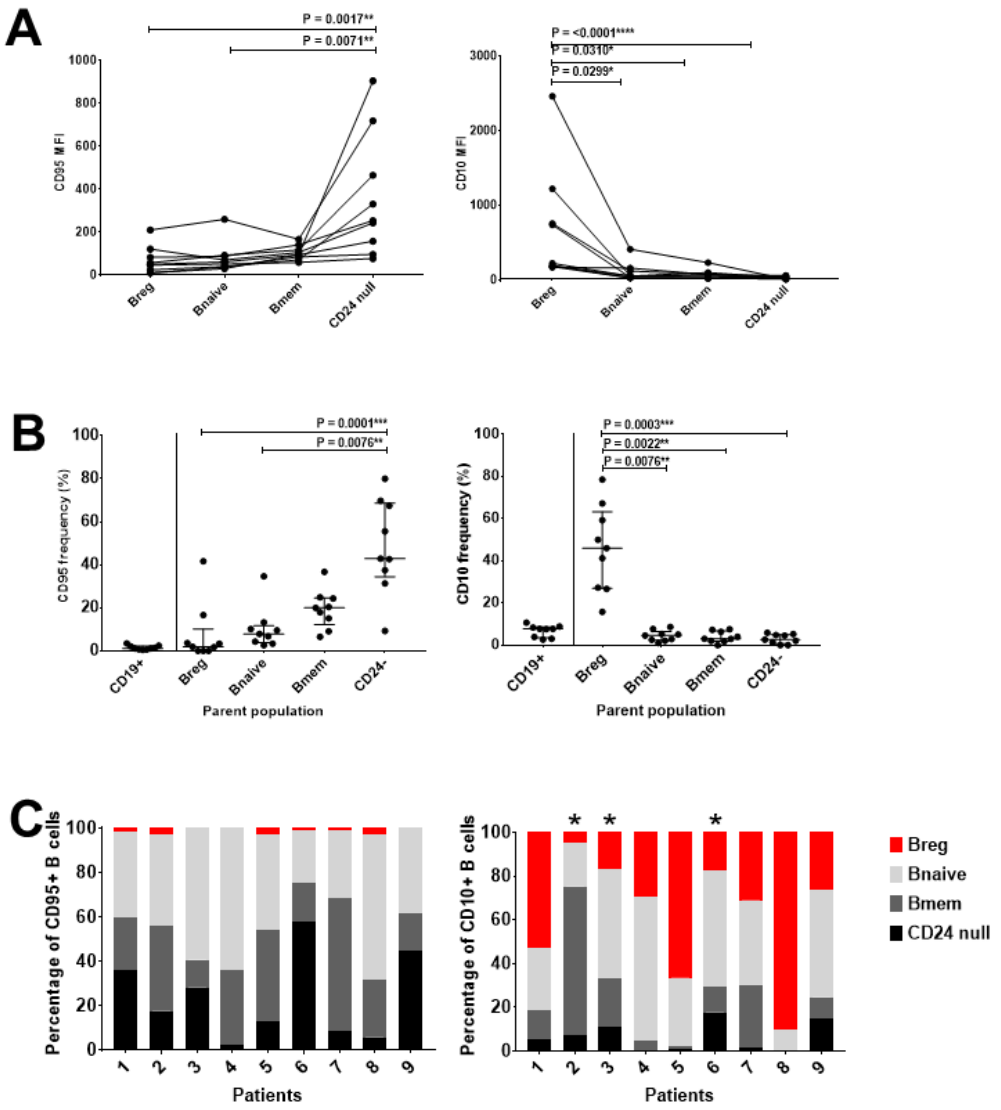

[A]. CD95 and CD10 geometric MFI in B cell subsets. CD24 null B cells have significantly higher CD95 MFI than Breg or Bnaive cells. Breg have higher CD10 MFI than all other B cells populations. [B]. CD95 and CD10 gates applied to B cell subsets. CD24 null cells have a higher proportion of CD95+ cells than Breg or Bnaive; Breg have a higher proportion of CD10+ cells than any of the other subsets. [C]. CD24 and CD38 gating applied to CD10 or CD95 B cells (results expressed as percentage of parent population, CD95+ or CD10+ B cells). There were few Breg in the CD95 B cell population, with more Bmem and CD24- B cells. Breg frequency was higher in CD10+ B cells but varied a lot. This may be partly due to low Breg frequency, asterisks denote samples with fewer than 50 Breg in the parental CD19+ population.

Figure 4.18 Flow cytometry plots of CD10 and CD95 expression profiles

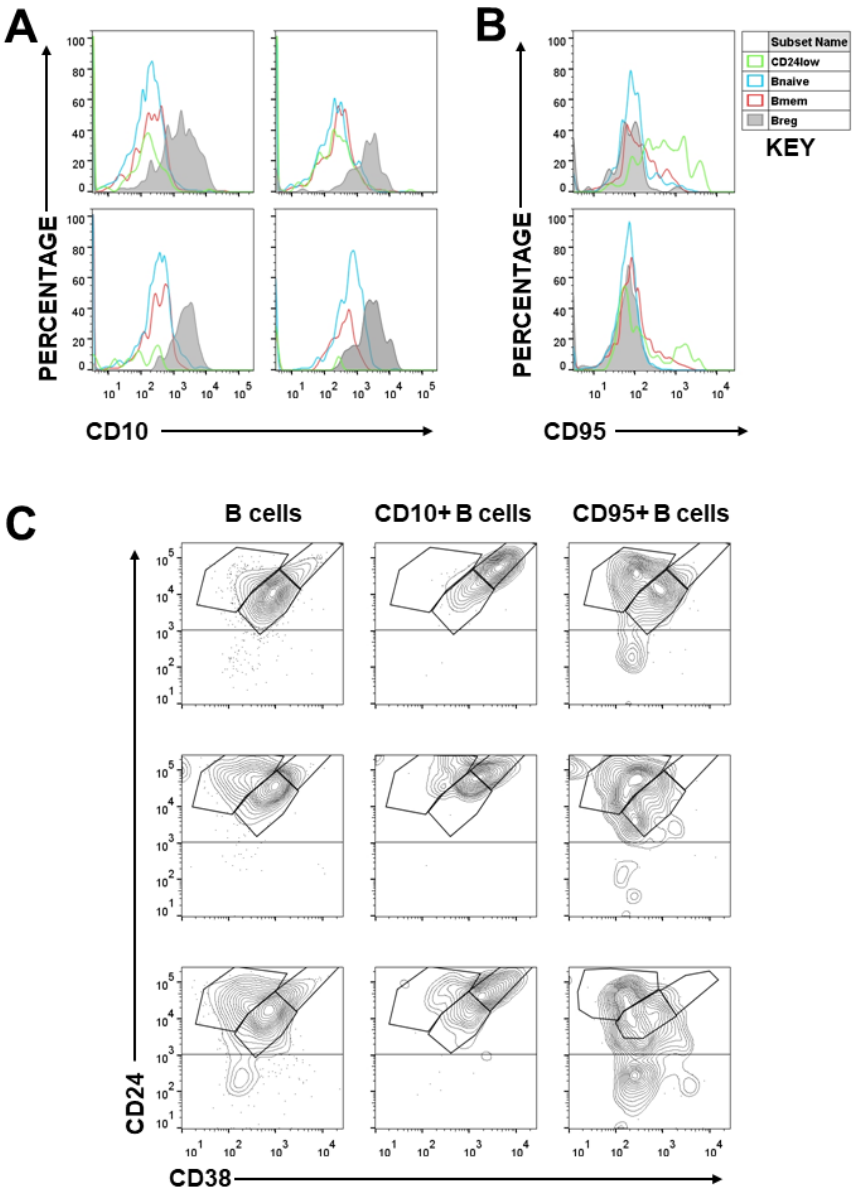

[A-B]. CD10 and CD95 overlays for B cell subsets. Breg shown in filled grey histograms, CD24- cells in green. CD10 expression is high on Breg and CD95 expression is low. CD95 expression is variable on Bmem and CD24- CD19+ cells. [C]. CD10 and CD95 B cells backgated on CD24 and CD38 biaxial plots. CD10+ B cells are predominately Breg. Bmem and CD24- B cell populations become more prominent within CD95+ B cells.

4.6 Key findings

4.6.1 There is little differential expression in CD1d in B cells

B cells express high levels of CD1d compared to CD19 null lymphocytes but there is little differential expression within CD19+ cells (CD5 and CD1d biaxial plots and CD1d staining in combination with CD24 and CD38).

4.6.2 CD5 B cells are reduced in AAV, but CD5 expression not limited to a single B cell subset and CD5 expression is inducible

CD5 B cells are reduced in patients compared to controls, irrespective of disease activity. When CD5 was stained in combination with CD24 and CD38, Breg had highest expression but this marker was not unique to one B cell subset. CD5 was shown to be induced in apoptotic cells, after freeze-thawing. In contrast CD24 and CD38 staining was very stable.

4.6.3 CD24 and CD38 B cell subsets are distinct

Additional phenotyping verified Breg were phenotypically distinct from other B cell subsets (results summarised in Table 4.3). Breg were CD27-, $CD10^{high}$ and $CD95^{low}$, concordant with Gary Sim's characterisation of T1 B cells (Sims, Ettinger et al. 2005). Breg were IgD+ and had the highest expression of IgM, corresponding to the Bm2' immature population.

CD27 staining was highly concordant with Bmem. IgD and IgM negative B cells were only observed in Bmem population. This is indicative of cells which have been involved in a germinal centre reaction undergone Ig class switch. CD95 positive B cells have positive correlation with Bmem. A CD24- population of putative

plasmablasts, with very low frequency in the CD19 population, is better resolved within the CD95+ subset. Results are summarised in Table 4.3.

CD24, CD38, CD10, CD5 and IgM are not discrete cell markers, these antigens are expressed in continuum. Breg have the highest expression, gradually downmodulated Bnaive cells and consistent with maturation (Figure 4.19),

Table 4.3 Verification that CD24 and CD38 B cell subsets are distinct

	Breg	**Bmem**	**Bnaive**
CD24	+++	+++	+
CD38	+++	Low	+
CD10	++	Negative	-/+
CD5	+	-/+	-/+
CD27	Negative	+++	Negative
CD95	Negative	+	-/+
IgM	+++	-/+	+
IgD	+	-/+	+

Figure 4.19 Verification that CD24 and CD38 B cell subsets are distinct

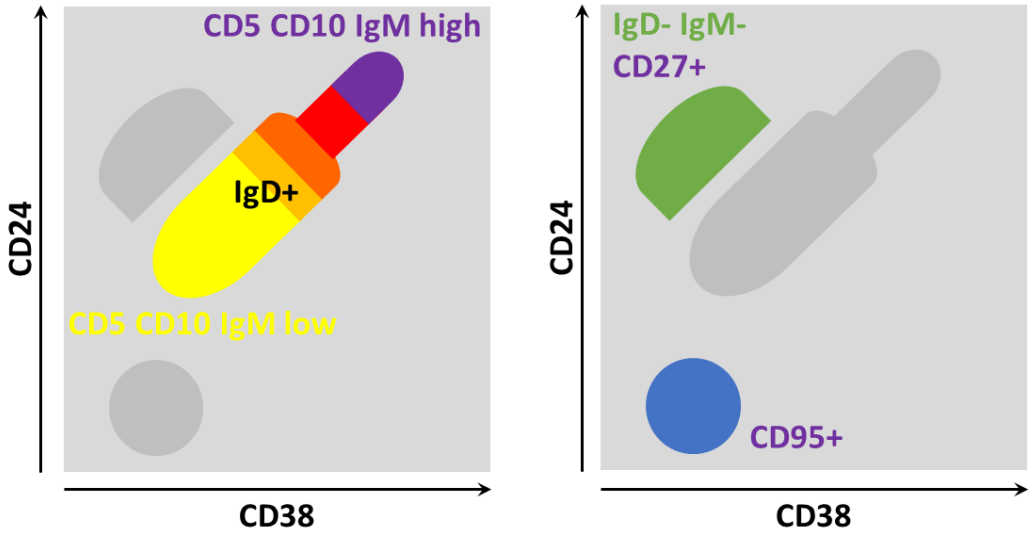

The left panel represents gradual reduction in CD24, CD38, CD10, CD5 and IgM, as antigen inexperienced, IgD+ B cells mature (highest expression shown in deepest colour, with gradual downmodulation). The other CD24 and CD38 B cell subpopulations are described in the right panel. IgD and IgM negative events are only observed in the Bmem population (shown in green), this cells also express high levels of CD27, indicative of B cells which have been involved in GC reaction and undergone Ig class switch. Back-gating of CD95+ B cells, revealed a CD24- CD38- putative plasmablast population (blue).

4.7 Discussion

Interaction of CD1d+ APC and iNKT is an important tolerogenic mechanism, with release of IL-10 and induction of Treg (Sonoda and Stein-Streilein 2002). iNKT are also reported to limit humoral responses; following NK1.1 antibody-mediated-cell-depletion in mice, antigen specific B cells, antibody titres and somatic hypermutation are reduced (Rydyznski, Daniels et al. 2015). iNKT are critical for clearance of apoptotic cells, limiting activation of autoreactive B cells and antibody production (Wermeling, Lind et al. 2010). In humans, a defect in CD1d cycling and reduced peripheral blood iNKT frequency is observed in SLE (Bosma, Abdel-Gadir et al. 2012) and CD5+ CD1d^{high} B cells are reduced in rheumatoid arthritis (Ma, Liu et al. 2013, Cui, Zhang et al. 2015).

In this study, CD1d was present on the CD19 population but a CD5+ CD1d^{high} B cells could not be detected (Figure 4.1). Uniform CD1d expression in peripheral B cell subsets is shown in Figure 4.10 and has been reported previously (Zeng, Ghnewa et al. 2013). CD1d staining was not increased on fixation and permeabilization, it was reduced (Figure 4.3). The reason for this was not clear; fixation affects cell-intrinsic autofluorescence and some markers are very susceptible to formaldehyde modification, with loss of key antigenic determinants.

Although not detected in peripheral blood, CD1d^{high} B cells may be present in lymphoid tissue. Splenic marginal zone B cells are reported to be CD1d^{high}, they bridge native and adaptive immunity, are particularly adept in capturing antigen, with rapid antibody production, conferring protection against blood borne infection. Following CD1d antigen capture B cells recruit iNKT, become activated, proliferate and produce antibodies (Galli, Nuti et al. 2003, Barral, Eckl-Dorna et al. 2008, Zeng, Ghnewa et al.

2013). B cell interaction with iNKT cells, bypasses the need for cognate peptide and TCR help.

This seemingly contradicts evidence that iNKT limit autoantibody responses, however B cells that have been activated by iNKT cannot induce antigen-specific proliferation of CD3+ T cells (Zeng, Ghnewa et al. 2013). This suggests existence of an intrinsic control mechanism, to prevent harmful autoreactive responses. Functional assessment of B cells and iNKT has not been conducted in AAV and is certainly warranted; it would be interesting to co-culture B cells in the presence of iNKT, assessing activation status and ANCA induction.

Differential expression of CD5 was observed in B cells, with reduction in AAV patients relative to controls. CD5 positive B cells have unique ontogeny in mice and are termed B1a B cells. They are enriched in peritoneal and pleural cavities, arise from a foetal precursor, are self-renewing and produce polyreactive antibodies (Gagro, McCloskey et al. 2000). CD5 promotes B-cell survival through stimulation of IL-10 production (Gary-Gouy, Harriague et al. 2002) and a subset of CD5+ B cells in human peripheral blood are even reported to express FoxP3 (Noh, Choi et al. 2010). Critically, CD5 is associated with the human B cell antigen receptor complex and negatively regulates signalling.

In addition to constitutive expression on B1a cells, CD5 null conventional B2 cells, can be induced to express CD5 with BCR and CD40 ligation (Gagro, McCloskey et al. 2000). The results showing induction of CD5 in frozen cells (Figure 4.4), verifies that CD5 is an activation marker, induced in apoptotic cells.

CD5 B cells are reported to be decreased in the aged (Colonna-Romano, Bulati et al. 2003), which could skew results however, low CD5 B cell frequencies were observed in AAV patients across the entire age range (17-85 years).

CD5 was suggested as a surrogate marker of Breg in AAV (Bunch, McGregor et al. 2013). $CD24^{high}$ and $CD38^{high}$ Breg designation is more stable and reveals greater heterogeneity in patient groups (Figure 4.2, panel C). There was no correlation between Breg and CD5+ in healthy controls (Figure 4.8, Panel C).Some additional immunophenotyping was conducted in healthy controls (CD24 and CD38 tested alongside CD5, CD1d, CD27), this extended flow cytometry panel showed that CD5 was not limited to a single CD24 CD38 subset (Figure 4.11). This testing was not extended to AAV patients. Previously, CD27+ CD5+ B cells were shown to be significantly reduced in remission and active GPA (Eriksson, Sandell et al. 2010); this population may correspond to circulating marginal zone B cells (IgD+ IgM^{high} CD27+), which positively correlate with serum IgM levels in AAV patients (Thiel, Salzer et al. 2013). CD5+ B cells (expressed as percentage of Breg), have also been shown to be reduced in active disease and restored in remission (Aybar, McGregor et al. 2015). The fact that CD5+ frequency showed considerable heterogeneity when expressed as a frequency of Breg in this study, further suggests CD5 alone is not a good surrogate marker for definition of $CD24^{high}$ $CD38^{high}$ Breg.

CD5 B cells did correlate with Breg in patients. CD5 B cell frequency was previously shown to correlate well with AAV disease activity after rituximab (Bunch, McGregor et al. 2013) but not after conventional treatment (Unizony, Lim et al. 2015). This is because the newly emerging B cells from the BM are phenotypically homogenous (Palanichamy, Barnard et al. 2009), verified in the preceding chapter Figure 3.13).

Increased CD5 frequency, was not more widely observed patients with generalised lymphopenia (Figure 4.9, Panel C). Stalling B cell maturation may protect from relapse after rituximab therapy, with reduced frequency of memory B cells (IgD- IgM- CD27+) and higher frequency naïve B cells (IgD^{high} IgM+ CD27-) conferring protection (Venhoff, Niessen et al. 2014).

There are no definitive markers of memory B cells; as many as 50% express IgM, with CD27- and IgD+ memory B cell subsets described. Heterogeneity in IgM and IgD in Bmem cells was indeed observed, but class-switched IgM- and IgD- cell were exclusively detected within the Bmem cell population (Figure 4.15).

CD25+ CD27+ and CD27+ $CD24^{high}$ B cells have also been attributed immunoregulatory function (Amu, Tarkowski et al. 2007, Iwata, Matsushita et al. 2011). A reduction in CD27 CD24high B cells was reported in AAV (Lepse, Abdulahad et al. 2013), unfortunately comparative testing was not conducted in patients to verify this finding (most testing pre-dated this publication). Bmem expression of CD27 was verified in 4 healthy controls, 67.9-88.3% of CD27+ cells fell within the Bmem gate (Figure 4.12).

Breg cells corresponded well with the Bm2' subset (Figure 4.15); this subset was previously shown to be reduced in active GPA (Eriksson, Sandell et al. 2010). Bm2' B cells are known to have very few mutations in Ig gene segments and to occupy the marginal B cell zone in tonsil (Pascual, Liu et al. 1994).

CD95 and CD10 was additionally assessed however, testing was carried out in patients only. High CD95 and low CD5 expression has previously been shown in SLE (Huck, Jamin et al. 1998). Gain of CD95 expression on naive B cells is associated with a

switch to double negative memory B cells (CD27- IgD-) and plasma cells (CD19+ CD20- CD38+) in SLE patients (Ducreux, Nieuwland et al. 2014).

CD95+ B cells positively correlated with Bmem and had an inverse relationship with Breg (Figure 4.16, Panel A). Because the balance of these two subsets is important in determining patient outcome, CD95 may be a good prognostic marker in AAV. Indeed, the frequency of CD95+ B cells at baseline, was shown to determine clinical outcome after rituximab in rheumatoid arthritis (Adlowitz, Barnard et al. 2015). Frequency of CD95+ double negative memory B cells has also been linked to increased SLEDAI and C' consumption in SLE (Jacobi, Reiter et al. 2008).

Back-gating onto CD24 and CD38 flow cytometry plots, also revealed a population of CD24- CD38- putative plasmablasts (Figure 4.18, Panel C), which not easily resolved from the CD19 parent population.

CD95 not only denotes B cell differentiation but is also a marker of cellular activation and exhaustion. CD95, CD80 and CD86 expression is increased in Systemic sclerosis (Sato, Fujimoto et al. 2004). CD95 expression is higher in B cells from aged individuals (Chong, Ikematsu et al. 2005) and exhaustion is inferred, due to the relationship with Ig levels in ulcerative colitis patients (Wang, Zhu et al. 2016). The concepts of cellular exhaustion and immunosenescence have not yet been explored in AAV.

Breg were also shown to be CD10+ (Figure 4.18, Panel A), the prototypic transitional B cell marker (Sims, Ettinger et al. 2005). Collectively the evidence places Breg as immature cells (CD27- CD10+, CD5+, IgD+ IgM^{high}), which are first repopulate the blood after rituximab therapy (Figure 3.13). In contrast Bmem cells are further advanced in their differentiation and show evidence of prior germinal centre reaction

and IgG class switch (CD27+, IgD-/low, IgM-/low). CD5 is not expressed by a single cell subset and can be induced on freeze-thawing. Both CD5 and CD95 indicate increased propensity to apoptosis and activation status.

B cell classification in AAV has been limited to ~6 colour flow cytometry panels and further classification would be of great benefit. Since completion this project, new advancements have been made in instrumentation, permitting simultaneous detection of 40+ parameters (Aurora^{TM} spectral analyser [Cytek Biosciences, Fremont, California], Helios^{TM} mass cytometer [Fluidigm, San Francisco, California] and Symphony^{TM} flow cytometer [BD Biosciences, San Jose, California]).

Chapter 5 Assessment of B cell function

5.1 Background

IL-10 is the prototypic immunoregulatory cytokine. It limits T cell responses indirectly by reducing monocyte antigen presentation (de Waal Malefyt, Haanen et al. 1991), production of inflammatory cytokines by macrophages (Fiorentino, Zlotnik et al. 1991), differentiation and maturation of dendritic cells.

IL-10 also acts directly on T cells, limiting intracellular signalling pathways downstream of CD28 and ICOS (Taylor, Akdis et al. 2007); it limits IL-2 production, the critical T survival factor, resulting in decreased proliferative capacity (de Waal Malefyt, Yssel et al. 1993). IL-10 maintains regulatory T cell function in mice preventing colitis (Murai, Turovskaya et al. 2009). In children with severe early-onset enterocolitis, loss of function mutations in the IL-10 receptor have been described; IL-10 fails to limit monocyte TNFα production *in vitro* in these patients (Glocker, Kotlarz et al. 2009). Adenoviral transfer of IL-10 limits collagen induced arthritis in mice (Whalen, Lechman et al. 1999).

When IL-10 deficiency is limited to B cells, mice develop more severe arthritis in the AIA model (Carter, Vasconcellos et al. 2011). IL-10 competent B cells were subsequently shown to induce Treg, resulting in reduced frequency of Th17 and Th1 T cells at the site of inflammation (Carter, Rosser et al. 2012).

This function is attributed to $CD24^{high}$ $CD38^{high}$ Breg in man, which are IL-10 competent, limit Th1 and Th17 differentiation, promote Treg differentiation and enhance their expression of FoxP3 (Blair, Chavez-Rueda et al. 2009, Flores-Borja,

Bosma et al. 2013). CD5+ B cells are also enriched in ability the produce IL-10 (Gary-Gouy, Harriague et al. 2002).

Immunomodulatory effect of B cells on T cells, can be modelled *in vitro* and role of IL-10 assessed. Bouaziz *et al* observed activated B cells or supernatants, limited CD4+ CD25- T cell proliferation, assessed by CFSE dilution (Bouaziz, Calbo et al. 2010). Blair *et al* reported Breg reduced IFNγ and TNFα production by CD4 T cells in a dose dependent manner (Blair, Norena et al. 2010). In both studies, the inhibitory effect was only particularly blocked by an agonistic IL-10 antibody. Additional modulatory mechanisms were at play, which relied in-part on direct B-T cell contact, demonstrated by blocking the co-stimulatory molecules CD80 and CD86 (Blair, Norena et al. 2010).

B cell IL-10 competency can also be assessed *in vitro*; IL-10 is induced in B cells by TLR ligands, CD154 or BCR ligation (Bouaziz, Calbo et al. 2010, Iwata, Matsushita et al. 2011). Tedder *et al* regard the induction of this cytokine so critical to immunomodulation by B cells, they classify cells solely on this basis (Tedder 2015). These B10 cells, have a memory phenotype, are enriched in autoimmunity and limit monocyte TNFα production *in vitro* (Iwata, Matsushita et al. 2011).

IL-10 B cells have subsequently been shown to be reduced in many autoinflammatory conditions, including type 1 diabetes, rheumatoid arthritis, psoriasis, juvenile dermatomyositis, primary Sjögren's syndrome, pemphigus and ankylosing spondylitis (Hirotani, Niino et al. 2010, Jagannathan, McDonnell et al. 2010, Knippenberg, Peelen et al. 2011, Li, Zhong et al. 2012, Daien, Gailhac et al. 2014, Zhu, Xu et al. 2015, Chen, Zhang et al. 2016, Hayashi, Yanaba et al. 2016, Piper, Wilkinson et al. 2018). IL-35 and TGFβ competent B cells have additionally been shown to be important in

limiting immune activation (Parekh, Prasad et al. 2003, Natarajan, Singh et al. 2012, Lee, Stott et al. 2014, Shen, Roch et al. 2014).

5.2 Aim

To assess whether B cells were dysfunctional in AAV, relative to healthy controls.

At the time of undertaking this research (samples isolated between 20/08/12 and 08/04/2013), the function of Breg in AAV had not been assessed. I had previously demonstrated an imbalance in B cell subsets, with reduction in Breg defined as CD5+ or $CD24^{high}$ and $CD38^{high}$. Blair *et al* had shown that Breg defined by expression of these markers, limited Th1 differentiation *in vitro* and had increased capacity to produce IL-10; these functions were defective in SLE (Blair, Norena et al. 2010). Assessment of immunoregulatory function in AAV, would therefore be judged on B cell IL-10 competency and effect on CD4+ CD25- T cells *in vitro*.

5.3 Methods in brief

A summary of the techniques employed is provided, detailed protocols can be found Chapter 2.

5.3.1.1 T and B cell co-cultures

Effects on T cell activation were assessed in a subset of individuals from the main cohort: 5 remission patients (1 male, 2 PR3-ANCA, 3 MPO-ANCA) and 5 controls (4 male). CD4+ CD25- T cells were magnetically isolated, cultured alone or with flow

cytometry sorted B cell subsets at a fixed ratio of 1:4 B:T. Cultures were conducted for 5 days, in the presence of plate bound anti-CD3 and soluble anti-CD28. For the last 4 hours, Brefeldin A, Monensin, PMA and ionomycin were added. Viability was assessed, CD4, IFN-γ and TNF-α staining conducted. Results were expressed as percentage change, relative to T cells cultured alone (normalised to zero).

5.3.1.2 IL-10 induction

B cell IL-10 production was assessed in a subset of individuals from the main cohort: 12 remission patients (5 male, 8 PR3-ANCA, 3 MPO-ANCA, 1 ANCA negative); 4 rituximab-treated patients (2 male, 4 PR3-ANCA) and 8 controls (4 male). Immunophenotyping was conducted at baseline. PBMCs were then cultured for 48 hours, alone, with CPG or with combined CPG and CD154. For the last 5 hours Brefeldin A, PMA and ionomycin were added. Viability was assessed, CD19, CD24, CD38, IL-10, LAP-TGFβ and TNF-α staining conducted. Supernatants were retained.

5.3.1.3 Measurement of soluble cytokine in supernatants

A cytometric bead array (CBA) and ELISAs were conducted to compare the profile of cytokines released into the supernatants, of PBMC stimulated to produce IL-10. The complete list of analytes and limits of detection are provided in (Table 2.1).

5.3.1.4 Effects of PBMC cell supernatants on T cells

The PBMC supernatants were pooled from patient or controls, incubated with anti-IL-10 or rat IgG isotope control. CD3+ CD25- T cells were magnetically isolated from 4 healthy controls. T cells were then cultured alone or with supernatants at 10% final volume, for 3 days with plate-bound anti-CD3. For the last 4 hours Brefeldin A, PMA and ionomycin were added. Viability was assessed, CD4, IFNγ and TNF-α staining conducted.

5.4 Results

5.4.1 Co-culture of B cell subsets and T cells

5.4.1.1 Selection of co-culture conditions

Co-cultures were optimised in a subset of patients and controls (antibodies titrated, anti-CD3 tested alone and in combination with anti-CD28, 3 and 5-day cultures). The chosen experimental conditions permitted robust detection of cytokines and verification, that Breg can limit T cell proliferation (results for 1 patient and control, shown in Figure 5.1, assessed by CFSE dilution).

The purity of isolated T cells and B cell subsets was assessed by flow cytometry. Representative flow cytometry profiles are shown in Figures 5.2 and 5.3.

5.4.1.2 Breg limit Th1 differentiation relative to Bnaive and Bmem subsets

Results were expressed relative to T cells cultured alone, as percentage change in geometric MFI or cytokine positive T cells (((value in co-culture condition/value in T cells culture alone) x 100) – 100). This meant the comparison was drawn within each individual and not across whole data set, in which a wide range of values may be observed.

Initially 2-way ANOVA was conducted to assess difference in patients and controls, in addition to B cell subsets. The only significant difference for patients and controls, was for relative IFNγ MFI. The other data sets were combined for patients and controls.

Figure 5.1 Breg limited CD4 cell proliferation in the 5-day culture system

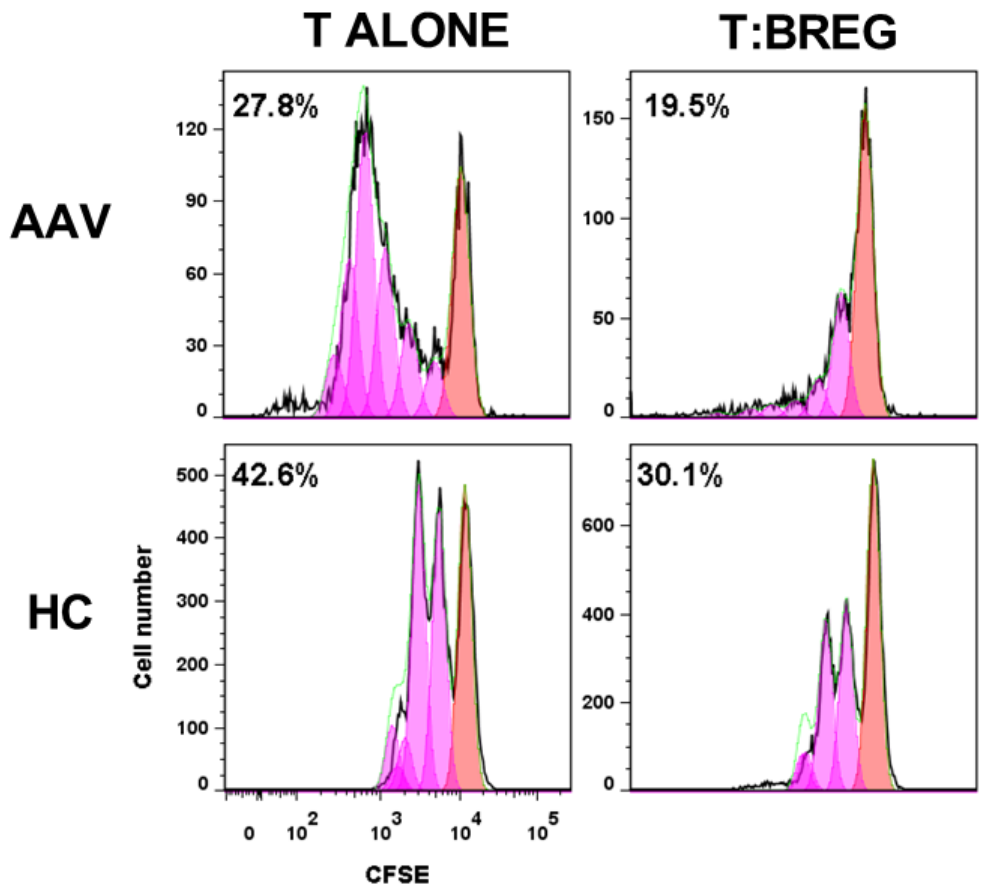

When the co-culture method was initially worked up, T cell proliferation was assessed in a subset of individuals by CFSE dilution. CFSE was used at 2.5µM, co-cultures conducted over 5 days in the presence of soluble anti-CD28 and plate bound anti-CD3. Panels show results for 1 patient and control; the percentage of divided cells is given in the top left corner of each pane (calculated using the proliferation modelling in Flow Jo Version 7.6). In both instances the percentage of T cells, that underwent division, was reduced on addition of Breg (same number of total cells in each condition, in co-cultures T and B cells combined at a 4:1 ratio). The software assigns a red colour the cells that have not divided, the peak furthest on the right with highest CFSE fluorescent intensity. On each round of division, the cytoplasmic dye is halved between 2 daughter cells, resulting in 50% reduction in fluorescent intensity. These peaks of cells that have undergone division are coloured magenta in the software.

Figure 5.2 Purity of magnetically isolated CD4+ CD25- T cells

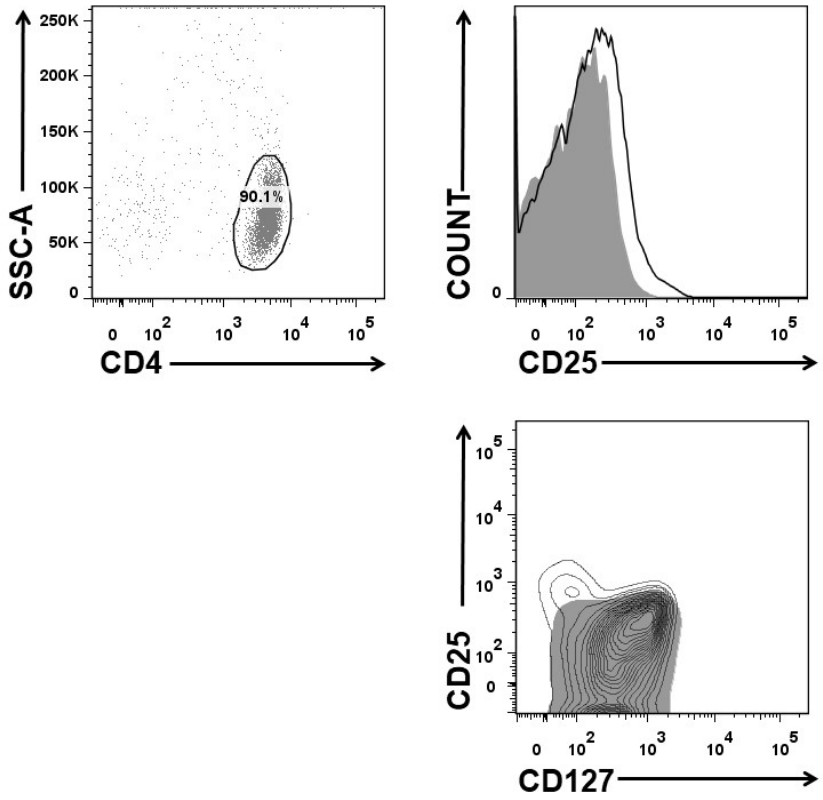

Representative flow cytometry plots for magnetically isolated T cells. In the example shown CD4+ T cells represent 90% of the events recorded in the fcs file, after enrichment. Overlaid histograms show CD25 expression in purified cells (grey filled histogram), relative to T cells in the replete PBMC sample. These population are also shown on a biaxial plot, CD25 and CD127 immunolabelling (T cells in replete PBMC sample shown as an unfilled contour plot and grey filled plot, shows purified CD4+ CD25- T cells). This demonstrates effective depletion of CD25^{high} T cells.

Figure 5.3 Purity of FACS sorted B cell subsets

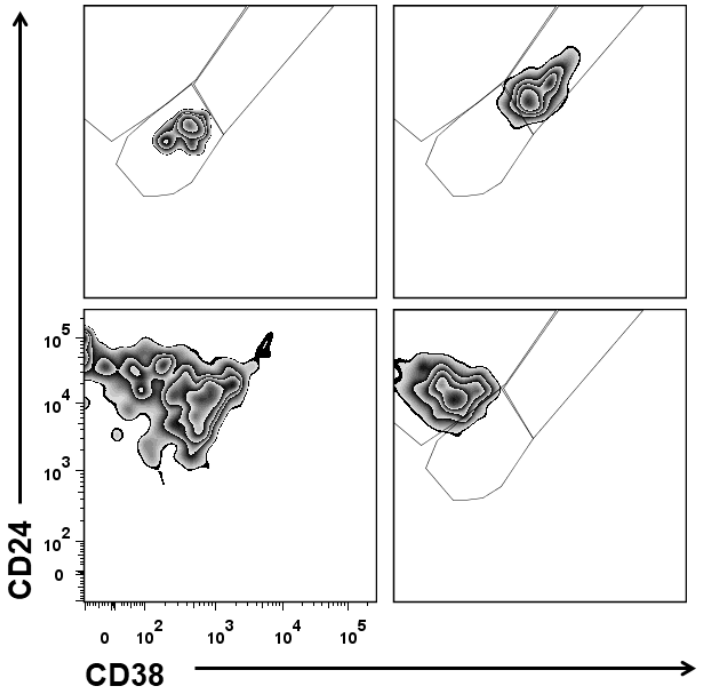

Representative flow cytometry plots for B cell sorts. B cells prior to sorting shown in the bottom left panel and isolated B cell subsets: Breg, top right; Bnaive, top left and Bmem bottom right.

Figure 5.4 Cytokine MFI in T cells cultured with B cell subsets

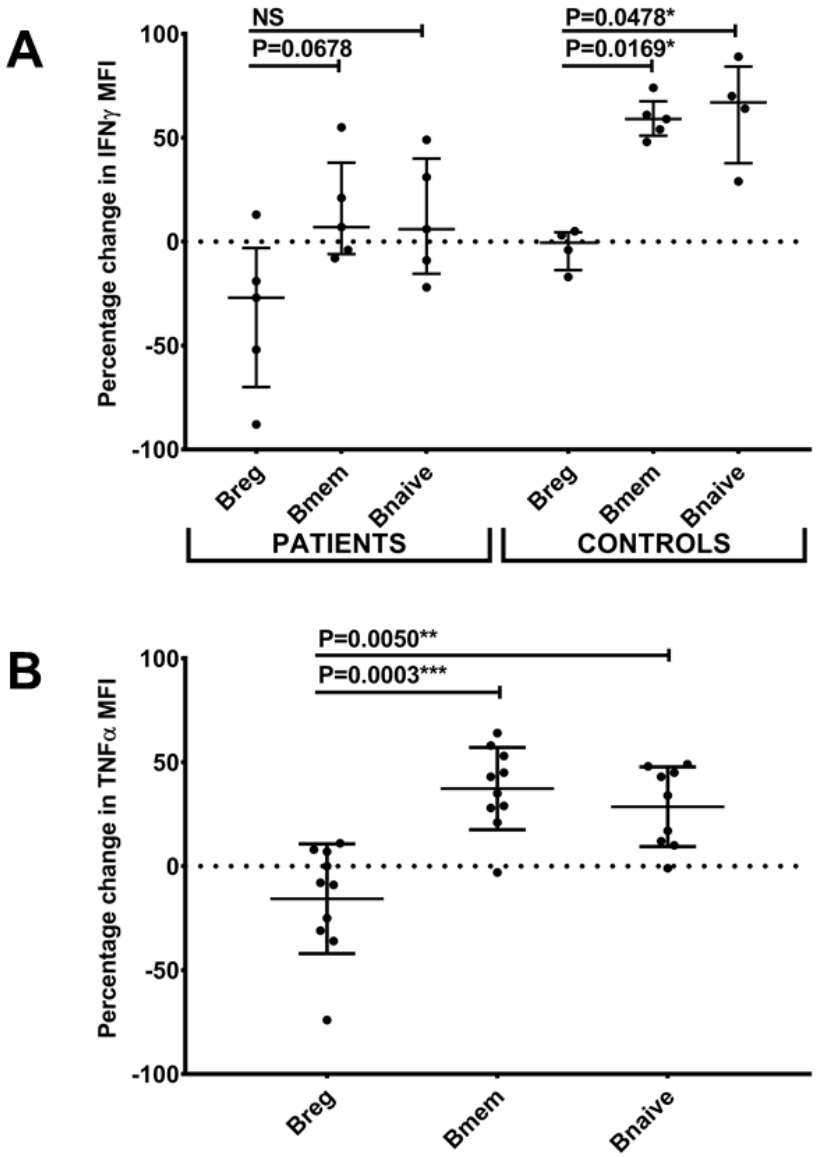

Percentage change relative to T cells alone (represented by dashed zero line in the Y axes). Median and interquartile range shown for B cell co-cultures. Change in IFNγ differed in patients and healthy controls, so analysis was conducted separately. [A] Addition of control Bmem and Bnaive to autologous CD4+ CD25- cells, resulted significantly higher T cell IFNγ MFI, compared to Breg (P=0.0169 and 0.0478*). A similar trend observed in patient Bmem co-cultures (P=0.0678). [B] In the mixed cohort of patients and controls, addition of Bmem or Bnaive resulted in significantly higher T cell TNFα MFI, relative to Breg (P=0.0003*** and P=0.0050**). Kruskal Wallis and Dunn's multiple comparison conducted.*

Mann Whitney U was used to compare patient and control B cell subsets for relative IFNγ MFI. Patient Bmem and Bnaive cells did not augment expression of IFNγ on a cellular level (percentage change in Geometric MFI). The median changes relative to T cells cultured alone, were negative for patients (Bmem -6.0 and Bnaive -15.5) however healthy control B cells did augment T cell IFNγ expression (positive median values, Bmem 51.0 and Bnaive 37.8). This difference in patients and controls was significant for Bmem (P=0.0317*) and trending towards significance for Bnaive (P=0.0635). This was not because patients had intrinsically higher T cell cytokine production. IFNγ geometric MFI of T cells cultured alone, had an IQR of 555-8697 in the patient cohort and 1086-5333 in healthy controls (Mann Whitney >0.9999). This difference in patients and controls might be due to immunosuppression or B cell exhaustion in patients. A T-bet+ CD11c+ CD21- Age Associated B Cell (ABC) phenotype, was recently linked to chronic inflammation in the context of viral infection and autoimmunity (this review article, includes a table comparing ABC and the markers that define B cell exhaustion Rubtsova, Rubtsov et al. 2015).

When relative IFNγ MFI was compared for B cell subsets in the healthy control cohort, Bmem (IQR 51.00-67.50) and Bnaive (IQR 37.75-84.25) induced expression, relative to Breg (IQR -13.50-4.50), P values were 0.0169* and 0.0478* for Bmem and Bnaive cells (Figure 5.4, Panel A). Patient Breg and Bmem showed a tendency to differ, but this did not reach statistical significance (Dunn's multiple comparison P=0.0678).

Relative TNFα MFI was highly significant when B cell subsets were compared (Kruskal Wallis P=0.0003***). Bmem (IQR 26.25-54.25) and Bnaive (IQR 11.00-46.50) significantly differed from Breg (IQR -32.35-7.25). Both B cell subsets

induced significantly higher TNFα expression in T cells, relative to Breg (Figure 5.4, Panel B, P=0.0003*** and P=0.0050**).

The relative frequency of IFNγ+ T cells was significantly higher in Bmem (IQR 12.75-37.75, P=0.0079**) and Bnaive (IQR 7.00-26.50, P=0.0321) co-cultures, compared to Breg (IQR -8.00-11.00, Figure 5.5, Panel A).

The relative frequency of TNFα T cells did not differ significantly between B cell co-cultures, but tended to be higher in Bmem (IQR 0.00-10.75, P=0.0614) and Bnaive (IQR 0.00-12.50, P=0.0531) cultures, compared to Breg (IQR -13.00-2.00, Figure 5.5, Panel B).

Collectively the evidence shows that there is no difference in Breg from patients and controls. Bnaive and Bmem cells from patients, induce less IFNγ in T cells on a cellular basis (geometric MFI). Breg do not augment T cell production (relative MFI or cell frequency), whilst B effector subsets (both Bnaive and Bmem cells), act to augment Th1 differentiation *in vitro.*

Figure 5.5 Comparison of cytokine positive T cells in B cell co-cultures

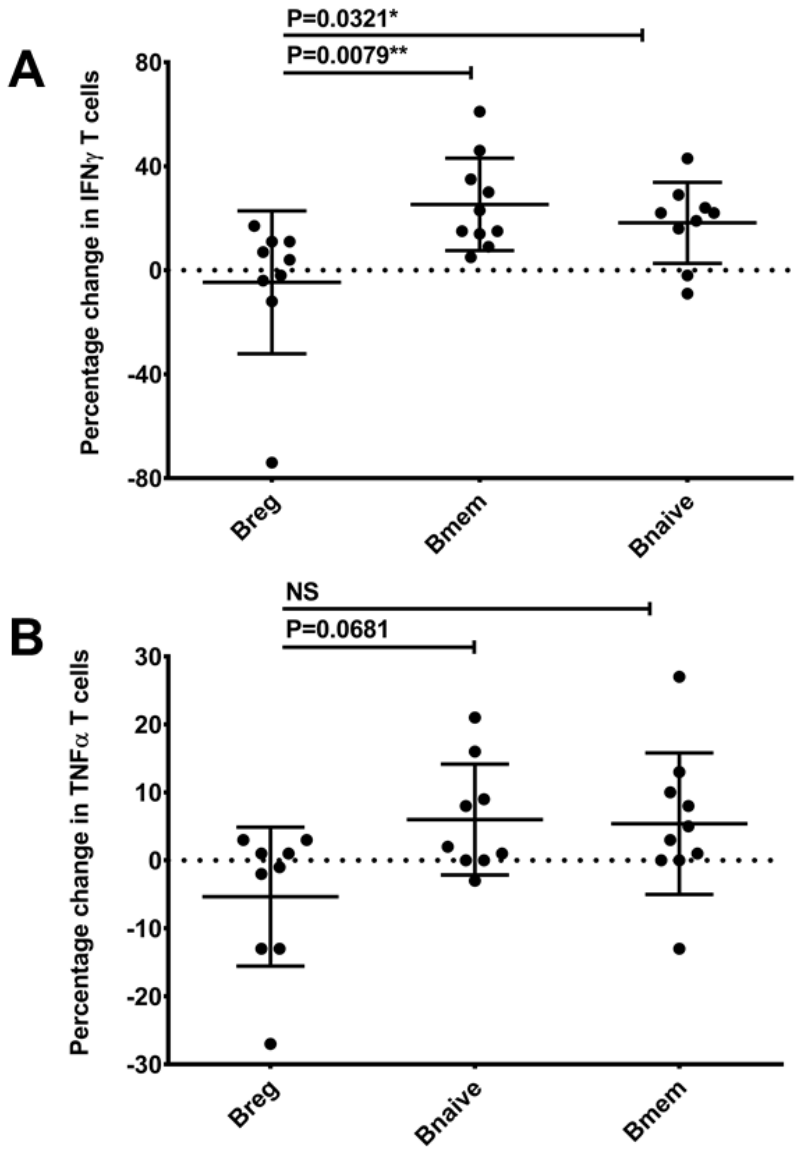

Percentage change relative to T cells alone (represented by dashed zero line in the Y axes), median and interquartile range shown for B cell co-cultures. There was no difference in patients and healthy controls, permitting data to be combined (2-way ANOVA). [A] Addition of control Bmem and Bnaive to autologous CD4+ CD25- cells, resulted significantly higher frequency of IFNγ+ T cell, compared to Breg (P=0.0079 and 0.321*). [B] There was a trend towards higher frequency of TNFα+ T cells in Bmem co-culture compared to Breg, but this did not reach the threshold for statistical significance (P=0.0681). Kruskal Wallis and Dunn's multiple comparison conducted.*

5.4.2 Intracellular flow cytometric detection of B cell cytokines

5.4.2.1 Induction of IL-10, TNFα and TGFβ

B cell IL-10 production was induced in B cells, by stimulating PBMC with CPG alone or in combination with CD154 (Figure 5.6). Results for IL-10 and TGFβ were expressed as percentage frequency of CD19+ live lymphocytes, with gates set to ≤1% in the untreated control (brefeldin A and test antibody, 48-hour culture, no stimulus). Maximum stimulation with combined CPG and CD154, also resulted in global TNF-α expression within the B cell population, a classical pro-inflammatory cytokine. For relative comparison of patients and controls, geometric MFI was used.

On initial analysis there was no difference in IL-10 frequency between the main remission cohort and healthy controls (Figure 5.7, Panel A). On CPG and CD154 stimulation, IL-10 frequency was higher in the rituximab treated patient group, compared to healthy controls (Kruskal Wallis test P=0.0106*and Dunn's multiple comparison P=0.0060*). This difference was maintained on removal of the outlying value in the rituximab group (without the data point at 88.2%, P=0.0135*).

There was also no difference in TNF-α geometric mean between the patient cohorts and healthy controls (Figure 5.7, Panel B). However, on CPG treatment TNF-α geometric mean was lower in rituximab treated patients (Median MFI 668, IQR 415-986) compared to main remission cohort (Median MFI 1370, IQR 917-1827, P=0.0268*).

TGFβ induction was significant in the subset of the individuals tested, with combined CPG and CD154 stimulus compared to unstimulated cells (Figure 5.8, n=19, Kruskal Wallis P<0.0001****). Some patients were resistant to B cell TGFβ induction, and this was not linked to IL-10 competency (Figure 5.8, Panels B and C).

Figure 5.6 IL-10 induction, also results in TNFα and TGFβ production

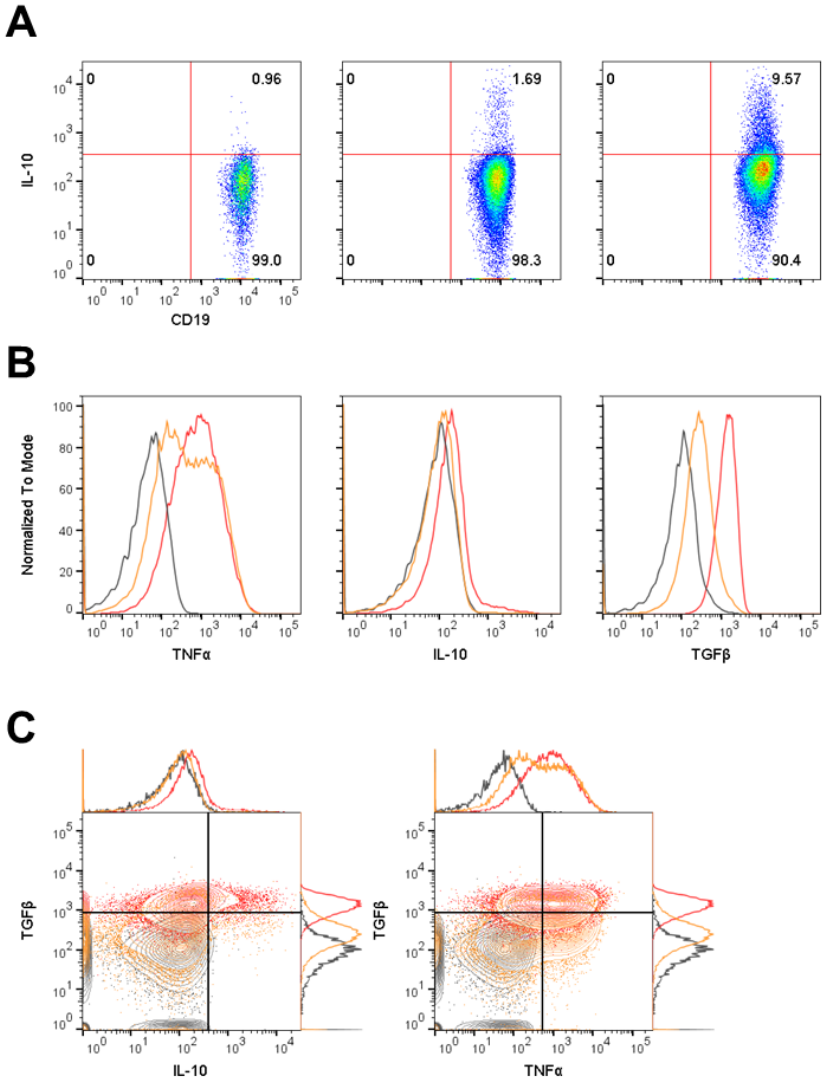

All plots show live B cells, gated on forward and side scatter, defined by CD19 expression and lack of live-dead exclusion dye. [A] Induction of B cell IL-10 shown. Biaxial plot on the left shows untreated PBMC gates were set to ≤1% IL-10+ (top right quadrant, Brefeldin A, test antibody). Middle plot shows IL-10 induction upon stimulation with CPG. Right plot shows IL-10 induction on combined stimulation with CPG and CD40 ligation. [B-C] Histograms and contour plots show B cells from untreated PBMC in grey, CPG stimulation in orange and combined CPG/CD40 stimulation in red. [C] Percentage of TGF+ B cells was calculated on biaxial plots, against TNFα and IL-10 (sum of the top 2 quadrants set to ≤1% and final TGFβ frequency, equal to the average of the 2 biaxial plots).

Figure 5.7 Remission patients' cytokine profile not significantly different from controls

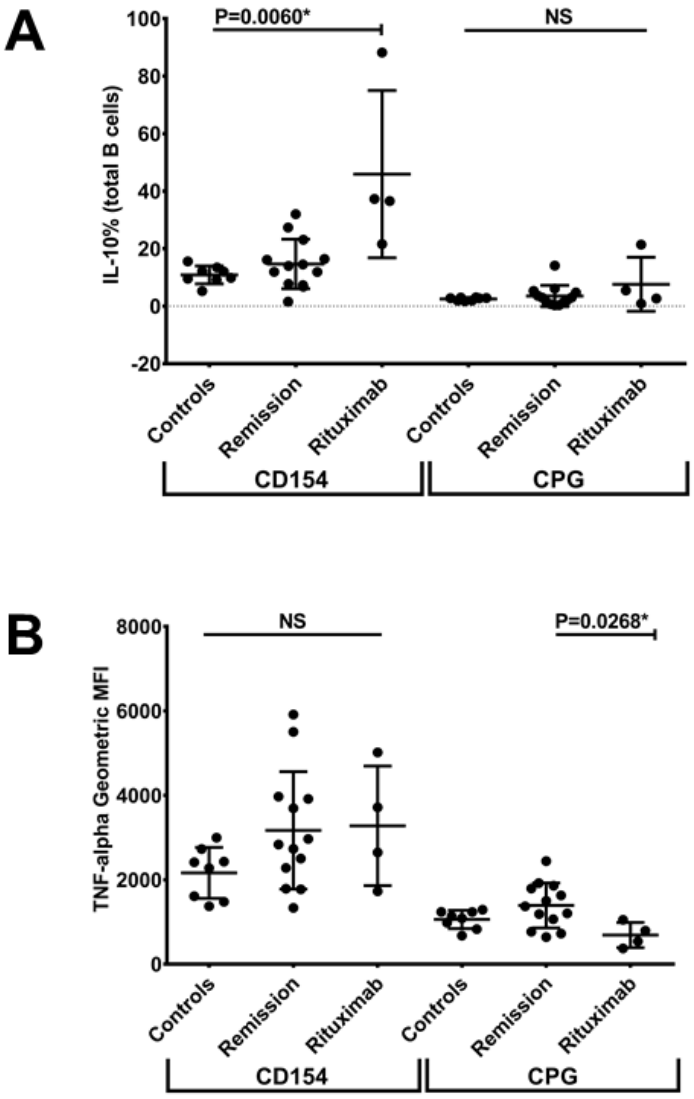

[A] IL-10 frequency, percentage of live CD19+ cells. Cohorts were compared by Kruskal Wallis test (P=0.0106), with Dunn's multiple comparison relative to healthy controls. The rituximab treated group had higher IL-10 frequency on CPG and CD154 stimulation (P=0.0060*). This difference was maintained on removal of the highest value (P=0.0135*). [B] On maximum stimulation B cells invariably expressed TNFα; for relative comparison of the groups, geometric TNFα MFI was used. Kruskal Wallis test was significant (P=0.0302*), with no difference in patients compared to controls. When Dunn's multiple comparison was conducted between all groups, rituximab treated patients had lower B cell TNFα geometric MFI, upon CPG stimulation, compared to the main remission cohort.*

Figure 5.8 B cell production of TGFβ

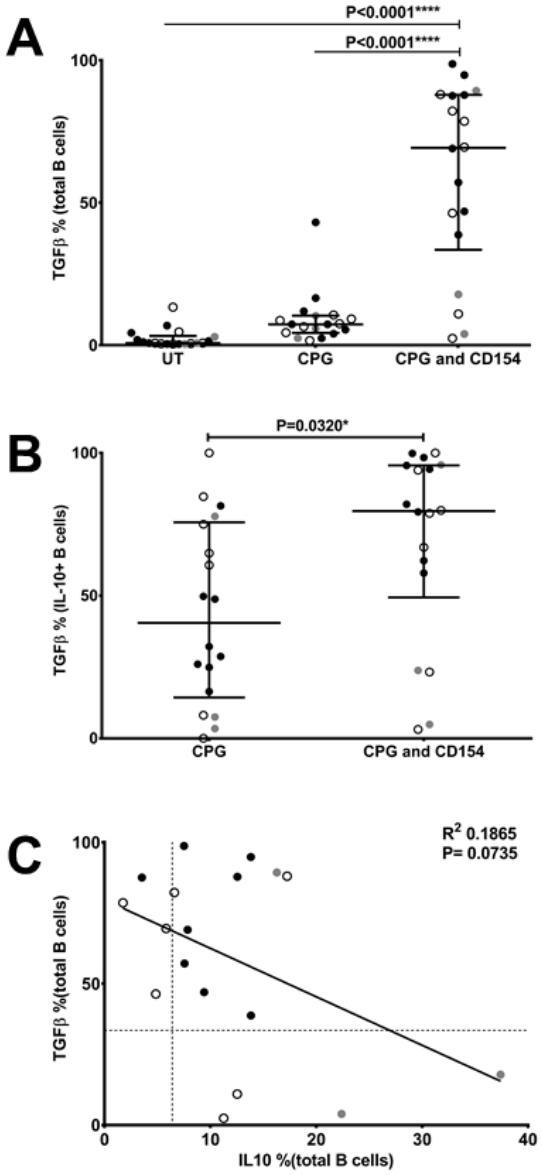

TGFβ induction was assessed in a subset of individuals, the combined data set is shown: 6/12 remission patients (unfilled data points, black outline), 3/4 rituximab treated patients (grey data points) and 8/8 healthy controls (black data points). [A] Although TGFβ B cell induction was highly significant upon CPG and CD154 stimulation, a subset of patients did not produce B cell TGFβ. This was not because these individuals had lower frequency of IL-10+ B cells; assessed by looking at [B] TGFβ B cells as a percentage of IL-10+ B cells and [C] correlation of IL-10+ and TGFβ B cells (lower 25th percentile shown for IL-10 and TGFβ).

5.4.2.2 Relationship between B subsets at baseline and cytokine induction

The balance of B cell subsets is profoundly affected after rituximab, resembling a tolerant state. It was interesting to observe that B cells from rituximab treated patients also had an increased frequency IL-10+ cells and reduced TNFα geometric MFI. To further assess the relationship between B cell subsets and cytokine competency, regression analysis was performed. B cell IL-10 induction upon CPG and CD154 stimulation was proportionate to Breg and inversely proportionate to Bmem frequency (Figure 5.9). Furthermore, on CPG stimulation B cell TNFα geometric MFI correlated with Bmem (P=0.0018**) and Breg had an inverse relationship (P=0.0079**, Figure 5.10). Significance was maintained on removal of rituximab treated patients. There was no relationship between B cell subsets and B cell TNFα geometric MFI on CPG and CD154 stimulation, until the rituximab treated patients were removed from analysis. In this combined cohort of remission patients and healthy controls, Breg had an inverse relationship B cell TNFα MFI (P=0.0348*, Figure 5.10, Panel C).

5.4.2.3 Relationship between B subsets and cytokine induction, revealed by CD24 and CD38 immunolabelling after stimulation

The starting frequency Breg and Bmem, determine frequency of IL-10 positive cells and intensity of TNFα staining in B cells, following CPG and CD154 stimulation (Figure 5.9 and 5.10). I wanted to further explore this relationship and did so by staining for B cell subsets in a subset of patients and controls, after culture (8 healthy controls, 8 remission patients and 3 rituximab treated patients). All 3 B cell subsets could still be resolved (Figure 5.12). There was no significant difference in the frequency of Breg, compared to baseline (freshly isolated PBMC) but relative frequency of Bmem was reduced and Bnaive increased upon treatment with CPG alone

Figure 5.9 Regression analysis starting frequency of Bmem and Breg, with IL-10 B cell frequency after maximum stimulation

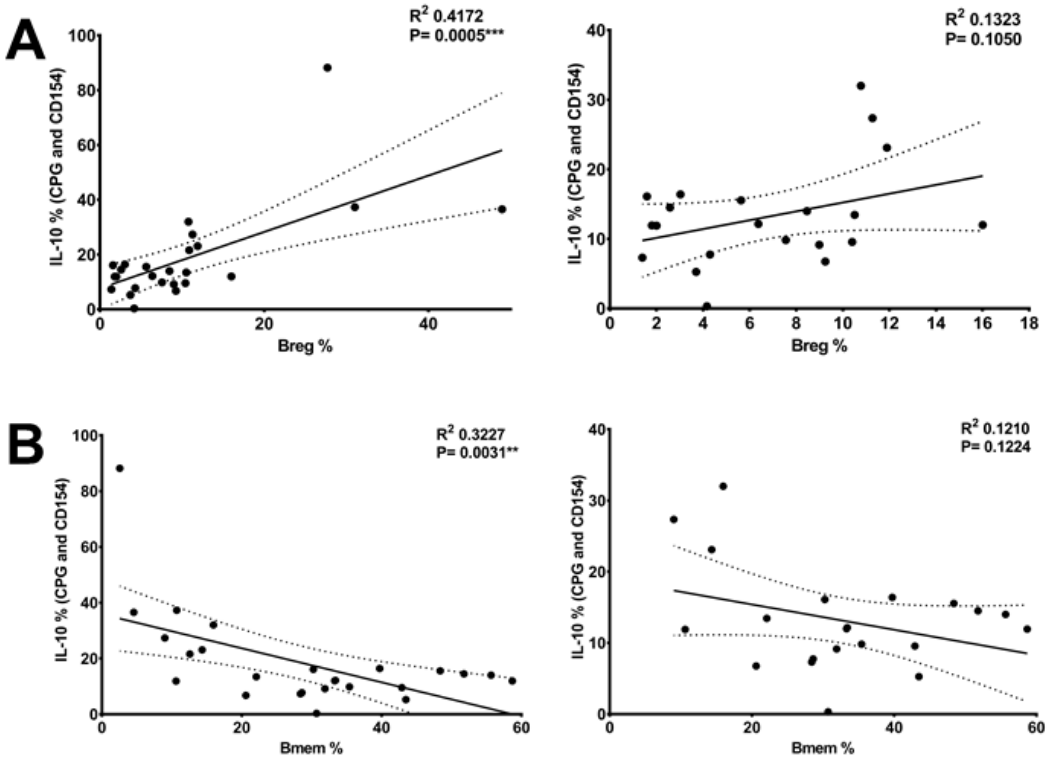

*To assess whether B cell subsets at baseline, were a good indication of IL-10 competency, correlation was performed. Panels on the left include rituximab treated patients n=24, rituximab treated patients excluded from graphs on the right, n=20. [A] Breg had a positive correlation with IL-10+ B cells on CPG and CD154 stimulation (P=0.0005***). This trend was still visible when analysis was conducted without the 4 rituximab-treated patients, although statistical significance was lost (right panel, P=0.1050). [B] Bmem had an inverse relationship with IL-10+ B cells on CPG and CD154 stimulation (P=0.0031**). Like Breg, this relationship was still apparent when analysis conducted without rituximab-treated patients, but significance lost (right panel, P=0.1224). The groups were mixed and relatively small.*

Figure 5.10 Regression analysis starting frequency of Bmem and Breg, with TNFα geometric MFI

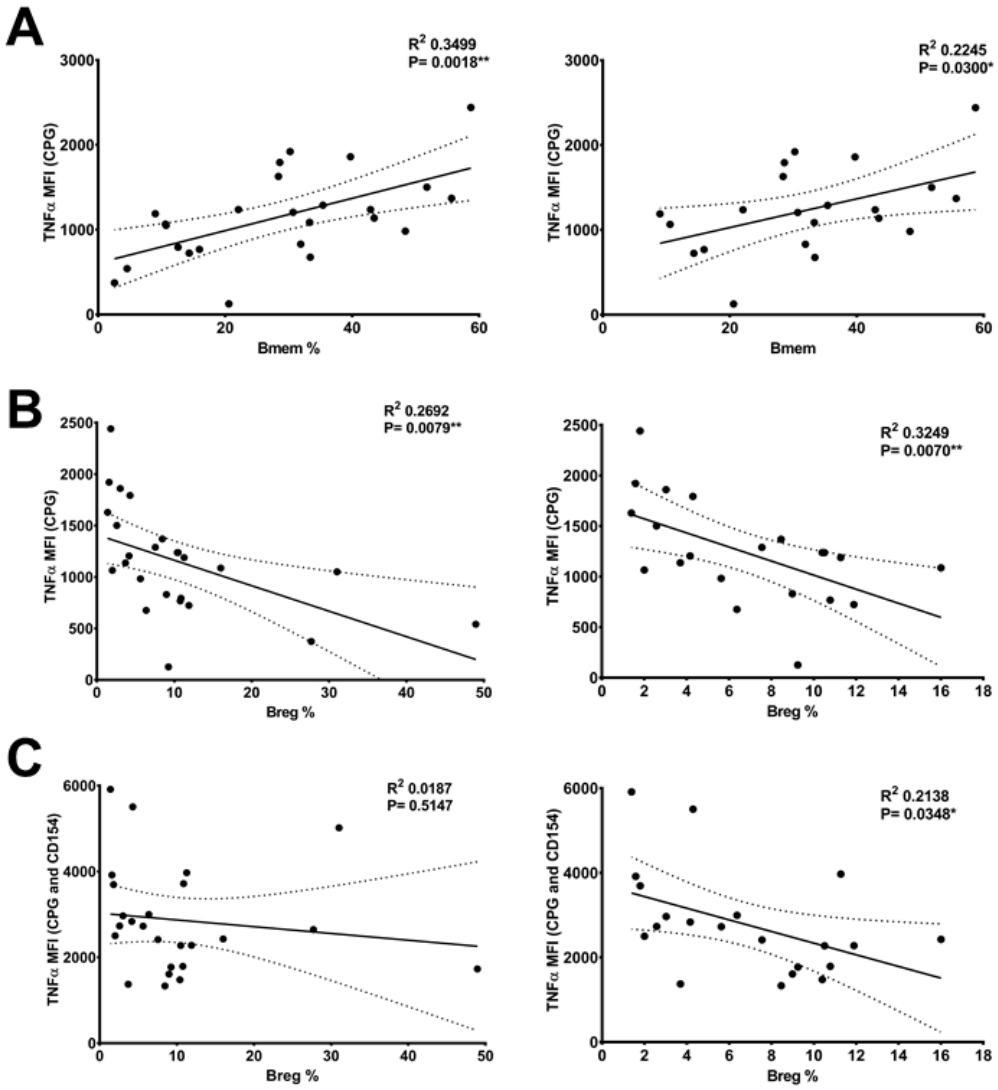

*Relationship between B cell subsets at baseline and B cell TNFα geometric MFI. Panels on the left include rituximab treated patients n=24, excluded from graphs on the right n=20. [A-B] In CPG stimulated PBMC, the frequency of Bmem positively correlated with TNFα MFI (P=0.0018**) and the inverse was observed with Breg (P=0.0079**). This was maintained on removal of rituximab treated patients. There was no relationship between B cell subsets and B cell TNFα geometric MFI on CPG and CD154 stimulation initially. [C] When rituximab treated patients were removed, Breg frequency had an inverse relationship B cell TNFα MFI (right panel, P=0.0348*)*

Figure 5.11 Stability of B cell subsets on stimulation

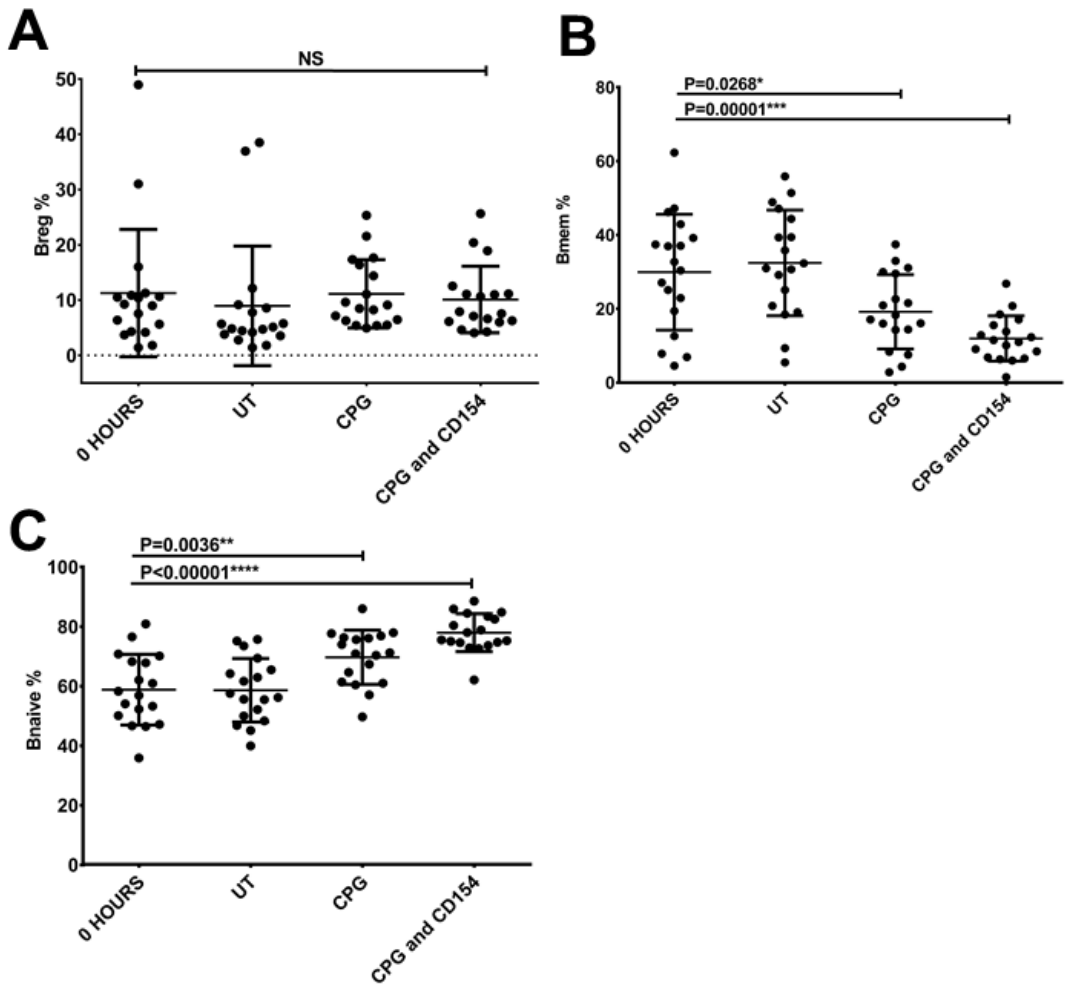

To evaluate how stable the B cell subsets were on stimulation, frequency was compared at baseline and after 48 hours culture. Assessed in a subset of individuals: 8/12 remission patients, 3/4 rituximab treated patients and 8/8 healthy controls. The relative frequency of Bnaive cells increased and Bmem decreased, there was no significant difference in Breg, compared to baseline.

or in combination with CD154 (Figure 5.11). On initial visualisation of flow cytometry plots, back gating of the IL-10 positive events onto CD24 and CD38 biaxial plots, showed that these cells were highly enriched within the Breg region, compared to untreated cells at 48 hours (Figure 5.12). Relative intensity of cytokine staining also varied for the B cell subsets at 48 hours; Breg also expressed highest levels of TGFβ and lowest TNFα (Figure 5.13). To objectively assess this, geometric MFI was compared across B cell subsets.

Distribution of the data sets (CPG alone or in combination with CD154), was assessed by D'Agostino and Pearson test. Breg and Bmem did not have a normal distribution pattern for cytokine MFI, consequently Friedman's test was conducted. IL-10 and TNFα MFI differed in B cell subsets on CPG stimulation (in both instances P<0.0001***). On combined CPG and CD154 stimulation, TNFα and IL-10 MFI also differed across the B cell subsets (P=0.0498* and P=0.0242*, respectively).

Wilcoxon matched pairs was used to further assess the difference between B cell subsets. On CPG stimulus IL-10 MFI was higher in Bmem and Breg, compared to Bnaive (P<0.0001****). The difference in Bmem and Breg was not significant (P=0.1508, Figure 5.14, Panel A), nor was significance gained on analysing patients and controls separately (P=0.5566 and P=0.2500). TNFα MFI was higher in Bmem and Breg, compared to Bnaive (P<0.0001**** and P=0.0062**). Breg had lower TNFα MFI than Bmem (P=0.0204*, Figure 5.14, Panel B). Interestingly, Breg had significantly lower TNFα MFI in controls (n=8, P=0.0156*) but significance was lost when patients were assessed alone, despite there being more data points in the latter group (Figure 5.15, n=11, P=0.2061). Median TNFα MFI was similar for patient and control Breg (850 and 1081), but a subset of patients had higher Breg TNFα MFI. The

Figure 5.12 B cell profile in unstimulated cells compared with IL-10+ B cells, after maximum stimulation

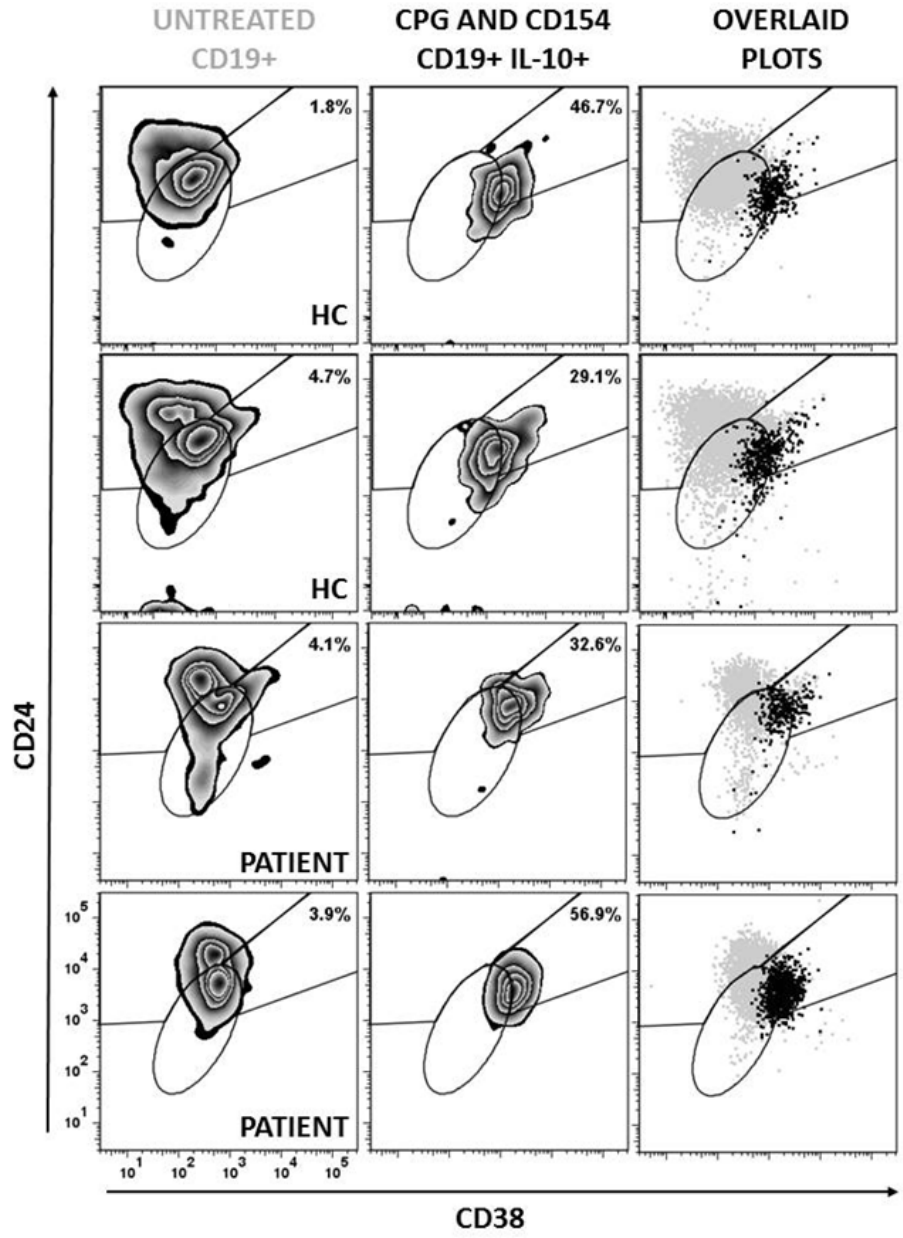

IL-10 positive cells were enriched within the Breg cell gate; plots compare untreated cells (zebra plot on the left) and IL-10 positive B cells (middle plot), after CPG and CD154 treatment (percentage of cells in the Breg gate shown in the top right corner). Overlaid dot plots show untreated B cells in grey and IL-10 positive B cells in black.

Figure 5.13 Different intensity of intracellular staining, in the B cell subsets

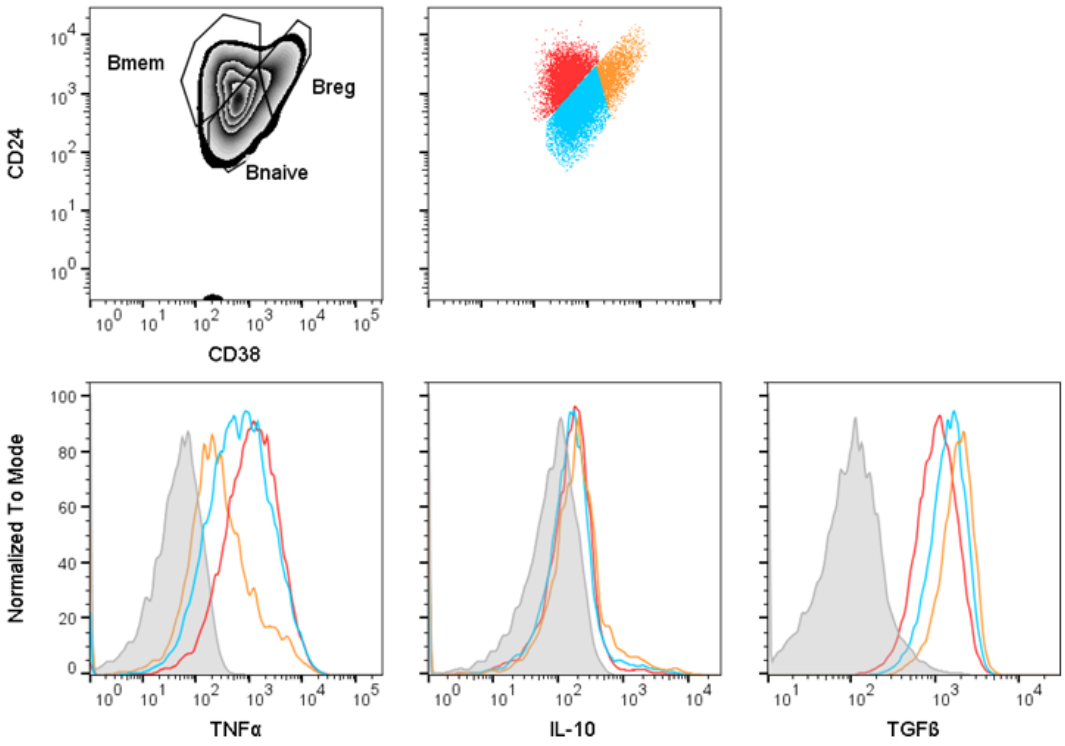

B cell subsets were assessed in a subset of individuals at 48 hours, a representative flow cytometry plot is shown on the top row (CPG and CD154 stimulation in a healthy control). In the second row the B cell subsets are shown relative to untreated cells (grey filled histogram), Bmem in red, Bnaive in blue and Breg in orange. The overlaid histograms seem to indicate that there is differential expression of cytokines in the B cell subsets.

range of TNFα MFIs, was much wider in patients than controls (490-4731 compared to 627-1489).

With combined CPG and CD154 stimulation, IL-10 was higher in Breg than Bmem (Wilcoxon matched pairs, P=0.0314*) and significance lost when separate analyses were conducted for patients and controls. IL-10 MFI did not differ significantly between Bnaive and Breg in the combined cohort (P=0.1336), controls alone (P=0.3125) or patients (P=0.2783). TNFα differed in the healthy control cohort alone (Figure 5.16). Bmem and Bnaive had higher TNFα MFI than Breg in healthy controls (P=0.0156* and P=0.0078**) and did not differ in patients (P=0.9658 and P=0.7002).

Figure 5.14 B cell subset cytokine intensity (geometric MFI), in CPG stimulated PBMC

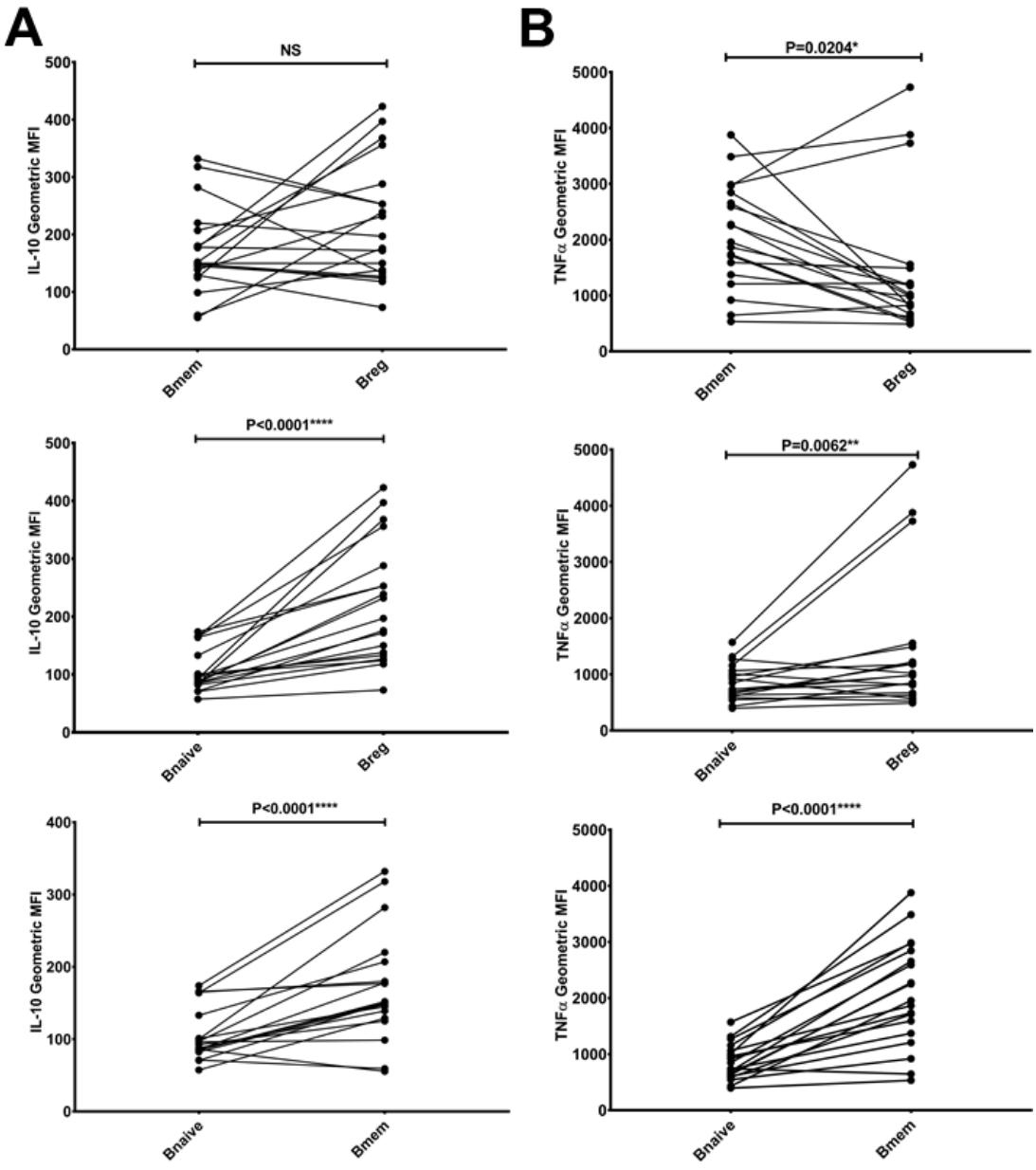

*Geometric MFI for [A] IL-10 (left panels) and [B] TNFα (right panels) was assessed in B cell subsets at 48 hours after CPG stimulation (n=19). This analysis followed Friedman's test, which showed highly significant differences in IL-10 and TNFα MFI across B cell subsets (P<0.0001****). Results of Wilcoxon matched pairs analysis are shown. The top row shows IL-10 MFI did not differ in Breg and Bmem (left panel) however, Breg had lower TNFα MFI than Bmem (right panel, P=0.0204*). Bnaive cells had significantly lower TNFα and IL-10 MFI, than Breg (middle row) or Bmem (bottom row); P values are shown on the graphs.*

Figure 5.15 Differences in patients and controls, upon CPG stimulation

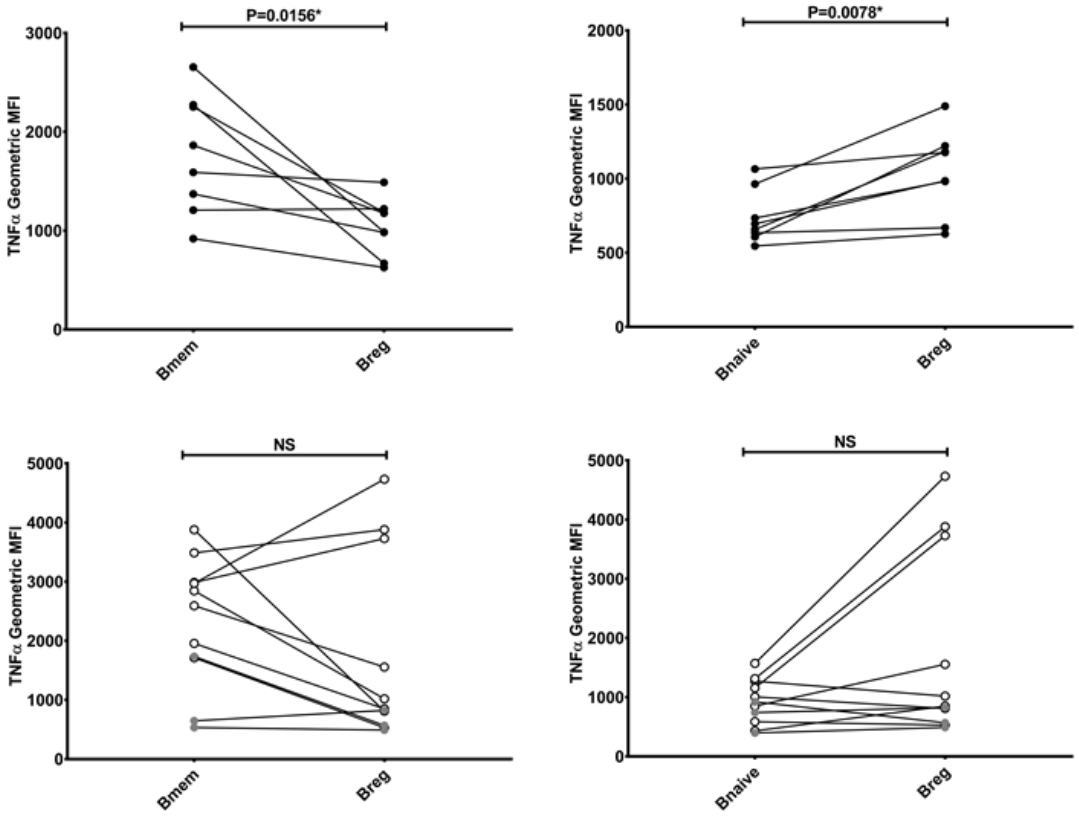

Geometric MFI TNFα in B cell subsets, after CPG stimulation. Separate analysis was conducted for healthy controls (n=8, top row) and patients (n=11, bottom row). Statistical significance was retained when Bmem or Bnaive were compared relative to Breg in healthy controls, but this effect was lost in patients. In the bottom row the 6 remission patients are shown with unfilled data points and black outline, the 3 rituximab treated patients are depicted with grey data points.

Figure 5.16 B cell subset cytokine intensity (geometric MFI), in CPG and CD154 stimulated PBMC

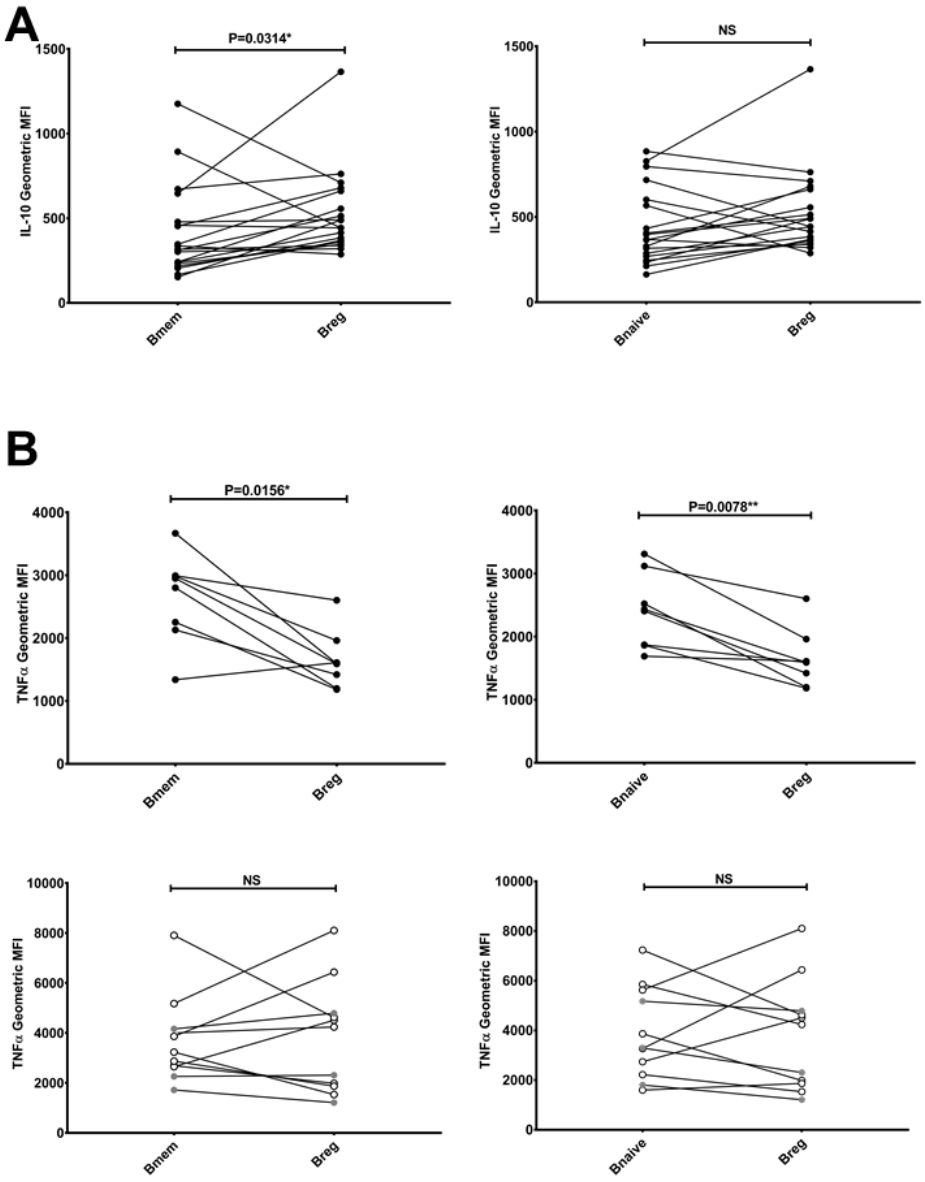

Geometric MFI in B cell subsets, after combined CPG and CD154 stimulation. [A] Breg had significantly higher IL-10 MFI than Bmem (Wilcoxon matched pairs, P-0.0314). [B] Breg had lower TNFα MFI in healthy controls, relative to Bmem and Bnaive (P=0.0156* and P=0.0078*). There was no difference in TNFα MFI in patient B cell subsets (in the bottom row, remission patients shown with unfilled data points and black outline, rituximab treated patients with grey filled data points).*

5.4.3 Soluble mediators detected in supernatants of PBMC stimulated with CPG alone or in combination with CD154

5.4.3.1 Analytes detected in supernatants

15 analytes were assessed in supernatants from PBMC stimulated for IL-10 induction by CBA and ELISA. IL-10, TGFβ, IL-2, IL-1β, IL-9, IL-6, IFNγ, TNFα and IL-17A were detected, most were induced on stimulation (Figure 5.17). Soluble TGFβ was not significantly different between PBMC which were untreated or stimulated with CPG or CPG and CD154 combined. This is likely because TGFβ remained undetectable with maximum stimulation in 7 out of 24 individuals (1 control, 2 rituximab treated and 4 remission patients). TGFβ was very robustly detected in the remaining 17 individuals (IQR 1514-3279 and median 2146pg/ml). Similarly, IL-9 was not induced on stimulation; this analyte was negative in 13/24 samples tested, unlike TGFβ, the levels of IL-9 in the supernatants was approaching the limit of detection in all the remaining samples (range 1.78-5.17 and median 2.76pg/ml). IL-9 detection was most robust in untreated samples, after 48-hour culture (Figure 5.19).

IL-10, IL-6, IL-1β, TNFα and IL-17A were significantly induced upon CPG and CD154 stimulation but not in CPG treated PBMC (Figure 5.18). In contrast, IFNγ and IL-2 were significantly induced in PBMC treated with CPG alone and CPG in combination with CD154 (Figure 5.18).

5.4.3.2 Analytes not detected in supernatants

The remaining 6 analytes were below the assay limit of detection (IL-5, IL-4, IL-22, IL-12p70, IL-13 and IL-35). There were very few IL-35 ELISA kits on the market at that time, and limit of detection was relatively high (0.13ng/ml).

5.4.3.3 Soluble TNFα results discordant with intracellular flow cytometry

Detection of TNFα was variable, it was not detected in 50% of individuals with maximum stimulation (3 controls, 7 remission patients and 2 rituximab treated patients) and values were low in the remaining individuals (median 15.54 and range 3.01-76.83pg/ml). Mean TNFα production represented less than 1% of the total cytokines, across all analytes detected (Figure 5.22). The low level of TNFα was surprising, given that B cells were invariably positive by flow cytometry and geometric MFI was high (Figure 5.7, Panel B). Supernatants were collected prior to final stimulated with PMA and ionomycin, B cell TNFα induction may therefore be a consequence of this treatment, not the CPG and CD154 stimulus that preceded it. This does not detract from the value of intracellular B cell TNFα as a prognostic measurement of rejection and graft outcome, which was demonstrated in the context of allogeneic kidney transplantation (Cherukuri, Rothstein et al. 2014).

5.4.3.4 Differences in patients and controls

Cytokine profiles were assessed by Kruskal Wallis and Dunn's multiple comparison test. Release of IL-10 was significantly lower in patients compared to controls, following CPG stimulation (P=0.0487*) and, was trending towards significance upon CPG and CD154 stimulation (P=0.0779, Figure 5.20, Panel A). There was no difference in the control and patient cohort on intracellular flow cytometry (IL-10+ viable B cells, expressed as a percentage of parent population, Figure 5.7, Panel A). AAV patients are on immunosuppression, which can result in B cell lymphopenia; IL-10 frequency may not be affected when expressed as a percentage of B cells but the absolute number of IL-10+ B cells and soluble IL-10 may still be reduced. Furthermore, IL-10 and TGFβ production are not limited to B cells, Breg can in fact

Figure 5.17 Detection of soluble cytokines in the supernatants of PBMCs, stimulated for maximum IL-10 induction in B cells

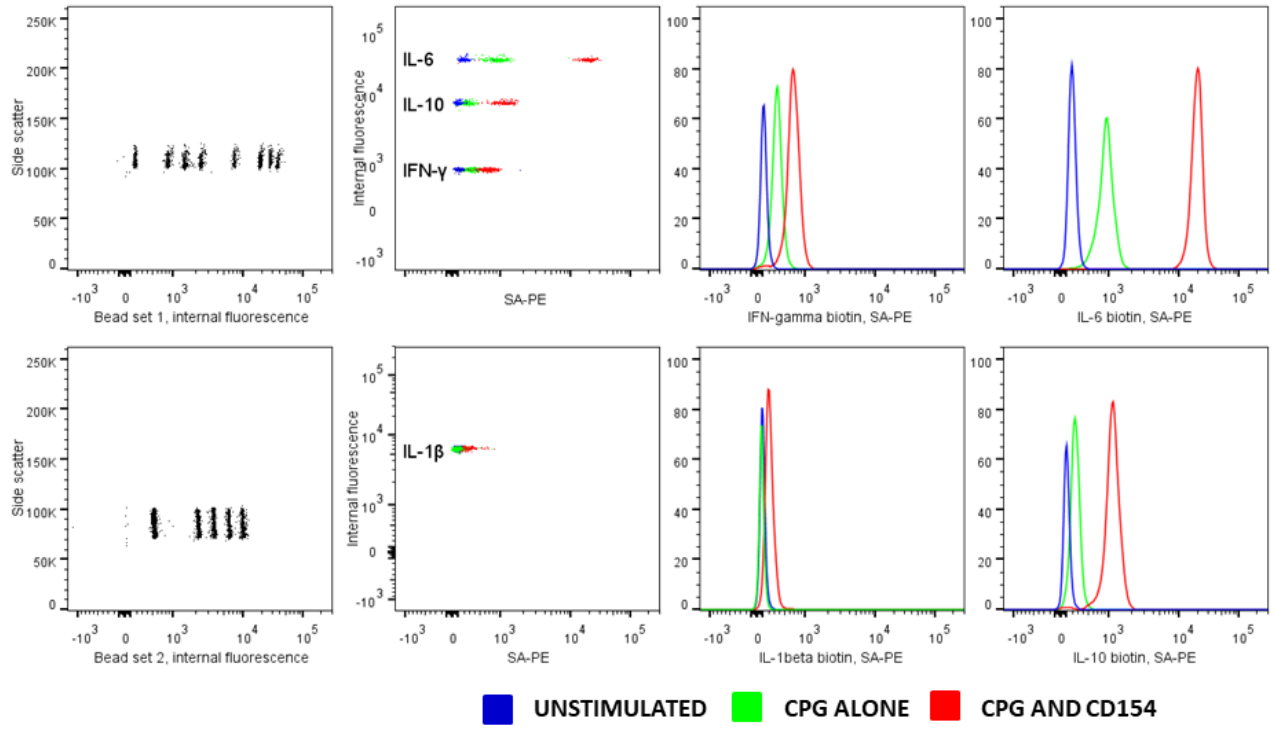

Cytometric Bead Array (CBA) was conducted on PBMC supernatants. The solid substrate are beads, coated with capture antibody; these are differentiated by size and internal fluorescence on flow cytometry. The detection antibody is biotinylated with detection by streptavidin-phycoerythrin (SA-PE). IL-6, IL-10, IL-1β and IFNγ beads are shown for one individual; supernatant from unstimulated PBMC in blue, CPG alone in green and CPG in combination with CD154 in red.

Figure 5.18 Cytokines detected in supernatants of stimulated PBMCs

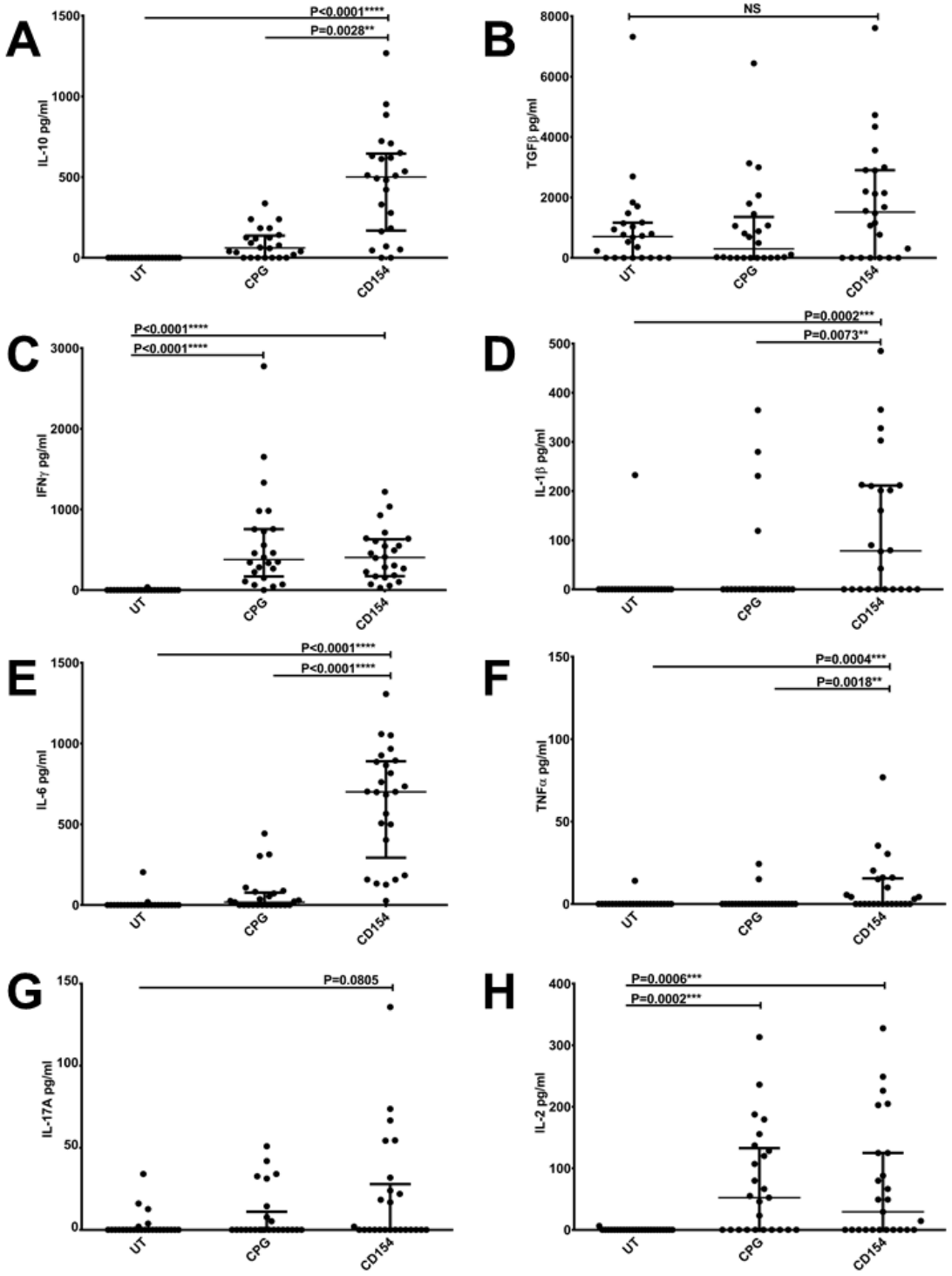

Induction of cytokines was assessed by Kruskal Wallis and Dunn's multiple comparison test (all conditions assessed relative to one another). Soluble IL-10, IL-6, IL-1β, TNFα and IL-17A were only significantly induced in CPG and CD154 treated PBMC. IFNγ and IL-2 were significantly induced in PBMC treated with CPG alone or in combination with CD154.

Figure 5.19 IL-9 not induced and approaching the limit of detection

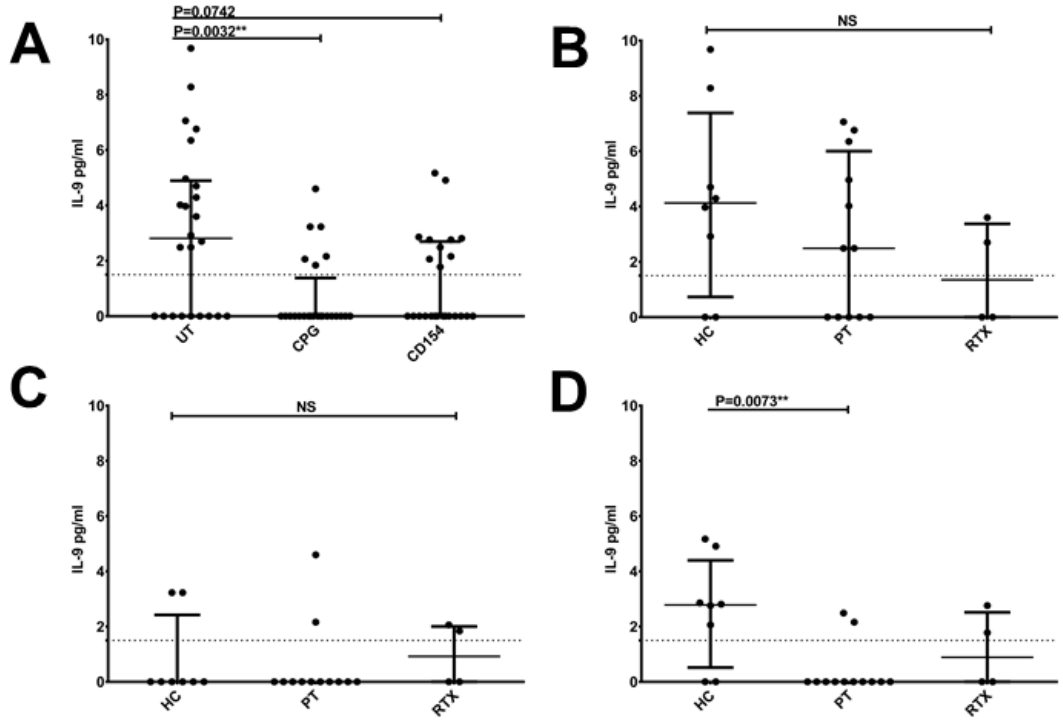

[A] Detection of IL-9 was most robust in untreated samples, but in all cases this analyte was approaching the limit of detection (dashed line, 1.5pg/ml). [B] In unstimulated PBMC, healthy controls (HC) were not more likely to produce IL-9, compared to remission (PT) or rituximab treated patents (RTX). [C] There was no difference on CPG stimulation. [D] IL-9 was detectable in more control supernatants than patients, upon maximum stimulation with CPG and CD154 combined.

induce Treg (Kessel, Haj et al. 2012, Flores-Borja, Bosma et al. 2013, Tarique, Naz et al. 2018), augmenting levels of these cytokines in a mixed PBMC culture. Soluble TGFβ also tended to be lower in patients compared to controls, on combined CPG and CD154 stimulation (P=0.0526, Figure 5.20, Panel B).

In terms of the more classical pro-inflammatory cytokines, soluble IFNγ was lower in rituximab treated patients, compared to healthy controls, with CPG stimulation alone or in combination with CD154 (Figure 5.20, Panel C). There was no significant difference in secreted IL-6, IL-1β and TNFα, between healthy controls, remission and rituximab treated patients (Figure 5.20, Panels D, E and F).

5.4.3.5 Net cytokine profile

All the raw data points for soluble analytes are presented together in Figure 5.21. After CPG treatment, production of both TGFβ and IFNγ production is high (the latter was previously described (Klinman, Yi et al. 1996)). Upon CPG and CD154 stimulation, the net production of anti-inflammatory cytokines typically represents more than 50% of the total soluble analytes assayed (shown in shades of blue in Figure 5.22, Panel A and C). There is no further induction of IFNγ (median and IQR are similar, Figure 5.18, Panel C) but now IL-6 is robustly detected. Although IL-6 and IL-1β are considered proinflammatory, cytokines are notoriously pleiotropic and this combination of cytokines, has also been shown to be important in the maintenance of regulatory B cells in mice (Rosser, Oleinika et al. 2014).

5.4.3.6 Relationship with B cell subsets

Although I controlled for the total number of PBMC in culture, the proportions of T cells, B cells and monocytes may differ between patients and controls, affecting net cytokine production. To assess this retrospectively, I conducted analysis of starting

Figure 5.20 Comparsion of soluble cytokines in patients and healthy controls

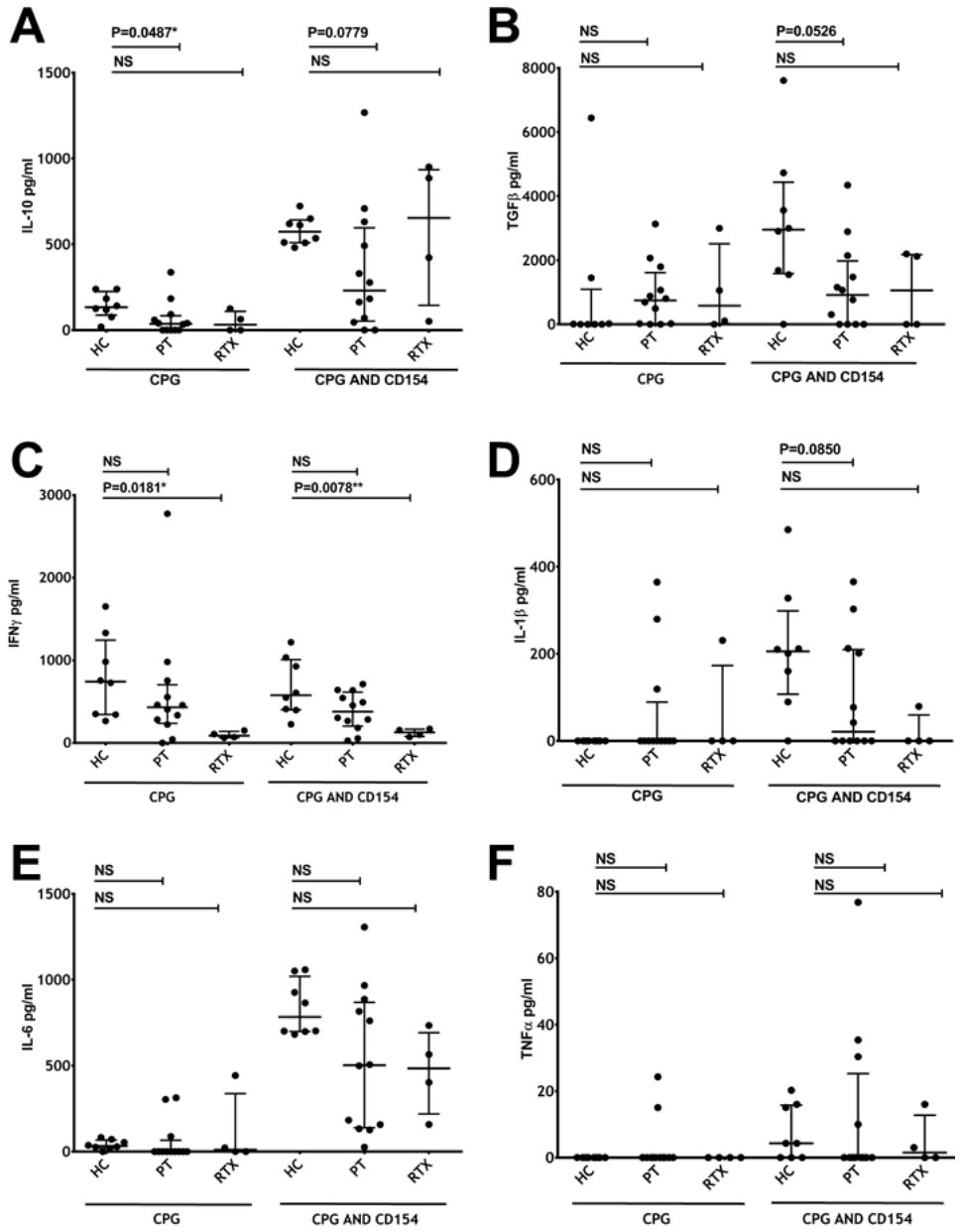

Kruskal Wallis and Dunn's multiple comparison conducted, P values less than 0.1000 shown. [A] Levels of soluble IL-10 were significantly lower in remission patients, compared to healthy controls on CPG stimulation (P=0.0487) and showed a similar trend on combined CPG and CD154 treatment (P=0.0779). [B]Maximally stimulated patient PBMCs also tended to have lower TGFβ than controls (P=0.0526). [C] IFNγ was significantly lower in rituximab treated patients, on stimulation with CPG alone (P=0.0181*) or with CD154 (P=0.0078**). [D-F] There was no significant difference in patients and controls cohorts for soluble IL-1β, IL-6 or TNFα.*

frequency of B cell subsets with secreted cytokine in PBMC supernatants. The results for the combined cohort of healthy controls and remission patients, excluding those patients treated with rituximab were convincing (Figure 5.23). The relationship of multiple B cell subsets with soluble IL-10, IL-6 and TGFβ were significant (supernatants from PBMC stimulated with CPG and CD154). The fact that these relationships were across multiple B cell subsets, suggests that this is a direct effect however, TLR-9 and CD40 expression is not limited to B cells.

Correlation with soluble IL-10, gave similar results IL-10+ B cells (Figure 5.9). Starting frequency of Breg correlated with secreted IL-10 (P=0.0023**) and tended to have the inverse relationship with Bmem (P=0.0925, Figure 5.23, Panel A). Soluble TGFβ did not correlate with Breg but showed positive correlation with Bmem and had an inverse relationship with Bnaive (P=0.0182* and P=0.0461*, Figure 5.23, Panel A). TGFβ has divergent roles, dependent on whether expressed in tandem with IL-6 or not (induction of Treg or of Th17 cells). Interestingly, the starting frequency of Bmem had an inverse relationship with secreted IL-6 (P=0.0584). Immunoregulatory function has also been attributed to CD27+ memory cells (Amu, Tarkowski et al. 2007, Iwata, Matsushita et al. 2011); perhaps they are particularly adept at inducing Treg and limiting Th17, unfortunately I only assessed Th1 cytokine production (Figures 5.4 and 5.5). Interesting, Bnaive cells had an inverse relationship with soluble TGFβ. Naïve B cells have not yet encountered their cognate antigen and reciprocal T cell activation, downstream of this. Activation of B cells has been proposed to be a mechanism whereby T cells induce their own regulation (Lemoine, Morva et al. 2011). This might be why there is an association between soluble TGFβ and Bmem but not Bnaive cells. The effect might also be indirect, FoxP3 and CTLA4 expression in Treg can be increased by B cells (Kessel, Haj et al. 2012).

Figure 5.21 Net cytokine profile in supernatants from stimulated PBMC

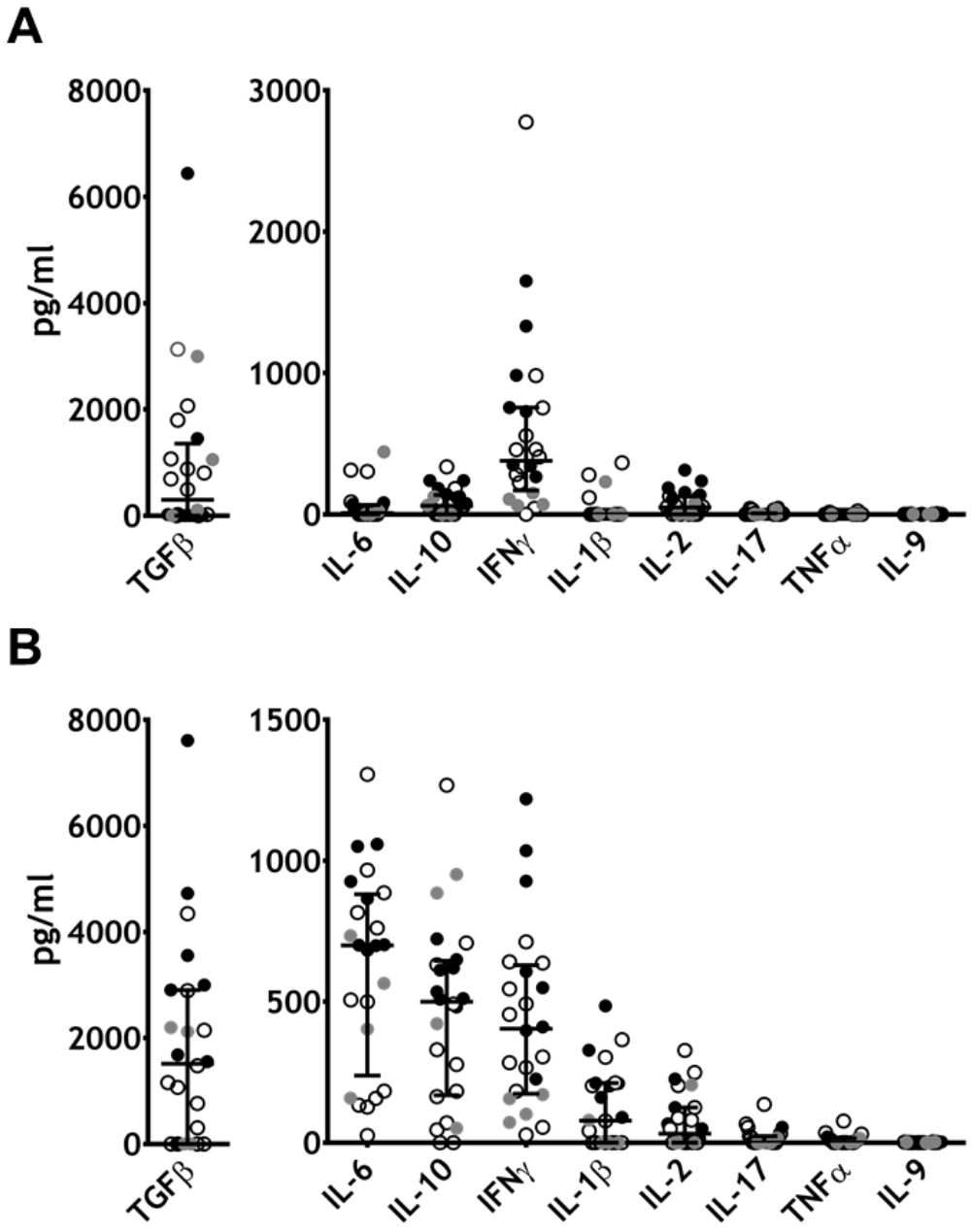

All the data points for cytokines detected in supernatants: controls are shown as black filled circles; rituximab treated patients, grey filled circles and remission patients, unfilled data points with a black outline. The median and interquartile range for each analyte is shown. [A] CPG alone and [B] CPG combined with CD154.

Figure 5.22 Cytokine profile, represented as percentage of all analytes detected

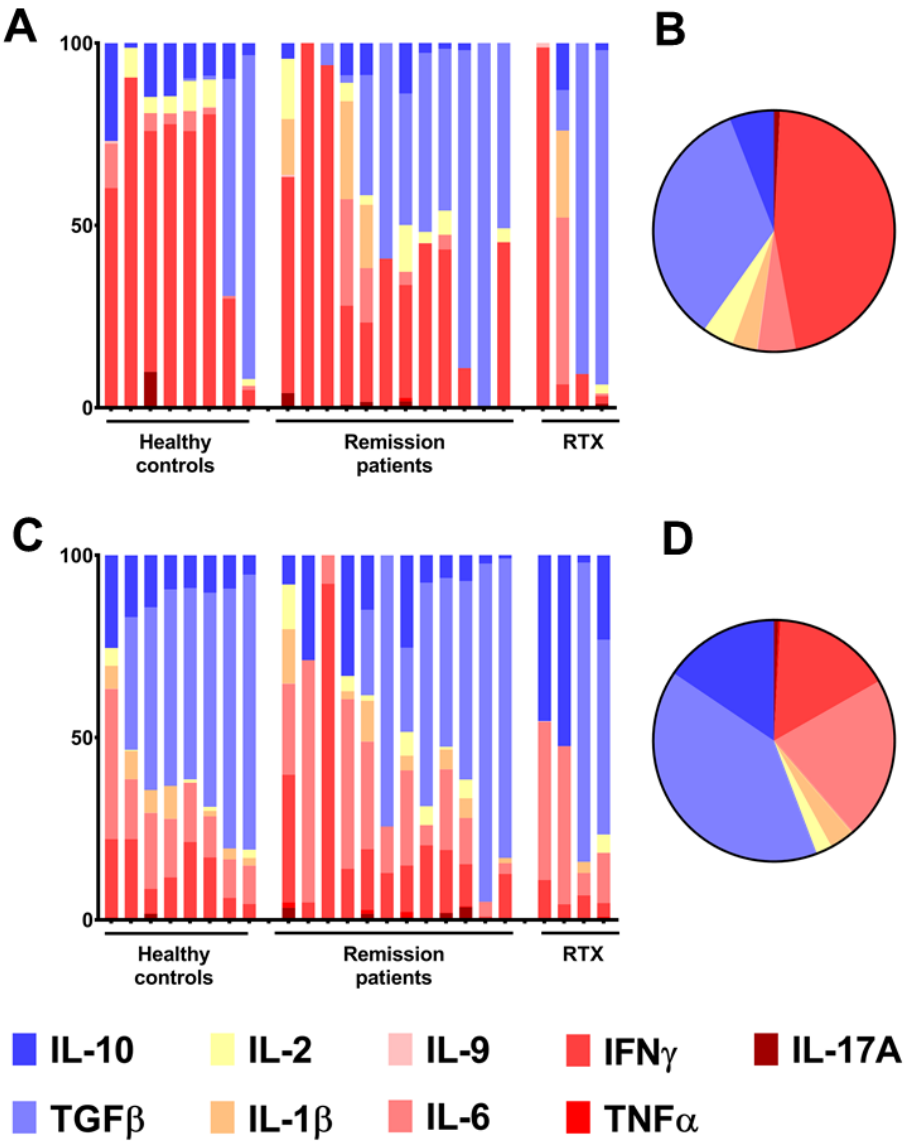

Proinflammatory cytokines shown in hot colours, IL-10 and TGFβ in shades of blue. [A and C] Cytokine profile for all individuals tested, the sum of the analytes detected (pg/ml), was normalised to 100. [B and D] Mean cytokine concentration for the cohort (n=24), normalised to 100 and presented in a pie chart. [A and B] On CPG stimulation, the profile is dominated by IFNγ production. [C and D] On combined CPG and CD154 stimulation, TGFβ and IL-10 represent more than 50% of the total analytes measured, IFNγ is diminished as proportion of the total and IL-6 is increased.

Figure 5.23 **Linear regression of B cell subsets with soluble IL-10, TGFβ and IL-6, from CPG and CD154 stimulated PBMC**

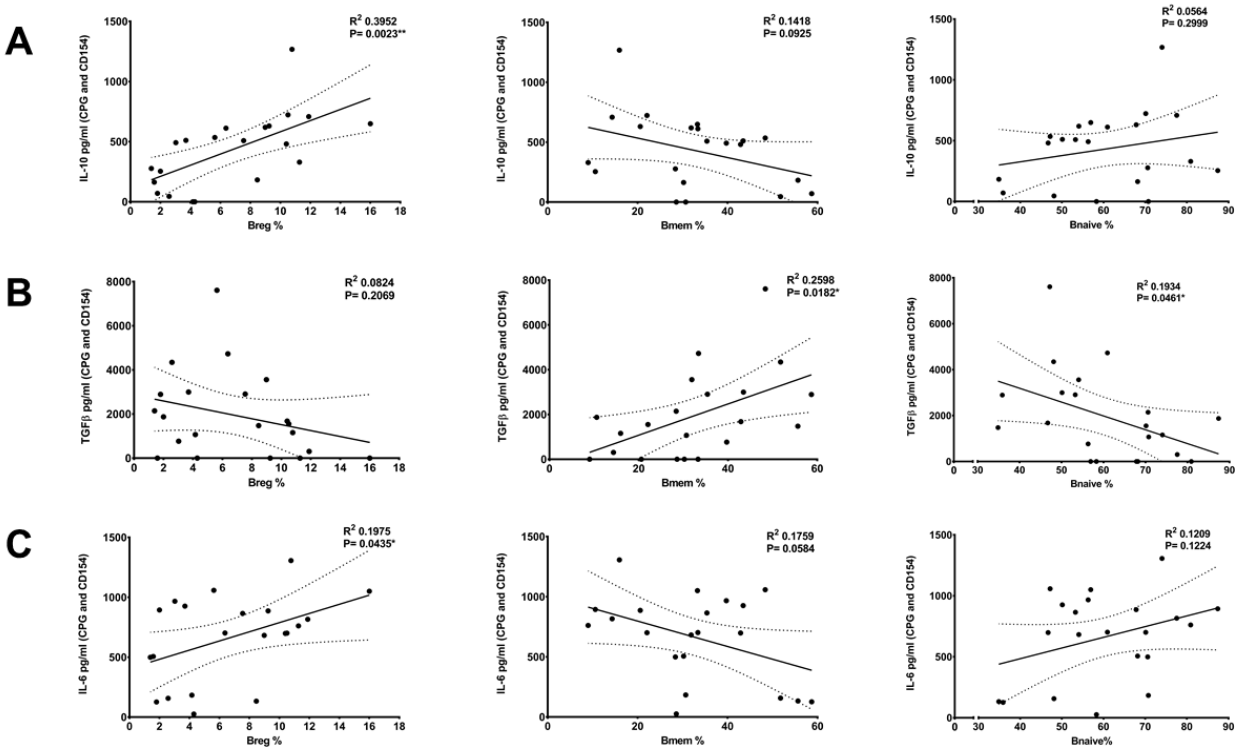

*B cell subsets at baseline and supernatant from CPG and CD154 stimulated PBMC (rituximab patients excluded from analysis). [A] Breg had a positive relationship with IL-10 (P=0.0023**). [B] Bmem had a positive correlation with TGFβ (P=0.0182*) and Bnaive, a negative relationship (P=0.0461*). [C] IL-6 and Breg correlated (P=0.0435*), Bmem were trending towards an inverse relationship with soluble IL-6 (P=0.0584).*

In contrast to Bmem, Breg frequency positively correlated with soluble IL-6. IL-10 and IL-6 together promote B cell survival, differentiation, germinal centre formation and immunoglobin production. Upon combined CPG and CD154 IL-6 was invariably detected (Figure 5.21, Panel B). Although the stimulation was perhaps not physiological, B cells are also reported to produce both IL-6 and IL-10, upon stimulation with autoantigen in healthy controls (Langkjaer, Kristensen et al. 2012). Further investigation is warranted, the net balance of these cytokines is critical in determining outcome in an animal model of MS, after B cell depletion (Barr, Shen et al. 2012). In addition, Tocilizumab an anti-IL6 receptor antibody, has been suggested as a suitable therapy for AAV (Sakai, Kondo et al. 2017).

5.4.4 Net effect of supernatants on T cells

Supernatants from CPG and CD154 stimulated PBMC, limited TNFα production in healthy control CD3+ CD25- cells (n=4), but not IFNγ at 10% final volume (representative flow cytometry plots shown in Figure 5.24, Panel A). The effect was comparable in pooled supernatants from patients and controls, permitting data to be combined. The median reduction in TNFα positive cells, relative to CD3 alone was: 69.5% and 60.1% for healthy control supernatants; 51.0 and 61.4% for patient supernatants. Mann Whitney was used to compare patient and control supernatants (IL-10 P=0.3429 and isotype P=0.6857).

Supernatants pre-incubated with anti-IL-10 monoclonal antibody or isotype control, were equally effective at limiting Th1 differentiation (Figure 5.24, Panel B). Statistical significance was assessed by Kruskal Wallis test (P=0.0097**) and Dunn's multiple comparison, relative to T cells alone (IL-10 P=0.0121* and isotype P=0.0299*). The

median percentage of TNFα T cells was 49.8% in T cells cultured alone and 22.34% in T cells cultured with any supernatant (Mann Whitney, P=0.0017**). TNFα geometric MFI for T cells had a median value of 278.8 (range 116.5-1120) in T cells cultured alone and 37.85 (range 22.5-86.7), in T cells cultured with any supernatant (Mann Whitney, P=0.0004**).

Figure 5.24 Net effect of PBMC supernatants on T cells

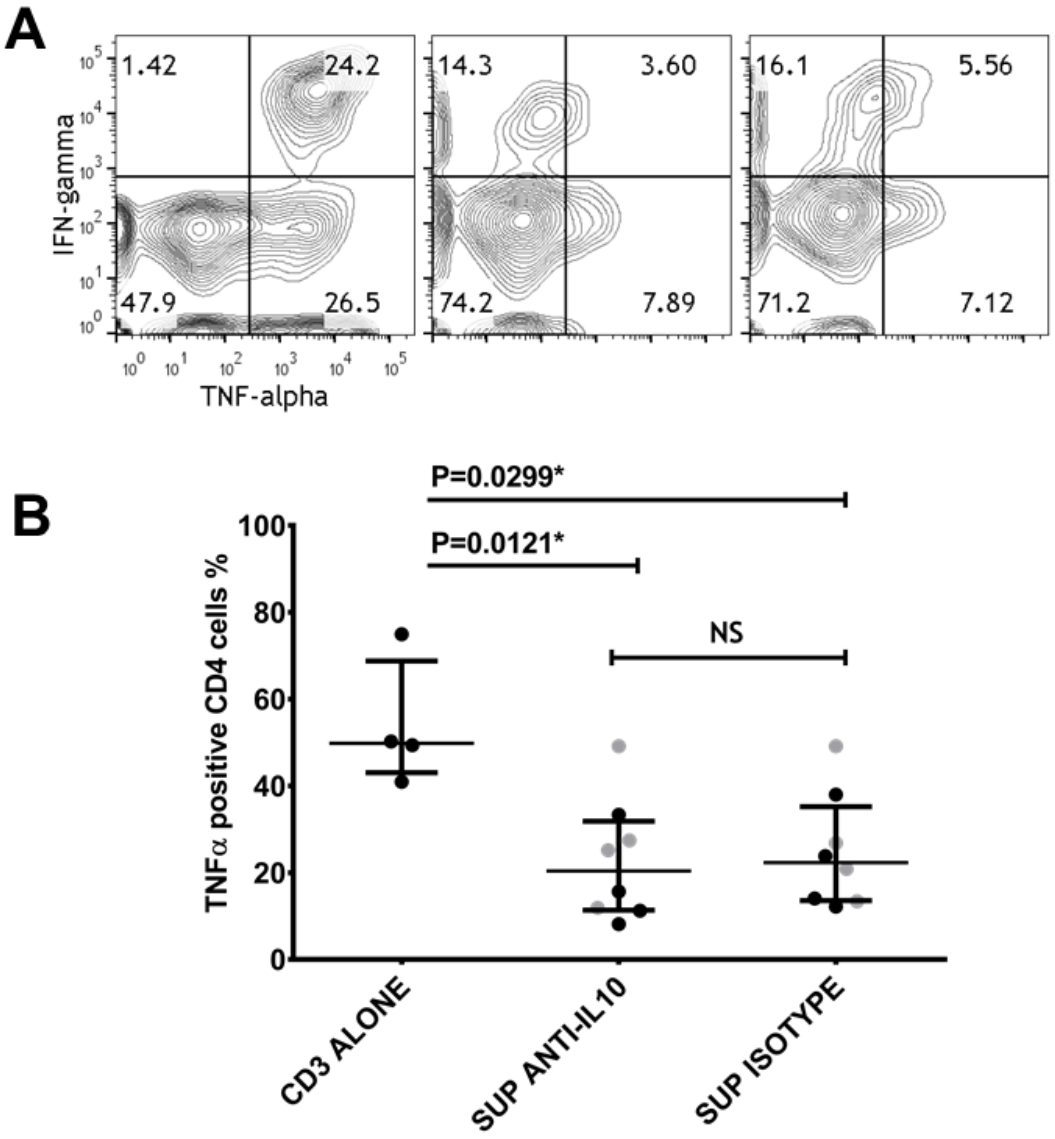

[A] Contour plots show T cells cultured without any supernatant on the left, cultured with supernatant preincubated with an IL-10 antibody (middle plot) or supernatant, preincubated with an isotype control (right plot). [B] The frequency of TNFα positive T cells after 3-day culture, was assessed in 4 healthy controls. T cells were either cultured alone or with 10% final volume of pooled PBMC supernatants. Supernatants from CPG and CD154 stimulated PBMC, significantly reduced frequency of TNFα positive T cells, whether IL-10 was neutralised (anti-IL10 P=0.0121) or not (incubated with a rat IgG isotype control P=0.0299*), assessed by Dunn's multiple comparison, relative to T cells alone. Grey circles, supernatant from non-rituximab treated patients; black circles, supernatant from healthy controls*

5.5 Key findings

5.5.1 Bmem and Bnaive cells augment Th1 differentiation, but Breg do not

The most striking observation was that Bnaive and Bmem augmented Th1 differentiation. Relative to Breg co-cultures, IFNγ and TNFα geometric MFI was significantly increased, as was frequency of IFNγ T cells (Figure 5.4 and 5.5).

There were only modest differences in patients and controls, specifically in relative IFNγ MFI for Bmem co-cultures (lower in patients than controls).

There were no differences between patients and control Breg and T cell co-cultures.

5.5.2 IL-10 B cell frequency is comparable in AAV remission patients and healthy controls

There were no differences between remission patients and healthy controls, however rituximab treated patients had higher frequency of IL-10+ B cells (Figure 5.7).

5.5.3 Conditions favouring B cell IL-10 production induce TNFα and TGFβ

Combined CPG and CD154 stimulation resulted in global B cell induction of TNFα (Figure 5.6, Panel B). Geometric MFI did not differ in remission patients and healthy controls on CPG and CD154 stimulus. Rituximab treated patients had significantly lower TNFα geometric MFI than the remission cohort, on CPG treatment (Figure 5.7).

TGFβ was also significantly induced, on treatment with CPG and CD154 (Figure 5.8).

5.5.4 Initial balance of B cell subsets, linked to B cell cytokine production

Immunophenotyping was conducted prior to IL-10 induction, which enabled balance of B cell subsets to be assessed relative to cytokine profile. Frequency of IL-10+ B cells on CPG and CD154 stimulation, positively correlated with Breg and had an inverse relationship with Bmem (Figure 5.9). Geometric TNFα MFI on CPG treatment, had a positive correlation with Bmem and the inverse relationship with Breg (Figure 5.10). Following CPG and CD154 stimulation, geometric TNFα MFI had a negative relationship with Breg when rituximab treated patients were removed from analysis (Figure 5.10, Panel C).

5.5.5 CD24 and CD38 immunophenotyping after stimulation, shows relative contribution of B cell subsets to cytokine induction

IL-10 B cells were highly enriched in the $CD24^{high}$ $CD38^{high}$ gate (Figure 5.12). B cell subsets also had differential expression of TNFα and TGFβ (Figure 5.13).

Following CPG and CD154 stimulation, Breg had higher IL-10 geometric MFI than Bmem (Figure 5.16). In healthy controls, TNFα geometric MFI was significantly higher in Bmem than Breg whether PBMC were treated with CPG alone or in combination with CD154; the same relationship was not observed in patient samples (Figure 5.14 and 5.15).

Although naïve B cells are more like Breg in terms of maturation than Bmem, having not encountered their cognate antigen, they differed in terms of cytokine geometric MFI. Bnaive cells had lower TNFα and IL-10 MFI than Breg or Bmem, on CPG treatment (Figure 5.14). Healthy control Bnaive had higher TNFα geometric MFI than Breg, upon combined CPG and CD154 stimulation.

5.5.6 Inflammatory and regulatory immune mediators detected in supernatants of PBMCs, stimulated for B cell IL-10 induction

IL-10, TGFβ, IL-2, IL-1β, IL-9, IL-6, IFNγ, TNFα and IL-17A were detected, in PBMC supernatants stimulated with CPG alone or in combination with CD154.

Very low levels of soluble TNFα were detected, which seemed discordant with intracellular flow cytometry results. TNFα may be induced by final treatment with PMA and ionomycin not prior stimulation with CPG and CD154; it would not be released into the supernatant, due to the presence of a Golgi-transport inhibitor.

5.5.7 Correlation between soluble analytes and B cell subsets at baseline

B cell subsets at baseline, influence net PBMC cytokine production on treatment with CPG and CD154.

There was correlation between the frequency of multiple B cell subsets, and secreted levels of IL-10, IL-6 and TGFβ after combined CPG and CD154 stimulation. Breg positively correlated with IL-10pg/ml (Figure 5.23, Panel A, P=0.0023**).

Some of the other findings were unexpected and warrant further investigation, for example there was positive correlation of Bmem with TGFβ and the inverse association with IL-6; the balance of these 2 cytokines is critical in determining whether Treg or Th17 cells are induced. Breg had no relationship with soluble TGFβ and Bnaive frequency had an inverse relationship. This might suggest divergent immunoregulatory roles for peripheral B cell subsets, with IL-10 production by Breg and TGFβ, by Bmem.

5.5.8 Effect of supernatants from PBMCs, stimulated for IL-10 induction

The net effect of B cell supernatants was to limit TNFα induction in T cells. This was not inhibited when supernatants were pre-incubated with an agonistic IL10 antibody, compared to a rat IgG isotype control.

5.5.9 Summary

Whilst there was little difference between AAV patients and controls, this chapter cumulatively builds evidence that Breg, Bnaive and Bmem are functionally different.

Bmem and Bnaive cells augment Th1 differentiation *in vitro,* relative to Breg.

The starting frequency of Breg cells positively correlates with IL-10+ B cells and has an inverse relationship with B cell TNFα MFI. The converse is true for Bmem.

On CPG stimulation, Breg have lower TNFα MFI than Bmem cells. IL-10 and TNFα expression is higher in Breg and Bmem, compared to Bnaive cells.

Following CPG and CD154 stimulation, IL-10 geometric MFI is higher in Breg than Bmem. In healthy controls, Breg have lower TNFα MFI than Bmem or Bnaive cells.

There is correlation between multiple B cell subsets and levels of soluble IL-6, IL-10 and TGFβ, detected in the supernatants from PBMC stimulated with CPG and CD154. Breg cells positively correlate with IL-10 and IL-6, with an opposing relationship observed with Bmem. Bmem have a positive relationship with TGFβ, whilst Bnaive cells have a negative relationship.

5.6 Discussion

5.6.1 B cell co-cultures

Effects on Th1 differentiation were assessed, as B cells had previously been shown to limit cytokine production, proliferation and induce apoptosis in CD4 T cells (Tretter, Venigalla et al. 2008, Blair, Norena et al. 2010, Bouaziz, Calbo et al. 2010, Kessel, Haj et al. 2012). Functional defects have been described in SLE, rheumatoid arthritis, Grave's disease, Pemphigus and Sjörgen's syndrome (Blair, Norena et al. 2010, Zha, Wang et al. 2012, Flores-Borja, Bosma et al. 2013, Lin, Jin et al. 2014, Zhu, Xu et al. 2015).

Under the culture conditions used, there was only modest differences in IFNγ and TNFα induction on addition of Breg to CD4+ CD25- T cells. Blair *et al* previously showed Breg reduced IFNγ and TNFα positive T cells in co-culture, with no effect observed with Bmem or Bnaive cells (Blair, Norena et al. 2010). Blair *et al* coated plates with anti-CD3 at a concentration of 0.5µg/ml and conducted co-cultures for 3 days, opposed to 1.0µg/ml plate bound anti-CD3, 2µg/ml soluble anti-CD28 and 5-day culture in this study. It is possible that this simulation may have masked any CD80- or CD86-dependent, regulatory effect (Blair, Chavez-Rueda et al. 2009).

In contrast, Bmem and Bnaive subsets significantly enhanced Th1 cytokine production. Harris *et al* first described cytokine producing B cells as effector 1 and 2 (Be1 or Be2) cells, which differed in their ability to augment Th1 or Th2 responses (Harris, Haynes et al. 2000). The balance of Bmem and Breg is affected in AAV and may determine clinical outcome by reciprocal interaction with T cells and monocytes.

Multiple Sclerosis (MS) is an antigenic specific, T cell mediated disease. In an animal model, B cells could both augment and limit autoimmunity (Matsushita, Yanaba et al. 2008). MS patients have an imbalance in peripheral B cell subsets (Knippenberg, Peelen et al. 2011), with greater propensity to produce GM-CSF (Li, Rezk et al. 2015). GM-CSF is a critical survival factor for granulocytic and myeloid cells, augmenting innate inflammatory responses. Indeed, these effector B cells in MS patients enhanced macrophage IL-12, IL-6 and IL-1β production in a GM-CSF specific manner (Li, Rezk et al. 2015). In contrast the regulatory $CD24^{high}$ CD27+ B cell population, limits TNFα production by monocytes *in vitro* (Iwata, Matsushita et al. 2011). Regulatory B cells also determine the net balance of Th17 and Treg in rheumatoid arthritis (Carter, Rosser et al. 2012, Flores-Borja, Bosma et al. 2013). Although I did not assess effect on B cells on monocytes or Th17 in AAV, this has subsequently been investigated.

Lepse *et al* assessed the ability of B cells to limit monocyte TNFα production in GPA patients and controls. Patient and control B cells both limited TNFα MFI in LPS stimulated monocytes (Lepse, Abdulahad et al. 2014). This function was previously shown to be impaired in idiopathic thrombocytopenic purpura (Li, Zhong et al. 2012).

Von Borstel *et al* recently reported that frequency of circulating Breg negatively correlates with Th17 in AAV patients and controls. When T:B co-cultures were performed, the depletion of Breg did not affect the induction of IFNγ in CD4 T cells but resulted in reduced frequency of Th17 T cells upon Staphylococcal enterotoxin B and CPG stimulation (Borstel, Lintermans et al. 2018).

5.6.2 IL-10, TNFα and TGFβ induction in B cells

CD5, CD24high CD27+ and Breg subsets have previously shown to be enriched for IL-10 competency (Gary-Gouy, Harriague et al. 2002, Blair, Norena et al. 2010, Iwata,

Matsushita et al. 2011). The balance of peripheral B cell subsets was perturbed in AAV, but I found no difference in the frequency of IL-10 B cells in remission patients and controls. I was not able to test patients with new onset disease, as IL-10 induction had to be conducted on fresh samples, and AAV patients present relatively infrequently (incidence of 30/million annually).

Lepse *et al* also found no deficiency in IL-10 B cells in AAV, assessed after 3-day stimulation with 500ng/ml CPG (Lepse, Abdulahad et al. 2014). In contrast, Wilde *et al*, found IL-10 B cells reduced in both active and remission AAV patients following stimulation with 0.1μM CPG. This was irrespective of whether patients were on immunosuppression or not (Wilde, Thewissen et al. 2013). Frequency of IL-10+ CD5+ Breg is reported to be linked to outcome in AAV (Aybar, McGregor et al. 2015), and high dose steroids actually improves IL-10 induction by CD5+ B cells (Hua, Ji et al. 2012).

Starting frequency of Bmem and Breg, was related to B cell IL-10 competency on regression analysis. This suggests patients with the most profound changes in alterations in these B cell subsets, would have altered frequency of IL-10+ B cells. Indeed, rituximab treated patients did have higher IL-10 frequency than controls, on CPG and CD154 stimulation. IL-10 frequency would be expected to be reduced in patients with high M:Rn.

Discrepancies in results might also be due to the differences in induction method. IL-10 is not uniquely expressed by any one B cell subset (Lighaam, Unger et al. 2018), with this cytokine also detected in CD27+ memory B cells (Iwata, Matsushita et al. 2011). In the other studies in AAV, B cells were stimulated with CPG alone (Wilde, Thewissen et al. 2013, Lepse, Abdulahad et al. 2014). After CPG treatment I found

IL-10 geometric MFI did not differ in Breg or Bmem, but was higher in both these subsets, compared to Bnaive cells. On CD154 and CPG stimulation, Breg had higher MFI IL-10 than Bmem and TGFβ was significantly induced.

TNFα was ubiquitously expressed by B cells on CPG and CD154 stimulation. The starting frequency of Bmem positively correlated with geometric TNFα MFI in B cells, Breg had an inverse relationship. When Breg were depleted in other study, B cells stimulated by BCR ligation secreted more IFNγ (Bautista-Caro, de Miguel et al. 2017). Although depletion experiments were not conducted in this study, B cell subset expression of TNFα and IL-10, was assessed after stimulation.

$CD24^{high}$ $CD38^{high}$ Breg are also reported to be heterogenous themselves, with variable CD21 expression (Suryani, Fulcher et al. 2010), CD27 (Simon, Pers et al. 2016) and cytokine production (Cherukuri, Rothstein et al. 2014). Net balance of anti- and pro-inflammatory cytokines may therefore be a better indicator of regulatory B cell function. To further assess this, I looked at soluble cytokines in PBMC simulated with CPG alone, or in combination with CD154.

5.6.3 Soluble mediators detected in supernatants

IL-10, TGFβ, IL-1β, IL-6, IFNγ were the major analytes detected in in supernatants from stimulated PBMC. IL-2, TNFα and IL-17A were detected to a lesser level and IL-9, was approaching the limit of detection. I did not verify that B cells produced all these cytokines by intracellular flow cytometry however, it has long been established that B cells can produce IL-1β, IL-6 and IFNγ (Pistoia 1997).

The net effect of these soluble mediators was to limit TNFα production in CD3+ CD25- T cells, at a final dilution of 1 in 10. This was not inhibited by an agonistic IL-10 antibody, so may be TGFβ dependent.

B cell subsets a baseline seemed to influence net cytokine production, even although supernatants were collected from mixed PBMC cultures, with expression of CD40 and TLR9 not limited to B cells.

On maximum stimulation, IL-10 and IL-6 levels positively correlated with starting frequency of Breg. Bmem had an inverse relationship with IL-10 and IL-6, but a positive relationship with TGFβ. Breg had no relationship with soluble TGFβ, whilst frequency of Bnaive had a negative relationship with soluble TGFβ levels. The fact that these relationships were observed across multiple B cell subsets, for the same analyte, gives more confidence in these results but effects may still be indirect. Breg induce Treg (Flores-Borja, Bosma et al. 2013) defined in-part by their production of IL-10 and TGFβ. Effector B cells promote secretion of IL-6 and IL-1β by macrophages (Li, Rezk et al. 2015). Degradation of ATP to adenosine has recently been proposed to be an important immunoregulatory mechanism in Breg (Menon, Smith et al. 2017); this could limit inflammasome activation, IL-1β and IL-6 release from myeloid cells. Myeloid suppressor cells also limit inflammation by production of IL-10, these cells are induced concomitantly with Breg, on culture with TFH, from non-small cell lung cancer patients (Qiu, Yu et al. 2018).

Use of various culture conditions would enable further dissection of the role of PBMC subsets on net cytokine production. This would be conducted by depletion (magnetic isolation, flow cytometry sorting or adherence of monocytes to plastic), irradiation and use of a trans-well culture system.

Chapter 6 Relationship with CD4 subsets

6.1 Background

The relationship between Breg and Treg frequency, was examined in a subset of AAV patients and healthy controls. Treg cells were defined as CD4+ CD25 high and CD127 low, with expression of CD39 and CD73 additionally assessed.

CD39 and CD73 are ectoenzymes that hydrolyse adenosine tri- di- or mono- phosphate (ATP, ADP and AMP) to adenosine. Degradation of ATP and adenosine generation is a key immunoregulatory mechanism used by Treg. ATP is a danger signal, which promotes migration and maturation of dendritic cells, whilst extracellular adenosine limits NK and T cell effector functions, promotes a switch to a tolerogenic DC phenotype and induces Treg (Cekic and Linden 2016). Upon stimulation, CD39+ Treg are less likely to transdifferentiate into Th1 or Th17 cells and have better preservation of FoxP3 expression (Gu, Ni et al. 2017). They have enhanced suppressive activity *in vitro*, compared to CD39- Treg (Borsellino, Kleinewietfeld et al. 2007).

Whilst CD4+ CD25+ T cells are widely reported to be increased in AAV (Popa, Marinaki, Free, Wilde, Abdulahad), there have been conflicting publications about the frequency of Treg in patients. These inconsistencies have likely arisen due to heterogeneity in patient groups in terms of ANCA-specificity, treatment and disease activity, compounded by differences in the methods used to classify Treg. Overall there is good evidence that Treg are functionally perturbed in AAV (Marinaki, Neumann et al. 2005, Abdulahad, Stegeman et al. 2007, Chavele, Shukla et al. 2010, Morgan, Day et al. 2010, Rimbert, Hamidou et al. 2011, Free, Bunch et al. 2013). The research findings are summarised in Table 6.1, below.

The relationship between Treg and B cell subsets has not been well characterised to-date, however B cells are reported to enhance Treg function *in vitro (Kessel, Haj et al. 2012, Flores-Borja, Bosma et al. 2013)*. Recently, the frequency of CD39 and CD73 positive lymphocytes was shown to be lower in AAV patients, compared to controls. CD39 frequency was reduced in both naïve and memory T cell populations (CD45RA- and CD45RA+), with CD73 expression reduced in memory T cells alone (Kling, Benck et al. 2017). In addition, CD39+ Treg frequency is reported to positively correlate with IL-10 B cell competency in AAV (Wilde, Thewissen et al. 2013).

6.2 Aims

The main aim was to establish whether there was any relationship between Treg and Breg frequency in AAV patients and controls in this mixed cohort. Most of the published case series, have a predominance of patients with GPA diagnosis (see table 6.1). Secondly, to define frequency of CD39 and CD73 positive cells within CD4 cells and Treg (CD4+ CD25 high and CD127-). It was also possible to define expression of these enzymes more broadly in CD4+ CD25 subsets, CD4- lymphocytes and monocytes (defined based on light scatter and intermediate expression of CD4).

T cell immunophenotyping was conducted in parallel to B cell testing; assessing T cell phenotypes, relative to frequency of B cell subsets and cytokine production. B cell subsets were classified on relative CD24 and CD38 expression and cytokines were induced in PBMC, stimulated with CPG alone or in combination with CD154. Intracellular FACS was conducted for TNFα, IL-10 and TFGβ production,

Table 6.1 Treg cells are numerically or functionally deficient in AAV

Reference	Experimental approach	Findings
Marinaki 2005	FoxP3 mRNA, in purified CD4+ cells relative Glucose-6-phosphate dehydrogenase (G6DP)	Infer **Treg frequency does not differ,** no difference in CD4 FoxP3 mRNA (22 GPA, 7 MPA)
	CD45RB high and low CD4 cell proliferation assessed in response to CD3 alone or in combination with IL2	Increased T cell proliferation in patients compared to HC, report due to persistently activated T cells –might infer **Treg dysfunctional**
Abdulahad 2007	Immunophenotyping to determine the frequency of Treg, defined as CD4+ $CD25^{high}$ FoxP3+	**Treg increased** in GPA, predominately CD45RO+ (52 patients and 27 HC)
	Suppression assay with CD25+ cells, thymidine uptake, anti-CD3 and CD28 stimulation 1:1 ratio	Treg **functionally impaired** (10 GPA patients and 10 HC)
Morgan 2010	Immunophenotyping to determine the frequency of Treg, defined as CD4+ $CD25^{high}$ FoxP3+	**Treg reduced** (55 GPA, 33 HC) Increased in rem compared to active (paired samples), inverse correlation time to relapse
	CFSE assay, 11-day stimulation with PR3 or PDD control antigen – in replete PBMC compared to CD25 depleted PBMC	Treg **functionally impaired**, did not suppress antigen induced proliferation or TNFα release, in ANCA+ patients
Rimbert 2011	Immunophenotyping, Treg were defined CD4+ CD127 $CD25^{high}$	Moderate **Treg reduction** in patients (25 GPA, 9 MPA, 18 HC
	FoxP3 and CD39 frequency in CD4+ CD127- $CD25^{high}$ cells	No difference in CD39 or FoxP3 expression
	CD4+ CD127- CD25 high FACS isolated cells, thymidine uptake, anti-CD3 and CD28, 1:1 ratio	**Treg dysfunctional** profoundly reduced ability to suppress proliferation of responder cells
Chavele 2012	FoxP3 mRNA, measured in whole blood relative to Glyceraldehyde 3-phosphate dehydrogenase (GAPDH)	Infer **Treg reduced**, FoxP3 mRNA reduced in whole blood of patients (10 MPO-ANCA, 10 HC
	Suppression CD25+ cells and CD25- responder cells, thymidine uptake, CD3 and CD28 beads	**No functional impairment** (11 MPO patients and 5 HC)
Free 2013	Immunophenotyping to determine Treg frequency, CD4+ $CD25^{high}$ $CD127^{low}$ FoxP3+	**Treg increased** in active disease (63 patients, 40% GPA, 48% MPA, 11% renal limited, 19 HC)
	Expression of FoxP3 splice variants assessed using 2 different clones PCH101 and 150D	Patients use an alternative FoxP3 isoform, lacking exon 2
	CD4+ CD127- CD25 high FACS isolated cells, CFSE assay, 4-day stimulation with anti-CD3 and CD28, 1:1 ratio	**Treg functionally impaired** (8 patients and 6 HC)

soluble analytes were measured by cytometric bead array and ELISA (see Table 2.1, for analytes and limit of detection).

6.3 Methods in brief

PBMC isolation, cryopreservation and flow cytometry staining protocols are described in the methods chapter. Briefly, cell surface immunostaining was performed on fresh cells or cryopreserved samples, thawed and stained immediately. Samples were stained with CD4 [RPA-T4], CD25 [BC96] and CD127 [A019D5] (Biolegend, San Diego, CA) and CD39 [eBioA1 (A1)] and CD73 [AD2] antibodies (eBiosciences, ThermoFisher Scientific, Loughborough). Staining was conducted between May 2013 and May 2015.

FACS acquisition was performed on a 4 laser BD LSR Fortessa instrument, with voltage correction to CST baseline (cytometer setup and tracking beads). Compensation was conducted on BD mouse IgG beads, with correction calculated automatically in BD Diva software (BD Biosciences, Berkshire, UK. Flow cytometry analysis was conducted using FlowJo (TreeStar, Ashland, OR, USA).

The additional methods were described in chapters 2 and 3, respectively. B cell subset characterisation was based on relative expression of CD24 and CD38. PBMC were stimulated *in vitro*, to induce maximum IL-10 induction in B cells. Following stimulation cytokine profiling was conducted by intracellular flow cytometry, CBA and ELISA.

6.3.1 Flow cytometric gating strategy

Flow cytometric gating strategy is shown in Figures 6.1 and 6.2. PBMC were stained for CD4, CD127, CD25, CD39 and CD73. Debris was excluded by applying a threshold gate, lymphocytes and monocytes were defined based on forward and side scatter of light (FSC-A:SSC-A, area parameter). The monocyte gate was further refined, as a compact population on side scatter (SSC-H, height parameter), with intermediate expression of CD4. CD4+ and CD4- populations were gated on expression of this marker, against SSC-H. Histograms show the refined monocyte population (dashed line), overlaid with CD4+ (filled grey histogram) and CD4 null lymphocytes (solid black line).

Treg cells were defined as CD4+ CD127- CD25 high. Additional populations could be resolved based on relative expression of CD25 alone, these were assigned CD25- , CD25+ and CD25 high. To exclude any contribution from Treg cells, whenever all these CD4 cell groups were compared, CD127+ cells were selected therein (gating for $CD25^{hi}$ CD127+ cells shown). Four groups were defined in total: 1. basal activation status CD4 T cells (CD25-), 2. activated CD4 T cells (CD25+ CD127+), 3. highly activated CD4+ T cells (CD25high CD127+) and 4. Treg (CD25 high CD127-).

Figure 6.1 Gating strategy for CD4, CD25 and CD127 stained PBMC

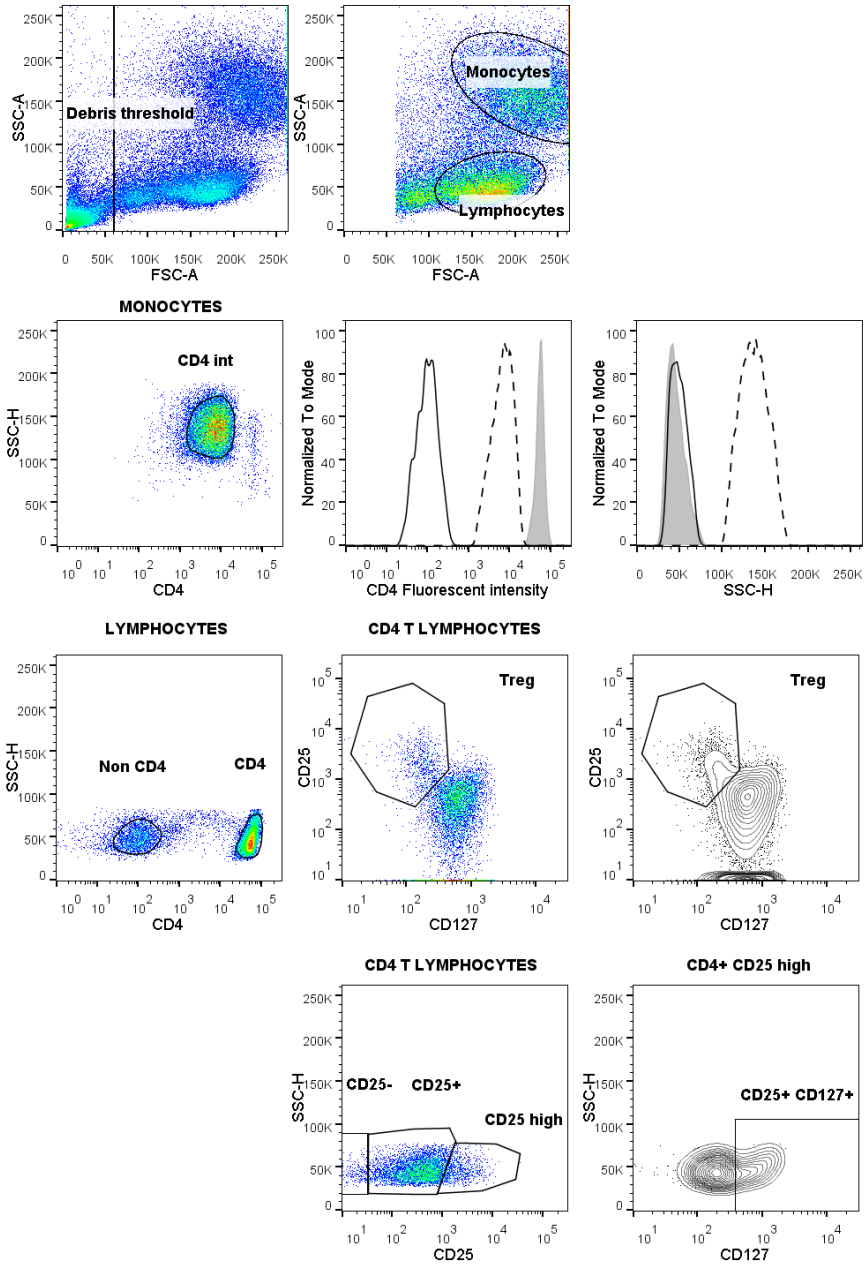

The top row shows exclusion of PBMC debris, with creation of lymphocyte and monocyte gates. The monocyte population was refined as a discrete population, with intermediate CD4 expression and similar side scatter (second row). Within the lymphocyte gate, CD4+ and CD4- gates were assigned. Treg were CD4+ CD25high and CD127low. 3 different CD4+ populations were classified base on relative CD25 expression. This permitted definition of a CD25high CD127+ population, of highly activated T cells (bottom row).

Figure 6.2 **Gating strategy for CD39 and CD73, within CD4, CD25 and CD127 stained PBMC**

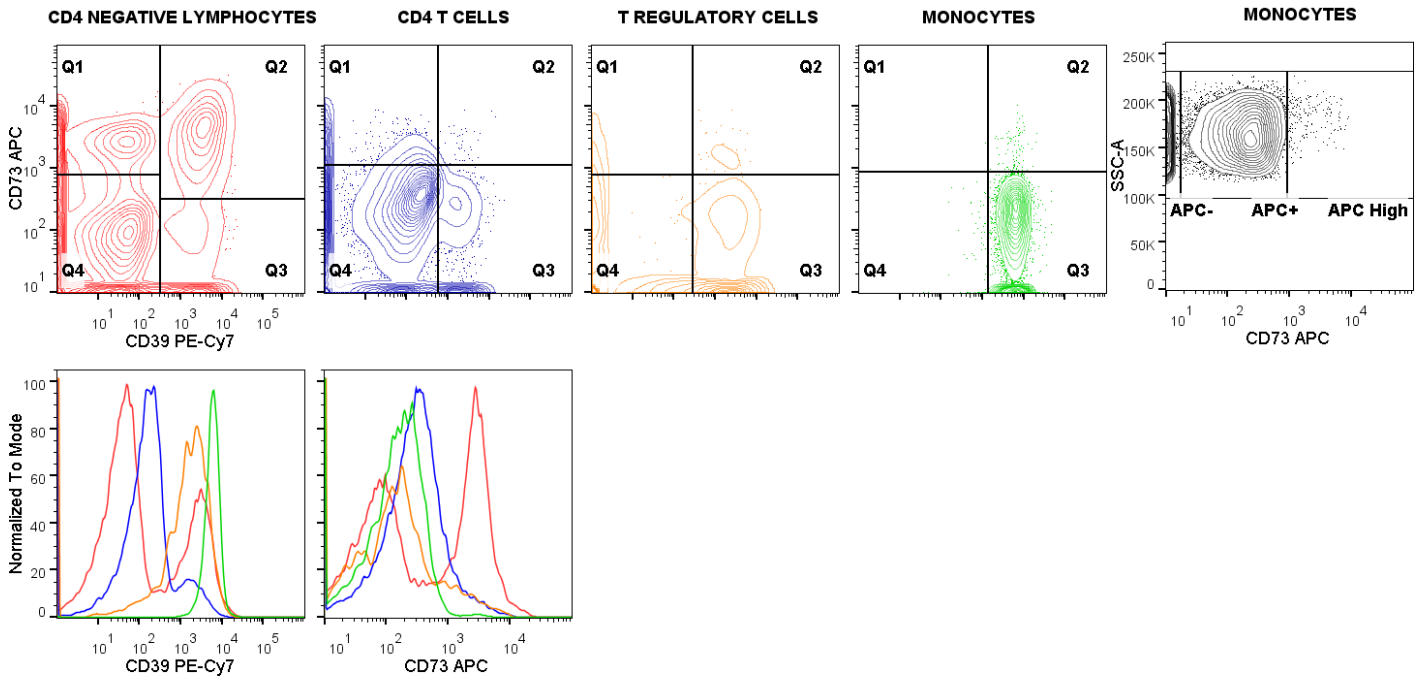

CD39 and CD73 gating was primarily based on quadrants, drawn for each subpopulation. In monocytes CD73 high cells were very low frequency, but 2 populations could be resolved with low and no expression of this marker. Colours used in contour plots, used to represent the same populations in overlaid histograms.

6.3.2 Patient and healthy control samples

The relationship between Breg and Treg frequencies, was examined in AAV patients (n=26) and healthy controls (n=12). The healthy controls were using fresh samples, 7 females and 5 males. Details of the AAV cohort are presented in brief in Table 6.2. A summary of the tests conducted on each patient is provided in Appendix 1.

The patient cohort comprised 13 individuals with grumbling or acute disease and with 13 in clinical remission (BVAS of zero). The remission group did not include any tolerant individuals or any showing lasting effects of rituximab treatment, on B cell immunophenotyping (p-054, 7 years after last infusion). Sex distribution was balanced, with 12 female and 14 male patients. In terms of ANCA specificity, 15 patients were PR3-ANCA, 8 MPO-ANCA and 3 were ANCA negative (2 GPA and 1 MPA diagnosis, also grouped as non-PR3 for analyses).

B cell subsets and Treg frequencies were determined for all patients (n=26). CD39 and CD73 analysis was conducted in CD4 and CD4 null lymphocytes populations for 24 individuals, and not tested (NT) in 2 individuals. CD39 and CD73 expression was further assessed in monocytes for 23 individuals (labelled Mon in Table 6.2). This cell subset could not be assigned for one patient (P_038) due to insufficient cell frequency relative to debris (denoted by a downwards arrow in Table 6.2).

Further CD4 subset analysis was not conducted if there were < 1000 Treg (represented with a downwards arrow in Table 6.2). In those patients with enough cells (n=17), CD39 and CD73 expression was assessed in CD4+ CD25 subsets namely: Treg (CD25 high CD127-), highly activated T cells (CD25 high CD127+), activated T cells (CD25+) and basal activation status T cells (CD25-). Some of the B cell subset data

Table 6.2 Patient cohort

ID	CELLS	COHORT GROUP	ANCA	SEX	AGE	CD39/73	
						Treg	Mon
P_002	Fresh	REPLICATE, REM	PR3	F	83	1	1
P_030	Frozen	Grumbling	PR3	M	59	1	1
P_033	Frozen	Grumbling, ANCA neg	None	M	47	1	1
P_034	Fresh	REPLICATE, REM	PR3	M	65	1	1
P_035	Frozen	Grumbling, ANCA neg	None	F	51	1	1
P_037	Frozen	*ACUTE	PR3	M	33	↓	1
P_038	Frozen	*ACUTE	PR3	F	52	↓	↓
P_039	Frozen	*ACUTE	MPO	M	38	↓	1
P_040	Frozen	Grumbling	MPO	M	56	1	1
P_042	Frozen	*ACUTE	PR3	M	22	1	1
P_043	Frozen	*ACUTE	MPO	M	41	↓	1
P_044	Frozen	*ACUTE	MPO	M	64	↓	1
P_045	Fresh	REPLICATE, REM	PR3	M	70	1	1
P_046	Frozen	*ACUTE	PR3	M	53	↓	1
P_048	Frozen	*ACUTE	MPO	F	62	1	1
P_049	Frozen	*ACUTE	MPO	F	74	↓	1
P_054	Fresh	*REM	PR3	F	54	1	1
P_057	Fresh	*REM	PR3	F	17	1	1
P_059	Frozen	*REM	MPO	F	69	NT	NT
P_061	Frozen	*REM	PR3	M	60	NT	NT
P_062	Fresh	REM, ANCA neg	None	F	68	1	1
P_063	Fresh	*REM	PR3	F	82	1	1
P_064	Fresh	*REM	MPO	F	64	1	1
P_065	Fresh	*REM	PR3	F	27	1	1
P_068	Fresh	*REM	PR3	M	67	1	1
P_070	Fresh	*REM	PR3	M	81	1	1

was previously presented in Chapter 3 (CD24 and CD38 immunophenotyping), prefixed by an asterix in the table (n=22). There were an additional 8 samples, included in this analysis: ANCA negative patients, grumbling disease opposed to acute and replicates (ANCA positive patients, now in remission, previously tested at initial presentation).

Although there was considerable overlap with the main case series, cohort selection was less stringent, and some samples were processed differently (11 samples tested fresh, 15 from frozen).

6.4 Results

6.4.1 Treg frequency is reduced in AAV patients compared to controls

Treg were lower in the combined patient group (n=26), compared to controls (n=12) (Figure 6.3). Both data sets passed D'Agostino and Pearson normality test, but it was apparent that the distribution differed in healthy controls, compared to patients (range 5.4-11.6 in controls and 2.87-11.33 in patients). Welch's 2 tailed unpaired t-test was used to compare patients and controls, this applies a correction for the difference in standard deviation; the mean Treg frequency in controls was 7.702% and 5.677% in patients (P=0.0167*).

Patient were further classified as PR3-ANCA (n=15) or non-PR3 (n=11). The mean Treg frequency in non-PR3 group was 5.035% and 6.148% for the PR3-ANCA patient group. The non-PR3 group were statistically different from controls (one-way ANOVA and Holm-Sidak's multiple comparison test P=0.0232*) however, the PR3-ANCA patients did not differ significantly from controls (Figure 6.3).

When patients were categorised according to disease activity, there were 13 with grumbling or acute disease and 13 in clinical remission with a BVAS of zero. The mean Treg frequency in grumbling or acute disease was 5.400% and 5.954% in clinical remission. The acute or grumbling group was statistically different from controls (one-way ANOVA and Holm-Sidak's multiple comparison test P=0.0472*) but the remission group did not differ significantly (Figure 6.3).

When patients were classified based on ANCA and disease activity, there were relatively few individuals in each group and statistical significance was not achieved (Kruskal-Wallis test P=0.1401). These data are summarised in Figure 6.3.

There was no correlation between age and Treg frequency when linear regression was performed (Figure 6.3, Panel B, P=0.3603). This analysis was conducted due to a significant difference in the age of controls and patients. Remission patients did not have a normal distribution of age, so Kruskal-Wallis and Dunn's multiple comparison test was conducted. Remission AAV patients were older than controls (P=0.0156*) but patients with active disease did not differ significantly compared to controls (P=0.8690). The median and age range for the respective groups were: 43 years and 31-62 for controls; 52 years and 22-74 years for patients with acute or grumbling disease; 67 years and 17-83 years for remission patients.

Treg frequencies were compared for the different processing techniques (not shown). There was no significant difference in Treg frequency in fresh and frozen patient samples, the mean and standard deviation was 6.66% $\pm$2.629 for fresh samples and 5.292% $\pm$2.786 for frozen samples (unpaired t-test P=0.2936). The spread of the data was very similar in fresh and frozen AAV patient samples, the range was 2.03-12.28 for fresh samples and 1.9-11.33 for frozen. The maximum value for controls was similar (11.6), however the minimum Treg frequency was higher (5.4%, opposed to 2.0 and 1.9).

Figure 6.3 Treg reduced in AAV, frequency not affected by age

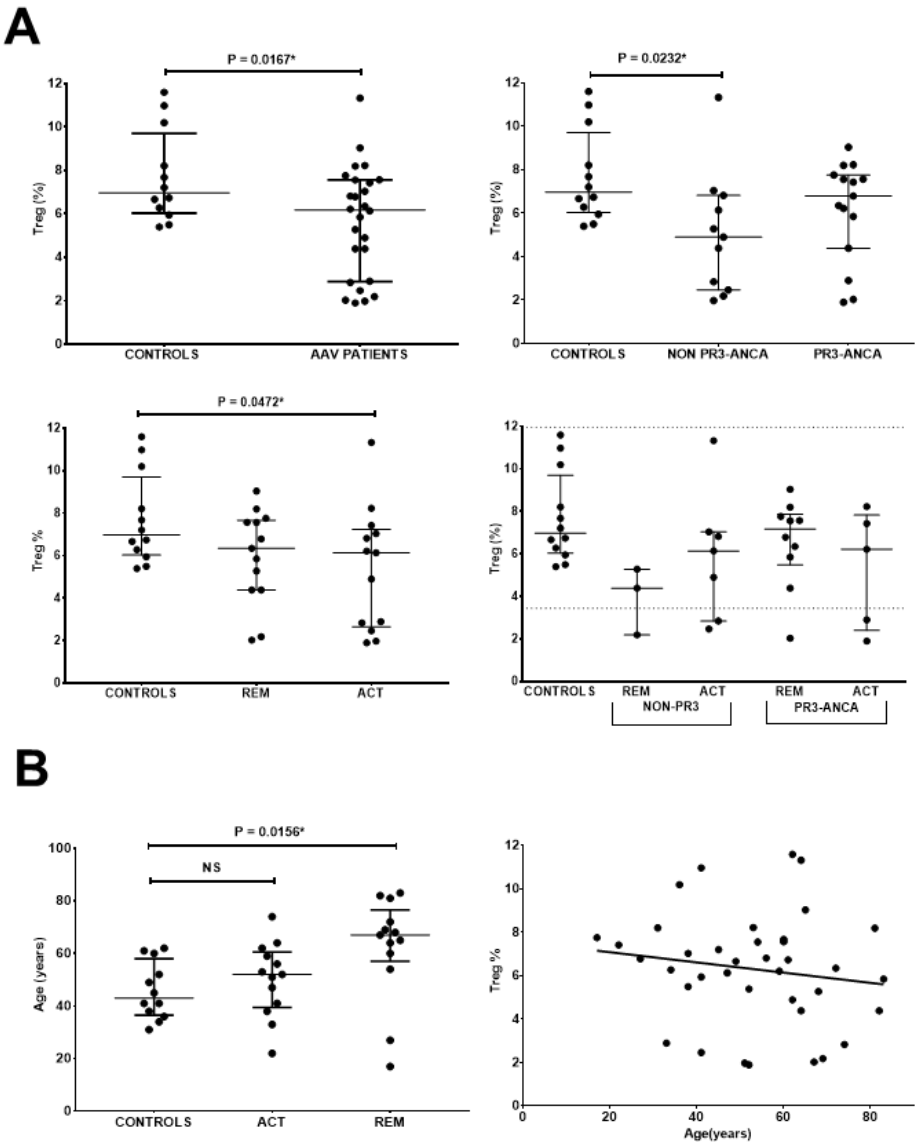

[A]Treg are reduced in patients compared to controls (Welch's unpaired t-test P=0.0167). When separated according to disease activity and ANCA, Non-PR3 and active (ACT) patient groups, still had lower Treg frequency than controls (Kruskal-Wallis and Dunn's multiple comparison conducted). In the lower right panel 2 dashed lines transecting the Y axis, these lines show the healthy control mean plus and minus 2 standard deviations; low Treg frequencies are observed in all patient groups. [B] Remission patients were significantly older than the controls, but the age of the patients with active disease was not different. There was no correlation between age and Treg frequency in the mixed patient and control cohort, comprising 38 individuals.*

6.4.2 Treg and B cell subset regression analysis

Treg frequency was compared to Breg, Bnaive and Bmem subsets, defined by relative expression of CD24 and CD38. This was a combined patient and control cohort, with 38 data points. There was an inverse correlation between frequency of naive B cells and Treg (P=0.0407* and R^2=0.1113), and a trend towards positive correlation between Bmem and Treg (P=0.0649 and R^2=0.09151, Figure 6.4). When analysis was conducted separately for controls (n=12) or patients (n=26), there was no relationship ($P \geq 0.1850$). This might be because the number of data points and the spread of data was reduced; for healthy controls the range of naïve B cells was 46.48-72.44, in the mixed cohort there were 38 data points distributed between 36.85 and 95.48.

The frequency of Breg and Treg in patients was further explored by plotting data with dashed lines, representing the mean of the healthy controls minus 2 standard deviations (Figure 6.5). The data for controls passed D'Agostino and Pearson normality test. Healthy control Breg mean was 7.783% and standard deviation was 2.605% (a dashed horizontal line intersects the Y axis at 2.573); Treg mean was equal to 7.702% and standard deviation was 2.130% (a dashed line has been drawn perpendicular to the X axis at 3.442). It has been established that Breg and Treg are both reduced in patients however, no AAV-patients had combined Breg and Treg frequency lower than the mean minus 2 standard deviations of the controls. This seems to indicate that patients are profoundly deficient in Breg or Treg relative to controls but not both cell types. The data was also presented in 2 by 2 tables (Figure 6.5, Panel B). Almost 70% of patients in this case series had profound reduction in Treg or Breg (lower than the healthy control mean, minus 2 standard deviations).

Figure 6.4 Treg correlation with B cell subsets

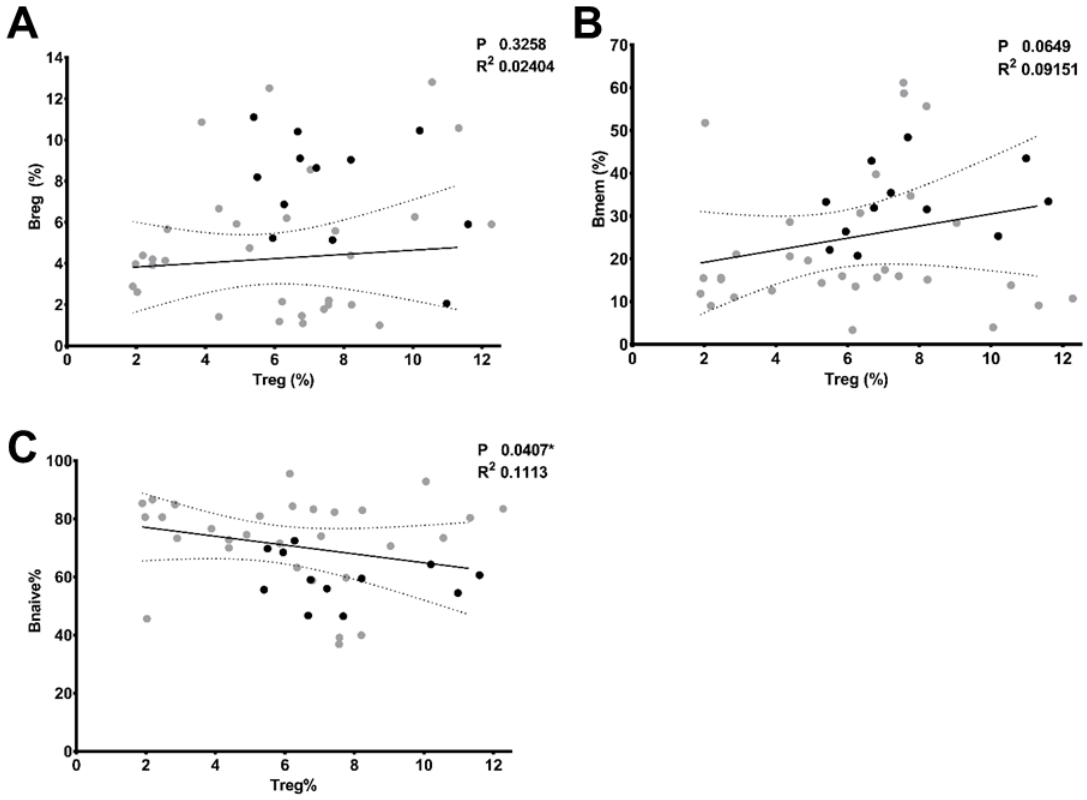

Data is shown for a mixed cohort of patients (grey filled circles) and controls (black filled circles). The lines show linearity and 95% confidence bands for the combined patient and control cohort. There was no relationship between the frequency of Treg and Breg [A], a trend towards positive correlation with memory B cells [B] and modest inverse correlation between peripheral Treg and naïve B cells [C]. The analysis for the mixed cohort is shown because there was no significant relationships when data was segregated for patients and controls.

Figure 6.5 **Colour coding to denote of ANCA specificity and disease activity**

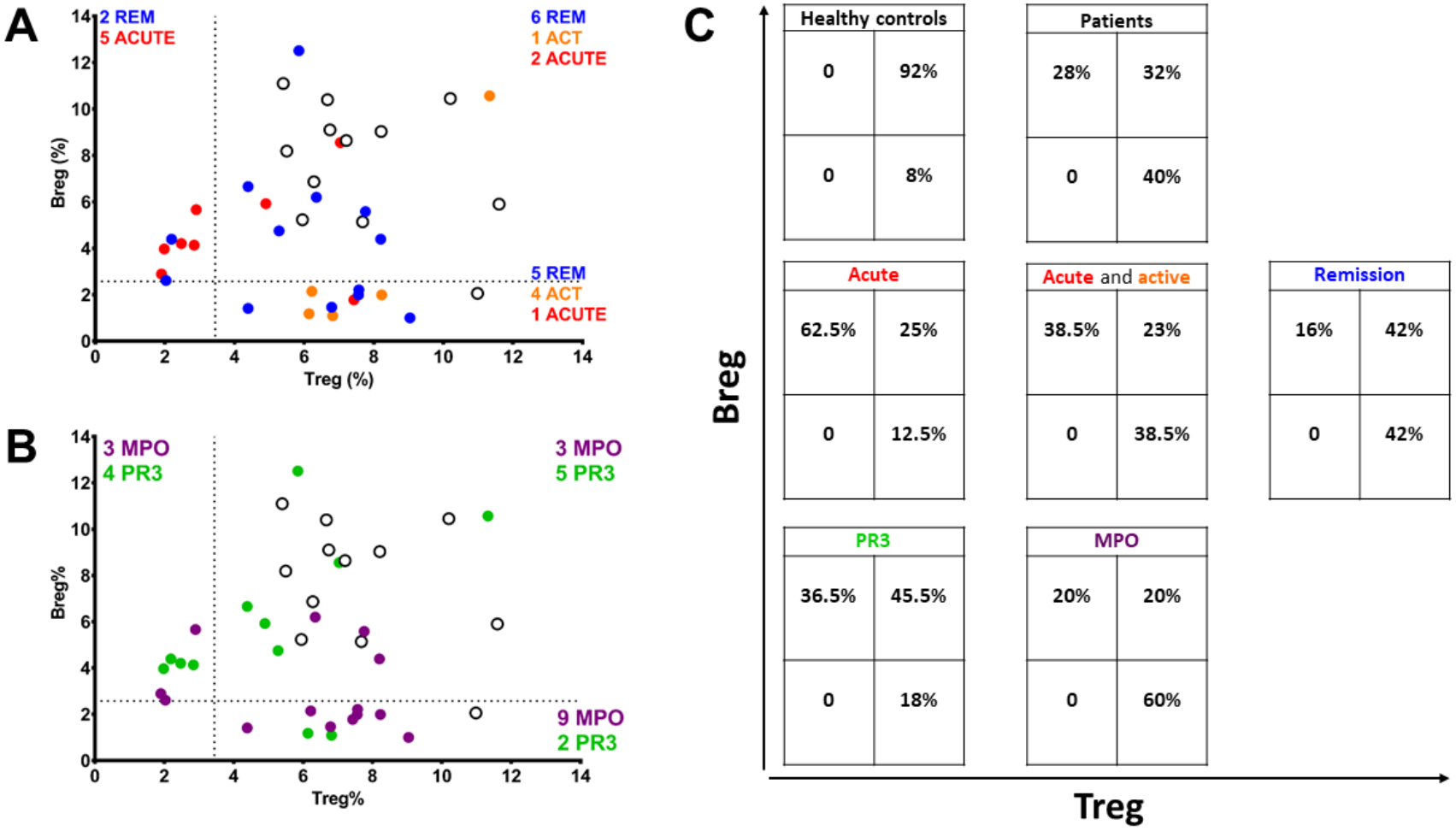

[A-B] Dashed lines represent the mean of the healthy controls minus 2 standard deviations. The data points are colour coded, controls unfilled circles with a black outline and patient data points coloured the same as the text, which indicates the tally of patients in each quadrant. Patients tend to be profoundly deficient in Breg or Treg relative to controls but not both cell types (no patients in the bottom left quadrant). [C] The data in panel B is also presented in 2 by 2 tables, with lines depicting the mean -2SD of healthy controls. Frequencies are percentage of total for each group (as labelled).

While 92% of HC had normal populations of both Breg and Treg only 32% of all patients did (42% of those in remission and only 25% of those with acute disease), potentially explaining propensity for relapse. Interestingly, MPO-ANCA patients appear to have greater normalisation of Treg compared to PR3-ANCA patients (80% vs 63.5%) and in PR3-ANCA more patients have normal Breg frequency compared to MPO-ANCA (82% vs 40%). Whether this underlies greater or lesser degrees of regulation, explaining difference in disease relapse propensity between the ANCA subtypes, needs to be further explored.

6.4.3 AAV patients had an increased frequency of highly activated CD4 T cells

Highly activated CD4 were defined as CD25 high and CD127+. Serial gating was conducted for CD25 versus side scatter height parameter (SSC-H), followed by CD127 versus SSC-H (Figure 6.1). Analysis of T cell subsets was only conducted when numbers of Treg were $\geq$1000 (17 patients and 12 controls), permitting ease of separation of Treg and highly activated T cell populations.

Patients had significantly more highly activated CD4 cells (mean and standard deviation 2.526 $\pm$1.409%), compared to controls (1.086 $\pm$0.4434%). Data passed D'Agostino and Pearson normality test, so Welch's unpaired t-test was conducted, P=0.0016** (Figure 6.6, Panel A). When separated according to disease activity or ANCA, non-PR3 and active disease (both grumbling and acute) had higher frequency of CD25 high CD127+ cells than controls (Kruskal-Wallis and Mann Whitney tests).

6.4.3.1 The net balance of CD25hi CD4 cells was skewed in AAV

The balance of CD25 high cells is perturbed in AAV, with more activated CD127+ cells and fewer regulatory CD127- cells. The ratio was calculated by taking the number of Treg CD127- CD25high CD4 cells and dividing by the number of highly activated,

CD127+ CD25high CD4 cells. Controls had 8-fold more Treg than highly activated T cells, this ratio was reduced to 3 in patients and differed significantly when Mann Whitney test was performed (P=0.0016**). The ratio was significantly lower in all patient groups, when 3-way analysis was conducted according to ANCA specificity or disease activity (Kruskal-Wallis test and Dunn's multiple comparison, Figure 6.6, Panel B).

6.4.3.2 Highly activated CD4 T cells and B cell subset regression analysis

Highly activated T cell frequency was compared to Breg, Bnaive and Bmem subsets, defined by relative expression of CD24 and CD38. This was a combined patient and control cohort, with 29 data points. There was a positive correlation between frequency of naive B cells and Treg (P=0.0207* and R^2=0.1892). Interestingly, there was an inverse relationship between frequency of highly activated T cells and Breg in peripheral blood (P=0.0479* and R^2=0.1422). Finally, there was a trend toward a negative correlation between highly activated T cells and Bmem (P=0.0676 and R^2=0.1227), which did not reach the threshold for statistical significance.

When segregated into patient and controls, statistical significance was lost for Breg and differences in the groups became apparent for Bmem and Bnaive. There was correlation between highly activated T cells and Bmem in controls (P=0.0095**) and the inverse relationship with Bnaive (p=0.0026**). Whilst some patients were closely aligned with controls, the active patients were not and were colour-coded in red (Figure 6.6, Panel C). The trend was towards positive correlation with Bnaive (P=0.0628) and inverse relationship with Bmem (P=0.0853) in patients.

Figure 6.6 Highly activated T cells are increased in AAV, balance with Treg is perturbed and there is relationship with B cell subsets

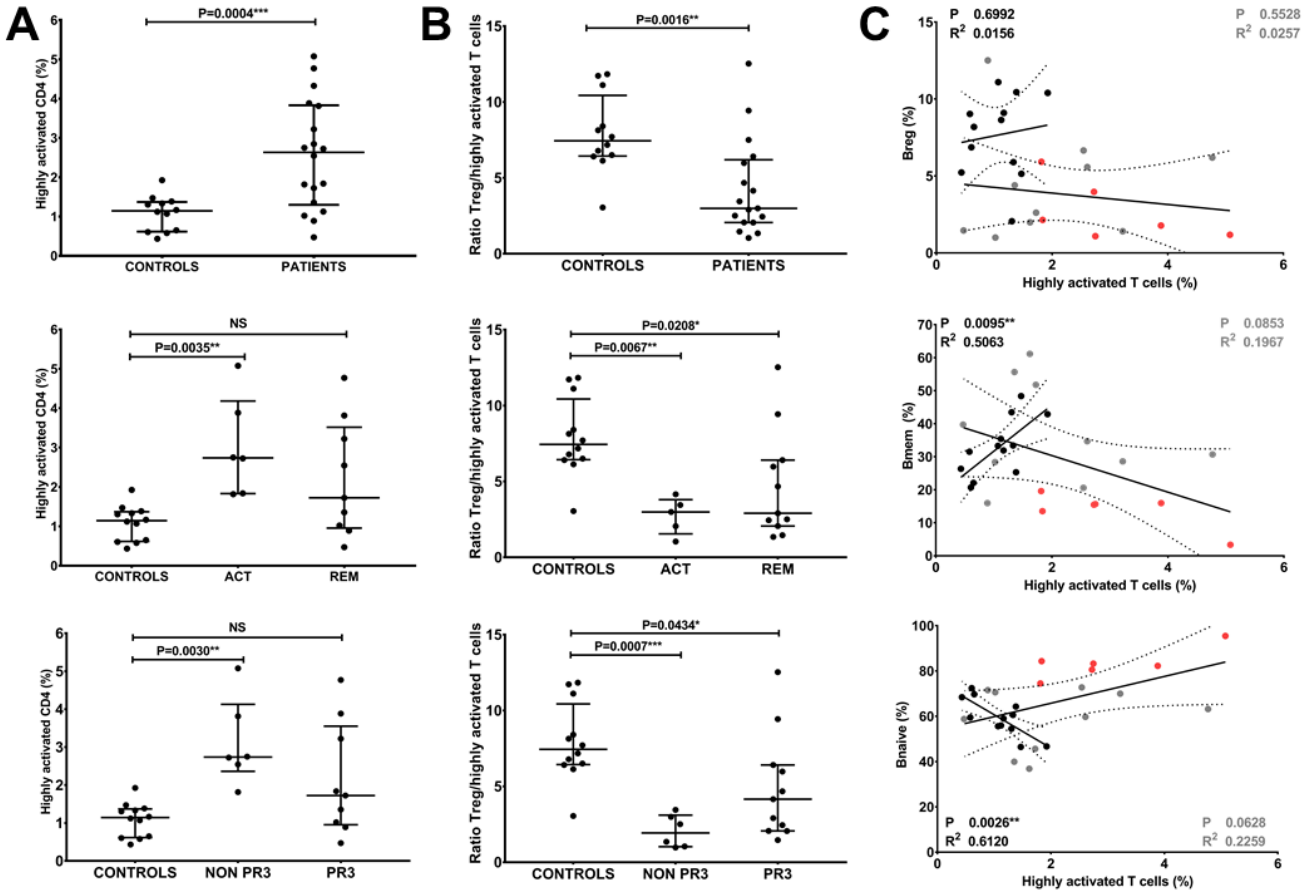

*[A] Patients have higher frequency of activated CD25 high CD127+ cells, compared to controls (Welch's unpaired t test P=0.0016**). When Kruskal-Wallis and Dunn's multiple comparison test conducted, active (ACT) and non-PR3 patients still had significantly more highly activated T cells, than controls. [B] A ratio was calculated by dividing the number of Treg by the number of highly activated, T cells. Controls had 8-fold more Treg than patients (Mann Whitney test P=0.0016**). The ratio was significantly lower in all patient groups compared to controls, Kruskal-Wallis test and Dunn's multiple comparison. [C]. Data is shown for a mixed cohort of remission patients (grey filled circles), patients with active disease (red filled circles) and controls (black filled circles). There was no correlation between highly activated Treg and Breg (P value for patients shown in grey and controls in black). There was positive correlation between highly activated Treg and Bmem (P=0.0095**) and inverse relationship between Bnaive (P=0.0026**) in the healthy control cohort. In patients, there tended to be an inverse relationship between highly activated T cells and Bmem (P=0.0853) and a positive correlation with Bnaive (P=0.0628). When analysis is conducted in the combined cohort of patients and controls highly activated T cells positively correlate with Bnaive cells (P=0.0207*).*

6.4.4 Expression of CD39 and CD73 in PBMC of AAV patients and controls

6.4.4.1 There was no difference in the frequency of CD39+ or CD73+ CD4 T cells in AAV patients and controls

The frequency of ATPase positive cells was calculated from quadrant plots (shown in Figure 6.2). There was no difference in percentage of CD73+ or CD39+ CD4 T cells in healthy controls and patients; data had a normal distribution, an unpaired Welch's t-test was conducted, which does not assume equal variance. The mean frequency and standard deviation for CD39+ CD4 T cells was 7.854% $\pm$ 3.956 for controls (n=12) and 7.602% $\pm$ 4.693 for AAV patients (n=24). There was no difference when 1-way ANOVA was conducted for controls, PR3-ANCA and non-PR3 (P=0.7355) or controls, active disease and clinical remission (P=0.2609, data summarised in Table 6.3).

The mean frequency and standard deviation for CD73+ CD4 T cells was 6.496% $\pm$ 3.802 for controls (n=8) and 6.474% SD $\pm$ 4.432 for AAV patients (n=24). In 4 out of 12 control samples CD73 APC data was atypical, due to signal from tandem antibody degradation (CD4 APC-Cy7 fluorophore on parent population, instead of PE). Consequently, only 8 data points were available for comparison with patients. Like CD39, there was no difference when patients further categorised according to ANCA (P=0.3749) or disease activity (P=0.9993). Kruskal-Wallis test conducted for patient subgroups categorised by ANCA (PR3 patients did not have normal distribution pattern) and 1-way ANOVA, for disease activity.

6.4.4.2 Frequency of CD39+ and CD73+ cells in B cells and CD8 T cells, was lower in AAV remission patients compared to active disease

Frequency of CD39+ and CD73+ cell was determined for CD4- lymphocytes, this population is primarily comprised of CD8 T cells and B cells. Unpaired Welch's t-test was used to compare patients and controls, there was no difference for CD39 (P=0.6480) or CD73 (P=0.1203). Remission patients did not have a normal distribution pattern for frequency of CD39 or CD73+ CD4 null lymphocytes (D'Agostino and Pearson normality test). Frequency of CD39 and CD73 CD4 null lymphocytes was significantly lower in remission patients, compared to active disease (Kruskal Wallis test comparing controls, remission and active disease; mean rank of all groups against compared against one another by Dunn's multiple comparison). CD39 median frequency in active disease was 25.72% and 5.86% in remission, P=0.0003***. CD73 median frequency in active disease was 30.6 and 10.69% in remission (P=0.0099**).

6.4.4.3 There was no difference in the frequency of CD39+ Treg in patients and controls

CD39 and CD73 analysis in Treg, was only conducted when this population numbered more than 1000 (17 patients and 12 controls for CD39, 8 controls for CD73). Frequencies were expressed as percentage of parent (Treg) and percentage of grandparent (CD4+ lymphocytes).

A significantly higher proportion of Treg express CD39, compared to non-Treg defined by use of a "Not Gate" in Flow Jo (Figure 6.7, Panel A, Welch's unpaired T test P<0.0001****). In contrast, there was no difference in frequency of CD73 cells in Treg and non-Treg (Figure 6.6, panel A). Treg have highest frequency of CD39

positive cells, so it would be anticipated that they would have the highest CD39 MFI and indeed, this was observed (Figure 6.7, Panel B). Unexpectedly, there was a lot of variability in CD73 MFI across CD25 T cell subsets. CD73 MFI was significantly higher for CD25- CD4+ cells, compared to all other populations. When flow cytometry plots were reviewed, CD25- cells were more uniform in expression, with no profoundly negative cells. The T cells with highest CD73 expression resided within the activated T cell populations (CD25 high or CD25 intermediate and CD127+), but this was on a subset of cells, so when MFI was represented as geometric mean the difference was lost (representative contour plots shown in Figure 6.7, Panel C).

The mean frequency and standard deviation for CD39+ Treg cells was 43.23 $\pm$19.98% for controls and 34.01 $\pm$21.82% for AAV patients (Welch's T test P=0.2500). There was also no difference in CD39+ Treg, when expressed as percentage frequency of CD4+ lymphocytes.

The mean and standard deviation in controls was 3.035 $\pm$1.472% and in patients, this was 2.160 $\pm$1.567% in patients (Welch's T test P=0.1372). There was no difference when further analysis conducted according to ANCA specificity or disease activity (6 active and 11 remission patients or 6 non-PR3 and 11 PR3-ANCA patients, compared to 12 healthy controls, Kruskal-Wallis and Dunn's multiple comparison).

6.4.4.4 No difference in the frequency of CD73+ Treg in patients and controls

CD73+ Treg cells had a normal distribution pattern in patients and controls. Mean and standard deviation for CD73+ Treg cells was 3.704 $\pm$2.144% for controls and 5.887 $\pm$3.642% for AAV patients (Welch's T test P=0.0744). Although mean was higher in patients, the spread of the data wider than controls and consequently, this did not meet

the threshold for statistical significance. The median value in controls was 2.83% with a range of 1.71-8.18 and median CD73+ Treg was 5.450% in patients, with range of 1.56-14.92%.

Median frequency of CD73+ Treg was higher in non-PR3 and grumbling or acute disease (Table 6.3) but did not differ significantly when Kruskal-Wallis and Dunn's multiple comparison tests were conducted for ANCA specificity and disease activity.

CD73+ Treg frequency was also expressed as percentage of CD4+ lymphocytes. Patients did not have normal distribution pattern, so comparison was by Mann-Whitney. The median and range for healthy controls was 0.2356% and 0.114-0.4927; in patients this was 0.2739 % and 0.02515-1.037, P=0.5486. There was no difference when Kruskal-Wallis and Dunn's multiple comparison tests were conducted for ANCA specificity and disease activity

6.4.4.5 Monocytes were invariably CD39 positive, with high geometric MFI

Monocytes were consistently CD39 positive, with no significant difference in patients and controls (range 92.96-99.83%, median 98.22). The geometric MFI for combined patients and controls had a normal distribution pattern, with mean value and standard deviation of 3512 $\pm$ 985.

6.4.4.6 Monocytes from patients had lower CD73 geometric MFI compared to controls, with a higher proportion of cells negative for this marker

In contrast cell surface CD73 expression was low on monocytes. Patients had lower CD73 geometric MFI (median 70.9), compared to controls (median 361.0, Mann Whitney test P=0.0178*). This required further analysis to determine whether there was a net shift in CD73 expression, or a difference in subpopulations. Patients had

lower frequency of CD73+ cells (Mann Whitney test P=0.0428*). When further categorised by disease activity, remission patients had significantly fewer CD73+ monocytes (median 0.864%) compared to controls (median 2.660%, P=0.0320*); there was no significant difference between acute or grumbling disease (median 1.115%) and controls (P=0.4769, Dunn's multiple comparison).

Within the CD73 low quadrant, some monocytes were stacked against the axis. These profoundly CD73 negative monocytes tended to be increased in patients compared to controls (P=0.0705). When further categorised by disease activity, grumbling or acute patients had more CD73 null monocytes (median 36.200%) compared to controls (median 5.810%, P=0.0142*); there was no significant difference in remission patients (median 9.455%) and controls (P>0.9999, Dunn's multiple comparison). This observation warrants further investigation in larger cohort, with a definitive monocyte marker and a single processing method (fresh or frozen samples).

Figure 6.7 Comparison of CD39 and CD73 expression in T cell subsets

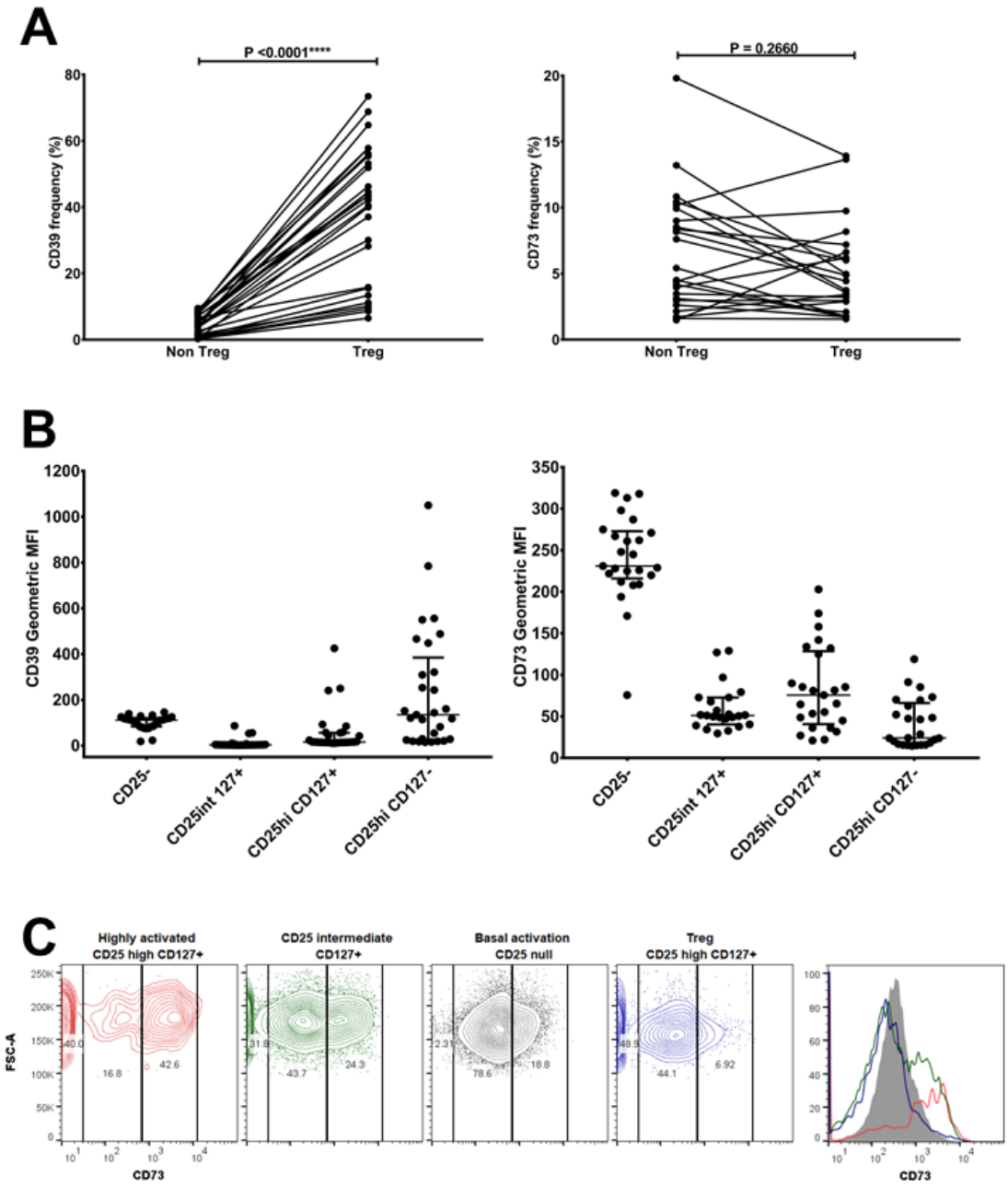

*[A]. ATPase positive cells in Treg and non-Treg. A not gate was applied in Flow Jo to define non-Treg cells (CD4 parent population, excluding CD127- CD25 high cells). CD39 frequency was significantly higher in Treg (Welch's t-test, P<0.0001****), but frequency of CD73 did not differ. [B]. ATPase MFI in CD4 subpopulations, defined based on relative CD25 and CD127 expression. In keeping with this observation, CD39 geometric was higher on Treg, compared to other CD4 subsets. There was*

considerable variation in CD73 geometric MFI, with maximum expression in CD25- CD4 T cells. [C]. A representative flow cytometry profile shows the variation in CD73 expression, observed in CD4 subpopulations. The CD25- CD4 population does not have profoundly negative CD73 cells, the entire population shifts to the right on histogram plot of CD73 MFI (grey filled histogram). A discrete CD73+ population is only observed in the activated CD4 cell populations, CD25+ or CD25high and CD127+ (red and green contour plots and histograms).

Table 6.3 Summary of analysis of CD39 and CD73 expression in PBMC

	Controls	Patients	PR3	Non-PR3	Active	Rem
CD4+ CD39+%	8.820	7.275	6.870	7.685	8.450	5.341
CD4+ CD73+%	4.701	5.965	3.825	8.107	6.010	4.200
CD4- CD39+%	14.870	11.890	9.040	24.760	**25.720**	**5.860**
CD4- CD73+%	18.220	24.820	24.400	24.400	**30.600**	**10.690**
Treg CD39+%	46.230	29.120	42.220	22.940	22.94	42.220
Treg CD73+%	2.825	5.450	4.880	6.325	6.070	4.440
Treg CD39+% GP	3.165	1.700	1.700	1.235	1.371	1.700
Treg CD73+% GP	0.2356	0.2739	0.3151	0.2482	0.2739	0.2951
Mono CD39+%	97.990	98.310	98.180	98.430	98.510	98.810
Mono CD73+%	**2.660**	**1.060**	1.027	1.080	1.115	**0.864**
Mono CD73 null%	**5.810**	34.600	31.400	36.200	**36.200**	13.300

Median frequencies for CD39 and CD73 PBMC subset are presented the above table, with significant differences shown in bold font and grey filled cells. Welch's unpaired t-test was conducted when control and patient data had normal distribution as assessed by D'Agostino and Pearson normality test. If distribution was not normal, Mann Whitney test was conducted. For comparison of PR3-ANCA, non-PR3 patients and controls, or active, remission patients and controls, Kruskal-Wallis test and

Dunn's multiple comparison test was conducted. This was because there were too few data points for non-PR3 and active patients to assess whether distribution normal or not.

*Within the CD4 negative lymphocyte gate, active patients had significantly fewer CD39 and CD73 positive cells, compared to remission patients (Kruskal Wallis test and Dunn's multiple comparison, CD39 P=0.0003*** and CD73 P=0.0099**).*

Within the monocyte population, patients had lower frequency of CD73+ cells (Mann Whitney test P=0.0428). When Kruskal Wallis test and Dunn's multiple comparison test were conducted, remission patients had lower frequency compared to controls (P=0.0320*). In monocytes, the CD73 negative population was further categorised into CD73 null cells (stacked against the axis) and cells with low expression. Active patients had more CD73 null monocytes compared to controls (P=0.0142*).*

6.4.5 Regression analysis of ATPase positive Treg, B cell subsets and cytokines

Previously it was reported that there is a positive correlation between IL-10 competent B cells and CD39 Treg frequency in AAV remission patients, when expressed as a percentage of CD4 lymphocytes. Therefore, regression analysis was conducted for CD73 and CD39 positive Treg, as percentage of parent and grandparent populations. The relationship between these ATPase positive Treg and B cell subsets, defined on relative expression of CD24 and CD38 was assessed in 29 individuals. Cytokine induction was conducted in 17 of these individuals; intracellular flow cytometry permitted frequency of IL-10 positive cells to be determined in B cells and soluble cytokines were additionally measured in supernatants. In maximally stimulated cells the cytokine profile included: IFNγ, IL-17A, IL-10, IL-6, IL-1β, TNF and TGFβ

6.4.5.1 CD39 or CD73 Treg do not correlate with B cell subsets (classified based on IL-10 competency or relative CD24 and CD38 expression)

In the combined patient and control cohort, there was no relationship between CD39+ or CD73+ Treg (expressed as percentage of parent or grandparent), and B cell subsets (Breg, Bnaive or Bmem). The relationship between Breg and these ATPase positive Treg was of particular interest (data shown in Figure 6.8, Panels A and B); a positive relationship was previously described between IL-10 competent B cells and CD39+ Treg as percentage of total CD4 cells, in AAV patients in clinical remission (Wilde, Thewissen et al. 2013) .

When patients were analysed alone, there was an inverse relationship between Breg and CD39+ Treg as percentage of parent (P=0.0496* and R^2=0.2337). There was also a tendency for patients to have an inverse relationship between CD39+ Treg as

percentage of CD4 and Breg (P=0.0536 and R^2=0.2264). One patient had a high Breg frequency of 12.509%, when this datapoint was removed the P-value was further increased (P=0.0905 and R^2=0.1911).

There was no relationship between CD39 or CD73 Treg and IL-10 B cell frequency, B cell TNFα or TGFβ MFI (assessed by intracellular flow cytometry after CPG and CD154 stimulation).

These results seemingly contradict the previous report (Wilde, Thewissen et al. 2013) however the patient cohorts, classification of Breg and method for induction of intracellular IL-10 differ considerably.

6.4.5.2 CD39 Treg as a percentage of CD4, correlate with TGFβ release, in maximally stimulated B cells

In supernatants collected from CD154 and CPG stimulated cells, there was positive correlation was between TGFβ (pg/ml) and CD39+ Treg (expressed as percentage of CD4, grandparent), P=0.0376* and R^2=0.2575 (Figure 6.8, Panel C). There was no significant relationship between the other soluble analytes assessed.

Correlation between CD39+ Treg and TGFβ release in PBMC cultures, might be a direct effect on CD39+ Treg. CD39+ Treg have a more stable regulatory phenotype under inflammatory conditions than CD39- Treg (Gu, Ni et al. 2017). Low CD39 expression in Treg has been associated with a defect in TGFβ signalling pathway in (Peres, Donate et al. 2018). Breg might indirectly enhance TGFβ production by CD39+ Treg. Breg produce TGFβ, induce Treg and enhance their function *in vitro* (Kessel, Haj et al. 2012, Lee, Stott et al. 2014, Tarique, Naz et al. 2018)

Figure 6.8 Regression analysis of ATPase positive Treg

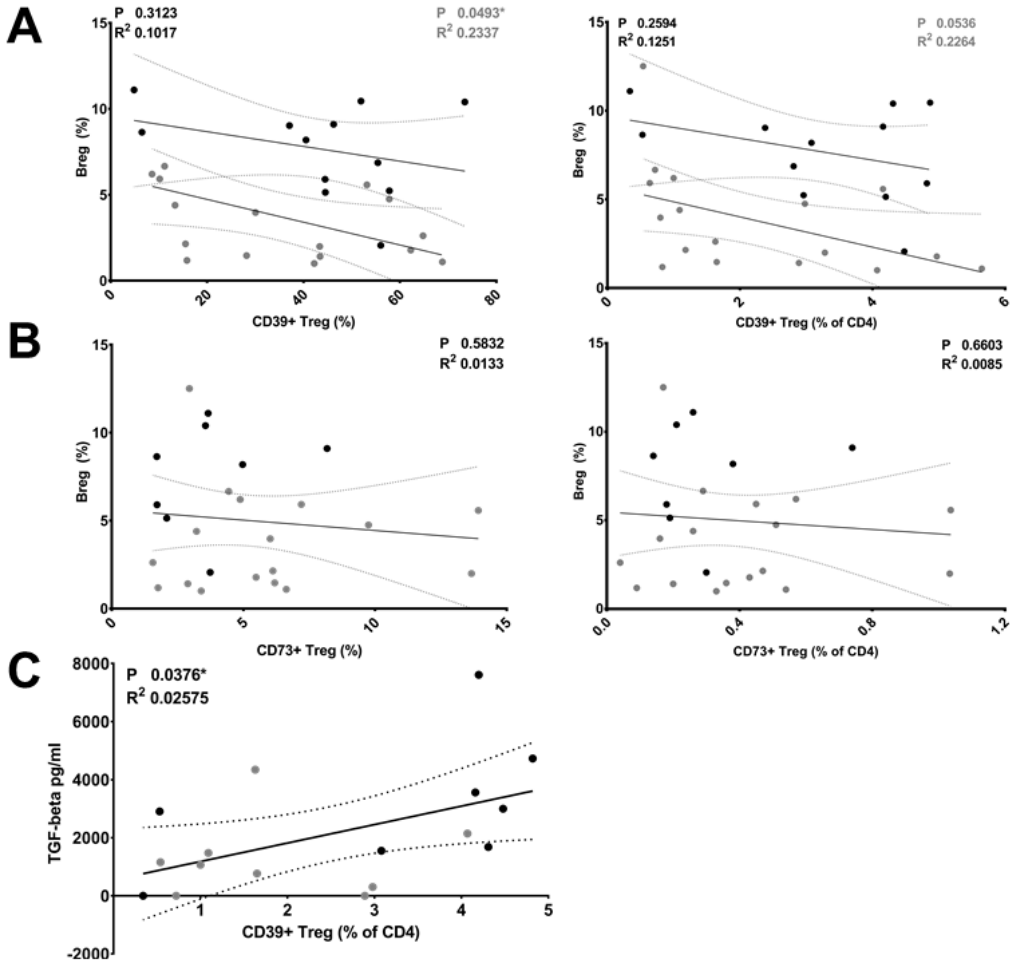

Data is shown for a mixed cohort of patients (grey filled circles) and controls (black filled circles). [A]. There was no correlation between frequency of Breg and CD39+ Treg, as percentage of parent population (CD4+ CD25high CD127- Treg) or grandparent (CD4+ lymphocytes) in healthy controls (P values in black). There tended to be an inverse relationship between in patients (P values shown in grey). [B] There was no correlation between frequency of Breg CD73+ Treg, as percentage of parent or grandparent. [C]. Regression analysis was conducted for ATPase+ Treg and cytokine profile in 17 individuals (8 controls and 9 patients, in remission with no history of Rituximab treatment). The only significant finding is shown. CD39+ Treg, as percentage of grandparent (CD4+ lymphocytes), positively correlated with TGFβ measured by ELISA in PBMC maximally stimulated to induce IL-10 production by B cells (CPG and CD40 ligation).

6.5 Discussion

This is a very comprehensive data set, in addition to definition of T cell subsets based on CD25 and CD127, CD39 and CD73 expression was assessed, immunophenotyping for B cell subsets was conducted (based on relative expression of CD24 and CD38) and cytokine profile defined, in PBMC maximally stimulated for B cell IL-10 induction (intracellular flow cytometry and measurement of 15 soluble analytes by CBA or ELISA).

Ideally patient and control groups would not differ significantly in terms of demographics or processing technique. Some patient PBMC were tested from frozen, whilst other patients and all the healthy controls were tested on fresh samples (Table 6.1). The purpose was so that some patients with acute or grumbling disease could be included; these would have been difficult to collect prospectively because individuals present relatively infrequently, with incidence of AAV 30 per a million in the general population, annually. Although there was no difference in Treg frequency in frozen relative to fresh patient samples, it would have been good to verify this in paired samples. In the literature the frequency of Treg defined as CD4+ $CD25^{hi}$ and $CD127^{lo}$, is reported to be more stable on freeze-thawing than frequency of Treg defined as CD4+ $CD25^{hi}$ FoxP3+ cells; CD39+ Treg frequency was stable in whole blood, fresh PBMC and cryopreserved PBMC (Zhang, Nilles et al. 2016).

In this case series, remission AAV patients were also significantly older than controls (P=0.0156*) but there was no correlation between age and Treg frequency (P=0.3603). In a prior publication, there was no correlation between age and Treg frequency in mixed cohort of 62 AAV patients (Free, Bunch et al. 2013). It is generally accepted

that Treg increase with age, with gradual loss of suppressive capacity (Gregg, Smith et al. 2005). If the control group had been more closely matched to the patients, the reduction in Treg frequency may have been even greater.

Treg were reduced and frequency of highly activated CD4+ T cells was increased in AAV patients, compared to controls. Reduction in Treg has been reported in some previous studies (Chavele, Shukla et al. 2010, Morgan, Day et al. 2010, Rimbert, Hamidou et al. 2011), but not all (Table 6.1). Increased T cell activation has been widely reported in AAV, with increased frequency of CD4+ CD25+ T cells (Popa, Stegeman et al. 1999, Tam, Sanders et al. 2004, Marinaki, Neumann et al. 2005, Abdulahad, Stegeman et al. 2007, Wilde, Dolff et al. 2009, Free, Bunch et al. 2013) and soluble markers of activation (Schmitt, Heesen et al. 1992, Schonermarck, Csernok et al. 2000, Chavele, Shukla et al. 2010).

There was no discernible relationship between frequency of Breg and Treg in peripheral blood. The evidence in the literature for such a relationship is limited and mainly from co-cultures *ex vivo*. There is one report, which showed a positive correlation between peripheral blood FoxP3+ CD4 T cell and Breg frequency, in gastric cancer patients (Wang, Yuan et al. 2015). Breg can certainly induce Treg in culture. CD24high CD38 high B cells convert CD4 CD25- cells into FoxP3 positive Treg, in controls but not arthritis patients (Flores-Borja, Bosma et al. 2013). A putative population of regulatory B cells, with high CD25 expression significantly enhance FoxP3 and CTLA4 MFI in Treg (Kessel, Haj et al. 2012). IL-10 positive B cells induce CD25, PD-1, IL-10 and TGF-β in CD4 CD25- T cells, isolated from human leprosy patients (Tarique, Naz et al. 2018). It would be interesting to test whether Breg from AAV patients induce FoxP3 in CD4+ CD25- cells.

Highly activated T cells had an inverse relationship with Breg (defined as CD19+ $CD38^{hi}$, $CD24^{hi}$) in the combined cohort of patients and controls. This might indicate that Breg can limit T cell activation *in vivo*. It was previously reported that B cells can downregulate CD25 expression *in vitro*, and CD25 expression was further reduced if B cells were activated through CD40 ligation (Lemoine, Morva et al. 2011).

In the combined cohort of patients and controls frequency of Treg had an inverse correlation with Bnaive, whilst positive correlation was observed between highly activated T cells and naïve B cells.

B cell homeostatic proliferation is the sustained proliferation of naive cells, in the absence of antigen and a consequence of lymphopenia. The net effect would be increased frequency of naïve B cells, with contraction of Bmem and Breg populations. Treg frequency reduction, might be incidental, no longer induced or lost as due to the immunosuppressive regimen.

In terms of the correlation with highly activated T cells, both Bmem and Bnaive cells can activate CD4 T cells by provision of cytokines, co-stimulatory signals or presentation of antigen. In co-culture experiments in the proceeding chapter both naïve and Bmem, augmented Th1 differentiation relative to T cells cultured alone (Figures 5.4 and 5.5).

When analysis was conducted separately for healthy controls and patients, the only significant correlation with highly activated T cells, was with Bmem cells in healthy individuals (Figure 6.6, Panel C). Perhaps this is indicative of generalised immune activation in patients, and more refined antigen specific responses in controls (with antigen experienced Bmem cells supporting T cell activation).

The frequency of CD39 and CD73 positive cells, did not differ in patient and control CD4 cells or Treg. CD39 and CD73 ectoenzymes are reported to be surrogate markers for Treg, however they were discordant, in the pattern of their expression. CD39 was highly enriched on Treg in this case series but CD73 was not (Figure 6.6, Panel A). This might have been anticipated, as CD73 is reported to be absent from human Treg and expression on T cells, independent of CD25 and CD39 (Dwyer, Hanidziar et al. 2010). Results may also have influenced by processing or method used to defined Treg. Firstly, the cells were not permeabilised and CD73 is predominantly intracellular in human Treg (Mandapathil, Hilldorfer et al. 2010). Arguably, CD73 would have to be at the cell surface to hydrolyse ATP, released from dead or dying cells and generate extracellular adenosine. Treg were defined as CD25high CD127- in this cohort and not on basis of FoxP3 expression. It is reported that 47% of FoxP3+ CD25+ cells co-express CD39 and CD73, with expression of the latter, highly inducible upon activation with anti-CD2, anti-CD3, and anti-CD28 beads (Alam, Kurtz et al. 2009).

There was no difference in the frequency of CD39 or CD73 positive Treg or CD4 cells in AAV patients and controls. A modest reduction in CD73 positive CD4 cells was previously reported in patients (Kling, Benck et al. 2017). The case series presented here, had a similar number of patients however, this cohort was more heterogenous with 11 patients in clinical remission and 13 with active disease.

In a report describing investigation of CD39 expression in CD4+ T cells and Treg (Free and Su 2013), AAV patients had higher frequency of CD39+ cells in the CD4 T cells (11.59% in patients versus 5.12% in controls) and Treg population. The frequency of CD39+ T cells did not differ significantly in this cohort; the median was 7.28% in patients and 8.82% in controls.

In remission the frequency of CD39 and CD73+ cells in the CD4 null lymphocyte gate, was reduced relative to active disease. We cannot exclude differences in immunosuppression or processing as a cause; certainly, CD73 can be induced on cells (Dwyer, Hanidziar et al. 2010) and this could occur due to freeze-thawing or the inflammatory process in vivo. It is interesting to note, that frequency in remission patients also tends to be lower than healthy controls (staining also conducted in fresh samples). In addition, Kling et al reported profound reduction in CD73+ cells in CD4- lymphocytes in their cohort of patients (mainly remission), with reduction in CD39+ cells in CD4- cells confined to the CD45RA- subset in patients. In that study the frequency of CD4- CD73+ cells had a positive correlation with eGFR and negative association with CRP (Kling, Benck et al. 2017).

ATPase positive CD4- lymphocytes have not been characterised further in AAV; they could be innate lymphoid cells, CD8+ T cells or B cells. CD39 and CD73 are highly expressed in B cells (Saze, Schuler et al. 2013), with reduced in MFI in $CD24^{hi}$ $CD38^{hi}$ B cells reported in SLE patients compared to controls (Menon , Smith et al. 2017). CD39 B cells are likely to be an important immunoregulatory cell type; CD39 high B cells reduce T cell activation and proliferation *in vitro*, as assessed by CD69 induction and Ki67 expression (Figueiro, Muller et al. 2016).

Monocytes invariably expressed CD39, in keeping with another report (Pulte year). Myeloid cells represent a high frequency of total ectoenzyme positive PBMC and are likely to be an important source of extracellular adenosine. It would be of value to assess whether CD39 is functional in patients; this could be determined by measuring breakdown of radiolabelled ATP.

There were more profoundly CD73 negative monocytes in active disease and reduced CD73+ monocytes in remission. Neutrophils additionally express CD39 and CD73 (Pulte, Broekman et al. 2007, Flogel, Burghoff et al. 2012). Myeloid cells and neutrophils are dominant in the renal infiltrate in AAV (Weidner, Carl et al. 2004), with urinary markers of vascular injury including MCP-1 and CD163 (Tam, Sanders et al. 2004, O'Reilly, Wong et al. 2016). Mice with a global deficiency in CD73, have enhanced monocyte adhesion to endothelium (Boring, Flogel et al. 2013), they are predisposed to renal endothelial injury and develop spontaneous proteinuria (Blume, Felix et al. 2012).

There is evidence that a higher frequency of CD73+ cells, is associated with improved renal function (Blume, Felix et al. 2012, Boring, Flogel et al. 2013, Kling, Benck et al. 2017). This was a relatively small cohort, with samples collected at a single timepoint and creatinine ranging from 54-665μmol/L; it would be interesting to look at an extended case series and more rigorously assess renal function and ATPase expression, longitudinally.

The relationship between ATPase positive Treg was assessed relative to B cell subsets and cytokine profile. It was previously reported that CD39+ Treg as percentage of CD4 (grandparent), had a positive correlation with IL-10 competent B cells (Wilde, Thewissen et al. 2013). There was no correlation between frequency of IL-10 positive B cells, following 48-hour stimulation with CPG alone, or in combination with CD154. Nor was there any relationship with Breg cells, defined as CD24 and CD38 high in the mixed cohort of patients and controls (Figure 6.8). In patients, unexpectedly there was a negative relationship between CD39+ Treg and Breg. The method to defined Breg

and to induce IL-10, differed from that employed by Wilde *et al* (66 hours with 0.1µm CPG followed by 6 hours stimulation with PMA and ionomycin).

Interesting, CD39 Treg expressed as a percentage of grandparent (CD4+ lymphocytes), positively correlated with TGFβ. Breg cells are thought to cause immunosuppression indirectly, by effects on T effector and regulatory cells (Blair, Norena et al. 2010, Carter, Rosser et al. 2012, Flores-Borja, Bosma et al. 2013). B cells also produce TGFβ, demonstrated by flow cytometry (Figures 5.6 and 5.8).

Chapter 7 Investigation of the role of B cells in an *in vivo* model

7.1 Background

I have shown that the balance of effector and regulatory B cell subsets seems to be important in determining clinical outcome in AAV. (Todd, Pepper et al. 2014)(Todd, Pepper et al. 2014)(Todd, Pepper et al. 2014). Breg were diminished in remission patients but Bmem frequency was the same as controls. In tolerant individuals, who did not require continued treatment, Breg frequency was restored but Bmem were diminished. Breg are known to limit antigen specific responses, primarily by production of IL-10. Bmem are antigen experienced cells, with a lower threshold for subsequent activation and differentiation to plasmablasts. In the preceding chapters, Bmem frequency was also shown to positively correlate with B cell TNFα geometric MFI and inversely, with IL-10 B cell frequency. Bmem and Bnaive augmented Th1 differentiation *in vitro*, whilst Breg did not.

In vivo models of ANCA vasculitis have been extensively reviewed elsewhere (Heeringa and Little 2011, Coughlan, Freeley et al. 2012, Salama and Little 2012, Hutton, Holdsworth et al. 2017). A table comparing the MPO-specific models of disease is provided below (Table 7.1). There has been limited success in generating a murine model for PR3 mediated disease. This is thought to be due to lack of PR3 sequence homology between human and mice, compounded by differences in frequency of circulating neutrophils.

In this thesis chapter the cell transfer model was used (Xiao, Heeringa et al. 2002), it is highly penetrative, resulting in severe glomerulonephritis. Splenocytes were isolated

Table 7.1 *In vivo* models of MPO-ANCA vasculitis

Model	Comments	References
MPO immunisation of MPO null mice, dissociation of splenocytes and transfer into *rag2-/-* mice	Multi-systemic and highly penetrative disease. Overt immunoglobulin deposition, unlike human disease. Enriched B cells pathological alone (conference report). MPO response, to an exogenous antigen. Disease induced in mice with no endogenous T or B cells; frequency of antigen specific lymphocytes not representative of human disease and, cells subject to homeostatic proliferation (lymphopenia a driver).	(Xiao, Heeringa et al. 2002, Xiao, Heeringa et al. 2003, Coughlan, Freeley et al. 2012)
MPO immunisation of MPO null mice, immunoglobulin isolation from peripheral blood and transferral to MPO replete mice (MEV)	Mild disease only, enhanced with LPS or use of 129 strain. Immunoglobulin paucci-immune. By-passes break in B cell tolerance. Essential role for innate immunity - neutrophils, TNFα and alternative C' pathway.	(Xiao, Heeringa et al. 2002, Huugen, Xiao et al. 2005, Xiao, Heeringa et al. 2005, Xiao, Ciavatta et al. 2013, Xiao, Dairaghi et al. 2014)
MPO immunisation of wild type mice with MPO antigen supplanted by sub-pathogenic NTS	Mild disease only. By-passes break in B cell tolerance. NTS broad reactivity, but disease can also be induced by MPO-ANCA linked to the immunodominant T cell epitope. Critical role for Ig, neutrophils, Th17 and Th1 cells. These T effector cells are controlled by IL-10 B cells in Antigen Induced Arthritis (AIA)	(Ruth, Kitching et al. 2006, Carter, Vasconcellos et al. 2011, Summers, Steinmetz et al. 2011, Ooi, Chang et al. 2012)
MPO immunisation of MPO-/- mice, irradiation and transplantation with MPO replete bone marrow	Multi-systemic and highly penetrative disease. By-passes break in B and T cell tolerance, essential role for innate immunity - mediated by Ig and neutrophils.	(Schreiber, Xiao et al. 2006)

The cell transfer model was used to further investigate the role of B regulatory and effector cells in AAV; the use of antibody in the other models by-passes the need for antigen specific B cells for induction of disease.

following immunisation of MPO null mice with native MPO isolated from MPRO cells, combined with the 20-mer immunodominant peptide (Ooi, Chang et al. 2012). The cell transfer model is the only one that permits the role of antigen specific B cells to be investigated; the other models rely on ANCA and deposition of MPO on renal endothelial, downstream of the break in B cell tolerance.

An essential role of B cells and immunoglobulin was previously demonstrated in this model (Xiao, Heeringa et al. 2002, Xiao, Heeringa et al. 2003). In the original publication native MPO wass immunised in an emulsion with adjuvant into knock out mice. Purified immunoglobulin was enriched in MPO reactivity and transferred disease to wild type animals. T cells and ANCA are essential to disease induction, but once the break in B cell tolerance is by-passed by antibody transfer, pathology can ensure in B cell deficient mice; this is due to antibody-mediated deposition of antigen on the renal microvasculature, resulting in a directed immune response (Ruth, Kitching et al. 2006).

Whole or B cell enriched splenocytes, from MPO null, immunised mice also results in disease in Rag2 mice. The resulting disease is multi-systemic with biochemical abnormalities, crescentic glomerulonephritis, necrotizing arteritis in the lung and haemorrhagic pulmonary capillaritis**.** The penetrance and severity of disease is reported to be high, which is essential in exploring a protective role of B cells. This cell transferral model, permits the role of antigen specific T and B cells to be dissected. However, the role of B cell subsets has not yet been explored.

A protective role of IL-10 has however been demonstrated in the nephrotoxic nephritis (NTN) model. In this model, mice are pre-immunised with sheep immunoglobulin and

disease is subsequently induced by administration of sheep anti-mouse basement membrane immunoglobulin (nephrotoxic serum or NTS). Animals develop thrombotic and crescentic glomeruli, with biochemical abnormalities. IL-10 limits Th1 response and macrophage induced glomerular injury in NTN (Huang, Kitching et al. 2000, Kitching, Tipping et al. 2000). Although IL-10 positive B cells were shown to infiltrate the kidney during NTN (Ostmann, Paust et al. 2013), conditional knockout of IL-10 in B cells alone, failed to significantly reduce disease (Kluger, Ostmann et al. 2014). Perhaps this is because other IL-10 producing cells are found within the kidney in the NTN model, including dendritic cells, monocytes and CD4 cells (Ostmann, Paust et al. 2013). Regulatory B cells also limit inflammation by production of TGFβ (Tian, Zekzer et al. 2001, Parekh, Prasad et al. 2003, Natarajan, Singh et al. 2012, Lee, Stott et al. 2014)

In an antigen specific model of arthritis, conditional knockout of IL-10 in B cells results in exacerbated disease. T cells from draining lymphnodes had reduced IL-10 competency and increased IFNγ and IL-17 production (Carter, Rosser et al. 2012). IL-10 B cells have also been shown to limit disease in murine models of multiple sclerosis and SLE (Matsushita, Yanaba et al. 2008, Watanabe, Ishiura et al. 2010).

Th17 and Th1 cells are implicated in another animal model of MPO-AAV, in which wild type animals are immunised with MPO and low dose NTS. The respective roles of these T cell subsets were elucidated on ligation of TLR-2 or 9 (Summers, Steinmetz et al. 2009). A 20mer amino acid linear MPO sequence was subsequently defined as the T cell immunodominant peptide (PRWNGEKLYQEA**RKIVGAMV**), with equivalent recall response to whole native MPO. Transfer of a T cell clone, with this peptide reactivity resulted in disease in immunodeficient mice (Ooi, Chang et al.

2012). Antigen deposition mediated by antibody, neutrophil recruitment and an adaptive T cell response, are the key pathogenic mechanisms in this model. Disease proceeds in B cell deficient mice, with their involvement by-passed by direct transferral of NTS (Summers, Steinmetz et al. 2011); interestingly disease is also induced by MPO-ANCA crosslinked to the immunodominant peptide sequence (Ooi, Chang et al. 2012). The T cell peptide defined in mice overlaps with a B cell epitope; antibodies to this epitope are only detected in human disease and not healthy controls (**RKIVGAMV**QIITY). Immunisation of this linear sequence induces ANCA and renal abnormalities in mice (Roth, Ooi et al. 2013). Despite the critical role of Th1, Th17 cells and antibody, the role of B regulatory cells and B cell derived IL-10 in limiting disease progression, has not been investigated in this model.

IL-10 immunoregulatory B cells are phenotypically defined as CD5+, $CD1d^{high}$ (Yanaba, Bouaziz et al. 2008), with most potent immunoregulatory potential attributed to a CD23low T2-MZP subset within this parental population (Evans, Chavez-Rueda et al. 2007). Normal gut microbiota is essential to the maintenance of these cells *in vivo* (Rosser, Oleinika et al. 2014).

The balance of B cell subsets has been shown to be important in determining disease course in animals with a generalised loss of immune tolerance and, in a model of antigen-specific autoimmunity (Matsushita, Yanaba et al. 2008, Haas, Watanabe et al. 2010).

7.2 Aims

The aim was to modulate regulatory and effector B cells, in cell transferral model of AAV, assessing impact on disease outcome.

7.3 Methods in brief

IL-10 induction was assessed in B cells, using defined experimental conditions (Matsushita and Tedder 2011).

Immunophenotyping of bone marrow, peritoneal, splenic and blood B cells was conducted by cell surface flow cytometry in the presence of FcR block. Acquisition and analysis as previously described.

Native MPO was isolated from MPRO cells, by Dounce homogenization and Con A affinity purification on the Äkta Prime FPLC system.

MPO null mice were immunised with 30µg of native MPO and 300µg immunodominant peptide over the course of 10 weeks (Table 2.3). Blood was collected and spleens retrieved for cell transfer experiments.

Splenocytes were injected intravenously into Rag2 mice, with intraperitoneal LPS. A subcutaneous antigen boost was conducted on day 6. At the end of the experiment urine and blood were collected, with kidney, lung and spleen retrieved post-mortem.

A portion of the spleen, the lungs and kidneys were processed into wax blocks, with PAS and H&E histological stains conducted (C&C Laboratory Services Ltd., London).

Additional sections were cut for immunofluorescence. Slides were dewaxed, rehydrated and antigen retrieval conducted. Staining was conducted with B220 [RA3-6B2] and CD3 [SP7] primary antibodies, with fluorescent secondaries and DAPI nuclear counterstain.

Biochemical analysis was conducted on plasma and urine at MRC Harwell testing centre (AU680 clinical chemistry analyser, Beckman Coulter). Urinary dipstick was additionally conducted at point of sample collection, after centrifugation (Multistix 10SG reagent sticks, Siemens).

MPO ELISA was conducted on all plasma samples. Total IgG was measured by ELISA (eBioscience). MPO specific Ig subtyping was performed with a modified ELISA protocol, outlined in the methods section.

7.4 Results

7.4.1 Assessment of B cell phenotype in mice

7.4.1.1 IL-10 induction in mice

IL-10 is a key immunoregulatory mediator, produced by regulatory B cells. Production was assessed by various methods, including treatment with LPS, CPG and anti-CD40 [FGK45 and HM40-3 clones]. Induction was always modest in mouse splenocytes, utilising live-dead exclusion and the same IL-10 clone as other research groups [JES5-16E3] (Evans, Chavez-Rueda et al. 2007, Yanaba, Bouaziz et al. 2008). A representative 5-hour experiment is shown in Figure 7.1 (more than 10 independent experiments conducted).

IL-10 was most potently induced in human PBMC by combining CPG and CD154. In these cultures, a histidine tagged CD154 was crosslinked with antibody to form multimers. Irradiated NIH-3T3 cells transfected with CD154, have also been used to crosslink CD40 on human B cells (Blair, Norena et al. 2010, Bouaziz, Calbo et al. 2010). CD154 exists as a trimer in nature. The anti-CD40 utilised in mouse cultures, may not be as efficacious as CD154 multimers assembled *in vitro* or trimers on the surface of mouse fibroblasts.

LPS serotype 026:B6 was used initially, which differed from that used in the many publications by Tedder *et al* (serotype 0111:B4). To assess whether detection was inhibited by choice of LPS serotype, 48-hour stimulation was conducted with 026:B6, 0111:B4 and R515 serotypes (Figure 7.2). IL-10 competent B cells represent a much higher proportion of peritoneal B cells; these cells were consequently included as a positive control. There was no difference between the different LPS serotypes tested and the results were not discordant with those previously reported. The mean frequency and SEM for IL-10 B cells observed across the 3 different LPS serotypes was 3.9%$\pm$0.26 in spleen and 28.7% +0.92 for peritoneal wash-out (Figure 7.2, Panel B). Matsushita *et al* reported 6.2% $\pm$0.03 in spleen and 30.2% +2.0 in the peritoneal cavity in 3 mice, 8-10 weeks old, stimulated with LPS 0111:B4 serotype (Matsushita and Tedder 2011). Although relative IL-10 frequency is higher in B cells from peritoneal wash-out, the total yield of cells from this source, is low relative to spleen and necessitates use of the latter for *in vivo* experiments (typically 30-fold higher cell yield in the spleen, which equates to a higher total number of IL-10 competent cells).

The findings presented here are important because they demonstrate that B cell IL-10

Figure 7.1 IL-10 induction in murine splenocytes, 5-hour stimulation

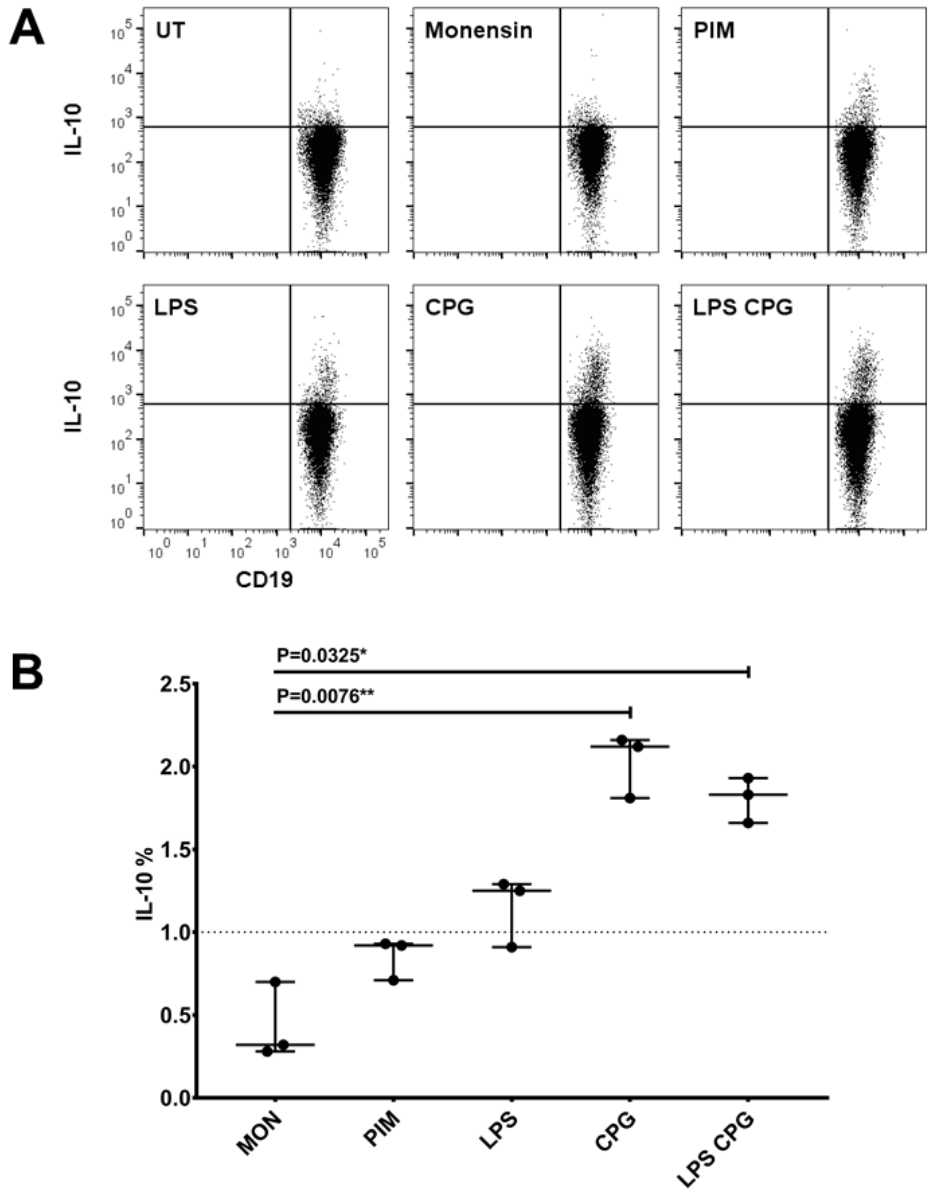

[A] Whole splenocytes were stimulated for 5 hours and frequency of IL-10 positive B cells assessed by intracellular flow cytometry. Controls conditions were untreated cells and monensin alone. All test conditions included PMA 50ng/ml, ionomycin 1µg/ml and monensin (PIM). PIM was combined with LPS (026:B6) at 10µg/ml or CPG DNA at 10µg/ml or both. [B] Triplicate wells were set up for each condition. Induction of IL-10 in B cells with CPG alone or CPG and LPS, was significant compared to monensin alone (Kruskal Wallis and Dunn's multiple comparison).

Figure 7.2 IL-10 induction in mice, 48-hour stimulation with LPS

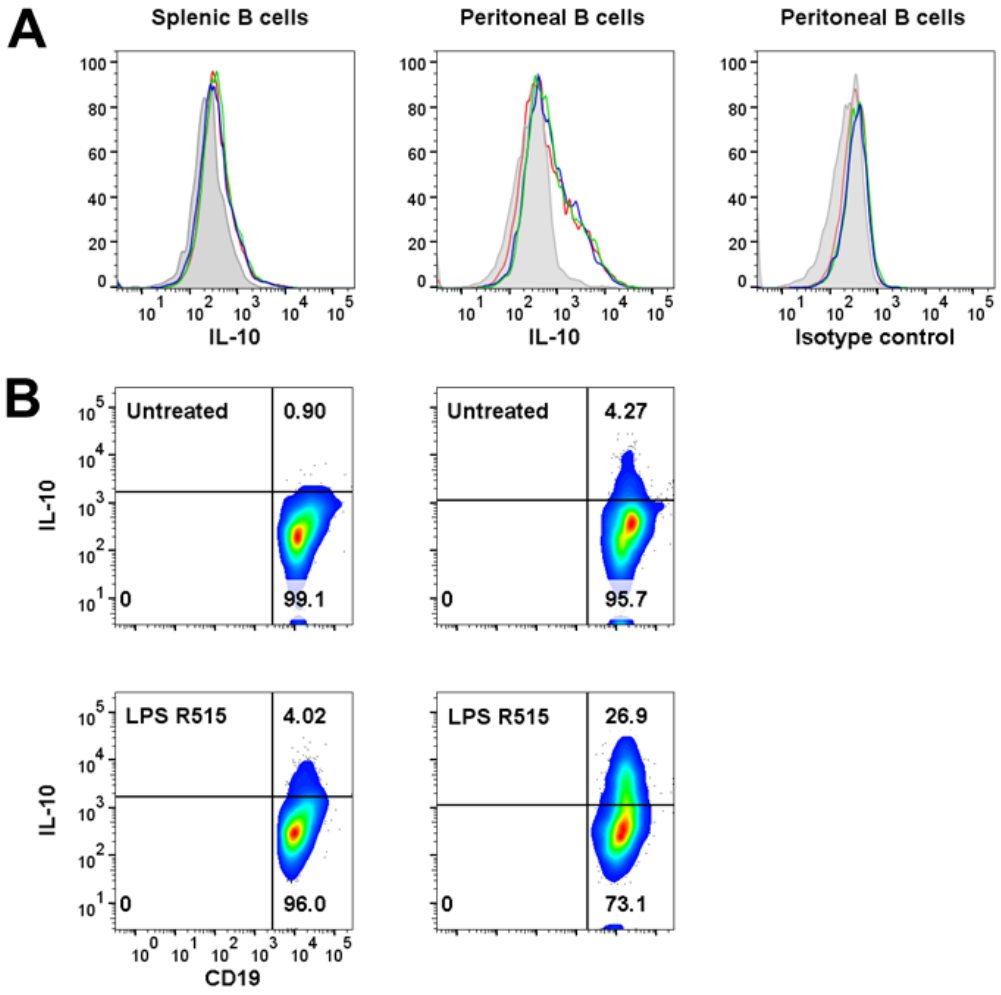

[A] Whole splenocytes and leukocytes from the peritoneal cavity were isolated and cultured for 48 hours. Cells were either untreated or stimulated LPS serotypes. Histograms show similar IL-10 induction in CD19+ B cells, with the different LPS isotypes assessed (0111:B4, 026:B6 and R515). There was no detection in untreated cells. IL-10 was much higher in peritoneal B cells, to verify that detection was specific an isotype control was used. [B] Smoothed pseudocolour biaxial plots for B cells, IL-10 shown against CD19. In peritoneal B cells there was some spontaneous IL-10 production (cells treated with monensin alone), gating was based on the isotope control and discrete positive population in stimulated cells. In spleen gates were set to ≤1% positivity with the test antibody, in untreated cells.

competency was intact in animals bred in our facility. In germ-free conditions, IL-10 competent B cells are lost; IL-6 and IL-1β, induced by gut microflora are essential for maintenance of these cells (Rosser, Oleinika et al. 2014). Induction of IL-10 is challenging in mice. Many researchers have since moved away from *in vitro* assays, to use of IL-10 eGFP reporter mice. Detection of CD9 mRNA is also reported to be predictive of IL-10 competency in murine B cells; CD9+ B cells inhibited T cell proliferation *in vitro*, produced TGFβ and limited contact hypersensitivity on oxazolone challenge in mice (Sun, Wang et al. 2015). Unfortunately, CD9 was not known to be a marker of IL-10 competency in B cells, when this work was undertaken. Other functional markers of regulatory B cells include Fas-L, PD-L1 and granzyme B; B cells expressing these markers can kill effector T cells directly.

7.4.1.2 B cell immunophenotyping in mice

Regulatory function had been attributed to two main B cell phenotypes at the time of this study, T2-MZP and B10. These cells express high levels of CD5 and CD1d, are IL-10 competent, readily isolated from mouse spleen and proven to limit inflammation *in vivo* (Evans, Chavez-Rueda et al. 2007, Yanaba, Bouaziz et al. 2008). Evans *et al* found the most potent immunoregulatory function resided within the $CD23^{low}$ subset within the CD1d+ B cell parent population.

To begin with, I verified that I could detect a CD5+ $CD1d^{high}$ population in mouse spleen. These cells expressed ubiquitously high levels of CD21 and IgM, with only a subset expressing CD23 (Figure 7.3). Although $CD23^{low}$ cells were enriched for CD1d+ B cells (18.9%), CD23+ cells were not profoundly deficient in CD1d+ cells

(5.06%). $CD23^{low}$ CD1d+ B cells only represented 3.87% of total B cells, whilst CD1d+ B cells had a frequency of 7.90%.

Isolation of cells based on CD5 and CD1d expression, was chosen forcell transfer experiments. Regulatory function of this subset was proven in an antigen specific model of autoimmunity (Matsushita, Yanaba et al. 2008). T2-MZP are a subset within this population and therefore highly enriched. CD1d has been shown to be essential to the immunoregulatory capacity of B regulatory cells, both in humans and mice (Bosma, Abdel-Gadir et al. 2012, Oleinika, Rosser et al. 2018). Many of the CD1d+ cells would not be isolated with $CD23^{low}$ expression set as a criterion, with number available for transfer reduced by 50%. Cell number is critical to penetrance and severity of the MPO animal model (Xiao, Heeringa et al. 2002).

Phenotype was further assessed in splenocytes, peritoneal and bone marrow B cells. Bone marrow B cells precede splenic B cells in terms of development, whilst peritoneal B cells have highest capacity to produce IL-10 (Matsushita and Tedder 2011). Focus was placed on putative immunoregulatory markers (CD11b, TIM-1) and those reported to overlap with human Breg (CD24, CD38, CD5, IgM and IgD).

Four population of B cells could be resolved based on relative expression of B220 and CD19 (Figure 7.4). In all compartments, B220+ and CD19+ cells represented approximately 70% of the total B cells. $B220^{low}$ and $CD19^{low}$ B cells were only detected in bone marrow. $B220^{high}$ and $CD19^{high}$ B cells were only detected in spleen. $B220^{low}$ and $CD19^{high}$ cells represented about 30% of the B cells in peritoneum cavity. CD1d+ B cells were only detected in mouse splenocytes, indicative of a specialised marginal zone niche in secondary lymphoid tissues. IgD and IgM null, pre-B cells

Figure 7.3 Immunophenotyping of mouse splenocytes

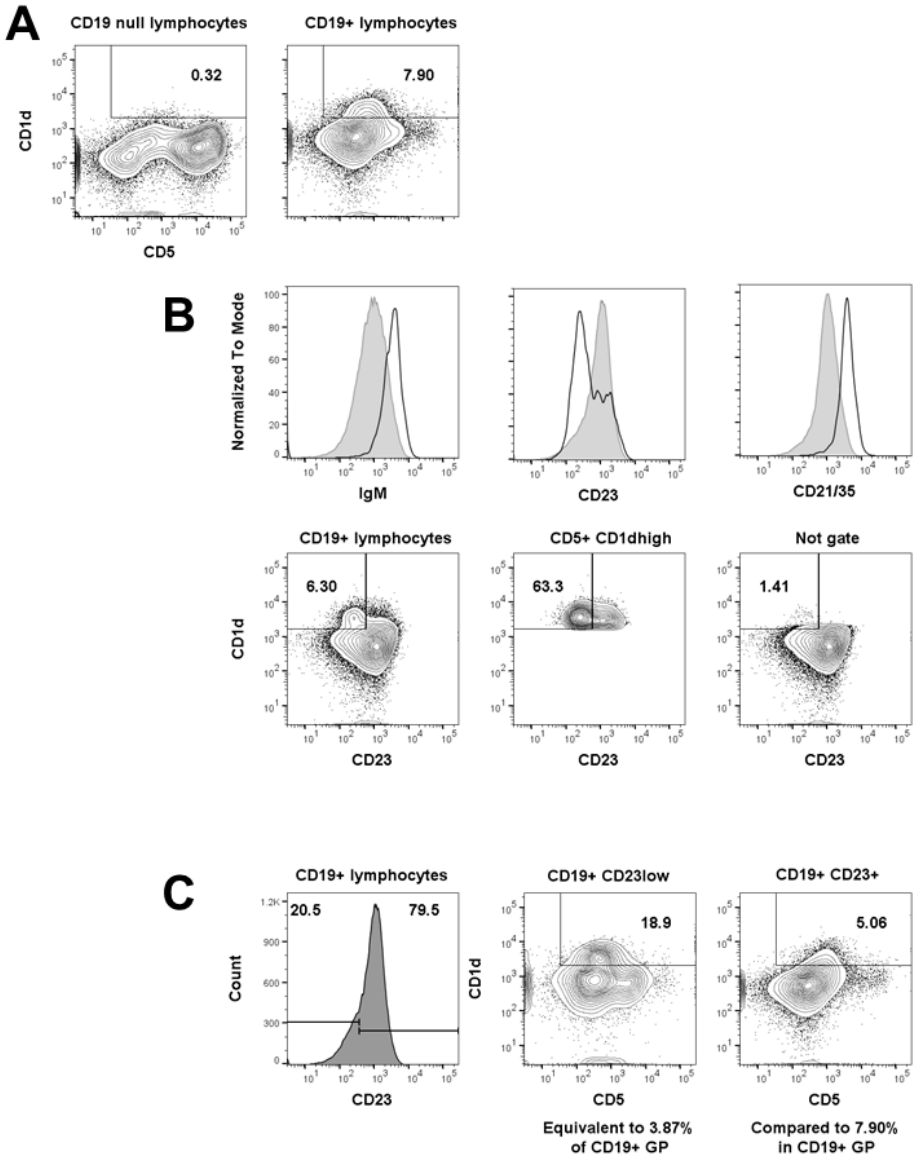

[A]Mouse splenocytes stained with CD19, CD5, CD1d, CD21, CD23 and IgM. Pattern of CD5 and CD1d staining as expected. [B] In overlaid histograms CD1d+ B cells are shown in black; the corresponding "Not-gate" (created with Boolean tool in Flow Jo) is depicted in grey. CD1d cells have high expression of IgM and CD21, but variable expression of CD23 compared to CD1d negative cells (contour plots also shown). [C] Although CD1d+ cells are highly enriched in CD23^{low} B cells, representing 18.9% of the parent population, there are twice as many CD1d+ B cells in the CD23+ fraction, when frequency of both, expressed as percentage of grandparent (CD19+ B cells)

Figure 7.4 Comparison of bone marrow, splenic and peritoneal B cells

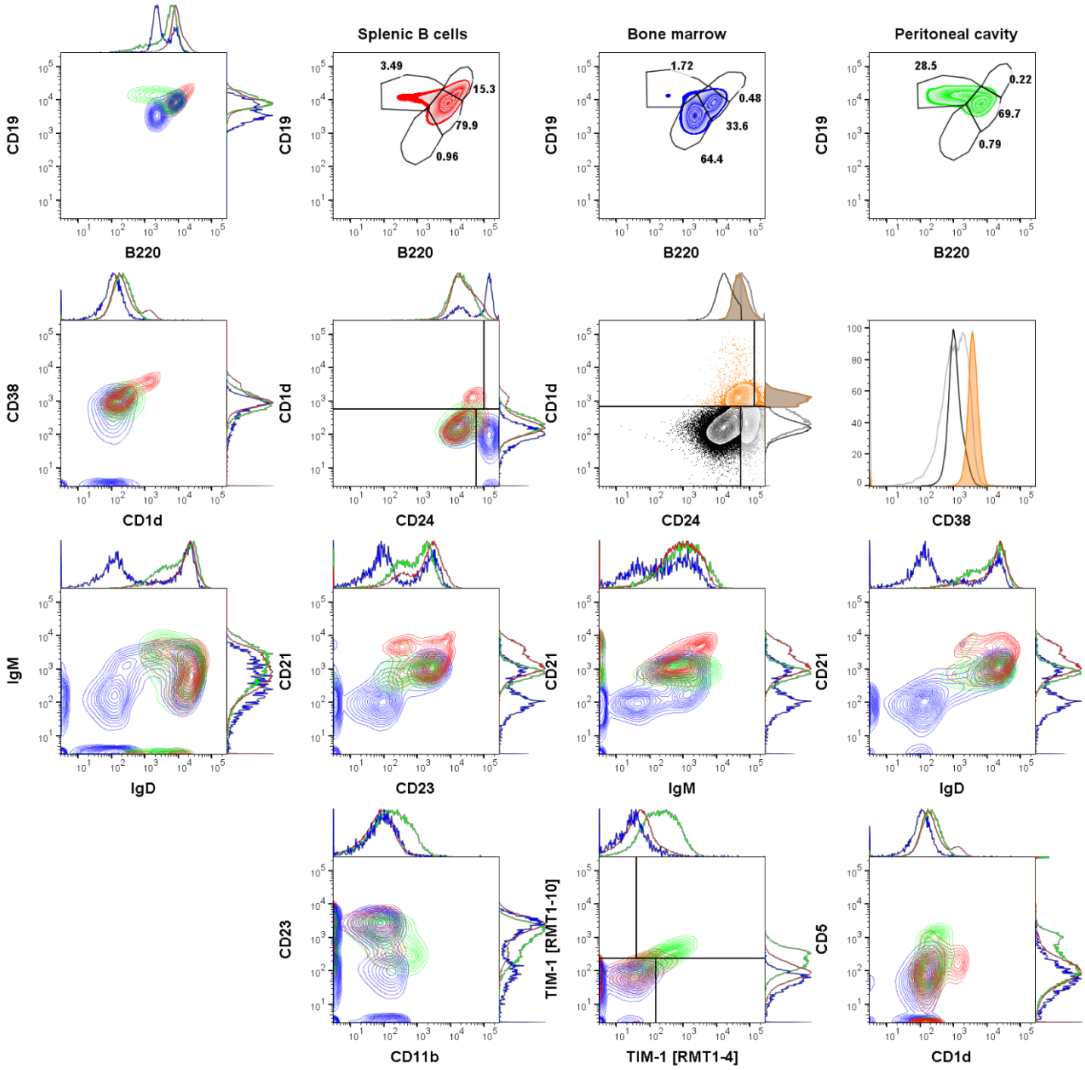

CD19+ B cells from spleen shown in red, bone marrow in blue and peritoneum in green. [Row 1] There was variation in CD19 and B220 expression, with 4 populations resolved. [Row 2] CD1d+ B cells are uniquely detected in spleen. Highest detection of CD24 is in bone marrow. CD24^{high} B splenocytes have higher expression of CD38, than CD24- CD1d- B splenocytes (black). Highest CD38 detection, was within CD24^{high} CD1d+ B cell population (orange). [Row 3] IgM and IgD double negative cells are only detected in the bone marrow (immature B cells). Complement receptors (CD21 and CD23) are most highly expressed in B splenocytes. [Row 4] Detection of TIM-1, CD5 and CD11b, regulatory B cell markers, was highest in peritoneal B cells.

were only detected in bone marrow, whilst immature IgM^{high} and IgD+ predominated in spleen. CD24 is a marker of immature B cells, expressed most highly in bone marrow and variably, in the other compartments. CD38^{high} B cells were only detected in the spleen; this marker segregated very well with CD1d and reasonably well with CD24. CD24 expression was not limited to CD1d cells in the spleen.

The CD21 antibody [7E9], detects an epitope shared between CD21 and CD35 (complement receptors 2 and 1). CD23 is the low affinity IgE receptor. These functional markers, which are shared with innate immune cells, were highest in splenic B cells. The capture of circulating bacteria and rapid release of cross-reactive, broadly neutralising antibody is an important function of the splenic marginal zone cells, conferring protection against encapsulated bacteria. CD21 expression was concordant with high IgM expression and IgD positivity, indicative of immature B cells, which have not undergone a germinal centre reaction. CD23 down-modulation is associated with differentiation to marginal zone B cells, with intermediary cell type T2-MZP.

The highest expression of CD11b, TIM-1 and CD5 was observed in peritoneal B cells. The ontogeny of peritoneal B cells is thought to be distinct from splenic B cells, with this compartment seeded in foetal development, an immunologically naïve phase of life. B1a cells are defined by CD5 expression and known to be enriched in serous cavities. CD11b expression is more classically associated innate immune cells, indeed these B1a cells are cross-reactive and have low avidity, consequently, they may not able to able to specifically modulate an antigen-driven immune response. In contrast, antigen receptor diversity or the check points associated with Ig rearrangement are essential to CD1d+ B regulatory cells, with efficacy in EAE demonstrated (Matsushita,

Yanaba et al. 2008) and impairment in mice with an oligoclonal HEL-BCR (Yanaba, Bouaziz et al. 2009).

Biaxial plots for all the analytes in the extended panel were generated against CD1d, for mouse B splenocytes (Figure 7.5). The markers that had best concordance with CD1d were IgM, CD21, CD38 and TIM-1 [clone RMT 1-10]. CD23 expression was biphasic in CD1d+ B cells, as previously discussed.

Overlaid plots for CD1d+ and CD1d- B splenocytes were generated next. CD1d B cells had markedly higher expression of IgM, CD21, CD24 and CD38 (Figure 7.6). When gated based on relative expression of CD24 and CD38, murine CD1d+ B cells had a very similar expression pattern (Figure 7.6, Panel B), to that previously shown in human PBMC.

The expression of TIM-1 is very low on splenic B cells, making it very hard to resolve a positive population. Detection was not enhanced when 2 clones with different fluorophores were combined. Clone RMT 1-10 gave better concordance with CD1d staining (Figure 7.5). B cells with higher geometric MFI for RMT 1-10, had a higher frequency of CD1d+ B cells than cells with low MFI. These cells also had higher geometric MFI for the other TIM-1 clone, RMT 1-4 (Figure 7.7). Collectively, this shows that TIM-1 is higher on CD1d+ B splenocytes but expression is still very low and this marker, would be unsuitable for cell isolation by flow cytometry sorting.

Figure 7.5 Extended immunophenotyping in splenic B cells

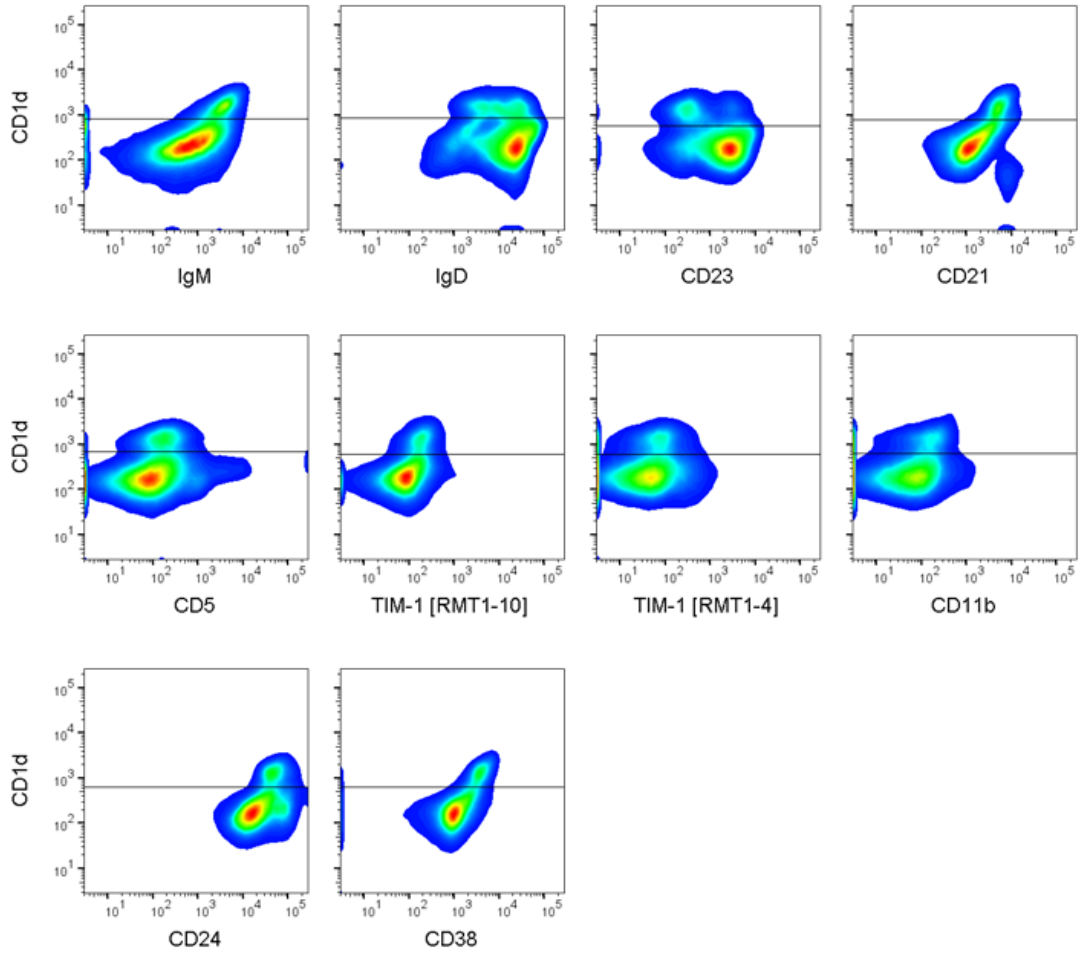

Smoothed pseudocolour biaxial plots of total CD19+ splenocytes. CD1d is presented in the Y-axis in all instances, against various markers in the X-axes (as labelled). CD1d+ cells have higher expression of IgM, CD21, CD38 and TIM-1 [RMT 1-10], with lower expression of CD23. CD24 and CD5 expression is not limited to CD1d+ B cells. The relationship of TIM-1 [RMT 1-4], CD11b and IgD, with CD1d, is less marked.

Figure 7.6 Comparison of CD1d+ and CD1d- splenic B cells

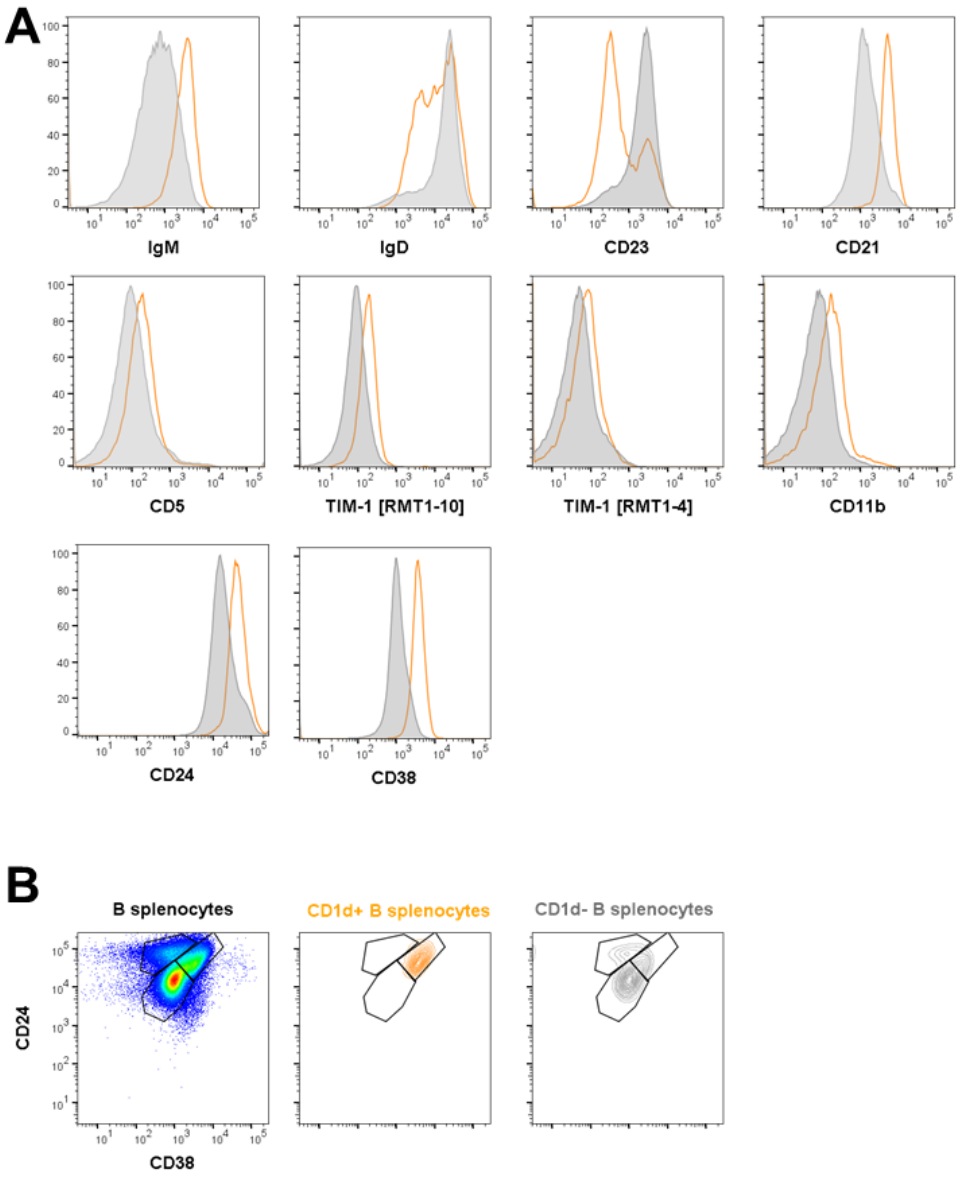

[A] Overlaid histograms for CD1d+ (orange) and CD1d- (filled grey) B *splenocytes. IgD and CD23 expression is variable. CD1d B cells express high levels of IgM, CD21, CD24 and CD38. TIM-1, CD5 and CD11b expression is only modestly increased, relative to CD1d null B cells. [B] Biaxial graphs for CD24 and CD38. Total B cells are shown with the pseudocolour dot-plot. CD1d+ B cells have high CD24 and CD38 expression (orange contour plot), relative to CD1d+ B cells (grey contour plot).*

Figure 7.7 TIM-1 expression in mouse splenocytes

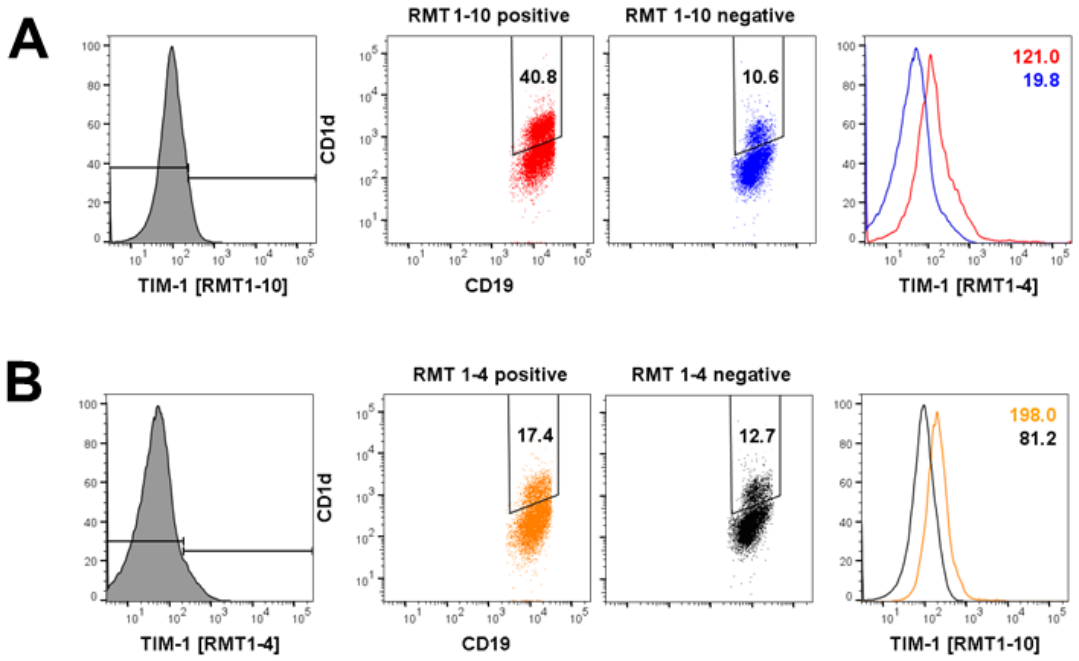

Two clones were used for detection of TIM-1, RMT 1-10 and RMT 1-4. B cells with the highest MFI for these 2 antibodies, were gated on histograms. [A] RMT 1-10 B cells were highly enriched for CD1d+ cells (40.8%, red dot plot). These cells also had 6-higher expression of RMT 1-4 (geometric MFI 121.0 and 19.8). [B] RMT 1-4 B cells were only modestly enriched for CD1d+ cells (17.4%, orange dot plot). These cells had 2.4 higher expression of RMT 1-10 (geometric MFI 198.0 and 81.2). RMT1-10 also had better concordance with CD1d immunostaining (Figure 7.5).

7.4.1.3 CD1d B cell isolation

Magnetic isolation of Breg was tested, using a CD1d PE conjugated antibody, anti-PE microbeads and LS-columns. Although CD1d B cells were enriched, the purity was low and many CD1d+ B cells, were still detected within the negative fraction (Figure 7.8). Purity can be negatively affected when target cells are low in frequency or, whenever there is little differential expression between positive and negative cells. This is likely to be true for CD1d. All B cells and in fact all antigen presenting cells, express CD1d, levels are variable and surface kinetics are dynamic, with endocytosis described (Bosma, Abdel-Gadir et al. 2012).

Ultimately, CD19+ B cells were enriched using microbeads and LS columns, with flow cytometry sorting for subsets. Purities approaching 100% can be obtained by this method. Flow cytometry was conducted to assess purity at each stage, sample plots are shown in Figure 7.8.

Figure 7.8 Magnetic isolation of CD1d B splenocytes

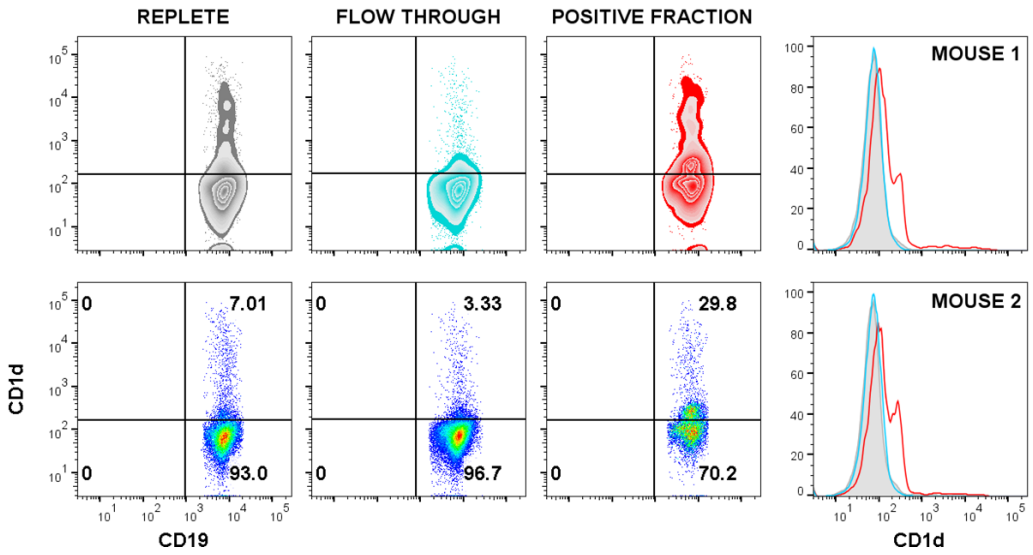

Magnetic isolation of Breg with an CD1d PE conjugated antibody, anti-PE microbeads. Although CD1d B cells were enriched, the purity was low and many CD1d+ B cells, were still detected within the negative fraction (flow through). Images show coloured zebra plots and pseudocolour dot plots for 1 mouse. CD1d frequency was increased from 7.01 to 29.8% in the example shown. CD1d expression was variable in the positive fraction. Overlaid histograms summarise the results for 2 mice, magnetic isolation conducted in tandem. The CD1d positive cells are shown in red, in addition to the discrete positive population, the histogram also shifted to the right

Figure 7.9 Magnetic enrichment of CD19+ B splenocytes and flow cytometry sorting for CD1d positive and negative fractions

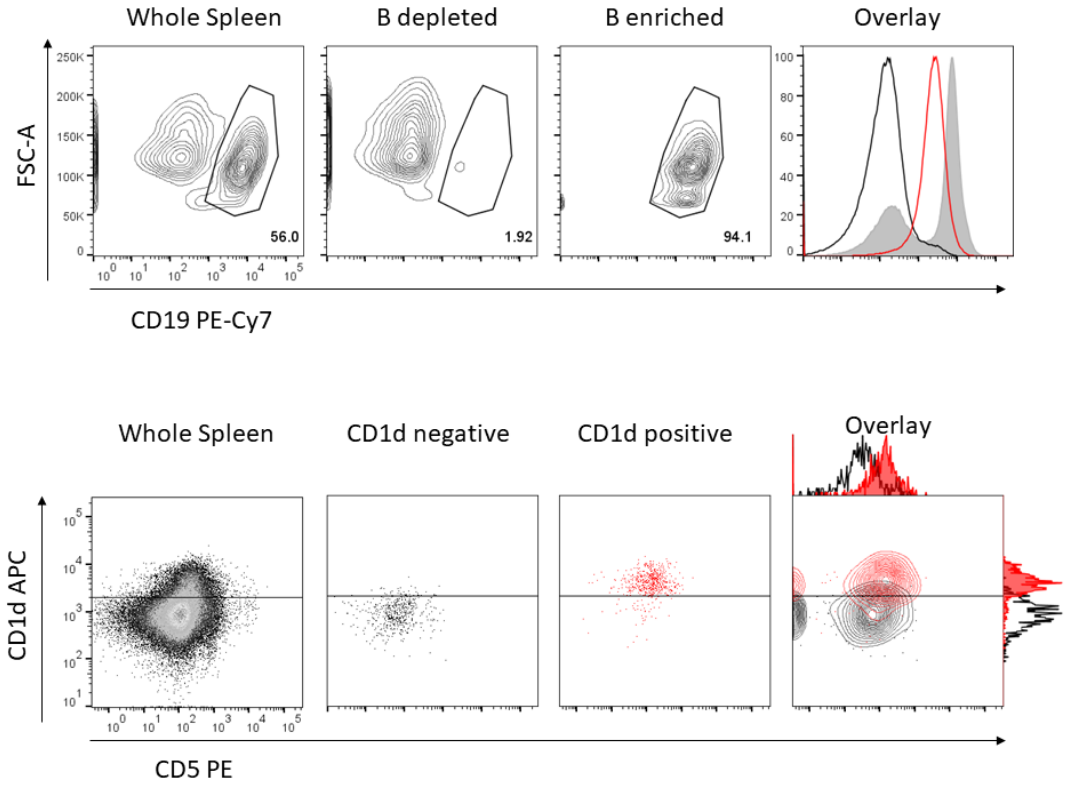

The top row shows magnetic isolation of murine B cells with CD19 microbeads. These were very effectively depleted from the flow through, frequencies shown and overlaid histograms (histograms show CD19+ fraction in red, CD19- in black and whole spleen grey filled histogram). The second row shows purity from fluorescent cell sorting. CD1d positive and negative cells could be very efficiently isolated by a 2-way flow cytometry sort. In the plot on the right, isolated CD1d+ cells and CD1d- cells are shown together (CD1d+ in red, CD1d- black contour plot and histogram).

7.4.2 Challenges of the MPO cell transfer model

Prior to my conducting this study, another researcher was working to set up the Murine Experimental Vasculitis (MEV) model at our facility. This involved establishing the MPO knock out colony (B6.129X1-Mpo$^{tm1Lus/J}$) and growing MPRO cells, with isolation of native MPO protein by affinity chromatography. To assist in this process, Professor Heeringa from Groningen University provided native MPO protein and positive control serum, pooled from 40 MPO-immunised mice. An HM-5 feeder cell line also was kindly gifted by Professor Robson, Kings College London.

In the MEV model, disease is induced in wild type animals upon passive transfer of IgG, isolated from MPO$^{-/-}$, immunised animals (Xiao, Heeringa et al. 2002). Splenocytes from MPO$^{-/-}$ immunised mice can also transfer disease to immunocompromised mice; B splenocytes are widely cited as being able induce disease alone (Xiao, Heeringa et al. 2003).

The mode of MPO immunisation is peritoneal, with protein injected in an emulsion with complete Freud's adjuvant initially then incomplete (CFA and IFA, respectively). Peritonitis consequently developed in these animals, with spleens becoming sclerotic and firmly attached to the surrounding membranes. This made post-mortem retrieval challenging; just 4 spleens were collected initially, yielding insufficient cells to proceed with flow cytometric cell sorting. Isolated splenocytes were introduced to Rag2-/- mice intravenously and detection of cells verified at 12 days by flow cytometry of whole blood leukocytes. A population of small, CD45+ leukocytes, with CD19+ cells within it, was observed after splenocyte transferral but was absent from untreated mice (data not shown). It was clear that the experimental approach needed to be refined

at this point. The first step was to change the route of antigen administration, amended to subcutaneous injection in the hind flank.

In the next experiment, spleens were dissociated from 8 MPO null mice, immunised subcutaneously with native MPO protein and immunodominant peptide. The total amount of protein injected was increased 100-fold, by administering with the synthetic linear amino acid sequence PRWNGEKLYQEARKIVGAMV (Activotec Ltd). This MPO T cell immunodominant peptide was first described by Ooi *et al*, who screened pools of overlapping MPO 20mer peptides to define pathological T cell epitopes. An equivalent T cell recall response was observed with peptide and whole native MPO in immunised mice (Ooi, Chang et al. 2012). This amino acid sequence was subsequently shown to overlap with a B cell epitope (**RKIVGAMV**QIITY), observed in AAV patients but not healthy controls. Mice immunised with a peptide containing the B cell epitope sequence, developed MPO-ANCA (p-ANCA with MPO replete neutrophils but not MPO-/- neutrophils) and urinary biochemical abnormalities (Roth, Ooi et al. 2013).

B cell isolation was conducted with CD19 magnetic microbeads. Whole splenocytes, B cell depleted cells or B cell enriched cells were transferred into Rag2 mice (2 mice per a condition and $6x10^7$ cells, each). Cell transfer was verified in spleen at the end of the experiment by flow cytometry (Figure 7.10, Panel A). Renal disease was unremarkable, with little pathology observed on immunohistochemistry (PAS stained sections). For each mouse, 25 glomeruli were scored by a renal physician, blinded to the experimental conditions. Most glomeruli were normal, with no crescents or thrombosis (frequency of normal glomeruli ranged from 80-100%). No crescents were observed in 4 animals and in the remaining 2 mice, just 8% of glomeruli had crescents

(1 mouse receiving whole splenocytes and in 1 mouse receiving enriched B cells). The pathological findings were verified by Professor Cook, Imperial College London and are shown in Figure 7.10, Panel B. MPO immunoglobulin titres in $MPO^{-/-}$ immunised mice and Rag2 mice, were very low relative to the pooled positive control serum (Figure 7.11). This is likely why little disease was observed. Highly penetrant and severe disease would be required, to verify a protective effect of B cells.

At this time, I took over maintenance of the cell lines and isolation of native MPO. The number of MPRO cells used in a single extraction was dramatically upscaled from $0.8x10^9$ to $5x10^9$ cells. The isolated protein was now viscous and visibly deep green, a property attributable to the heme moiety in MPO. The quantity and purity of isolated MPO had historically been assessed by RZ ratio (ratio of absorbance at 430nm/280nm). In addition to spectrophotometry, quality was now assessed by SDS-PAGE relative to recombinant MPO (Figure 7.12, Panel A). The isolated protein was also assessed as an ELISA substrate, with positive control serum. Optical density on titration was highly comparable with recombinant protein and the native protein, gifted by Professor Heeringa (Figure 7.12, Panel B). There was very little reactivity with immunodominant peptide. The number of MPO knock out mice immunised was also increased. 15 mice were immunised with this new batch of native protein, either 2 or 3 subcutaneous injections. Final antibody titres dramatically improved, proving that immune response was not inhibited by mode of antigen introduction (Figure 7.13).

Figure 7.10 Successful B cell transfer and pathology on initial testing

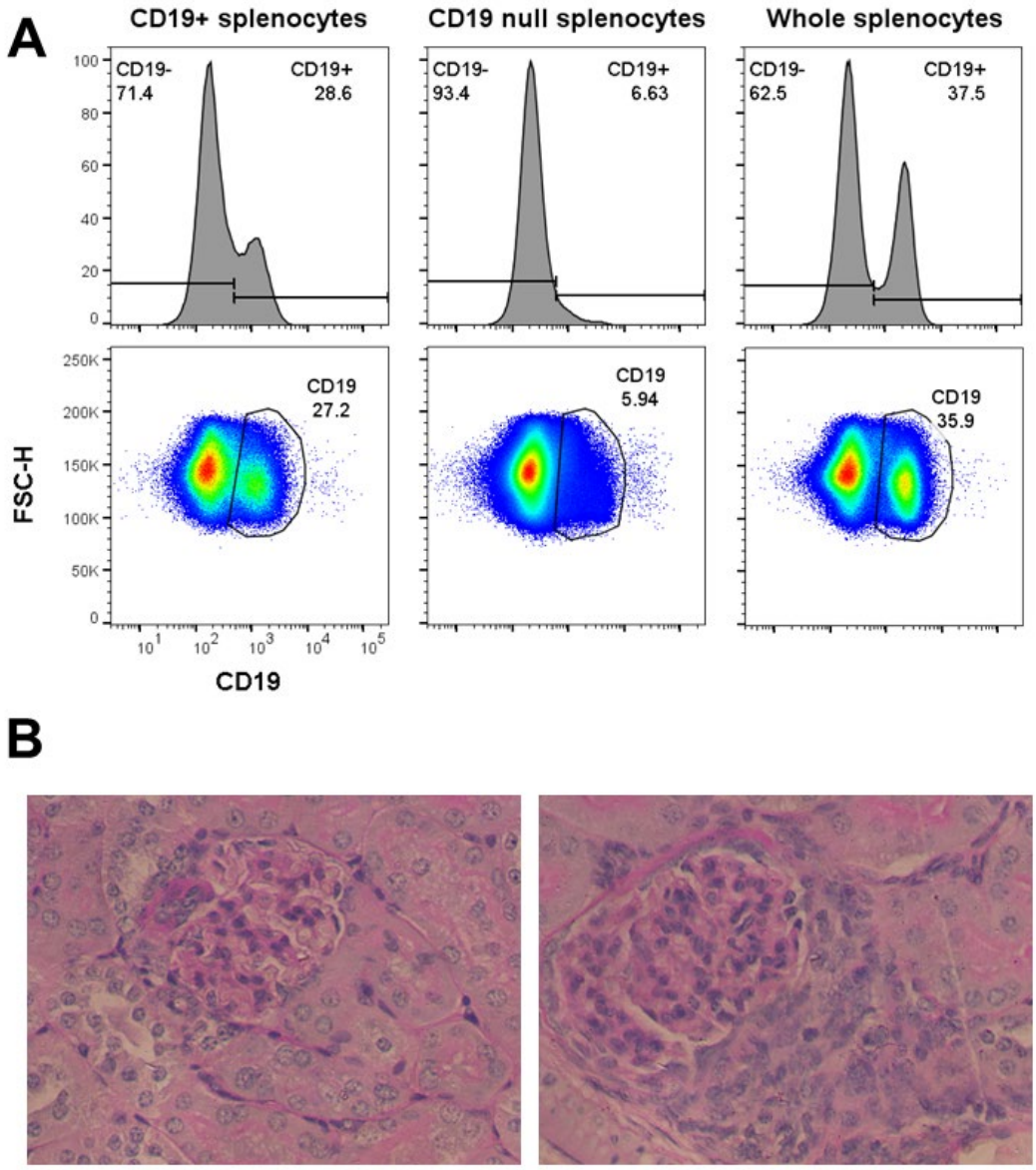

[A] Spleens from the treatment groups were combined and flow cytometry conducted. B cells were detected within the small CD45+ population. Frequency would be more accurately assessed with the inclusion of an additional B cell marker and CD3. [B] Renal pathology was observed. The panel on the left shows a deep pink area of fibrinoid necrosis. The panel on the right shows a crescent within Bowman's space (x63 magnification, PAS stain).

Figure 7.11 Low MPO antibodies titres in the initial experiment

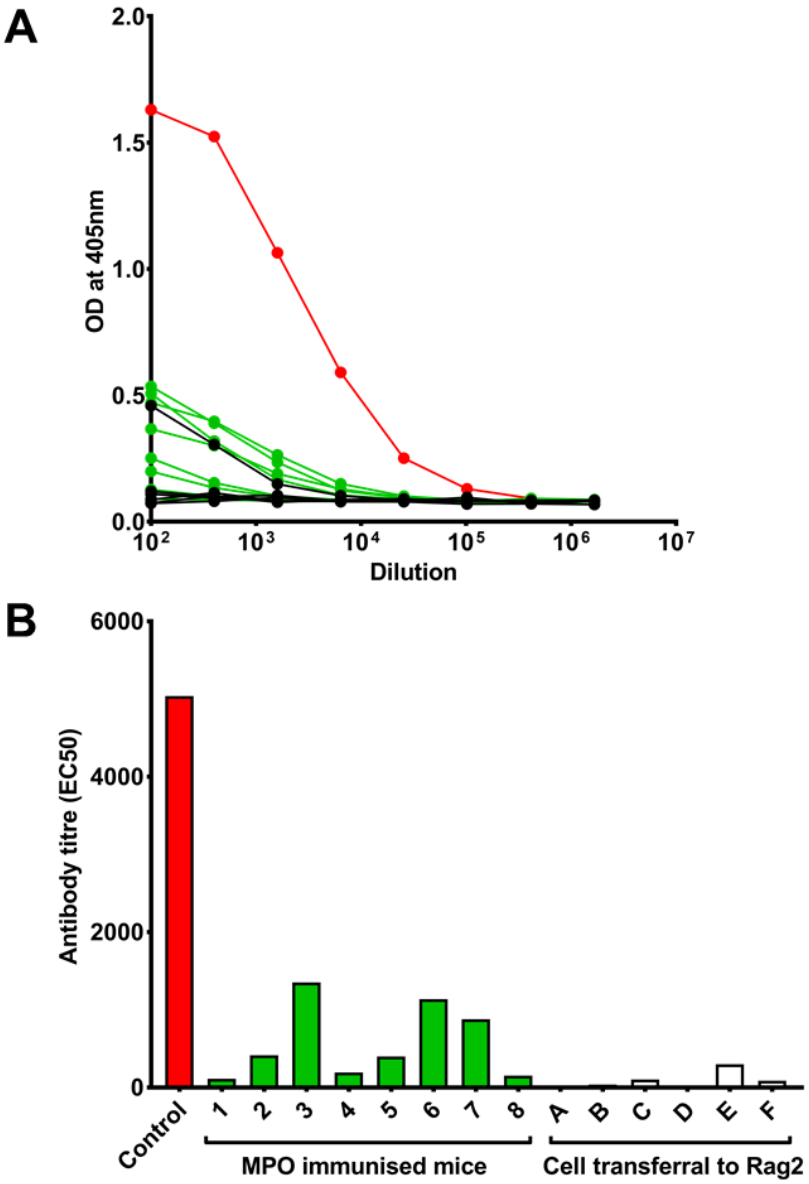

ELISA was conducted on serially diluted plasma (1x103 - 1.64x106). The data was transformed, creating a sigmoidal curve from which EC50 was calculated. EC50 is the dilution factor, which results in half the maximum optical density. [A] Sigmoidal curves are shown for MPO null immunised (green) and the Rag2 mice (black), relative to known positive control (red). The positive control was pooled serum from 40 mice, provided by Professor Heeringa. [B] The EC50s were very low in MPO null immunised and Rag2 mice compared to the control.

In the final round of immunisations, 12 MPO null mice and 1 wild type mouse were immunised. Antibody titres were high, with many readings over the limit of detection at a 1 in 6400 dilution (Figure 7.14, Panel A). ELISAs were conducted in parallel with the new batch of native MPO and recombinant mouse MPO, as capture reagents. Results were highly concordant, increasing confidence in the antigen specificity of the response (Figure 7.14, Panel B). It is interesting that there was no humoral response to the immunodominant peptide. The T cell peptide sequence is not synonymous to the B cell epitope but does overlap considerably. The B cell epitope was previously shown to induce renal pathology in mice, with p-ANCA detection by indirect immunofluorescence (Roth, Ooi et al. 2013).

I proceeded with flow cytometric sorting of splenocytes from these MPO null, immunised mice. CD1d+ (Breg) and CD1d- (Beff) cells were isolated. This took a long time and cells consequently had to be rested in replete media in the incubator overnight, which negatively affected yield. With low total number, the highly purified B cells were combined with CD19 depleted splenocytes. Comparator groups included CD19 depleted splenocytes without sorted cells, splenocytes enriched for B cells and whole splenocytes. The results of this experiment are presented in detail, section 7.5.3.

Figure 7.12 Quality assessment of a new batch of murine MPO

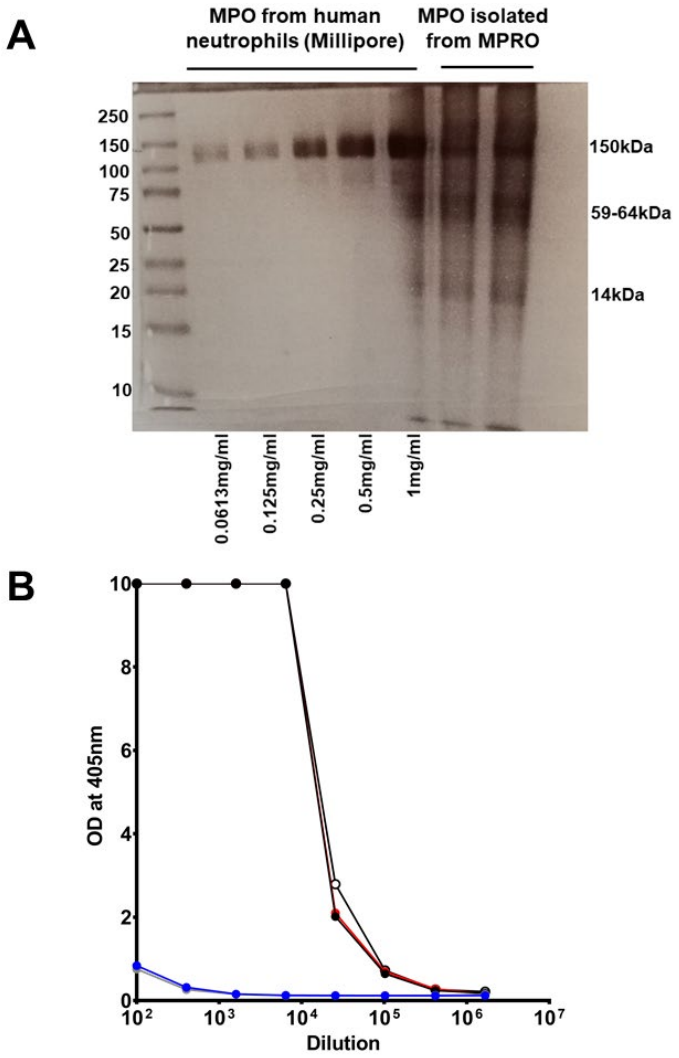

[A] The murine MPO isolated by affinity chromatography, 20µg was run against commercially available native, human MPO (Millipore). 1.25-20µg of control protein was loaded. The protein as resolved on a 10% SDS-PAGE hand poured gel and stained with Bio-Safe™ Coomassie (BioRad). Results were concordant with the expected molecular weight; MPO is a 150kDa tetrameric protein, composed of 2 59-64kDa α-chains and 2 14kDa β-chains. [B] The new batch of MPO was also compared as an ELISA substrate, with positive control serum. New MPO (black filled data points), existing ELISA substrate (red, native protein gifted by Professor Heeringa), recombinant MPO (unfilled data points, RnD Systems) and immunodominant peptide (shown in blue, manufactured by Activotec Ltd, sequence published by Ooi et al).

Figure 7.13 Response upon immunisation, with the new batch of MPO

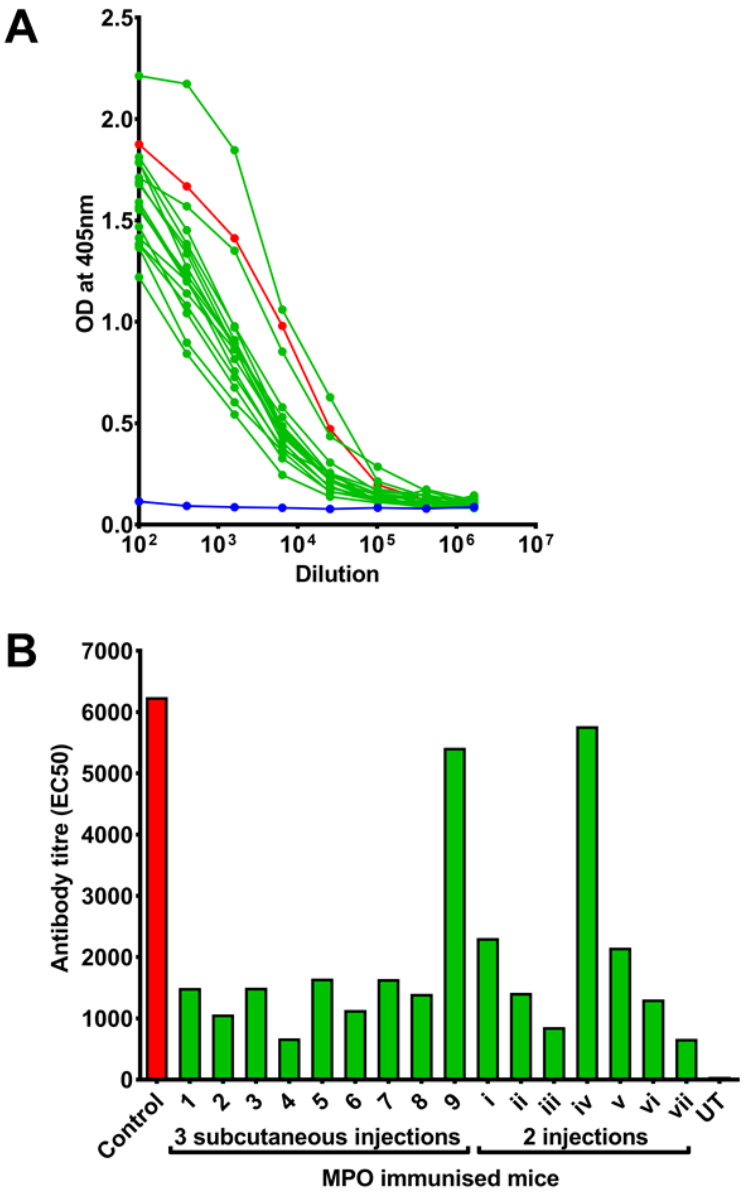

The new batch of protein was effective at inducing an MPO antibody response in null mice, upon subcutaneous immunisation. [A] Sigmodal curves are shown for MPO null immunised mice (green data points), relative to serum from an un-immunised mouse (blue data points) and the positive control (red data points, pooled serum gifted by Professor Heeringa). [B] The response was variable, but this was not due to the immunisation schedule. EC50s were much higher than those previously observed.

Figure 7.14 MPO titres of mice, used for final splenocyte transfer experiment

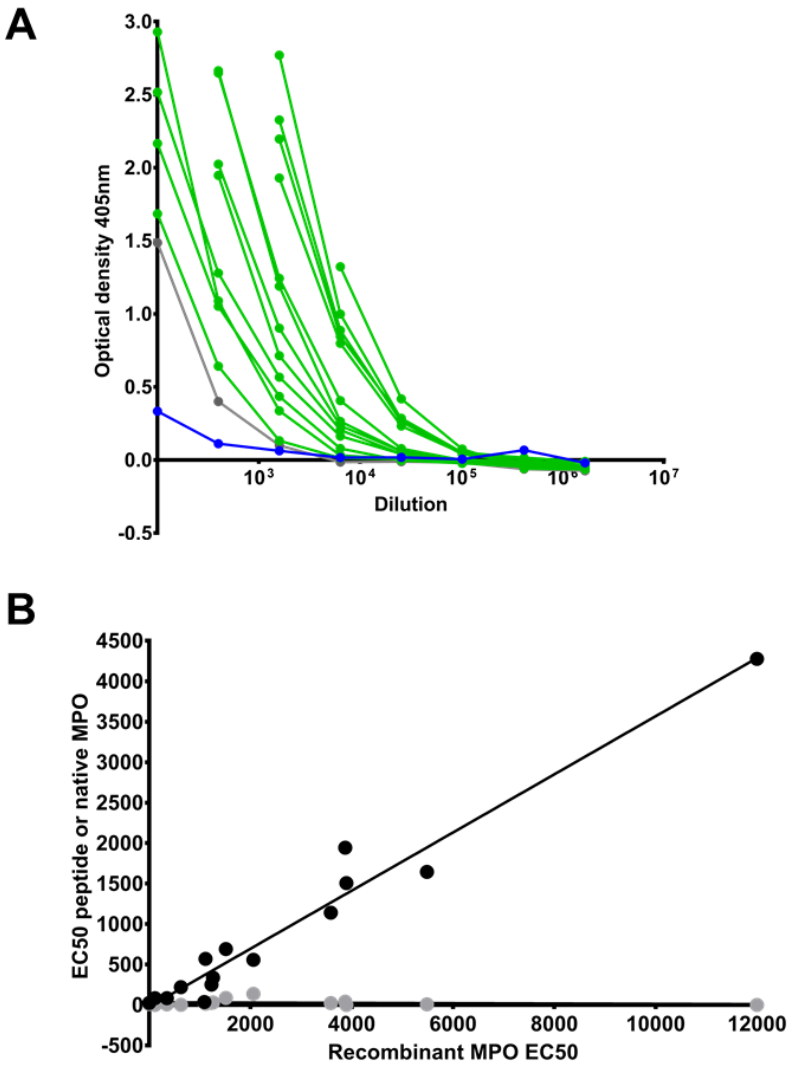

[A] ELISA results with plates coated with native antigen. Sigmodal curves are shown for MPO null immunised mice (green data points), relative to an immunised wild type mouse (blue) and MPO null animal that was not immunised (grey). Optical densities were high, with many data points above the upper limit of detection. [B] ELISA was additionally conducted with plates coated in recombinant murine MPO (RnD Systems) and immunodominant peptide. There was very good concordance with EC50 calculated with recombinant murine MPO and the new batch of native antigen. This shows that the response is specific for MPO.

Xiao *et al* found the highest penetrance of disease in Rag2 mice was with $1x10^8$ splenocytes (Xiao, Heeringa et al. 2002). Even with CD19 pre-enrichment, it is not feasible to obtain enough purified B cells by flow cytometric sort to transfer these alone. It is also difficult to modulate the balance of B cell subsets when adding a relatively small proportion of highly purified B cells to a mixed, parental cell population.

The CD1d fraction could be depleted from total splenocytes by cell sorting however, at the event rate of 10,000 cells per second (recommended by BD Biosciences), this sort would take a prohibitively long time (25 hours, based on an estimated yield of $9x10^9$ splenocytes, from 15 mouse spleens). I assessed whether CD1d-PE microbeads might be used instead of flow cytometry sorting, but this strategy was not successful (see Figure 7.8).

Another strategy might be use of conditional knock-out mice, with B cells lacking IL-10 competency or CD1d expression. Alternatively, *in vitro* expansion of Breg (Yoshizaki, Miyagaki et al. 2012) or short activation of B cells with anti-CD40 or LPS, to promote regulatory function prior to transfer (Tian, Zekzer et al. 2001, Mauri, Gray et al. 2003).

7.4.3 Investigation of the role of B cells in the MPO cell transfer model

7.4.3.1 Cell transfer

This was a small pilot study, with splenocytes pooled from MPO null, immunised animals transferred into 14 Rag2 mice. On day 1 splenocytes were injected into the tail vein and mice injected intraperitoneally with 0.018µg LPS (R515 serotype, Enzo). An antigen boost was delivered on day 6 (10µg of native MPO in an emulsion with

CFA), injected subcutaneously. One control Rag2 mouse received LPS and antigen boost but no splenocytes. Animals were transferred to metabolic cages on day 14 to collect urine and culled on day 15. 3 mice received 30 $x10^6$ whole splenocytes and 2 received 25 $x10^6$ CD19-enriched splenocytes. CD19 null cells were infused alone (30 $x10^6$ into 2 mice) or with highly purified CD1d+ (Breg) or CD1d- B cells (Beff) (29 $x10^6$ T cells and 1 $x10^6$ regulatory or effector B cells, 3 mice for each condition). Purity was assessed by flow cytometry (Figure 7.9), this permitted robust calculation of the final number of each cell type transferred (Figure 7.15). Because starting purity of CD19 positive and negative fractions was very good, the proportion of Breg could be manipulated as desired. CD1d+ B cells were 10-fold higher in CD19 depleted cells with Breg added (850,621), compared to CD19 null cells (73,762) or CD19 depleted cells with B effector cells added (75,304).

7.4.3.2 Verification of successful cell transferral

Flow cytometry was conducted on blood and spleen at the end of the experiment, to verify that the cells were successfully transferred and had survived *in vivo.*

For staining of whole blood leukocytes, red blood cell lysis was conducted. There remained a lot of debris, which was excluded from analysis on FSC and SSC biaxial plot. CD45 stain then used to gate small leukocytes, with further rounds of debris and duplet exclusion (FSC and SSC, height and area parameters). Despite this rigorous gating strategy, there was still a large population of CD3- CD19- small leukocytes in peripheral blood (Figure 7.16, Panel A). The frequency of B and T cells as percentage of lymphocytes, was therefore calculated from relative to the sum of these 2

Figure 7.15 Transfer of splenocytes into Rag2 mice

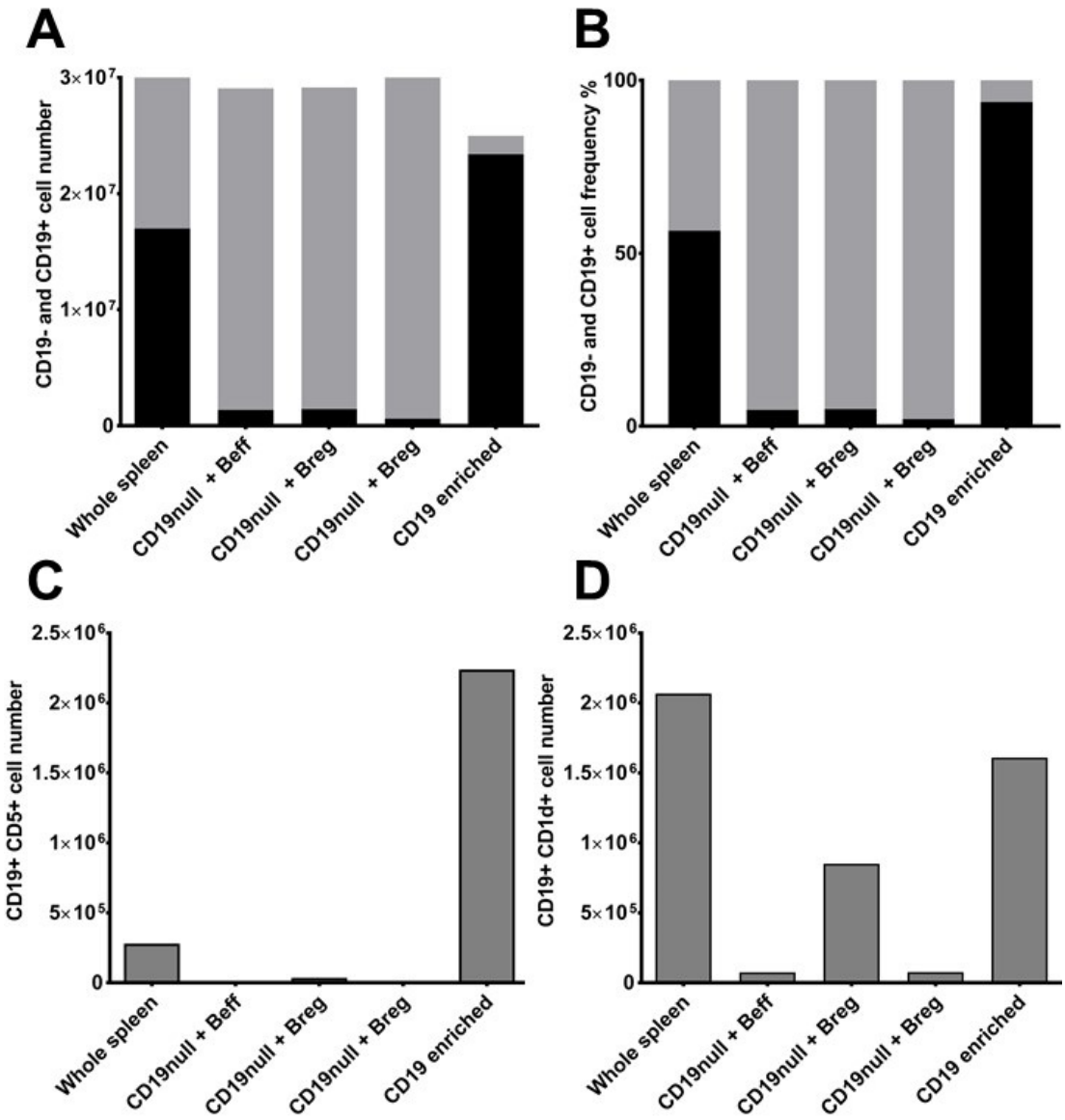

The cell numbers transferred into the Rag2 mice were calculated from purities, determined by flow cytometry. [A] Actual B cell numbers (black) and T cell numbers (grey) injected into Rag2 mice. [B] Relative proportions of B (black) and T cells (grey), injected into Rag2 mice. [C] CD5 B cell number injected into each group. [D] CD1d B cell number injected into each group. More than 10-fold higher in CD19null + Breg, compared to CD19 null cells alone or with B effector cells added (defined as CD1d-).

Figure 7.16 Verification of cell transfer in Rag2 mouse blood

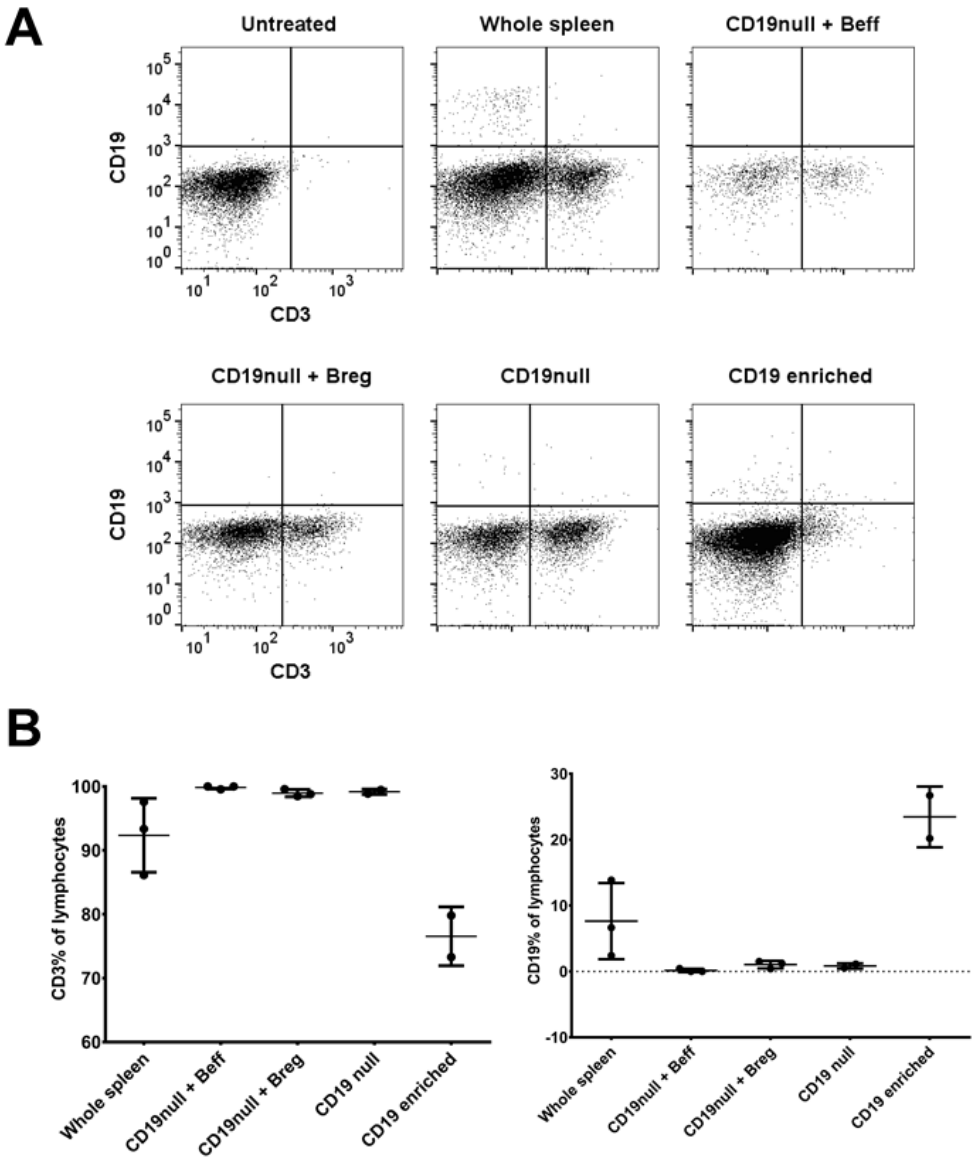

Red cell lysis was conducted for whole blood flow cytometry. [A] Biaxial plots show CD19 and CD3 expression in small, CD45+ cells (these are overlaid, data for the mice in each group, combined into a single dot plot). Despite stringent debris and duplet exclusion criteria, most small leukocytes were double negative for CD19 and CD3. No B or T cells were detected in the untreated Rag2 mouse. [B] CD19 and CD3 frequency was corrected, so the sum of these 2 populations was equal to 100%. T cell frequency remained high in all groups. The highest proportion of B cells was observed in mice receiving CD19 enriched splenocytes.

populations (Figure 7.16, Panel B). There were relatively few lymphocytes in mice that received CD19 enriched splenocytes; most B cells are not found in circulation and reside within secondary lymphoid tissues, so analysis was also conducted on spleen.

On flow cytometric analysis of spleen, T cells were more numerable than expected in mice receiving CD19 enriched splenocytes. A CD3 CD19 double positive population was also visible. This population was not present in untreated mice and instead appears to be an artefact of the cell processing or staining protocol (Figure 7.18). Dissociation of leukocytes from tissue, can result in higher rate of duplets and cell death; multiple antibodies can bind non-specifically and result in diagonal pattern observed in these 2 discrete lineage markers.

To verify correct classification of B cells, expression of B220 was assessed. The CD19+ CD3- population expressed high levels of this additional B cell marker, with low levels in other small, CD45+ leukocytes. B cells were enumerated based on expression of CD19 alone or CD19 and B220 double positivity (Figure 7.18, Panel B). There were more CD19 single positive cells than CD19, B220 double positive.

In another tube CD19, B220, CD43 and IgD were stained in combination. Biaxial plots verified the existence of a CD19+ $B220^{low}$ $CD43^{high}$ population in Rag2 mice. CD19+ $B220^{high}$ $CD43^{int}$ B cells were only detected after splenocyte transferral. The intrinsic population in Rag2 mice had low expression of IgD, like the phenotype observed in bone marrow B cells (Figure 7.4). IgD is a marker of mature B cells in the periphery. Low expression of IgD and high CD43 (Figure 7.19), suggest that these cells in the Rag2 mice are B cell precursors and not associated with a “leaky” Rag phenotype (mature B cells, previously reported in the periphery of aged Rag2 mice).

Figure 7.17 Verification of cell transfer in Rag2 mouse spleen

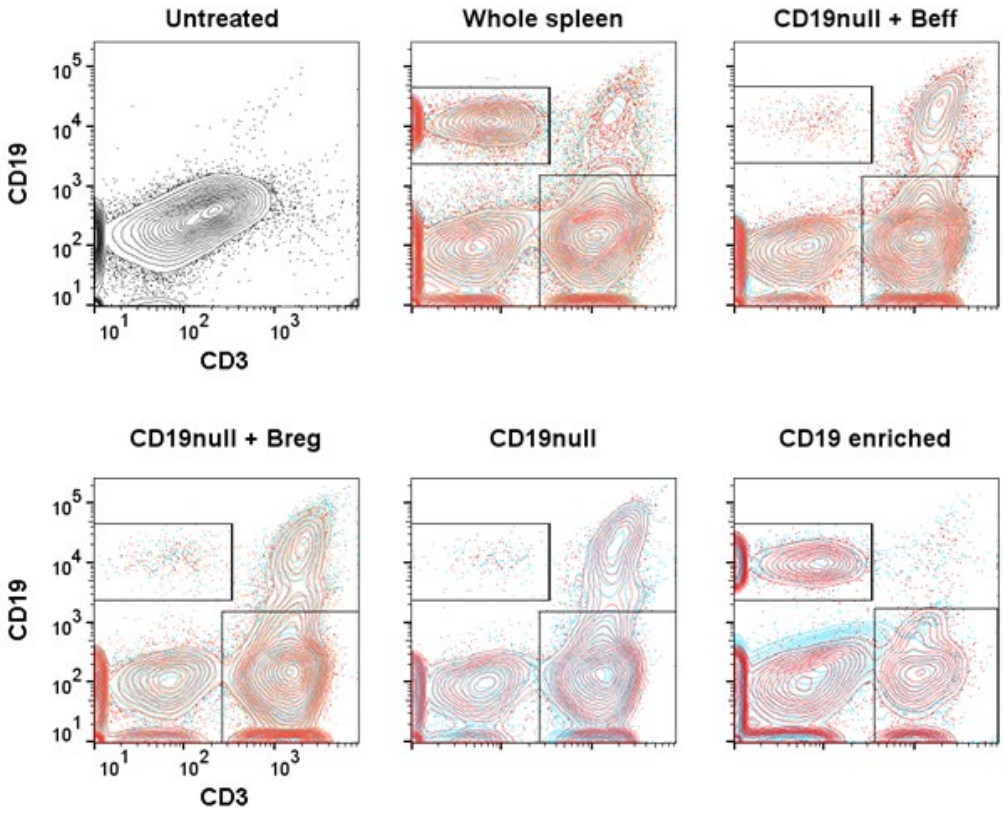

Splenocytes were dissociated, passed through a cell strainer and red cell lysis conducted prior to flow cytometry. Biaxial plots show CD19 and CD3 expression in small, CD45+ cells. Overlaid contour plots show data for all the mice in the named group, individual mice are depicted in separate colours. There were no B or T cells in the untreated Rag2 mouse. In addition to the CD19 and CD3 double negative population of small leukocytes observed in blood, there was also a double positive population in spleen.

Figure 7.18 Different frequency of CD19+ and B220+ B cells in spleen

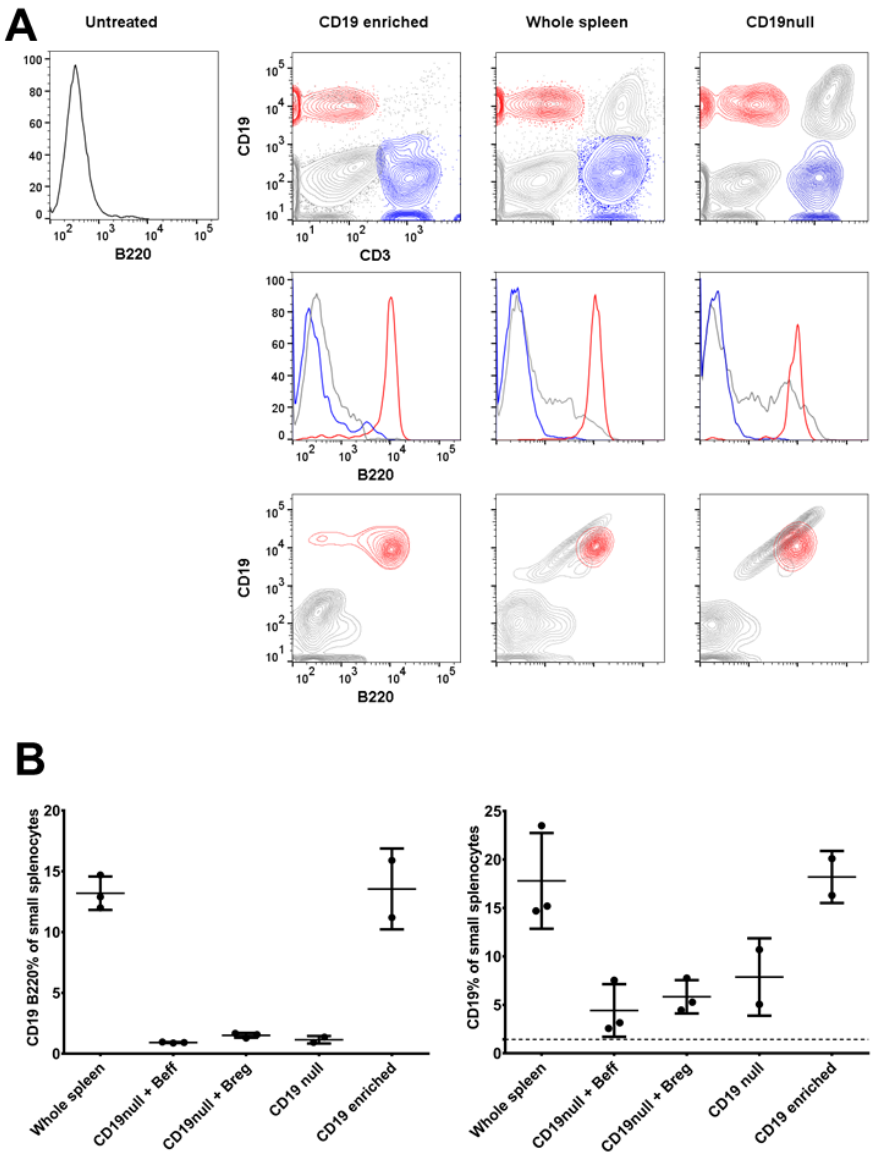

[A] CD19 and CD3 double positive cells, were combined in a single gate with double negative cells (grey). CD19+ CD3- cells (red) also had high expression of B220, absent from CD19- CD3+ cells (blue). Some of the double staining may be due to inclusion of dead T cells in this gate, as it was not observed with highly enriched CD19+ cells. Compensation was adequate in this cell population and biaxial plots, revealed variable expression of B220. [B] Across of the animal groups, CD19+ B cells represent a higher proportion of small leukocytes, than B220 high CD19+ B cells. CD19+ cells are even detected in untreated Rag2 mice at low frequency (dashed line)

Figure 7.19 Phenotype of the B220^{low} CD19^{high} splencoytes

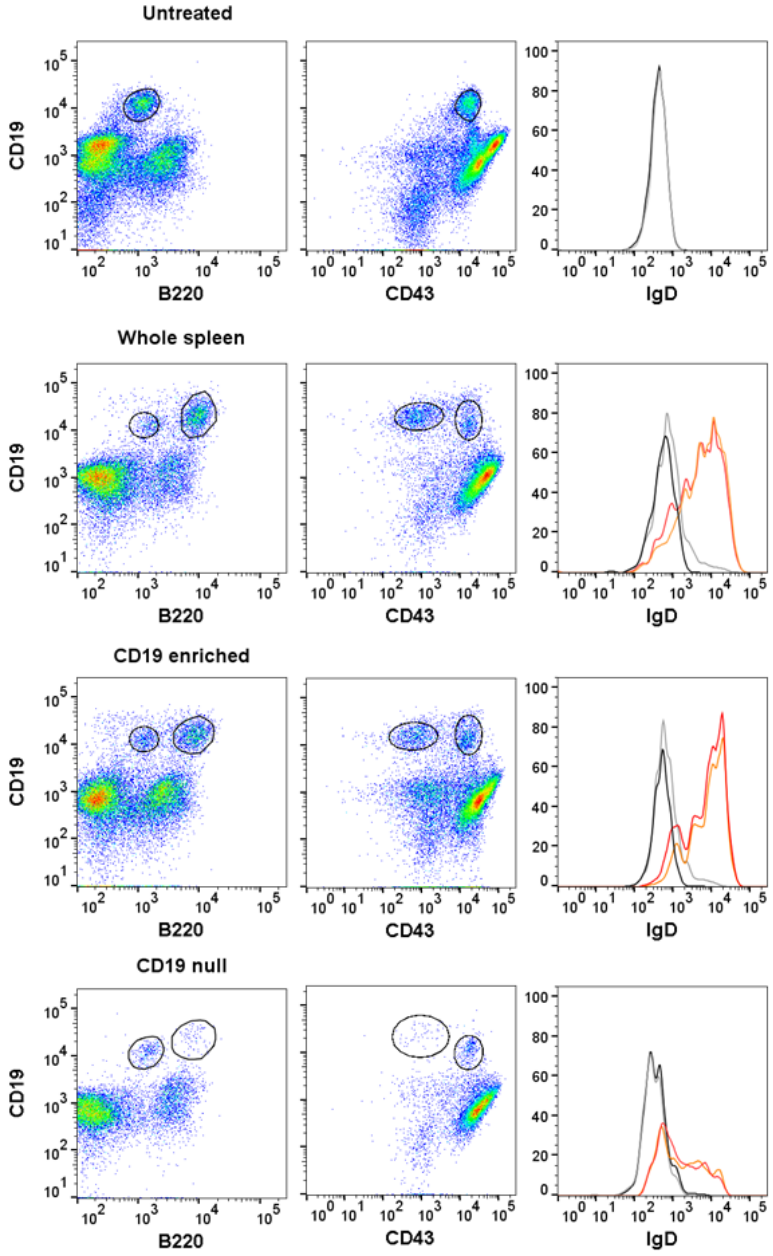

CD19^{high}B220^{low} cells were detected in the untreated Rag2 mouse. CD19^{high}B220^{high} cells were only detected after splenocyte transferral. The CD19^{high} population also expresses higher levels of CD43, a marker of immature B cells. B220^{low}and CD43^{high} B cells (grey and black) were overlaid with B220^{high}and CD43^{int} cells (orange and red histograms). B220^{low}and CD43^{high} cells express low levels of the B cell maturation marker IgD, which is in keeping with a pre-B cell phenotype.

7.4.3.3 MPO antibody titres in Rag2 mice

The response in $MPO^{-/-}$ immunised and Rag2 immunised mice was variable (Figure 7.20). When Rag2 mice were separated according to experimental conditions, the response in Rag2 mice receiving whole splenocytes, was greater than the mean for $MPO^{-/-}$ mice (Figure 7.21, Panel A). The sigmoidal curve of the transformed data was steeper and the lowest dilution factors, exceeded the assay upper limit of detection. The response for Rag2 mice receiving CD19 depleted cells and Beff, was not profoundly diminished despite transfer of very few B cells. There appeared to very little antibody response in mice receiving CD19 enriched cells alone, CD19 depleted cells alone or CD19 depleted cells combined with Breg. This suggests B cells alone, cannot sustain an antibody response, even although many were likely antigen specific memory cells, with a lower threshold of activation.

Statistical analysis was performed on EC50 values, relative to MPO-/- immunised mice (Figure 7.21, Panel B). Mice receiving CD19 depleted or CD19 enriched splenocytes, had significantly lower EC50. Mice receiving whole splenocyte, CD19 depleted cells with Beff or Breg, did not differ from MPO immunised mice (Kruskal Wallis and Dunn's multiple comparison conducted).

7.4.3.4 Biochemistry

Animals were placed in metabolic cages overnight for collection of urine, samples were collected for 13 out of 14 mice, with none for 1 mouse receiving B cells alone. Blood was collected into 0.8% sodium citrate and plasma separated by centrifugation.

Overall biochemistry was unremarkable. Urinary dipstick was conducted (Siemens Multistix 8 SG reagent strips). Traces of leukocytes were detected in 7 urines, with

Figure 7.20 Variable MPO response in MPO-/- immunised and Rag2 mice

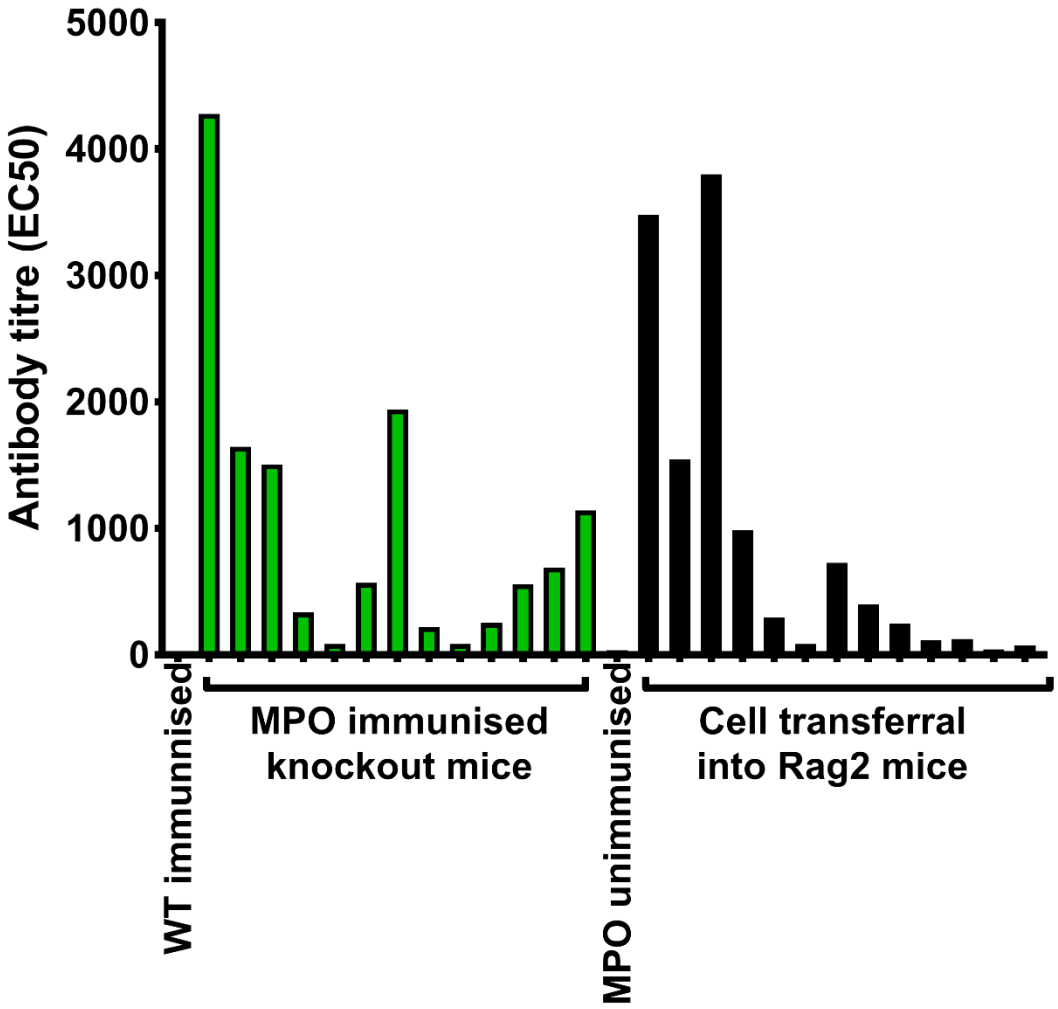

ELISA was conducted on serially diluted plasma ($1x10^3$ - $1.64x10^6$). The data was transformed, creating a sigmoidal curve from which EC50 was calculated in Prism GraphPad. EC50 is the dilution factor, which results in half the maximum optical density. EC50 were variable in MPO null immunised mice and controls. No response was observed in wildtype mice, receiving MPO immunisation not in MPO null mice that were unimmunised.

Figure 7.21 MPO antibody levels in Rag2 mice and MPO$^{-/-}$ immunised

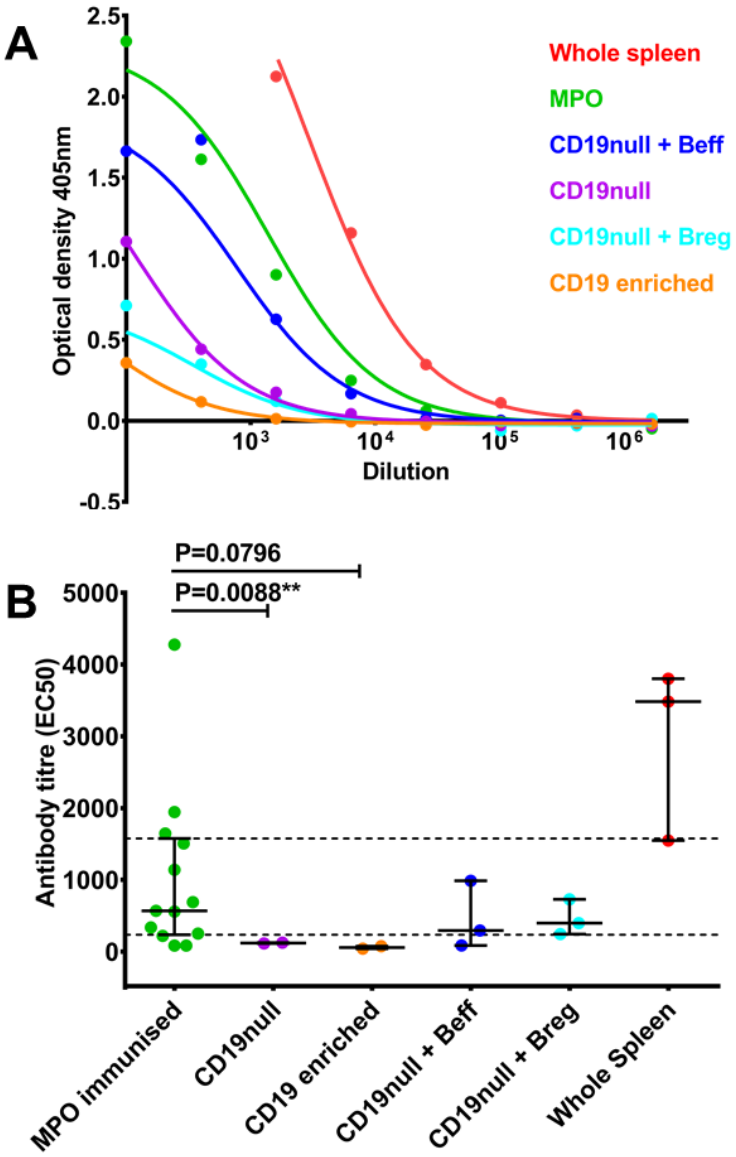

*[A] Sigmoidal curves are shown for MPO null immunised mice and the Rag2 treatment groups. A robust MPO response was observed with whole splenocytes. [B] The EC50 values were compared by Kruskal Wallis and Dunn's multiple comparison, relative to MPO null immunised mice (25th and 75th percentile shown). The only group with significantly different EC50, was the Rag2 group receiving CD19null splenocytes (P=0.0088**). The only mice with EC50 $\geq$ the 75th percentile of the null immunised mice, were in the whole spleen cohort.*

blood in 4 (Figure 7.24, Panel A). Samples were sent to MRC Harwell for additional testing. There was no difference in urinary creatinine between the groups Kruskal Wallis (P=0.1019). Proteinuria differed significantly between the groups, however all values in the test groups were lower than the untreated Rag2 mouse. When the results were expressed as protein to creatinine ratio, no difference was found. Creatinine, urea and albumin were measured in plasma, with no difference in the test groups (Kruskal Wallis P=0.3884, P=0.1177 and P=0.7791).

7.4.3.5 Histological findings in kidney and lung

Pattern of organ involvement was as previously described, with lung and kidney pathological findings (Xiao, Heeringa et al. 2002). In the lungs, cellular infiltrate was observed in most animals receiving splenocytes (Figure 7.22, shows densely packed leukocytes in 11/13 mice). The cellular infiltrate was most severe in Rag2 receiving whole splenocytes. Overt pulmonary haemorrhage was observed in 2 animals from this group (lungs were deep red in colour, opposed to pale pink on organ retrieval), and red cells are also visible microscopically. Higher resolutions images were captured on PAS stained sections, these showed that the immune infiltrate was primarily innate, with neutrophils, exudate and goblet cell hyperplasia (Figure 7.23).

The severity of renal disease was lower than previously reported, despite extensive optimisation of the MPO immunisation. There was a very low frequency of crescentic glomeruli, defined as two or more layers of cells within bowman's space. Scoring was conducted by 3 clinicians, blinded to experimental conditions (50 glomeruli for each mouse). There was good concordance in results, with highest incidence of crescents in Rag2 mice receiving whole splenocytes and CD19 depleted cells +Beff.

Figure 7.22 Overview of pulmonary pathology observed in Rag2 mice

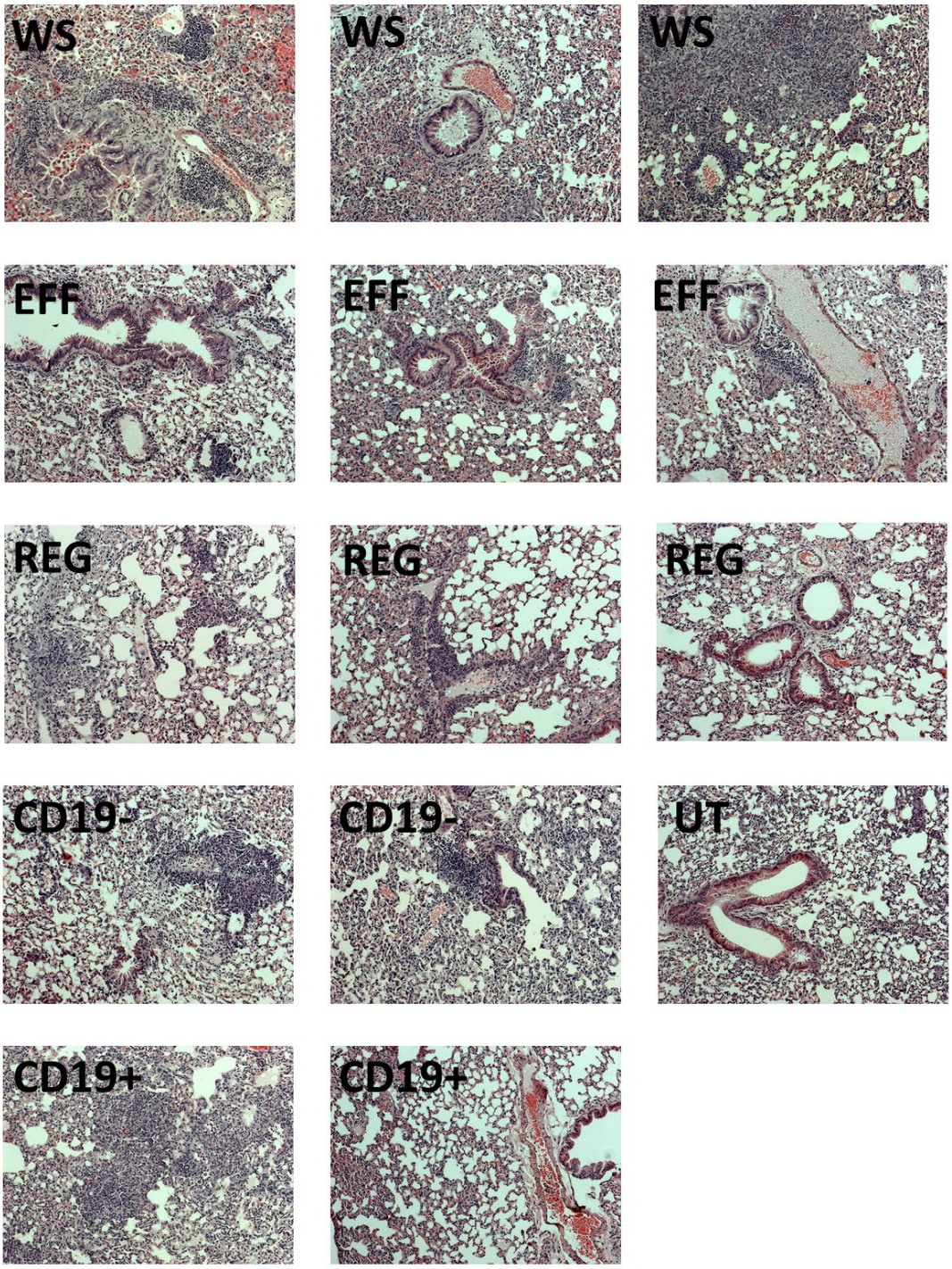

H&E stained lung images captured with a 10x objective. Patent alveoli visible in all images apart from the top left, which has the most infiltrating leukocytes and pulmonary haemorrhage. Leukocyte infiltrate was variable, in terms of area occupied and density.

Figure 7.23 Further characterisation of lung pathology

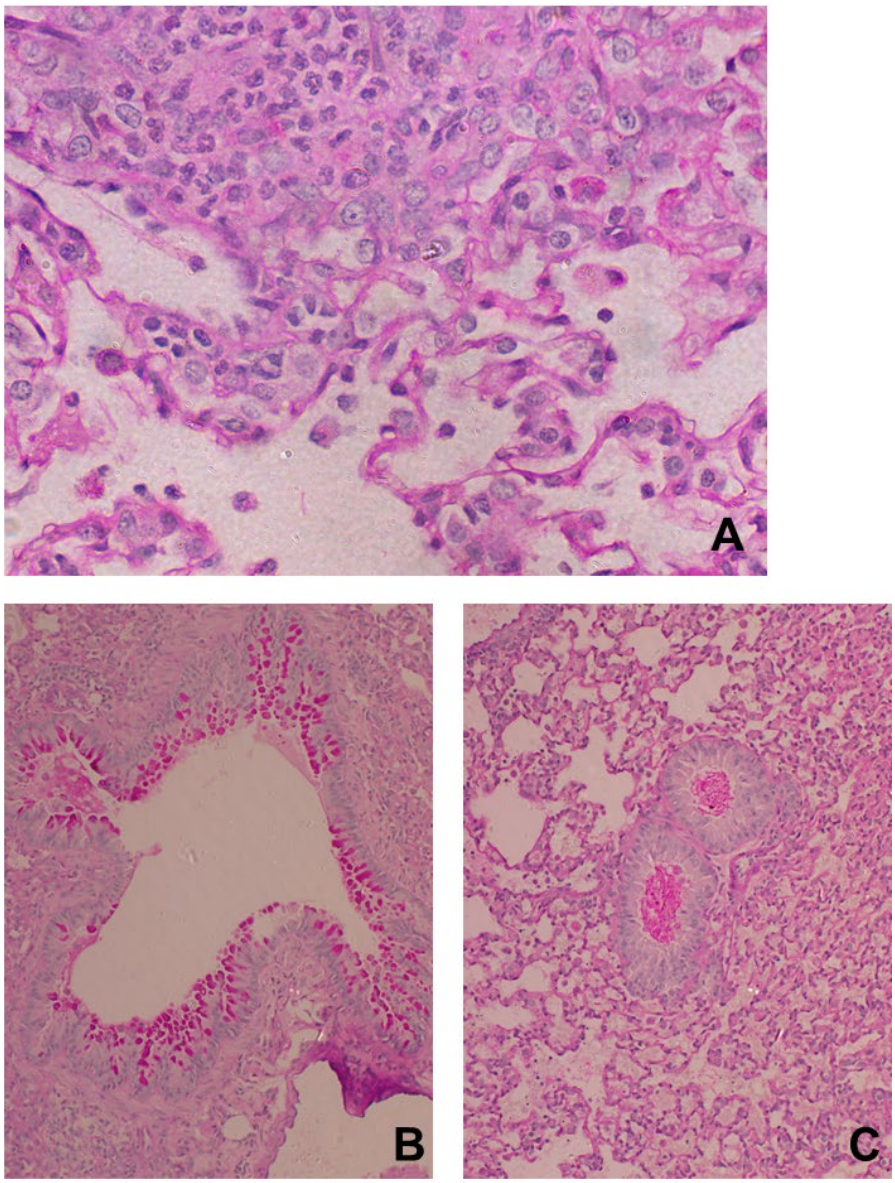

PAS stained lung sections of Rag2 mice receiving whole splenocytes. [A] Imaging at 63x magnification, shows a dense area of neutrophils in the top left corner, identifiable by their lobed nuclei. This was accompanied by [B] goblet cell hyperplasia (cells in the bronchiole lining staining deep pink) and [C] accumulation of pulmonary exudate (bottom 2 images captured with a 20x objective).

Figure 7.24 Summary of renal pathology in rag2 mice

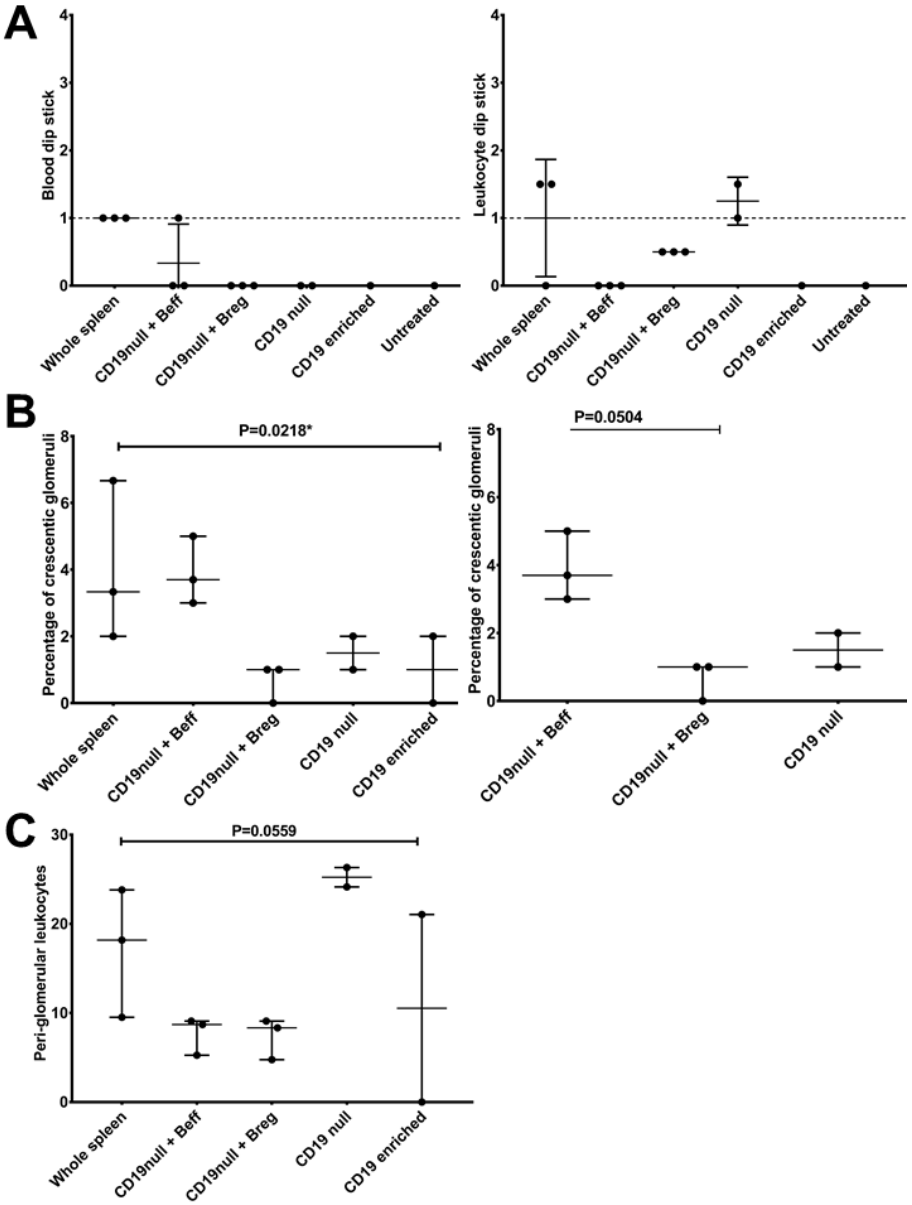

[A] Traces of leukocytes and blood were detected on urinary dipstick. [B] Frequency of crescents, expressed as percentage of total glomeruli scored was low. Kruskal Wallis test was significant, but Dunn's multiple comparison was not. Further analysis was conducted for animals receiving CD19null cells alone and in combination with Beff or Breg. Mice receiving Breg, tended to have fewer crescents than those receiving Beff (Dunn's multiple comparison P=0.0504). [C] The percentage of glomeruli with leukocytes surrounding them ranged from 0-26% but did not differ across the groups.

Figure 7.25 Representative images of pathological renal findings in Rag2 mice

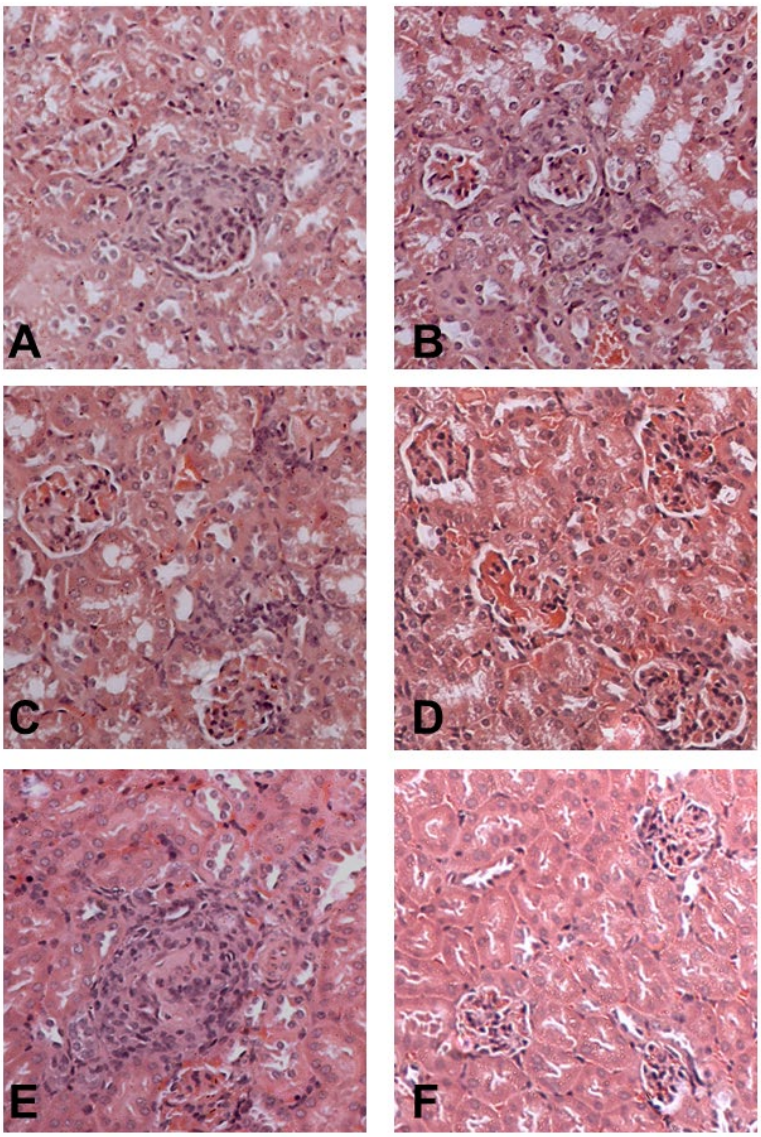

H&E stained slides, images captured with a 20x objective on a light microscope. The pathological findings included: [A] crescentic glomeruli, [B] peri-glomerular, leukocytes and tubular vacuolation, [C] interstitial leukocytes, [D] glomerular thrombosis and a granulomatous lesion [E]. Normal histology is depicted in panel [F].

When Kruskal Wallis test was conducted, a difference was observed across the experimental conditions (Figure 7.24, Panel B P=0.0218*), but no further differences were resolved when Dunn's multiple comparison was performed. When analysis was limited to CD19 depleted cells alone or in combination with B regulatory or B effector cells, the latter 2 groups tended to differ (Figure 7.24, Panel B P=0.0504).

Many more glomeruli were encircled by lymphocytes than crescentic (Figure 7.24, Panel C), and interstitial leukocytes were visible in all mice receiving splenocytes. To further assess the extra-glomerular infiltrate confocal microscopy was performed for CD3(data follows in the next section), this was important in establishing the involvement of the adaptive immune system.

There was no difference in glomerular thrombosis between the treatment groups. Thrombosis was rarely observed, with similar incidence in the untreated mouse. Where seen, the thrombi typically occupied less than 10% of the total glomerular area and never more than 25%. Tubular dilation was observed in 2/3 mice receiving whole splenocyte and 1/2 receiving CD19 depleted splenocytes. Tubular vacuolation was observed in 13/14 mice that received splenocytes, not in the untreated Rag2 mouse or 1 receiving CD19 depleted + Beff. This was assessed across an average of 4 microscope fields, captured with a 10x objective (Figure 7.25).

7.4.3.6 Immunofluorescent detection of T cells in kidney

To verify that the adaptive immune response was contributing to the renal pathology, FFPE kidney sections were stained with CD3 and DAPI. Large, stitched fluorescent images were captured for enumeration of infiltrating T cells. A grid was applied in ImageJ and T cells counted with the multipoint tool. Cells were defined by bright

Figure 7.26 Enumeration of infiltrating T cells in Rag2 kidney

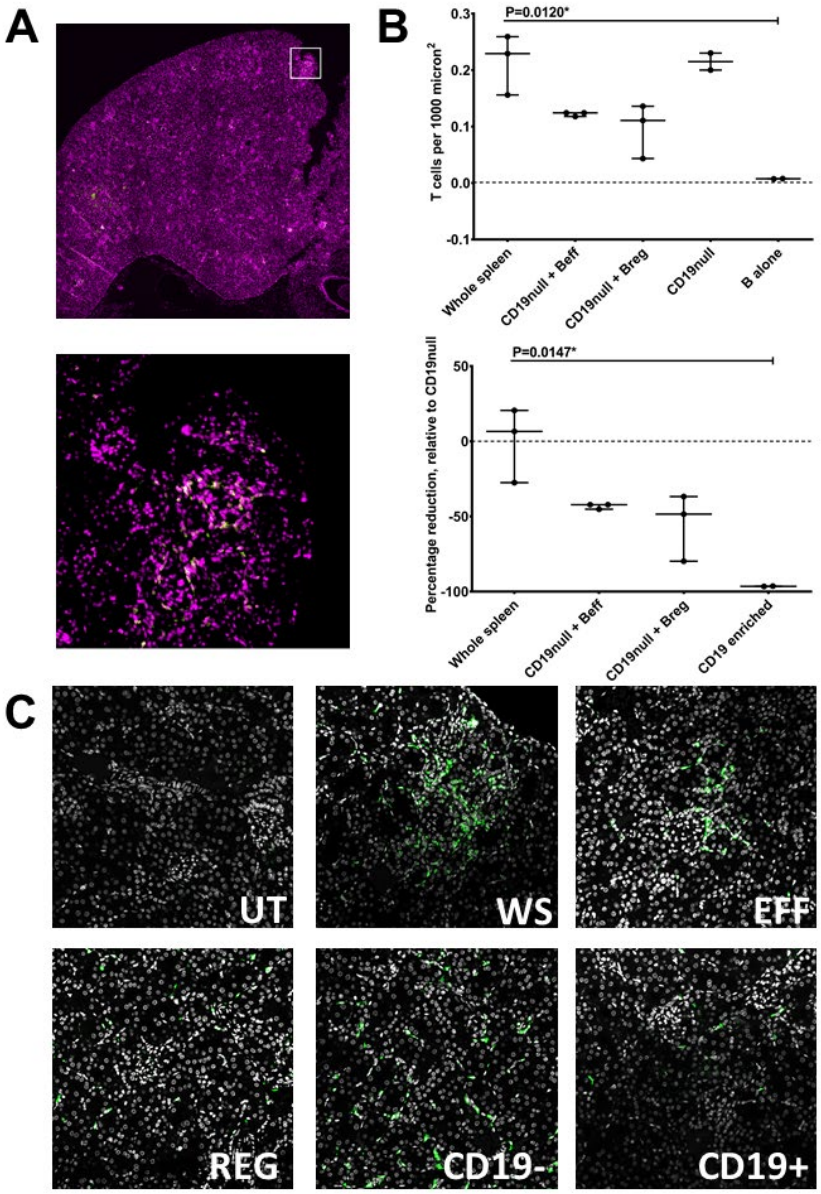

Panel A shows a large fluorescent stitched image, 16 x10 objective fields captured on the Nikon Ti microscope. Analysis of images was conducted in ImageJ, with individual CD3+ cell bodies counted (green) and correction for total area applied (area defined by DAPI nuclear stain, shown in purple). [B] T cells counted per 1000µm^2, with percentage change relative to CD19null cells alone. There were significantly fewer in Rag2 mice receiving CD19 enriched cells, compared to whole splenocytes. [C] Representative 20x confocal images (CD3 in grey and DAPI in grey).

discrete expression of CD3, around a nuclei. The median number of T cells counted per a mouse was 224 (IQR 122-313) and median area scored was 1.86x10^6µm2 (IQR 1.66-5.20x10^6µm^2). The data was presented as T cells per a 1000µm^2 and percentage change relative to Rag2 mice receiving CD19 depleted splenocytes alone (Figure 7.26, Panel B). Mice receiving CD19 enriched splenocytes had significantly fewer T cell infiltrating the kidney than observed in mice, receiving whole splenocytes. The density of T cells also appeared to differ, representative 20x confocal images are shown in Figure 7.26, Panel C.

7.4.3.7 Assessment of spleens

Spleens were dissected, all fat and connective tissue removed prior to photographing and weighing. Spleens were macroscopically different in size (Figure 7.27, Panel B). Weight was increased in 11/13 Rag2 mice receiving splenocytes, compared to the untreated mouse. If this was normal variance, it would not be expected to be unidirectional. When the treatment groups were compared by Kruskal Wallis test and Dunn's multiple comparison, mice receiving CD19 depleted cells had significantly lower splenic weight, compared to those receiving whole splenocytes (Figure 7.27, Panel A, P=0.0301*). Spleen architecture was abnormal in untreated Rag2 mice, but histology was normal after cell transfer, with germinal centres surrounded by red pulp (Figure 7.27, Panel D).

Spleens were stained with B220 and CD3 antibodies, fluorescent secondaries and DAPI nuclear counterstain. Large, stitched fluorescent images were captured to measure B and T cells areas (Figure 7.28, Panel D). B220 areas were measured in ImageJ; areas composed of cells (defined by their discrete membranous stain) were

Figure 7.27 Increase in splenic mass and restoration of normal architecture

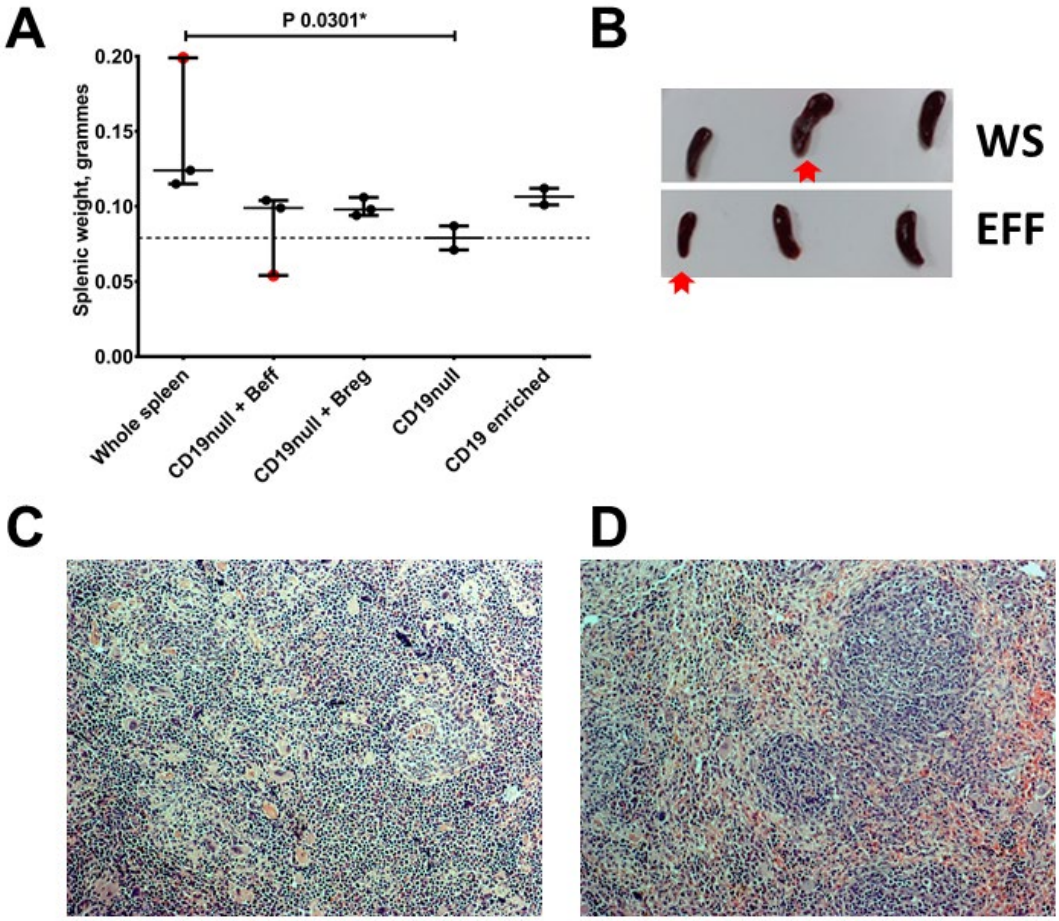

[A] Rag2 mice receiving whole splenocytes, had significantly heavier spleens than those receiving CD19 depleted cells. The dotted line shows the splenic weight of the untreated Rag2 mouse. [B] The spleens with greatest and smallest mass are shown, they were visibly different in size (the red arrows correspond with the red data points in panel A). [C] Rag2 mice have abnormal splenic histology, untreated mouse shown. [D] In mice receiving splenocytes, normal architecture is recapitulated, with organised germinal centres surrounded by red cell pulp (H&E sections, with images captured at 10x magnification on a light microscope).

measured, excluding any diffusely stained regions. 25th and 75th percentiles were calculated for all the B cell areas measured and data plotted relative to this (Figure 7.28, Panel A). B cell follicle size was significantly larger in Rag2 mice that received whole splenocytes, relative to CD19 depleted + Beff or CD19 enriched splenocytes. The total spleen area occupied by T and B cells remained low (Figure 7.28, Panels B and C). The tendency was for more area to be occupied by lymphocytes in the Rag2 mice, that received whole splenocytes. This was a small data set, on statistical analysis, mice receiving whole splenocytes only had a significantly greater area of T cells compared to the CD19 depleted cohort (P=0.0392*, Kruskal Wallis and Dunn's multiple comparison).

Representative 20x confocal images are additionally shown (Figure 7.28, Panels D). The B cell follicles are looser or less well defined in mice receiving non-replete splenocytes. A rare B220+ population was visible in the untreated mouse on confocal; in keeping with the characterisation of a low abundance CD19^{high}, B220^{int}, CD43^{high}, IgD- pre-B cell population on flow cytometric analysis of mouse spleen (Figure 7.19).

7.4.3.8 Subtyping of the MPO antibody response

Total IgG was quantified in the MPO null and Rag2 mice by ELISA. The median IgG was 0.1833mg/ml in MPO null immunised mice (IQR 0.161-0.2166). Levels in Rag2 mice receiving whole splenocytes, were very similar with a median value of 0.2005mg/ml. IgG levels were significantly higher in MPO null immunised mice than Rag2 mice receiving CD19 depleted + Breg (P=0.0424*) or Beff (Figure 7.29, Panel A, P=0.0184*). The other Rag2 groups receiving splenocytes, did not significantly differ significantly from MPO null immunised mice (Dunn's multiple comparison).

Figure 7.28 Analysis of B and T cell splenic composition in Rag2 mice

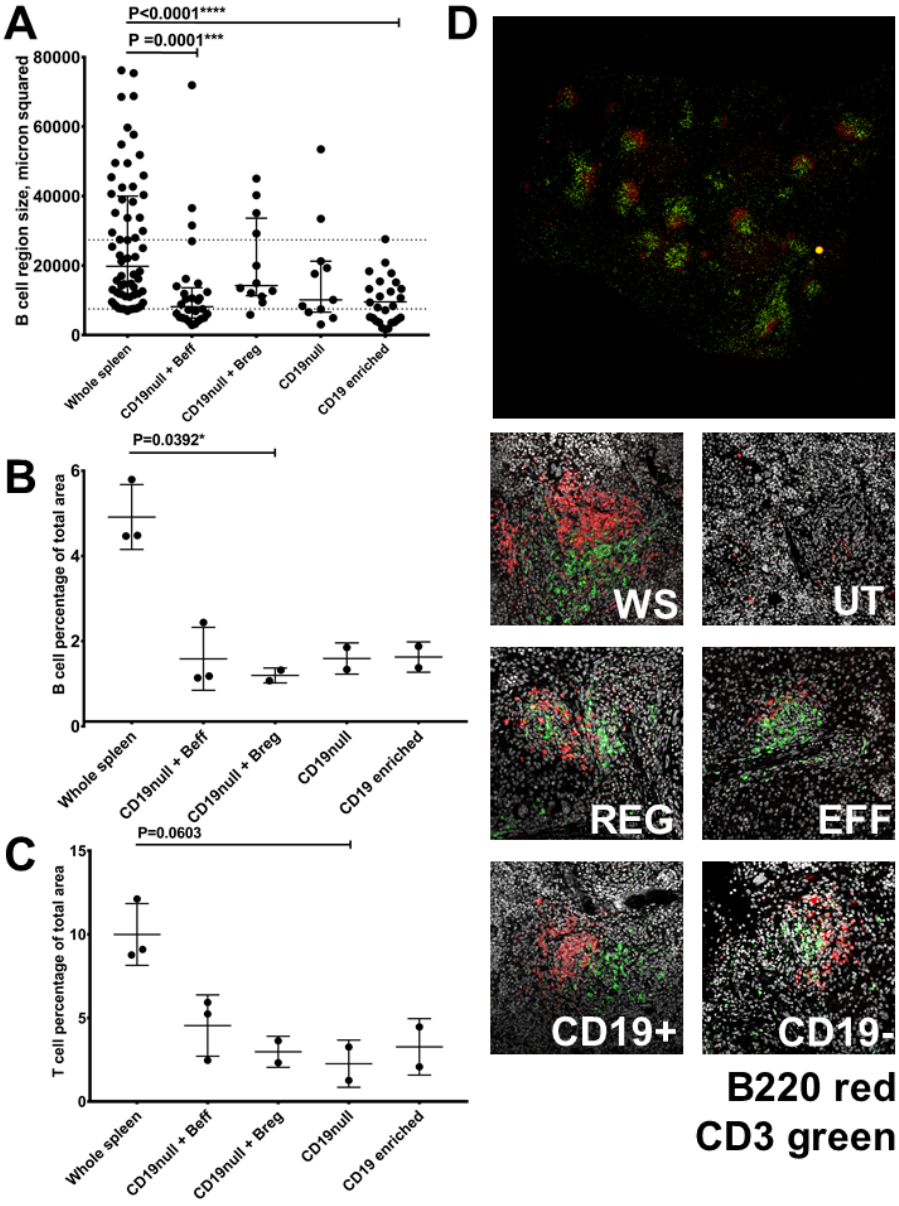

*[A] B cell areas in the spleen were measured, IQR is shown for the entire data set (dashed lines). B cell follicle size was significantly larger in mice receiving whole splenocytes, compared to CD19null + Beff (P<0.0001****) or CD19 enriched splenocytes (P=0.0001***). Panels B and C show the total splenic area occupied by lymphocytes, which tended to be higher in mice receiving whole splenocytes. [D]The top image shows a large stitched fluorescent image of spleen. Representative B cell staining pattern is shown in the lower 6 images, 20x magnification on confocal.*

Figure 7.29 Total IgG levels and Ig subtyping in Rag2 mice

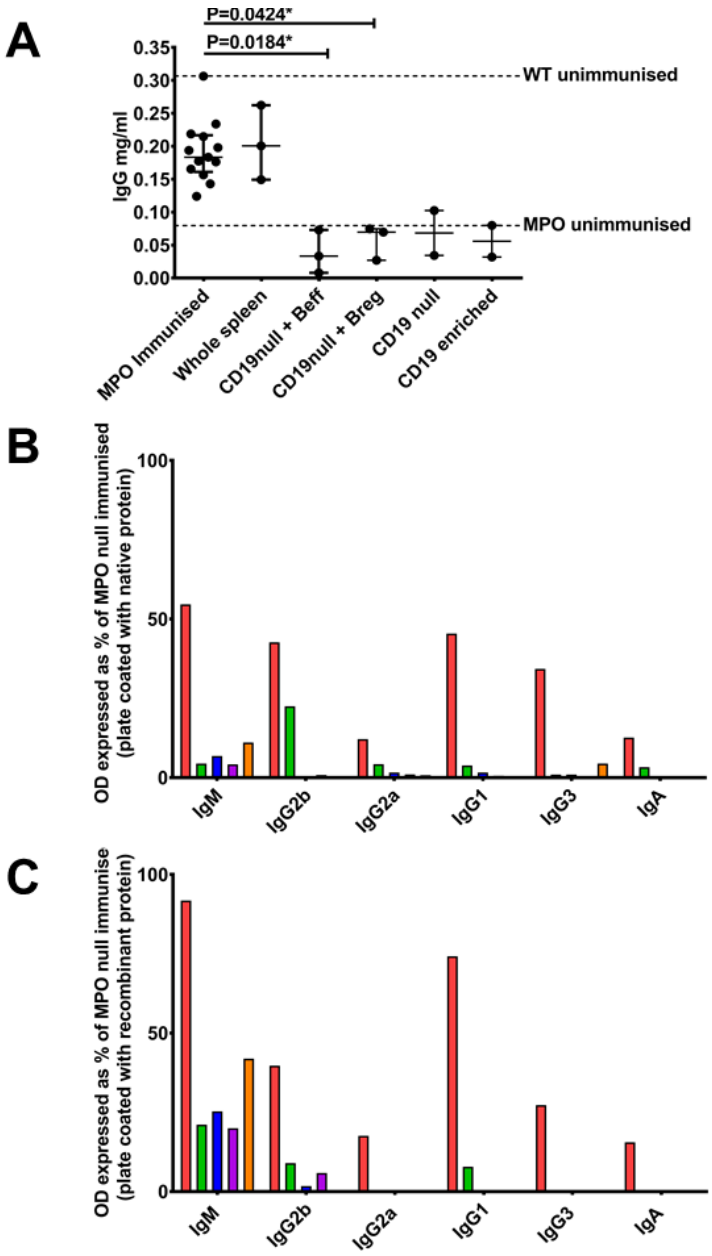

[A] Total IgG was quantified in the MPO null and Rag2, median and IQR shown. Rag2 mice receiving CD19null + Breg or Beff had significantly lower IgG levels than MPO null immunised mice (Dunn's multiple comparison, P=0.0424 and 0.0184*). Panels B and C show, the percentage difference in mean optical densities for Rag2 mice, relative to MPO null immunised mice. Bars denote Rag2 mice receiving: whole splenocytes, CD19null + Beff, CD19null + Breg, CD19null and CD19 enriched splenocytes. ELISAs were conducted with native MPO [A] and recombinant [B].*

MPO specific Ig subtyping was conducted (Figure 7.29, Panel B and C). The kit was not directly quantitative, as it was intended for subclass definition of monoclonal antibodies. The median optical densities for MPO null and Rag2 mice receiving whole splenocytes did not differ for any of the analytes tested (IgG1, IgG2a, IgG2b, IgG3, IgA, IgM and kappa light chains). Mean optical densities were calculated and results for Rag2 mice expressed as a percentage of MPO null immunised. A complex immunological response was seen in Rag2 mice receiving whole splenocytes, which can be inferred to be polyclonal. In the other groups an IgM response predominated, with little Ig class switching. The threshold of B cells and supporting splenocytes required to sustain a robust immunological response, was not met in these groups. This was also apparent on immunofluorescent analysis of B cell follicle area and structure (Figure 7.28).

7.5 Key findings

7.5.1 Phenotyping of candidate immunoregulatory B cells

IL-10 production was verified in a subset of B splenocytes. Although a higher percentage of peritoneal B cells produce IL-10, total number of IL-10 competent B cells is highest in spleen.

CD1d+ B cells were only present in the spleen, they expressed high CD21, IgM, CD38 and CD24. TIM-1, CD11b and CD5 expression was highest in peritoneal B cells.

These finding are in keeping with the BM origin of splenic B cells with separate foetal ontogeny of peritoneal B1a cells and, the proposed existence of more than 1 B cell regulatory population.

7.5.2 Precursor B cells are present in Rag2 mouse spleen

Rag2 mice have a pre-B cell population in the spleen ($B220^{low}$, $CD43^{high}$ IgD-), detectable on flow cytometry. Presence of B220+ cells was verified in untreated Rag2 mice by confocal microscopy.

7.5.3 Successful cell transferral into Rag2 mice

Cell transfer into Rag2 was successful, verified by flow cytometry of blood and spleen. Active B cell follicles were observed, with total IgG and MPO titres, equivalent in mice receiving whole splenocytes and MPO null immunised mice.

7.5.4 Disease penetrance and severity less, than previously described.

Despite successful cell transferral, only mild renal disease was induced. T cells had however infiltrated the kidney. Leukocyte infiltrate and haemorrhage was observed in the lung.

7.5.5 B cells alone are unlikely to be pathological

MPO Ig subtyping showed that B cells alone, cannot sustain a complex antibody response. B cell follicles were fewer in number and more diffuse, than in mice receiving replete splenocytes.

7.6 Discussion

In the initial experiments IL-10 competency was verified and immunophenotyping for regulatory B cells conducted. Peritoneal B cells were assessed a potential source of regulatory B cells, these cells have the greatest IL-10 competency (Tedder 2015) and limit inflammation in an *in vivo* model of colitis (Maseda, Candando et al. 2013). CD5 is a putative marker for Breg cells in man and the peritoneum cavity, is a specialised niche for B1a CD5+ cells (Baumgarth 2011).

I verified that peritoneal B cells expressed high levels of CD5, with the majority producing IL-10 *in vitro.* Peritoneal B cells also had higher expression of TIM-1 a putative regulatory marker (Ding, Yeung et al. 2011) and CD11b, a classical myeloid cell marker. In a CD11b B cell conditional knockout mouse, autoimmunity ensues, suggesting that CD11b B cells are critical for establishing immune tolerance (Ding, Ma et al. 2013). CD11b regulatory B cells are also described in man (Griffin and Rothstein 2012). Collectively, the results suggested peritoneal B cell were immunoregulatory. However, total B cell yield from the peritoneal cavity was variable and low, relative to spleen. Numerically more IL-10 competent B cells reside in the spleen than the peritoneal cavity. Peritoneal B cells also lack expression of CD1d, the most widely used marker of regulatory B cells in mice (Evans, Chavez-Rueda et al. 2007, Yanaba, Bouaziz et al. 2008). CD1d can modulate antigen specific autoimmunity (Matsushita, Horikawa et al. 2010), and functional importance of this marker was recently proven, with induction of tolerogenic iNKT *in vivo* (Oleinika, Rosser et al. 2018). Detailed immunophenotyping of CD1d+ B splenocytes, showed they shared high expression of IgM, CD24 and CD38 with human Breg.

With a candidate B regulatory subset identified, an isolation strategy was defined. Combination of CD19 magnetic enrichment of B cells and 2-way CD1d flow cytometric sorting, yielded highly purified B regulatory (CD19+ CD1d+) and effector cells (CD19+ CD1d-).

Modulating effector and regulatory B cell subsets in the cell transfer model of AAV with these cells, was an attractive prospect. Human disease is relatively uncommon and patient cohorts heterogenous. Studies in mice remove many confounding variables, there are no comorbidities, variation in genetics, age, sex or environment. Access to tissues is improved (secondary lymph, lungs and kidney), disease follows a defined course (initial insult, duration and disease severity) and any interventions are controlled. The differing contribution of antibody and B cells to pathogenesis can be explored. There is the potential to labels B cells, re-infuse and track them *in vivo.* Therapeutic potential can be assessed in a safe manner, with *in vitro* expansion previously described (Yoshizaki, Miyagaki et al. 2012).

Severe glomerulonephritis was previously shown in the cell transfer model. This was dose-dependent with no crescents in mice receiving 1 $x10^7$ splenocytes and incidence ranging from 35-99% in mice receiving 5 or 10 $x10^7$ splenocytes (Xiao, Heeringa et al. 2002). I transferred 3 $x10^7$ splenocytes, which may not have been adequate. However, anti-MPO antibody titres were comparable in Rag2 mice receiving replete splenocytes and the MPO null, immunised mice.

Native MPO is a xeno-antigen in knock out mice and would be expected to induce a very robust, high affinity, polyclonal B response. The humoral response was equivalent to the known positive control (pooled serum gifted by Professor Heeringa)

and specificity, was verified by conducting ELISA with recombinant, biologically active protein (RnD Systems). Ig subtyping showed the MPO response in null immunised mice and Rag2 mice receiving whole splenocytes, spanned multiple Ig isotypes. This is indicative of an adaptive and polyclonal B cell response, spanning multiple epitopes. The antibody response included IgG2a and IgG2b MPO-ANCA, isotypes that are associated with most severe pathology, upon transfer into the 129 mice (Van der Veen B.S, doctorate thesis, University of Groningen, 2010, https://www.rug.nl/research/portal/files/14663229/05c5.pdf, accessed 16/01/2019). The MPO null and Rag2 used in the experiments detailed in this chapter, were on a C57/Bl6 background. The 129S6 strain has the highest incidence of crescents on passive transferral of MPO antibody, approximately 60%. Incidence is around 20% in 129S1 mice and just 10% in the C57/Bl6 strain (Xiao, Ciavatta et al. 2013). Severity of disease might therefore have been increased by backcrossing onto the 129S6 strain, however the initial cell transfer experiments were conducted on C57/Bl6 mice, with high penetrance described.

Although MPO antibody titre was comparable in mice receiving whole splenocytes, T cell number may have been insufficient. I verified that T cells formed part of the renal infiltrate on immunofluorescence but there were few crescents and no biochemical renal abnormalities. Importantly, Ruth *et al* also showed non-redundant roles for T cells and antibodies in AAV pathogenesis (Ruth, Kitching et al. 2006).

In the Rag2 mice iNKT are not reduced, since they have an invariant TCR. Immunophenotyping revealed a precursor B cell population also resides within the

spleen. These cell subsets might also act to limit disease induction in mice, with high ANCA titre.

B cells alone are reported to transfer disease to Rag2 mice (Xiao, Heeringa et al. 2003). More B cells were transferred to the CD19 enriched mice than those receiving replete splenocytes. When B cells were transferred alone the total area occupied by B cells in the spleen was reduced, there was no disease and a limited, IgM antibody response. The reciprocal interaction between CD4 and B cells is essential for antibody production. T cell independent responses are low avidity, cross reactive and wane quickly, with no memory cell generated. T cells are absolutely required for a high affinity, class switched response. B cells are the key APC in initiating a primary CD4 T cell response (Janeway, Ron et al. 1987) and are essential for normal splenic architecture.

The cell transfer model is not widely used due to overt complement and Ig deposition, in contrast to the paucci immune human disease. Antibody transfer into wildtype mice or bone marrow transplant into MPO null immunised mice (Schreiber, Xiao et al. 2006), have been used more extensively. The transplant model has shown that the key antibody target, is bone marrow in origin. MPO is a constituent of azurophilic neutrophil granules and monocyte lysosomes. ANCA has been shown to activate these cells *in vitro* (Falk, Terrell et al. 1990, Mulder, Stegeman et al. 1995, Nowack, Schwalbe et al. 2000).

Although B cells are essential to the production of high affinity, class switched antibody, the effector functions of antibodies are primarily mediated by cells of the innate immune system which express complement and Fc receptors. Immunoglobulin

mediated disease in mice can be inhibited by targeting the alternative complement pathway (Xiao, Schreiber et al. 2007, Schreiber, Xiao et al. 2009) and is exacerbated on intraperitoneal injection of LPS (Huugen, Xiao et al. 2005, Summers, van der Veen et al. 2010). The role of LPS and TNFα in precipitating disease, suggests that cells of myeloid origin are the principle effector cells in this model.

Systemic administration of LPS induces acute kidney injury and if sustained, this leads to chronic kidney disease with mTOR signalling in macrophages critical to pathogenesis (Chen, Zhu et al. 2015). The dose of LPS administered in the MPO cell transferral model is comparatively low, with intraperitoneal introduction. However, without LPS introduction, crescent frequency is 5-10% and biochemistry normal (Heeringa and Little 2011). Mice received 0.018µg of TLR grade LPS (R515 serotype), the amount was determined by prior work on the NTN model in our laboratory. This was a lower amount than previously administered in the MEV model, 0.5µg/g body weight (Huugen, Xiao et al. 2005). This initiating event mimics the role of infection in autoimmune disease; innate immune cells are first to arrive at the site of inflammation.Monocytes, macrophages and neutrophil represent a cellular source of antigen, upon degranulation, the MPO antigen is supplanted onto renal endothelial cells.

Murine disease is observed whenever the only source of antigen expressing cells, is haematopoietic in origin (Schreiber, Xiao et al. 2006). Moreover, neutrophils alone are a sufficient source of auto-antigen, demonstrated by Ly-6c and Ly-6g antibody mediated depletion of these cells in the MEV model (Xiao, Heeringa et al. 2005).

MPO is highly cationic and upon degranulation and the MPO antigen is supplanted onto renal endothelial cells, with retention of peroxidase activity. Other extracellular sources of MPO include NETs and micro-vesicles, which may increase the persistence of antigen locally. Extracellular MPO is also frequently observed in renal biopsies from patients with AAV (O'Sullivan, Lo et al. 2015).

The severity of the initial LPS insult may not have been enough in this pilot study, to recruit sufficient neutrophils to the kidneys. Low crescent frequency observed despite equivalent antibody titres in Rag2 mice receiving whole splenocytes and MPO null immunised mice.

The disease was subclinical biochemically, but with circulating MPO-ANCA and T cells infiltrating the kidney, perhaps disease would have become progressive if end point had been extended. Unlike the cell transferral model (Xiao, Heeringa et al. 2002), the course of the bone marrow transplant and NTS-supplanted antigen models of disease are 6-8 weeks (Schreiber, Xiao et al. 2006, Ooi, Chang et al. 2012) .

In this MEV model, antibody and LPS are critical in the initiation phase. In the subsequent phase of disease, Th17 cells are of key importance (Gan, Steinmetz et al. 2010), with a role also described in the NTS-supplanted antigen model (Summers, Steinmetz et al. 2011). IL-10 B cells limit Th17 responses in arthritis in animal models and human disease (Carter, Rosser et al. 2012, Flores-Borja, Bosma et al. 2013).

Breg cells are critical in limiting autoimmune disease in the initiation phase of EAE (Matsushita, Yanaba et al. 2008), with Treg important in resolution (Matsushita, Horikawa et al. 2010). EAE is induced by antigen immunisation, with de novo

generation of a T cell response and antibodies, with disease onset between 9 and 14 days.

In the MPO cell transfer model, antigen experienced splenocytes are transferred, this secondary response is detectable from 3 days and antibody titres rising until sacrifice (Xiao, Heeringa et al. 2002). This initiation phase differs from MEV, suggesting that the role of B cells beyond antibody production, could be resolved. With the novel immunoregulatory functions attributed to B cells, and therapeutic potential (Mauri and Menon 2017), this certainly warrants further investigation. In the experiments presented in this chapter, antibody titres were not comparable between the groups and disease penetrance was low, making it difficult to resolve any protective role of Breg.

Chapter 8 Final summary

8.1 There is an imbalance in memory and regulatory B cells in AAV

This study adds to cumulating evidence that Breg are numerically deficient in AAV. I detected reduction in both $CD24^{high}$ $CD38^{high}$ (Breg) and CD5 B cells. Overall there is an imbalance in memory and regulatory cells, which is corrected in patients who re-establish immune tolerance and following rituximab therapy. This might explain why rituximab is so efficacious in AAV.

8.2 Potential for M:Rn to be used as a predictive measure of clinical outcome

I represented the imbalance as ratio memory to regulatory cells (M:Rn). In remission memory B cells rebound but Breg do not, and this may predispose to relapse. Propensity to relapse is greatest in PR3-ANCA patients, they had significantly higher M:Rn compared to MPO-ANCA patients, during the acute phase of disease and in clinical remission.

8.3 CD5 population less stable than Breg, making it an unsuitable for isolating B cells for functional studies

Although CD5+ cells were enriched in Breg gate, there was no correlation between these B cell subsets in controls. There was no differential detection of CD1d in B cells, although they expressed higher levels than CD19null lymphocytes.

CD24 and CD38 markers are expressed on a continuum, making assignment of gates subjective. However, the populations I defined corresponded very well with other markers of transitional B cells (CD10+ and IgM^{high}) or memory B cells (CD27+).

CD24 and CD38 staining was more stable than CD5, which was inducible on freeze thawing. CD24 and CD38 subsets were consequently used for functional experiments.

8.4 The imbalance in B cells in AAV, represents a proinflammatory profile

Bmem augment Th1 differentiation *in vitro*, whilst Breg do not. Bmem frequency is associated with reduced B IL-10 competency and increased TNFα production, the converse is true for Breg.

There was no difference in T cell cultures, with control or patient B cell subsets. B cell cytokine induction did not differ in the main remission cohort compared controls, however IL-10 B cells were dramatically increased after rituximab treatment. Unfortunately, I was limited to assessing this in remission patients because acute patients seldom present (incidence of 20-30/million annually).

TNFα, IL-10 and TGFβ were induced in B cell on CPG and CD154 stimulation, a mixture of inflammatory and regulatory B cell cytokines. This led to further testing, with the purpose of resolve the soluble mediators released on PBMC simulation (15 analytes measured in total).

8.5 Inhibitory and inflammatory cytokines are released from PBMC, maximally stimulated for IL-10 induction, but the net effect is inhibitory

IL-10, IL-6, IL-1β, TNFα, IL-17A, IFNγ and IL-2 were significantly induced in PBMC, simulated with CPG and CD154. TGFβ was only detected in a subset of samples. The net effect of these supernatants was to limit T cell TNFα production, this was not impaired on blockade of IL-10 with an agonistic antibody. This demonstrates

that it is important not to look at any one cytokine in isolation, with additional benefit conferred by defining net profile and effect *in vitro.*

8.6 Bmem and Breg, distinct immunomodulatory profiles on CPG and CD154 stimulation?

Breg frequency positively correlated with IL-10 release in the supernatants, the converse was observed with Bmem. Bmem positively correlated with TGFβ release into the supernatant and inversely with IL-6. The balance of these 2 cytokines is critical is determining balance of Treg and Th17 T cells. Bmem also tended to have a positive relationship with circulating Tregs. Whilst both Bmem and Breg had an inverse relationship with high activated T cells (CD127+ $CD25^{high}$).

The differing relationship between IL-10 and TGFβ, might be indicative of existence of 2 distinct regulatory functions which modulate frequency of activated and regulatory T cells in the periphery. Although these are interesting observations, they are difficult to interpret in a mixed PBMC culture, with analysis of soluble mediators. Further investigation would be warranted, with intracellular flow cytometry or cell culture, to see if Bmem are particularly adept at inducing or maintaining Treg *ex vivo*.

8.7 No relationship between Treg and Breg

Treg were reduced in patients, but there was no relationship with Breg. Treg or Breg were reduced (< the mean of the controls minus 2 standard deviations), but not both in combination. This warrants further investigation, to see how these 2 key immunomodulatory cell types, modulate patient outcome.

There was no relationship between Breg and ATPase positive T cells and Breg. CD39+ Treg had a positive relationship with TGFβ release in CPG and CD154 stimulated PBMC. These cells might be targets of Bmem cell induction, since positive correlation was observed with CD39+ Treg and soluble TGFβ. Equally, the relationship between Bmem, soluble TGFβ and CD39 Treg might be casual or indirect, a consequence of generalised immune activation for example. It would be interesting to look at these parameters, in an extended cohort, longitudinally.

8.8 Low disease on splenocyte transferral into Rag2 mice

Despite normal splenic architecture, infiltration of T cells in the kidney and antibody titres, equivalent to those in MPO-/- immunised mice, very limited disease was observed in Rag2 mice on transfer of whole splenocytes.

When purified B cells were transferred alone, antibody response could not be maintained and was predominantly IgM. This contradicts a previous conference report, which is extensively cited but the finding is not wholly unexpected. T cell co-stimulation through CD154, is essential for production of high affinity, class switch antibody. When this is perturbed, patients develop hyper IgM syndrome.

8.9 Antibody or B cells alone are insufficient to cause disease

An initiating event is crucial, with TNFα and LPS effective in animal models. This results in a directed innate immune response, with local inflammatory cascade and deposition of MPO on the microvasculature, which results in tissue damage. Without this inciting damage, ignorance is maintained. T cells were observed in the interstitium but there were few crescentic lesions. MPO deposition in the glomeruli and damage to

the microvasculature mediated by the innate immune cells, are essential initiating steps in pathogenesis.

8.10 Merits of revisiting the cell transfer model of disease

Effector functions of antibodies are predominately modulated by innate immune cells, with antigen release resulting in an inflammatory cascade. The role of B cells extends far beyond antibody production, but this has not been assessed in the antigen specific models of AAV to date.

IL-10 deletion restricted to B cells does not limit NTN, however that too is an antibody mediated disease with T cells and macrophages, the central mediators of pathology.

With the newly appreciated effector and regulatory roles of B cells in autoimmunity, combined with increasing interest in novel B cell targeted therapies, this would be of great value. The cell transfer model might finally enable us to the separate the roles of B cells and antibody in pathogenesis of AAV.

Studies in humans are typically conducted after development of symptoms, when central and peripheral tolerance checkpoints have been by-passed. It is therefore difficult to investigate the complex role of B cells in induction, maintenance and resolution of disease. Investigation is typically limited to peripheral blood, however only 5-10% of B cells exist in circulation, with the vast majority residing in secondary lymphoid tissues.

References

Abdulahad, W. H., C. A. Stegeman, Y. M. van der Geld, B. Doornbos-van der Meer, P. C. Limburg and C. G. Kallenberg (2007). "Functional defect of circulating regulatory CD4+ T cells in patients with Wegener's granulomatosis in remission." Arthritis Rheum **56**(6): 2080-2091.

Adlowitz, D. G., J. Barnard, J. N. Biear, C. Cistrone, T. Owen, W. Wang, A. Palanichamy, E. Ezealah, D. Campbell, C. Wei, R. J. Looney, I. Sanz and J. H. Anolik (2015). "Expansion of Activated Peripheral Blood Memory B Cells in Rheumatoid Arthritis, Impact of B Cell Depletion Therapy, and Biomarkers of Response." PLoS One **10**(6): e0128269.

Alam, M. S., C. C. Kurtz, R. M. Rowlett, B. K. Reuter, E. Wiznerowicz, S. Das, J. Linden, S. E. Crowe and P. B. Ernst (2009). "CD73 is expressed by human regulatory T helper cells and suppresses proinflammatory cytokine production and Helicobacter felis-induced gastritis in mice." J Infect Dis **199**(4): 494-504.

Amel Kashipaz, M. R., M. L. Huggins, P. Lanyon, A. Robins, R. J. Powell and I. Todd (2003). "Assessment of Be1 and Be2 cells in systemic lupus erythematosus indicates elevated interleukin-10 producing CD5+ B cells." Lupus **12**(5): 356-363.

Amu, S., A. Tarkowski, T. Dorner, M. Bokarewa and M. Brisslert (2007). "The human immunomodulatory CD25+ B cell population belongs to the memory B cell pool." Scand J Immunol **66**(1): 77-86.

Anolik, J. H., J. W. Friedberg, B. Zheng, J. Barnard, T. Owen, E. Cushing, J. Kelly, E. C. Milner, R. I. Fisher and I. Sanz (2007). "B cell reconstitution after rituximab treatment of lymphoma recapitulates B cell ontogeny." Clinical immunology **122**(2): 139-145.

Arkatkar, T., S. W. Du, H. M. Jacobs, E. M. Dam, B. Hou, J. H. Buckner, D. J. Rawlings and S. W. Jackson (2017). "B cell-derived IL-6 initiates spontaneous germinal center formation during systemic autoimmunity." J Exp Med **214**(11): 3207-3217.

Artis, D. and H. Spits (2015). "The biology of innate lymphoid cells." Nature **517**(7534): 293-301.

Aybar, L. T., J. G. McGregor, S. L. Hogan, Y. Hu, C. E. Mendoza, E. J. Brant, C. J. Poulton, C. D. Henderson, R. J. Falk and D. O. Bunch (2015). "Reduced CD5(+) CD24(hi) CD38(hi) and interleukin-10(+) regulatory B cells in active anti-neutrophil cytoplasmic autoantibody-associated vasculitis permit increased circulating autoantibodies." Clin Exp Immunol **180**(2): 178-188.

Bader, L., W. Koldingsnes and J. Nossent (2010). "B-lymphocyte activating factor levels are increased in patients with Wegener's granulomatosis and inversely correlated with ANCA titer." Clin Rheumatol **29**(9): 1031-1035.

Baker, N. and M. R. Ehrenstein (2002). "Cutting edge: selection of B lymphocyte subsets is regulated by natural IgM." J Immunol **169**(12): 6686-6690.

Baldus, S., J. P. Eiserich, A. Mani, L. Castro, M. Figueroa, P. Chumley, W. Ma, A. Tousson, C. R. White and D. C. Bullard (2001). "Endothelial transcytosis of myeloperoxidase confers specificity to vascular ECM proteins as targets of tyrosine nitration." Journal of Clinical Investigation **108**(12): 1759-1770.

Bansal, P. J. and M. C. Tobin (2004). "Neonatal microscopic polyangiitis secondary to transfer of maternal myeloperoxidase-antineutrophil cytoplasmic antibody resulting

in neonatal pulmonary hemorrhage and renal involvement." Ann Allergy Asthma Immunol **93**(4): 398-401.
Barr, T. A., P. Shen, S. Brown, V. Lampropoulou, T. Roch, S. Lawrie, B. Fan, R. A. O'Connor, S. M. Anderton, A. Bar-Or, S. Fillatreau and D. Gray (2012). "B cell depletion therapy ameliorates autoimmune disease through ablation of IL-6-producing B cells." J Exp Med **209**(5): 1001-1010.
Barral, P., J. Eckl-Dorna, N. E. Harwood, C. De Santo, M. Salio, P. Illarionov, G. S. Besra, V. Cerundolo and F. D. Batista (2008). "B cell receptor-mediated uptake of CD1d-restricted antigen augments antibody responses by recruiting invariant NKT cell help in vivo." Proc Natl Acad Sci U S A **105**(24): 8345-8350.
Baumgarth, N. (2011). "The double life of a B-1 cell: self-reactivity selects for protective effector functions." Nat Rev Immunol **11**(1): 34-46.
Bautista-Caro, M. B., E. de Miguel, D. Peiteado, C. Plasencia-Rodriguez, A. Villalba, I. Monjo-Henry, A. Puig-Kroger, P. Sanchez-Mateos, E. Martin-Mola and M. E. Miranda-Carus (2017). "Increased frequency of circulating CD19+CD24hiCD38hi B cells with regulatory capacity in patients with Ankylosing spondylitis (AS) naive for biological agents." PLoS One **12**(7): e0180726.
Benard, A., I. Sakwa, P. Schierloh, A. Colom, I. Mercier, L. Tailleux, L. Jouneau, P. Boudinot, T. Al-Saati, R. Lang, J. Rehwinkel, A. G. Loxton, S. H. E. Kaufmann, V. Anton-Leberre, A. O'Garra, M. D. C. Sasiain, B. Gicquel, S. Fillatreau, O. Neyrolles and D. Hudrisier (2018). "B Cells Producing Type I IFN Modulate Macrophage Polarization in Tuberculosis." Am J Respir Crit Care Med **197**(6): 801-813.
Bennett, S. R., F. R. Carbone, T. Toy, J. F. Miller and W. R. Heath (1998). "B cells directly tolerize CD8(+) T cells." J Exp Med **188**(11): 1977-1983.
Berden, A., A. Goceroglu, D. Jayne, R. Luqmani, N. Rasmussen, J. A. Bruijn and I. Bajema (2012). "Diagnosis and management of ANCA associated vasculitis." BMJ **344**: e26.
Bergtold, A., D. D. Desai, A. Gavhane and R. Clynes (2005). "Cell surface recycling of internalized antigen permits dendritic cell priming of B cells." Immunity **23**(5): 503-514.
Berland, R. and H. H. Wortis (2002). "Origins and functions of B-1 cells with notes on the role of CD5." Annu Rev Immunol **20**: 253-300.
Berti, A., R. Warner, K. Johnson, D. Cornec, D. Schroeder, B. Kabat, C. A. Langford, G. S. Hoffman, F. C. Fervenza, C. G. M. Kallenberg, P. Seo, R. Spiera, E. W. St Clair, P. Brunetta, J. H. Stone, P. A. Merkel, U. Specks, P. A. Monach and R.-I. R. Group (2018). "Brief Report: Circulating Cytokine Profiles and Antineutrophil Cytoplasmic Antibody Specificity in Patients With Antineutrophil Cytoplasmic Antibody-Associated Vasculitis." Arthritis Rheumatol **70**(7): 1114-1121.
Blair, P. A., K. A. Chavez-Rueda, J. G. Evans, M. J. Shlomchik, A. Eddaoudi, D. A. Isenberg, M. R. Ehrenstein and C. Mauri (2009). "Selective targeting of B cells with agonistic anti-CD40 is an efficacious strategy for the generation of induced regulatory T2-like B cells and for the suppression of lupus in MRL/lpr mice." J Immunol **182**(6): 3492-3502.
Blair, P. A., L. Y. Norena, F. Flores-Borja, D. J. Rawlings, D. A. Isenberg, M. R. Ehrenstein and C. Mauri (2010). "CD19(+)CD24(hi)CD38(hi) B cells exhibit regulatory capacity in healthy individuals but are functionally impaired in systemic Lupus Erythematosus patients." Immunity **32**(1): 129-140.

Blume, C., A. Felix, N. Shushakova, F. Gueler, C. S. Falk, H. Haller and J. Schrader (2012). "Autoimmunity in CD73/Ecto-5'-nucleotidase deficient mice induces renal injury." PLoS One **7**(5): e37100.
Bohnhorst, J. O., M. B. Bjorgan, J. E. Thoen, J. B. Natvig and K. M. Thompson (2001). "Bm1-Bm5 classification of peripheral blood B cells reveals circulating germinal center founder cells in healthy individuals and disturbance in the B cell subpopulations in patients with primary Sjogren's syndrome." J Immunol **167**(7): 3610-3618.
Booth, A. D., M. K. Almond, A. Burns, P. Ellis, G. Gaskin, G. H. Neild, M. Plaisance, C. D. Pusey, D. R. Jayne and G. Pan-Thames Renal Research (2003). "Outcome of ANCA-associated renal vasculitis: a 5-year retrospective study." Am J Kidney Dis **41**(4): 776-784.
Boring, Y. C., U. Flogel, C. Jacoby, M. Heil, W. Schaper and J. Schrader (2013). "Lack of ecto-5'-nucleotidase (CD73) promotes arteriogenesis." Cardiovasc Res **97**(1): 88-96.
Borsellino, G., M. Kleinewietfeld, D. Di Mitri, A. Sternjak, A. Diamantini, R. Giometto, S. Hopner, D. Centonze, G. Bernardi, M. L. Dell'Acqua, P. M. Rossini, L. Battistini, O. Rotzschke and K. Falk (2007). "Expression of ectonucleotidase CD39 by Foxp3+ Treg cells: hydrolysis of extracellular ATP and immune suppression." Blood **110**(4): 1225-1232.
Borstel, A. v., L. L. Lintermans, P. Heeringa, A. Rutgers, C. A. Stegeman, J. S. Sanders and W. H. Abdulahad (2018). "Circulating CD24hi CD38hi regulatory B cells influence Th17 cell responses in patients with ANCA-associated vasculitides." Ann Rheum Dis **77**(Supplement 2): 75.
Bosma, A., A. Abdel-Gadir, D. A. Isenberg, E. C. Jury and C. Mauri (2012). "Lipid-antigen presentation by CD1d(+) B cells is essential for the maintenance of invariant natural killer T cells." Immunity **36**(3): 477-490.
Bouaziz, J. D., S. Calbo, M. Maho-Vaillant, A. Saussine, M. Bagot, A. Bensussan and P. Musette (2010). "IL-10 produced by activated human B cells regulates CD4(+) T-cell activation in vitro." Eur J Immunol **40**(10): 2686-2691.
Brisslert, M., M. Bokarewa, P. Larsson, K. Wing, L. V. Collins and A. Tarkowski (2006). "Phenotypic and functional characterization of human CD25+ B cells." Immunology **117**(4): 548-557.
Bruchfeld, A., M. Wendt, J. Bratt, A. R. Qureshi, S. Chavan, K. J. Tracey, K. Palmblad and I. Gunnarsson (2011). "High-mobility group box-1 protein (HMGB1) is increased in antineutrophilic cytoplasmatic antibody (ANCA)-associated vasculitis with renal manifestations." Mol Med **17**(1-2): 29-35.
Buffa, S., M. Pellicano, M. Bulati, A. Martorana, D. Goldeck, C. Caruso, G. Pawelec and G. Colonna-Romano (2013). "A novel B cell population revealed by a CD38/CD24 gating strategy: CD38(-)CD24 (-) B cells in centenarian offspring and elderly people." Age (Dordr) **35**(5): 2009-2024.
Bunch, D. O., J. G. McGregor, N. B. Khandoobhai, L. T. Aybar, M. E. Burkart, Y. Hu, S. L. Hogan, C. J. Poulton, E. A. Berg, R. J. Falk and P. H. Nachman (2013). "Decreased CD5+ B Cells in Active ANCA Vasculitis and Relapse after Rituximab." Clin J Am Soc Nephrol.
Bunch, D. O., C. E. Mendoza, L. T. Aybar, E. S. Kotzen, K. R. Colby, Y. Hu, S. L. Hogan, C. J. Poulton, J. L. Schmitz, R. J. Falk, P. H. Nachman, W. F. Pendergraft and J. G. McGregor (2015). "Gleaning relapse risk from B cell phenotype: decreased CD5+

B cells portend a shorter time to relapse after B cell depletion in patients with ANCA-associated vasculitis." Ann Rheum Dis **74**(9): 1784-1786.
Carrasco, Y. R. and F. D. Batista (2007). "B cells acquire particulate antigen in a macrophage-rich area at the boundary between the follicle and the subcapsular sinus of the lymph node." Immunity **27**(1): 160-171.
Carsetti, R., G. Kohler and M. C. Lamers (1995). "Transitional B cells are the target of negative selection in the B cell compartment." J Exp Med **181**(6): 2129-2140.
Carsetti, R., M. M. Rosado and H. Wardmann (2004). "Peripheral development of B cells in mouse and man." Immunol Rev **197**: 179-191.
Carter, N. A., E. C. Rosser and C. Mauri (2012). "Interleukin-10 produced by B cells is crucial for the suppression of Th17/Th1 responses, induction of T regulatory type 1 cells and reduction of collagen-induced arthritis." Arthritis Res Ther **14**(1): R32.
Carter, N. A., R. Vasconcellos, E. C. Rosser, C. Tulone, A. Munoz-Suano, M. Kamanaka, M. R. Ehrenstein, R. A. Flavell and C. Mauri (2011). "Mice lacking endogenous IL-10-producing regulatory B cells develop exacerbated disease and present with an increased frequency of Th1/Th17 but a decrease in regulatory T cells." J Immunol **186**(10): 5569-5579.
Casellas, R., T. A. Shih, M. Kleinewietfeld, J. Rakonjac, D. Nemazee, K. Rajewsky and M. C. Nussenzweig (2001). "Contribution of receptor editing to the antibody repertoire." Science **291**(5508): 1541-1544.
Cekic, C. and J. Linden (2016). "Purinergic regulation of the immune system." Nat Rev Immunol **16**(3): 177-192.
Chavele, K. M., D. Shukla, T. Keteepe-Arachi, J. A. Seidel, D. Fuchs, C. D. Pusey and A. D. Salama (2010). "Regulation of myeloperoxidase-specific T cell responses during disease remission in antineutrophil cytoplasmic antibody-associated vasculitis: the role of Treg cells and tryptophan degradation." Arthritis Rheum **62**(5): 1539-1548.
Chen, H., J. Zhu, Y. Liu, Z. Dong, H. Liu, Y. Liu, X. Zhou, F. Liu and G. Chen (2015). "Lipopolysaccharide Induces Chronic Kidney Injury and Fibrosis through Activation of mTOR Signaling in Macrophages." Am J Nephrol **42**(4): 305-317.
Chen, M., G.-Q. Xing, F. Yu, G. Liu and M.-H. Zhao (2009). "Complement deposition in renal histopathology of patients with ANCA-associated pauci-immune glomerulonephritis." Nephrology Dialysis Transplantation **24**(4): 1247-1252.
Chen, M., L. Zhang, Y. Ren, K. Zhang, Y. Yang, Y. Fang, X. Yan, D. Peng, C. Gao and S. Li (2016). "Defective Function of CD24(+)CD38(+) Regulatory B Cells in Ankylosing Spondylitis." DNA Cell Biol **35**(2): 88-95.
Cherukuri, A., D. M. Rothstein, B. Clark, C. R. Carter, A. Davison, M. Hernandez-Fuentes, E. Hewitt, A. D. Salama and R. J. Baker (2014). "Immunologic human renal allograft injury associates with an altered IL-10/TNF-alpha expression ratio in regulatory B cells." J Am Soc Nephrol **25**(7): 1575-1585.
Chong, Y., H. Ikematsu, K. Yamaji, M. Nishimura, S. Nabeshima, S. Kashiwagi and J. Hayashi (2005). "CD27(+) (memory) B cell decrease and apoptosis-resistant CD27(-) (naive) B cell increase in aged humans: implications for age-related peripheral B cell developmental disturbances." Int Immunol **17**(4): 383-390.
Cohen, P. L. and R. A. Eisenberg (1991). "Lpr and gld: single gene models of systemic autoimmunity and lymphoproliferative disease." Annu Rev Immunol **9**: 243-269.
Colonna-Romano, G., M. Bulati, A. Aquino, G. Scialabba, G. Candore, D. Lio, M. Motta, M. Malaguarnera and C. Caruso (2003). "B cells in the aged: CD27, CD5, and CD40 expression." Mech Ageing Dev **124**(4): 389-393.

Cooper, M. D., R. D. Peterson and R. A. Good (1965). "Delineation of the Thymic and Bursal Lymphoid Systems in the Chicken." Nature **205**: 143-146.
Coughlan, A. M., S. J. Freeley and M. G. Robson (2012). "Animal models of anti-neutrophil cytoplasmic antibody-associated vasculitis." Clin Exp Immunol **169**(3): 229-237.
Crawford, A., M. Macleod, T. Schumacher, L. Corlett and D. Gray (2006). "Primary T cell expansion and differentiation in vivo requires antigen presentation by B cells." J Immunol **176**(6): 3498-3506.
Cui, D., L. Zhang, J. Chen, M. Zhu, L. Hou, B. Chen and B. Shen (2015). "Changes in regulatory B cells and their relationship with rheumatoid arthritis disease activity." Clin Exp Med **15**(3): 285-292.
Culton, D. A., M. W. Nicholas, D. O. Bunch, Q. L. Zhen, T. B. Kepler, M. A. Dooley, C. Mohan, P. H. Nachman and S. H. Clarke (2007). "Similar CD19 dysregulation in two autoantibody-associated autoimmune diseases suggests a shared mechanism of B-cell tolerance loss." J Clin Immunol **27**(1): 53-68.
Cyster, J. G., S. B. Hartley and C. C. Goodnow (1994). "Competition for follicular niches excludes self-reactive cells from the recirculating B-cell repertoire." Nature **371**(6496): 389-395.
Daien, C. I., S. Gailhac, T. Mura, R. Audo, B. Combe, M. Hahne and J. Morel (2014). "Regulatory B10 cells are decreased in patients with rheumatoid arthritis and are inversely correlated with disease activity." Arthritis Rheumatol **66**(8): 2037-2046.
Dambuza, I. M., C. He, J. K. Choi, C. R. Yu, R. Wang, M. J. Mattapallil, P. T. Wingfield, R. R. Caspi and C. E. Egwuagu (2017). "IL-12p35 induces expansion of IL-10 and IL-35-expressing regulatory B cells and ameliorates autoimmune disease." Nat Commun **8**(1): 719.
Dass, S., E. M. Vital and P. Emery (2007). "Development of psoriasis after B cell depletion with rituximab." Arthritis & Rheumatism **56**(8): 2715-2718.
De Bandt, M., O. Meyer, L. Dacosta, C. Elbim and C. Pasquier (1999). "Anti-proteinase-3 (PR3) antibodies (C-ANCA) recognize various targets on the human umbilical vein endothelial cell (HUVEC) membrane." Clin Exp Immunol **115**(2): 362-368.
de Waal Malefyt, R., J. Haanen, H. Spits, M. G. Roncarolo, A. te Velde, C. Figdor, K. Johnson, R. Kastelein, H. Yssel and J. E. de Vries (1991). "Interleukin 10 (IL-10) and viral IL-10 strongly reduce antigen-specific human T cell proliferation by diminishing the antigen-presenting capacity of monocytes via downregulation of class II major histocompatibility complex expression." J Exp Med **174**(4): 915-924.
de Waal Malefyt, R., H. Yssel and J. E. de Vries (1993). "Direct effects of IL-10 on subsets of human CD4+ T cell clones and resting T cells. Specific inhibition of IL-2 production and proliferation." J Immunol **150**(11): 4754-4765.
Delong, T., T. A. Wiles, R. L. Baker, B. Bradley, G. Barbour, R. Reisdorph, M. Armstrong, R. L. Powell, N. Reisdorph, N. Kumar, C. M. Elso, M. DeNicola, R. Bottino, A. C. Powers, D. M. Harlan, S. C. Kent, S. I. Mannering and K. Haskins (2016). "Pathogenic CD4 T cells in type 1 diabetes recognize epitopes formed by peptide fusion." Science **351**(6274): 711-714.
Ding, C., Y. Ma, X. Chen, M. Liu, Y. Cai, X. Hu, D. Xiang, S. Nath, H. G. Zhang, H. Ye, D. Powell and J. Yan (2013). "Integrin CD11b negatively regulates BCR signalling to maintain autoreactive B cell tolerance." Nat Commun **4**: 2813.

Ding, Q., M. Yeung, G. Camirand, Q. Zeng, H. Akiba, H. Yagita, G. Chalasani, M. H. Sayegh, N. Najafian and D. M. Rothstein (2011). "Regulatory B cells are identified by expression of TIM-1 and can be induced through TIM-1 ligation to promote tolerance in mice." J Clin Invest **121**(9): 3645-3656.
Dongen, J. v., T. Szczepanski and H. Adriaansen (2002). Leukemia. New York, Saunders.
Ducreux, J., S. Nieuwland, F. A. Houssiau and B. R. Lauwerys (2014). "Increased CD95 (Fas) Expression on Naive B Cells Is Associated with a Switch to Double Negative and Plasma Cells in the Peripheral Blood, and Correlates with Disease Activity in Systemic Lupus Erythematosus." Arthritis and rheumatism, Abstracts from The 2014 ACR/ARHP Annual Meeting **66**(S716).
Duddy, M., M. Niino, F. Adatia, S. Hebert, M. Freedman, H. Atkins, H. J. Kim and A. Bar-Or (2007). "Distinct effector cytokine profiles of memory and naive human B cell subsets and implication in multiple sclerosis." J Immunol **178**(10): 6092-6099.
Dunleavy, K., F. Hakim, H. K. Kim, J. E. Janik, N. Grant, T. Nakayama, T. White, G. Wright, L. Kwak, R. Gress, G. Tosato and W. H. Wilson (2005). "B-cell recovery following rituximab-based therapy is associated with perturbations in stromal derived factor-1 and granulocyte homeostasis." Blood **106**(3): 795-802.
Dwyer, K. M., D. Hanidziar, P. Putheti, P. A. Hill, S. Pommey, J. L. McRae, A. Winterhalter, G. Doherty, S. Deaglio, M. Koulmanda, W. Gao, S. C. Robson and T. B. Strom (2010). "Expression of CD39 by human peripheral blood CD4+ CD25+ T cells denotes a regulatory memory phenotype." Am J Transplant **10**(11): 2410-2420.
Eckl-Dorna, J. and F. D. Batista (2009). "BCR-mediated uptake of antigen linked to TLR9 ligand stimulates B-cell proliferation and antigen-specific plasma cell formation." Blood **113**(17): 3969-3977.
Eriksson, P., C. Sandell, K. Backteman and J. Ernerudh (2010). "B cell abnormalities in Wegener's granulomatosis and microscopic polyangiitis: role of CD25+-expressing B cells." J Rheumatol **37**(10): 2086-2095.
Evans, J. G., K. A. Chavez-Rueda, A. Eddaoudi, A. Meyer-Bahlburg, D. J. Rawlings, M. R. Ehrenstein and C. Mauri (2007). "Novel suppressive function of transitional 2 B cells in experimental arthritis." J Immunol **178**(12): 7868-7878.
Falk, R. J., R. S. Terrell, L. A. Charles and J. C. Jennette (1990). "Anti-neutrophil cytoplasmic autoantibodies induce neutrophils to degranulate and produce oxygen radicals in vitro." Proceedings of the National Academy of Sciences **87**(11): 4115-4119.
Fauci, A. S., P. Katz, B. F. Haynes and S. M. Wolff (1979). "Cyclophosphamide therapy of severe systemic necrotizing vasculitis." N Engl J Med **301**(5): 235-238.
Fecteau, J. F., G. Cote and S. Neron (2006). "A new memory CD27-IgG+ B cell population in peripheral blood expressing VH genes with low frequency of somatic mutation." J Immunol **177**(6): 3728-3736.
Ferry, H., M. Jones, D. J. Vaux, I. S. Roberts and R. J. Cornall (2003). "The cellular location of self-antigen determines the positive and negative selection of autoreactive B cells." J Exp Med **198**(9): 1415-1425.
Figueiro, F., L. Muller, S. Funk, E. K. Jackson, A. M. Battastini and T. L. Whiteside (2016). "Phenotypic and functional characteristics of CD39(high) human regulatory B cells (Breg)." Oncoimmunology **5**(2): e1082703.

Fillatreau, S., C. H. Sweenie, M. J. McGeachy, D. Gray and S. M. Anderton (2002). "B cells regulate autoimmunity by provision of IL-10." Nature immunology **3**(10): 944-950.
Finkielman, J. D., P. A. Merkel, D. Schroeder, G. S. Hoffman, R. Spiera, E. W. St Clair, J. C. Davis, Jr., W. J. McCune, A. K. Lears, S. R. Ytterberg, A. M. Hummel, M. A. Viss, T. Peikert, J. H. Stone, U. Specks and W. R. Group (2007). "Antiproteinase 3 antineutrophil cytoplasmic antibodies and disease activity in Wegener granulomatosis." Ann Intern Med **147**(9): 611-619.
Fiorentino, D. F., A. Zlotnik, T. R. Mosmann, M. Howard and A. O'Garra (1991). "IL-10 inhibits cytokine production by activated macrophages." J Immunol **147**(11): 3815-3822.
Flogel, U., S. Burghoff, P. L. van Lent, S. Temme, L. Galbarz, Z. Ding, A. El-Tayeb, S. Huels, F. Bonner, N. Borg, C. Jacoby, C. E. Muller, W. B. van den Berg and J. Schrader (2012). "Selective activation of adenosine A2A receptors on immune cells by a CD73-dependent prodrug suppresses joint inflammation in experimental rheumatoid arthritis." Sci Transl Med **4**(146): 146ra108.
Flores-Borja, F., A. Bosma, D. Ng, V. Reddy, M. R. Ehrenstein, D. A. Isenberg and C. Mauri (2013). "CD19+CD24hiCD38hi B cells maintain regulatory T cells while limiting TH1 and TH17 differentiation." Sci Transl Med **5**(173): 173ra123.
Flossmann, O., A. Berden, K. de Groot, C. Hagen, L. Harper, C. Heijl, P. Hoglund, D. Jayne, R. Luqmani, A. Mahr, C. Mukhtyar, C. Pusey, N. Rasmussen, C. Stegeman, M. Walsh, K. Westman and G. European Vasculitis Study (2011). "Long-term patient survival in ANCA-associated vasculitis." Ann Rheum Dis **70**(3): 488-494.
Free, M. E., D. O. Bunch, J. A. McGregor, B. E. Jones, E. A. Berg, S. L. Hogan, Y. Hu, G. A. Preston, J. C. Jennette, R. J. Falk and M. A. Su (2013). "Patients with antineutrophil cytoplasmic antibody-associated vasculitis have defective Treg cell function exacerbated by the presence of a suppression-resistant effector cell population." Arthritis Rheum **65**(7): 1922-1933.
Free, M. E. and M. A. Su (2013). "Reply to the editor." Arthritis Rheumatism **65**(12): 3316-3318.
Fries, J. F., G. G. Hunder, D. A. Bloch, B. A. Michel, W. P. Arend, L. H. Calabrese, A. S. Fauci, R. Y. Leavitt, J. T. Lie, R. W. Lightfoot, Jr. and et al. (1990). "The American College of Rheumatology 1990 criteria for the classification of vasculitis. Summary." Arthritis Rheum **33**(8): 1135-1136.
Gagro, A., N. McCloskey, A. Challa, M. Holder, G. Grafton, J. D. Pound and J. Gordon (2000). "CD5-positive and CD5-negative human B cells converge to an indistinguishable population on signalling through B-cell receptors and CD40." Immunology **101**(2): 201-209.
Galli, G., S. Nuti, S. Tavarini, L. Galli-Stampino, C. De Lalla, G. Casorati, P. Dellabona and S. Abrignani (2003). "CD1d-restricted help to B cells by human invariant natural killer T lymphocytes." J Exp Med **197**(8): 1051-1057.
Gan, P. Y., O. M. Steinmetz, D. S. Tan, K. M. O'Sullivan, J. D. Ooi, Y. Iwakura, A. R. Kitching and S. R. Holdsworth (2010). "Th17 cells promote autoimmune anti-myeloperoxidase glomerulonephritis." J Am Soc Nephrol **21**(6): 925-931.
Gao, J., X. Ma, W. Gu, M. Fu, J. An, Y. Xing, T. Gao, W. Li and Y. Liu (2012). "Novel functions of murine B1 cells: active phagocytic and microbicidal abilities." Eur J Immunol **42**(4): 982-992.

Gary-Gouy, H., J. Harriague, G. Bismuth, C. Platzer, C. Schmitt and A. H. Dalloul (2002). "Human CD5 promotes B-cell survival through stimulation of autocrine IL-10 production." Blood **100**(13): 4537-4543.
Gaudin, E., Y. Hao, M. M. Rosado, R. Chaby, R. Girard and A. A. Freitas (2004). "Positive selection of B cells expressing low densities of self-reactive BCRs." J Exp Med **199**(6): 843-853.
Giannoukakis, N. and M. Trucco (2012). "A role for tolerogenic dendritic cell-induced B-regulatory cells in type 1 diabetes mellitus." Curr Opin Endocrinol Diabetes Obes **19**(4): 279-287.
Glocker, E. O., D. Kotlarz, K. Boztug, E. M. Gertz, A. A. Schaffer, F. Noyan, M. Perro, J. Diestelhorst, A. Allroth, D. Murugan, N. Hatscher, D. Pfeifer, K. W. Sykora, M. Sauer, H. Kreipe, M. Lacher, R. Nustede, C. Woellner, U. Baumann, U. Salzer, S. Koletzko, N. Shah, A. W. Segal, A. Sauerbrey, S. Buderus, S. B. Snapper, B. Grimbacher and C. Klein (2009). "Inflammatory bowel disease and mutations affecting the interleukin-10 receptor." N Engl J Med **361**(21): 2033-2045.
Goetz, M., R. Atreya, M. Ghalibafian, P. R. Galle and M. F. Neurath (2007). "Exacerbation of ulcerative colitis after rituximab salvage therapy." Inflammatory bowel diseases **13**(11): 1365-1368.
Gordon, J. R., Y. Ma, L. Churchman, S. A. Gordon and W. Dawicki (2014). "Regulatory dendritic cells for immunotherapy in immunologic diseases." Front Immunol **5**: 7.
Gou, S.-J., J. Yuan, M. Chen, F. Yu and M.-H. Zhao (2012). "Circulating complement activation in patients with anti-neutrophil cytoplasmic antibody–associated vasculitis." Kidney International **83**(1): 129-137.
Gregg, R., C. M. Smith, F. J. Clark, D. Dunnion, N. Khan, R. Chakraverty, L. Nayak and P. A. Moss (2005). "The number of human peripheral blood CD4+ CD25high regulatory T cells increases with age." Clin Exp Immunol **140**(3): 540-546.
Griffin, D. O. and T. L. Rothstein (2012). "Human "orchestrator" CD11b(+) B1 cells spontaneously secrete interleukin-10 and regulate T-cell activity." Mol Med **18**: 1003-1008.
Grimsholm, O., W. Ren, A. I. Bernardi, H. Chen, G. Park, A. Camponeschi, D. Chen, B. Bergmann, N. Hook, S. Andersson, A. Stromberg, I. Gjertsson, S. Cardell, U. Yrlid, A. De Riva and I. L. Martensson (2015). "Absence of surrogate light chain results in spontaneous autoreactive germinal centres expanding V(H)81X-expressing B cells." Nat Commun **6**: 7077.
Groom, J., S. L. Kalled, A. H. Cutler, C. Olson, S. A. Woodcock, P. Schneider, J. Tschopp, T. G. Cachero, M. Batten, J. Wheway, D. Mauri, D. Cavill, T. P. Gordon, C. R. Mackay and F. Mackay (2002). "Association of BAFF/BLyS overexpression and altered B cell differentiation with Sjogren's syndrome." J Clin Invest **109**(1): 59-68.
Gu, J., X. Ni, X. Pan, H. Lu, Y. Lu, J. Zhao, S. Guo Zheng, K. L. Hippen, X. Wang and L. Lu (2017). "Human CD39(hi) regulatory T cells present stronger stability and function under inflammatory conditions." Cell Mol Immunol **14**(6): 521-528.
Gu, P., J. F. Gao, C. A. D'Souza, A. Kowalczyk, K. Y. Chou and L. Zhang (2012). "Trogocytosis of CD80 and CD86 by induced regulatory T cells." Cell Mol Immunol **9**(2): 136-146.
Guerry, M. J., P. Brogan, I. N. Bruce, D. P. D'Cruz, L. Harper, R. Luqmani, C. D. Pusey, A. D. Salama, D. G. Scott, C. O. Savage, R. A. Watts and D. R. Jayne (2012).

"Recommendations for the use of rituximab in anti-neutrophil cytoplasm antibody-associated vasculitis." Rheumatology (Oxford) **51**(4): 634-643.
Haas, K. M., R. Watanabe, T. Matsushita, H. Nakashima, N. Ishiura, H. Okochi, M. Fujimoto and T. F. Tedder (2010). "Protective and pathogenic roles for B cells during systemic autoimmunity in NZB/W F1 mice." J Immunol **184**(9): 4789-4800.
Haas, M. and J. A. Eustace (2004). "Immune complex deposits in ANCA-associated crescentic glomerulonephritis: a study of 126 cases." Kidney international **65**(6): 2145-2152.
Habib, J., J. Deng, N. Lava, W. Tyor and J. Galipeau (2015). "Blood B Cell and Regulatory Subset Content in Multiple Sclerosis Patients." J Mult Scler (Foster City) **2**(2).
Hakkim, A., B. G. Furnrohr, K. Amann, B. Laube, U. A. Abed, V. Brinkmann, M. Herrmann, R. E. Voll and A. Zychlinsky (2010). "Impairment of neutrophil extracellular trap degradation is associated with lupus nephritis." Proc Natl Acad Sci U S A **107**(21): 9813-9818.
Han, W. K., H. K. Choi, R. M. Roth, R. T. McCluskey and J. L. Niles (2003). "Serial ANCA titers: useful tool for prevention of relapses in ANCA-associated vasculitis." Kidney Int **63**(3): 1079-1085.
Hardy, R. R., C. E. Carmack, S. A. Shinton, J. D. Kemp and K. Hayakawa (1991). "Resolution and characterization of pro-B and pre-pro-B cell stages in normal mouse bone marrow." The Journal of Experimental Medicine **173**(5): 1213-1225.
Harris, D. P., S. Goodrich, A. J. Gerth, S. L. Peng and F. E. Lund (2005). "Regulation of IFN-gamma production by B effector 1 cells: essential roles for T-bet and the IFN-gamma receptor." J Immunol **174**(11): 6781-6790.
Harris, D. P., L. Haynes, P. C. Sayles, D. K. Duso, S. M. Eaton, N. M. Lepak, L. L. Johnson, S. L. Swain and F. E. Lund (2000). "Reciprocal regulation of polarized cytokine production by effector B and T cells." Nat Immunol **1**(6): 475-482.
Harwood, N. E. and F. D. Batista (2010). "Early events in B cell activation." Annu Rev Immunol **28**: 185-210.
Hayakawa, K., M. Asano, S. A. Shinton, M. Gui, D. Allman, C. L. Stewart, J. Silver and R. R. Hardy (1999). "Positive selection of natural autoreactive B cells." Science **285**(5424): 113-116.
Hayashi, M., K. Yanaba, Y. Umezawa, Y. Yoshihara, S. Kikuchi, Y. Ishiuji, H. Saeki and H. Nakagawa (2016). "IL-10-producing regulatory B cells are decreased in patients with psoriasis." J Dermatol Sci **81**(2): 93-100.
He, B., X. Qiao and A. Cerutti (2004). "CpG DNA induces IgG class switch DNA recombination by activating human B cells through an innate pathway that requires TLR9 and cooperates with IL-10." J Immunol **173**(7): 4479-4491.
Heeringa, P. and M. A. Little (2011). "In vivo approaches to investigate ANCA-associated vasculitis: lessons and limitations." Arthritis Res Ther **13**(1): 204.
Heidt, S., J. Hester, S. Shankar, P. J. Friend and K. J. Wood (2012). "B cell repopulation after alemtuzumab induction-transient increase in transitional B cells and long-term dominance of naive B cells." Am J Transplant **12**(7): 1784-1792.
Heinemann, K., B. Wilde, A. Hoerning, B. Tebbe, A. Kribben, O. Witzke and S. Dolff (2016). "Decreased IL-10(+) regulatory B cells (Bregs) in lupus nephritis patients." Scand J Rheumatol **45**(4): 312-316.
Hippen, K. L., L. E. Tze and T. W. Behrens (2000). "CD5 maintains tolerance in anergic B cells." J Exp Med **191**(5): 883-890.

Hirotani, M., M. Niino, T. Fukazawa, S. Kikuchi, I. Yabe, S. Hamada, Y. Tajima and H. Sasaki (2010). "Decreased IL-10 production mediated by Toll-like receptor 9 in B cells in multiple sclerosis." J Neuroimmunol **221**(1-2): 95-100.
Hogan, S. L., G. S. Cooper, D. A. Savitz, L. A. Nylander-French, C. G. Parks, H. Chin, C. E. Jennette, S. Lionaki, J. C. Jennette and R. J. Falk (2007). "Association of silica exposure with anti-neutrophil cytoplasmic autoantibody small-vessel vasculitis: a population-based, case-control study." Clin J Am Soc Nephrol **2**(2): 290-299.
Hogan, S. L., P. H. Nachman, A. S. Wilkman, J. C. Jennette and R. J. Falk (1996). "Prognostic markers in patients with antineutrophil cytoplasmic autoantibody-associated microscopic polyangiitis and glomerulonephritis." J Am Soc Nephrol **7**(1): 23-32.
Holden, N., J. Williams, M. Morgan, A. Challa, J. Gordon, R. Pepper, A. Salama, L. Harper and C. Savage (2011). "ANCA-stimulated neutrophils release BLyS and promote B cell survival: a clinically relevant cellular process." Annals of the rheumatic diseases **70**(12): 2229-2233.
Hollsberg, P., V. Batra, A. Dressel and D. A. Hafler (1996). "Induction of anergy in CD8 T cells by B cell presentation of antigen." J Immunol **157**(12): 5269-5276.
Hsu, B. L., S. M. Harless, R. C. Lindsley, D. M. Hilbert and M. P. Cancro (2002). "Cutting edge: BLyS enables survival of transitional and mature B cells through distinct mediators." J Immunol **168**(12): 5993-5996.
Hua, F., L. Ji, Y. Zhan, F. Li, S. Zou, X. Wang, D. Song, Z. Min, S. Gao, Y. Wu, H. Chen and Y. Cheng (2012). "Pulsed high-dose dexamethasone improves interleukin 10 secretion by CD5+ B cells in patients with primary immune thrombocytopenia." J Clin Immunol **32**(6): 1233-1242.
Huang, X. R., A. R. Kitching, P. G. Tipping and S. R. Holdsworth (2000). "Interleukin-10 inhibits macrophage-induced glomerular injury." J Am Soc Nephrol **11**(2): 262-269.
Huang, Y., L. Perrin, P. Miescher and R. Zubler (1988). "Correlation of T and B cell activities in vitro and serum IL-2 levels in systemic lupus erythematosus." The Journal of Immunology **141**(3): 827-833.
Huck, S., C. Jamin, P. Youinou and M. Zouali (1998). "High-density expression of CD95 on B cells and underrepresentation of the B-1 cell subset in human lupus." J Autoimmun **11**(5): 449-455.
Hussain, S. and T. L. Delovitch (2005). "Dysregulated B7-1 and B7-2 expression on nonobese diabetic mouse B cells is associated with increased T cell costimulation and the development of insulitis." J Immunol **174**(2): 680-687.
Hutton, H. L., S. R. Holdsworth and A. R. Kitching (2017). "ANCA-Associated Vasculitis: Pathogenesis, Models, and Preclinical Testing." Semin Nephrol **37**(5): 418-435.
Huugen, D., A. Van Esch, H. Xiao, C. Peutz-Kootstra, W. Buurman, J. C. Tervaert, J. Jennette and P. Heeringa (2007). "Inhibition of complement factor C5 protects against anti-myeloperoxidase antibody-mediated glomerulonephritis in mice." Kidney international **71**(7): 646-654.
Huugen, D., H. Xiao, A. van Esch, R. J. Falk, C. J. Peutz-Kootstra, W. A. Buurman, J. W. Tervaert, J. C. Jennette and P. Heeringa (2005). "Aggravation of anti-myeloperoxidase antibody-induced glomerulonephritis by bacterial lipopolysaccharide: role of tumor necrosis factor-alpha." Am J Pathol **167**(1): 47-58.

Iwata, Y., T. Matsushita, M. Horikawa, D. J. Dilillo, K. Yanaba, G. M. Venturi, P. M. Szabolcs, S. H. Bernstein, C. M. Magro, A. D. Williams, R. P. Hall, E. W. St Clair and T. F. Tedder (2011). "Characterization of a rare IL-10-competent B-cell subset in humans that parallels mouse regulatory B10 cells." Blood **117**(2): 530-541.
Jacobi, A. M., K. Reiter, M. Mackay, C. Aranow, F. Hiepe, A. Radbruch, A. Hansen, G. R. Burmester, B. Diamond, P. E. Lipsky and T. Dorner (2008). "Activated memory B cell subsets correlate with disease activity in systemic lupus erythematosus: delineation by expression of CD27, IgD, and CD95." Arthritis Rheum **58**(6): 1762-1773.
Jagannathan, M., M. McDonnell, Y. Liang, H. Hasturk, J. Hetzel, D. Rubin, A. Kantarci, T. E. Van Dyke, L. M. Ganley-Leal and B. S. Nikolajczyk (2010). "Toll-like receptors regulate B cell cytokine production in patients with diabetes." Diabetologia **53**(7): 1461-1471.
Janeway, C. A., Jr., J. Ron and M. E. Katz (1987). "The B cell is the initiating antigen-presenting cell in peripheral lymph nodes." J Immunol **138**(4): 1051-1055.
Jayne, D. R., G. Gaskin, N. Rasmussen, D. Abramowicz, F. Ferrario, L. Guillevin, E. Mirapeix, C. O. Savage, R. A. Sinico and C. A. Stegeman (2007). "Randomized trial of plasma exchange or high-dosage methylprednisolone as adjunctive therapy for severe renal vasculitis." Journal of the American Society of Nephrology **18**(7): 2180-2188.
Jennette, J., R. Falk, P. Bacon, N. Basu, M. Cid, F. Ferrario, L. Flores-Suarez, W. Gross, L. Guillevin and E. Hagen (2013). "2012 Revised International Chapel Hill Consensus Conference Nomenclature of Vasculitides." Arthritis & Rheumatism **65**(1): 1-11.
Jennette, J. C., R. J. Falk, K. Andrassy, P. A. Bacon, J. Churg, W. L. Gross, E. C. Hagen, G. S. Hoffman, G. G. Hunder, C. G. Kallenberg and et al. (1994). "Nomenclature of systemic vasculitides. Proposal of an international consensus conference." Arthritis Rheum **37**(2): 187-192.
Jennette, J. C., R. J. Falk, P. A. Bacon, N. Basu, M. C. Cid, F. Ferrario, L. F. Flores-Suarez, W. L. Gross, L. Guillevin, E. C. Hagen, G. S. Hoffman, D. R. Jayne, C. G. Kallenberg, P. Lamprecht, C. A. Langford, R. A. Luqmani, A. D. Mahr, E. L. Matteson, P. A. Merkel, S. Ozen, C. D. Pusey, N. Rasmussen, A. J. Rees, D. G. Scott, U. Specks, J. H. Stone, K. Takahashi and R. A. Watts (2013). "2012 revised International Chapel Hill Consensus Conference Nomenclature of Vasculitides." Arthritis Rheum **65**(1): 1-11.
Jennette, J. C., H. Xiao and R. J. Falk (2006). "Pathogenesis of vascular inflammation by anti-neutrophil cytoplasmic antibodies." J Am Soc Nephrol **17**(5): 1235-1242.
Jiang, W., M. M. Lederman, C. V. Harding, B. Rodriguez, R. J. Mohner and S. F. Sieg (2007). "TLR9 stimulation drives naive B cells to proliferate and to attain enhanced antigen presenting function." Eur J Immunol **37**(8): 2205-2213.
Johnson, B. A., 3rd, D. J. Kahler, B. Baban, P. R. Chandler, B. Kang, M. Shimoda, P. A. Koni, J. Pihkala, B. Vilagos, M. Busslinger, D. H. Munn and A. L. Mellor (2010). "B-lymphoid cells with attributes of dendritic cells regulate T cells via indoleamine 2,3-dioxygenase." Proc Natl Acad Sci U S A **107**(23): 10644-10648.
Johnson, K., T. Hashimshony, C. M. Sawai, J. M. Pongubala, J. A. Skok, I. Aifantis and H. Singh (2008). "Regulation of immunoglobulin light-chain recombination by the transcription factor IRF-4 and the attenuation of interleukin-7 signaling." Immunity **28**(3): 335-345.

Jones, R. B., J. W. Tervaert, T. Hauser, R. Luqmani, M. D. Morgan, C. A. Peh, C. O. Savage, M. Segelmark, V. Tesar, P. van Paassen, D. Walsh, M. Walsh, K. Westman, D. R. Jayne and G. European Vasculitis Study (2010). "Rituximab versus cyclophosphamide in ANCA-associated renal vasculitis." N Engl J Med **363**(3): 211-220.
Kaku, H., K. F. Cheng, Y. Al-Abed and T. L. Rothstein (2014). "A novel mechanism of B cell-mediated immune suppression through CD73 expression and adenosine production." J Immunol **193**(12): 5904-5913.
Katz, S., D. Parker and J. Turk (1974). "B-cell suppression of delayed hypersensitivity reactions." Nature **251**: 550-551.
Keenan, R. A., A. De Riva, B. Corleis, L. Hepburn, S. Licence, T. H. Winkler and I. L. Martensson (2008). "Censoring of autoreactive B cell development by the pre-B cell receptor." Science **321**(5889): 696-699.
Kessel, A., T. Haj, R. Peri, A. Snir, D. Melamed, E. Sabo and E. Toubi (2012). "Human CD19(+)CD25(high) B regulatory cells suppress proliferation of CD4(+) T cells and enhance Foxp3 and CTLA-4 expression in T-regulatory cells." Autoimmun Rev **11**(9): 670-677.
Kessenbrock, K., M. Krumbholz, U. Schonermarck, W. Back, W. L. Gross, Z. Werb, H. J. Grone, V. Brinkmann and D. E. Jenne (2009). "Netting neutrophils in autoimmune small-vessel vasculitis." Nat Med **15**(6): 623-625.
Khan, A. R., E. Hams, A. Floudas, T. Sparwasser, C. T. Weaver and P. G. Fallon (2015). "PD-L1hi B cells are critical regulators of humoral immunity." Nat Commun **6**: 5997.
Khare, S. D., I. Sarosi, X. Z. Xia, S. McCabe, K. Miner, I. Solovyev, N. Hawkins, M. Kelley, D. Chang, G. Van, L. Ross, J. Delaney, L. Wang, D. Lacey, W. J. Boyle and H. Hsu (2000). "Severe B cell hyperplasia and autoimmune disease in TALL-1 transgenic mice." Proc Natl Acad Sci U S A **97**(7): 3370-3375.
Kil, L. P., O. B. Corneth, M. J. de Bruijn, P. S. Asmawidjaja, A. Krause, E. Lubberts, P. F. van Loo and R. W. Hendriks (2015). "Surrogate light chain expression beyond the pre-B cell stage promotes tolerance in a dose-dependent fashion." J Autoimmun **57**: 30-41.
Kim, K. W., B. H. Chung, E. J. Jeon, B. M. Kim, B. S. Choi, C. W. Park, Y. S. Kim, S. G. Cho, M. L. Cho and C. W. Yang (2012). "B cell-associated immune profiles in patients with end-stage renal disease (ESRD)." Exp Mol Med **44**(8): 465-472.
Kim, Y., G. Kim, H. J. Shin, J. W. Hyun, S. H. Kim, E. Lee and H. J. Kim (2018). "Restoration of regulatory B cell deficiency following alemtuzumab therapy in patients with relapsing multiple sclerosis." J Neuroinflammation **15**(1): 300.
Kitching, A. R., P. G. Tipping, J. R. Timoshanko and S. R. Holdsworth (2000). "Endogenous interleukin-10 regulates Th1 responses that induce crescentic glomerulonephritis." Kidney Int **57**(2): 518-525.
Kling, L., U. Benck, A. Breedijk, L. Leikeim, M. Heitzmann, S. Porubsky, B. K. Kramer, B. A. Yard and A. I. Kalsch (2017). "Changes in CD73, CD39 and CD26 expression on T-lymphocytes of ANCA-associated vasculitis patients suggest impairment in adenosine generation and turn-over." Sci Rep **7**(1): 11683.
Klinker, M. W. and S. K. Lundy (2012). "Multiple mechanisms of immune suppression by B lymphocytes." Mol Med **18**: 123-137.

Klinman, D. M., A. K. Yi, S. L. Beaucage, J. Conover and A. M. Krieg (1996). "CpG motifs present in bacteria DNA rapidly induce lymphocytes to secrete interleukin 6, interleukin 12, and interferon gamma." Proc Natl Acad Sci U S A **93**(7): 2879-2883.
Kluger, M. A., A. Ostmann, M. Luig, M. C. Meyer, B. Goerke, H. J. Paust, C. Meyer-Schwesinger, R. A. Stahl, U. Panzer, G. Tiegs and O. M. Steinmetz (2014). "B-cell-derived IL-10 does not vitally contribute to the clinical course of glomerulonephritis." Eur J Immunol **44**(3): 683-693.
Knippenberg, S., E. Peelen, J. Smolders, M. Thewissen, P. Menheere, J. W. Cohen Tervaert, R. Hupperts and J. Damoiseaux (2011). "Reduction in IL-10 producing B cells (Breg) in multiple sclerosis is accompanied by a reduced naive/memory Breg ratio during a relapse but not in remission." J Neuroimmunol **239**(1-2): 80-86.
Kondo, T. and K. Amano (2018). "Era of steroid sparing in the management of immune-mediated inflammatory diseases." Immunological Medicine **41**(1): 6-11.
Krumbholz, M., U. Specks, M. Wick, S. L. Kalled, D. Jenne and E. Meinl (2005). "BAFF is elevated in serum of patients with Wegener's granulomatosis." Journal of autoimmunity **25**(4): 298-302.
Kuravi, S. J., A. Bevins, S. C. Satchell, L. Harper, J. M. Williams, G. E. Rainger, C. O. Savage and S. P. Tull (2012). "Neutrophil serine proteases mediate inflammatory cell recruitment by glomerular endothelium and progression towards dysfunction." Nephrology Dialysis Transplantation **27**(12): 4331-4338.
Land, J., W. H. Abdulahad, J. S. Sanders, C. A. Stegeman, P. Heeringa and A. Rutgers (2016). "Regulatory and effector B cell cytokine production in patients with relapsing granulomatosis with polyangiitis." Arthritis Res Ther **18**: 84.
Langkjaer, A., B. Kristensen, B. E. Hansen, H. Schultz, L. Hegedus and C. H. Nielsen (2012). "B-cell exposure to self-antigen induces IL-10 producing B cells as well as IL-6- and TNF-alpha-producing B-cell subsets in healthy humans." Clin Immunol **145**(1): 1-10.
Lanzavecchia, A. (1985). "Antigen-specific interaction between T and B cells." Nature **314**(6011): 537-539.
Le Texier, L., P. Thebault, A. Lavault, C. Usal, E. Merieau, T. Quillard, B. Charreau, J. P. Soulillou, M. C. Cuturi, S. Brouard and E. Chiffoleau (2011). "Long-term allograft tolerance is characterized by the accumulation of B cells exhibiting an inhibited profile." Am J Transplant **11**(3): 429-438.
Lee, J. H., J. Noh, G. Noh, W. S. Choi, S. Cho and S. S. Lee (2011). "Allergen-specific transforming growth factor-beta-producing CD19+CD5+ regulatory B-cell (Br3) responses in human late eczematous allergic reactions to cow's milk." J Interferon Cytokine Res **31**(5): 441-449.
Lee, J. H., J. Noh, G. Noh, W. S. Choi and S. S. Lee (2011). "IL-10 is predominantly produced by CD19(low)CD5(+) regulatory B cell subpopulation: characterisation of CD19 (high) and CD19(low) subpopulations of CD5(+) B cells." Yonsei Med J **52**(5): 851-855.
Lee, K. M., R. T. Stott, G. Zhao, J. SooHoo, W. Xiong, M. M. Lian, L. Fitzgerald, S. Shi, E. Akrawi, J. Lei, S. Deng, H. Yeh, J. F. Markmann and J. I. Kim (2014). "TGF-beta-producing regulatory B cells induce regulatory T cells and promote transplantation tolerance." Eur J Immunol **44**(6): 1728-1736.
Lemoine, S., A. Morva, P. Youinou and C. Jamin (2011). "Human T cells induce their own regulation through activation of B cells." J Autoimmun **36**(3-4): 228-238.

Lepse, N., W. Abdulahad, A. Rutgers, C. Stegeman, C. Kallenberg and P. Heeringa (2013). "Characterization of regulatory B cells in ANCA-associated vasculitis (AAV)." La Presse Médicale **42**(4): 755-756.
Lepse, N., W. H. Abdulahad, A. Rutgers, C. G. Kallenberg, C. A. Stegeman and P. Heeringa (2014). "Altered B cell balance, but unaffected B cell capacity to limit monocyte activation in anti-neutrophil cytoplasmic antibody-associated vasculitis in remission." Rheumatology (Oxford) **53**(9): 1683-1692.
Li, R., A. Rezk, Y. Miyazaki, E. Hilgenberg, H. Touil, P. Shen, C. S. Moore, L. Michel, F. Althekair, S. Rajasekharan, J. L. Gommerman, A. Prat, S. Fillatreau, A. Bar-Or and B. c. i. M. S. T. Canadian (2015). "Proinflammatory GM-CSF-producing B cells in multiple sclerosis and B cell depletion therapy." Sci Transl Med **7**(310): 310ra166.
Li, X., H. Zhong, W. Bao, N. Boulad, J. Evangelista, M. A. Haider, J. Bussel and K. Yazdanbakhsh (2012). "Defective regulatory B-cell compartment in patients with immune thrombocytopenia." Blood **120**(16): 3318-3325.
Lighaam, L. C., P. A. Unger, D. W. Vredevoogd, D. Verhoeven, E. Vermeulen, A. W. Turksma, A. Ten Brinke, T. Rispens and S. M. van Ham (2018). "In vitro-Induced Human IL-10(+) B Cells Do Not Show a Subset-Defining Marker Signature and Plastically Co-express IL-10 With Pro-Inflammatory Cytokines." Front Immunol **9**: 1913.
Lin, W., L. Jin, H. Chen, Q. Wu, Y. Fei, W. Zheng, Q. Wang, P. Li, Y. Li, W. Zhang, Y. Zhao, X. Zeng and F. Zhang (2014). "B cell subsets and dysfunction of regulatory B cells in IgG4-related diseases and primary Sjogren's syndrome: the similarities and differences." Arthritis Res Ther **16**(3): R118.
Lionaki, S., E. R. Blyth, S. L. Hogan, Y. Hu, B. A. Senior, C. E. Jennette, P. H. Nachman, J. C. Jennette and R. J. Falk (2012). "Classification of antineutrophil cytoplasmic autoantibody vasculitides: the role of antineutrophil cytoplasmic autoantibody specificity for myeloperoxidase or proteinase 3 in disease recognition and prognosis." Arthritis Rheum **64**(10): 3452-3462.
Little, M. A., B. Al-Ani, S. Ren, H. Al-Nuaimi, M. Leite Jr, C. E. Alpers, C. O. Savage and J. S. Duffield (2012). "Anti-proteinase 3 anti-neutrophil cytoplasm autoantibodies recapitulate systemic vasculitis in mice with a humanized immune system." PloS one **7**(1): e28626.
Little, M. A., L. Nazar and K. Farrington (2004). "Outcome in glomerulonephritis due to systemic small vessel vasculitis: effect of functional status and non-vasculitic co-morbidity." Nephrol Dial Transplant **19**(2): 356-364.
Little, M. A., C. L. Smyth, R. Yadav, L. Ambrose, H. T. Cook, S. Nourshargh and C. D. Pusey (2005). "Antineutrophil cytoplasm antibodies directed against myeloperoxidase augment leukocyte-microvascular interactions in vivo." Blood **106**(6): 2050-2058.
Liu, X. and N. Quan (2015). "Immune Cell Isolation from Mouse Femur Bone Marrow." Bio Protoc **5**(20).
Lund, F. E. and T. D. Randall (2010). "Effector and regulatory B cells: modulators of CD4(+) T cell immunity." Nat Rev Immunol **10**(4): 236-247.
Lyons, P. A., T. F. Rayner, S. Trivedi, J. U. Holle, R. A. Watts, D. R. Jayne, B. Baslund, P. Brenchley, A. Bruchfeld and A. N. Chaudhry (2012). "Genetically distinct subsets within ANCA-associated vasculitis." New England Journal of Medicine **367**(3): 214-223.

Ma, L., B. Liu, Z. Jiang and Y. Jiang (2013). "Reduced numbers of regulatory B cells are negatively correlated with disease activity in patients with new-onset rheumatoid arthritis." Clin Rheumatol.
Ma, L., B. Liu, Z. Jiang and Y. Jiang (2014). "Reduced numbers of regulatory B cells are negatively correlated with disease activity in patients with new-onset rheumatoid arthritis." Clin Rheumatol **33**(2): 187-195.
Mackay, F., S. A. Woodcock, P. Lawton, C. Ambrose, M. Baetscher, P. Schneider, J. Tschopp and J. L. Browning (1999). "Mice transgenic for BAFF develop lymphocytic disorders along with autoimmune manifestations." J Exp Med **190**(11): 1697-1710.
Mandapathil, M., B. Hilldorfer, M. J. Szczepanski, M. Czystowska, M. Szajnik, J. Ren, S. Lang, E. K. Jackson, E. Gorelik and T. L. Whiteside (2010). "Generation and accumulation of immunosuppressive adenosine by human CD4+CD25highFOXP3+ regulatory T cells." J Biol Chem **285**(10): 7176-7186.
Mannoor, K., A. Matejuk, Y. Xu, M. Beardall and C. Chen (2012). "Expression of natural autoantibodies in MRL-lpr mice protects from lupus nephritis and improves survival." J Immunol **188**(8): 3628-3638.
Manson, J. J., C. Mauri and M. R. Ehrenstein (2005). "Natural serum IgM maintains immunological homeostasis and prevents autoimmunity." Springer Semin Immunopathol **26**(4): 425-432.
Marie-Cardine, A., F. Divay, I. Dutot, A. Green, A. Perdrix, O. Boyer, N. Contentin, H. Tilly, F. Tron, J. P. Vannier and S. Jacquot (2008). "Transitional B cells in humans: characterization and insight from B lymphocyte reconstitution after hematopoietic stem cell transplantation." Clin Immunol **127**(1): 14-25.
Marinaki, S., I. Neumann, A. I. Kalsch, P. Grimminger, A. Breedijk, R. Birck, W. Schmitt, R. Waldherr, B. A. Yard and F. J. Van Der Woude (2005). "Abnormalities of CD4 T cell subpopulations in ANCA-associated vasculitis." Clin Exp Immunol **140**(1): 181-191.
Marino, E., B. Tan, L. Binge, C. R. Mackay and S. T. Grey (2012). "B-cell cross-presentation of autologous antigen precipitates diabetes." Diabetes **61**(11): 2893-2905.
Maseda, D., K. M. Candando, S. H. Smith, I. Kalampokis, C. T. Weaver, S. E. Plevy, J. C. Poe and T. F. Tedder (2013). "Peritoneal cavity regulatory B cells (B10 cells) modulate IFN-gamma+CD4+ T cell numbers during colitis development in mice." J Immunol **191**(5): 2780-2795.
Matsuda, T., T. Hirano and T. Kishimoto (1988). "Establishment of an interleukin 6 (IL 6)/B cell stimulatory factor 2-dependent cell line and preparation of anti-IL 6 monoclonal antibodies." Eur J Immunol **18**(6): 951-956.
Matsumoto, M., A. Baba, T. Yokota, H. Nishikawa, Y. Ohkawa, H. Kayama, A. Kallies, S. L. Nutt, S. Sakaguchi, K. Takeda, T. Kurosaki and Y. Baba (2014). "Interleukin-10-producing plasmablasts exert regulatory function in autoimmune inflammation." Immunity **41**(6): 1040-1051.
Matsumoto, M., Y. Fujii, A. Baba, M. Hikida, T. Kurosaki and Y. Baba (2011). "The calcium sensors STIM1 and STIM2 control B cell regulatory function through interleukin-10 production." Immunity **34**(5): 703-714.
Matsushita, T., M. Horikawa, Y. Iwata and T. F. Tedder (2010). "Regulatory B cells (B10 cells) and regulatory T cells have independent roles in controlling experimental autoimmune encephalomyelitis initiation and late-phase immunopathogenesis." J Immunol **185**(4): 2240-2252.

Matsushita, T. and T. F. Tedder (2011). "Identifying regulatory B cells (B10 cells) that produce IL-10 in mice." Methods Mol Biol **677**: 99-111.
Matsushita, T., K. Yanaba, J.-D. Bouaziz, M. Fujimoto and T. F. Tedder (2008). "Regulatory B cells inhibit EAE initiation in mice while other B cells promote disease progression." The Journal of clinical investigation **118**(10): 3420.
Matsushita, T., K. Yanaba, J. D. Bouaziz, M. Fujimoto and T. F. Tedder (2008). "Regulatory B cells inhibit EAE initiation in mice while other B cells promote disease progression." J Clin Invest **118**(10): 3420-3430.
Mauri, C. (2010). "Regulation of immunity and autoimmunity by B cells." Curr Opin Immunol **22**(6): 761-767.
Mauri, C., D. Gray, N. Mushtaq and M. Londei (2003). "Prevention of arthritis by interleukin 10-producing B cells." J Exp Med **197**(4): 489-501.
Mauri, C., D. Gray, N. Mushtaq and M. Londei (2003). "Prevention of arthritis by interleukin 10–producing B cells." The Journal of experimental medicine **197**(4): 489-501.
Mauri, C. and M. Menon (2015). "The expanding family of regulatory B cells." Int Immunol **27**(10): 479-486.
Mauri, C. and M. Menon (2017). "Human regulatory B cells in health and disease: therapeutic potential." J Clin Invest **127**(3): 772-779.
Mayet, W. J., E. Csernok, C. Szymkowiak, W. L. Gross and K. H. Meyer zum Buschenfelde (1993). "Human endothelial cells express proteinase 3, the target antigen of anticytoplasmic antibodies in Wegener's granulomatosis." Blood **82**(4): 1221-1229.
McAdoo, S. P., N. Medjeral-Thomas, S. Gopaluni, A. Tanna, N. Mansfield, J. Galliford, M. Griffith, J. Levy, T. D. Cairns, D. Jayne, A. D. Salama and C. D. Pusey (2018). "Long-term follow-up of a combined rituximab and cyclophosphamide regimen in renal anti-neutrophil cytoplasm antibody-associated vasculitis." Nephrol Dial Transplant **33**(5): 899.
McAdoo, S. P., F. W. Tam and C. D. Pusey (2010). "Disease models of rapidly progressive glomerulonephritis." Drug Discovery Today: Disease Models **7**(1): 43-50.
Meng, X., B. Grotsch, Y. Luo, K. X. Knaup, M. S. Wiesener, X. X. Chen, J. Jantsch, S. Fillatreau, G. Schett and A. Bozec (2018). "Hypoxia-inducible factor-1alpha is a critical transcription factor for IL-10-producing B cells in autoimmune disease." Nat Commun **9**(1): 251.
Menon, M., P. A. Blair, D. A. Isenberg and C. Mauri (2016). "A Regulatory Feedback between Plasmacytoid Dendritic Cells and Regulatory B Cells Is Aberrant in Systemic Lupus Erythematosus." Immunity **44**(3): 683-697.
Menon, M., E. Smith, E. Jury and C. Mauri (2017). "323. IMMUNE SIGNATURE OF CD19+CD24HICD38HI REGULATORY B CELLS IN PATIENTS WITH SYSTEMIC LUPUS ERYTHEMATOSUS." Rheumatology **56**(suppl_2): kex062.325-kex062.325.
Menon , M., E. Smith, E. Jury and C. Mauri (2017). "Immune signature CD19+ CD24hi CD38hi Regulatory B cells in patients with systemic lupus erythematosus." Rheumatology **56**(Supplement 2): Abstract 323.
Merkenschlager, J., M. J. Ploquin, U. Eksmond, R. Andargachew, G. Thorborn, A. Filby, M. Pepper, B. Evavold and G. Kassiotis (2016). "Stepwise B-cell-dependent expansion of T helper clonotypes diversifies the T-cell response." Nat Commun **7**: 10281.

Mingari, M., F. Gerosa, G. Carra, R. Accolla, A. Moretta, R. Zubler, T. Waldmann and L. Moretta (1984). "Human interleukin-2 promotes proliferation of activated B cells via surface receptors similar to those of activated T cells."
Mizoguchi, A., E. Mizoguchi, R. N. Smith, F. I. Preffer and A. K. Bhan (1997). "Suppressive role of B cells in chronic colitis of T cell receptor α mutant mice." The Journal of experimental medicine **186**(10): 1749-1756.
Mizoguchi, A., E. Mizoguchi, H. Takedatsu, R. S. Blumberg and A. K. Bhan (2002). "Chronic intestinal inflammatory condition generates IL-10-producing regulatory B cell subset characterized by CD1d upregulation." Immunity **16**(2): 219-230.
Mizoguchi, E., A. Mizoguchi, F. I. Preffer and A. K. Bhan (2000). "Regulatory role of mature B cells in a murine model of inflammatory bowel disease." Int Immunol **12**(5): 597-605.
Molberg, O., S. N. McAdam, R. Korner, H. Quarsten, C. Kristiansen, L. Madsen, L. Fugger, H. Scott, O. Noren, P. Roepstorff, K. E. Lundin, H. Sjostrom and L. M. Sollid (1998). "Tissue transglutaminase selectively modifies gliadin peptides that are recognized by gut-derived T cells in celiac disease." Nat Med **4**(6): 713-717.
Molina, M., L. M. Allende, L. E. Ramos, E. Gutierrez, D. E. Pleguezuelo, E. R. Hernandez, F. Rios, C. Fernandez, M. Praga and E. Morales (2018). "CD19(+) B-Cells, a New Biomarker of Mortality in Hemodialysis Patients." Front Immunol **9**: 1221.
Moran, S. M., P. A. Monach, L. Zgaga, D. Cuthbertson, S. Carette, N. A. Khalidi, C. L. Koening, C. A. Langford, C. A. McAlear, L. Moreland, C. Pagnoux, P. Seo, U. Specks, A. Sreih, J. Wyse, S. R. Ytterberg, P. A. Merkel and M. A. Little (2018). "Urinary soluble CD163 and monocyte chemoattractant protein-1 in the identification of subtle renal flare in anti-neutrophil cytoplasmic antibody-associated vasculitis." Nephrol Dial Transplant.
Morgan, M. D., C. J. Day, K. P. Piper, N. Khan, L. Harper, P. A. Moss and C. O. Savage (2010). "Patients with Wegener's granulomatosis demonstrate a relative deficiency and functional impairment of T-regulatory cells." Immunology **130**(1): 64-73.
Morva, A., S. Lemoine, A. Achour, J. O. Pers, P. Youinou and C. Jamin (2012). "Maturation and function of human dendritic cells are regulated by B lymphocytes." Blood **119**(1): 106-114.
Mosmann, T. R., H. Cherwinski, M. W. Bond, M. A. Giedlin and R. L. Coffman (1986). "Two types of murine helper T cell clone. I. Definition according to profiles of lymphokine activities and secreted proteins." J Immunol **136**(7): 2348-2357.
Mukhtyar, C., R. Lee, D. Brown, D. Carruthers, B. Dasgupta, S. Dubey, O. Flossmann, C. Hall, J. Hollywood, D. Jayne, R. Jones, P. Lanyon, A. Muir, D. Scott, L. Young and R. A. Luqmani (2009). "Modification and validation of the Birmingham Vasculitis Activity Score (version 3)." Ann Rheum Dis **68**(12): 1827-1832.
Mulder, A., C. Stegeman and C. Kallenberg (1995). "Activation of granulocytes by anti-neutrophil cytoplasmic antibodies (ANCA) in Wegener's granulomatosis: a predominant role for the IgG3 subclass of ANCA." Clinical and experimental immunology **101**(2): 227.
Murai, M., O. Turovskaya, G. Kim, R. Madan, C. L. Karp, H. Cheroutre and M. Kronenberg (2009). "Interleukin 10 acts on regulatory T cells to maintain expression of the transcription factor Foxp3 and suppressive function in mice with colitis." Nat Immunol **10**(11): 1178-1184.

Nagai, M., K. Hirayama, I. Ebihara, H. Shimohata, M. Kobayashi and A. Koyama (2011). "Serum levels of BAFF and APRIL in myeloperoxidase anti-neutrophil cytoplasmic autoantibody-associated renal vasculitis: association with disease activity." Nephron Clinical Practice **118**(4): c339-c345.
Nakayamada, S. and Y. Tanaka (2016). "BAFF- and APRIL-targeted therapy in systemic autoimmune diseases." Inflamm Regen **36**: 6.
Natarajan, P., A. Singh, J. T. McNamara, E. Secor, L. A. Guernsey, R. S. Thrall and C. M. Schramm (2012). "Regulatory B cells from hilar lymph nodes of tolerant mice in a murine model of allergic airway disease are CD5+, express TGF-β, and co-localize with CD4+ Foxp3+ T cells." Mucosal immunology **5**(6): 691-701.
Natarajan, P., A. Singh, J. T. McNamara, E. R. Secor, Jr., L. A. Guernsey, R. S. Thrall and C. M. Schramm (2012). "Regulatory B cells from hilar lymph nodes of tolerant mice in a murine model of allergic airway disease are CD5+, express TGF-beta, and co-localize with CD4+Foxp3+ T cells." Mucosal Immunol **5**(6): 691-701.
Naumov, Y. N., K. S. Bahjat, R. Gausling, R. Abraham, M. A. Exley, Y. Koezuka, S. B. Balk, J. L. Strominger, M. Clare-Salzer and S. B. Wilson (2001). "Activation of CD1d-restricted T cells protects NOD mice from developing diabetes by regulating dendritic cell subsets." Proc Natl Acad Sci U S A **98**(24): 13838-13843.
Newell, K. A., A. Asare, A. D. Kirk, T. D. Gisler, K. Bourcier, M. Suthanthiran, W. J. Burlingham, W. H. Marks, I. Sanz and R. I. Lechler (2010). "Identification of a B cell signature associated with renal transplant tolerance in humans." The Journal of clinical investigation **120**(6): 1836.
Noh, J., W. S. Choi, G. Noh and J. H. Lee (2010). "Presence of Foxp3-expressing CD19(+)CD5(+) B Cells in Human Peripheral Blood Mononuclear Cells: Human CD19(+)CD5(+)Foxp3(+) Regulatory B Cell (Breg)." Immune Netw **10**(6): 247-249.
Norvell, A., L. Mandik and J. G. Monroe (1995). "Engagement of the antigen-receptor on immature murine B lymphocytes results in death by apoptosis." J Immunol **154**(9): 4404-4413.
Nouel, A., P. Pochard, Q. Simon, I. Segalen, Y. Le Meur, J. O. Pers and S. Hillion (2015). "B-Cells induce regulatory T cells through TGF-beta/IDO production in A CTLA-4 dependent manner." J Autoimmun **59**: 53-60.
Nova-Lamperti, E., G. Fanelli, P. D. Becker, P. Chana, R. Elgueta, P. C. Dodd, G. M. Lord, G. Lombardi and M. P. Hernandez-Fuentes (2016). "IL-10-produced by human transitional B-cells down-regulates CD86 expression on B-cells leading to inhibition of CD4+T-cell responses." Sci Rep **6**: 20044.
Nowack, R., K. Schwalbe, L.-F. Flores-Suarez, B. Yard and F. J. VAN DER WOUDE (2000). "Upregulation of CD14 and CD18 on monocytes in vitro by antineutrophil cytoplasmic autoantibodies." Journal of the American Society of Nephrology **11**(9): 1639-1646.
O'Reilly, V. P., L. Wong, C. Kennedy, L. A. Elliot, S. O'Meachair, A. M. Coughlan, E. C. O'Brien, M. M. Ryan, D. Sandoval, E. Connolly, G. J. Dekkema, J. Lau, W. H. Abdulahad, J. S. Sanders, P. Heeringa, C. Buckley, C. O'Brien, S. Finn, C. D. Cohen, M. T. Lindemeyer, F. B. Hickey, P. V. O'Hara, C. Feighery, S. M. Moran, G. Mellotte, M. R. Clarkson, A. J. Dorman, P. T. Murray and M. A. Little (2016). "Urinary Soluble CD163 in Active Renal Vasculitis." J Am Soc Nephrol **27**(9): 2906-2916.
O'Sullivan, K. M., C. Y. Lo, S. A. Summers, K. D. Elgass, P. J. McMillan, A. Longano, S. L. Ford, P. Y. Gan, P. G. Kerr, A. R. Kitching and S. R. Holdsworth (2015). "Renal

participation of myeloperoxidase in antineutrophil cytoplasmic antibody (ANCA)-associated glomerulonephritis." Kidney Int **88**(5): 1030-1046.
Ochsenbein, A. F., T. Fehr, C. Lutz, M. Suter, F. Brombacher, H. Hengartner and R. M. Zinkernagel (1999). "Control of early viral and bacterial distribution and disease by natural antibodies." Science **286**(5447): 2156-2159.
Olalekan, S. A., Y. Cao, K. M. Hamel and A. Finnegan (2015). "B cells expressing IFN-gamma suppress Treg-cell differentiation and promote autoimmune experimental arthritis." Eur J Immunol **45**(4): 988-998.
Oleinika, K., E. C. Rosser, D. E. Matei, K. Nistala, A. Bosma, I. Drozdov and C. Mauri (2018). "CD1d-dependent immune suppression mediated by regulatory B cells through modulations of iNKT cells." Nat Commun **9**(1): 684.
Ooi, J. D., J. Chang, M. J. Hickey, D. B. Borza, L. Fugger, S. R. Holdsworth and A. R. Kitching (2012). "The immunodominant myeloperoxidase T-cell epitope induces local cell-mediated injury in antimyeloperoxidase glomerulonephritis." Proc Natl Acad Sci U S A **109**(39): E2615-2624.
Ostmann, A., H. J. Paust, U. Panzer, C. Wegscheid, S. Kapffer, S. Huber, R. A. Flavell, A. Erhardt and G. Tiegs (2013). "Regulatory T cell-derived IL-10 ameliorates crescentic GN." J Am Soc Nephrol **24**(6): 930-942.
Palanichamy, A., J. Barnard, B. Zheng, T. Owen, T. Quach, C. Wei, R. J. Looney, I. Sanz and J. H. Anolik (2009). "Novel human transitional B cell populations revealed by B cell depletion therapy." J Immunol **182**(10): 5982-5993.
Pankhurst, T., G. Nash, J. Williams, R. Colman, A. Hussain and C. Savage (2011). "Immunoglobulin subclass determines ability of immunoglobulin (Ig) G to capture and activate neutrophils presented as normal human IgG or disease-associated anti-neutrophil cytoplasm antibody (ANCA)-IgG." Clinical & Experimental Immunology **164**(2): 218-226.
Papadimitraki, E. D., C. Choulaki, E. Koutala, G. Bertsias, C. Tsatsanis, I. Gergianaki, A. Raptopoulou, H. D. Kritikos, C. Mamalaki, P. Sidiropoulos and D. T. Boumpas (2006). "Expansion of toll-like receptor 9-expressing B cells in active systemic lupus erythematosus: implications for the induction and maintenance of the autoimmune process." Arthritis Rheum **54**(11): 3601-3611.
Pape, K. A., D. M. Catron, A. A. Itano and M. K. Jenkins (2007). "The humoral immune response is initiated in lymph nodes by B cells that acquire soluble antigen directly in the follicles." Immunity **26**(4): 491-502.
Parekh, V. V., D. V. Prasad, P. P. Banerjee, B. N. Joshi, A. Kumar and G. C. Mishra (2003). "B cells activated by lipopolysaccharide, but not by anti-Ig and anti-CD40 antibody, induce anergy in CD8+ T cells: role of TGF-beta 1." J Immunol **170**(12): 5897-5911.
Pasare, C. and R. Medzhitov (2005). "Control of B-cell responses by Toll-like receptors." Nature **438**(7066): 364-368.
Pascual, V., Y.-J. Liu, A. Magalski, O. De Bouteiller, J. Banchereau and J. D. Capra (1994). "Analysis of somatic mutation in five B cell subsets of human tonsil." The Journal of experimental medicine **180**(1): 329-339.
Pascual, V., Y. J. Liu, A. Magalski, O. de Bouteiller, J. Banchereau and J. D. Capra (1994). "Analysis of somatic mutation in five B cell subsets of human tonsil." J Exp Med **180**(1): 329-339.
Pepper, R. J., S. Hamour, K. M. Chavele, S. K. Todd, N. Rasmussen, S. Flint, P. A. Lyons, K. G. Smith, C. D. Pusey, H. T. Cook and A. D. Salama (2013). "Leukocyte

and serum S100A8/S100A9 expression reflects disease activity in ANCA-associated vasculitis and glomerulonephritis." Kidney Int **83**(6): 1150-1158.
Peres, R. S., P. B. Donate, J. Talbot, N. T. Cecilio, P. R. Lobo, C. C. Machado, K. W. A. Lima, R. D. Oliveira, V. Carregaro, H. I. Nakaya, T. M. Cunha, J. C. Alves-Filho, F. Y. Liew, P. Louzada-Junior and F. Q. Cunha (2018). "TGF-beta signalling defect is linked to low CD39 expression on regulatory T cells and methotrexate resistance in rheumatoid arthritis." J Autoimmun **90**: 49-58.
Petro, J. B., R. M. Gerstein, J. Lowe, R. S. Carter, N. Shinners and W. N. Khan (2002). "Transitional type 1 and 2 B lymphocyte subsets are differentially responsive to antigen receptor signaling." J Biol Chem **277**(50): 48009-48019.
Piper, C. J. M., M. G. L. Wilkinson, C. T. Deakin, G. W. Otto, S. Dowle, C. L. Duurland, S. Adams, E. Marasco, E. C. Rosser, A. Radziszewska, R. Carsetti, Y. Ioannou, P. L. Beales, D. Kelberman, D. A. Isenberg, C. Mauri, K. Nistala and L. R. Wedderburn (2018). "CD19(+)CD24(hi)CD38(hi) B Cells Are Expanded in Juvenile Dermatomyositis and Exhibit a Pro-Inflammatory Phenotype After Activation Through Toll-Like Receptor 7 and Interferon-alpha." Front Immunol **9**: 1372.
Pistoia, V. (1997). "Production of cytokines by human B cells in health and disease." Immunol Today **18**(7): 343-350.
Poe, J. C., S. H. Smith, K. M. Haas, K. Yanaba, T. Tsubata, T. Matsushita and T. F. Tedder (2011). "Amplified B lymphocyte CD40 signaling drives regulatory B10 cell expansion in mice." PLoS One **6**(7): e22464.
Popa, E. R., C. A. Stegeman, N. A. Bos, C. G. Kallenberg and J. W. C. Tervaert (1999). "Differential B-and T-cell activation in Wegener's granulomatosis." Journal of allergy and clinical immunology **103**(5): 885-894.
Pulte, E. D., M. J. Broekman, K. E. Olson, J. H. Drosopoulos, J. R. Kizer, N. Islam and A. J. Marcus (2007). "CD39/NTPDase-1 activity and expression in normal leukocytes." Thromb Res **121**(3): 309-317.
Qiu, L., Q. Yu, Y. Zhou, S. Zheng, J. Tao, Q. Jiang and G. Yuan (2018). "Functionally impaired follicular helper T cells induce regulatory B cells and CD14(+) human leukocyte antigen-DR(-) cell differentiation in non-small cell lung cancer." Cancer Sci **109**(12): 3751-3761.
Rao, S. P., J. Sancho, J. Campos-Rivera, P. M. Boutin, P. B. Severy, T. Weeden, S. Shankara, B. L. Roberts and J. M. Kaplan (2012). "Human peripheral blood mononuclear cells exhibit heterogeneous CD52 expression levels and show differential sensitivity to alemtuzumab mediated cytolysis." PLoS One **7**(6): e39416.
Ray, A., S. Basu, C. B. Williams, N. H. Salzman and B. N. Dittel (2012). "A novel IL-10-independent regulatory role for B cells in suppressing autoimmunity by maintenance of regulatory T cells via GITR ligand." J Immunol **188**(7): 3188-3198.
Ray, A. and B. N. Dittel (2010). "Isolation of mouse peritoneal cavity cells." J Vis Exp(35).
Relle, M., H. Cash, N. Schommers, K. Reifenberg, P. R. Galle and A. Schwarting (2013). "PR3 antibodies do not induce renal pathology in a novel PR3-humanized mouse model for Wegener's granulomatosis." Rheumatology international **33**(3): 613-622.
Ren, W., O. Grimsholm, A. I. Bernardi, N. Hook, A. Stern, N. Cavallini and I. L. Martensson (2015). "Surrogate light chain is required for central and peripheral B-cell tolerance and inhibits anti-DNA antibody production by marginal zone B cells." Eur J Immunol **45**(4): 1228-1237.

Rimbert, M., M. Hamidou, C. Braudeau, X. Puechal, L. Teixeira, H. Caillon, A. Neel, M. Audrain, L. Guillevin and R. Josien (2011). "Decreased numbers of blood dendritic cells and defective function of regulatory T cells in antineutrophil cytoplasmic antibody-associated vasculitis." PLoS One **6**(4): e18734.
Rivera, A., C. C. Chen, N. Ron, J. P. Dougherty and Y. Ron (2001). "Role of B cells as antigen-presenting cells in vivo revisited: antigen-specific B cells are essential for T cell expansion in lymph nodes and for systemic T cell responses to low antigen concentrations." Int Immunol **13**(12): 1583-1593.
Rodriguez-Pinto, D. (2005). "B cells as antigen presenting cells." Cell Immunol **238**(2): 67-75.
Rosser, E. C., K. Oleinika, S. Tonon, R. Doyle, A. Bosma, N. A. Carter, K. A. Harris, S. A. Jones, N. Klein and C. Mauri (2014). "Regulatory B cells are induced by gut microbiota-driven interleukin-1beta and interleukin-6 production." Nat Med **20**(11): 1334-1339.
Roth, A. J., J. D. Ooi, J. J. Hess, M. M. van Timmeren, E. A. Berg, C. E. Poulton, J. McGregor, M. Burkart, S. L. Hogan, Y. Hu, W. Winnik, P. H. Nachman, C. A. Stegeman, J. Niles, P. Heeringa, A. R. Kitching, S. Holdsworth, J. C. Jennette, G. A. Preston and R. J. Falk (2013). "Epitope specificity determines pathogenicity and detectability in ANCA-associated vasculitis." J Clin Invest **123**(4): 1773-1783.
Roubaud-Baudron, C., C. Pagnoux, N. Meaux-Ruault, A. Grasland, A. Zoulim, L. E. G. J, A. Prud'homme, B. Bienvenu, M. de Menthon, S. Camps, L. E. G. V, A. Aouba, P. Cohen, L. Mouthon, L. Guillevin and G. French Vasculitis Study (2012). "Rituximab maintenance therapy for granulomatosis with polyangiitis and microscopic polyangiitis." J Rheumatol **39**(1): 125-130.
Rubtsova, K., A. V. Rubtsov, M. P. Cancro and P. Marrack (2015). "Age-Associated B Cells: A T-bet-Dependent Effector with Roles in Protective and Pathogenic Immunity." J Immunol **195**(5): 1933-1937.
Ruth, A. J., A. R. Kitching, R. Y. Kwan, D. Odobasic, J. D. Ooi, J. R. Timoshanko, M. J. Hickey and S. R. Holdsworth (2006). "Anti-neutrophil cytoplasmic antibodies and effector CD4+ cells play nonredundant roles in anti-myeloperoxidase crescentic glomerulonephritis." J Am Soc Nephrol **17**(7): 1940-1949.
Rydyznski, C., K. A. Daniels, E. P. Karmele, T. R. Brooks, S. E. Mahl, M. T. Moran, C. Li, R. Sutiwisesak, R. M. Welsh and S. N. Waggoner (2015). "Generation of cellular immune memory and B-cell immunity is impaired by natural killer cells." Nat Commun **6**: 6375.
Sakai, R., T. Kondo, T. Kurasawa, E. Nishi, A. Okuyama, K. Chino, A. Shibata, Y. Okada, H. Takei, H. Nagasawa and K. Amano (2017). "Current clinical evidence of tocilizumab for the treatment of ANCA-associated vasculitis: a prospective case series for microscopic polyangiitis in a combination with corticosteroids and literature review." Clin Rheumatol **36**(10): 2383-2392.
Sakkas, L. I., D. Daoussis, A. Mavropoulos, S. N. Liossis and D. P. Bogdanos (2018). "Regulatory B cells: New players in inflammatory and autoimmune rheumatic diseases." Semin Arthritis Rheum.
Salama, A. D. and M. A. Little (2012). "Animal models of ANCA associated vasculitis." Current opinion in rheumatology **24**(1): 1.
Sanders, J. S., C. A. Stegeman and C. G. Kallenberg (2003). "The Th1 and Th2 paradigm in ANCA-associated vasculitis." Kidney Blood Press Res **26**(4): 215-220.

Sanz, I., C. Wei, F. E. Lee and J. Anolik (2008). "Phenotypic and functional heterogeneity of human memory B cells." Semin Immunol **20**(1): 67-82.
Sater, R. A., P. C. Sandel and J. G. Monroe (1998). "B cell receptor-induced apoptosis in primary transitional murine B cells: signaling requirements and modulation by T cell help." Int Immunol **10**(11): 1673-1682.
Sato, S., M. Fujimoto, M. Hasegawa and K. Takehara (2004). "Altered blood B lymphocyte homeostasis in systemic sclerosis: expanded naive B cells and diminished but activated memory B cells." Arthritis Rheum **50**(6): 1918-1927.
Saze, Z., P. J. Schuler, C. S. Hong, D. Cheng, E. K. Jackson and T. L. Whiteside (2013). "Adenosine production by human B cells and B cell-mediated suppression of activated T cells." Blood **122**(1): 9-18.
Schindelin, J., I. Arganda-Carreras, E. Frise, V. Kaynig, M. Longair, T. Pietzsch, S. Preibisch, C. Rueden, S. Saalfeld, B. Schmid, J. Y. Tinevez, D. J. White, V. Hartenstein, K. Eliceiri, P. Tomancak and A. Cardona (2012). "Fiji: an open-source platform for biological-image analysis." Nat Methods **9**(7): 676-682.
Schlieben, D. J., S. M. Korbet, R. E. Kimura, M. M. Schwartz and E. J. Lewis (2005). "Pulmonary-renal syndrome in a newborn with placental transmission of ANCAs." Am J Kidney Dis **45**(4): 758-761.
Schmitt, W. H., C. Heesen, E. Csernok, A. Rautmann and W. L. Gross (1992). "Elevated serum levels of soluble interleukin-2 receptor in patients with Wegener's granulomatosis. Association with disease activity." Arthritis Rheum **35**(9): 1088-1096.
Schonermarck, U., E. Csernok, A. Trabandt, H. Hansen and W. L. Gross (2000). "Circulating cytokines and soluble CD23, CD26 and CD30 in ANCA-associated vasculitides." Clin Exp Rheumatol **18**(4): 457-463.
Schreiber, A., H. Xiao, R. J. Falk and J. C. Jennette (2006). "Bone marrow-derived cells are sufficient and necessary targets to mediate glomerulonephritis and vasculitis induced by anti-myeloperoxidase antibodies." J Am Soc Nephrol **17**(12): 3355-3364.
Schreiber, A., H. Xiao, J. C. Jennette, W. Schneider, F. C. Luft and R. Kettritz (2009). "C5a receptor mediates neutrophil activation and ANCA-induced glomerulonephritis." Journal of the American Society of Nephrology **20**(2): 289-298.
Seifert, M. and R. Kuppers (2016). "Human memory B cells." Leukemia **30**(12): 2283-2292.
Shalapour, S., J. Font-Burgada, G. Di Caro, Z. Zhong, E. Sanchez-Lopez, D. Dhar, G. Willimsky, M. Ammirante, A. Strasner, D. E. Hansel, C. Jamieson, C. J. Kane, T. Klatte, P. Birner, L. Kenner and M. Karin (2015). "Immunosuppressive plasma cells impede T-cell-dependent immunogenic chemotherapy." Nature **521**(7550): 94-98.
Shanebeck, K. D., C. R. Maliszewski, M. K. Kennedy, K. S. Picha, C. A. Smith, R. G. Goodwin and K. H. Grabstein (1995). "Regulation of murine B cell growth and differentiation by CD30 ligand." European journal of immunology **25**(8): 2147-2153.
Shen, P. and S. Fillatreau (2015). "Suppressive functions of B cells in infectious diseases." Int Immunol **27**(10): 513-519.
Shen, P., T. Roch, V. Lampropoulou, R. A. O'Connor, U. Stervbo, E. Hilgenberg, S. Ries, V. D. Dang, Y. Jaimes, C. Daridon, R. Li, L. Jouneau, P. Boudinot, S. Wilantri, I. Sakwa, Y. Miyazaki, M. D. Leech, R. C. McPherson, S. Wirtz, M. Neurath, K. Hoehlig, E. Meinl, A. Grutzkau, J. R. Grun, K. Horn, A. A. Kuhl, T. Dorner, A. Bar-Or, S. H. E. Kaufmann, S. M. Anderton and S. Fillatreau (2014). "IL-35-producing B cells are critical regulators of immunity during autoimmune and infectious diseases." Nature **507**(7492): 366-370.

Shi, Y., K. Agematsu, H. D. Ochs and K. Sugane (2003). "Functional analysis of human memory B-cell subpopulations: IgD+CD27+ B cells are crucial in secondary immune response by producing high affinity IgM." Clin Immunol **108**(2): 128-137.
Shinkai, Y., G. Rathbun, K. P. Lam, E. M. Oltz, V. Stewart, M. Mendelsohn, J. Charron, M. Datta, F. Young, A. M. Stall and et al. (1992). "RAG-2-deficient mice lack mature lymphocytes owing to inability to initiate V(D)J rearrangement." Cell **68**(5): 855-867.
Silva, H. M., M. C. Takenaka, P. M. Moraes-Vieira, S. M. Monteiro, M. O. Hernandez, W. Chaara, A. Six, F. Agena, P. Sesterheim, F. M. Barbe-Tuana, D. Saitovitch, F. Lemos, J. Kalil and V. Coelho (2012). "Preserving the B-cell compartment favors operational tolerance in human renal transplantation." Mol Med **18**: 733-743.
Simon, Q., J. O. Pers, D. Cornec, L. Le Pottier, R. A. Mageed and S. Hillion (2016). "In-depth characterization of CD24(high)CD38(high) transitional human B cells reveals different regulatory profiles." J Allergy Clin Immunol **137**(5): 1577-1584 e1510.
Sims, G. P., R. Ettinger, Y. Shirota, C. H. Yarboro, G. G. Illei and P. E. Lipsky (2005). "Identification and characterization of circulating human transitional B cells." Blood **105**(11): 4390-4398.
Sonoda, K. H. and J. Stein-Streilein (2002). "CD1d on antigen-transporting APC and splenic marginal zone B cells promotes NKT cell-dependent tolerance." Eur J Immunol **32**(3): 848-857.
Stegeman, C. A., J. W. Tervaert, W. J. Sluiter, W. L. Manson, P. E. de Jong and C. G. Kallenberg (1994). "Association of chronic nasal carriage of Staphylococcus aureus and higher relapse rates in Wegener granulomatosis." Ann Intern Med **120**(1): 12-17.
Steinmetz, O. M., J. Velden, U. Kneissler, M. Marx, A. Klein, U. Helmchen, R. A. Stahl and U. Panzer (2008). "Analysis and classification of B-cell infiltrates in lupus and ANCA-associated nephritis." Kidney Int **74**(4): 448-457.
Stoehr, A. D., C. T. Schoen, M. M. Mertes, S. Eiglmeier, V. Holecska, A. K. Lorenz, T. Schommartz, A. L. Schoen, C. Hess, A. Winkler, H. Wardemann and M. Ehlers (2011). "TLR9 in peritoneal B-1b cells is essential for production of protective self-reactive IgM to control Th17 cells and severe autoimmunity." J Immunol **187**(6): 2953-2965.
Stone, J. H., P. A. Merkel, R. Spiera, P. Seo, C. A. Langford, G. S. Hoffman, C. G. Kallenberg, E. W. St Clair, A. Turkiewicz, N. K. Tchao, L. Webber, L. Ding, L. P. Sejismundo, K. Mieras, D. Weitzenkamp, D. Ikle, V. Seyfert-Margolis, M. Mueller, P. Brunetta, N. B. Allen, F. C. Fervenza, D. Geetha, K. A. Keogh, E. Y. Kissin, P. A. Monach, T. Peikert, C. Stegeman, S. R. Ytterberg, U. Specks and R.-I. R. Group (2010). "Rituximab versus cyclophosphamide for ANCA-associated vasculitis." N Engl J Med **363**(3): 221-232.
Stone, J. H., P. A. Merkel, R. Spiera, P. Seo, C. A. Langford, G. S. Hoffman, C. G. Kallenberg, E. W. St. Clair, A. Turkiewicz and N. K. Tchao (2010). "Rituximab versus cyclophosphamide for ANCA-associated vasculitis." New England Journal of Medicine **363**(3): 221-232.
Strasser, A., S. Whittingham, D. L. Vaux, M. L. Bath, J. M. Adams, S. Cory and A. W. Harris (1991). "Enforced BCL2 expression in B-lymphoid cells prolongs antibody responses and elicits autoimmune disease." Proc Natl Acad Sci U S A **88**(19): 8661-8665.

Summers, S. A., O. M. Steinmetz, P. Y. Gan, J. D. Ooi, D. Odobasic, A. R. Kitching and S. R. Holdsworth (2011). "Toll-like receptor 2 induces Th17 myeloperoxidase autoimmunity while Toll-like receptor 9 drives Th1 autoimmunity in murine vasculitis." Arthritis Rheum **63**(4): 1124-1135.
Summers, S. A., O. M. Steinmetz, M. Li, J. Y. Kausman, T. Semple, K. L. Edgtton, D. B. Borza, H. Braley, S. R. Holdsworth and A. R. Kitching (2009). "Th1 and Th17 cells induce proliferative glomerulonephritis." J Am Soc Nephrol **20**(12): 2518-2524.
Summers, S. A., B. S. van der Veen, K. M. O'Sullivan, P. Y. Gan, J. D. Ooi, P. Heeringa, S. C. Satchell, P. W. Mathieson, M. A. Saleem, K. Visvanathan, S. R. Holdsworth and A. R. Kitching (2010). "Intrinsic renal cell and leukocyte-derived TLR4 aggravate experimental anti-MPO glomerulonephritis." Kidney Int **78**(12): 1263-1274.
Sun, J., J. Wang, E. Pefanis, J. Chao, G. Rothschild, I. Tachibana, J. K. Chen, Ivanov, II, R. Rabadan, Y. Takeda and U. Basu (2015). "Transcriptomics Identify CD9 as a Marker of Murine IL-10-Competent Regulatory B Cells." Cell Rep **13**(6): 1110-1117.
Suryani, S., D. A. Fulcher, B. Santner-Nanan, R. Nanan, M. Wong, P. J. Shaw, J. Gibson, A. Williams and S. G. Tangye (2010). "Differential expression of CD21 identifies developmentally and functionally distinct subsets of human transitional B cells." Blood **115**(3): 519-529.
Tadema, H., W. H. Abdulahad, N. Lepse, C. A. Stegeman, C. G. Kallenberg and P. Heeringa (2011). "Bacterial DNA motifs trigger ANCA production in ANCA-associated vasculitis in remission." Rheumatology (Oxford) **50**(4): 689-696.
Tam, F. W., J. S. Sanders, A. George, T. Hammad, C. Miller, T. Dougan, H. T. Cook, C. G. Kallenberg, G. Gaskin, J. B. Levy and C. D. Pusey (2004). "Urinary monocyte chemoattractant protein-1 (MCP-1) is a marker of active renal vasculitis." Nephrol Dial Transplant **19**(11): 2761-2768.
Tang, Y., Q. Jiang, Y. Ou, F. Zhang, K. Qing, Y. Sun, W. Lu, H. Zhu, F. Gong, P. Lei and G. Shen (2016). "BIP induces mice CD19(hi) regulatory B cells producing IL-10 and highly expressing PD-L1, FasL." Mol Immunol **69**: 44-51.
Tarique, M., H. Naz, S. V. Kurra, C. Saini, R. A. Naqvi, R. Rai, M. Suhail, N. Khanna, D. N. Rao and A. Sharma (2018). "Interleukin-10 Producing Regulatory B Cells Transformed CD4(+)CD25(-) Into Tregs and Enhanced Regulatory T Cells Function in Human Leprosy." Front Immunol **9**: 1636.
Taylor, A., M. Akdis, A. Joss, T. Akkoc, R. Wenig, M. Colonna, I. Daigle, E. Flory, K. Blaser and C. A. Akdis (2007). "IL-10 inhibits CD28 and ICOS costimulations of T cells via src homology 2 domain-containing protein tyrosine phosphatase 1." J Allergy Clin Immunol **120**(1): 76-83.
Tedder, T. F. (2015). "B10 cells: a functionally defined regulatory B cell subset." J Immunol **194**(4): 1395-1401.
Terrier, B., C. Pagnoux, E. Perrodeau, A. Karras, C. Khouatra, O. Aumaitre, P. Cohen, O. Decaux, H. Desmurs-Clavel, F. Maurier, P. Gobert, T. Quemeneur, C. Blanchard-Delaunay, B. Bonnotte, P. L. Carron, E. Daugas, M. Ducret, P. Godmer, M. Hamidou, O. Lidove, N. Limal, X. Puechal, L. Mouthon, P. Ravaud, L. Guillevin and G. French Vasculitis Study (2018). "Long-term efficacy of remission-maintenance regimens for ANCA-associated vasculitides." Ann Rheum Dis **77**(8): 1150-1156.
Tervaert, J. W., J. D. Elema and C. G. Kallenberg (1990). "Clinical and histopathological association of 29kD-ANCA and MPO-ANCA." APMIS Suppl **19**: 35.

Thai, T. H., D. P. Calado, S. Casola, K. M. Ansel, C. Xiao, Y. Xue, A. Murphy, D. Frendewey, D. Valenzuela, J. L. Kutok, M. Schmidt-Supprian, N. Rajewsky, G. Yancopoulos, A. Rao and K. Rajewsky (2007). "Regulation of the germinal center response by microRNA-155." Science **316**(5824): 604-608.
Thiel, J., M. Rizzi, M. Engesser, A. K. Dufner, A. Troilo, R. Lorenzetti, R. E. Voll and N. Venhoff (2017). "B cell repopulation kinetics after rituximab treatment in ANCA-associated vasculitides compared to rheumatoid arthritis, and connective tissue diseases: a longitudinal observational study on 120 patients." Arthritis Res Ther **19**(1): 101.
Thiel, J., U. Salzer, F. Hässler, N. M. Effelsberg, C. Hentze, H. Sic, M. Bartsch, N. Miehle, H. H. Peter and K. Warnatz (2013). "B cell homeostasis is disturbed by immunosuppressive therapies in patients with ANCA-associated vasculitides." Autoimmunity(0): 1-10.
Thompson, S. A., J. L. Jones, A. L. Cox, D. A. Compston and A. J. Coles (2010). "B-cell reconstitution and BAFF after alemtuzumab (Campath-1H) treatment of multiple sclerosis." J Clin Immunol **30**(1): 99-105.
Tian, J., D. Zekzer, L. Hanssen, Y. Lu, A. Olcott and D. L. Kaufman (2001). "Lipopolysaccharide-activated B cells down-regulate Th1 immunity and prevent autoimmune diabetes in nonobese diabetic mice." The Journal of Immunology **167**(2): 1081-1089.
Todd, S., S. Henderson, R. Pepper, J. Draibe and A. D. Salama (2015). Cytokine profiles of B Cells conditioned to produce IL-10 in ANCA Associated vasculitis patients and controls, and their functional immune effects. Nephron.
Todd, S., R. Pepper, A. Tanna, C. Mauri and A. Salama (2013). B regulatory cells are numerically but not functionally impaired in AAV. La Presse Medicale.
Todd, S. K., R. J. Pepper, J. Draibe, A. Tanna, C. D. Pusey, C. Mauri and A. D. Salama (2014). "Regulatory B cells are numerically but not functionally deficient in anti-neutrophil cytoplasm antibody-associated vasculitis." Rheumatology (Oxford) **53**(9): 1693-1703.
Tretter, T., R. K. Venigalla, V. Eckstein, R. Saffrich, S. Sertel, A. D. Ho and H. M. Lorenz (2008). "Induction of CD4+ T-cell anergy and apoptosis by activated human B cells." Blood **112**(12): 4555-4564.
Tuin, J., J. Sanders, A. de Joode and C. Stegeman (2012). "Pregnancy in women diagnosed with Antineutrophil cytoplasmic antibody–associated vasculitis: Outcome for the mother and the child." Arthritis Care & Research **64**(4): 539-545.
Turnbull, J. and L. Harper (2009). "Adverse effects of therapy for ANCA-associated vasculitis." Best Pract Res Clin Rheumatol **23**(3): 391-401.
Unizony, S., N. Lim, D. J. Phippard, V. J. Carey, E. M. Miloslavsky, N. K. Tchao, D. Ikle, A. L. Asare, P. A. Merkel, P. A. Monach, P. Seo, E. W. St Clair, C. A. Langford, R. Spiera, G. S. Hoffman, C. G. Kallenberg, U. Specks and J. H. Stone (2015). "Peripheral CD5+ B cells in antineutrophil cytoplasmic antibody-associated vasculitis." Arthritis Rheumatol **67**(2): 535-544.
Unizony, S., M. Villarreal, E. M. Miloslavsky, N. Lu, P. A. Merkel, R. Spiera, P. Seo, C. A. Langford, G. S. Hoffman, C. M. Kallenberg, E. W. St Clair, D. Ikle, N. K. Tchao, L. Ding, P. Brunetta, H. K. Choi, P. A. Monach, F. Fervenza, J. H. Stone, U. Specks and R.-I. R. Group (2016). "Clinical outcomes of treatment of anti-neutrophil cytoplasmic antibody (ANCA)-associated vasculitis based on ANCA type." Ann Rheum Dis **75**(6): 1166-1169.

van de Veen, W., B. Stanic, G. Yaman, M. Wawrzyniak, S. Sollner, D. G. Akdis, B. Ruckert, C. A. Akdis and M. Akdis (2013). "IgG4 production is confined to human IL-10-producing regulatory B cells that suppress antigen-specific immune responses." J Allergy Clin Immunol **131**(4): 1204-1212.
van der Geld, Y. M., T. Hellmark, D. Selga, P. Heeringa, M. G. Huitema, P. C. Limburg and C. G. Kallenberg (2007). "Rats and mice immunised with chimeric human/mouse proteinase 3 produce autoantibodies to mouse Pr3 and rat granulocytes." Annals of the rheumatic diseases **66**(12): 1679-1682.
Varani, J., I. Ginsburg, L. Schuger, D. Gibbs, J. Bromberg, K. Johnson, U. Ryan and P. Ward (1989). "Endothelial cell killing by neutrophils. Synergistic interaction of oxygen products and proteases." The American journal of pathology **135**(3): 435.
Vas, J., C. Gronwall and G. J. Silverman (2013). "Fundamental roles of the innate-like repertoire of natural antibodies in immune homeostasis." Front Immunol **4**: 4.
Venhoff, N., N. M. Effelsberg, U. Salzer, K. Warnatz, H. H. Peter, D. Lebrecht, M. Schlesier, R. E. Voll and J. Thiel (2012). "Impact of rituximab on immunoglobulin concentrations and B cell numbers after cyclophosphamide treatment in patients with ANCA-associated vasculitides." PLoS One **7**(5): e37626.
Venhoff, N., L. Niessen, M. Kreuzaler, A. G. Rolink, F. Hassler, M. Rizzi, R. E. Voll and J. Thiel (2014). "Reconstitution of the peripheral B lymphocyte compartment in patients with ANCA-associated vasculitides treated with rituximab for relapsing or refractory disease." Autoimmunity **47**(6): 401-408.
Vignali, D. A., L. W. Collison and C. J. Workman (2008). "How regulatory T cells work." Nat Rev Immunol **8**(7): 523-532.
Vigorito, E., K. L. Perks, C. Abreu-Goodger, S. Bunting, Z. Xiang, S. Kohlhaas, P. P. Das, E. A. Miska, A. Rodriguez, A. Bradley, K. G. Smith, C. Rada, A. J. Enright, K. M. Toellner, I. C. Maclennan and M. Turner (2007). "microRNA-155 regulates the generation of immunoglobulin class-switched plasma cells." Immunity **27**(6): 847-859.
Voswinkel, J., G. Assmann, G. Held, S. Pitann, W. L. Gross, K. Holl-Ulrich, K. Herlyn and A. Mueller (2008). "Single cell analysis of B lymphocytes from Wegener's granulomatosis: B cell receptors display affinity maturation within the granulomatous lesions." Clin Exp Immunol **154**(3): 339-345.
Walsh, M., A. Chaudhry and D. Jayne (2008). "Long-term follow-up of relapsing/refractory anti-neutrophil cytoplasm antibody associated vasculitis treated with the lymphocyte depleting antibody alemtuzumab (CAMPATH-1H)." Ann Rheum Dis **67**(9): 1322-1327.
Walsh, M., O. Flossmann, A. Berden, K. Westman, P. Höglund, C. Stegeman and D. Jayne (2012). "Risk factors for relapse of antineutrophil cytoplasmic antibody–associated vasculitis." Arthritis & Rheumatism **64**(2): 542-548.
Wang, R. X., C. R. Yu, I. M. Dambuza, R. M. Mahdi, M. B. Dolinska, Y. V. Sergeev, P. T. Wingfield, S. H. Kim and C. E. Egwuagu (2014). "Interleukin-35 induces regulatory B cells that suppress autoimmune disease." Nat Med **20**(6): 633-641.
Wang, W. W., X. L. Yuan, H. Chen, G. H. Xie, Y. H. Ma, Y. X. Zheng, Y. L. Zhou and L. S. Shen (2015). "CD19+CD24hiCD38hiBregs involved in downregulate helper T cells and upregulate regulatory T cells in gastric cancer." Oncotarget **6**(32): 33486-33499.

Wang, X., Y. Zhu, M. Zhang, H. Wang, Y. Jiang and P. Gao (2016). "Ulcerative Colitis Is Characterized by a Decrease in Regulatory B Cells." J Crohns Colitis **10**(10): 1212-1223.
Wardemann, H., S. Yurasov, A. Schaefer, J. W. Young, E. Meffre and M. C. Nussenzweig (2003). "Predominant autoantibody production by early human B cell precursors." Science **301**(5638): 1374-1377.
Watanabe, R., N. Ishiura, H. Nakashima, Y. Kuwano, H. Okochi, K. Tamaki, S. Sato, T. F. Tedder and M. Fujimoto (2010). "Regulatory B cells (B10 cells) have a suppressive role in murine lupus: CD19 and B10 cell deficiency exacerbates systemic autoimmunity." J Immunol **184**(9): 4801-4809.
Watts, R. A., J. Mooney, J. Skinner, D. G. Scott and A. J. MacGregor (2012). "The contrasting epidemiology of granulomatosis with polyangiitis (Wegener's) and microscopic polyangiitis." Rheumatology **51**(5): 926-931.
Watts, R. A. and D. G. Scott (2012). "ANCA vasculitis: to lump or split?" Rheumatology **51**(12): 2115-2117.
Weidner, S., M. Carl, R. Riess and H. D. Rupprecht (2004). "Histologic analysis of renal leukocyte infiltration in antineutrophil cytoplasmic antibody-associated vasculitis: importance of monocyte and neutrophil infiltration in tissue damage." Arthritis Rheum **50**(11): 3651-3657.
Wermeling, F., S. M. Lind, E. D. Jordo, S. L. Cardell and M. C. Karlsson (2010). "Invariant NKT cells limit activation of autoreactive CD1d-positive B cells." J Exp Med **207**(5): 943-952.
Whalen, J. D., E. L. Lechman, C. A. Carlos, K. Weiss, I. Kovesdi, J. C. Glorioso, P. D. Robbins and C. H. Evans (1999). "Adenoviral transfer of the viral IL-10 gene periarticularly to mouse paws suppresses development of collagen-induced arthritis in both injected and uninjected paws." J Immunol **162**(6): 3625-3632.
Wilde, B., S. Dolff, X. Cai, C. Specker, J. Becker, M. Totsch, U. Costabel, J. Durig, A. Kribben, J. W. Tervaert, K. W. Schmid and O. Witzke (2009). "CD4+CD25+ T-cell populations expressing CD134 and GITR are associated with disease activity in patients with Wegener's granulomatosis." Nephrol Dial Transplant **24**(1): 161-171.
Wilde, B., Z. Jiqiao, S. Dolff, A. Bienholz, A. Kribben, J. W. C. Tervaert and O. Witzke (2016). "Granzyme B producing B-cells have immunoregulatory function and are diminished in patients with ANCA-vasculitis." Nephrol Dial Transplant **31**(Supplement 1): i103.
Wilde, B., M. Thewissen, P. Van Paassen, M. Hilhorst, J. Damoiseaux, O. Witzke and J. Cohen Tervaert (2013). "IL-10 producing regulatory B-cells are diminished in ANCA-associated vasculitis." La Presse Médicale **42**(4): 758-759.
Wilde, B., O. Witzke and J. W. Cohen Tervaert (2014). "Rituximab and B-cell return in ANCA-associated vasculitis." Am J Kidney Dis **63**(6): 1066.
Wolf, S. D., B. N. Dittel, F. Hardardottir and C. A. Janeway (1996). "Experimental autoimmune encephalomyelitis induction in genetically B cell–deficient mice." The Journal of experimental medicine **184**(6): 2271-2278.
Xiang, F. F., J. M. Zhu, X. S. Cao, B. Shen, J. Z. Zou, Z. H. Liu, H. Zhang, J. Teng, H. Liu and X. Q. Ding (2016). "Lymphocyte depletion and subset alteration correlate to renal function in chronic kidney disease patients." Ren Fail **38**(1): 7-14.
Xiao, H., D. Ciavatta, D. L. Aylor, P. Hu, F. P. de Villena, R. J. Falk and J. C. Jennette (2013). "Genetically determined severity of anti-myeloperoxidase glomerulonephritis." Am J Pathol **182**(4): 1219-1226.

Xiao, H., D. J. Dairaghi, J. P. Powers, L. S. Ertl, T. Baumgart, Y. Wang, L. C. Seitz, M. E. Penfold, L. Gan, P. Hu, B. Lu, N. P. Gerard, C. Gerard, T. J. Schall, J. C. Jaen, R. J. Falk and J. C. Jennette (2014). "C5a receptor (CD88) blockade protects against MPO-ANCA GN." J Am Soc Nephrol **25**(2): 225-231.
Xiao, H., P. Heeringa, P. Hu, Z. Liu, M. Zhao, Y. Aratani, N. Maeda, R. J. Falk and J. C. Jennette (2002). "Antineutrophil cytoplasmic autoantibodies specific for myeloperoxidase cause glomerulonephritis and vasculitis in mice." J Clin Invest **110**(7): 955-963.
Xiao, H., P. Heeringa, P. Q. Hu, Z. Liu and R. J. Falk (2003). "Neutrophils but not T lymphocytes are important in the induction of necrotizing and crescentic glomerulonephritis by antineutrophil cytoplasmic autoantibodies specific for myeloperoxidase (MPO-ANCA) in mice." Journal of the American Society of Nephrology **14**: 634A-634A.
Xiao, H., P. Heeringa, Z. Liu, D. Huugen, P. Hu, N. Maeda, R. J. Falk and J. C. Jennette (2005). "The role of neutrophils in the induction of glomerulonephritis by anti-myeloperoxidase antibodies." Am J Pathol **167**(1): 39-45.
Xiao, H., A. Schreiber, P. Heeringa, R. J. Falk and J. C. Jennette (2007). "Alternative complement pathway in the pathogenesis of disease mediated by anti-neutrophil cytoplasmic autoantibodies." The American journal of pathology **170**(1): 52-64.
Xiao, H., A. Schreiber, P. Heeringa, R. J. Falk and J. C. Jennette (2007). "Alternative complement pathway in the pathogenesis of disease mediated by anti-neutrophil cytoplasmic autoantibodies." Am J Pathol **170**(1): 52-64.
Yanaba, K., J.-D. Bouaziz, K. M. Haas, J. C. Poe, M. Fujimoto and T. F. Tedder (2008). "A Regulatory B Cell Subset with a Unique CD1d< sup> hi</sup> CD5< sup>+</sup> Phenotype Controls T Cell-Dependent Inflammatory Responses." Immunity **28**(5): 639-650.
Yanaba, K., J.-D. Bouaziz, T. Matsushita, T. Tsubata and T. F. Tedder (2009). "The development and function of regulatory B cells expressing IL-10 (B10 cells) requires antigen receptor diversity and TLR signals." The Journal of Immunology **182**(12): 7459-7472.
Yanaba, K., J. D. Bouaziz, K. M. Haas, J. C. Poe, M. Fujimoto and T. F. Tedder (2008). "A regulatory B cell subset with a unique CD1dhiCD5+ phenotype controls T cell-dependent inflammatory responses." Immunity **28**(5): 639-650.
Yanaba, K., J. D. Bouaziz, T. Matsushita, T. Tsubata and T. F. Tedder (2009). "The development and function of regulatory B cells expressing IL-10 (B10 cells) requires antigen receptor diversity and TLR signals." J Immunol **182**(12): 7459-7472.
Yang, M., L. Sun, S. Wang, K. H. Ko, H. Xu, B. J. Zheng, X. Cao and L. Lu (2010). "Novel function of B cell-activating factor in the induction of IL-10-producing regulatory B cells." J Immunol **184**(7): 3321-3325.
Yim, S. H., Y. J. Chung, E. H. Jin, S. C. Shim, J. Y. Kim, Y. S. Kim, H. J. Hu, S. H. Shin, H. O. Pae, M. Zouali and H. T. Chung (2011). "The potential role of VPREB1 gene copy number variation in susceptibility to rheumatoid arthritis." Mol Immunol **48**(11): 1338-1343.
Yoshizaki, A., T. Miyagaki, D. J. DiLillo, T. Matsushita, M. Horikawa, E. I. Kountikov, R. Spolski, J. C. Poe, W. J. Leonard and T. F. Tedder (2012). "Regulatory B cells control T-cell autoimmunity through IL-21-dependent cognate interactions." Nature **491**(7423): 264-268.

Zarek, P. E., C. T. Huang, E. R. Lutz, J. Kowalski, M. R. Horton, J. Linden, C. G. Drake and J. D. Powell (2008). "A2A receptor signaling promotes peripheral tolerance by inducing T-cell anergy and the generation of adaptive regulatory T cells." Blood **111**(1): 251-259.
Zeng, S. G., Y. G. Ghnewa, V. P. O'Reilly, V. G. Lyons, A. Atzberger, A. E. Hogan, M. A. Exley and D. G. Doherty (2013). "Human invariant NKT cell subsets differentially promote differentiation, antibody production, and T cell stimulation by B cells in vitro." J Immunol **191**(4): 1666-1676.
Zha, B., L. Wang, X. Liu, J. Liu, Z. Chen, J. Xu, L. Sheng, Y. Li and Y. Chu (2012). "Decrease in proportion of CD19+ CD24(hi) CD27+ B cells and impairment of their suppressive function in Graves' disease." PLoS One **7**(11): e49835.
Zhang, J., M. Wan, J. Ren, J. Gao, M. Fu, G. Wang, Y. Liu and W. Li (2016). "Positive selection of B10 cells is determined by BCR specificity and signaling strength." Cell Immunol **304-305**: 27-34.
Zhang, W., T. L. Nilles, J. R. Johnson and J. B. Margolick (2016). "The effect of cellular isolation and cryopreservation on the expression of markers identifying subsets of regulatory T cells." J Immunol Methods **431**: 31-37.
Zhang, X., E. Deriaud, X. Jiao, D. Braun, C. Leclerc and R. Lo-Man (2007). "Type I interferons protect neonates from acute inflammation through interleukin 10-producing B cells." J Exp Med **204**(5): 1107-1118.
Zhang, Y., J. Li, N. Zhou, Y. Zhang, M. Wu, J. Xu, C. Shen, X. An, G. Shen, M. Yang, C. Zhang and J. Tao (2017). "The Unknown Aspect of BAFF: Inducing IL-35 Production by a CD5(+)CD1d(hi)FcgammaRIIb(hi) Regulatory B-Cell Subset in Lupus." J Invest Dermatol **137**(12): 2532-2543.
Zhao, M., C. Jiang and M. Diaz (2009). "Amelioration of Lupus Nephritis in MRL/lpr mice by Adoptive Transfer of IgM Anti-dsDNA antibodies (50.28)." The Journal of Immunology **182**(50 (S1)).
Zhao, Y., E. Odell, L. M. Choong, F. Barone, P. Fields, B. Wilkins, F. M. Tungekar, P. Patel, J. D. Sanderson and S. Sangle (2012). "Granulomatosis with polyangiitis involves sustained mucosal inflammation that is rich in B-cell survival factors and autoantigen." Rheumatology **51**(9): 1580-1586.
Zhu, H. Q., R. C. Xu, Y. Y. Chen, H. J. Yuan, H. Cao, X. Q. Zhao, J. Zheng, Y. Wang and M. Pan (2015). "Impaired function of CD19(+) CD24(hi) CD38(hi) regulatory B cells in patients with pemphigus." Br J Dermatol **172**(1): 101-110.

Appendix Summary of all tests conducted in AAV patients

PID	DATE BLED	B cell subsets	Treg	39/73	CD5	SORT	IL-10	CBA	TGF	Subsets
P_001	04/08/2011	**rh REM**								
P_002	02/06/2011	**rh REM**								
P_002	29/04/2013	**REPLICATE**	**1**	**1**	**1**		**1**	**1**	**0**	**0**
P_003	07/04/2011	**rh REM**								
P_004	21/07/2011	**rh REM**								
P_005	30/06/2011	**MPO AND PR3**			**1**					
P_006	17/03/2011	**rh REM**			**1**					
P_007	03/03/2011	**rh REM**			**1**					
P_008	30/06/2011	**rh REM**								
P_009	23/06/2011	**rh REM**			**1**					
P_010	18/03/2013	**rh RTX**	**1**		**1**		**1**	**1**	**1**	**0**
P_011	05/01/2012	**rh REM**			**1**					
P_012	30/06/2011	**rh REM**								
P_013	04/08/2011	**rh REM**								
P_014	28/07/2011	**NO ANCA**								
P_016	11/08/2011	**rh REM**								
P_017	04/08/2011	**rh REM**								
P_018	17/03/2011	**rh REM**			**1**					
P_019	17/03/2011	**rh REM**			**1**					

PID	DATE BLED	B cell subsets	Treg	39/73	CD5	SORT	IL-10	CBA	TGF	Subsets
P_020	17/03/2011	**rh REM**			**1**					
P_021	14/07/2011	**rh REM**								
P_021	08/04/2013	**REPLICATE**		**1**			**1**	**1**	**1**	**1**
P_022	23/06/2011	**rh REM**								
P_023	30/06/2011	**rh TOL**			**1**					
P_024	10/03/2011	**rh TOL**			**1**					
P_026	14/07/2011	**rh TOL**	**1**	**1**	**1**					
P_027	14/07/2011	**rh TOL**								
P_029	08/04/2013	**rh RTX**	**1**		**1**		**1**	**1**	**1**	**1**
P_030	30/06/2011	**GRUMBLING**	**1**	**1**	**1**					
P_031	14/07/2011	**GRUMBLING**								
P_031	18/03/2013	**rh RTX**			**1**		**1**	**1**	**1**	**0**
P_033	09/06/2011	**GRUMBLING**	**1**	**1**	**1**					
P_034	12/01/2012	**rh ACUTE**			**1**					
P_034	08/04/2013	**REPLICATE**	**1**	**1**			**1**	**1**	**1**	**1**
P_035	09/06/2011	**NO ANCA**	**1**	**1**	**1**					
P_036	08/12/2011	**GRUMBLING**								
P_037	18/08/2011	**rh ACUTE**	**1**							
P_037	17/09/2012	**rh RTX**								
P_038	05/01/2012	**rh ACUTE**	**1**							
P_039	09/01/2012	**rh ACUTE**	**1**							
P_040	12/05/2011	**GRUMBLING**	**1**	**1**	**1**					

PID	DATE BLED	B cell subsets	Treg	39/73	CD5	SORT	IL-10	CBA	TGF	Subsets
P_041	07/07/2011	**ATYPICAL ANCA**								
P_042	15/06/2011	**rh ACUTE**	**1**	**1**	**1**					
P_043	12/01/2012	**rh ACUTE**	**1**		**1**					
P_044	13/12/2011	**rh ACUTE**	**1**							
P_045	06/10/2011	**rh ACUTE**								
P_045	08/10/2012	**REPLICATE**								
P_045	08/04/2013	**REPLICATE**	**1**	**1**		**1**	**1**	**1**	**1**	**1**
P_046	22/12/2011	**rh ACUTE**	**1**							
P_047	07/10/2011	**rh ACUTE**								
P_048	23/03/2012	**rh ACUTE**	**1**	**1**						
P_048	03/09/2012	**REPLICATE**	**1**			**1**				
P_048	29/04/2013	**REPLICATE**					**1**	**1**	**0**	**0**
P_049	15/05/2012	**rh ACUTE**	**1**							
P_050	18/06/2012	**rh RTX**								
P_051	10/09/2012	**rh REM**				**1**				
P_053	01/10/2012	**rh RTX**				**1**				
P_054	15/10/2012	**rh REM**	**1**			**1**				
P_057	26/11/2012	**rh REM**	**1**							
P_058	04/02/2013	**rh REM**			**1**					
P_059	18/03/2013	**rh REM**	**1**		**1**		**1**	**1**	**1**	**0**
P_061	18/03/2013	**rh REM**	**1**		**1**		**1**	**1**	**1**	**0**
P_062	08/04/2013	**NO ANCA**	**1**	**1**			**1**	**1**	**1**	**1**

PID	DATE BLED	B cell subsets	Treg	39/73	CD5	SORT	IL-10	CBA	TGF	Subsets
P_063	08/04/2013	**rh REM**	**1**	**1**			**1**	**1**	**1**	**1**
P_064	08/04/2013	**rh REM**	**1**	**1**			**1**	**1**	**1**	**1**
P_065	29/04/2013	**rh REM**	**1**	**1**	**1**		**1**	**1**	**0**	**0**
P_067	29/04/2013	**rh RTX**			**1**		**1**	**1**	**0**	**0**
P_068	29/04/2013	**rh REM**	**1**	**1**	**1**		**1**	**1**	**0**	**0**
P_070	29/04/2013	**rh REM**	**1**	**1**	**1**		**1**	**1**	**0**	**0**
P_070	29/04/2013	**rh REM**	**1**	**1**	**1**		**1**	**1**	**0**	**0**
P_071	12/03/2013	**rh REM**								
Rheumatology		**53**	**30**	**17**	**29**	**5**	**17**	**17**	**11**	**7**
Unique individuals		**63**								
Unique samples		**70**								

B cell subsets were defined in all samples, based on relative CD38 and CD24 expression. For the Rheumatology publication, each patient was represented in the B cell analysis group once only (in column 3 the prefix rh is used to denote the published data series, REM, RTX, ACUTE and TOL denote patient groups). 17 samples were not included in the published data set, these are shaded in dark grey; these included replicates samples (n=7); those patients with grumbling disease opposed to acute (n=5) and those who were not PR3-ANCA or MPO-ANCA single positive (1 atypical, 3 negative, 1 double positive).

Treg frequency was determined by CD4, CD127 and CD25 immunostaining in 30 individuals (22 samples were paired with the published B cell data series). Treg CD73 and CD39 analysis was conducted for 17 of these individuals; ATPases were not stained in all incidences and analysis was only conducted when >1000 Treg (defined as CD4+ CD25high CD127low).

CD19, CD5 and CD1d staining was conducted in parallel to CD19, CD24 and CD38 in 29 samples, 23 overlapped with Rheumatology case series.

The sort column denotes the samples used for B cell co-cultures, this functional assessment was conducted for 5 individuals, 2 of these samples were replicates (acute B cell subset data included in publication, individuals in remission at the time of resampling).

The final 4 columns denote patients whose PBMC were stimulated in vitro, inducing B cell IL-10 production (n=17). 1 was excluded from the Rheumatology data set, due to no history of ANCA. Cell supernatant were assessed in all individual and intracellular flow cytometry was conducted for IL-10 and TNFα (n=17), TGFβ intracellular staining was conducted for 11 of these, in combination with CD24 and CD38 in 7 individuals (subsets column). B cell subsets included in the main analyses for 11 of these samples and 5 samples were replicates.